frontiers | Research Topics

Transcriptome & metabolic profiling: An insight into the abiotic stress response crosstalk in plants

Edited by
Poonam Yadav, Guanlin Li
and Jose M. Mulet

Published in
Frontiers in Plant Science

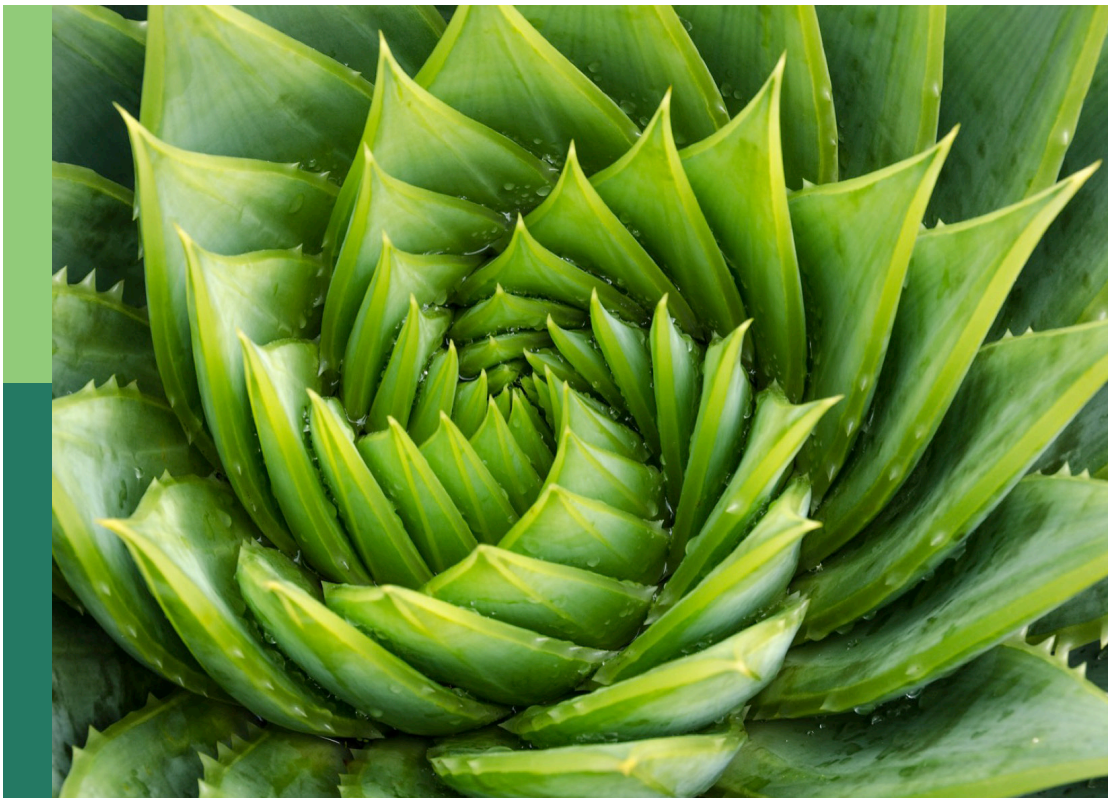

ISSN 1664-8714
ISBN 978-2-8325-4505-8
DOI 10.3389/978-2-8325-4505-8

About Frontiers

Frontiers is more than just an open access publisher of scholarly articles: it is a pioneering approach to the world of academia, radically improving the way scholarly research is managed. The grand vision of Frontiers is a world where all people have an equal opportunity to seek, share and generate knowledge. Frontiers provides immediate and permanent online open access to all its publications, but this alone is not enough to realize our grand goals.

Frontiers journal series

The Frontiers journal series is a multi-tier and interdisciplinary set of open-access, online journals, promising a paradigm shift from the current review, selection and dissemination processes in academic publishing. All Frontiers journals are driven by researchers for researchers; therefore, they constitute a service to the scholarly community. At the same time, the *Frontiers journal series* operates on a revolutionary invention, the tiered publishing system, initially addressing specific communities of scholars, and gradually climbing up to broader public understanding, thus serving the interests of the lay society, too.

Dedication to quality

Each Frontiers article is a landmark of the highest quality, thanks to genuinely collaborative interactions between authors and review editors, who include some of the world's best academicians. Research must be certified by peers before entering a stream of knowledge that may eventually reach the public - and shape society; therefore, Frontiers only applies the most rigorous and unbiased reviews. Frontiers revolutionizes research publishing by freely delivering the most outstanding research, evaluated with no bias from both the academic and social point of view. By applying the most advanced information technologies, Frontiers is catapulting scholarly publishing into a new generation.

What are Frontiers Research Topics?

Frontiers Research Topics are very popular trademarks of the *Frontiers journals series*: they are collections of at least ten articles, all centered on a particular subject. With their unique mix of varied contributions from Original Research to Review Articles, Frontiers Research Topics unify the most influential researchers, the latest key findings and historical advances in a hot research area.

Find out more on how to host your own Frontiers Research Topic or contribute to one as an author by contacting the Frontiers editorial office: frontiersin.org/about/contact

Transcriptome & metabolic profiling: An insight into the abiotic stress response crosstalk in plants

Topic editors
Poonam Yadav — Banaras Hindu University, India
Guanlin Li — Jiangsu University, China
Jose M. Mulet — Universitat Politècnica de València, Spain

Citation
Yadav, P., Li, G., Mulet, J. M., eds. (2024). *Transcriptome & metabolic profiling: An insight into the abiotic stress response crosstalk in plants*.
Lausanne: Frontiers Media SA. doi: 10.3389/978-2-8325-4505-8

Table of contents

frontiers | Frontiers in Plant Science

TYPE Editorial
PUBLISHED 13 February 2024
DOI 10.3389/fpls.2024.1370817

OPEN ACCESS

EDITED AND REVIEWED BY
Douglas S Domingues,
University of São Paulo, Brazil

*CORRESPONDENCE
Poonam Yadav
poonamyadav.b.h.u@gmail.com

RECEIVED 15 January 2024
ACCEPTED 29 January 2024
PUBLISHED 13 February 2024

CITATION
Yadav P, Li G and Mulet JM (2024) Editorial: Transcriptome & metabolic profiling: an insight into the abiotic stress response crosstalk in plants.
Front. Plant Sci. 15:1370817.
doi: 10.3389/fpls.2024.1370817

Editorial: Transcriptome & metabolic profiling: an insight into the abiotic stress response crosstalk in plants

Poonam Yadav[1]*, Guanlin Li[2] and Jose M. Mulet[3]

[1]Institute of Environment and Sustainable Development, Banaras Hindu University, Uttar Pradesh, Varanasi, India, [2]School of Emergency Management, School of Environment and Safety Engineering, Jiangsu Province Engineering Research Center of Green Technology and Contingency Management for Emerging Pollutants, Jiangsu University, Zhenjiang, China, [3]Instituto de Biología Molecular y Celular de Plantas, Universitat Politècnica de València-Consejo superior de investigaciones científicas (CSIC), Valencia, Spain

KEYWORDS

salt stress, drought stress, crops, transcriptome, metabolome

Editorial on the Research Topic

Transcriptome & metabolic profiling: an insight into the abiotic stress response crosstalk in plants

Global warming is menacing natural ecosystems (Taïbi et al., 2015) and food production systems (Melino and Tester, 2023). Abiotic stress usually affects the normal plant developmental program at several points. Drought and salt stress, i.e., less water than is required and a sodium concentration in soil of approximately 20-30 mM (glycophytes) or 100-200 mM (halophytes), induce abscisic acid, which arrests plant development (Chevilly et al., 2021). In addition, salt stress in the soil increases osmotic potential, makes water uptake more difficult for plants, and competes with the uptake of potassium, the major mineral nutrient (Yadav and Jaiswal, 2021; Mulet et al., 2023). Inside the plant, sodium is toxic and interferes with many biochemical processes, and plants must divert energy from the developmental program to maintain correct ion homeostasis (Flowers and Colmer, 2015). Similar constraints for the developmental program occur with temperature stress: freezing (below 0°C), chilling (usually between 0°C to 5°C), or heating (usually above 30°C, but depends on the plant). Heat stress also increases photorespiration and thus increases oxidation (Busch, 2020). Whereas under heavy metal toxicity overproduction of reactive oxygen species (ROS) and redox imbalance alters the energetic ratio of ATD/ADP, NADP/NADPH and NAD/NADH. Plant's compromised energetic balance are suggested as major factors related to heavy metal stress (Srivastava et al., 2013; Yadav et al., 2021). It becomes clear that the study of abiotic stress in plants cannot be carried out as a single effect but as a whole, and the crosstalk between the different signal transduction responses must be considered to obtain a general picture (Yadav et al., 2021). Systems biology, specifically technological advances in bioinformatics, and mass spectrometry, among other techniques, have allowed us to study the impact of abiotic stress on the whole transcriptome or metabolome, and thus investigate how different pathways are affected by the applied stress.

In this Research Topic, we collected twelve excellent contributions that bring new light to this complex subject and emphasize the significance of the transcriptomic and

metabolomic profile in solving the complex puzzle of stress management and mechanisms in plants. Additionally, this may help the biotechnologist involved in breeding or genetic engineering to better understand the stress management mechanism and complex role of the metabolic mechanism and develop stress and climate-resilient crops in the near future.

Abiotic stress in cereal crops

One of the advantages of recent technological advances is that abiotic stress can be studied at the molecular level not only in model organisms such as *Arabidopsis thaliana* but also in wild or cultivated plants. There is no study investigating model plants in this Research Topic but there are two that focus on barley and one that features maize. Mahalingam et al. take an original approach by comparing the transcriptome of stress-tolerant (Otis) and stress-sensitive (Golden Promise) barley genotypes subjected to drought, heat, and combined heat and drought stress for 5 days during the heading stage. The stress-sensitive phenotype presented a higher number of differentially expressed genes than the stress-resistant phenotype. Genes associated with RNA metabolism and *Hsp70* chaperones were the most upregulated; therefore, the authors suggested that these may be targets for biotechnological improvement.

It is known that during drought, plants close their stomata at a critical soil water content (SWC), and this induces diverse physiological, developmental, and biochemical responses. Paul et al. investigated this phenomenon in different genotypes of barley and found that the different responses among genotypes could suggest a specific adaptation to different rain patterns and the prominent role of the retrotransposon *BARE1*, as well as the identification of novel genes participating in the drought stress response.

Zhang et al. showed the response-related mechanism of a low phosphorus (LP)-induced gene *ZmG6PE* and its stress impact on maize (*Zea mays ssp. mays*) yield. It was advocated that the *ZmG6PE* gene was required under the LP response by mediating the expression of the *SPX6* and *PHT1.13* genes in maize plants. Additionally, the *ZmG6PE* gene contributed to the grain yield of maize through sugar and starch synthesis under LP stress. A combined transcriptomic and metabolomic study also revealed that the plant's immune regulation was activated in response to the LP stress under the influence of carbon metabolism, fatty acid metabolism, and amino acid metabolism.

Abiotic stress in horticultural crops

Vegetables are essential for a healthy diet. Horticultural crops are prone to abiotic stress due to their high water requirement. In this Research Topic, two studies have contributed with advances in onion (*Allium cepa*). Onion is another important global vegetable/spice crop and faces various challenges in the field. Gedam et al., investigated the impact of waterlogging (hypoxia) stress on onion. The study included in this Research Topic describes the transcriptomic response in leaves of two contrasting genotypes of onion under waterlogging stress and reports that several key biological processes were affected, such as phytohormone production, antioxidant enzymes, programmed cell death, and aerenchyma development. Additionally, changes were observed in the regulation of energy production under the stress response. Antioxidant enzyme activity was also higher in the tolerant variety than in the sensitive W-344 variety. Furthermore, they reported that some genes related to waterlogging tolerance, such as *RAP2-12* and *RAP2-3*, were highly expressed in the tolerant variety. Manape et al. identified and validated the probable genes governing wax accumulation in onion through transcriptomic profiling of the glossy mutant and its wild-type counterpart. The study revealed significant differences in the genes involved in the wax biosynthesis pathway in two different types of onions, the glossy mutant and the wild type. The study represents a significant contribution to onion resistance breeding against stress imposed by thrips (pest attack) or drought.

Contributions to woody plants

In this Research Topic, we have also gained some insight into the abiotic stress response in woody plants. We present a report on grapevine, a woody crop of major importance, and an industrial crop, *Hevea brasiliensis*. Drought is seen as a common stress for grape cultivation. Yang et al. quantified the effect of drought stress on 'Shine Muscat' grapevine, presented the related consequences, and provided insights into the new growth regulator 5-aminolevulinic acid (ALA) in stress mitigation. The study reported a decline in MDA production, glutathione, ascorbic acid, and betaine along with the activation of POD and SOD to better manage stress under the application of ALA. Reduction in abscisic acid by upregulating *CYP707A1* gene helped in relieving the closure of stomata and also induced changes in some chlorophyll synthesis genes. This finding can pave the way for better drought stress management of grapes and other crops in the future.

Mao et al. explored new insights regarding the metabolomic and transcriptomic profiling of rubber plants (*Hevea brasiliensis*) under cold stress. The study presented a detailed analysis of transcriptomics and metabolomics that revealed the role of cold-stress-responsive genes and metabolite molecules in rubber trees. The finding was promising as two rubber tree clones, temperature-sensitive and cold-resistant, were studied, and their transcriptomic and metabolomic responses through RNA-seq and LCMS-based metabolite profiling were mapped. Additionally, they highlighted key pathways, such as flavonoid, arginine, and anthocyanin metabolism involved with cold resistance. It is very important to track the modulation of gene expression due to cold stress and its effect on the metabolome. Finally, we also included a study on the Chinese tree *qing qian liu*, or wheel wingnut (*Cyclocarya paliurus*). Zhang et al. investigated and demonstrated the role of two stress signaling molecules, nitric oxide (NO) and hydrogen sulfide (H_2S), in salt stress tolerance in *Cyclocarya paliurus*. They described the intricate role of exogenous application of NO and H_2S in salt

tolerance in *C. paliurus*. The mechanisms is based in maintaining the photosynthetic ability and energetics, as evidenced by reduced leaf biomass loss. The study also reports increased cellular NO synthesis and decreased oxidative damage through the activation of the antioxidant enzymatic machinery and by increasing the soluble protein and flavonoid content.

Abiotic stress and medicinal herbs

Medicinal plants are of major economic and social interest. Metabolomic and transcriptomic profiling is a very useful technology for identifying active ingredients and investigating how environmental conditions affect their accumulation. Zhou et al. addressed a specific problem. *Gynostemma pentaphyllum*, also called Southern Ginseng, Miracle Plant, or Jiaogulan, is an important medicinal herb but can absorb high amounts of cadmium (Cd), which may be deleterious for consumers. The study included in this Research Topic investigated the genomic and metabolomic response of this plant to cadmium stress to develop a novel cultivar that accumulates cadmium less. The authors found that phenylpropanoid biosynthesis, starch, sucrose metabolism, alpha-linolenic acid metabolism, and the ABC transporter were significantly enriched at the gene and metabolic levels.

Illicium difengpi is an endangered medicinal plant, native to the karst mountains of the Guangxi region of China. This plant is highly adapted to drought stress. Zhang et al. performed transcriptomic and metabolomic profiling to obtain new insights into its drought tolerance mechanism. The joint transcriptome and metabolome analyses showed that under drought there was an increase in glutathione, flavonoids, polyamines, soluble sugars, and amino acids, contributing to cell osmotic potential and antioxidant activity.

The *Pueraria* genus includes more than 20 plants species, which are economically important food and medicinal plants in South-East Asia. Fu et al. analyzed the flavonoids, dietary fiber, total starch, and crude protein of one *P. lobatae* and three *P. thomsonii* varieties by combining various chemical analysis methods. Based on their findings, they proposed *P. lobata* is better for medicinal use, whereas *P. thomsonii* is a better option as edible food.

And finally, we also contribute with a review on zinc fingers. Moulick et al. put good effort into collecting literature about the detailed molecular involvement of Zn-finger motifs in abiotic stress management in crop plants. They comprehensively reviewed Zn-finger motifs and provided deep insights into the role of Zn fingers in various abiotic stress tolerance mechanisms. The review covers structural to functional aspects of zinc finger motifs/proteins and their involvement in various signaling transduction pathways, triggering the action of plant transcription factors and controlling the expression of various stress-regulated genes.

Outlook

It becomes crystal-clear that abiotic stress cannot be studied as an isolated process but must be considered as the different effects that are exerted on the essential processes of plant physiology and the multiple read-outs. Metabolomic and transcriptional studies have allowed us to study this process in general and unveil how different signal transduction pathways, many previously unrelated to the studied stress, are affected. These studies provide novel and valuable information on the crosstalk of different abiotic stresses and their interplay with developmental processes in crops and medicinal and woody plants. We hope that future investigations will convert this information into improved crops with increased tolerance to abiotic stress or increased nutritional content.

Author contributions

PY: Writing – original draft, Writing – review & editing. GL: Writing – original draft, Writing – review & editing. JM: Writing – original draft, Writing – review & editing.

Acknowledgments

The authors are thankful to the senior speciality editor of Frontiers in Plant Science for their valued input during the entire Research Topic process. The authors are thankful to the Institute of Environment and Sustainable Development, Banaras Hindu University, Varanasi, India; Jiangsu University, Zhenjiang, China; and Instituto de Biología Molecular y Celular de Plantas, Universitat Politècnica de València-CSIC, Camino de Vera, 46022 Valencia, Spain, which helped make this Research Topic successful.

Conflict of interest

The authors declare that the research was conducted in the absence of any commercial or financial relationships that could be construed as a potential conflict of interest.

Publisher's note

References

Busch, F. A. (2020). Photorespiration in the context of Rubisco biochemistry, CO_2 diffusion and metabolism. *Plant J.* 101, 919–939. doi: 10.1111/tpj.14674

Chevilly, S., Dolz-Edo, L., Martínez-Sánchez, G., Morcillo, L., Vilagrosa, A., López-Nicolás, J. M., et al. (2021). Distinctive traits for drought and salt stress tolerance in melon (Cucumis melo L.). *Front. Plant Sci.* 12. doi: 10.3389/fpls.2021.777060

Flowers, T. J., and Colmer, T. D. (2015). Plant salt tolerance: Adaptations in halophytes. *Ann. Bot.* 115, 327–331. doi: 10.1093/aob/mcu267

Melino, V., and Tester, M. (2023). Salt-tolerant crops: time to deliver. *Annu. Rev. Plant Biol.* 74, 671–696. doi: 10.1146/annurev-arplant-061422-104322

Mulet, J. M., Porcel, R., and Yenush, L. (2023). Modulation of potassium transport to increase abiotic stress tolerance in plants. *J. Exp. Botany* 74, 5989–6005. doi: 10.1093/jxb/erad333

Srivastava, S., Srivastava, A. K., Suprasanna, P., and D'souza, S. F. (2013). Identification and profiling of arsenic stress-induced microRNAs in Brassica juncea. *J. Exp. Bot.* 64, 303–315. doi: 10.1093/jxb/ers333

Taïbi, K., del Campo, A. D., Aguado, A., and Mulet, J. M. (2015). The effect of genotype by environment interaction, phenotypic plasticity and adaptation on Pinus halepensis reforestation establishment under expected climate drifts. *Ecol. Eng.* 84, 218–228. doi: 10.1016/j.ecoleng.2015.09.005

Yadav, P., and Jaiswal, D. K. (2021). *Effects of Salt Stress on Biochemistry of Crop Plants. Physiology of Salt Stress in Plants: Perception, Signalling, Omics and Tolerance Mechanism*. pp.38–pp.52.

Yadav, P., Srivastava, S., Patil, T., Raghuvanshi, R., Srivastava, A. K., and Suprasanna, P. (2021). Tracking the time-dependent and tissue-specific processes of arsenic accumulation and stress responses in rice (*Oryza sativa* L.). *J. Hazard. Mater.* Hoboken, NJ: Wiley. 406, 124307. doi: 10.1016/j.jhazmat.2020.124307

frontiers | Frontiers in Plant Science

TYPE Original Research
PUBLISHED 08 December 2022
DOI 10.3389/fpls.2022.1066421

OPEN ACCESS

EDITED BY
Jose M. Mulet,
Universitat Politècnica de València,
Spain

REVIEWED BY
Yuri Shavrukov,
Flinders University, Australia
Sotirios Fragkostefanakis,
Goethe University Frankfurt, Germany
Xinghong Yang,
Shandong Agricultural University,
China

*CORRESPONDENCE
Ramamurthy Mahalingam
mali.mahalingam@usda.gov

SPECIALTY SECTION
This article was submitted to
Plant Abiotic Stress,
a section of the journal
Frontiers in Plant Science

RECEIVED 10 October 2022
ACCEPTED 28 October 2022
PUBLISHED 08 December 2022

CITATION
Mahalingam R, Duhan N, Kaundal R, Smertenko A, Nazarov T and Bregitzer P (2022) Heat and drought induced transcriptomic changes in barley varieties with contrasting stress response phenotypes.
Front. Plant Sci. 13:1066421.
doi: 10.3389/fpls.2022.1066421

Heat and drought induced transcriptomic changes in barley varieties with contrasting stress response phenotypes

Ramamurthy Mahalingam[1]*, Naveen Duhan[2], Rakesh Kaundal[2], Andrei Smertenko[3], Taras Nazarov[3] and Phil Bregitzer[4]

[1]Cereal Crops Research Unit, USDA-ARS, Madison, WI, United States, [2]Department of Plant, Soils and Climate, Utah State University, Logan, UT, United States, [3]Institute of Biological Chemistry, Washington State University, Pullman, WA, United States, [4]National Small Grains Germplasm Research Facility, USDA-ARS, Aberdeen, ID, United States

Drought and heat stress substantially impact plant growth and productivity. When subjected to drought or heat stress, plants exhibit reduction in growth resulting in yield losses. The occurrence of these two stresses together intensifies their negative effects. Unraveling the molecular changes in response to combined abiotic stress is essential to breed climate-resilient crops. In this study, transcriptome profiles were compared between stress-tolerant (Otis), and stress-sensitive (Golden Promise) barley genotypes subjected to drought, heat, and combined heat and drought stress for five days during heading stage. The major differences that emerged from the transcriptome analysis were the overall number of differentially expressed genes was relatively higher in Golden Promise (GP) compared to Otis. The differential expression of more than 900 transcription factors in GP and Otis may aid this transcriptional reprogramming in response to abiotic stress. Secondly, combined heat and water deficit stress results in a unique and massive transcriptomic response that cannot be predicted from individual stress responses. Enrichment analyses of gene ontology terms revealed unique and stress type-specific adjustments of gene expression. Weighted Gene Co-expression Network Analysis identified genes associated with RNA metabolism and Hsp70 chaperone components as hub genes that can be useful for engineering tolerance to multiple abiotic stresses. Comparison of the transcriptomes of unstressed Otis and GP plants identified several genes associated with biosynthesis of antioxidants and osmolytes were higher in the former that maybe providing innate tolerance capabilities to effectively combat hostile conditions. Lines with different repertoire of innate tolerance

mechanisms can be effectively leveraged in breeding programs for developing climate-resilient barley varieties with superior end-use traits.

KEYWORDS

Barley, combined stress, drought, differential gene expression, gene networks, gene ontologies, heat, RNA-seq

Introduction

Among the most consequential impacts of the ongoing global climate change, drought and high temperatures will adversely affect agricultural production world-wide (Fedoroff et al., 2010; Mahalingam et al., 2021). While singly occurring drought or heat stress can lead to yield reduction, the concomitant occurrence of these two abiotic stressors in field can be devastating (Barnabas et al., 2008; Awasthi et al., 2014; Cohen et al., 2021). Five or more recurring days of heat in which the daily maximum temperature is 5°C higher than the average maximum temperature is considered a heatwave (W.M.O, 2015). In the two decades spanning 1990-2010, in the US, combined heat waves and drought have increased compared to earlier decades (Mazdiyasni and AghaKouchak, 2015). Furthermore, climate models predict the intensity and frequency of such incidents will further increase (Lobell and Gourdji, 2012).

For breeding climate change resilient crop plants, a better understanding of the responses to combined drought and heat stress is important (Zandalinas et al., 2018). Responses to combined drought and heat stress in different crop species have previously been reviewed recently (Mahalingam et al., 2021). Combined heat and drought stress generate unique metabolic signatures in maize that are otherwise unaffected when the stressors are applied singly (Obata et al., 2015). In wheat lines subjected to combined heat and drought stress during pre-anthesis stage, proline content and number of tillers were identified as key attributes of tolerance to combined stress (Qaseem et al., 2019). In chick peas, the starch and sucrose content of seeds was significantly reduced in the combined heat and drought stress treatment during seed-filling stage when compared to singly applied stress (Awasthi et al., 2014). Apart from a reduction in yield in response to combined heat and drought stress, seed nitrogen was reported to be high and starch content was low in two Australian malting barley varieties (Savin and Nicolas, 1996). Combined heat and drought stress negatively impacted malting quality of US barley varieties (Mahalingam, 2017). These studies focused on the agronomic and physiological impacts of combined stress. There is gap in the knowledge about the molecular mechanisms of tolerance in plants operative during combined stress.

Photosynthesis machinery can recover once drought and heat stress is removed; however, flower, ovary or seed abortion are irreversible processes. Hence, drought and heat stress combination during the reproductive stages are more detrimental to crop yields (Barnabas et al., 2008; Mahalingam and Bregitzer, 2019). Drought and heat combination restricts the life cycle, decreases overall carbon assimilation and drastically shortens the grain filling period in crops (Awasthi et al., 2014). Meta-analysis of more than 120 case studies of heat and drought stress combination confirmed its negative impacts on harvest index, seed number and single seed size (Cohen et al., 2021). A key strategy to alleviate the influence of drought and heat stress on crop production and quality is identification of germplasm that can tolerate these stresses during post-anthesis and using them in breeding programs or identifying the genetic mechanisms of tolerance and moving those favorable genes/alleles into the current germplasm using modern biotechnological tools.

The main obstacle in the selection of genes conferring drought and heat tolerance is the complexity of plant responses to these types of stresses. Coping strategies to overcome abiotic stress like drought may be transient, such as reduced transpiration or hydrotropism, or entail developmental reprogramming such as deeper root system, reduction of leaf area or biochemical alterations such as osmotic adjustments to minimize water loss and improve water uptake (Hu and Xiong, 2014). Transient responses, developmental changes and biochemical modifications require a substantial rebuilding of plant metabolism and gene expression changes that keep changing with the onset and as the stress persists (Wiegmann et al., 2019). Insight into the complexity of plant response to combined stress can be appreciated *via* transcriptome profiling.

The majority of studies of drought induced transcriptome changes in barley focused on leaf tissue (Talame et al., 2007; Guo et al., 2009; Bedada et al., 2014; Wehner et al., 2016; Zeng et al., 2016) while few studies analyzed spikelets, awns, seeds (Abebe et al., 2010; Hubner et al., 2015), or crowns (Svoboda et al., 2016) and one examined leaves and roots (Janiak et al., 2018). Heat stress in different parts of the seeds were examined using microarrays (Mangelsen et al., 2011). Transcriptome changes in leaves and inflorescence in response to drought and combined heat and drought stress (Cantalapiedra et al., 2017) and

proteomic alterations in young leaves subjected to heat, drought and combined stress have been reported (Ashoub et al., 2015).

In this study, drought, heat and combined heat and drought was imposed during heading stages in the tolerant barley variety Otis and a sensitive variety Golden Promise. Physiological traits were monitored during the stress regime and agronomic traits were compared at maturity. Transcriptomic differences associated with heat, drought, and combined heat and drought stress in these two contrasting lines were examined 1-day after initiating the stress and at the end of the 5-day treatment. RNA-Seq analysis revealed a greater number of differentially expressed genes in response to combined heat and drought stress compared to heat or drought stress in both GP and Otis. Interestingly, several genes with proven roles in abiotic stress tolerance such as trehalose biosynthesis, linolenic acid and glutathione metabolism were expressed at higher levels in Otis under non-stress conditions compared to Golden Promise. Identification of innately expressed genes with proven roles in abiotic stress tolerance in advanced breeding lines and modern varieties can accelerate the pace of climate-resilient cultivar development with superior end-use traits.

Materials and methods

Plant growth conditions

Seeds of Barley varieties Golden Promise (GP) and Otis were imbibed in water for three hours and three seeds were sown in each 2.5 L pots containing the potting mix as described earlier (Mahalingam and Bregitzer, 2019). Plants were maintained in the greenhouse till the first spikelet of the head had completely emerged corresponding to Zadok's scale 5.9. This plant grow-out scheme was followed precisely for the three biological replications.

Stress treatments

Pots with plants at heading stage were moved into growth chambers for heat stress and combined heat and drought stress experiments. The growth chambers were programmed to approximate the light intensity in the greenhouse (450 µmol m^{-2} s^{-1}; 16 h of light and 8 h of darkness; 50% humidity). Plants were acclimated in the growth chamber for 48 h before the imposition of the stress treatments. The heat, drought and combined stress treatments were conducted as described previously (Mahalingam and Bregitzer, 2019), when the head on the main tiller became visible. During the heat stress, plants were manually irrigated with 550 ml of water, the same amount as control plants in the greenhouse under auto-irrigation. Plants were maintained in these stress conditions for five days. On the sixth day, the chamber was reprogrammed to simulate the conditions in the greenhouse. On day seven the plants were moved into the greenhouse until physiological maturity.

Physiological measurements

Flag leaf and the leaf underneath the flag leaf from each plant were used for measuring the physiological traits with a Li-Cor 6400 Portable Photosynthesis system (Li-Cor, Lincoln, NE) as described previously (Mahalingam and Bregitzer, 2019). Stomatal conductance, net transpiration rates and net photosynthetic rates were recorded before the stress treatment and after the end of the stress treatments.

The leaf relative water content (LRWC) was calculated as described earlier (Schonfeld et al., 1988). LRWC% = (Fresh weight-Dry weight)/(Turgid weight-Dry weight) X 100. The LRWC measurements were conducted from the leaves sampled on the fifth day of the stress treatment.

For the physiological measurements with Li-Cor and the LRWC, two leaves were sampled from two different plants for each stress treatment and each genotype in each replication. Averages reported are based on data collected from at least five plants. The average measurements for the physiological traits of plants before the imposition of stress were compared with measurements from the same plants after five-days of stress treatment to determine statistically significant differences.

Sample harvesting for RNA analysis

Flag leaf and heads were harvested from each plant and frozen immediately in liquid nitrogen. For each stress and corresponding controls, tissues were collected from five individual plants. Frozen tissue samples were wrapped in aluminum foils and stored in -80 °C. Tissues were collected one day into the stress treatment (early time point) and at the end of the five days of stress treatment (late time point).

Agronomic traits

The weight of dry shoots and dry roots were recorded for each plant at maturity. The dry mature heads from each plant were collected in brown bags and threshed using a benchtop thresher (Model LT15; Haldrup, Poneto, IN). The seed weight was recorded for each plant and seed yield of five plants from each treatment were averaged.

RNA isolations

Total RNA was isolated from the flag leaf and head tissues using the RNeasy plant mini kit (Qiagen). Two independent RNA

isolations were done for each tissue from each of the biological replicates. Two genotypes, three different stress treatment (drought, heat, combined stress) and three corresponding non-stressed controls, two different tissue types (flag leaf and developing head), two time points (1 day into stress and 5th day of stress treatment) equates to 48 RNA samples for one replication. Three replications of this entire experiment accounted for 144 RNA samples.

Library construction and sequencing

QuantSeq method was used to generate 144 next-generation sequencing (NGS) libraries as described in the kit protocol at the University of Idaho sequencing facility.

Read quality assessment and mapping to barley genome

The raw reads were trimmed to remove adapter sequences and ambiguous nucleotides and assessed for quality by running through several programs such as feature counts, STAR, Gene Counts, Cutadapt, SortMeRNA, and FastQC. The output from these various programs were summarized into a single report using MultiQC (version 1.8). The filtered reads were then mapped to the barley reference genome IBGS_version 3. The read mapping data were then combined with gene feature file to obtain the feature counts. This helped to identify uniquely mapped reads and reads that mapped to multiple genes. The uniquely mapped reads were used for identifying the differentially expressed genes (DEGs) by pair-wise comparisons to corresponding controls.

Data analysis

Samples (libraries) were clustered in a multidimensional scaling plot (MDS plot) by the plotMDS function implemented in the Bioconductor package Limma in R (R Version 3.4.0, limma_3.32.2).

Identification of DEGs

The gene expression levels were estimated using RNA-Seq by Expectation–Maximization (RSEM) (Li and Dewey, 2011). To perform differential expression analysis the DESeq2 R package (1.10.1) was used. This provides statistical routines based on the negative binomial distribution model for identifying differential expression. To control false discovery rate (FDR) the P-values were adjusted using the Benjamin and Hochberg's approach (Benjamini and Hochberg, 1995). Both the q-value ≤ 0.05 and $\log_2$ (fold-change) ≥ 1 was set as the threshold for significant differential expression.

Gene Ontology (GO) enrichment analysis of DEGs

GO analysis for biological process, cellular component, and molecular function of the DEGs was implemented by the GOseq R package. GO annotations for the entire barley genome determined based on the GOMAP strategy (Wimalanathan et al., 2018) was used as the reference for enrichment analysis using the Fisher's Exact test and an FDR cutoff of 0.05. Genes within the enriched GOs from heat, drought and combined stress were compared for the leaf and head tissues separately.

KEGG pathway enrichment analysis of DEGs

Statistical enrichment of genes in KEGG (http://www.genome.jp/kegg/) pathways was conducted using KOBAS software (Kanehisa and Goto, 2000; Mao et al., 2005). For the KEGG enrichment of the DEGs, a R package, ClusterProfiler was used (Yu et al., 2012).

Weighted Gene Co-expression Network Analysis (WGCNA)

The raw reads counts were normalized using DESeq2 package and the signed co-expression network was created using WGCNA package (Langfelder and Horvath, 2008). The adjacency matrix was created by calculating the Pearson's correlations between each gene. A value of nine was used as power parameter (β) on the scale-free topology requirement (Zhao et al., 2010). Then the adjacency matrix was used to calculate the topological overlap measure (TOM) and associated dissimilarity (1-TOM). Gene modules were then identified using a dynamic tree cutoff algorithm (minimum cluster size of 30, merging threshold function of 0.25) (Langfelder et al., 2008). Module membership (MM) was computed using Pearson correlations between expression levels and module eigengenes. A relatively high MM suggests that certain genes are well-connected inside the module.

Module-traits relationships and functional categorization of modules

The module eigengenes (ME) was used to estimate the module-traits relationships by calculating the Pearson's

correlations between the ME and the traits of interest. Gene significance (GS) was used to correlate the trait of interest with the expression data of individual genes. The module-characteristics associations were calculated using the ME by computing Pearson's correlations between the ME and the traits of interest. The modules were selected based on correlation >=0.05 and *p*-value <=0.05 in control vs treatments. Genes in the module were chosen when their intra-modular connection with that module was more than 0.2, and their intra-modular connectivity with all other modules was less than 0.2. The correlation between the gene's expression profile and the ME's expression profile was used to calculate intra-modular connectivity. Only the differentially expressed genes were extracted from each module and the network visualization was done using Cytoscape (Shannon et al., 2003). Using the pySeqRNA package (Duhan and Kaundal, 2020), the uniqueness of all the modules was determined based on gene ontology.

Peroxisome abundance

Peroxisome abundance was measured using small fluorescent probe Nitro-BODIPY according to previously published procedure (Hickey et al., 2022). A 2-cm piece of the leaf was placed into 2 cm deep 96-well plate, immersed in a liquid nitrogen bath and ground with a tissue grinder (TissueLyser II, Qiagen, Venlo, Netherlands). The tissue powder was mixed with 0.8 ml of the extraction buffer A (EBA) containing 20 mM Tris HCl, pH7.4, 500 mM NaCl, 7M Urea, then the plate was rotated for one hour to extract total protein. The debris was removed by centrifugation at 3,000 *g* for 30 minutes and the supernatant was aspirated into a fresh plate. The reaction contained 20 µl of the extract, 80 µl of freshly prepared 2 µM solution of N-BODIPY, and 100 µl of water in 96-well plates and incubated for 10 min. The fluorescence intensity (490 nm excitation wavelength and 530 nm emission wavelength) was measured using Synergy Neo B spectrofluorometer (Biotek Instrument, Inc). Extracts from five individual plants (biological replicates), each three technical replicates, were measured per genotype and treatment. Two background values were measured per each 96-well plate: 20 µl of the protein extract in 180 µl of water; and 20 µl of 2 M N-BODIPY solution with 180 µl of water. These values were subtracted from the N-BODIPY fluorescence signal. The protein concentration was measured in each extract using the Bradford Reagent (Biorad Laboratories) with a calibration curve of known concentrations of Bovine Serum Albumin. The N-BODIPY fluorescence intensity was normalized by the protein concentration and calculated in arbitrary units per mg of protein.

Results

Growth and physiological responses to drought, heat, and combined stress

The stress experiments described in this study were conducted using barley plants that were in their heading stage. There were basic morphological differences between GP and Otis with the former bearing a lot more tillers during their vegetative growth phase. The leaves of Otis were broader, and the plants were taller than GP. Flag leaves of GP plants were smaller compared to the flag leaves of Otis.

Leaf relative water content (LRWC) was reduced in both the lines in response to heat, drought, and combined stresses. Overall, the reduction in the LRWC was greater in GP leaves compared to Otis (Figure 1A). Pre-stress stomatal conductance (SC) showed significant difference between the two varieties, with Otis registering values that were nearly 50% higher than GP (Figure 1B). In response to drought, both varieties showed significant reduction in their SC. On the contrary, heat and combined stress increased the SC of leaf by nearly 45% in Otis. Interestingly SC of GP leaf subjected to heat stress were like that of control leaves. Patterns of changes in net transpiration rates were identical to the pattens observed for SC in both varieties (Figure 1C). Net photosynthesis rates declined by nearly 50% in response to heat and 84% in response to drought in GP (Figure 1D). Leaves of Otis showed a 25% reduction in photosynthesis in response to heat, a 32% decrease in response to drought and 50% reduction in response to combined stress. In the GP plants the impact of the combined stress on the leaf was too severe and did not provide reliable measurements for SC, net photosynthesis, and transpiration rates.

Agronomic impact of drought, heat, and combined stress

In both varieties there was no significant difference in the root biomass in response to singly applied heat or drought stress. However, in response to combined stress both lines showed a nearly 40% reduction in their root biomass (Figure 2A). In GP the shoot biomass doubled in response to drought stress and by 30% in response to heat stress. Interestingly, combined stress did not cause any significant change in GP (Figure 2B). On the contrary, in Otis, the shoot biomass decreased by more than 40% in response to combined stress and a similar decreasing trend was observed in response to singly applied heat or drought stress but was not statistically significant.

Given the profuse tillering habit of GP the seed yield per plant was 60% higher compared to Otis plants under control conditions (Figure 2C). However, the seed yields of GP were reduced by 75% in response to heat or drought and by nearly

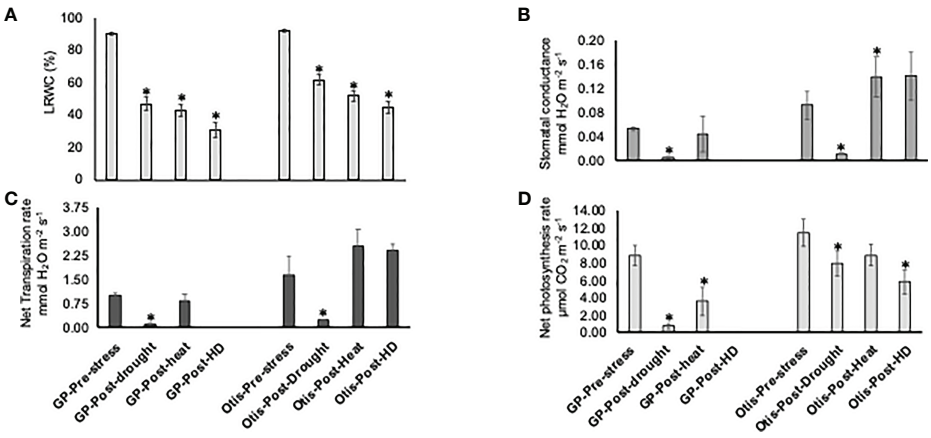

FIGURE 1
Physiological changes in Golden Promise and Otis under heat, drought and combined heat and drought stress **(A)** Leaf Realtive Water Content (LRWC). **(B)** Stomatal conductance. **(C)** Net transpiration rate. **(D)** Net photosynthetic rate. Values are the means of five plants. Bars represent standard errors of the means. *P < 0.05.

95% in response to combined stress. In Otis the reduction in yield per plant was about 40% for the singly applied stress and about 60% for the combined stress. Based on the seed yield data, Otis was nearly 50% and 300% higher yielding compared to GP in response to singly applied stresses and combined stress, respectively.

The average length of Otis seeds was nearly 18% longer than the GP seeds under control conditions (Figure 3). Interestingly, heat stress increased the average seed length of GP seeds. Though the average seed length of GP and Otis seeds were reduced in response to combined stress, there was significant variation. GP seeds did not show any significant change in seed length in response to drought stress. An overall tendency towards reduction in seed length in response to stress was seen in Otis but was not statistically significant. The reduction in seed width was more obvious in Otis seeds subjected to heat stress (~23%) compared to GP (~11%). In response to combined stress, both varieties showed a reduction of more than 30% in seed width. GP seeds showed a slight increase in seed width in response to drought while Otis seeds showed a slight decrease in width. However, these differences were not statistically significant.

Mapping of the RNA-seq reads to the barley genome

After quality trimming, an average of 79.4% of the sequences per library in Golden Promise and 78.4% of sequences from Otis were aligned to the barley reference genome (Supplementary Table 1). More than 96% of reads were mapped to unique genes in the barley genome.

Overview of the relationships among the RNA-seq samples

Transcriptomic relationships between the type of stress and tissue sample were determined in a multidimensional scaling (MDS) plot (Figure 4). Resulting distances between control and treatment samples are displayed as the leading log2-fold change (i.e., estimated root-mean-square deviation for the top 500 genes with the largest standard deviation among all samples). This analysis visually displays relationships among samples (stress treatment and tissue types) based on their spatial arrangement. The clustering of the control samples in the top left and top right was expected and represent the diversity in the biological material used for the analysis - flag leaf and head tissues, grouped near the left and the right side, respectively. Combined stress samples showed the most significant separation. The later time point of the drought stress showed a significant separation compared to the early time point. Heat stressed samples seemed to show the least separation and were found in closer proximity to the controls.

Differentially Expressed Genes (DEGs) in response to heat, drought, and combined stress

For each of the stress treatments, comparisons were made to time-matched non-stress controls for both the flag leaf and head tissues. A log2-fold cutoff ≥ 1 and an FDR of 5% were used as the defining criteria for DEGs. Of the 24 comparisons in this study (Supplementary Table 2), the lowest number of DEGs was in 1-day drought samples in both lines and in both tissues (Figure 5

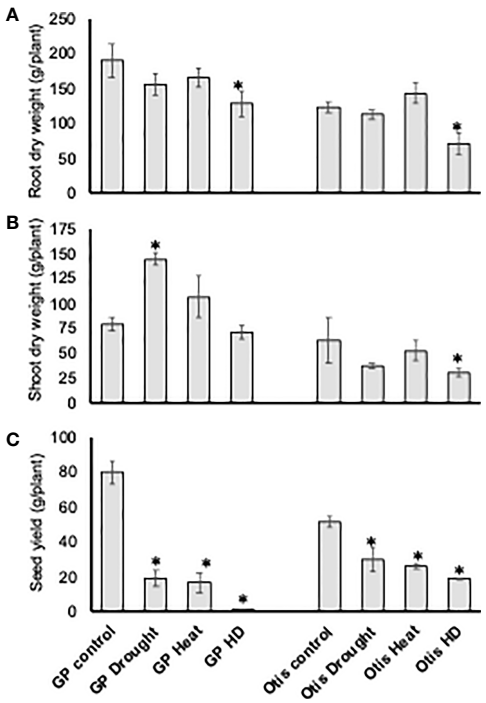

FIGURE 2
Analysis of dry root biomass **(A)**, shoot biomass **(B)**, and seed yield **(C)** in response to heat, drought and combined stress in Golden Promise and Otis. Error bars represent standard deviations of the mean of five observations from five different plants for each treatment (n = 5). Statistically significant differences in measured traits when compared to non-stressed control plants are denoted by '*' above the bars (**P*-value <0.05).

and Supplementary Figure 1). However, by the end of the fifth day of stress 4650 genes were differentially expressed in flag leaves of GP and 3905 in Otis, while the corresponding numbers in head tissue were 2467 and 1576, respectively (Figure 5).

In response to heat stress, both GP and Otis showed some marked differences in their tissue-specific and temporal transcriptional responses. In GP, more genes were differentially expressed in head compared to flag leaf at the early time point. On the contrary, in Otis nearly three-fold more genes were differentially expressed in the leaf compared to the heads at this timepoint. In the 5-day heat-stressed samples, the number of DEGs in the head and leaf tissue of Otis were similar. The very low number of DEGs observed in GP could be due to the severe heat stress damage incurred to flag leaf and the developing heads. Despite the minimal response to drought at one day, the strong response evoked by 5-days of drought was significantly higher than the transcriptional responses evoked after 5-days of heat stress.

Combined heat and drought stress caused massive changes in the transcriptomes of both these varieties. Within 1-day of combined stress, more than 9300 genes were differentially expressed in GP and 7500 genes in Otis and the number of genes differentially expressed genes was greater in the leaf tissue compared to heads. By five days of combined stress, the number of differentially expressed genes increases to more than 15,000 genes in GP while these numbers were nearly 50% less (6789) in Otis. These results clearly showed massive transcriptional changes in response to combined stress, in both genotypes and tissues when compared to heat or drought stress. Furthermore, the transcriptional changes observed in the sensitive GP was significantly larger compared to the tolerant Otis.

Comparing DEGs responsive to drought, heat, and combined stress

The number of differentially expressed genes that were common for the early (1-day) and later stages (5 days) of singly applied heat stress in GP and drought stress in Otis did not show any overlap (Figure 6). This observation was consistent for flag leaf and head tissues. Thirty genes in the flag leaf and 55 genes in the head tissues showed an overlap between 1 and 5-days of drought in GP, while 414 genes in leaf and 196 genes in head tissues overlapped between the 1 and 5-days of heat stress in Otis (Figure 6). On the contrary, there were significantly more genes that were common to 1 and 5 days in response to combined stress when compared to singly applied stresses. Furthermore, significant differences were observed in the pattern of overlap in the two varieties. In flag leaf of GP more than 4400 differentially expressed genes were common between 1 and 5 days, while in Otis around 1000 genes were found to overlap between the two time points. Consistent with this observation, the number of uniquely differentially expressed genes at early stage in GP was 470 genes, while in Otis this was close to 2450 genes. This pattern was reversed at the 5-day time point with GP recording 2222 genes while in Otis 660 genes were uniquely differentially expressed. In the head tissue, GP had 2600 commonly differentially expressed genes between 1 and 5 days compared to 1750 genes in Otis. Like the pattern in the flag leaf, in GP heads 3416 genes were uniquely expressed at the 5-day time point compared to 360 genes observed at 1 day. In Otis head tissues, approximately about 600 genes were unique for the 1-day and 400 at the 5-day time point. Based on these observations the transcriptional response to counter combined stress in Otis appears to be regulated and consistent while GP appears to unleash a massive reprogramming especially during the later time point.

Gene Ontology (GO) enrichment analysis of DEGs

The GO terms with an FDR cutoff of 0.05 containing five or more genes were identified for further analysis and are presented

FIGURE 3
Seed physical characteristics of Golden Promise (GP) and Otis collected from plants subjected to heat (Ht), drought (Drt), combined heat and drought stress (HD) and control (C). Ten seeds randomly sampled from the seed bags were placed on a paper and arranged on a straight line and photographed using a Nikon camera.

in Figure 7 (Supplementary Table 3). GOs wherein most genes that were differentially expressed were either in GP or Otis are described below for each of the three stresses.

Combined stress: Peroxisomal genes were enriched in the DEGs in response to combined heat and drought stress in leaves of both GP and Otis at the early time point (Supplementary Table 4). This enrichment was observed even at the later time point in GP in response to combined stress and drought alone. Among the differentially expressed genes associated with peroxisomes, 25 genes were up and 15 were down in GP, while 22 were up and 9 down in Otis. At the end of the 5-day stress regime this pattern was maintained with 32 genes being up

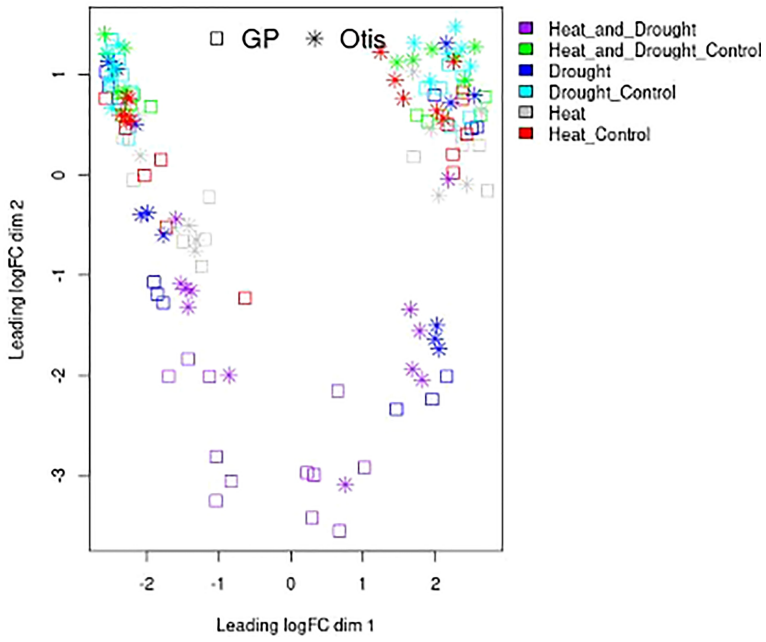

FIGURE 4
Multidimensional scaling plot of replicated RNA-Seq samples. Features on the plot represent libraries of control, drought, heat and combined stress treatments from flag leaves and head tissues collected after 1 day and 5 days of treatment. Spatial arrangement of the various RNA-seq libraries is based on their calculated distances estimated using root-mean-square deviation for the top 500 genes with the largest standard deviation among all samples. The square represents GP libraries while the * represent Otis libraries. The color code for the heat, drought and combined heat and drought and corresponding controls is shown on the right.

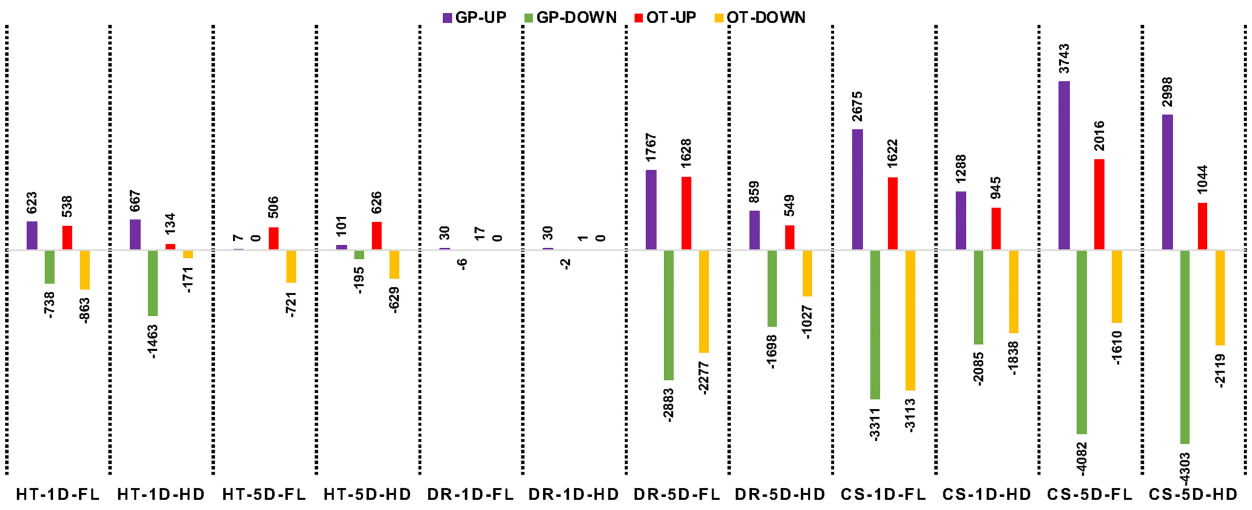

FIGURE 5
Number of differentially expressed genes in the flag leaf (FL) and head (HD) tissues at 1-day after stress (1D) or 5 days after stress (5D) in Golden Promise (GP) and Otis (OT) observed in response to heat (HT), drought (D), and combined stress (CS). Upward pointing bars represent upregulated genes and the downward facing bars represent the down regulated genes. Normalized counts for a gene from a stressed sample library is divided by the corresponding normalized counts for the same gene from the matched control sample library. A $\log_2 > 1.0$ and FDR of 0.05 was used as the cutoff to call a gene as being differentially expressed.

and 14 down in GP. One catalase gene was down only in GP while another catalase gene was induced in both genotypes at the early time point. At the 5-day time point two catalases were down in GP and one was induced in both the genotypes. One of the genes annotated as PEX11 was down in both GP and Otis while two other PEX11 genes were upregulated in both genotypes at 1- and 5-day after stress. It was observed that the extent of downregulation of the catalases and peroxin genes were stronger in GP compared to Otis. In the 5-day drought leaf sample, three PEX11 genes were identified, of which two were up in both GP and Otis while one was down only in the former. The extent of differential expression was stronger in GP than in Otis. Intriguingly, quantification of peroxisomes in the leaves showed a larger reduction in peroxisome abundance in GP compared to Otis at 5-days of combined stress (Figure 8).

Autophagy genes were strongly enriched in the DEGs in the 5-day leaf samples of GP. Of the 19 genes that were identified as being associated with this GO, six genes had annotations indicating they were ATG family genes. In particular, ATG8 which is a marker gene for peroxisome degradation was found to be induced strongly in GP compared to Otis. This suggests that GP may be experiencing higher levels of oxidative stress that leads to oxidation of proteins and turnover of organelles that trigger the autophagic flux. This is further supported by the enrichment of the GO for unfolded protein binding in the stress sensitive GP.

In Otis, the GO for oxido-reductase activity is enriched in the set of DEGs (Supplementary Table 4). Of the 241 genes associated with this category there were 74 genes that were differentially expressed only in Otis. Noteworthy genes among the induced ones were a gene involved in proline biosynthesis, several peroxidases, dioxygenases, flavin monooxygenase, and genes in the GABA shunt pathway. Among the repressed genes were Rubisco, GA20 Oxidase, and chlorophyll biosynthesis genes.

In the head tissue of GP, combined stress evoked differential expression of six different genes annotated as cyclin-dependent protein ser/thr protein kinase inhibitors of which one gene was induced and five genes were repressed.

In the head tissue of Otis plants, the GO xylan biosynthesis was enriched. Analysis of the 14 DEGs associated with this GO showed that seven were repressed only in Otis. The remaining seven genes were repressed in both GP and Otis, but the extent of repression was stronger in the latter.

Similar patterns of stronger repression of eight genes associated with GO for cellulose catabolic process was observed in Otis. Among the repressed genes were three endoglucanases that were strongly downregulated only in Otis. In GP heads the GO for cellulose synthase (UDP-forming) activity was enriched and again 11 of the 12 genes were repressed. Among the repressed genes, four were only identified in GP. Interestingly, this GO was identified in the heads of Otis at the 5-day time point. Among the 13 DEGs associated with this GO, 12 were repressed and one was induced in Otis and none of these genes were differentially expressed in the heads of GP.

Drought stress: The GO for peroxisomes was enriched in response to drought in GP leaves (Supplementary Table 5). Of

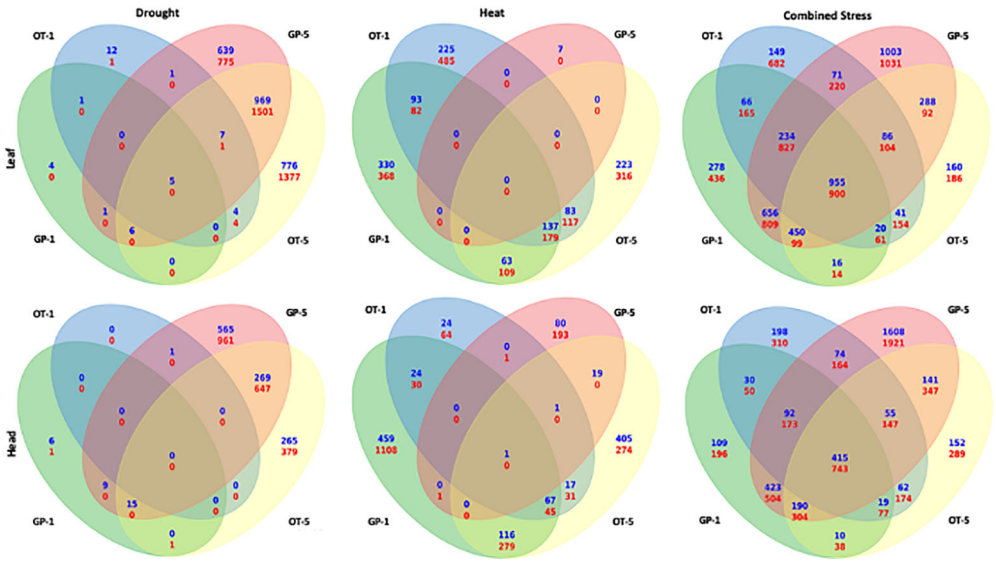

FIGURE 6
Venn diagram showing the overlap between DEGs responsive to drought (left), heat (middle), and combined stress (right). The top panel shows the comparisons from the leaf libraries and the bottom panel shows the comparisons from head libraries. In each Venn diagram the left side ovals represents the 1-day tissue sample and the right-side ovals represent the 5-day tissue sample.

the 29 DEGs associated with this GO, nine were repressed and 20 were induced. Notable among the induced genes that showed significant upregulation in GP compared to Otis were two genes – urate oxidase and acyl-CoA oxidase whose activities can lead to generation of hydrogen peroxide.

Among the 70 genes associated with the GO mRNA binding, 64 were repressed in GP and six were induced. Many of these genes were associated with rRNA processing, and proteins associated with forming larger complexes such as WD-40 repeat containing proteins, tetra and pentatricopeptide repeat containing proteins.

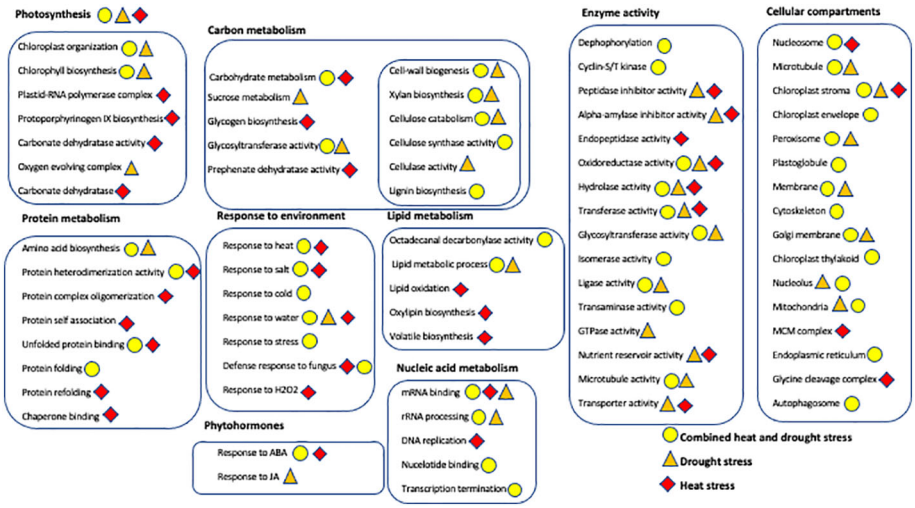

FIGURE 7
Overview of the Gene Ontology enrichment analysis showing the major biological processes, molecular functions, and cellular compartments of differentially expressed genes from leaves and head of Golden Promise and Otis in response to drought (brown triangles), heat (red diamond) and combined stress (yellow circle). Metabolic processes, molecular functions and genes encoding for proteins with specific activities are grouped within boxes. Only statistically significant GOs (P-value <0.001 and FDR<0.05) and those containing three or more DEGs were used for creating this illustration.

In Otis, there were 166 genes associated with the transmembrane transport process. Of these 87 were repressed and 79 were induced. Among the induced genes that were unique to Otis several were annotated as ABCG type transporter that are implicated in hormonal transport especially ABA. Interestingly there were two sugar transporters that were unique to Otis but showed opposites patterns of expression.

The octadecanal decarbonylase activity was enriched among genes differentially expressed in response to drought in Otis. Of the 11 genes associated with this GO, eight were induced and three were repressed. Two genes that were uniquely induced only in Otis, *Glossy1* and *Eceriferum1* homologs have been known to be involved in the biosynthesis of long chain fatty acids leading to enhanced wax production and rendering plants tolerant to drought.

The oxygen evolving complex (OEC) was an enriched GO cellular compartment in response to drought in Otis. Subunits of all three major genes (psbO, psbP and psbQ) of the OEC were identified and all these genes were repressed in both Otis and GP. Two subunit genes of the psbP domain important for binding of the chloride and calcium ions and making them available to PSII was downregulated only in Otis.

One of the most interesting GO terms that was identified in Otis heads was the negative regulation of endopeptidase activity. All the 18 genes associated with this GO were strongly induced in Otis and more importantly 14 of these genes were only observed in Otis but not in GP. Twelve of these were annotated as the serine type endopeptidase inhibitors, five were cysteine endopeptidase inhibitors and one gene contained the soybean trypsin inhibitor domain.

Sucrose metabolism was enriched in Otis heads. Six genes were associated with this GO of which four were induced and two were repressed in Otis in response to drought. Of the three genes that were uniquely induced only in Otis, two were annotated as sucrose synthase and one was a sucrose symporter.

In GP heads, the GO for response to JA was significant and included seven genes of which five were induced and two were repressed. Among induced genes were three transcription factors-two ERFs and a WRKY type TF, ornithine aminotransferase, important for proline biosynthesis, and an Inositol-polyphosphate phosphatase that can be crucial for stress signaling.

Heat stress: The GO for transmembrane transport was enriched in GP and comprised of a set of 76 genes of which 15 were induced and 61 were down regulated (Supplementary Table 6). Only two of the GP-induced genes associated with this GO was identified in Otis and one of them encoding a major intrinsic protein showed opposite pattern of expression. Of the 61 down regulated genes, 50 were unique to GP and only 11 genes were identified in Otis and showed similar changes in their expression in response to heat.

The GO for lipid transport was enriched in Otis and included a set of 15 genes of which 14 were down regulated. Only three of the genes associated with this GO was identified as differentially expressed in GP. Interestingly, all the genes

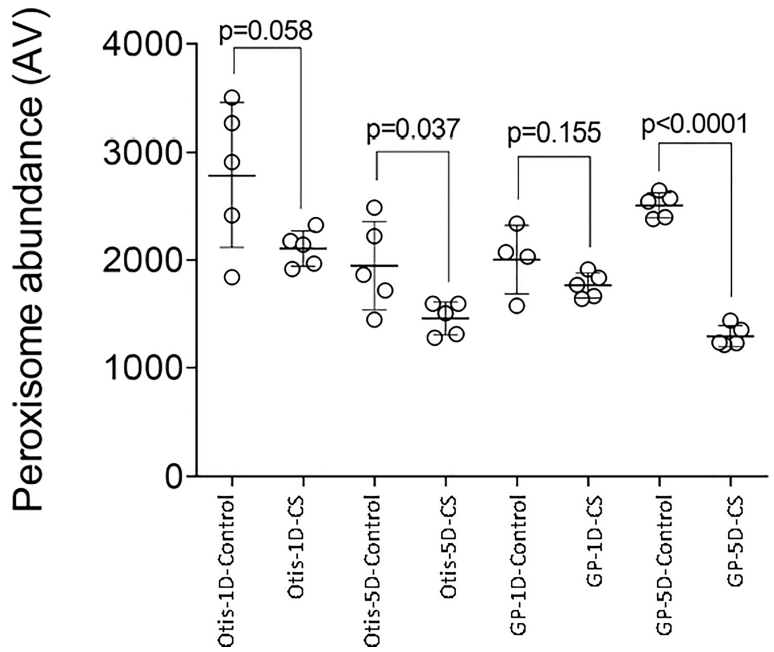

FIGURE 8
Impact of combined heat and drought stress (CS) on peroxisome abundance in Golden Promise (GP) and Otis. Values are from five different samples. P-values represent the pair-wise comparison of control and stressed leaf samples for each time point and genotype.

associated with this GO were annotated as the non-specific lipid transfer proteins (nsLTPs). In the 5-day leaves of Otis, there were six genes associated with the zinc ion transport and all of them were down regulated.

In GP heads the ABA response GO was enriched one day after heat stress. Of the 17 genes identified as differentially expressed 11 were induced and six were repressed. Notable among the induced were the LEA, dehydrin8 and HVA22 genes. Among the repressed genes was a bZIP46-like TF that includes the well-known ABI5 gene.

Carbonate dehydratase activity was enriched in Otis heads. Of the seven genes associated with this GO, two were induced while five were strongly down regulated. The differential regulation of the members of this gene family only in Otis suggests a role for these genes in the heat tolerance trait. Since these genes are affected strongly by the zinc, it is possible that the observed differential expression could be indirectly mediated by zinc, wherein we observed a strong downregulation of zinc transporter genes only in Otis.

The GO for negative regulation of peptidase activity was enriched in the leaves of GP at the 1- day time point and in the heads of Otis at the end of treatment. Of the 20 genes associated with this GO in GP, 6 were up regulated, 14 were downregulated and none of these genes were identified in Otis. Of the 14 genes associated with this GO in Otis heads, 13 were strongly induced and one was down regulated. Only two of these genes were identified in GP and interestingly, these two genes showed opposite patterns of expression when compared to Otis. These two genes (HORVU.MOREX.R3.2HG0122620 and HORVU.MOREX.R3.3HG0309490) were down regulated in GP heads. As described earlier this GO was also identified in response to drought stress in Otis and hence, we compared the genes associated with this GO in the two stresses. Nine genes associated with this GO were common between heat and drought stress and eight of these showed similar patterns of gene expression in the head tissue. One gene (HORVU.MOREX.R3.3HG0309490) that was strongly induced in GP in response to drought was down regulated in heat stress.

Weighted gene co-expression network analysis

The WGCNA analysis clustered the genes identified in this study into 41 modules (Supplementary Figure 2). The module-trait specifications using Pearson correlation to link modules to stresses identified 55 significant correlations (Figure 9). The largest number of significant correlations (18) were associated with the combined stress. In the individually applied heat or drought stress, five significant correlations were identified. For the construction of gene networks, two selection parameters were considered. The first criterion was the number of genes in the module. Of the 41 modules, 19 contained less than 100 genes, 12 had more than 100 but less than 1000 and 3 had more than 1000 genes (Supplementary Figure 3). Secondly, we focused on those modules which showed opposite patterns of correlations between the stress and corresponding stress modules. Nine modules passed these criteria. The darkred module was identified in heat, drought, and combined stress. Black, green, magenta, red, blue, brown, pink, and tan modules were associated with the combined stress but not the singly applied stresses.

In the darkred module with 108 genes, networks comprising 101, 87 and 48 genes were identified among differentially expressed genes in combined stress (Figure 10A), heat

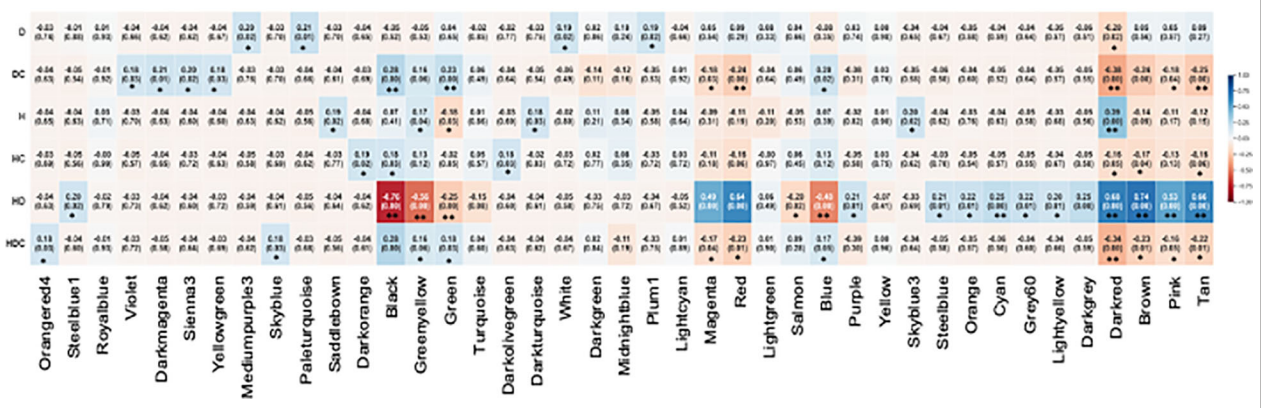

FIGURE 9
Matrix showing Module-Trait Relationships (MTRs) of different WGCNA modules under drought (D), heat (H) and combined heat and drought stress (HD) and the corresponding control modules for drought (DC), heat (HC) and combined heat and drought (HDC). The colors represent the various modules (Supplementary Figure 2). The numbers represent Pearson correlation coefficients, and the p-values are in parenthesis. Positive correlation is colored in blue while negative correlation is colored in red. Statistically significant correlations are indicated by *p-value <0.05 and >0.01, **p-values <0.01.

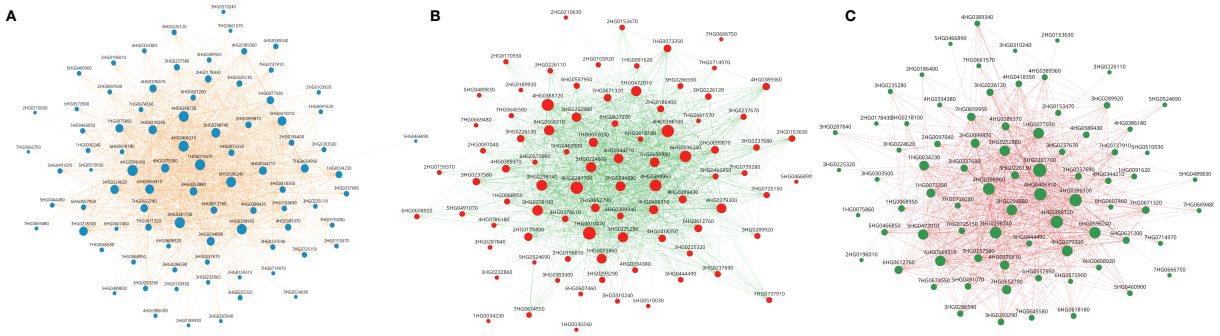

FIGURE 10
(A) Gene networks for 102 DEGs involved under heat and drought stress in the Dark red module (108 genes). Size of the node represent the degree. All genes' nodes are represented in blue color while edges are represented by tan color. **(B)** Gene networks for 87 DEGs in response to heat stress in the Dark red module (108 genes). Size of the node represent the degree. All genes are represented in tomato color while edges are represented by green color. **(C)** Gene networks for 42 DEGs involved under drought stress in the Dark red module (108 genes). Size of the node represent the degree. All genes are represented in green color while edges are represented by pink color.

(Figure 10B) and drought stresses (Figure 10C) respectively. Of the 48 genes in the drought network, 44 were also identified in the heat and combined stress networks. Between the heat and combined stress networks there were 42 common genes.

The network analysis indicated there were six hub genes in the heat, drought and the combined stress networks based on clustering and topological coefficient (Supplementary Table 7). Three were identified as hub genes in all three stress conditions, three were identified in two stress states (heat and combined stress or drought and combined stress), two genes were associated only with drought and one hub gene was associated only with heat stress. Four genes associated with RNA metabolism were identified as hub genes and included two genes associated with alternate splicing, a polyA polymerase and an RNA binding protein of unknown function. HSP family chaperones such as HsP70, ClpB and Hsp70-dependent nucleotide exchange factor were identified as the hub genes in these networks associated with heat, drought, and combined stress (Figure 11).

Transcription Factors (TFs) responsive to heat, drought, and combined stress

Between the two varieties there were more than 1000 genes encoding TFs that were differentially expressed and consistent with the patterns observed for the whole DEG data set (Supplementary Table 8). Combined stress caused extensive up-regulation (232 in GP and 130 in Otis after 1 day; 179 in GP and 193 in Otis at 5 days) as well as down-regulation of TFs (269 in GP and 250 in Otis after 1 day; 226 in GP and 218 in Otis after 5 days). One day after drought stress evoked the lowest number of TFs in both lines. In contrast to drought stress, 1 day of heat stress caused upregulation of 71 TFs and downregulation of 110 TFs in GP while 50 were up and 48 were down in Otis. However, 5 days after drought stress, 181 TFs were up in GP and 150 in Otis, while 229 in GP and 177 in Otis were down regulated. In the 5-day heat stress samples the leaf tissues from GP were severely damaged and in the head tissue only two were up regulated and 26 were down, while 52 were up and 82 were down in Otis heads.

	1GL-C	1OL-C	1GH-C	1OH-C	5GL-C	5OL-C	5GH-C	5OH-C	1GL-D	1OL-D	1GH-D	1OH-D	5GL-D	5OL-D	5GH-D	5OH-D	1GL-H	1OL-H	1GH-H	1OH-H	5GL-H	5OL-H	5GH-H	5OH-H	
HORVU.MOREX.R3.1HG0010470	2.0	1.5	1.1	1.2	2.4	1.3	0.0	1.1	0.0	0.0	0.0	0.0	0.0	0.0	0.0	0.0	1.0	0.0	0.0	0.0	0.0	0.0	0.0	0.0	Arginine/serine-rich splicing factor
HORVU.MOREX.R3.1HG0034230	2.2	1.3	0.0	0.0	2.8	0.0	0.0	1.4	0.0	0.0	0.0	0.0	0.0	1.2	0.0	0.0	0.0	0.0	0.0	0.0	0.0	0.0	0.0	0.0	Poly(A) RNA polymerase cid11
HORVU.MOREX.R3.1HG0077030	6.7	4.7	3.1	3.9	7.1	4.1	0.0	3.0	0.0	0.0	0.0	0.0	2.7	3.2	1.9	2.1	5.3	2.5	2.2	2.1	0.0	4.4	0.0	2.2	ATP-dependent chaperone ClpB
HORVU.MOREX.R3.3HG0281700	2.7	2.4	1.8	1.5	2.9	2.3	0.0	1.6	0.0	0.0	0.0	0.0	2.0	2.3	1.3	1.1	1.1	0.0	1.9	0.0	0.0	1.2	-1.1	0.0	splicing factor-like protein
HORVU.MOREX.R3.4HG0388720	6.3	4.4	3.6	3.3	7.7	5.0	0.0	3.2	0.0	0.0	0.0	0.0	1.4	0.0	0.0	0.0	3.6	3.1	3.0	2.7	0.0	3.2	0.0	2.9	Hsp70 nucleotide exchange factor fes1
HORVU.MOREX.R3.4HG0396100	7.0	7.4	5.6	6.3	7.6	5.8	0.0	5.8	0.0	0.0	0.0	0.0	0.0	0.0	4.1	4.0	4.3	2.0	3.8	4.0	0.0	5.4	0.0	3.7	Heat shock 70 kDa protein
HORVU.MOREX.R3.4HG0398960	2.9	2.0	2.1	1.8	3.6	1.8	0.0	2.2	0.0	0.0	0.0	0.0	0.0	1.4	1.0	1.4	1.2	0.0	1.4	0.0	0.0	1.6	0.0	1.8	Bifunctional protein HldE
HORVU.MOREX.R3.4HG0406310	2.5	1.2	1.2	0.0	2.7	1.4	0.0	1.2	0.0	0.0	0.0	0.0	2.2	0.0	0.0	0.0	0.0	0.0	0.0	0.0	0.0	0.0	0.0	0.0	WD and tetratricopeptide repeat protein
HORVU.MOREX.R3.6HG0596240	3.7	3.5	2.8	2.1	4.4	2.8	0.0	2.4	0.0	0.0	0.0	0.0	0.0	1.1	1.2	0.0	1.8	1.8	1.7	1.5	0.0	3.2	0.0	1.5	RNA binding protein

FIGURE 11
The nine hub genes identified in the darkred module for heat, drought, and combined stress in barley. Hub genes were selected based on the topological coefficients (<0.4) and closeness-connectivity values (>0.8). The matrix shows the differential expression values for each time point (1 or 5), genotype (Golden Promise-G and Otis-O), tissue type (L-Leaf; H-Head) and stress (D: Drought; H: Heat; C: Combined stress). The intensity of the color within each (brown: combined stress; Yellow: Heat; Red: Drought) indicates the extent of differential expression of the hub genes. The left column shows the gene identifiers, and the right column shows the IPK gene descriptions.

To get a better appreciation for the major transcription factor families associated with abiotic stress, an arbitrary cutoff of five or more members of a TF family was used as a selection criterion. This led to the identification of 23 TF families in the leaf tissues and 21 in the head tissues (Figure 12 and Supplementary Figures 4-7). All the identified members of the ERF, GRAS, HD-Zip, HSF, NAC, and Trihelix family TFs were up regulated. All the identified members of ARF, B3, CO-like, GATA, MIKC-MADS, TALE, TCP and ZF-HD were down regulated. TFs belonging to the bHLH, bZIP, C2H2, C3H, Dof, G2-like, Myb, Myb-related and WRKY contained family members that were up or down regulated. The C3H family TFs were up in GP and down in Otis in response to combined stress (Supplementary Figure 6). In the head tissue the patterns of differential expression were like that observed in the leaf samples, except for few exceptions. The number of genes associated with the HD-Zip and Myb were substantially high in the heads compared to the leaf tissues.

Innate differences in the transcriptomes of GP and Otis

Since GP is a malting variety and Otis is a feed barley, we set out to identify the innate differences in gene expression these two varieties in their leaf and head tissues. Since the tissue sampling was done at 1 and 5 days of stress treatments, control samples were also collected at the corresponding time points. For identifying genes differentially expressed between the two barley varieties, control samples were considered without respect to their timepoint (1-day, 5-day). Genes that were differentially expressed in two or more biological replicates were used for this analysis. In the flag leaf of GP 534 genes were differentially expressed (down in Otis) while 502 were identified in Otis (down in GP). In the head tissue of GP, 218 genes were differentially expressed compared to 238 in Otis (Supplementary Table 9).

KEGG pathway enrichment analysis was undertaken to identify the key differences that are associated with these two barley varieties. The comparisons between GP and Otis leaf samples identified three pathways that were reproducibly different between the biological replicates. The pathways were associated with glutathione metabolism, alpha-linolenic acid metabolism and starch-sucrose metabolism (Table 1). The glutathione pathway was also the lone pathway that was consistently differentially regulated in the head tissues.

Glutathione metabolism: Of the 16 genes that were identified with this pathway in the leaves there were several interesting genes in ascorbate-glutathione pathway that were up in Otis compared to GP. This included key genes like the ascorbate peroxidase, dehydroascorbate reductase, glutathione peroxidase, gamma-glutamyl cyclotransferase and a predicted 5-oxoprolinase. It was interesting to note that a phosphogluconate dehydrogenase gene was up in Otis and could play a role in imparting stress tolerance by reducing oxidative stress. There were five GST genes that were upregulated in GP compared to Otis leaves. In the head tissue the most noteworthy genes identified as up in Otis were ascorbate peroxidase, ribonucleotide diphosphate reductase and spermidine synthase.

Alpha-linolenic acid metabolism: Eight genes were identified associated with this pathway. Interestingly, four genes were up in GP and four were up in Otis. Allene oxide synthase, lipoxygenase and Acyl-CoA oxidase are three genes identified in Otis that are associated with JA signaling. While 12-oxophytodienoic acid reductase 2, a lipoxygenase and an alcohol dehydrogenase were identified in GP.

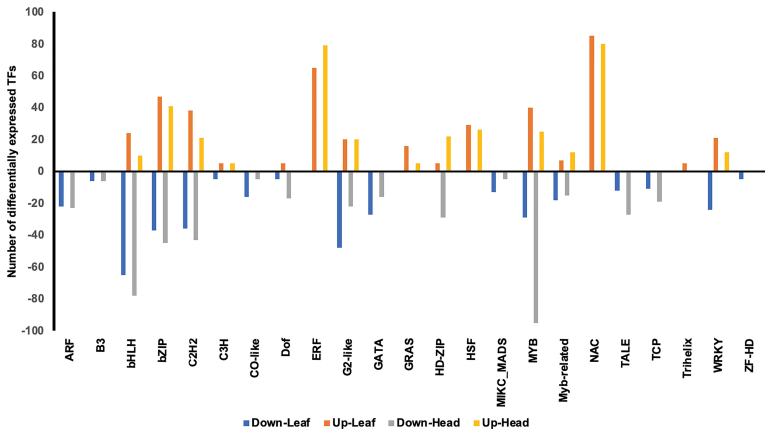

FIGURE 12
Transcription factors (TF) in leaf and head tissues that are differentially expressed in response to heat, drought and combined stress in Golden Promise and Otis. Only families of TFs with >5 expressed members are shown.

TABLE 1 KEGG pathways enriched among differentially expressed genes in GP and Otis under non-stress conditions.

Gene Ids[1]	GP:Otis[2]	Description
Glutathione metabolism		
1HG0021340	3.73	GST
1HG0023640	3.97	predicted protein
1HG0051740	3.56	glutathione S-transferase U17-like
1HG0051870	2.82	Tau GST
1HG0051910	4.80	glutathione S-transferase GSTU6
4HG0336870	1.75	glutathione S-transferase 3
2HG0169250	1.42	predicted protein
1HG0081150	*-2.13*	6-Phosphogluconate dehydrogenase
2HG0193390	*-1.71*	predicted protein
2HG0202910	*-1.17*	glutathione S-transferase GSTU6
2HG0214080	*-1.77*	glutathione peroxidase GPX15Hv
6HG0615590	*-1.47*	5-oxoprolinase
7HG0666960	*-1.64*	dehydroascorbate reductase
7HG0687590	*-1.59*	Ascorbate peroxidase
4HG0386180	*-1.60*	Glutathione-S-transferase
6HG0549380	*-1.42*	Gamma-glutamylcyclotransferase
Starch and sugar metabolism		
7HG0643810	1.94	nudix hydrolase 14
7HG0751660	2.18	starch branching enzyme
4HG0413910	2.61	Invertase, GH32 family
2HG0200340	3.51	Beta-fructofuranosidase
3HG0292350	2.20	Glycoside hydrolase family 3 GH3
5HG0478650	2.39	Endoglucanase
3HG0287930	*-2.38*	Hexokinase
7HG0735650	*-1.62*	Alpha-glucosidase
3HG0312760	*-2.31*	beta-glucosidase 5-like
7HG0712530	*-2.14*	1,4-alpha-glucan-branching enzyme
3HG0309930	*-3.15*	sucrose-phosphate synthase 1
5HG0525230	*-1.03*	adenylyltransferase
4HG0333180	*-2.17*	predicted protein
5HG0476550	*-1.87*	Trehalose-phosphatase
7HG0666870	*-1.27*	pfkB-like carbohydrate kinase
4HG0340370	*-1.90*	Glycoside hydrolase family 9
Liniolenic acid metabolism		
1HG0040000	2.46	3-ketoacyl-CoA thiolase 2
1HG0056730	1.39	Lipoxygenase
4HG0406770	2.95	alcohol dehydrogenase
2HG0170580	1.92	12-oxophytodienoic acid reductase
4HG0394970	*-3.49*	Allene oxide synthase
7HG0674860	*-1.41*	Acyl-CoA oxidase peroxisomal
5HG0420500	*-3.17*	Lipoxygenase
5HG0493180	*-1.90*	Alcohol dehydrogenase

[1] Each of the gene identifiers should be preceded by HORVU.MOREX.R3.
[2] The differential expression in GP:Otis non-stress plants. Regular font refers to genes that are up in GP while the negative italicized values represent genes that are up in Otis.

Starch and sugar metabolism: Of the 16 genes associated with this pathway, 10 were up in Otis and six were up in GP. Among the genes that were up in Otis were a hexokinase, trehalose phosphatase, sucrose phosphate synthase, carbohydrate kinase, alpha and beta-glucosidase. In GP, a gene annotated as a starch branching enzyme, nudix hydrolase 14, invertase, and a glycoside hydrolase 3 family gene were identified.

Discussion

In this study we chose to use the heat and drought stress tolerant Otis variety, a feed barley suited for the US-western drylands (with high temperatures and low moisture) and Golden Promise, a good malting variety, but sensitive to heat and drought stresses. Using model genotypes of *Hordeum vulgare* for identifying abiotic stress tolerance mechanisms will provide valuable genetic information for accelerating commercial cultivar development that can cater to the needs of the malting and brewing industries.

The physiological responses in both the varieties indicated a significant reduction in their stomatal conductance and transpiration rates in response to drought stress and higher than control levels in response to heat stress (Figure 1). Since the response to combined stress is like that of singly applied heat stress based on the increased stomatal conductance and transpiration rates it suggests that barley plants have innate abilities to withstand water deficits. However, based on the severe reduction in leaf water content, net photosynthesis rates and significantly higher seed yield loss observed in response to combined stress we speculate that barley plants perceive the combined heat and drought as an entirely different threat (Figures 1, 2).

Pot-based experiments, such as the one described in this study, have the inherent disadvantage of not mimicking natural conditions, especially related to edaphic factors. On the contrary, experiments in controlled growth chamber settings aid in limiting variation due to interaction with environment. For example, rooting depth is not a trait for consideration, since the roots in these plants at heading stage readily explored all soil volume (although the pots were large). Thus, differences in soil exploring capacity (rooting depth) of these two varieties cannot be a factor for the genotypic disparities in physiological measurements. In fact, the root biomass data did not show any significant differences in the two varieties in response to heat or drought stress (Figure 2). Since the soil conditions and water availability were similar for the two genotypes, the more significant reduction in root biomass in response to combined stress in Otis compared to GP may be a stress tolerance strategy to divert the valuable resources for producing more seeds.

During terminal stresses such as heat and drought, shoot characteristics contribute to grain weight (Kobata et al., 1992; Sallam et al., 2014; Sallam et al., 2019). Drought or heat stresses during grain filling rapidly reduces photosynthesis which in turn reduces the available assimilates leading to significant reduction in kernel weight (Wardlaw and Willenbrink, 2000) (Figure 2). Therefore, reserves assimilated pre-anthesis is needed during grain filling (Gent, 1994). Shoot traits especially shoot dry weight has a strong linear relationship with the amount of carbohydrate remobilization under heat and drought stress (Kobata et al., 1992; Ehdaie et al., 2006; Xue et al., 2008). The higher shoot dry weight of GP observed in response to drought and heat stress suggests that poor remobilization of stem reserves could contribute to the lower seed yields. On the same lines, the significantly lower shoot dry weight in Otis in response to combined stress suggests efficient remobilization of stem reserves that contribute to the higher seed yields when compared to GP plants under stress (Figure 2).

A careful examination of the individual seeds shows significant differences between these two varieties. Otis is a two-row barley and in general has longer and plump seeds compared to GP which has much smaller grain size. The overall impact on seed length and width in response to drought was less pronounced compared to heat stress again indicating that the barley plants have innate ability to withstand water stress compared to temperature stresses (Figure 3). Duration of grain filling and the grain-filling rate are major contributors of grain plumpness. Reduction of nonstructural carbohydrates in the stems and vascular bundle impairment was associated with reduction in rice grain plumpness by heat stress during the early reproductive phase (Zhang et al., 2009; Wu et al., 2019). The significant reduction in both the seed length and width observed in GP compared to Otis in response to combined stress suggests grain filling processes such as synthesis and distribution of carbohydrates could be negatively impacted in the former. The increase in the seed length and the reduction in seed width in response to heat stress in GP is interesting and suggests changes associated with cell wall properties in this variety.

We chose QuantSeq method since it provides an easy protocol to generate strand-specific next-generation sequencing (NGS) libraries close to the 3' end of polyadenylated RNAs. The main advantage of this strategy is that only one fragment per transcript is generated, directly linking the number of reads mapping to a gene to its expression. QuantSeq enables a higher level of multiplexing per run and provides accurate and affordable gene expression measurement. When compared with the normal RNA-seq wherein multiple reads can map to the same transcript thus tending to over-represent the longer transcripts, the 3'mRNA-seq method used in this study is set up to give one read per transcript and hence it is unbiased for transcript length. However, compared with normal RNA-seq libraries the total number of reads generated by this strategy is lower (Supplementary Table 1). The nearly 97% mapping of the reads from these libraries is significantly higher compared to other recent RNA-seq studies (Osthoff et al., 2019) wherein only 60% of the reads were mapped uniquely to the barley genome. We speculate that this improved

mapping efficiency of the RNA-seq reads in this study was facilitated by the recently updated assembly of the barley genome (Morex V3) using the PacBio HiFi long read sequencing strategy (Mascher et al., 2021).

Among our three stress conditions and two timepoints, we found the least changes in gene expression at the end of 1-day of drought stress (Figures 4, 5) similar to results reported on prolonged drought stress in a barley landrace (Cantalapiedra et al., 2017). Although related studies found more gene expression changes in leaves during early responses (Guo et al., 2009), plant responses to water deficit are different depending on genotype, phenology adjustment, acclimation, and developmental stage during which the stress is evaluated (Ashoub et al., 2015). Leaves from adult plants, like the ones in this study, will show different responses to drought than those of seedlings (Blum, 2005). Limited transcriptional response to drought stress in mature flowering plants could be due to acclimation or enhanced tolerance, maybe conferred by senescence of older leaves (Blum, 2009). No changes in leaf proteome of mature barley plants were reported under drought stress sampled three days into the treatment (Rollins et al., 2013). The importance of sampling tissues at different time-points is evident based on the significant changes in transcriptional responses that were observed in both genotypes at the end of the 5-day drought stress treatment (Figures 5, 6).

Some processes that were found to be regulated in previous drought studies in barley were also identified in our analysis. This includes genes associated with carbohydrate metabolism, antioxidant enzymes like catalases, components of photosystem II (Krasensky and Jonak, 2012), proteases (Ford et al., 2011; Ashoub et al., 2013), lipoxygenases (Wendelboe-Nelson and Morris, 2012; Ashoub et al., 2015), and wax biosynthesis genes. Some common genes identified in drought studies in other plant species that came up in this study included transcription factors (TFs) from various families such as AP2/ERF, bZIP, DREB, NAC, WRKY (Sahoo et al., 2013; Janiak et al., 2016), genes associated with calcium signaling such as calcium sensor proteins, calmodulin, calcium-dependent protein kinases, and protein phosphatases class 2C (PP2C) (Molina et al., 2008; Guo et al., 2009; Ranjan and Sawant, 2015) and different members of the LEA family (Shinozaki and Yamaguchi-Shinozaki, 2007; Talame et al., 2007).

As reported in several other studies comparing barley genotypes with contrasting responses to drought (Rollins et al., 2013; Cantalapiedra et al., 2017; Harb et al., 2020), the sensitive variety in this study (GP) exhibited a higher number of differentially expressed genes than the tolerant one (Figure 5). However, some genes were found to be differentially expressed due to drought specifically in the relatively drought tolerant variety, Otis. Noteworthy genes included a calcium-dependent protein kinase, kynurenine formamidase, eceriferum 3, fatty acid hydroxylases, serine hydroxymethyltransferase, aspartate aminotransferase, sucrose synthase, sucrose symporter, several sugar transporters, 13 different genes associated with endopeptidase inhibitors that included two alpha-amylase inhibitors, four cysteine-type inhibitors, and seven serine-type endopeptidase inhibitors.

Biosynthesis of epicuticular waxes under stress conditions is mediated by *Eceriferum (CER)*s, an important gene family that plays key role in elongation of fatty acids chains (Ahmad et al., 2022). This gene was reported to be highly induced in Otis leaves in response to drought imposed during vegetative stage (Harb et al., 2020). In Arabidopsis overexpression of CER1 increased the very long chain alkenes in the cuticle and rendered the plants drought tolerant by preventing water loss from the leaves (Bourdenx et al., 2011). Elevated expression of two other genes annotated as fatty acid hydroxylase involved in wax biosynthesis in Otis may provide a mechanism for imparting the observed drought tolerance in this variety (Figure 7).

Proteases and Protease Inhibitors have been suggested to play a key role in adaptation to stress since it requires the active involvement of regulated proteolysis and the inhibition of uncontrolled proteolysis (Kidric et al., 2014). Lower proteolytic activity and decreased expression of certain cysteine protease genes under water deficit during early developmental stage are regarded as indicators for drought tolerance of winter wheat cultivars (Simova-Stoilova et al., 2010). Thus, the up regulation of cysteine protease inhibitors in Otis in response to drought could be involved in lowering the proteolytic activities (Figure 7).

The upregulation of four alpha-amylase inhibitor genes in Otis heads in response to drought is novel and exciting. It was reported that overexpression of wheat alpha-amylase inhibitor increased salt and drought tolerance (Xiao et al., 2013). It is known that, once amylase activity decreases (due to increased expression of alpha-amylase inhibitors), there is a concomitant reduction in the amount of glucose that is generated from starch breakdown. Subsequently, this lowers phosphoenolpyruvate (PEP) and oxaloacetate levels leading to a reduction in malic acid and cell turgor (Mansfield and Jones, 1971). This ultimately results in reduced stomatal apertures and/or its closure in leaves. However, the functional role of these inhibitors expressed in the heads needs further investigation.

Heat Stress associated GOs

When compared to drought stress, heat stress evoked a larger transcriptional response by the end of the first day of treatment in both the genotypes. As a temperate cereal crop, it is not surprising that an increase in the temperature evoked substantial changes in the transcriptomes of these barley varieties. In contrast to drought stress, we identified enriched GOs wherein all the DEGs were identified in only one variety. For example, in Otis, there were seven carbonic anhydrase (CA) genes that were differentially expressed in response to heat of which two were up and five were down. Moderate stress, in

general, leads to increased expression of CAs (Polishchuk, 2021). CAs plays a role in stress adaptation through its involvement in stomatal closure, ROS scavenging and partial compensation for reduced CO_2 conductance in mesophyll. At high temperatures, CA gene expression was upregulated (Kaul et al., 2011), but its protein abundance and enzymatic activity were reportedly decreased (Ahsan et al., 2010; Chaki et al., 2013). Deactivation of CAs by high temperature (Boyd et al., 2015) could trigger a compensatory mechanism leading to their transcriptional upregulation. The association between CA and Rubisco enables interaction with CO_2 and maintains the functional machinery of Rubisco (Badger and Price, 1994). Since photosynthesis is downregulated during severe stresses, suppression of CAs seems logical. Photosynthesis was reduced in both Otis and GP in response to heat stress, and it is still not clear why CAs are suppressed only in the former.

The enrichment of the GO for response to ABA in GP suggests higher levels of ABA. Of the 17 genes associated with this GO, 15 were differentially expressed only in GP and several of them have been shown to be induced in response to ABA. For example, HVA22 was initially identified as an ABA-induced transcript in barley aleurone layers (Shen et al., 1993). Another gene, Multiprotein Bridging Factor (MBF1), a key link that forms a bridge between stress responsive TFs and the basal transcription machinery (Jaimes-Miranda and Montes, 2020) has been reported to be induced by ABA (Yan et al., 2014) and heat in Arabidopsis (Suzuki et al., 2005), rice (Qin et al., 2015) and other plants. Upregulation of MBF1 in heads of GP agrees with the above-mentioned studies.

Combined stress

In marked contrast to drought or heat stress, combination of drought and heat evoked a very extensive transcriptional reprogramming in both genotypes even within 24 hours after the treatment initiation. This clearly demonstrates that combined stress is not just an additive effect of heat and drought, but barley plants perceive this as a new threat. Combined heat and drought stress has been shown to evoke such massive transcriptional responses in other plants as well (Mahalingam, 2015; Mahalingam et al., 2021).

The GO term integral component of membrane contained the largest number of differentially expressed genes, exceeding more than 1000 in the sensitive GP leaves within 1-day of combined stress initiation and observed at the later time point. This GO is described as component of a membrane consisting of gene products with some part of their peptide sequence implanted in the hydrophobic region of the membrane. This suggests that changes in membrane composition and structure in GP could be a key factor for its susceptibility to combined heat and drought stress. Membrane damage is usually due to excess generation of reactive oxygen species (ROS) which attack lipid bilayers (Mahalingam and Fedoroff, 2003). Consistent with this hypothesis we identified that the GO for peroxisomes is significant in GP at both the early and later time points. Peroxisomes are ubiquitous subcellular organelles that are the major sites of ROS production in plants (del Rio and Lopez-Huertas, 2016). Several genes associated with H_2O_2 production in peroxisomes such as glycolate oxidase (GOX), amine oxidase, Acyl-CoA oxidases were unique to GP, or their expression was higher compared to Otis. It is important to note that the rate of H_2O_2 production by the peroxisomal GOX is several fold higher than that reported for chloroplasts and mitochondria (Foyer et al., 2009). Furthermore, superoxide generating enzymes such as uricase or urate oxidase and the superoxide dismutase were also differentially expressed suggesting a significant increase in the H_2O_2 production in response to combined stress. Several abiotic stresses are known to increase peroxisome abundance in Arabidopsis (Desai and Hu, 2008; Sinclair et al., 2009; Rodriguez-Serrano et al., 2016; Fahy et al., 2017), wheat (Sanad et al., 2019) and quinoa (Hinojosa et al., 2019). Peroxisomes were proposed as a cellular proxy for induction of ROS during stresses (Smertenko, 2017). In contrast to the above-mentioned studies where in stresses were imposed singly, the significantly lower peroxisome abundance observed in GP and Otis in response to combined stress merits scrutiny and this was also observed in quinoa in response to combined heat and drought stress (Hinojosa et al., 2019). In the light of the observation that several peroxins, genes associated with peroxisome proliferation such as PEX11, dynamin and PEX16 (Lingard et al., 2008) were higher in GP compared to Otis, it begs the question why the peroxisome abundance is significantly lower in GP compared to Otis in response to combined stress (Figure 8). Since upregulation of peroxisome proliferation genes did not reflect in higher peroxisome abundance under the combination of heat and drought, we speculate it may be offset by the higher rate of peroxisome degradation. Damaged peroxisomes (due to excess ROS) are eliminated by a process called pexophagy, a specialized type of autophagy (Farmer et al., 2013; Shibata et al., 2013). Higher autophagic flux could contribute to the reduced peroxisome abundance under the combination of drought and heat stress which is further supported by the enrichment of the GO for autophagy in the leaves of GP. Of the 19 genes associated with this GO, 11 were unique to GP and included several autophagy related genes such as ATG5, ATG9, ATG13, Beclin1, cysteine proteases (Shibata et al., 2013).

An interesting GO, cyclin-dependent protein ser/thr protein kinase inhibitor activity was identified in GP. One of the CDKI, was a Siamese-related protein that has been shown to restrict cell proliferation during leaf growth (Churchman et al., 2006). It has been shown in rice that these genes act as negative regulators of seed size and seed weight. CDKIs are also referred to as Kinase Inhibitor Proteins (KIPs) and Kip-related proteins (KRPs). *KRP1* overexpression transgenic lines (*OxKRP1*), *krp2* mutant *(crkrp2)*, and *krp1/krp2* double mutant *(crkrp1/krp2)* exhibited significantly reduced grain weight. Further, the seeds from these lines had seed

germination issues and early seedling growth was retarded. This suggested that disturbing the normal steady state of KRP1 or KRP2 blocks seed development by impeding cell proliferation during grain filling and germination (Ajadi et al., 2020). Based on this rice study, it is tempting to speculate that the down regulation of the CDKIs (five in GP compared to two in Otis) could contribute to the reduced seed size in response to combined stress in GP.

Several genes associated with oxidoreductase activity that was induced early only in Otis in response to combined stress were very interesting and have documented roles in improving abiotic stresses. This includes genes involved in secondary metabolite production such as sorbitol, isoflavonoids, and atropine alkaloid, three ACC oxidase genes involved in the biosynthesis of phytohormone ethylene and two genes involved in the production of proline, a well-documented osmolyte (Al-Quraan and Al-Share, 2016). The upregulation of G3PDH gene in Otis is also consistent with a report on a wheat GAPDH gene that improved drought tolerance in a H_2O_2-mediated ABA-signaling pathway (Li et al., 2019).

WGCNA provides another strategy for identifying key genes important in response to abiotic stresses based on co-expression patterns that presumes interaction with other genes in the module (Figure 9). In gene networks, a subset of genes interacts with many other genes, and it is suggested that these hub genes are more likely to be essential than genes that have fewer interaction partners (Yokotani et al., 2008). It was interesting to find that four of the nine hub genes were associated with RNA metabolism including two different splicing factors, a polyA RNA polymerase and a RRM containing protein (Figure 10, 11). Alternate splicing of key genes involved in abiotic stress such as HsfA2 in Arabidopsis (Liu et al., 2013), HvDRF1 in barley (Xue and Loveridge, 2004) and DREB in wheat (Egawa et al., 2006), maize (Qin et al., 2007) and tomato (Liu et al., 2017) have been reported. More than 300 genes were identified as being uniquely regulated by alternate splicing in response to drought in barley (Harb et al., 2020). Regulation of alternative splicing provides a mechanism to fine-tune gene expression that may save the time required for changes in transcriptional activation and pre-mRNA accumulation, thus facilitating rapid plant adaptation to adverse environmental conditions.

The removal of non-functional polypeptides due to aggregation, misfolding, denaturation is important for cellular homeostasis. Disassembly of heat shock-induced protein aggregates is aided by the Hsp100/ClpB (casein lytic protease) family proteins in conjunction with the Hsp70/Hsp40 system (Schirmer et al., 1996; Schilke et al., 2017). Heat shock induces the expression of plastid ClpB proteins in soybeans (Lee et al., 1994), lima bean (Keeler et al., 2000), and *A. thaliana* (Agarwal et al., 2001). Furthermore, the seedling-lethal phenotype exhibited by *clpb* mutants suggests an essential role for ClpB3 in normal development (Lee et al., 2007). The Hsp70 chaperone system is involved in folding and quality control of unfolded proteins (Schilke et al., 2017). It is a complex consisting of chaperone Hsp70 (DnaK), co-chaperone Hsp40 (DnaJ-type), and a nucleotide exchange factor (NEF). The binding and release of the substrate proteins are regulated by a cycle of ATP/ADP exchange. ATP hydrolysis on Hsp70 is accelerated by Hsp40 and substrate binding. Dissociation of ADP and rebinding of ATP causes the release of the bound substrate and this rate-limiting step in the ATPase cycle is regulated by the NEFs (Bukau and Horwich, 1998). In rice, Fes1, a NEF was found to directly interact with a salt responsive protein and Bip, an ER ortholog of HsP70 family and over/under-expression of Fes1 affected grain length and weight and improved salt tolerance (Qian et al., 2021). The Fes1 gene identified in barley is annotated as being localized to membranes and further functional analysis is warranted to confirm its role in abiotic stress tolerance.

Transcription factors

The observed reprogramming of the transcriptome in response to heat, drought and combined stress involving nearly 10,000 genes in GP and more than 6000 genes in Otis is probably mediated by the differential expression of genes from 23 different transcription factor families (Figure 12).

Heat shock factors (HSFs) were identified in heat, drought, and combined stress in both genotypes. The expression of Heat-Shock-Proteins (HSPs) that function as chaperones to protect proteins under various stresses (Bartels and Sunkar, 2005) is regulated by HSFs (Rizhsky et al., 2004; Swindell et al., 2007; Guo et al., 2016). HSFs were more strongly induced in GP compared to Otis and the differential expression was highest in combined stress compared to drought or heat (Supplementary Figures 4, 6). This type of modulation was also observed in Arabidopsis, wherein stronger induction of HSFA7B was reported in response to a combination of salt, osmotic and heat stress, when compared to its expression under heat stress (Sewelam et al., 2014). Thus, HSF and HSPs has been regarded as plausible targets for breeding or engineering plants with improved tolerance to abiotic stresses.

ERF TFs were another over-represented family that were identified in both single and combined stresses across time points (Supplementary Figures 5–7 and Supplementary Table 8). In addition to their role in several developmental and physiological processes (Nakano et al., 2006) ERFs also act in response to wounding and in abiotic stresses (Mizoi et al., 2012; Heyman et al., 2018). Transgenic plants overexpressing certain ERFs are more resistant to several abiotic stresses including salinity, cold and water stress (Xu et al., 2008; Morran et al., 2011). In the present study, genes identified as ERF were both up and down-regulated (Supplementary Figures 5–7). DREB1A and DREB2A, two well studied ERFs were induced in rice in response to high salinity and water deficit (Dubouzet et al., 2003). In barley, the expression of DREB1A was significantly down-regulated in response to both short and long-term water deficit treatments while DREB2A was only slightly

induced in long-term water deficit and combined salt and water-deficit stress (Osthoff et al., 2019). The precise functions of these barley ERFs need to be elucidated in future genetic analyses.

Genes shaping stress tolerance in barley

Our study showed that the sensitive cultivar Golden Promise exhibited far more expression changes after combined heat and drought stress than the tolerant Otis genotype. This observation led to the hypothesis that Otis may have a "primed" transcriptome that is active under optimal conditions and hence does not need to instigate massive transcriptome changes when the stress occurs, as observed in the sensitive cultivar. This hypothesis was tested by the KEGG pathway enrichment analysis. The higher expression of key genes of the ascorbate-glutathione cycle in Otis can facilitate efficient ROS detoxification (Hasanuzzaman et al., 2019). Secondly, the innately higher expression of genes that are important for biosynthesis of osmolytes such as trehalose (Kosar et al., 2018) can provide a leg up for Otis in combating abiotic stresses. Thirdly the higher expression of key JA biosynthesis genes Allene oxide synthase, lipoxygenase and acyl-CoA oxidase could lead to higher levels of JA which has been shown to improve abiotic stress by enhancing antioxidants, osmolytes and cross-talk with other key phytohormones (Raza et al., 2021).

In addition to KEGG enrichment analysis of the innate differentially expressed genes we selected candidate genes based on two criteria (i) genes were differentially expressed only after application of stress in GP and (ii) the differential gene expression in GP in response to stress is like the expression pattern observed in Otis. It was surmised that such DEGs may be involved in better adaptation to stressful conditions.

Interestingly a gene annotated as a member of the universal stress response protein (USP) family (HORVU.MOREX.r3.6HG0618180) was identified in response to heat, drought, and combined stress. In plants USP functions include acting as protein and RNA chaperone, modulate ROS production, ABA-induced stomatal movement, Ethylene-mediated stress adaptation (Chi et al., 2019). In the barley genome there are 42 USPs and the identification of the USP in this study provides a strong rationale for its further functional characterization.

AP2/ERF gene family members in wheat were reported to show significant down regulation in response to heat and drought and one of the RAV subfamily members (TtAP2/ERF-117) contained a repressor motif (R/KLFGV) was down regulated in response to heat and drought stress (Faraji et al., 2020). The AP2/ERF gene (HORVU.MOREX.r3.1HG0083340) in barley had the same repressor motif and was down regulated in Otis under control conditions (compared with GP) and was repressed in response to heat and drought.

Homogentisate Phytyltransferase is a key enzyme for tocopherol biosynthesis (Collakova and DellaPenna, 2003). Tocopherols are well known lipid soluble antioxidants protecting cellular components from increased oxidative stress (Havaux et al., 2000; Munne-Bosch and Alegre, 2002). Identification of HPT as an innate gene with higher abundance in Otis adds one more important antioxidant metabolite that could aid in providing tolerance to abiotic stresses in this variety. In a previous study we have screened the wild barley diversity collection and the mini-core collection for all the eight isoforms of tocols (Mahalingam et al., 2020). Selecting lines with higher levels of tocopherols from these collections will provide additional novel barley lines for expanding the abiotic stress tolerance germplasm in barley.

Another novel transcription factor is the FAR1 (FAR-RED-Impaired Response 1), initially identified in Arabidopsis as crucial component of the phytochrome A-mediated far-red light signaling that has multifaceted roles in UV-B signaling, flowering, chloroplast biogenesis, ROS homeostasis, ABA signaling (Wang and Wang, 2015). Most of these studies have only been done in model systems and their functional studies in crops has not been reported. This study provides a strong rationale for pursuing functional characterization of this family of transcription factor in barley and is particularly fascinating given their extensive similarity to mutator-like transposase, indicative of molecular domestication (Hudson et al., 2003; Lin et al., 2007).

Starch is a key determinant of plant fitness especially during abiotic stresses (Thalmann and Santelia, 2017) since its remobilization can provide an alternate source of carbon which is limiting factor due to reduced photosynthesis. Alpha-amylases are important for starch breakdown in the leaves that can provide the much-needed energy supply and aid in the accumulation of compatible solutes. Increased amylase activity has been reported in response to abiotic stresses in rice, potato, Arabidopsis (Sicher, 2011; Valerio et al., 2011; Sitnicka and Orzechowski, 2014). Higher alpha-amylase activities in Otis may efficiently hydrolyze the transitory starch in the leaves to attenuate the impact of reduced photosynthesis in response to stress. This remobilization strategy could provide an alternate source of energy and carbon, promoting seed filling even during abiotic stress.

Conclusions and future directions

Several well-known stress responsive genes and pathways associated with abiotic stress were found to be elevated in the feed barley variety Otis that could be conferring its tolerance to these stresses. Similar studies using commercial varieties (malting and feed barley) and advanced breeding lines with tolerance to abiotic stresses is warranted. Such pan-transcriptomics approach will enable identifying suites of stress tolerance genes that are innately expressed at higher levels. This information can be leveraged for selecting lines for

breeding programs focused on developing malting and feed barley varieties with improved abiotic stress tolerance.

Engineering endogenous enzymes of barley could provide a direct approach to improving stress tolerance. For example, increased drought tolerance was reported in a CRISPR-generated Arabidopsis trehalase line wherein the edit mimicked the substrate binding site of an orthologous enzyme from the drought-tolerant *Selaginella lepidophylla* (Nunez-Munoz et al., 2021). We anticipate the innate stress responsive genes identified in Otis in conjunction with enzyme engineering offers an opportunity to accelerate success in producing climate-resilient barley varieties.

Data availability statement

The data presented in the study are deposited in the SRA database, accession number PRJNA898434.

Author contributions

RM and PB conceived the research project and approved the plan. PB provided the seeds and provided the fiscal support for the RNA-seq. RM, ND, and RK conducted the transcriptome analysis. AS and TN conducted peroxisome analysis and provided novel insights into the data analysis. RM wrote the manuscript with inputs from RK and AS. All authors contributed to the article and approved the submitted version.

Funding

This research was funded by the USDA-ARS and partially supported by the American Malting Barley Association Inc.

Acknowledgments

Authors thank Dr. Sarah Whitcomb for providing insightful comments and critiques to improve the manuscript. Authors thank Danielle Graham (USDA-ARS) for her technical assistance and Michelle Andrews (Idaho State University Molecular Research Core Facility) for helping with RNA-seq libraries and sequencing. Mention of trade names or commercial products in this publication is solely for the purpose of providing specific information and does not imply recommendation or endorsement by the U.S. Department of Agriculture. USDA is an equal opportunity provider and employer.

Conflict of interest

The authors declare that the research was conducted in the absence of any commercial or financial relationships that could be construed as a potential conflict of interest.

Publisher's note

Supplementary material

The Supplementary Material for this article can be found online at: https://www.frontiersin.org/articles/10.3389/fpls.2022.1066421/full#supplementary-material

References

Abebe, T., Melmaiee, K., Berg, V., and Wise, R. P. (2010). Drought response in the spikes of barley: gene expression in the lemma, palea, awn, and seed. *Funct. Integr. Genomics* 10, 191–205. doi: 10.1007/s10142-009-0149-4

Agarwal, M., Katiyar-Agarwal, S., Sahi, C., Gallie, D. R., and Grover, A. (2001). Arabidopsis thaliana Hsp100 proteins: kith and kin. *Cell Stress Chaperones* 6, 219–224. doi: 10.1379/1466-1268(2001)006<0219:ATHPKA>2.0.CO;2

Ahmad, H. M., Wang, X. K., Mahmood-Ur-Rahman, F., S., A., and Shaheen, T. (2022). Morphological and physiological response of helianthus annuus l. to drought stress and correlation of wax contents for drought tolerance traits. *Arabian J. Sci. Eng.* 47, 6747–6761. doi: 10.1007/s13369-021-06098-1

Ahsan, N., Donnart, T., Nouri, M. Z., and Komatsu, S. (2010). Tissue-specific defense and thermo-adaptive mechanisms of soybean seedlings under heat stress revealed by proteomic approach. *J. Proteome Res.* 9, 4189–4204. doi: 10.1021/pr100504j

Ajadi, A. A., Tong, X. H., Wang, H. M., Zhao, J., Tang, L. Q., Li, Z. Y., et al. (2020). Cyclin-dependent kinase inhibitors KRP1 and KRP2 are involved in grain filling and seed germination in rice (Oryza sativa l.). *Int. J. Mol. Sci.* 21, 245. doi: 10.3390/ijms21010245

Al-Quraan, N. A., and Al-Share, A. T. (2016). Characterization of the gamma-aminobutyric acid shunt pathway and oxidative damage in arabidopsis thaliana pop 2 mutants under various abiotic stresses. *Biol. Plantarum* 60, 132–138. doi: 10.1007/s10535-015-0563-5

Ashoub, A., Baeumlisberger, M., Neupaertl, M., Karas, M., and Bruggemann, W. (2015). Characterization of common and distinctive adjustments of wild barley leaf proteome under drought acclimation, heat stress and their combination. *Plant Mol. Biol.* 87, 459–471. doi: 10.1007/s11103-015-0291-4

Ashoub, A., Beckhaus, T., Berberich, T., Karas, M., and Bruggemann, W. (2013). Comparative analysis of barley leaf proteome as affected by drought stress. *Planta* 237, 771–781. doi: 10.1007/s00425-012-1798-4

Awasthi, R., Kaushal, N., Vadez, V., Turner, N. C., Berger, J., Siddique, K. H. M., et al. (2014). Individual and combined effects of transient drought and heat stress

on carbon assimilation and seed filling in chickpea. *Funct. Plant Biol.* 41, 1148–1167. doi: 10.1071/FP13340

Badger, M. R., and Price, G. D. (1994). The role of carbonic-anhydrase in photosynthesis. *Annu. Rev. Plant Physiol. Plant Mol. Biol.* 45, 369–392. doi: 10.1146/annurev.pp.45.060194.002101

Barnabas, B., Jager, K., and Feher, A. (2008). The effect of drought and heat stress on reproductive processes in cereals. *Plant Cell Environ.* 31, 11–38. doi: 10.1111/j.1365-3040.2007.01727.x

Bartels, D., and Sunkar, R. (2005). Drought and salt tolerance in plants. *Crit. Rev. Plant Sci.* 24, 23–58. doi: 10.1080/07352680590910410

Bedada, G., Westerbergh, A., Muller, T., Galkin, E., Bdolach, E., Moshelion, M., et al. (2014). Transcriptome sequencing of two wild barley (Hordeum spontaneum l.) ecotypes differentially adapted to drought stress reveals ecotype-specific transcripts. *BMC Genomics* 15, 995. doi: 10.1186/1471-2164-15-995

Benjamini, Y., and Hochberg, Y. (1995). Controlling the false discovery rate - a practical and powerful approach to multiple testing. *J. R. Stat. Soc. Ser. B-Statistical Method.* 57, 289–300. doi: 10.1111/j.2517-6161.1995.tb02031.x

Blum, A. (2005). Drought resistance, water-use efficiency, and yield potential - are they compatible, dissonant, or mutually exclusive? *Aust. J. Agric. Res.* 56, 1059–1118. doi: 10.1071/AR05069

Blum, A. (2009). Effective use of water (EUW) and not water-use efficiency (WUE) is the target of crop yield improvement under drought stress. *Field Crops Res.* 112, 119–123. doi: 10.1016/j.fcr.2009.03.009

Bourdenx, B., Bernard, A., Domergue, F., Pascal, S., Leger, A., Roby, D., et al. (2011). Overexpression of arabidopsis ECERIFERUM1 promotes wax very-Long-Chain alkane biosynthesis and influences plant response to biotic and abiotic stresses. *Plant Physiol.* 156, 29–45. doi: 10.1104/pp.111.172320

Boyd, R. A., Gandin, A., and Cousins, A. B. (2015). Temperature responses of c-4 photosynthesis: Biochemical analysis of rubisco, phosphoenolpyruvate carboxylase, and carbonic anhydrase in setaria viridis. *Plant Physiol.* 169, 1850–1861. doi: 10.1104/pp.15.00586

Bukau, B., and Horwich, A. L. (1998). The Hsp70 and Hsp60 chaperone machines. *Cell* 92, 351–366. doi: 10.1016/S0092-8674(00)80928-9

Cantalapiedra, C. P., Garcia-Pereira, M. J., Gracia, M. P., Igartua, E., Casas, A. M., and Contreras-Moreira, B. (2017). Large Differences in gene ex pression responses to drought and heat stress between elite barley cultivar Scarlett and a Spanish landrace. *Front. Plant Sci.* 8, 647. doi: 10.3389/fpls.2017.00647

Chaki, M., Carreras, A., Lopez-Jaramillo, J., Begara-Morales, J. C., Sanchez-Calvo, B., Valderrama, R., et al. (2013). Tyrosine nitration provokes inhibition of sunflower carbonic anhydrase (beta-CA) activity under high temperature stress. *Nitric. Oxide-Biology Chem.* 29, 30–33. doi: 10.1016/j.niox.2012.12.003

Chi, Y. H., Koo, S. S., Oh, H. T., Lee, E. S., Park, J. H., Phan, K. A. T., et al. (2019). The physiological functions of universal stress proteins and their molecular mechanism to protect plants from environmental stresses. *Front. Plant Sci.* 10. doi: 10.3389/fpls.2019.00750

Churchman, M. L., Brown, M. L., Kato, N., Kirik, V., Hulskamp, M., Inze, D., et al. (2006). SIAMESE, a plant-specific cell cycle regulator, controls endoreplication onset in arabidopsis thaliana. *Plant Cell* 18, 3145–3157. doi: 10.1105/tpc.106.044834

Cohen, I., Zandalinas, S. I., Huck, C., Fritschi, F. B., and Mittler, R. (2021). Meta-analysis of drought and heat stress combination impact on crop yield and yield components. *Physiol. Plant* 171, 66–76. doi: 10.1111/ppl.13203

Collakova, E., and Dellapenna, D. (2003). The role of homogentisate phytyltransferase and other tocopherol pathway enzymes in the regulation of tocopherol synthesis during abiotic stress. *Plant Physiol.* 133, 930–940. doi: 10.1104/pp.103.026138

Del Rio, L. A., and Lopez-Huertas, E. (2016). ROS generation in peroxisomes and its role in cell signaling. *Plant Cell Physiol.* 57, 1364–1376. doi: 10.1093/pcp/pcw076

Desai, M., and Hu, J. (2008). Light induces peroxisome proliferation in arabidopsis seedlings through the photoreceptor phytochrome a, the transcription factor HY5 HOMOLOG, and the peroxisomal protein PEROXIN11b. *Plant Physiol.* 146, 1117–1127. doi: 10.1104/pp.107.113555

Dubouzet, J. G., Sakuma, Y., Ito, Y., Kasuga, M., Dubouzet, E. G., Miura, S., et al. (2003). OsDREB genes in rice, oryza sativa l., encode transcription activators that function in drought-, high-salt- and cold-responsive gene expression. *Plant J.* 33, 751–763. doi: 10.1046/j.1365-313X.2003.01661.x

Duhan, N., and Kaundal, R. (2020). "pySeqRNA: an automated Python package for RNA sequencing data analysis," in . *28th International Conference on Intelligent Systems for Molecular Biology (ISMB).*

Egawa, C., Kobayashi, F., Ishibashi, M., Nakamura, T., Nakamura, C., and Takumi, S. (2006). Differential regulation of transcript accumulation and alternative splicing of a DREB2 homolog under abiotic stress conditions in common wheat. *Genes Genet. Syst.* 81, 77–91. doi: 10.1266/ggs.81.77

Ehdaie, B., Alloush, G. A., and Waines, J. G. (2006). Genotypic variation for stem reserves and mobilization in wheat: II. postanthesis changes in internode water-soluble carbohydrates. *Crop Sci.* 46, 2093–2103. doi: 10.2135/cropsci2006.01.0013

Fahy, D., Sanad, M. N. M. E., Duscha, K., Lyons, M., Liu, F. Q., Bozhkov, P., et al. (2017). Impact of salt stress, cell death, and autophagy on peroxisomes: quantitative and morphological analyses using small fluorescent probe n-BODIPY. *Sci. Rep.* 7, 39069. doi: 10.1038/srep39069.

Faraji, S., Filiz, E., Kazemitabar, S. K., Vannozzi, A., Palumbo, F., Barcaccia, G., et al. (2020). The AP2/ERF gene family in triticum durum: Genome-wide identification and expression analysis under drought and salinity stresses. *Genes* 11, 1464. doi: 10.3390/genes11121464

Farmer, L. M., Rinaldi, M. A., Young, P. G., Danan, C. H., Burkhart, S. E., and Bartel, B. (2013). Disrupting autophagy restores peroxisome function to an arabidopsis lon2 mutant and reveals a role for the LON2 protease in peroxisomal matrix protein degradation. *Plant Cell* 25, 4085–4100. doi: 10.1105/tpc.113.113407

Fedoroff, N. V., Battisti, D. S., Beachy, R. N., Cooper, P. J. M., Fischhoff, D. A., Hodges, C. N., et al. (2010). Radically rethinking agriculture for the 21st century. *Science* 327, 833–834. doi: 10.1126/science.1186834

Ford, K. L., Cassin, A., and Bacic, A. (2011). Quantitative proteomic analysis of wheat cultivars with differing drought stress tolerance. *Front. Plant Sci.* 2. doi: 10.3389/fpls.2011.00044

Foyer, C. H., Bloom, A. J., Queval, G., and Noctor, G. (2009). Photorespiratory metabolism: Genes, mutants, energetics, and redox signaling. *Annu. Rev. Plant Biol.* 60, 455–484. doi: 10.1146/annurev.arplant.043008.091948

Gent, M. P. N. (1994). Photosynthate reserves during grain filling in winter wheat. *Agron. J.* 86, 159–167. doi: 10.2134/agronj1994.00021962008600010029x

Guo, P. G., Baum, M., Grando, S., Ceccarelli, S., Bai, G. H., Li, R. H., et al. (2009). Differentially expressed genes between drought-tolerant and drought-sensitive barley genotypes in response to drought stress during the reproductive stage. *J. Exp. Bot.* 60, 3531–3544. doi: 10.1093/jxb/erp194

Guo, M., Liu, J. H., Ma, X., Luo, D. X., Gong, Z. H., and Lu, M. H. (2016). The plant heat stress transcription factors (HSFs): Structure, regulation, and function in response to abiotic stresses. *Front. Plant Sci.* 7. doi: 10.3389/fpls.2016.00114

Harb, A., Simpson, C., Guo, W. B., Govindan, G., Kakani, V. G., and Sunkar, R. (2020). The effect of drought on transcriptome and hormonal profiles in barley genotypes with contrasting drought tolerance. *Front. Plant Sci.* 11. doi: 10.3389/fpls.2020.618491

Hasanuzzaman, M., Bhuyan, M., Anee, T. I., Parvin, K., Nahar, K., Mahmud, J. A., et al. (2019). Regulation of ascorbate-glutathione pathway in mitigating oxidative damage in plants under abiotic stress. *Antioxidants (Basel)* 8, 384. doi: 10.3390/antiox8090384

Havaux, M., Bonfils, J. P., Lutz, C., and Niyogi, K. K. (2000). Photodamage of the photosynthetic apparatus and its dependence on the leaf developmental stage in the npq1 arabidopsis mutant deficient in the xanthophyll cycle enzyme violaxanthin de-epoxidase. *Plant Physiol.* 124, 273–284. doi: 10.1104/pp.124.1.273

Heyman, J., Canher, B., Bisht, A., Christiaens, F., and De Veylder, L. (2018). Emerging role of the plant ERF transcription factors in coordinating wound defense responses and repair. *J. Cell Sci.* 131, jcs208215. doi: 10.1242/jcs.208215

Hickey, K., Wood, M., Sexton, T., Sahin, Y., Nazarov, T., Fisher, J., et al. (2022). Drought tolerance strategies and autophagy in resilient wheat genotypes. *Cells* 11, 1765. doi: 10.3390/cells11111765

Hinojosa, L., Sanad, M. N. M. E., Jarvis, D. E., Steel, P., Murphy, K., and Smertenko, A. (2019). Impact of heat and drought stress on peroxisome proliferation in quinoa. *Plant J.* 99, 1144–1158. doi: 10.1111/tpj.14411

Hubner, S., Korol, A. B., and Schmid, K. J. (2015). RNA-Seq analysis identifies genes associated with differential reproductive success under drought-stress in accessions of wild barley hordeum spontaneum. *BMC Plant Biol.* 15, 134. doi: 10.1186/s12870-015-0528-z

Hudson, M. E., Lisch, D. R., and Quail, P. H. (2003). The FHY3 and FAR1 genes encode transposase-related proteins involved in regulation of gene expression by the phytochrome a-signaling pathway. *Plant J.* 34, 453–471. doi: 10.1046/j.1365-313X.2003.01741.x

Hu, H., and Xiong, L. (2014). Genetic engineering and breeding of drought-resistant crops. *Annu. Rev. Plant Biol.* 65, 715–741. doi: 10.1146/annurev-arplant-050213-040000

Jaimes-Miranda, F., and Montes, R. A. C. (2020). The plant MBF1 protein family: a bridge between stress and transcription. *J. Exp. Bot.* 71, 1782–1791. doi: 10.1093/jxb/erz525

Janiak, A., Kwasniewski, M., Sowa, M., Gajek, K., Zmuda, K., Koscielniak, J., et al. (2018). No time to waste: Transcriptome study reveals that drought tolerance in barley may be attributed to stressed-like expression patterns that exist before the occurrence of stress. *Front. Plant Sci.* 8. doi: 10.3389/fpls.2017.02212

Janiak, A., Kwasniewski, M., and Szarejko, I. (2016). Gene expression regulation in roots under drought. *J. Exp. Bot.* 67, 1003–1014. doi: 10.1093/jxb/erv512

Kanehisa, M., and Goto, S. (2000). KEGG: Kyoto encyclopedia of genes and genomes. *Nucleic Acids Res.* 28, 27–30. doi: 10.1093/nar/28.1.27

Kaul, T., Reddy, P. S., Mahanty, S., Thirulogachandar, V., Reddy, R. A., Kumar, B., et al. (2011). Biochemical and molecular characterization of stress-induced beta-carbonic anhydrase from a c-4 plant, pennisetum glaucum. *J. Plant Physiol.* 168, 601–610. doi: 10.1016/j.jplph.2010.08.007

Keeler, S. J., Boettger, C. M., Haynes, J. G., Kuches, K. A., Johnson, M. M., Thureen, D. L., et al. (2000). Acquired thermotolerance and expression of the HSP100/ClpB genes of lima bean. *Plant Physiol.* 123, 1121–1132. doi: 10.1104/pp.123.3.1121

Kidric, M., Kos, J., and Sabotic, J. (2014). Proteases and their endogenous inhibitors in the plant response to abiotic stresses. *Botanica Serbica* 38, 139–158.

Kobata, T., Palta, J. A., and Turner, N. C. (1992). Rate of development of postanthesis water deficits and grain filling of spring wheat. *Crop Sci.* 32, 1238–1242. doi: 10.2135/cropsci1992.0011183X003200050035x

Kosar, F., Akram, N. A., Ashraf, M., Sadiq, M., and Al-Qurainy, F. (2018). Trehalose-induced improvement in growth, photosynthetic characteristics and levels of some key osmoprotectants in sunflower (Helianthus annuus l.) under drought stress. *Pakistan J. Bot.* 50, 955–961.

Krasensky, J., and Jonak, C. (2012). Drought, salt, and temperature stress-induced metabolic rearrangements and regulatory networks. *J. Exp. Bot.* 63, 1593–1608. doi: 10.1093/jxb/err460

Langfelder, P., and Horvath, S. (2008). WGCNA: an r package for weighted correlation network analysis. *BMC Bioinf.* 9, 559. doi: 10.1186/1471-2105-9-559

Langfelder, P., Zhang, B., and Horvath, S. (2008). Defining clusters from a hierarchical cluster tree: the dynamic tree cut package for r. *Bioinformatics* 24, 719–720. doi: 10.1093/bioinformatics/btm563

Lee, Y. R. J., Nagao, R. T., and Key, J. L. (1994). A soybean 101-kd heat-shock protein complements a yeast Hsp104 deletion mutant in acquiring thermotolerance. *Plant Cell* 6, 1889–1897. doi: 10.1105/tpc.6.12.1889

Lee, U., Rioflorido, I., Hong, S. W., Larkindale, J., Waters, E. R., and Vierling, E. (2007). The arabidopsis ClpB/Hsp100 family of proteins: chaperones for stress and chloroplast development. *Plant J.* 49, 115–127. doi: 10.1111/j.1365-313X.2006.02940.x

Li, B., and Dewey, C. N. (2011). RSEM: accurate transcript quantification from RNA-seq data with or without a reference genome. *BMC Bioinf.* 12, 323. doi: 10.1186/1471-2105-12-323

Lin, R. C., Ding, L., Casola, C., Ripoll, D. R., Feschotte, C., and Wang, H. Y. (2007). Transposase-derived transcription factors regulate light signaling in arabidopsis. *Science* 318, 1302–1305. doi: 10.1126/science.1146281

Lingard, M. J., Gidda, S. K., Bingham, S., Rothstein, S. J., Mullen, R. T., and Trelease, R. N. (2008). Arabidopsis PEROXIN11c-e, FISSION1b, and DYNAMIN-RELATED PROTEIN3A cooperate in cell cycle-associated replication of peroxisomes. *Plant Cell* 20, 1567–1585. doi: 10.1105/tpc.107.057679

Liu, Y., Huang, W., Xian, Z., Hu, N., Lin, D. , Ren, H., et al. (2017). Overexpression of SlGRAS40 in tomato enhances tolerance to abiotic stresses and influences auxin and gibberellin signaling. *Front. Plant Sci.* 81659. doi: 10.3389/fpls.2017.01659

Liu, J. J., Sun, N., Liu, M., Liu, J. C., Du, B. J., Wang, X. J., et al. (2013). An autoregulatory loop controlling arabidopsis HsfA2 expression: Role of heat shock-induced alternative Splicing(1[C]). *Plant Physiol.* 162, 512–521. doi: 10.1104/pp.112.205864

Li, X., Wei, W., Li, F., Zhang, L., Deng, X., Liu, Y., et al. (2019). The plastidial glyceraldehyde-3-Phosphate dehydrogenase is critical for abiotic stress response in wheat. *Int. J. Mol. Sci.* 20, 1104. doi: 10.3390/ijms20051104

Lobell, D. B., and Gourdji, S. M. (2012). The influence of climate change on global crop productivity. *Plant Physiol.* 160, 1686–1697. doi: 10.1104/pp.112.208298

Mahalingam, R. (2015). "Consideration of combined stress: A crucial paradigm for improving multiple stress tolerance in plants," in *Combined stresses in plants: Physiological, molecular and biochemical aspects*. Ed. R. MAHALINGAM (Switzerland: Springer).

Mahalingam, R. (2017). Phenotypic, physiological and malt quality analyses of US barley varieties subjected to short periods of heat and drought stress. *J. Cereal Sci.* 76, 199–205. doi: 10.1016/j.jcs.2017.06.007

Mahalingam, R., and Bregitzer, P. (2019). Impact on physiology and malting quality of barley exposed to heat, drought and their combination during different growth stages under controlled environment. *Physiologia Plantarum* 165, 277–289. doi: 10.1111/ppl.12841

Mahalingam, R., and Fedoroff, N. (2003). Stress response, cell death and signalling: the many faces of reactive oxygen species. *Physiologia Plantarum* 119, 56–68. doi: 10.1034/j.1399-3054.2003.00156.x

Mahalingam, R., Pandey, P., and Senthil-Kumar, M. (2021). Progress and prospects of concurrent or combined stress studies in plants. *Annu. Plant Rev.* 4, 813–868. doi: 10.1002/9781119312994.apr0783

Mahalingam, R., Sallam, A. H., Steffenson, B. J., Fiedler, J. D., and Walling, J. G. (2020). Genome-wide association analysis of natural variation in seed tocochromanols of barley. *Plant Genome* 13, e20039. doi: 10.1002/tpg2.20039

Mangelsen, E., Kilian, J., Harter, K., Jansson, C., Wanke, D., and Sundberg, E. (2011). Transcriptome analysis of high-temperature stress in developing barley caryopses: Early stress responses and effects on storage compound biosynthesis. *Mol. Plant* 4, 97–115. doi: 10.1093/mp/ssq058

Mansfield, T. A., and Jones, R. J. (1971). Effects of abscisic acid on potassium uptake and starch content of stomatal guard cells. *Planta* 101, 147–14+. doi: 10.1007/BF00387625

Mao, X. Z., Cai, T., Olyarchuk, J. G., and Wei, L. P. (2005). Automated genome annotation and pathway identification using the KEGG orthology (KO) as a controlled vocabulary. *Bioinformatics* 21, 3787–3793. doi: 10.1093/bioinformatics/bti430

Mascher, M., Wicker, T., Jenkins, J., Plott, C., Lux, T., Koh, C. S., et al. (2021). Long-read sequence assembly: a technical evaluation in barley. *Plant Cell* 33, 1888–1906. doi: 10.1093/plcell/koab077

Mazdiyasni, O., and Aghakouchak, A. (2015). Substantial increase in concurrent droughts and heatwaves in the united states. *Proc. Natl. Acad. Sci. United States America* 112, 11484–11489. doi: 10.1073/pnas.1422945112

Mizoi, J., Shinozaki, K., and Yamaguchi-Shinozaki, K. (2012). AP2/ERF family transcription factors in plant abiotic stress responses. *Biochim. Et Biophys. Acta-Gene Regul. Mech.* 1819, 86–96. doi: 10.1016/j.bbagrm.2011.08.004

Molina, C., Rotter, B., Horres, R., Udupa, S. M., Besser, B., Bellarmino, L., et al. (2008). SuperSAGE: the drought stress-responsive transcriptome of chickpea roots. *BMC Genomics* 9, 553. doi: 10.1186/1471-2164-9-553

Morran, S., Eini, O., Pyvovarenko, T., Parent, B., Singh, R., Ismagul, A., et al. (2011). Improvement of stress tolerance of wheat and barley by modulation of expression of DREB/CBF factors. *Plant Biotechnol. J.* 9, 230–249. doi: 10.1111/j.1467-7652.2010.00547.x

Munne-Bosch, S., and Alegre, L. (2002). Plant aging increases oxidative stress in chloroplasts. *Planta* 214, 608–615. doi: 10.1007/s004250100646

Nakano, T., Suzuki, K., Fujimura, T., and Shinshi, H. (2006). Genome-wide analysis of the ERF gene family in arabidopsis and rice. *Plant Physiol.* 140, 411–432. doi: 10.1104/pp.105.073783

Nunez-Munoz, L., Vargas-Hernandez, B., Hinojosa-Moya, J., Ruiz-Medrano, R., and Xoconostle-Cazares, B. (2021). Plant drought tolerance provided through genome editing of the trehalase gene. *Plant Signaling Behav.* 16, 4. doi: 10.1080/15592324.2021.1877005

Obata, T., Witt, S., Lisec, J., Palacios-Rojas, N., Florez-Sarasa, I., Yousfi, S., et al. (2015). Metabolite profiles of maize leaves in drought, heat, and combined stress field trials reveal the relationship between metabolism and grain yield. *Plant Physiol.* 169, 2665–2683. doi: 10.1104/pp.15.01164

Osthoff, A., Rose, P. D. D., Baldauf, J. A., Piepho, H. P., and Hochholdinger, F. (2019). Transcriptomic reprogramming of barley seminal roots by combined water deficit and salt stress. *BMC Genomics* 20, 325. doi: 10.1186/s12864-019-5634-0

Polishchuk, O. V. (2021). Stress-related changes in the expression and activity of plant carbonic anhydrases. *Planta* 253, 76. doi: 10.1007/s00425-020-03553-5

Qaseem, M. F., Qureshi, R., and Shaheen, H. (2019). Effects of pre-anthesis drought, heat and their combination on the growth, yield and physiology of diverse wheat (Triticum aestivum l.) p genotypes varying in sensitivity to heat and drought stress. *Sci. Rep.* 9, 6955. doi: 10.1038/s41598-019-43477-z

Qian, D. D., Xiong, S., Li, M., Tian, L. H., and Qu, L. Q. (2021). OsFes1C, a potential nucleotide exchange factor for OsBiP1, is involved in the ER and salt stress responses. *Plant Physiol.* 187, 396–408. doi: 10.1093/plphys/kiab263

Qin, F., Kakimoto, M., Sakuma, Y., Maruyama, K., Osakabe, Y., Tran, L. S. P., et al. (2007). Regulation and functional analysis of ZmDREB2A in response to drought and heat stresses in zea mays l. *Plant J.* 50, 54–69. doi: 10.1111/j.1365-313X.2007.03034.x

Qin, D. D., Wang, F., Geng, X. L., Zhang, L. Y., Yao, Y. Y., Ni, Z. F., et al. (2015). Overexpression of heat stress-responsive TaMBF1c, a wheat (Triticum aestivum l.) multiprotein bridging factor, confers heat tolerance in both yeast and rice. *Plant Mol. Biol.* 87, 31–45. doi: 10.1007/s11103-014-0259-9

Ranjan, A., and Sawant, S. (2015). Genome-wide transcriptomic comparison of cotton (Gossypium herbaceum) leaf and root under drought stress. *3 Biotech.* 5, 585–596. doi: 10.1007/s13205-014-0257-2

Raza, A., Charagh, S., Zahid, Z., Mubarik, M. S., Javed, R., Siddiqui, M. H., et al. (2021). Jasmonic acid: a key frontier in conferring abiotic stress tolerance in plants. *Plant Cell Rep.* 40, 1513–1541. doi: 10.1007/s00299-020-02614-z

Rizhsky, L., Liang, H. J., Shuman, J., Shulaev, V., Davletova, S., and Mittler, R. (2004). When defense pathways collide. the response of arabidopsis to a combination of drought and heat stress. *Plant Physiol.* 134, 1683–1696. doi: 10.1104/pp.103.033431

Rodriguez-Serrano, M., Romero-Puertas, M. C., Sanz-Fernandez, M., Hu, J. P., and Sandalio, L. M. (2016). Peroxisomes extend peroxules in a fast response to stress *via* a reactive oxygen species-mediated induction of the peroxin PEX11a. *Plant Physiol.* 171, 1665–1674. doi: 10.1104/pp.16.00648

Rollins, J. A., Habte, E., Templer, S. E., Colby, T., Schmidt, J., and Von Korff, M. (2013). Leaf proteome alterations in the context of physiological and morphological responses to drought and heat stress in barley (Hordeum vulgare l.). *J. Exp. Bot.* 64, 3201–3212. doi: 10.1093/jxb/ert158

Sahoo, K. K., Tripathy, A. K., Pareek, A., and Singla-Pareek, S. (2013). Taming drought stress in rice through genetic engineering and transcription factors and protein kinases. *Plant Stress* 1, 60–72.

Sallam, A., Alqudah, A. M., Dawood, M. F. A., Baenziger, P. S., and Borner, A. (2019). Drought stress tolerance in wheat and barley: Advances in physiology, breeding and genetics research. *Int. J. Mol. Sci.* 20, 3137. doi: 10.3390/ijms20133137

Sallam, A., Hamed, E.-S., Hashad, M., and Omara, M. (2014). Inheritance of stem diameter and its relationship to heat and drought inheritance in wheat (Triticum aestivum l.). *J. Plant Breed. Crop Sci.* 6, 11–23. doi: 10.5897/JPBCS11.017

Sanad, M. N. M. E., Smertenko, A., and Garland-Campbell, K. A. (2019). Differential dynamic changes of reduced trait model for analyzing the plastic response to drought phases: A case study in spring wheat. *Front. Plant Sci.* 10. doi: 10.3389/fpls.2019.00504

Savin, R., and Nicolas, M. E. (1996). Effects of short periods of drought and high temperature on grain growth and starch accumulation of two malting barley cultivars. *J. Plant Physiol.* 23, 201–210. doi: 10.1071/PP9960201

Schilke, B. A., Ciesielski, S. J., Ziegelhoffer, T., Kamiya, E., Tonelli, M., Lee, W., et al. (2017). Broadening the functionality of a J-protein/Hsp70 molecular chaperone system. *PLoS Genet.* 13, e1007084. doi: 10.1371/journal.pgen.1007084

Schirmer, E. C., Glover, J. R., Singer, M. A., and Lindquist, S. (1996). HSP100/Clp proteins: A common mechanism explains diverse functions. *Trends Biochem. Sci.* 21, 289–296. doi: 10.1016/S0968-0004(96)10038-4

Schonfeld, M. A., Johnson, R. C., Carver, B. F., and Mornhinweg, D. W. (1988). Water relations in winter wheat as drought resistance indicator. *Crop Sci.* 28, 526–531. doi: 10.2135/cropsci1988.0011183X002800030021x

Sewelam, N., Oshima, Y., Mitsuda, N., and Ohme-Takagi, M. (2014). A step towards understanding plant responses to multiple environmental stresses: a genome-wide study. *Plant Cell Environ.* 37, 2024–2035. doi: 10.1111/pce.12274

Shannon, P., Markiel, A., Ozier, O., Baliga, N. S., Wang, J. T., Ramage, D., et al. (2003). Cytoscape: A software environment for integrated models of biomolecular interaction networks. *Genome Res.* 13, 2498–2504. doi: 10.1101/gr.1239303

Shen, Q. X., Uknes, S. J., and Ho, T. H. D. (1993). Hormone response complex in a novel abscisic-acid and cycloheximide-inducible barley gene. *J. Biol. Chem.* 268, 23652–23660. doi: 10.1016/S0021-9258(19)49512-4

Shibata, M., Oikawa, K., Yoshimoto, K., Kondo, M., Mano, S., Yamada, K., et al. (2013). Highly oxidized peroxisomes are selectively degraded *via* autophagy in arabidopsis. *Plant Cell* 25, 4967–4983. doi: 10.1105/tpc.113.116947

Shinozaki, K., and Yamaguchi-Shinozaki, K. (2007). Gene networks involved in drought stress response and tolerance. *J. Exp. Bot.* 58, 221–227. doi: 10.1093/jxb/erl164

Sicher, R. (2011). Carbon partitioning and the impact of starch deficiency on the initial response of arabidopsis to chilling temperatures. *Plant Sci.* 181, 167–176. doi: 10.1016/j.plantsci.2011.05.005

Simova-Stoilova, L., Vaseva, I., Grigorova, B., Demirevska, K., and Feller, U. (2010). Proteolytic activity and cysteine protease expression in wheat leaves under severe soil drought and recovery. *Plant Physiol. Biochem.* 48, 200–206. doi: 10.1016/j.plaphy.2009.11.003

Sinclair, A. M., Trobacher, C. P., Mathur, N., Greenwood, J. S., and Mathur, J. (2009). Peroxule extension over ER-defined paths constitutes a rapid subcellular response to hydroxyl stress. *Plant J.* 59, 231–242. doi: 10.1111/j.1365-313X.2009.03863.x

Sitnicka, D., and Orzechowski, S. (2014). Cold-induced starch degradation in potato leaves - intercultivar differences in the gene expression and activity of key enzymes. *Biol. Plantarum* 58, 659–666. doi: 10.1007/s10535-014-0453-2

Smertenko, A. (2017). Can peroxisomes inform cellular response to drought? *Trends Plant Sci.* 22, 1005–1007. doi: 10.1016/j.tplants.2017.09.021

Suzuki, N., Rizhsky, L., Liang, H. J., Shuman, J., Shulaev, V., and Mittler, R. (2005). Enhanced tolerance to environmental stress in transgenic plants expressing the transcriptional coactivator multiprotein bridging factor 1c. *Plant Physiol.* 139, 1313–1322. doi: 10.1104/pp.105.070110

Svoboda, P., Janska, A., Spiwok, V., Prasil, I. T., Kosova, K., Vitamvas, P., et al. (2016). Global scale transcriptional profiling of two contrasting barley genotypes exposed to moderate drought conditions: Contribution of leaves and crowns to water shortage coping strategies. *Front. Plant Sci.* 7. doi: 10.3389/fpls.2016.01958

Swindell, W. R., Huebner, M., and Weber, A. P. (2007). Transcriptional profiling of arabidopsis heat shock proteins and transcription factors reveals extensive overlap between heat and non-heat stress response pathways. *BMC Genomics* 8, 125. doi: 10.1186/1471-2164-8-125

Talame, V., Ozturk, N. Z., Bohnert, H. J., and Tuberosa, R. (2007). Barley transcript profiles under dehydration shock and drought stress treatments: a comparative analysis. *J. Exp. Bot.* 58, 229–240. doi: 10.1093/jxb/erl163

Thalmann, M., and Santelia, D. (2017). Starch as a determinant of plant fitness under abiotic stress. *New Phytol.* 214, 943–951. doi: 10.1111/nph.14491

Valerio, C., Costa, A., Marri, L., Issakidis-Bourguet, E., Pupillo, P., Trost, P., et al. (2011). Thioredoxin-regulated beta-amylase (BAM1) triggers diurnal starch degradation in guard cells, and in mesophyll cells under osmotic stress. *J. Exp. Bot.* 62, 545–555. doi: 10.1093/jxb/erq288

Wang, H., and Wang, H. Y. (2015). Multifaceted roles of FHY3 and FAR1 in light signaling and beyond. *Trends Plant Sci.* 20, 453–461. doi: 10.1016/j.tplants.2015.04.003

Wardlaw, I. F., and Willenbrink, J. (2000). Mobilization of fructan reserves and changes in enzyme activities in wheat stems correlate with water stress during kernel filling. *New Phytol.* 148, 413–422. doi: 10.1046/j.1469-8137.2000.00777.x

Wehner, G., Balko, C., Humbeck, K., Zyprian, E., and Ordon, F. (2016). Expression profiling of genes involved in drought stress and leaf senescence in juvenile barley. *BMC Plant Biol.* 16, 3. doi: 10.1186/s12870-015-0701-4

Wendelboe-Nelson, C., and Morris, P. C. (2012). Proteins linked to drought tolerance revealed by DIGE analysis of drought resistant and susceptible barley varieties. *Proteomics* 12, 3374–3385. doi: 10.1002/pmic.201200154

Wiegmann, M., Thomas, W. T. B., Bull, H. J., Flavell, A. J., Zeyner, A., Peiter, E., et al. (2019). "Wild barley serves as a source for biofortification of barley grains". *Plant Sci.* 283, 83–94. doi: 10.1016/j.plantsci.2018.12.030

Wimalanathan, K., Friedberg, I., Andorf, C. M., and Lawrence-Dill, C. J. (2018). Maize GO annotation-methods, evaluation, and review (maize-GAMER). *Plant Direct* 2, e00052. doi: 10.1002/pld3.52

W.M.O (2015) *Guidelines on the definition and monitoring of extreme weather and climate events - draft version - first review by TT-DEWCE [Online]*. Available at: http://www.wmo.int/pages/prog/wcp/ccl/opace/opace2/documents/DraftversionoftheGuidelinesontheDefinitionandMonitoringofExtremeWeatheranClimateEvents.pdf.

Wu, C., Tang, S., Li, G., Wang, S., Fahad, S., and Ding, Y. (2019). Roles of phytohormone changes in the grain yield of rice plants exposed to heat: a review. *PeerJ* 11, e7792. doi: 10.7717/peerj.7792

Xiao, Y. H., Huang, X., Shen, Y. Z., and Huang, Z. J. (2013). A novel wheat -amylase inhibitor gene, TaHPS, significantly improves the salt and drought tolerance of transgenic arabidopsis. *Physiologia Plantarum* 148, 273–283. doi: 10.1111/j.1399-3054.2012.01707.x

Xu, Z. S., Chen, M., Li, L. C., and Ma, Y. Z. (2008). Functions of the ERF transcription factor family in plants. *Botany* 86, 969–977. doi: 10.1139/B08-041

Xue, G. P., and Loveridge, C. W. (2004). HvDRF1 is involved in abscisic acid-mediated gene regulation in barley and produces two forms of AP2 transcriptional activators, interacting preferably with a CT-rich element. *Plant J.* 37, 326–339. doi: 10.1046/j.1365-313X.2003.01963.x

Xue, G. P., Mcintyre, C. L., Jenkins, C. L., Glassop, D., Van Herwaarden, A. F., and Shorter, R. (2008). Molecular dissection of variation in carbohydrate metabolism related to water-soluble carbohydrate accumulation in stems of wheat. *Plant Physiol.* 146, 441–454. doi: 10.1104/pp.107.113076

Yan, Q., Hou, H. M., Singer, S. D., Yan, X. X., Guo, R. R., and Wang, X. P. (2014). The grape VvMBF1 gene improves drought stress tolerance in transgenic arabidopsis thaliana. *Plant Cell Tissue Organ Culture* 118, 571–582. doi: 10.1007/s11240-014-0508-2

Yokotani, N., Ichikawa, T., Kondou, Y., Matsui, M., Hirochika, H., Iwabuchi, M., et al. (2008). Expression of rice heat stress transcription factor OsHsfA2e enhances tolerance to environmental stresses in transgenic arabidopsis. *Planta* 227, 957–967. doi: 10.1007/s00425-007-0670-4

Yu, G. C., Wang, L. G., Han, Y. Y., and He, Q. Y. (2012). clusterProfiler: an r package for comparing biological themes among gene clusters. *Omics-a J. Integr. Biol.* 16, 284–287. doi: 10.1089/omi.2011.0118

Zandalinas, S. I., Mittler, R., Balfagon, D., Arbona, V., and Gomez-Cadenas, A. (2018). Plant adaptations to the combination of drought and high temperatures. *Physiol. Plant* 162, 2–12. doi: 10.1111/ppl.12540

Zeng, X. Q., Bai, L. J., Wei, Z. X., Yuan, H. J., Wang, Y. L., Xu, Q. J., et al. (2016). Transcriptome analysis revealed the drought-responsive genes in Tibetan hulless barley. *BMC Genomics* 17, 386. doi: 10.1186/s12864-016-2685-3

Zhang, G. L., Zhang, S. T., Xiao, L. T., Tang, W. B., Xiao, Y. H., and Chen, L. Y. (2009). Effects of high temperature stress on microscopic and ultrastructural characteristics of mesophyll cells in flag leaf of rice. *Rice Sci.* 16, 65–71. doi: 10.1016/S1672-6308(08)60058-X

Zhao, W., Langfelder, P., Fuller, T., Dong, J., Li, A., and Hovarth, S. (2010). Weighted gene coexpression network analysis: State of the art. *J. Biopharmaceutical Stat* 20, 281–300. doi: 10.1080/10543400903572753

frontiers | Frontiers in Plant Science

TYPE Review
PUBLISHED 04 January 2023
DOI 10.3389/fpls.2022.1083960

OPEN ACCESS

EDITED BY
Poonam Yadav,
Institute of Environment and Sustainable Development, Banaras Hindu University, India

REVIEWED BY
Munish Kumar Upadhyay,
Indian Institute of Technology Kanpur, India
Arnab Majumdar,
Jadavpur University, India
Sudhakar Srivastava,
Banaras Hindu University, India

*CORRESPONDENCE
Viliam Barek
viliam.barek@uniag.sk
Akbar Hossain
akbar.hossain@bwmri.gov.bd

SPECIALTY SECTION
This article was submitted to Plant Abiotic Stress, a section of the journal Frontiers in Plant Science

RECEIVED 29 October 2022
ACCEPTED 22 November 2022
PUBLISHED 04 January 2023

CITATION
Moulick D, Bhutia KL, Sarkar S, Roy A, Mishra UN, Pramanick B, Maitra S, Shankar T, Hazra S, Skalicky M, Brestic M, Barek V and Hossain A (2023) The intertwining of Zn-finger motifs and abiotic stress tolerance in plants: Current status and future prospects. *Front. Plant Sci.* 13:1083960. doi: 10.3389/fpls.2022.1083960

The intertwining of Zn-finger motifs and abiotic stress tolerance in plants: Current status and future prospects

Debojyoti Moulick[1], Karma Landup Bhutia[2], Sukamal Sarkar[3], Anirban Roy[3], Udit Nandan Mishra[4], Biswajit Pramanick[5,6], Sagar Maitra[7], Tanmoy Shankar[7], Swati Hazra[8], Milan Skalicky[9], Marian Brestic[9,10], Viliam Barek[11]* and Akbar Hossain[12]*

[1]Department of Environmental Science, University of Kalyani, Nadia, West Bengal, India, [2]Department of Agricultural Biotechnology & Molecular Breeding, College of Basic Science and Humanities, Dr. Rajendra Prasad Central Agricultural University, Samastipur, India, [3]School of Agriculture and Rural Development, Faculty Centre for Integrated Rural Development and Management (IRDM), Ramakrishna Mission Vivekananda Educational and Research Institute, Ramakrishna Mission Ashrama, Narendrapur, Kolkata, India, [4]Department of Crop Physiology and Biochemistry, Sri University, Cuttack, Odisha, India, [5]Department of Agronomy, Dr. Rajendra Prasad Central Agricultural University, PUSA, Samastipur, Bihar, India, [6]Department of Agronomy and Horticulture, University of Nebraska Lincoln, Scottsbluff, NE, United States, [7]Department of Agronomy and Agroforestry, Centurion University of Technology and Management, Paralakhemundi, Odisha, India, [8]School of Agricultural Sciences, Sharda University, Greater Noida, Uttar Pradesh, India, [9]Department of Botany and Plant Physiology, Faculty of Agrobiology, Food, and Natural Resources, Czech University of Life Sciences Prague, Prague, Czechia, [10]Institute of Plant and Environmental Sciences, Slovak University of Agriculture, Nitra, Slovakia, [11]Department of Water Resources and Environmental Engineering, Faculty of Horticulture and Landscape Engineering, Slovak University of Agriculture, Nitra, Slovakia, [12]Division of Agronomy, Bangladesh Wheat and Maize Research Institute, Dinajpur, Bangladesh

Environmental stresses such as drought, high salinity, and low temperature can adversely modulate the field crop's ability by altering the morphological, physiological, and biochemical processes of the plants. It is estimated that about 50% + of the productivity of several crops is limited due to various types of abiotic stresses either presence alone or in combination (s). However, there are two ways plants can survive against these abiotic stresses; a) through management practices and b) through adaptive mechanisms to tolerate plants. These adaptive mechanisms of tolerant plants are mostly linked to their signalling transduction pathway, triggering the action of plant transcription factors and controlling the expression of various stress-regulated genes. In recent times, several studies found that Zn-finger motifs have a significant function during abiotic stress response in plants. In the first report, a wide range of Zn-binding motifs has been recognized and termed Zn-fingers. Since the zinc finger motifs regulate the function of stress-responsive genes. The Zn-finger was first reported as a repeated Zn-binding motif, comprising conserved cysteine (Cys) and histidine (His) ligands, in *Xenopus laevis* oocytes as a transcription factor (TF) IIIA (or TFIIIA). In the proteins where Zn^{2+} is mainly attached to amino acid residues and thus espousing a tetrahedral coordination

geometry. The physical nature of Zn-proteins, defining the attraction of Zn-proteins for Zn^{2+}, is crucial for having an in-depth knowledge of how a Zn^{2+} facilitates their characteristic function and how proteins control its mobility (intra and intercellular) as well as cellular availability. The current review summarized the concept, importance and mechanisms of Zn-finger motifs during abiotic stress response in plants.

KEYWORDS

abiotic stresses, Zn-finger proteins, mechanisms, plants, gene signalling ABA - abscisic acid

1 Introduction

Crops usually encounter a wide range of hostile climatic fluctuations during their life cycles. Such abnormal environmental fluctuations are covered by stressors of both biotic origins, including infection by pathogens (virus, bacteria, fungi, etc.), attack by weeds, and insects, as well as by abiotic components also (Moulick et al., 2018d; Ghosh et al., 2020a; Ghosh et al., 2020b; Ghosh et al., 2021; Ghosh et al., 2022a; Ghosh et al., 2022b; Mateos Fernández et al., 2022; Tonnang et al., 2022; Jain et al., 2022a; Jain et al., 2022b). Among the abiotic stress including heat and chilling stress (Aslam et al., 2022; Haider et al., 2022; Ullah et al., 2022; Verma et al., 2022), limitation of water (drought), limitation of nutrients, elevated levels of salt, and hazardous/toxic metals and metalloids in the soil (Hernandez et al., 2000; Moulick et al., 2019; Saha et al., 2019; Sahoo et al., 2019; Moulick et al., 2021; Choudhury et al., 2022a; Choudhury et al., 2022b; Choudhury and Moulick, 2022; Mazumder et al., 2022).

Environmental stress can adversely modulate the field crop's ability to maintain its yield potential, i.e., their determining yield despite satisfactory inputs and other factors. A field crop/plant's vulnerability to adverse deviations from (maximum yield) yield potential is usually calculated by measuring the respective crop's yield stability (Bhadra et al., 2021). The difference between the actual yield and yield potential of a particular site (agro-environment) is regarded as the yield gap (Mueller et al., 2012). Crops seldom touch their real yield potential in most broad-acre agri-environmental systems due to experiencing stress (s) during crop's life cycle. Stress-affected plants exhibited three primary response segments: first is the alarm or apprehension phase, sometimes also called the initiation of stress; the next phase, i.e., the second phase is characterized by resistance or fight phase through the initiation of defence systems; and the last or third phase is the exhaustion phase or collapse stage where loss due to stress is evident (Larcher, 2003; Moulick et al., 2019; Sahoo et al., 2019).

Among the stresses, salinity (high Na^{+}) is the critical agro-environmental factor that limits growth and yield/productivity. Under salinity stress, crops usually modulate their physiological processes by endorsing water acquisition and retention, and shifting the ion homeostasis management process (Parida and Das, 2005; Barman et al., 2022; Roy et al., 2022). At the same time, scarcity of available water to plants or drought stress results in decreased survival of plants, growth, and development due to metabolic imbalances. Drought is often linked with a lack of accessibility of groundwater in the land/soil but can also be worsened by greater evapotranspiration (Jaleel et al., 2009; Choudhury et al., 2022c; Jadhav et al., 2022). Such stress (drought) may occur under dry/humid conditions and with elevated air temperatures. The disparity in the water loss due to evapotranspiration flux and water uptake from soil may attribute to the key reason behind imposing drought stress (Lipiec et al., 2013; Dash et al., 2022; Sagar et al., 2022). On the other hand, toxic heavy metals and metalloids are also posing a serious threat to achieving agricultural sustainability in crop production with significant accumulation in the edible parts imposing a menace to the food chain (Moulick et al., 2016a; Moulick et al., 2016b; Moulick et al., 2018a; Moulick et al.,

Abbreviations: ABA, abscisic acid; APX, ascorbate peroxidase; AtERF5, a class I ERF protein; CAT, catalase; COR, cold-regulated genes; DREB/CBF, C-repeat binding factors; EIN3, ethylene-induced 3; ENA1, Na+- exporting P-type ATPase gene; FIT, fer-like iron deficiency-induced transcription factor; FSD1, iron superoxide dismutase 1; GR, glutathione reductase; GSH1/2, glutathione 1/2; LP2, plasma membrane receptor-like kinase leaf panicle 2; MAPK, mitogen-activated protein kinase; MDA, malonaldehyde; NCED, 9-cis-epoxy-carotenoid dioxygenase; OsDREB2A, dehydration-responsive element-binding 2A; OsP5CS, pyrroline 5 carboxylate synthetase; OsProT, proline transporter; PCS1/2, phytochelatin synthases 1/2; PMR2, Ca^{2+} ATPase gene; POD, peroxidase; PRXZ4, peroxidase 24 precursor; RbohD, respiratory burst oxidase homologue; RD29A, a classical stress-response gene; ROS, reactive oxygen species; SOD, superoxide dismutase.

2018b; Moulick et al., 2018c; Saha et al., 2019; Chowardhara et al., 2019a; Chowardhara et al., 2019b; Saha et al., 2022).

From a genetic point of view, stress is a set of certain environmental conditions that prevent a crop from experiencing its complete genetic expression. An abiotic component-induced stress, not only due to the exchanges (mainly with signalling) with other organisms and that can negatively impact particular organisms in an agro-environment, is regarded as abiotic stress. The effect of abiotic stresses on the agro-environmental sector is a crucial threat presently intensified by anthropogenic activities and global warming (Kang et al., 2017; Mukherjee and Hazra, 2022).

Reports indicate that abiotic stresses not only impose adverse on a crop's anatomy, physiology, biochemistry and but subsequently limit essential metabolic processes like respiration, photosynthesis, and growth when lingered for a long time often inducing death also (Hirayama and Shinozaki, 2010; Lima et al., 2015; Basu et al., 2016). Plants are equipped with mechanisms (physiological and metabolic) that may be crucial in lightening/mitigating agro-environmental stresses. These stress-induced shuffling crops' metabolic machinery is controlled using the initiation of genetic networks or pathways. The outcome of this genetic alternation is imparting greater/better tolerance or resistance to certain stress (s) (Claeys and Inzéand Inzé, 2013; Thorpe et al., 2013). Upon exposure to environmental stresses, dangerous by-products to crop health were found to be instrumental to plants' normal health and wellbeing. H_2O_2 (hydrogen peroxide), superoxide radicals, OH-radicals (hydroxyl radicals), are regarded as reactive oxygen species (ROS), generated as a result of leakage of electrons that occurs during the photorespiration and photosynthesis process (Thorpe et al., 2013; Kao, 2017; Moulick et al., 2021). Within the plant cells, the proper antioxidant defense machinery and ROS build-up sustain a steady-state balance (Hasanuzzaman et al., 2012). Keeping a satisfactory level of ROS within the cell permits adequate operation of redox biology (metabolic reactions) and the management of numerous phycio-biochemical processes vital for plant's growth and development. This kind of harmony among ROS formation and ROS quenching is an example of intermediate level of ROS management/homeostasis (Hasanuzzaman et al., 2019).

These reduced oxygen radicals or ROS were reported to adversely influence key components of a crop's metabolic cycle resulting in significant damage to cellular processes and death (Nouman et al., 2014). In order to lessen the excessive ROS production and subsequent oxidative stress, plants/crops have well-maintained anti-oxidative machinery that consists of non-enzymatic as well as an enzymatic unit that can bring equilibrium among ROS generation and quenching and protection of cellular damage even PCD or programed cell death also (Raja et al., 2017; Duan et al., 2012; Das and Roychoudhury, 2014; Choudhury et al., 2021a; Hossain et al., 2021).

The magnitude of ROS induced damage to biomolecules subjected to many factors like the concentration of target biomolecule(s), site of the particular biomolecule(s) in relation to the ROS production site, the rate constant of the reaction among biomolecules and ROS, efficacy ROS quenching components are to name a few (Davies, 2005). Increasing the antioxidant level within the plant cells can be achieved by spontaneously through use of genetic engineering or by supplementing can boost up the defense system of the plant and saving them from the adverse impact of ROS generated as a result of environmental stress (Mishra et al., 2006; Gupta et al., 2009; Kaur et al., 2022; Upadhyay et al., 2022). SOD (superoxide dismutase), CAT (catalase), and POX or peroxides are well-recognized enzymes involved in antioxidant systems that adjust the ROS homeostasis by reducing OH• into H_2O_2 of crops (Gill and Tuteja, 2010; Nouman et al., 2016). Whereas, in coordination, with enzymatic components, the non-enzymatic units of the antioxidant system (glutathione, flavanoid, lipids carotenoids, etc.) work on H_2O_2 through various means (Duan et al., 2012; Yin et al., 2020; Choudhury et al., 2022c).

At present, the main concern for the researchers working on developing suitable strategies to mitigate abiotic stress in crops, the main challenge is the complexities regarding stressor (s), i.e., abiotic components and the responses by crops towards the stressors. Apart from agronomic practices, irrigation management comparatively newer avenues like seed priming technology (Moulick et al., 2016a; Moulick et al., 2017; Moulick et al., 2018a; Moulick et al., 2018b; Moulick et al., 2018c), potentials of wild relatives (Hossain et al., 2022) potentials of metabolomics and next generation sequences are to name a few (Choudhury et al., 2021b; Hossain et al., 2021).In order to properly understand how stressors and crops interact at the molecular level, i.e. replication, transcription and translation. One such exciting topic of how the information imposed upon exposure to a stressor communicates at the cellular level is to illustrate the contributions made by transcription factors or Tfs. Among the well-known TFs, Zn-Fingers are of prime interest.

The Zn-finger was first reported as a repeated Zn-binding motif, comprising conserved cysteine (Cys) and histidine (His) ligands, in *Xenopus laevis* oocytes as a transcription factor (TF) IIIA (TFIIIA) (Miller et al., 1985). Since its first report, a wide range of Zn-binding motifs has been recognized and termed Zn-fingers. To meet the cellular demand, many proteins employ non-protein (often metallic ions) as cofactors. Among the metallic ions considered cofactors, transition metal ions are the most important due to their significant influence on modulating a wide range of cellular activities. From the periodic table's perspective, d-block elements are found to be more actively involved as cofactors. Zn is one cofactor that can influence as much as >10% of human proteins with a pronounced impact on structural and catalytic activities (Andreini et al., 2006; Maret and Li, 2009; Kochańczyk et al., 2015). In the proteins where Zn^{2+} is mostly attached to amino

acid residues and thus espousing a tetrahedral coordination geometry. The physical nature of Zn-proteins, defining the attraction of Zn-proteins for Zn2+is crucial for knowing how a Zn^{2+} facilitates their characteristic function and how proteins control its mobility (intra and intercellular) as well as cellular availability. In the mammalian genomes, encoded Zn-finger proteins dominate in number and are known as TF-regulators. A specific number and variety within Zn-finger or Zn-containing domains contribute to different cellular processes like regulation of transcription, binding to nucleic acid, and folding of proteins. Intermolecular attachment spots are the most significant and sort after when compared with similar intermolecular bindings. Due to having structural complexities (peptide chain composition, orientation, etc.), the intermolecular attachment of ligands and their respective targets poses serious challenges to analysis analyze (Maret et al., 2004; Kochańczyk et al., 2016). Findings have shown that an optimum level of Zn^{2+} concentration is essential to maintaining the stability and folding of protein subunits and for satisfactory performance of the catalytic activity of a particular enzyme (Keilin and Mann, 1940; Vallee and Neurath, 1954; Parraga et al., 1988). This innovative concept of small Zn^{2+}-stabilized domains was further supported by the in-depth analysis of the TFIIIA sequence, which exhibited that a continuous stretch of nine tandemly repeated 30 amino acid residues (13 to 276) having two invariant pairs of Cys along with His residues coordinating one Zn^{2+}. This particular pattern was later coined as ZF/zinc finger (Miller et al., 1985; Fairall et al., 1986; Rhodes and Klug, 1986).

In this review, we are going to assess the contributions made by ZFs in elaborating and imparting abiotic stress tolerance in field crops with unique references to salinity, water stress, thermos-stress, heavy metals, irradiation and elevated CO_2 levels.

2 Zn-finger acellular perspective

2.1 Sub-cellular localization of Zinc Finger Proteins

Zinc Finger Proteins (ZFPs) contain a highly conserved signature domain consisting of 20–30 amino acid residues having the consensus sequence of CX2–4CX3FX5LX2HX3–5H (X denotes any amino acid). Structural differences in different ZFPs are basically due to the differences in positions and numbers of cysteine (Cys) and histidine (His) residues that interacts and bind to the zinc ion and are constituted of several sub-groups which are designated as Cys4/C4 (GATA-1), Cys6/C6 (GAL4), Cys8/C8, Cys2HisCys/C2HC (Retroviral nucleocapsid), Cys2His2/C2H2 (TFIIIA), Cys2HisCys5/C2HC5 (LIM domain), Cys3His/C3H/CCCH, Cys3HisCys4/C3HC4 (RING finger) and Cys4HisCys3/C4HC3 (Requium), DnaJ-like zinc finger protein and many others (Lyu and Cao, 2018; Han et al., 2020; Yuce and Ozkan, 2020; Ali et al., 2022). As ZFPs are basically the members of the most prominent transcription factor family having a DNA binding domain, they are generally localized to the nucleus after translation. However, the zinc finger domain, an important structural motif, is also reported to be involved in other cellular activities such as RNA binding, membrane association and protein-protein recognitions and interaction (Han et al., 2020). Thus, different types of ZFPs are localized to cellular compartments as per their specific role in cellular activities. Protein sorting in a cell can also offer clues about the functions of these proteins (Wang et al., 2020).

Among all the sub-groups of ZFPs, the C_2H_2 (TFIIIA) has been extensively studied in plants. It represents the large proportions of ZFPs in plants where 189 members in rice (Agarwal et al., 2007), 321 in Soybean (Yuan et al., 2018), 122 in *Cucumis sativus* (Yin et al., 2020) and many more members in other crops have been reported. Its DNA-binding motif is one of the best-characterized motifs having two residues each of Cys and His amino acids tetrahedrally combined into a zinc ion (Xie et al., 2019). Focussing on plant-specific C_2H_2 type ZFPs (Q-type C_2H_2-ZFPs), it is reported to have different lengths of long spacer between two Zn finger motifs as compared to other eukaryotic organisms. Apart from the Zn finger motif, the core sequence KXKRSKRXR, which is present in the N-terminal of protein sequences, acts as an NLS for sorting of C_2H_2 type ZFPs to the nucleus (Xie et al., 2019) and the QALGGH motif present in the helical region is required for binding to DNA (Kielbowicz-Matuk, 2012). Having multiple functions in the nucleus, most of the reported C_2H_2-type ZFPs in plants were found to be localized in the nucleus. Several experiments were conducted with the C_2H_2 type ZFP genes to confirm the nuclear localization, such as FEMU2 of *Chlamydomonas reinhardtii*, fused with the β-glucuronidase (GUS) reporter gene was bombarded into onion epidermal cell and found that FEMU2 protein was in fact localized to the nucleus. A similar experiment was conducted with *JcZFP8* gene of *Jatropha curcas* fused with the GFP reporter gene under the control of the CaMV35S promoter. The 35Sp : *JcZFP8:GFP* gene construct was injected into tobacco protoplast for transient expression, and the fluorescence signal results clearly showed the localization of 35Sp : JcZFP8:GFP fusion protein into the nucleus of the tobacco cells (Shi et al., 2018). WRKYs with its conserved consensus sequence of WRKYGQK along with zinc-finger-like motifs of C_2H_2 and C_2HC type ZFPs also have a NLS for their localization to the nucleus (Bakshi and Oelmüller, 2014). In the nucleus, it acts as a transcription factor and binds to the TTGAC(C/T) W-box cis-element in the promoter of their target genes (Bakshi and Oelmüller, 2014; Chen W et al., 2019) and transcriptionally regulates the expression of target genes (Cheng et al., 2017).

Similarly, another extensively studied sub-class of plant ZFPs is Cys3His/C3H/CCCH type. Plant genome encodes large numbers of CCCH type ZFPs and has been identified

and characterized in crop plants such as Chickpea (Pradhan et al., 2017), *Brassica rapa* (Pi et al., 2018) and many other plants. The CCCH-type ZFPs of plants have conserved CCCH motifs ranging from one to six copies, with the most prevalent consensus sequence of the C-X7–8-C-X5-C-X3-H motif in the middle of the protein sequence (Pi et al., 2018; Chen et al., 2020). Although C-X7–8-C-X5-C-X3-H is the most common motif in CCCH-type ZFPs in plants, other structural variations in the consensus sequences suggest different cellular localisation patterns and roles in cellular activities (Han et al., 2020). Many of the CCCH-type ZFPs are localized to the nucleus, such as AtZFP1, KHZ1 and KHZ2 of Arabidopsis (Han et al., 2014), SAW1 and OsC3H10 of rice (Wang et al., 2020; Seong et al., 2020). CCCH-type ZFPs such as AtTZF2/3, ZFP36L3 and ZC3H12a are localized to the cytoplasm [84-86), where some of the CCCH-type ZFPs, namely OsC3H10, AtTZF4-6, etc. gets co-localized with stress granules (SGs) and processing bodies (PBs) (Seong et al., 2020). Likewise, some CCCH-type ZFPs are localized to plasma membranes such as AtOZF1and AtOZF2 (Oxidation-related Zinc Finger 1) of Arabidopsis and PeC3H74 of *Moso bamboo* (Huang TL et al., 2012; Chen et al., 2020) where some of the members are involved in secondary wall synthesis in response to biotic and abiotic stresses (Zhang et al., 2018; Chen et al., 2020), while several other members of CCCH type ZFPs such as OsLIC of rice, AtTZF of Arabidopsis shuttle between the nucleus and the cytoplasm (Wang et al., 2008; Bogamuwa and Jang, 2013). Shuttling of CCCH type ZFPs between cytoplasm and nucleus is due to the presence of leucine-rich NESs (Nuclear Export Signals) and NLSs (Nuclear Localization Signals) which are mainly present in their N- or C- terminal of the protein sequence (Han et al., 2020). These shuttle signals are current in several CCCH-type ZFPs across the crop species indicating their potential role in stress responses and signal transduction (Wang et al., 2008; Chai et al., 2012). Sub-cellular localization to cytoplasm and membrane was observed in another class of ZFPs called RING ZFPs. Arabidopsis RING ZFPs, *AtRZFP* fused with *GFP* under the control of 35S promoter was transformed into onion epidermal cells, and the signal of *AtRZFP-GFP* was clearly observed in the cytoplasm and plasma membrane (Zang et al., 2016). Some of the RING ZFPs located in the plasma membrane and cytoplasm include *AtAIRP1, RHA2a*, *AtATL78* of Arabidopsis, *OsRDCP1, OsSIRH2-14, OsRFPv6* of rice, *LjCZF1* of *Lotus japonicas*, VpRH2 of grape are located to the plasma membrane (Han et al., 2021) and *ZmXerico2* of maize (Gao et al., 2012), *OsSIRH2-14* and *OsSIRP1* of rice (Hwang et al., 2016), *AtAIRP4, EMR* of Arabidopsis (Park et al., 2018), *CaDSR1, CaASRF1* of pepper (Lim et al., 2018; Joo et al., 2019) are located in the cytoplasm. Other studies suggested that other than plasma membrane and cytoplasm, RING ZFPs are also localized to nucleus and other cellular compartments. For instance, *CaASRF1, CaAIRF1, CaDSR1* of pepper (Lim et al., 2017), *AtHOS1, AtATRF1* of Arabidopsis (Tian et al., 2015; Kim et al., 2017; Qin et al., 2017) and *OsSADR1* of rice (Park et al., 2018) were located to nucleus, whereas, *OsSIRH2-14* of rice was not only located in the cytoplasm and plasma membrane but was also found to be localized to Golgi bodies (Park et al., 2019). Likewise, wheat *TaDIS1* was also reported to be localized to Golgi bodies (Lv et al., 2020). Rice RING-H2 zinc finger proteins *OsHCI-1* and *OsMAR-1* were found to be localized to the cytoskeleton particularly in microtubules (Lim et al., 2013; Park et al., 2018) and RING-H2 ZFPs of wild tomato *SpRING* was found to be localized to the endoplasmic reticulum.

GATA-1 which is one of the sub-group members of ZFPs conserved families of transcription factors regulating the expression genes involved in cellular processes (Zhang et al., 2015). With the consensus sequence of CX2CX17−20CX2C along with DNA binding domain, it binds to the WGATAR (W = T/A, R = G/A) sequence in the promoter region of the target genes (Behringer and Schwechheimer, 2015; Gupta et al., 2017). As a transcription factor family, it has to be localized to the nucleus for its activities and to confirm it a study was conducted using the GATA gene of Poplar (*P. deltoids*) where Arabidopsis plant was transformed with *PdGNC-GFP* gene fusion under the control of CaMV35S promoter. Its nuclear localization was confirmed as the 35S: *PdGNC-GFP* fusion protein was detected in the nucleus (An et al., 2014).

Likewise, *Brachpodium distachyon BdGATA13-eGFP* gene fusion under the control of 35S promoter which was used for the transformation of tobacco leaves was found to be localized into the nucleus (Guo et al., 2021). However, reports on *FIP* (FtsH5 Interacting Protein), which is a type of GATA-1 ZFPs highlighted its localization to plastid as well specifically to thylakoid membrane in response to abiotic stress signals (Lopes et al., 2018). Similarly, DnaJ-like ZFPs with their characteristic C-terminal tandem 4× repeats of the CxxCxxxG are reported to have roles in the accumulation of carotenoids in plastids of non-pigmented tissues (Osorio, 2019) and inducing chromoplast biogenesis and simultaneously repressing the chloroplast biogenesis and chlorophyll biosynthesis in the nucleus of de-etiolating cotyledons cells (Sun et al., 2019). With its functions specific to the nucleus and chloroplast, *DnaJ-like ZFPs are localized to both the nu*cleus and chloroplast. Chloroplast localization of DnaJ like ZFPs is due to the presence of N-terminal chloroplast transit peptide (cTP) along with C-terminal zinc finger domain (ZF) which is separated by two trans-membrane domains (TMs) (Chen et al., 2021a). For nuclear localization, ubiquitination of lysine58 in ORANGE/OR (a type of DnaJ like ZFPs) by UBC19 was reported to be essential to generate truncated OR ZFPs proteins (Chen et al., 2021a). Sub-cellular localization studies of another class of ZFPs called as FCS-like ZFPs (FLZs) were conducted as it was found to be active both in cytoplasm and nucleus. FCS-like ZFPs are reported to act as scaffold proteins for plant-specific SnRK1 complex which is involved in various stress responses and are reported to be

localized to both cytoplasm and the nucleus in plants like Arabidopsis and Maize (Jamsheer et al., 2018a; Chen et al., 2021b). The distribution of ZFPs to different compartments of plant cell clearly indicates that this class of proteins are involved in several cellular processes either at both transcriptional and post-transcriptional level.

2.2 Transcription and post-transcriptional roles of Zn finger proteins

Many ZFPs acts as critical transcriptional regulators that correlate with their localization into the nucleus. However, it also interacts with RNA and other proteins to regulate the post-transcriptional expression of the target genes at RNA and protein levels, respectively (Han et al., 2020). As a transcription factor, it binds to the cis-acting element and subsequently activates or represses the expression of downstream target genes. The conserved zinc finger structure helps it bind to DNA double helix at specific sites to act as a transcription factor (Han et al., 2021). In plants like Arabidopsis, durum wheat and rice, a highly conserved sequence QALGGH of Q-type C2H2-ZFPs provide the ability for ZFPs to recognize the target sites and to further regulate the expression of downstream genes through activator or repressor domain (Lyu and Cao, 2018; Xie et al., 2019). However, the QALGGH sequence is not the only key and ubiquitous sequence for binding to target genes (Liu et al., 2022), the C_2H_2 type ZFPs may bind to the target site of the genes through DNA binding domain which is present in long spacers between the two adjacent zinc finger motifs (Sakamoto et al., 2004).

Apart from binding to DNA as a transcription factor, C_2H_2 ZFPs can also bind to RNA based on their bases and folding backbones, which recognize variants of phosphoric acid skeletons in RNA (Lin and Lin, 2018; Han et al., 2020). It is found that amino acid residues of C_2H_2 zinc finger proteins positioned at -1 and +2 of the a-helix play a vital role in its binding to RNA (Han et al., 2020). Upon binding to RNA, some of the members of ZFPs such as cleavage and polyadenylation specificity factor 30 (CPSF30) belonging to CCCH/Cys3His/C3H type ZFPs are involved in the polyadenylation step of pre-mRNA processing after forming a complex which is collectively called as CPSF (Shimberg et al., 2016). The RNA binding *AtCPSF30* known for involvement in the polyadenylation step of pre-mRNA also interacts with other molecules like calmodulin, however, its RNA binding activity gets reduced in presence of its other interacting molecules like calmodulin (Lee et al., 2012). For interacting with other proteins including other zinc finger proteins, ZFPs like the C2H2 type utilize domains such as L-box motif and EAR motif for interaction resulting in binding/prevention of binding of the target protein to DNA which in turn regulates the expression of downstream genes (Gamsjaeger et al., 2007; Brayer and Segal, 2008). Among the two motifs, the EAR motif which is the smallest known repressor domain in plants is reported to be essential for the inhibition of transcriptional activities (Hiratsu et al., 2004).

Correspondingly, WRKY proteins which are the type of Cys (2)-His(2) (C2H2) or Cys(2)-HisCys (C2HC) ZFPs, have two highly conserved domains with WRKYGQK sequences of WRKY domain and C-terminal zinc finger domain (Rushton et al., 2010). The target DNA binding site generally recognizes W-box cis-elements in the promoter region of target genes. For instance, a WRKY protein of *Hylocereus polyrhizus HpWRKY44* was found to be directly binding to the W-box element present in the promoter of *HpCytP450-like1* and transcriptionally activated the *HpCytP450-like1*, resulting into induced betalain biosynthesis in pitaya fruit (Cheng et al., 2017). However, some WRKY proteins bind to the promoter region other than W-box cis-elements (Chen et al., 2019). The selective binding of different WRKY TF members to W-box cis-element is based on neighboring DNA sequences outside of the W-box core motif (Bakshi and Oelmüller, 2014). Several experiments highlighted the role of the WRKY gene family to be associated with the regulation of transcriptional reprogramming in response to environmental stresses. For example, *PROPER* genes of Arabidopsis which encodes for small peptides which act as molecular patterns associated with injury or damage are perceived by *PEPR1* and *PEPR2* (leucine-rich repeat receptor kinases) and amplify the defense responses. Upon receiving the stress signal WRKY TF binds to the promoter of these two kinases and regulates their expression (Logemann et al., 2013).

Advancement in molecular techniques has helped to characterize various TF and regulatory element functions on a genome-wide scale, such as the utilization of the DAP-seq technique to discover the binding sites of TFs in DNA (O'Malley et al., 2016). Similarly, transcriptional role and binding sites of ZFPs like *AtWRKY33* under biotic were successfully identified using the techniques like ChIP-seq and revealed that *AtWRKY33* negatively regulates the *NCED3* and *NCED5* (ABA biosynthesis genes) to impart resistance against biotic stress like necrotrophic fungus (Liu et al., 2015). Some C2H2 type ZFPs are reported to transcriptionally regulate the expression of genes involved in programme cell death of the plants, thereby inducing PCD of plant cells (Yin et al., 2020).

Similar to C_2H_2 type ZFPs, many C_3H/CCCH type ZFPs are keys to regulating transcriptional activities with the presence of its conserved activator or repressor domains. For instance, rice *OsLIC* and *Ehd4* protein have a conserved EELR domain in its C terminal, which acts as the key component for transcriptional activation of the target genes (Wang et al., 2008). CCCH type ZFPs such as *OsLIC* and *Ehd4* of rice, *AtTZF1* and *AtTZF6* (*PEI1*) of Arabidopsis can bind to the promoter region of target genes (Wang et al., 2008; Bogamuwa and Jang, 2013; Wang et al., 2020). However, in some of the CCCH-type ZFPs, the

transcriptional activator domain, called EELR-like, was found to be in N-terminal. This EELR-like domain of ZFPs such as *AtC3H17* and *AtZFP1*were found to play an essential role in transcriptional activation of downstream salt-responsive genes like *AtP5CS1, AtGSTU5, SOS1* and ABA-dependent responsive genes *RD22, COR15A* and *RAB18* (Seok et al., 2016; Seok et al., 2018). In addition to transcriptional activators, some other proteins are transcriptional repressors. For negatively regulating the transcription of target genes, CCCH ZFPs like *GLUB-1-BINDING ZINC FINGER 1 (OsGZF1)* and *ILA1-interacting protein 4 (IIP4)* of rice have repressor motifs. After binding of ZFPs in the promoter region of target genes like *MYB61, CESAs* and *GluB-1*, it negatively regulates the expression of *CESAs* and *MYB61* for secondary wall synthesis and *GluB-1* for accumulation of gluten (Chen et al., 2014; Zhang et al., 2018). In addition to its involvement in transcriptional activities, CCCH ZFPs like *AtTZF1, KHZ1* and *KHZ2* of Arabidopsis also has been reported to be involved in post-transcriptional regulation of gene expression by binding to mRNA through its RNA binding motif (Yan et al., 2017; Pi et al., 2018). It is reported that with the help of the RNA binding domain, ZFPs namely, *OsTZF1* bind to mRNA at the 3' un-translated region specifically at AU-rich elements (AREs) (Jan et al., 2013). In plants like Arabidopsis, ZFPs like *HUA1* with its RNA binding ability regulates flower development through pre-mRNA processing of *AGAMOUS* (Rodriguezcazorla et al., 2018) and *FRIGIDA-ESSENTIAL 1 (FES1)* promotes the winter annual growth habits in a FRIGIDA-dependent manner by regulating mRNA levels of *FLOWERING LOCUS C (FLC)* (Schmitz et al., 2005). A recent study has found that the splicing efficiency of *FLC* pre-mRNA can be inhibited by *KHZ1* and *KHZ2* (RNA binding ZFPs) and promotes flowering in Arabidopsis through other independent pathways (Yan et al., 2020). Likewise, it has been reported that zinc finger homeodomain proteins (ZF-HD) another class of ZFPs are essential for the induction of flowers in plants like Arabidopsis. As the induction of flowers is affected by environmental stresses, *ZF-HD1* proteins over-expresses during such stress condition and helps in coping with stress through transcriptional activation of genes like *ERD1* (Shalmani et al., 2019).

In plants, through *in vitro* studies, KTEL (V) residue at the N terminus of ZFPs was observed in each zinc finger motif proving to be a key interface for RNA binding (Wang et al., 2008) and plant-specific TZF motif (RR-TZF) & RR sequence in AtTZF1 were found to be the essential motifs for binding to AREs of RNA leading to mRNA degradation (Qu et al., 2014). More recently two putative mRNA binding domains namely RRM and OST-HTH/LOTUS were identified in CCCH type ZFP (*AtC3H18L*) sequence (Xu et al., 2020).

Some ZFPs are co-localized to PBs and SGs. These PBs and SGs have essential roles in the post-transcriptional regulation of several genes, more importantly, during plant tolerance against environmental stresses (Bogamuwa and Jang, 2016). Some ZFPs, namely *AtTZF1, AtTZF4, AtTZF5*, and *AtTZF6* of Arabidopsis, with their cytoplasmic shuttling characteristics, work in association with these PBs and SGs for post-transcriptional regulation of target proteins (Jang, 2016; Seong et al., 2020). Different from the rest of the ZFPs, most of the RING zinc finger proteins have E3 ubiquitin ligase activity and it is involved in post-transcriptional activities of the ubiquitin-proteasome pathway. In this pathway, E3 RING ZFPs help in the recognition of the substrate proteins and degrades or change the activity of target proteins through ubiquitination (Swatek et al., 2019). For instance, *AtATL78, StRFP2*, *AtRZF1, DRIP1, DRIP2, OsDIS1* and *HOS1* post-transcriptionally regulate the target proteins such as *DREB2A, OsNek6, OsSKIPa, AtERF53, ICE1, OsARK4, OsHRK1, AtRma1* and *CaRma1H1*, etc. through ubiquitination (Han et al., 2021) of which many of the target proteins like *CaRma1H1* and *AtRma1* are involved in the transport of the aquaporin PIP2;1 from the ER. It is also reported to have roles in transcriptional and post-transcriptional regulations of different genes involved in ABA-dependent pathways, ROS and Ca^{2+} signalling pathways (Han et al., 2021). Transcriptionally it is involved in the activation of genes encoding enzymes of ABA pathways such as *ABA aldolase, NCED, ZEP* and *short-chain dehydrogenase/reductase* (Vaičiukynė et al., 2019) and post-transcriptionally it is involved in forming a complex with other proteins such as *PP2Cs* and *SnRK2s* for ubiquitination and phosphorylation of other proteins and transcription factors like *protein phosphatase 1* (*CaADIP1*), *CaATBZ1*, *AtAIRP3, bZIP, AtKPNB1, TaSTP, GDU1* and *RD21* which further activates or represses the transcription of ABA-responsive genes (Sah et al., 2016; Joo et al., 2020; Lv et al., 2020; Oh et al., 2020). In the MAPK signalling pathway, zinc finger proteins such as RGLG1 and RGLG2 have been involved in post-transcriptional modification of *MAPKKK18* in response to environmental stress like drought. In ROS and Ca^{2+} signalling pathways, it is involved in transcriptional activation of genes encoding antioxidant enzymes like *SOD* and *POD* in response to environmental stresses (Zang et al., 2016). The ORANGE or OR proteins which are the type of DnaJ type ZFPs with their dual sub-cellular localization abilities, perform transcriptional and post-transcriptional activities in the nucleus and plastids. In the nucleus, it interacts with *eRF1-2* (*eukaryotic release factor 1-2*) for transcriptional regulation of the downstream gene involved in cell elongation of petiole and plastids. It plays a role in post-transcriptional regulation by interacting with *phytoene synthase* to induce biogenesis of chromoplast and accumulation of carotenoid in non-pigmented tissues, simultaneously interacting with *TCP14*, a type of TFs to repress *ELIPs* (*Early Light Induced Proteins*) and biogenesis of chloroplast in de-etiolating cotyledons (Sun et al., 2019; Chen et al., 2021b). Whereas, some reports suggest that DnaJ ZFPs function as molecular chaperones in post-transcriptional or rather post-translational maintenance of structures and functions of its

interacting proteins (Ali et al., 2022). The FCS-like zinc finger (FLZ) proteins which are reported to be localized to the cytoplasm and nucleus extensively interact with the kinase subunit of the *SnRK1* complex and act as an adaptor to facilitate the interactions of effector proteins with the *SnRK1* complex. In plants, it was found to be acting as a transcriptional activator by mediating the interactions of *SnRK1* and effector proteins under various environmental stresses, however many of them are reported as negative regulators of *SnRK1* signalling (Jamsheer et al., 2018a and Jamsheer et al., 2018b).

3 Role of Zn finger in conferring tolerance to abiotic stress and possible mode of action

Zinc finger proteins play an extensive role in plant tolerance to various abiotic stress, such as drought, high salt, cold, high light, and osmotic and oxidative stresses (Wang et al., 2019; Han et al., 2020). In the process of external stress resistance, plants have evolved a set of complex and effective defence mechanisms, including signal perception, signal transduction, transcriptional regulation and response, to reduce or avoid damage to plants and ensure their average growth (Figures 1, 2) (Noman et al., 2019; Liu et al., 2022).

Several studies found that Zn-finger motifs significantly function during abiotic stress response in plants. In the first report, a wide range of Zn-binding motifs has been recognized and termed as Zn-fingers. Since the zinc finger motifs regulate the function of stress-adaptation genes. The Zn-finger was first reported as a repeated Zn-binding motif, comprising conserved cysteine (Cys) and histidine (His) ligands, in *Xenopus laevis* oocytes as a transcription factor (TF) IIIA (TFIIIA) (Laity et al., 2001; Ciftci-Yilmaz and Mittler, 2008; Kielbowicz-Matuk, 2012; Lyu and Cao, 2018). In the proteins where Zn^{2+} is mainly attached to amino acid residues and thus espousing a tetrahedral coordination geometry. The physical nature of Zn-proteins, defining the attraction of Zn-proteins for Zn^{2+}, is crucial for having an in-depth knowledge of how a Zn^{2+} facilitates their characteristic function and how proteins control its mobility (intra and intercellular) as well as cellular availability.

Many C_2H_2-type zinc finger proteins involved in the abiotic stress signalling pathway were identified based on stress induction, mutant, compliment, and ectopic expression analysis. Phytohormones are responsible for abiotic stress resistance and participate in the process of response to various stresses *via* C_2H_2-type zinc finger proteins, especially ABA (Abscisic acid) (Roychoudhury et al., 2013; Ku et al., 2018; Takahashi et al., 2018; Chong et al., 2020). ABA, acting as a pivotal regulator of abiotic stress responses in plants, induces the expression of stress-related genes and triggers a range of adaptive physiological responses under abiotic stress conditions in the plant (Ku et al., 2018; Takahashi et al., 2018; Chong et al., 2020). C_2H_2 zinc finger proteins regulate plants in response to abiotic stresses through two ABA-mediated signal pathways: ABA-dependent and ABA-independent signal pathways (Smekalova et al., 2014; Ku et al., 2018; Takahashi et al., 2018; Chong et al., 2020). In addition to the ABA signal pathway, C2H2 zinc finger proteins enhance abiotic stress resistance by the MAPK (mitogen-activated protein kinase) signaling pathway (Smekalova et al., 2014; Ku et al., 2018;

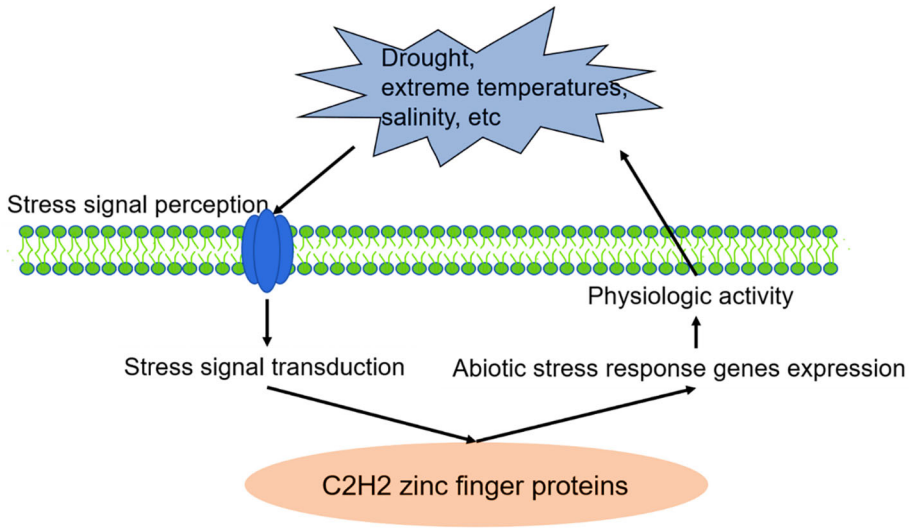

FIGURE 1
C2H2 zinc finger proteins are involved in plant stress responses. Source: (Liu et al., 2022).

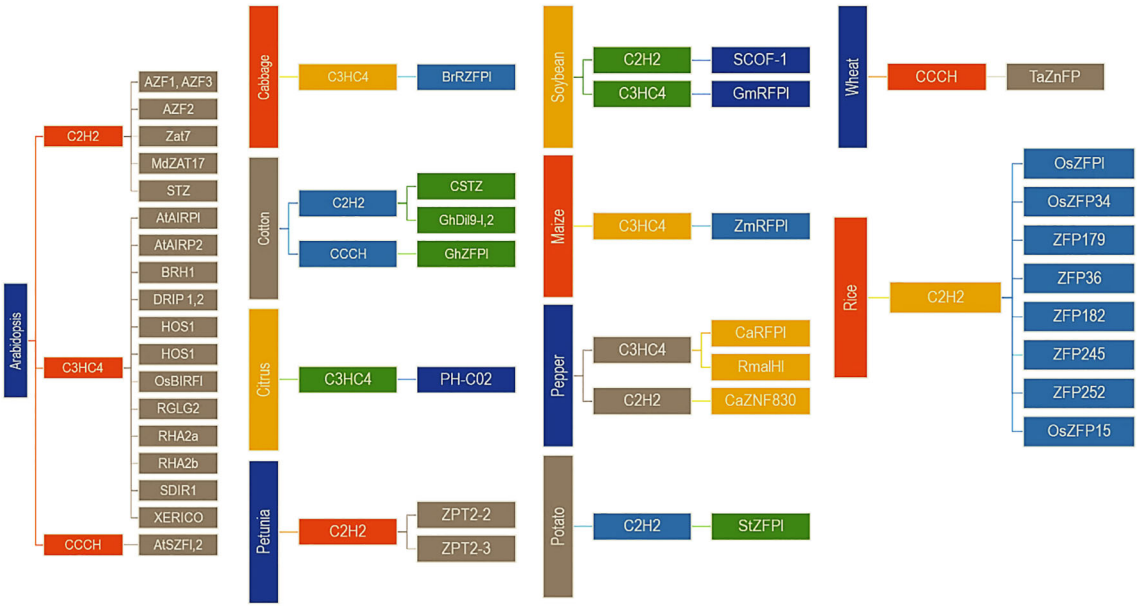

FIGURE 2
Some important Zinc Finger Proteins (ZNPs) involved in abiotic stress factors of the plants (1st order of the hierarchy is the name of the crop/plant, 2nd order is the type of the protein and 3rd order is the name of the ZNPs) (Source: Modified after Noman et al. (2019) with the permission from the Elsevier Rights Links (https://s100.copyright.com/), Licence No.: 5371200779212, Dated 17th August 2022).

Takahashi et al., 2018; Chong et al., 2020; He et al., 2020; Lin et al., 2021). MAPKs, as highly conserved signaling transduction modules, play an essential role in regulating responses to adverse environmental stresses (Lin et al., 2021). Typically, a MAPK module is composed of at least three protein kinases, including MAPK (MPK), MAPK kinase (MAPKK/MAP2K/MKK/MEK) and MAPK kinase (MAPKKK/MAP3K/MEKK). The MAPK cascade amplifies and conveys stress signals from signaling receptors to downstream stress response factors through a sequential phosphorylation manner (De Zelicourt et al., 2016; He et al., 2020; Lin et al., 2021). Thus, C_2H_2 zinc finger proteins regulate abiotic stress responses *via* both the ABA signaling pathway and MAPK signaling transduction pathway and constitute a certain degree of crosstalk and a complex regulatory network (Figure 3) (Liu et al., 2022).

3.1 Salinity

In many regions of the globe, soil salinity is significant abiotic stress that inhibits plant production. Salinity stress creates nutrient imbalances, is a source of harmful ions, and alters the osmotic condition of plants (Yaghoubian et al., 2021). It has been reported that more than 108 × 108 km^2 of land throughout the world are affected by salinity (Riaz et al., 2019). Due to salinity and problematic soils, millions of hectares in the humid areas of South and Southeast Asia that are technically suitable for various field crops, particularly rice cultivation, are left uncultivated or are cultivated with extremely poor yields. (Mainuddin et al., 2019; Mainuddin et al., 2020). In addition, mineral shortages and toxicity often exacerbate the issue of salinity since it seldom occurs alone. These soil stresses change in magnitude and interactions throughout time and space, making long-term adaptation dependent on its degree of tolerance to all environmental stresses (Sarkar et al., 2022). Moreover, the ill response of soil and water salinity in the different crops varied significantly.

As transcription factors, zinc finger proteins (ZNPs) play an essential part in a wide variety of cellular processes, including RNA binding, transcription control, stress tolerance, and plant growth and development in response to phytohormones) (Noman et al., 2019). Scientists have identified a large number of zinc finger proteins in higher plants that can regulate the various environmental cues (Yu et al., 2015). Around 189 stress-induced zinc finger proteins especially for indica rice and maize have been classified and amongst them, Cys2/His2- and CCCH-types have received greater attention (Agarwal et al., 2007) Multiple C2H2-type zinc finger proteins in rice, including ZFP36, ZFP179, ZFP182, ZFP245, and ZFP252, have been implicated in salt, drought, and oxidative stress responses (Xu et al., 2008; Wang et al., 2015; Wang et al., 2022a). It has been found that drought and salt tolerance in rice are improved by overexpressing the ZFP252 zinc finger protein gene by elevated synthesis of free proline and soluble sugars (Xu et al., 2008) and

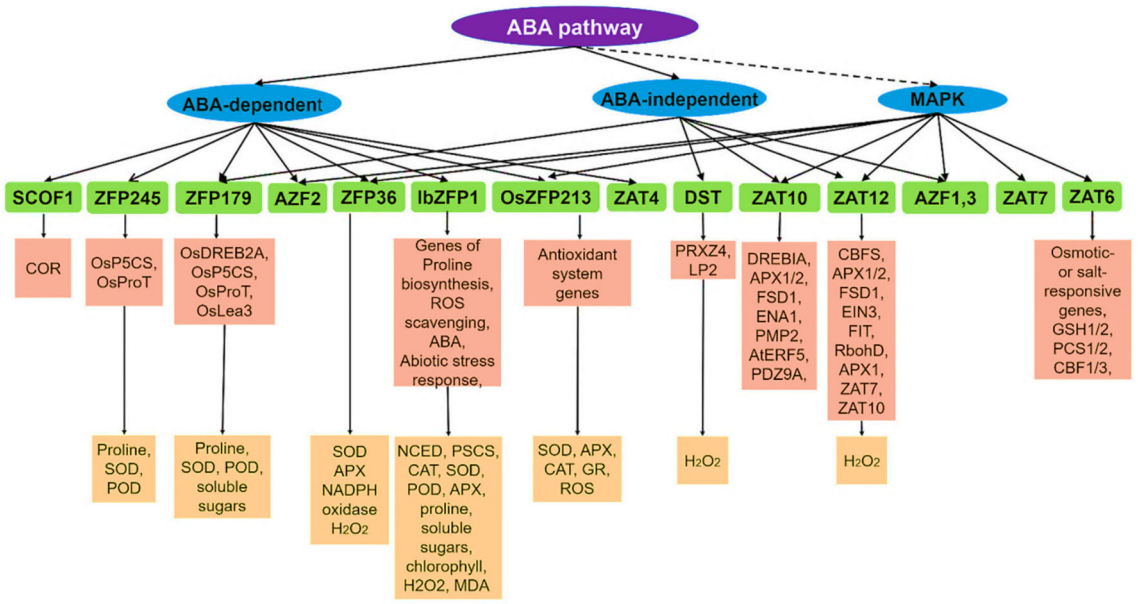

FIGURE 3
The signalling pathways of zinc finger proteins during abiotic stress response in plants. Note: The lines marked as solid indicate regulation, and the dashed lines indicate putatively. The C2H2 zinc finger proteins are SCOF-1, ZFP245, ZFP179, AZF1/2/3, ZFP36, IbZFP1, OsZFP213, ZAT4, DST, ZAT10/STZ, ZAT12, ZAT7 and ZAT6. Source: (Liu et al., 2022).

increased ROS scavenging activity (Huang et al., 2009). Huang et al. (2007) found that the production of ZFP182 in transgenic tobacco or overexpression in rice plants boosted their salt tolerance, ZFP182 may have a curative function in salt tolerance in plants. Wang et al. (2022a) reported that some C_2H_2 type Zinc finger protein plays a significant role in salinity tolerance in rice seedlings by enhancing ABA catabolism. They also stated that overexpression of OsZFP15-like Zinc finger protein increased the production of reactive oxygen species (ROS) and decreased tolerance to oxidative stress, resulting in increased salinity stress tolerance in rice seedlings. The A20/AN1-type (ZmZnF1) and ring-binding type (ZmZnF2) zinc finger proteins found in maize kernels are reported to induce by ABA, mannitol and NaCl stresses. Similarly, simultaneous overexpression of these zinc finger proteins in transgenic lines of rice significantly increased the Na induced stress tolerance (Yu et al., 2015). It has been observed that transgenic Arabidopsis plants that constitutively produce the Cys2/His2 zinc finger protein Zat7 exhibit slower growth and development and a higher degree of tolerance for the effects of salt stress and the ability to tolerate high salinity is lost when the EAR motif of Zat7 has a mutation or deletion (Ciftci-Yilmaz et al., 2007). Wang et al. (2022b) found that the overexpression of C_2H_2-type zinc finger protein 'MdZAT17' in transgenic apple and Arabidopsis reduces the sensitivity to abscisic acid (ABA) and regulates salt tolerance positively. They also reported that the growth of both wild-type and transgenic *Arabidopsis* seedlings was inhibited under salt stress, but the growth shyness of transgenic plants was pointedly lower than that of wild-type seedlings. In another study (Xu et al., 2022) has been identified 36 B-box (BBX) family of proteins in maize consists of zinc-finger transcription factors that have a significant role in the regulation of different abiotic stresses, including drought and salinity.

3.2 Soil moisture

Water is one of the fundamental inputs for the growth and yield of any arable crop. Still, both excess and deficit water supply in different growth stages can significantly reduce crop production. In the present era of climate change, aberrant weather conditions have increased the excess and deficit supply of soil moisture in most growing regions worldwide. Crop physiological and biological adaptability with the excess and deficiency supply of soil moisture has emerged as a potential research question (Osakabe et al., 2014). Multiple Zinc finger proteins have been identified from various crops has a definite role concerning drought and excess moisture stress of the field crops. Numbers of ZFPs have been identified in transgenic rice that has significant functions in enhancing drought, and excess moisture tolerance (Huang et al., 2009; Li et al., 2013; Wang et al., 2022a). Huang et al. (2009) reported that ZFP245 type ZNPs have significantly enhanced the cold and drought tolerance in rice by augmenting free proline and antioxidant

concentration in transgenic rice plants. They further suggested that ZFP245 transgenic rice plants under 14 days drought stressed condition has survived at 70-80% with 7 days recovery period. It has been postulated that under cold or drought stress, ZFPs boost the SOD and POD enzymatic activities in transgenic rice seedlings and thereby help to enhance the abiotic stress tolerance by triggering the ROS-scavenging mechanism (Rizhsky et al., 2004). In harmony to the previous findings, (Sakamoto et al., 2004) found that two Cys-2/His-2-type ZNPs viz. AZP2 and STZ in transgenic Arabidopsis have significantly overexpressed under drought-stressed conditions and facilitated the plant to tolerate drought stress. (Gao et al., 2012) reported that 'CgZFP1', a Cys2/His2 type ZFP isolated from Chrysanthemum has a significant role in regulating drought and salinity stress in transgenic Arabidopsis. In severer drought conditions, abscisic acid plays an important role in enhancing the plant's leaf senescence rate, reducing the yield. It has been found that a Cys-2/His-2-type ZNP, ′ MdZAT10′, reduced the sensitivity to abscisic acid in apples and in addition to that, MdZAT10 (overexpressed in *Arabidopsis*) has a beneficial effect on seed germination and seedling growth (Yang et al., 2021). In another study, Mukhopadhyay et al. (2004) isolated a ZNP from rice viz. "OSISAP1" (induced by abscisic acid) overexpressed in transgenic tobacco increased tolerance to cold, dehydration, and salt stress at early growing stages. Giri et al. (2011) reported that Stress-associated ZNP isolated from rice viz. A20-AN1 increased the abiotic stress tolerance in transgenic *Arabidopsis* plants.

Most of the study suggested that ZNPs isolated from various plant sources involved in regulating abiotic stress factors has manually controlled the drought and salinity stress simultaneously (Huang et al., 2009; Lawrence et al., 2022). But application or overexpression of ZNPs in different transgenic crops is precise in nature.

3.3 Temperature

Temperature stress due to both cold and high temperatures is considered a vital abiotic stress a plant faces during its growth and development (Liu et al., 2018). Thus, a clear-cut concept about the bio-physical-chemical impacts of temperature on a plant and its subsequent response mechanism is crucial to breeding improved stress-tolerant cultivars (Liu et al., 2018). Many Zn-finger proteins are responsible for mitigating the different temperature-related stresses in plants. CCCH Zn-finger proteins can control the expression of cold-induced genes; these proteins can improve cold tolerance in plants. Lin et al. (2011) found that the expressions of the cold-temperature genes viz. COR15A, RD29A, KIN1 etc. were upregulated in the cold-stress tolerant different Arabidopsis lines. Enhancement of the cold-stress tolerance in the plants can also be explained through signalling pathways of ABA, which are controlled by CCCH Zn-finger proteins (Xie et al., 2019). Transgenic switchgrass lines with induced Zn-finger protein, PvC3H72, survived even at −5°C temperature, while the lines with the low Zn-finger proteins could not survive (Xie et al., 2019). Zn-finger protein, DgC3H1, can improve the proline and soluble sugar levels in *Chrysanthemum* plants along with increased-level of SOD and POD, which ultimately make the plants able to survive under cold stress (Bai et al., 2021). C_2H_2 Zn-finger proteins also play a pivotal part in mitigating cold stress by regulating the ABA pathways. Kim et al. (2001) reported that the overexpression of C_2H_2 Zn-finger proteins results in cold-stress tolerance in soybean and tobacco by controlling ABA-response elements which facilitate COR gene-expression responsible for developing the plant cold-tolerance. The ABA-independent pathway for cold tolerance through C2H2 Zn-finger proteins is represented in Figure 4. In addition to the above two Zn-finger proteins, the AZF: Arabidopsis Zn-finger protein and STZ: salt-tolerance Zn-finger proteins are also responsible for cold-stress tolerance in Arabidopsis (Kodaira et al., 2011). The AZF genes, AZF, AZF2, AZF3, and STZ gene regulate the ABA-dependant pathway of Arabidopsis by regulating the ATPase gene, Na+, and Li+ outflows in plants (Lippuner et al., 1996).

3.4 Heavy metal (HM)

3.4.1 HM-tolerance through cellular layer modification

For any HM stress, the plant has a three-tier strategy including absorption or isolation of HM inside the plant, HM removal through a series of chelating mechanisms and ROS removal which are accumulated during HM stress. Other than this a few subsidiary events of the HM-tolerance mechanism include an impedance of HM transport within the plant through HM binding to the cytoderm (composed of cellulosic material) (Chen et al., 2019). Few HM ions bind to the active groups (-COOH, -OH) of cellulose (inside cytoderm) which reduces the quantity of HM that enters the protoplasm resulting in damage alleviation caused by HM (Nedelkoska and Doran, 2000; Clemens et al., 2013). Three types of zinc finger transcription factors (ZF-TFs) (GATA-type, CCCH-type, and C2H2-type) are expressed differentially and reported to be up-regulated under cadmium stress in cotton roots, some of which are shown to be associated with secondary cell wall biosynthesis (Chen et al., 2019). Up-regulation in the homologs of cellulose synthase genes during cadmium stress reveals the involvement of ZF-TF in cellular layer modification as one of the possible modes of action for imparting HM-stress tolerance in cotton plants.

In *Arabidopsis thaliana*, upon exposure to HMs exhibited some interesting findings. With the help of yeast-two-hybrid model when interaction among the different members of the HIPP family and the related zinc finger TF or transcription factors, have borne a particular interaction pattern of ATHB29 and HIPP proteins (of

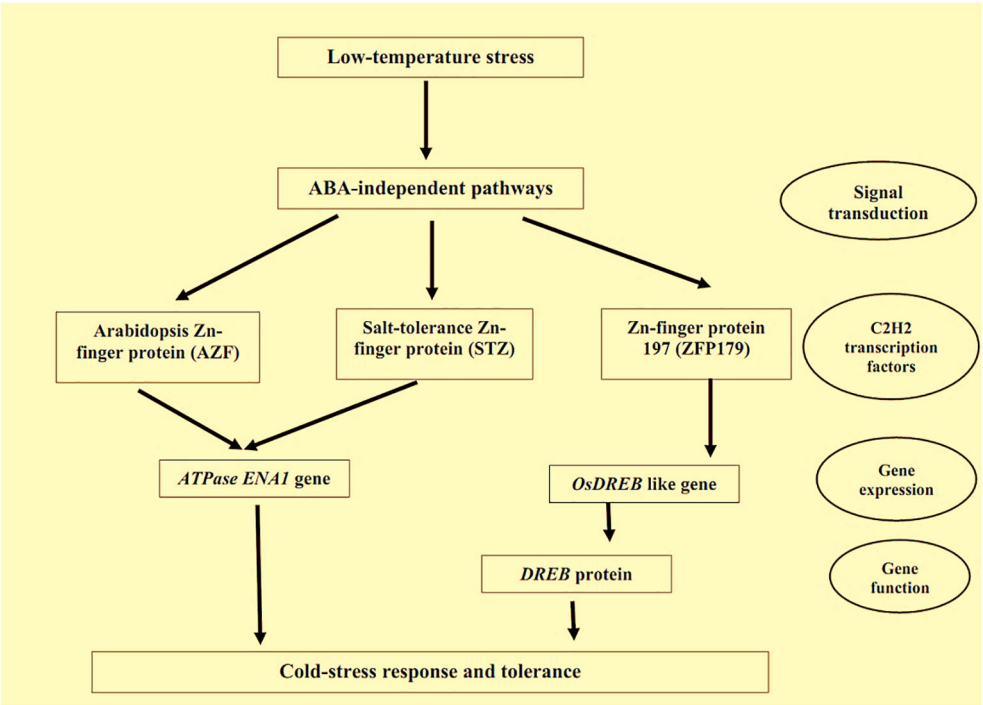

FIGURE 4
ABA-independent pathways for cold-tolerance by C2H2 Zn-finger proteins. Note: Zn-finger proteins also regulate the several pathways of plants under heat-induced stresses. Huang et al. (2008) found A20/AN1-type Zn-finger proteins in japonica rice regulating the heat-induced stresses in the plants. Moreover, they reported that Zn-finger protein, ZFP177 was responsive to heat stress tolerance in plants. Overexpression of Zn-finger protein, ZFP177, is also responsible for the heat tolerance in tobacco plants (Mukhopadhyay et al., 2004).

cluster III). Thus, a purposeful connection among ATHB29 and HIPP26 is also shown by experiments conducted with HIPP26 (mutants), displayed reformed expression pattern levels of such genes earlier known to be controlled by ATHB29 (Barth et al., 2009). Chakrabarty et al. (2009) while investigating genome-wide expression pattern of Zn-finger proteins in plants exposed to As^{3+} and As^{5+} reported a contrasting scenario. Proteins of the zinc-finger family were found to be downregulated under As^{5+} stressed situation whereas, Zinc-finger C3HC4-type proteins were found to exhibited both up and down regulated expression profile upon exposed to As^{3+} stressed situation. Authors like Abercrombie et al. (2008); Chakrabarty et al. (2009); Tripathi et al. (2012) have presented the expression profile of *Oryza sativa* (monocot) and *Arabidopsis thaliana* (dicot). Under As stressed condition both exhibited a downregulated Zn-finger protein expression profile. Shah et al. (2022) observed that spermine (Spm), a polyamine compound upon supplanting in common bean (*P. vulgaris*) exposed to As stress have enhanced the expression of PvC3H24, PvC3H25, PvC3H26 and PvC3H27 (Zn-finger proteins). The authors concluded that, Spm confer tolerance to As induced phyto-toxicity by modulating polyamine metabolism, antioxidant defense system along with facilitating (as enhancer) for zinc-finger proteins related genes expressions. Huang et al. (2012) reported some interesting findings while analysing the transcriptomic profile of rice roots exposed to As stress. among the 231 TFs, the zinc-finger protein (expressed particularly in inflorescence meristem or ZIM) had a share of only 3.46%. The authors have concluded that under As stress ZIM-TF were enhanced in a noteworthy fashion.

3.4.2 HM-tolerance through HM-homeostasis strategies

HM homeostasis strategies mainly involve the phytochelatin, metallothionein and metallochaperones (responsible for safe transport of metal ions inside the cell) induction (Harrison et al., 2000; de Abreu-Neto et al., 2013; Zhang et al., 2014) as well as vacuolar sequestration mediated by phytochelatin binding (Yang and Chuand Chu, 2011). Barth et al. (2009) found a functional association between a ZF-homeodomain (ZF-HD) TF (known as ATHB29) and arrays of HIPP26 (a type of metallochaperone protein) in *A. thaliana* under HM stress by double checking mutant line assay (mutated for HIPP26 functional loss) for the expression of stress-responsive genes which showed that the genes up-regulated under the influence of ATHB29 are inhibited in the absence of functional interaction between HIPP26 and ZF-HD.

3.4.3 HM-tolerance through protein-protein interactions (PPIs) and signal transduction

Plant stress-associated proteins (SAPs) contain ZF domains (either $[Cys2\text{-}Cys2]_n$ finger motifs or $[Cys\ and\ His]_n$ residues; 'n' represents multiple numbers of motif repeat) at the N- or C-terminal (Jin et al., 2007). These SAPs can be a key player in stress signaling through protein-protein interactions (PPIs) *via* their ZF-domain (Opipari et al., 1990; Kanneganti and Gupta, 2008). Additionally, SAP10 of A. thaliana was found to be coding for a nuclear or cytoplasmic protein that might act early in the signal transduction of the HM-stress tolerance response (Ströher et al., 2009; Dixit and Dhankher, 2011). Many of the HM defense responses shown by the plants are due to the major contribution of cellular receptors involved in signaling cascades like MAPK (three-tier phosphorylation module) (Rodriguez et al., 2010; Sinha et al., 2011; Jalmi and Sinha, 2015) which modulates downstream WRKY and ZAT TFs (containing ZF motifs) (Ogawa et al., 2009; Opdenakker et al., 2012). PPI (protein-protein interaction) study performed by Nguyen et al. (2012) between ZAT-TF (ZAT10; a ZF-containing TF) and Arabidopsis MAPK (MPK3, MPK6) under HM stress has paved a conceptual understanding that MAPKs are involved in HM stress signaling either through ZF-TFs or transcription factors containing ZF-motifs. Major plant stress tolerance responsive signaling factors includes EF-Tu receptor, ETR1/ETR2, SIT1, ER etc. Ca signaling is important in heavy metal stress hormone signaling, as is MAPK signaling, which uses Calmodulin, a Calcineurin B-like protein, and Ca dependent kinase (Steinhorst and Kudla, 2014). Among these, MAPK signalling is one of the major signalling pathways involved in alleviating heavy metal stress. Two transcription factors, viz., MPK3 and MPK6, get activated under high Cd stress mediated by ROS signalling (Liu et al., 2010). Calcium- and cadmium-responsive mitogen activated protein kinase (MAPKKK) in Arabidopsis remains a major signal transduction protein component (Suzuki et al., 2001).

3.4.4 HM-tolerance through ROS-detoxification

HM stress always generates oxidative stress and causes destabilization in the balance between ROS and the antioxidant system (Zhang et al., 2013; Jin et al., 2016; Yin et al., 2016; Xu et al., 2019). Different transcription factors (TFs) families including zinc finger-TFs are involved in such ROS-mediated stress responses (Singh et al., 2019). HM accumulation ROS mediated functional disruption of biomolecules among several other damages (Stohs and Bagchi, 1995; Cuypers et al., 2009; Haider et al., 2021). Under HM-stress SlRING1-ZFP overexpression in tomatoes led to more chlorophyll content and photosynthetic rate. Moreover, the maximal photochemical efficiency of photosystem II was evidently improved by SlRING1-ZFP mediated minimization of ROS levels and electrolyte leakage (Ahammed et al., 2020). Soybean ZFP (GmRZFP1) and Arabidopsis ZFP (AtOHRP) are reported to be involved in oxidative stress (activity induced by ROS) in plants thereby promoting ROS scavenging enzyme systems (Wu et al., 2010; Li et al., 2015). Putting together, zinc finger protein (ZFP) is involved in HM stress alleviation and detoxification of ROS as two underlined strategies of HM tolerance. Abscisic acid enhances plant stress response mechanisms under drought stress. Ring-zinc finger protein overexpression enhances genes like AtNECD3, which codes for a key enzyme in ABA biosynthesis (Ko et al., 2006). Zinc finger protein also enhances major genes' expression (ABA3, ABI5, etc.) responsible for ABA biosynthesis in rice (Zeng et al., 2015). Zinc finger protein ZFP-185 regulates ABA and GA synthesis modulation, which enhances stress response (Zhang et al., 2016). Flowering and gibberellin biosynthesis are also controlled by ZFP in *Chrysanthemum* (Yang et al., 2014). The effect of different Zinc finger protein in mitigating various abiotic stresses has been presented in Table 1.

3.4.5 HM-tolerance through ubiquitin proteosome-mediated degradation of misfolded or altered protein

Under abiotic stress, including HM, many functional proteins undergo the ubiquitin proteosome-mediated degradation process due to the altered quaternary structure of the protein (resulting in misfolded design) and hence no longer required for average growth and development (Blasiak et al., 2019). This way of aberrant protein identification and removal ensures better survival of plants under stress conditions (Stone, 2019). Most RING zinc finger proteins have E3 ubiquitin ligase activity (Joazeiro and Weissman, 2000; Ahammed et al., 2020) similar to the last enzyme of the ubiquitin-proteasome pathway (which plays a specific role in recognising target substrates and then degrades the target protein or changes the activity of the target protein). Hence RING-ZFP can be engaged in ubiquitin proteosome-mediated degradation of the misfolded or altered protein (Swatek et al., 2019) as a stress tolerance mechanism.

3.4.6 HM-tolerance through domain interaction with metal ions

Further bioinformatics analysis on RING-ZFP (possess intra- and extra-cellular domains) has already revealed research findings on extracellular domain binding (negatively charged) of RING-ZFP to the positively charged extracellular harmful metal ions suggesting a sensor-like activity of ZFP upon HM accumulation. Additionally, the intracellular domain of RING-ZFP interacts with and promotes ROS-mediated ABA signalling (Suh et al., 2016).

3.4.7 HM-tolerance through GSH-dependent pathway and chelation-based vacuolar sequestration

A GSH-dependent pathway and phytochelatin (polymerized GSH encoded by PCS)-conjugated vacuolar sequestration are two established mechanisms contributing to

TABLE 1 The effect of different Zinc finger protein in mitigating various abiotic stresses.

Stress	Crops	Mechanism involved	Effect	Reference
Heavy Metal	*Arabidopsis thaliana*	MAPKKK	Alterations in Auxin Homeostasis	Kovtun et al. (2000)
	Arabidopsis thaliana	PIN	Auxin transport	Tognetti et al. (2010)
	Oryza sativa	MAPK	Decreased ROS induced root cell death	Tsai and Huang (2006)
	Oryza sativa	GSH and Sodium nitropruside	By product S nitrosoglutathione generates bioactive NO	Mostofa et al. (2015)
	Medicago sativa	MAPKs	Cellular Signal induction	Jonak et al. (2004)
	Gossypium hirsutum	Reduced Glutathione (GSH)	Multivesicular body formation induced, structural integrity of cellular components	Khan et al. (2020)
Drought	*Oryza sativa*	OsC3H47, OsTZF1, OsTZF2	Involves in ABA and JA Production modulation	Han et al. (2021)
	Oryza sativa	OsC3H10	Enhances expression of LEAs, GLPs and PR protein	Seong et al. (2020)
	Glycine soja	GsZFP, a new cis2/His2 type Zinc finger protein	Plant development and stress response	Luo et al. (2012)
	Arabidopsis thaliana	AetTZF1	Enhances expression of CBF1, CBF2, DREB2A, COR47	Jiang et al. (2014)
	Malus domestica	MdZAT10	Negative regulator of Drought resistance	Yang et al. (2021)
	Malus domestica	MdDof54	Development and stress response	Chen et al. (2020)
Salinity	*Festuca arundinacea*	FaZNF	Regulation of Salt stress response pathway	Martin et al. (2012)
	Arabidopsis thaliana	ZAt7	Senescence and defense	Ciftci-Yilmaz et al. (2007)
	Chrysanthemum sp	CgZFP1	Osmotic adjustment, ROS scavenging, and ion homeostasis	Gao et al. (2012)
	Arabidopsis thaliana	ZPT2	Transcriptional repressor	Sakamoto et al. (2004)
	Ipomea batatus	IbZFP	Growth, developemnt and homeostasis	Wang et al. (2016)
Cold	*Petunia hybrida*	PhZFP1	Modulation of galactinol synthase	Zhang et al. (2022)
	Gossipium hirsutum	GhZAT	Transcription regulator	Fan et al. (2021)
	Panicum virgatum	PvC3H72	Transcriptional Activator factor	Xie et al. (2019)
	Arabidopsis thaliana	GmZF1	Modulates cold responsive genes	Yu et al. (2014)
	Nicotiana tabacum	OSISAP1	Stress response inducer	Mukhopadhyay et al. (2004)

HM-tolerance (Flores-Cáceres et al., 2015; Hernández et al., 2015; Jozefczak et al., 2015). Cd-tolerant Arabidopsis phenotypes resulted from ZAT6 over-expression, when undergoing BSO (an irreversible inhibitor of GSH biosynthesis; γ-glutamylcysteine synthetase; Reliene and Schiestl (2006) treatment, completely loses its HM-tolerance ability which implies that the ZAT6-mediated enhanced Cd tolerance is GSH-dependent (Chen et al., 2016). Furthermore, Chen and his co-workers have also found GSH1 (encoding γ-glutamylcysteine synthetase) as the transcriptional target of ZAT6 through qRT-PCR (outcome: positive regulation of GSH1 by ZAT6) and transient expression analysis (outcome: activation of GSH1 promoter activity by ZAT6). Putting together, it is clear that GSH1 which regulates HM tolerance in Arabidopsis is under transcriptional control of ZAT6, a ZF-TF. Phytochelatin synthesis was found to be under ZAT6 (acts as TF for gene encoding PCS1 and PCS2) transcriptional regulation too under HM-stress (Chen et al., 2016). Phytochelatin synthesis additionally augments the effect of GSH towards Cd-tolerance by accumulating Cd followed by phytochelatin-conjugated vacuolar sequestration (Wawrzynski et al., 2006; Lin and Aarts, 2012). Saad et al. (2018) demonstrated that LmSAP overexpression in tobacco seedlings enhanced the expression of several genes encoding metallothionein proteins (thiol group of cysteine amino acid residue binds with metal ions and/or ROS, (Yuan et al., 2008; Hassinen et al., 2009).

3.4.8 HM-tolerance findings through QTL analysis

Out of twenty-three sequences of sorghum gene homologs identified by BLASTP searches of the Xtxp270-*QTL* genomic region on chromosome 10, two gene homologs encoding ZFPs

(SbZFP17 and SbZFP346) were found to be up-regulated under HM stress (Abou-Elwafa et al., 2019). Another HM-tolerance study on Arabidopsis reported decreased HM-tolerance upon mutation in the gene encoding a ZFP (ZAT6) (Chen et al., 2016).

3.5 Radiation/high light stress

Over-expression of a gene encoding an HM (Si) transporter in rice was found to promote strong cell membrane structure and activate regulators (ZF protein *viz*. Lsd1 and dof, protein kinase domain) of the UV-B tolerance signal transduction pathway (Fang et al., 2011), suggesting the possible involvement of zinc finger motif in irradiance-induced signalling.

The B-box (BBX) proteins are a family of zinc finger TFs containing one or two BBX motifs, which has already elucidated its role in PPI (Gangappa and Botto, 2014; Zhang et al., 2017). Fang et al. (2019) monitored the transcript levels of eight BBX genes in the apple, which were significantly induced by UV-B radiation. Further, MdBBX20 overexpression in apple callus promoted the expression of structural genes encoding anthocyanin pigments and their subsequent accumulation under UV-B radiation, possibly by its transcriptional coactivator role (promoter modulation of several proteins) that coordinates with MdHY5 (Fang et al., 2019). In fact, the direct relationship between the expression profile of rhl41 (encode for a ZFP) and collective accumulation of anthocyanin and chlorophyll under UV irradiation suggests the disguised role of zinc finger in photo-protection and increased level of photosynthetic efficiency (both are evolved as strategies of light and radiation tolerance in plants) respectively (Iida et al., 2000).

Exposure of plants to light intensities that exceed the electron utilization capacity of the chloroplastic photosystem (PS) and light-harvesting complex (LHC) dramatically impacts nuclear gene expression. In this regard, the interaction and genetically association (binding component unknown to date) between GATA-type zinc finger-TF (ZML) and CryR1 (cryptochrome involved in growth and regulation) induce the formation of ZML heterodimer regulating the expression of photo-protective genes (Shaikhali et al., 2012).

Protective role (as a shield of LHC of PS-I, II and as an antioxidant; quenching of excited electrons during an imbalanced state of excitation transfer at the LHC) of flavonoid (anthocyanin) class of metabolites are very prominent under light and irradiance stress (Hughes et al., 2014; Tattini et al., 2014). HY5 (a type of Leucine zipper TF) positively regulates light-responsive gene expression (Nawkar et al., 2017) through interaction (*via* phytochrome interacting factor) with BBX-ZFP resulting in anthocyanin accumulation under light and/or radiation stress (Wei et al., 2016; Zhang et al., 2017). MdBBX20 responds to UV-B signaling and forms an active heterodimer with HY5 (one of the key regulatory factors for UV-B response; facilitating the transcriptional activity of HY5 (An et al., 2019; Fang et al., 2019).

Modulation in antenna size of LHC is another approach adopted by the plant to tolerate incoming high light and radiation stress (Rossel et al., 2002; Kimura et al., 2003; Mittler et al., 2004). Genetic alteration of ZAT10 (ZF-TF) has a modulatory impact on high light-induced transcriptome (Rossel et al., 2002) whose products are targeted to chloroplast suggesting the involvement of ZF-TF (zinc finger motif) in plants' manipulation of chloroplastic apparatus.

3.6 Elevated CO_2 stress

The experiment setup (95% CO_2+1% O_2 treatment; Artificial high-CO_2 atmosphere) designed by Jamil et al. (2019) reported abundant levels of C_2H_2-type ZFP (DkZF1-5) transcripts. Even though there are no direct *in-vivo* reports on ZF-motif-mediated stress tolerance under the influence of elevated CO_2 to date but still, the existing elucidated protein-protein interactions among the expressed product of DkZF1-5 transcripts might have some synergistic regulatory role under CO_2 stress. Notably, comparative transcriptome analysis had already unveiled up-regulation in stress-related TFs (WRKY; domain containing C2HC ZF motif) (Rushton et al., 2010) in immature California grapes under CO_2 gaseous treatment (Rosales et al., 2016; Romero et al., 2019). ABA phytohormone maintenance (balance between anabolism and catabolism) and their optimal levels are influenced by elevated CO_2 (linear relationship between CO_2 concentration and ABA synthesis) (Seo et al., 2000; Iuchi et al., 2001; Xiong et al., 2001; Xiong et al., 2002; Xiong and Zhu, 2003; Zou et al., 2007). Both of the above concepts indicate the possible involvement of WRKY with ABA-inducible and -repressible genes (under the influence of HVA22 promoter; Zou et al. (2004) under elevated CO_2 suggesting ABA-mediated stomatal response to CO_2 stress in plants. The present interpretation and previously made elucidations suggest the involvement of WRKY-TF as a functional node integrating stress signaling. Non-fluctuating concentrations of existing intracellular monosaccharides and disaccharides (soluble sugars like glucose and sucrose) (Katny et al., 2005; Zou et al., 2007)and increased accumulation of storage polysaccharides (starch) (Poorter et al., 1997) under elevated CO_2 remain a mystery which can be taken up as future research to establish the link between ABA-signaling and intracellular starch proportion of the cell under elevated CO_2 situation.

4 Conclusion

From the discussion of the current overview of the recent study, it can be concluded that abiotic stresses, particularly drought, high salinity, heavy metal, photo-stress, and high and low temperatures, are the major hindrances that limit crop productivity. After overviewing various earlier studies, the current study revealed that Zn-finger motifs have a significant

role in the better understanding of abiotic stress. The study also recognized that a wide range of Zn-binding motifs, termed Zn-fingers' proteins, had been identified. However, the function of stress-adaptation Zn-finger motifs is fully controlled by various genes. Speaking of abiotic stress and illustration the role of ZFP in wide range of plants, drought, salinity, temperatures etc. seems to be predominated. However, the involvements of ZFP in heavy metal stress are comparatively less than the other stresses. Moreover, the consequences of radio-nucleotides exposure to plants and the behaviour of ZFs will be an area of interest in the near future, as there is hardly any article addressing this issue. On the other hand, there is an ample scope to work on the effect of HM on the yield of crops as associated with various zinc finger protein. Another area of interest will be the documentation of the role of ZFP when plants were exposed to multiple stresses in different magnitudes. The information on the concept, importance, and mechanisms of Zn-finger motifs during abiotic stress response in plants will be helpful for the sustainability of crop production in the modern era of the changing climate.

Author contributions

Conceptualization, DM, KB, BP, SM, TS, MS, UM, MB, and AH; writing—original draft preparation, DM, UM, SS, AR, KB, BP, SM, TS, MS, MB, VB, and AH; writing—review and editing, MB, MS, VB, SM, SH, and AH; Funding, MB, VB, MS, SM, and AH; All authors have read and agreed to submit the manuscript in Front. Plant Sci.

Funding

This is a collaborative write-up to prove information on abiotic stress response in plants. This publication was supported by the Slovak University of Agriculture, Nitra, Tr. A. Hlinku 2, 949 01 Nitra, Slovak Republic, under the projects 'APVV-20-0071 and EPPN2020-OPVaI-VA-ITMS313011T813'.

Acknowledgments

We gratefully acknowledge to the funded project 'APVV-20-0071 and EPPN2020-OPVaI-VA-ITMS313011T813'.

Conflict of interest

The authors declare that the research was conducted in the absence of any commercial or financial relationships that could be construed as a potential conflict of interest.

Publisher's note

References

Abercrombie, J. M., Halfhill, M. D., Ranjan, P., Rao, M. R., Saxton, A. M., Yuan, J. S., et al. (2008). Transcriptional responses of arabidopsis thaliana plants to as (V) stress. *BMC Plant Biol.* 8, 87. doi: 10.1186/1471-2229-8-87

Abou-Elwafa, S. F., Amin, A. E. E. A. Z., and Shehzad, T. (2019). Genetic mapping and transcriptional profiling of phytoremediation and heavy metals responsive genes in sorghum. *Ecotoxicol. Environ. Safety.* 173, 366–372. doi: 10.1016/j.ecoenv.2019.02.022

Agarwal, P., Arora, R., Ray, S., Singh, A. K., Singh, V. P., Takatsuji, H., et al. (2007). Genome-wide identification of C2H2 zinc-finger gene family in rice and their phylogeny and expression analysis. *Plant Mol. Biol.* 65, 467–485. doi: 10.1007/S11103-007-9199-Y

Ahammed, G. J., Li, C. X., Li, X., Liu, A., Chen, S., and Zhou, J. (2020). Overexpression of tomato RING E3 ubiquitin ligase gene SlRING1 confers cadmium tolerance by attenuating cadmium accumulation and oxidative stress. *Physiol. Plant* 173, 449–459. doi: 10.1111/ppl.13294

Ali, F., Wang, Q., Fazal, A., Wang, L. J., Song, S., Kong, M. J., et al. (2022). The DnaJ-like zinc finger protein ORANGE promotes proline biosynthesis in drought-stressed arabidopsis seedlings. *Int. J. Mol. Sci.* 23 (7), 3907. doi: 10.3390/ijms23073907

Andreini, C., Banci, L., Bertini, I., and Rosato, A. (2006). Counting the zinc-proteins encoded in the human genome. *J. Proteome Res.* 5 (1), 196–201. doi: 10.1021/pr050361j

An, Y., Han, X., Tang, S., Xia, X., and Yin, W. (2014). Poplar GATA transcription factor PdGNC is capable of regulating chloroplast ultrastructure, photosynthesis, and vegetative growth in arabidopsis under varying nitrogen levels. *Plant Cell Tissue Organ Culture.* 119 (2), 313–327. doi: 10.1007/s11240-014-0536-y

An, J. P., Zhang, X. W., Bi, S. Q., You, C. X., Wang, X. F., and Hao, Y. J. (2019). MdbHLH93, an apple activator regulating leaf senescence, is regulated by ABA and MdBT2 in antagonistic ways. *New Phytol.* 222, 735–751. doi: 10.1111/nph.15628

Aslam, M., Fakher, B., Ashraf, M. A., Cheng, Y., Wang, B., and Qin, Y. (2022). Plant low-temperature stress: Signaling and response. *Agron.* 12 (3), 702. doi: 10.3390/agronomy12030702

Bai, H., Lin, P., Li, X., Liao, X., Wan, L., Yang, X., et al. (2021). DgC3H1, a CCCH zinc finger protein gene, confers cold tolerance in transgenic chrysanthemum. *Sci. Hortic.* 281, 109901. doi: 10.1016/j.scienta.2021.109901

Bakshi, M., and Oelmüller, R. (2014). WRKY transcription factors: Jack of many trades in plants. *Plant Signal Behav.* 9 (2), e27700. doi: 10.4161/psb.27700

Barman, D., Sathee, L., Padhan, B. K., and Watts, A. (2022). "Compatible solutes engineering to balance salt (Na+) and ROS-induced changes in potassium homeostasis". In *Response of field crops to abiotic stress: Current status and future prospects* Eds. S Choudhury and D Moulick (Boca Raton, USA: CRC Press), 139–152.

Barth, O., Vogt, S., Uhlemann, R., Zschiesche, W., and Humbeck, K. (2009). Stress induced and nuclear localized HIPP26 from arabidopsis thaliana interacts *via* its heavy metal associated domain with the drought stress related zinc finger transcription factor ATHB29. *Plant Mol. Biol.* 69 (1–2), 213–226. doi: 10.1007/s11103-008-9419-0

Basu, S., Ramegowda, V., Kumar, A., and Pereira, A. (2016). Plant adaptation to drought stress. *F1000 Res.* 5, 1554. doi: 10.12688/f1000research.7678.1

Behringer, C., and Schwechheimer, C. (2015). B-GATA transcription factors – insights into their structure, regulation, and role in plant development. *Front. Plant Sci.* 6. doi: 10.3389/fpls.2015.00090

Bhadra, P., Maitra, S., Shankar, T., Hossain, A., Praharaj, S., and Aftab, T. (2012). "Climate change impact on plants: Plant responses and adaptations," in *Plant perspectives to global climate changes*. Eds. T. Aftab and A. Roychoudhury (Elsevier Inc., Academic Press), 1–24. doi: 10.1016/B978-0-323-85665-2.00004-2

Blasiak, J., Pawlowska, E., Szczepanska, J., and Kaarniranta, K. (2019). Interplay between autophagy and the ubiquitin-proteasome system and its role in the pathogenesis of age-related macular degeneration. *Int. J. Mol. Sci.* 20, 210. doi: 10.3390/ijms20010210

Bogamuwa, S., and Jang, J. (2013). The arabidopsis tandem CCCH zinc finger proteins AtTZF4, 5 and 6 are involved in light-, abscisic acid and gibberellic acid-mediated regulation of seed germination. *Plant Cell Environ.* 36, 1507–1519. doi: 10.1111/pce.12084

Bogamuwa, S., and Jang, J. (2016). Plant tandem CCCH zinc finger proteins interact with ABA, drought, and stress response regulators in processing-bodies and stress granules. *PloS One* 11, e0151574. doi: 10.1371/journal.pone.0151574

Brayer, K. J., and Segal, D. J. (2008). Keep your fingers off my DNA: Protein-protein interactions mediated by C2H2 zinc finger domains. *Cell Biochem. Biophys.* 50, 111–131. doi: 10.1007/s12013-008-9008-5

Chai, G., Hu, R., Zhang, D., Qi, G., Zuo, R., Cao, Y., et al. (2012). Comprehensive analysis of CCCH zinc finger family in poplar (*Populus trichocarpa*). *BMC Genom.* 13, 253. doi: 10.1186/1471-2164-13-253

Chakrabarty, D., Trivedi, P. K., Misra, P., Tiwari, M., Shri, M., Shukla, D., et al. (2009). Comparative transcriptome analysis of arsenate and arsenite stresses in rice seedlings. *Chemosphere* 74 (5), 688–702. doi: 10.1016/j.chemosphere.2008.09.082

Cheng, M. N., Huang, Z. J., Hua, Q. Z., Shan, W., Kuang, J. F., Lu, W. J., et al. (2017). The WRKY transcription factor HpWRKY44 regulates CytP450-like1 expression in red pitaya fruit (*Hylocereus polyrhizus*). *Hortic. Res.* 4, 17039. doi: 10.1038/hortres.2017.39

Chen, W. F., Wei, X. B., Rety, S., Huang, L. Y., Liu, N. N., Dou, S. X., et al. (2019). Structural analysis reveals a "molecular calipers" mechanism for a LATERAL ORGAN BOUNDARIES DOMAIN transcription factor protein from wheat. *Journal of Biological Chemistry* 294 (1), 142–156.

Chen, F., Liu, H. L., Wang, K., Gao, Y. M., Wu, M., and Xiang, Y. (2020). Identification of CCCH zinc finger proteins family in moso bamboo (*Phyllostachys edulis*), and PeC3H74 confers drought tolerance to transgenic plants. *Front.Plant Sci.* 11, 579255. doi: 10.3389/fpls.2020.579255

Chen, S., Li, X., Yang, C., Yan, W., Liu, C., Tang, X., et al. (2021a). Genome-wide identification and characterization of FCS-like zinc finger (FLZ) family genes in maize (*Zea mays*) and functional analysis of ZmFLZ25 in plant abscisic acid response. *Int. J. Mol. Sci.* 22 (7), 3529. doi: 10.3390/ijms22073529

Chen, Y., Sun, A., Wang, M., Zhu, Z., and Ouwerkerk, P. B. F. (2014). Functions of the CCCH type zinc finger protein OsGZF1 in regulation of the seed storage protein GluB-1 from rice. *Plant Mol. Biol.* 84, 621–634. doi: 10.1007/s11103-013-0158-5

Chen, W. C., Wang, Q., Cao, T. J., and Lu, S. (2021b). UBC19 is a new interacting protein of ORANGE for its nuclear localization in arabidopsis thaliana. *Plant Signal Behav.* 16 (11), 1964847. doi: 10.1080/15592324.2021.1964847

Chen, J., Yang, L., Yan, X., Liu, Y., Wang, R., Fan, T., et al. (2016). Zinc-finger transcription factor ZAT6 positively regulates cadmium tolerance through the glutathione-dependent pathway in arabidopsis. *Plant Physiol.* 171, 707–719. doi: 10.1104/pp.15.01882

Chong, L., Guo, P., and Zhuand Zhu, Y. (2020). Mediator complex: A pivotal regulator of ABA signaling pathway and abiotic stress response in plants. *Int. J. Mol. Sci.* 21, 7755. doi: 10.3390/ijms21207755

Choudhury, S., Mazumder, M. K., Moulick, D., Sharma, P., Tata, S. K., Ghosh, D., et al. (2022a). Computational study of the role of secondary metabolites for mitigation of acid soil stress in cereals using dehydroascorbate and mono-dehydroascorbate reductases. *Antioxidant*. 11 (3), 458. doi: 10.3390/antiox11030458

Choudhury, S., and Moulick, D. (2022). *Response of field crops to abiotic stress: Current status and future prospects*. (Boca Raton, USA: CRC Press), 1–332 doi: 10.1201/9781003258063

Choudhury, S., Moulick, D., Ghosh, D., Soliman, M., Alkhedaide, A., Gaber, A., et al. (2022b). Drought-induced oxidative stress in pearl millet (*Cenchrus americanus* l.) at seedling stage: Survival mechanisms through alteration of morphophysiological and antioxidants activity. *Life.* 12 (8), 1171. doi: 10.3390/life12081171

Choudhury, S., Moulick, D., Mazumder, M. K., Pattnaik, B. K., Ghosh, D., Vemireddy, L. R., et al. (2022c). An *In vitro* and in silico perspective study of seed priming with zinc on the phytotoxicity and accumulation pattern of arsenic in rice seedlings. *Antioxidants* 11 (8), 1500. doi: 10.3390/antiox11081500

Choudhury, S., Moulick, D., and Mazumder, M. K. (2021a). Secondary metabolites protect against metal and metalloid stress in rice: An in silico investigation using dehydroascorbate reductase. *Acta Physiol. Plantarum.* 43 (1), 1–10. doi: 10.1007/s11738-020-03173-2

Choudhury, S., Sharma, P., Moulick, D., and Mazumder, M. K. (2021b). Unrevealing metabolomics for abiotic stress adaptation and tolerance in plants. *J.Crop Sci. Biotechnol.* 24, 5479–5493. doi: 10.1007/s12892-021-00102-8

Chowardhara, B., Borgohain, P., Saha, B., Awasthi, J. P., Moulick, D., and Panda, S. K. (2019a). Phytotoxicity of cd and zn on three popular Indian mustard varieties during germination and early seedling growth. *Biocatalysis Agric. Biotechnol.* 21, 101349. doi: 10.1016/j.bcab.2019.101349

Chowardhara, B., Borgohain, P., Saha, B., Prakash, J., Awasthi, D. M., and Panda, S. K. (2019b). Assessment of phytotoxicity of zinc on Indian mustard (*Brassica juncea*) varieties during germination and early seedling growth. *Ann. Plant Soil Res.* 21 (3), 239–244. doi: 10.1016/j.bcab.2019.101349

Ciftci-Yilmaz, S., and Mittler, R. (2008). The zinc finger network of plants. *Cell Mol. Life Sci.* 65, 1150–1160. doi: 10.1007/s00018-007-7473-4

Ciftci-Yilmaz, S., Morsy, M. R., Song, L., Coutu, A., Krizek, B. A., Lewis, M. W., et al. (2007). The EAR-motif of the Cys2/His2-type zinc finger protein Zat7 plays a key role in the defense response of arabidopsis to salinity stress. *J.Biol. Chem.* 282 (12), 9260–9268. doi: 10.1074/jbc.M611093200

Claeys, H., and Inzéand Inzé, D. (2013). The agony of choice: How plants balance growth and survival under water-limiting conditions. *Plant Physiol.* 162, 1768–1779. doi: 10.1104/pp.113.220921

Clemens, S., Aarts, M. G. M., Thomine, S., and Verbruggen, N. (2013). Plant science: the key to preventing slow cadmium poisoning. *Trend. Plant Sci.* 18, 92–99. doi: 10.1016/j.tplants.2012.08.003

Cuypers, A., Smeets, K., and Vangronsveld, J. (2009). "Heavy metal stress in plants," in *Plant stress biology: From genomics to systems biology*. Ed. H. Hirt (Weinheim: Wiley-VCH Verlag GmbH & Co. KGaA), 161–178.

Dash, G. K., Barik, M., Parida, S., Baig, M. J., Swain, P., Sahoo, S. K., et al. (2022). "Drought and high-temperature stress tolerance in field crops", in *Response of field crops to abiotic stress: Current status and future prospects*. Eds. S. Choudhury and D. Moulick. (Boca Raton, USA: CRC Press) 103-109.

Das, K., and Roychoudhury, A. (2014). Reactive oxygen species (ROS) and response of antioxidants as ROS-scavengers during environmental stress in plants. *Front. Environ. Sci.* 2, 53. doi: 10.3389/fenvs.2014.00053

Davies, M. J. (2005). The oxidative environment and protein damage. *Biochim. Biophys. Acta* 1703 (2), 93–109. doi: 10.1016/j.bbapap.2004.08.007

de Abreu-Neto, J. B., Turchetto-Zolet, A. C., de Oliveira, L. F. V., Bodanese Zanettini, M. H., and Margis Pinheiro, M. (2013). Heavy metal-associated isoprenylated plant protein (HIPP): characterization of a family of proteins exclusive to plants. *FEBS J.* 280 (7), 1604–1616. doi: 10.1111/febs.12159

De Zelicourt, A., Colcombet, J., and Hirtand Hirt, H. (2016). The role of MAPK modules and ABA during abiotic stress signaling. trends. *Plant Sci.* 21, 677–685. doi: 10.1016/j.tplants.2016.04.004

Dixit, A. R., and Dhankher, O. P. (2011). A novel stress-associated protein 'AtSAP10' from arabidopsis thaliana confers tolerance to nickel, manganese, zinc, and high temperature stress. *PloS One* 6 (6), e20921. doi: 10.1371/journal.pone.0020921

Duan, J., Zhang, M., Zhang, H., Xiong, H., Liu, P., Ali, J., et al. (2012). OsMIOX, a myo-inositol oxygenase gene, improves drought tolerance through scavenging of reactive oxygen species in rice (*Oryza sativa* l.). *Plant Sci.* 196, 143–151. doi: 10.1016/j.plantsci.2012.08.003

Fairall, L., Rhodes, D., and Klug, A. (1986). Mapping of the sites of protection on a 5 s RNA gene by the xenopus transcription factor IIIA: A model for the interaction. *J. Mol. Biol.* 192 (3), 577–591. doi: 10.1016/0022-2836(86)90278-0

Fan, Y., Zhang, Y., Rui, C., et al. (2021). Zinc finger transcription factor ZAT family genes confer multi-tolerances in gossypium hirsutum l. . *J. Cotton Res.* 4, 24. doi: 10.1186/s42397-021-00098-0

Fang, H., Dong, Y., Yue, X., Hu, J., Jiang, S., Xu, H., et al. (2019). The b-box zinc finger protein MdBBX20 integrates anthocyanin accumulation in response to ultraviolet radiation and low temperature. *Plant Cell Environ.* 42 (7), 2090–2104. doi: 10.1111/pce.13552

Fang, C. X., Wang, Q. S., Yu, Y., Li, Q. M., Zhang, H. L., Wu, X. C., et al. (2011). Suppression and overexpression of Lsi1 induce differential gene expression in rice under ultraviolet radiation. *Plant Growth Reg.* 65 (1), 1–10. doi: 10.1007/s10725-011-9569-y

Flores-Cáceres, M. L., Hattab, S., Hattab, S., Boussetta, H., Banni, M., and Hernández, L. E. (2015). Specific mechanisms of tolerance to copper and cadmium are compromised by a limited concentration of glutathione in alfalfa plants. *Plant SciPlant Sci.* 233, 165–173. doi: 10.1016/j.plantsci.2015.01.013

Gamsjaeger, R., Liew, C. K., Loughlin, F. E., Crossley, M., and Mackay, J. P. (2007). Sticky fingers: Zinc-fingers as protein-recognition motifs. *Trends Biochem. Sci.* 32, 63–70. doi: 10.1016/j.tibs.2006.12.007

Gangappa, S. N., and Botto, J. F. (2014). The BBX family of plant transcription factors. *Trends Plant Sci.* 19 (7), 460–470. doi: 10.1016/j.tplants.2014.01.010

Gao, H., Song, A., Zhu, X., Chen, F., Jiang, J., Chen, Y., et al. (2012). The heterologous expression in arabidopsis of a chrysanthemum Cys2/His2 zinc finger protein gene confers salinity and drought tolerance. *Plant.* 235 (5), 979–993. doi: 10.1007/s00425-011-1558-x

Ghosh, D., Brahmachari, K., Brestic, M., Ondrisik, P., Hossain, A., Skalicky, M., et al. (2020a). Integrated weed and nutrient management improve yield, nutrient uptake and economics of maize in the rice-maize cropping system of Eastern India. *Agron* 10 (12), 1906. doi: 10.3390/agronomy10121906

Ghosh, D., Brahmachari, K., Das, A., Hassan, M. M., Mukherjee, P. K., Sarkar, S., et al. (2021). Assessment of energy budgeting and its indicator for sustainable nutrient and weed management in a rice-Maize-Green gram cropping system. *Agron.* 11 (1), 166. doi: 10.3390/agronomy11010166

Ghosh, D., Brahmachari, K., Sarkar, S., Dinda, N. K., Das, A., and Moulick, D. (2022a). Impact of nutrient management in rice-maize-greengram cropping system and integrated weed management treatments on summer greengram productivity. *Ind. J. Weed Sci.* 54 (1), 25–30. doi: 10.5958/0974-8164.2022.00004.1

Ghosh, D., Brahmachari, K., Skalicky, M., Hossain, A., Sarkar, S., Dinda, N. K., et al. (2020b). Nutrients supplementation through organic manures influence the growth of weeds and maize productivity. *Molecules* 25 (21), 4924. doi: 10.3390/molecules25214924

Ghosh, D., Brahmachari, K., Skalický, M., Roy, D., Das, A., Sarkar, S., et al. (2022b). The combination of organic and inorganic fertilizers influence the weed growth, productivity and soil fertility of monsoon rice. *PloS One* 17 (1), e0262586. doi: 10.1371/journal.pone.0262586

Gill, S. S., and Tuteja, N. (2010). Reactive oxygen species and antioxidant machinery in abiotic stress tolerance in crop plants. *Plant Physiol. Biochem.* 48, 909–930. doi: 10.1016/j.plaphy.2010.08.016

Giri, J., Vij, S., Dansana, P. K., and Tyagi, A. K. (2011). Rice A20/AN1 zinc-finger containing stress-associated proteins (SAP1/11) and a receptor-like cytoplasmic kinase (OsRLCK253) interact *via* A20 zinc-finger and confer abiotic stress tolerance in transgenic arabidopsis plants. *New Phytol.* 191 (3), 721–732. doi: 10.1111/j.1469-8137.2011.03740.x

Guo, J., Bai, X., Dai, K., Yuan, X., Guo, P., Zhou, M., et al. (2021). Identification of GATA transcription factors in *Brachypodium distachyon* and functional characterization of BdGATA13 in drought tolerance and response to gibberellins. *Front. Plant Sci.* 11, 2386. doi: 10.3389/fpls.2021.763665

Gupta, D. K., Nicoloso, F. T., Schetinger, M. R. C., Rossato, L. V., Pereira, L. B., Castro, G. Y., et al. (2009). Antioxidant defense mechanism in hydroponically grown zea mays seedlings under moderate lead stress. *J. Hazardous Materials* 172 (1), 479–484. doi: 10.1016/j.jhazmat.2009.06.141

Gupta, P., Nutan, K. K., Singla-Pareek, S. L., and Pareek, A. (2017). Abiotic stresses cause differential regulation of alternative splice forms of GATA transcription factor in rice. *Front. Plant Sci.* 8, 1944. doi: 10.3389/fpls.2017.01944

Haider, F. U., Liqun, C., Coulter, J. A., Cheema, S. A., Wu, J., Zhang, R., et al. (2021). Cadmium toxicity in plants: Impacts and remediation strategies. *Ecotoxicol. Environ. Safety.* 211, 111887. doi: 10.1016/j.ecoenv.2020.111887

Haider, S., Raza, A., Iqbal, J., Shaukat, M., and Mahmood, T. (2022). Analyzing the regulatory role of heat shock transcription factors in plant heat stress tolerance: A brief appraisal. *Mol. Biol. Rep.* ;49 (6), 1–15. doi: 10.1007/s11033-022-07190-x

Han, G., Lu, C., Guo, J., Qiao, Z., Sui, N., Qiu, N., et al. (2020). C2H2 zinc finger proteins: Master regulators of abiotic stress responses in plants. *Front. Plant Sci.* 11, 115. doi: 10.3389/fpls.2020.00115

Han, G., Qiao, Z., Li, Y., Wang, C., and Wang, B. (2021). The roles of CCCH zinc-finger proteins in plant abiotic stress tolerance. *Int. J. Mol. Sci.* 22 (15), 8327. doi: 10.3390/ijms22158327

Han, G., Wang, M., Yuan, F., Sui, N., Song, J., and Wang, B. (2014). The CCCH zinc finger protein gene AtZFP1 improves salt resistance in arabidopsis thaliana. *Plant Mol. Biol.* 86, 237–253. doi: 10.1007/s11103-014-0226-5

Harrison, M. D., Jones, C. E., Solioz, M., and Dameron, C. T. (2000). Intracellular copper routing: the role of chaperones. *Trends Biochem. Sci.* 25, 29–32. doi: 10.1016/S0968-0004(99)01492-9

Hasanuzzaman, M., Bhuyan, M. H. M. B., Anee, T. I., Parvin, K., Nahar, K., Mahmud, J. A., et al. (2019). Regulation of ascorbate-glutathione pathway in mitigating oxidative damage in plants under abiotic stress. *Antioxidants* 8 (9), 384. doi: 10.3390/antiox8090384

Hasanuzzaman, M., Hossain, M. A., Silva, J. A., and Fujita, M. (2012). "Plant response and tolerance to abiotic oxidative stress: Antioxidant defense is a key factor," in *Crop stress and its management: Perspectives and strategies* (Singapore: Springer), 261–315.

Hassinen, V., Vallinkoski, V.-M., Issakainen, S., Tervahauta, A., Kärenlampi, S., and Servomaa, K. (2009). Correlation of foliar MT2b expression with cd and zn concentrations in hybrid aspen (*Populus tremula×tremuloides*) grown in contaminated soil. *Environ. pollut.* 157, 922–930. doi: 10.1016/j.envpol.2008.10.023

Hernandez, J. A., Jimenez, A., Mullineaux, P. M., and Sevilla, F. (2000). Tolerance of pea (Pisum sativum l.) to long term salt stress is associated with induction of antioxidant defenses. *Plant Cell Environ.* 23, 853–862. doi: 10.1046/j.1365-3040.2000.00602.x

Hernández, L. E., Sobrino-Plata, J., Montero-Palmero, M. B., Carrasco-Gil, S., Flores-Cáceres, M. L., Ortega-Villasante, C., et al. (2015). Contribution of glutathione to the control of cellular redox homeostasis under toxic metal and metalloid stress. *J. Exp. Bot.* 66, 2901–2911. doi: 10.1093/jxb/erv063

He, X., Wang, C., Wang, H., Li, L., and Wang, C. (2020). The function of MAPK cascades in response to various stresses in horticultural plants. *Front. Plant Sci.* 11, 952. doi: 10.3389/fpls.2020.00952

Hiratsu, K., Mitsuda, N., Matsui, K., and Ohme-Takagi, M. (2004). Identification of the minimal repression domain of SUPERMAN shows that the DLELRL hexapeptide is both necessary and sufficient for repression of transcription in arabidopsis. *Biochem. Biophys. Res. Commun.* 321, 172–178. doi: 10.1016/j.bbrc.2004.06.115

Hirayama, T., and Shinozaki, K. (2010). Research on plant abiotic stress responses in the post-genome era: past, present and future. *Plant J.* 61, 1041–1052. doi: 10.1111/j.1365-313X.2010.04124.x

Hossain, A., Maitra, S., Pramanick, B., Bhutia, K. L., Ahmad, Z., Moulik, D., et al. (2022). "Wild relatives of plants as sources for the development of abiotic stress tolerance in plants," in *Plant perspectives to global climate changes* (Springer, Singapore: Academic Press), 471–518. doi: 10.1016/B978-0-323-85665-2.00011-X

Hossain, A., Pramanick, B., Bhutia, K. L., Ahmad, Z., Moulick, D., Maitra, S., et al. (2021). "Emerging roles of osmoprotectant glycine betaine against salt-induced oxidative stress in plants: A major outlook of maize (Zea mays l.)," in *Frontiers in plant-soil interaction* (Springer, Singapore: Academic Press), 567–587. doi: 10.1016/B978-0-323-90943-3.00015-8

Huang, P., Ju, H., Min, J., Zhang, X., Chung, J., Cheong, H., et al. (2012). Molecular and physiological characterization of the arabidopsis thaliana oxidation-related zinc finger 2, a plasma membrane protein involved in ABA and salt stress response tThrough the ABI2-mediated signaling pathway. *Plant Cell Physiol.* 53, 193–203. doi: 10.1093/pcp/pcr162

Huang, T. L., Nguyen, Q. T. T., Fu, S. F., Lin, C. Y., Chen, Y. C., and Huang, H. J. (2012). Transcriptomic changes and signalling pathways induced by arsenic stress in rice roots. *Plant Mol. Biol.* 80 (6), 587–608. doi: 10.1007/s11103-012-9969-z

Huang, J., Sun, S. J., Xu, D. Q., Yang, X., Bao, Y. M., Wang, Z. F., et al. (2009). Increased tolerance of rice to cold, drought and oxidative stresses mediated by the overexpression of a gene that encodes the zinc finger protein ZFP245. biochem. *Biophy. Res. Commun.* 389 (3), 556–561. doi: 10.1016/j.bbrc.2009.09.032

Huang, J., Wang, M., Jiang, Y., Bao, Y., Huang, X., Sun, H., et al. (2008). Expression analysis of rice A20/AN1-type zinc finger genes and characterization of ZFP177 that contributes to temperature stress tolerance. *Gene.* 420, 135–144. doi: 10.1016/j.gene.2008.05.019

Huang, J., Yang, X., Wang, M. M., Tang, H. J., Ding, L. Y., Shen, Y., et al. (2007). A novel rice C2H2-type zinc finger protein lacking DLN-box/EAR-motif plays a role in salt tolerance. *Biochim. Biophys. Acta* 1769, 220–227. doi: 10.1016/j.bbaexp.2007.02.006

Hughes, N. M., Carpenter, K. L., Keidel, T. S., Miller, C. N., Waters, M. N., and Smith, W. K. (2014). Photosynthetic costs and benefits of abaxial versus adaxial anthocyanins in colocasia esculenta 'Mojito'. *Plant.* 240 (5), 971–981. doi: 10.1007/s00425-014-2090-6

Hwang, S. G., Kim, J. J., Lim, S. D., Park, Y. C., Moon, J. C., and Jang, C. S. (2016). Molecular dissection of *Oryza sativa* salt-induced RING finger protein 1 (OsSIRP1): possible involvement in the sensitivity response to salinity stress. *Physiol. Plant* 158 (2), 168–179. doi: 10.1111/ppl.12459

Iida, A., Kazuoka, T., Torikai, S., Kikuchi, H., and Oeda, K. (2000). A zinc finger protein RHL41 mediates the light acclimation response in arabidopsis. *Plant J.* 24, 191–203. doi: 10.1046/j.1365-313x.2000.00864.x

Iuchi, S., Kobayashi, M., Taji, T., Naramoto, M., Seki, M., Kato, T., et al. (2001). Regulation of drought tolerance by gene manipulation of 9-cis-epoxycarotenoid dioxygenase, a key enzyme in abscisic acid biosynthesis in arabidopsis. *Plant J.* 27 (4), 325–333. doi: 10.1046/j.1365-313x.2001.01096.x

Jadhav, S. S., Kumari, R., Mahtha, S. K., Purama, R. K., Lamba, V., and Yadav, G. (2022). "Metabolomics and molecular physiology perspective for drought and salinity stress tolerance. response of field crops to abiotic stress: Current status and future prospects", in *Response of field crops to abiotic stress: Current status and*

future prospects. Eds. S Choudhury and D Moulick (Boca Raton, USA: CRC Press), 153–166.

Jain, R. G., Fletcher, S. J., Manzie, N., Robinson, K. E., Li, P., Lu, E., et al. (2022b). Foliar application of clay-delivered RNA interference for whitefly control. *Nat. Plant* 8 (5), 535–548. doi: 10.1038/s41477-022-01152-8

Jain, R., Fletcher, S., and Mitter, N. (2022a). Effective RNAi-mediated control of the crop pest whitefly. *Nat. Plant* 8 (5), 461–462. doi: 10.1038/s41477-022-01160-8

Jaleel, C. A., Manivannan, P., Wahid, A., Farooq, M., Al-Juburi, H. J., and Somasundaram, R. (2009). Drought stress in plants: A review on morphological characteristics and pigments composition. *Int. J. Agric. Biol.* 11, 100–105.

Jalmi, S. K., and Sinha, A. K. (2015). ROS mediated MAPK signaling in abiotic and biotic stress-striking similarities and differences. *Front. Plant Sci. Plant Sci.* 6. doi: 10.3389/fpls.2015.00769

Jamil, W., Wu, W., Gong, H., Huang, J. W., Ahmad, M., Zhu, Q. G., et al. (2019). C2H2-type zinc finger proteins (DkZF1/2) synergistically control persimmon fruit deastringency. *Int. J. Mol. Sci.* 20 (22), 5611. doi: 10.3390/ijms20225611

Jamsheer, K. M., Sharma, M., Singh, D., Mannully, C. T., Jindal, S., Shukla, B. N., et al. (2018a). FCS-like zinc finger 6 and 10 repress SnRK1 signalling in arabidopsis. *Plant J.* 94 (2), 232–245. doi: 10.1111/tpj.13854

Jamsheer, K. M., Shukla, B. N., Jindal, S., Gopan, N., Mannully, C. T., and Laxmi, A. (2018b). The FCS-like zinc finger scaffold of the kinase SnRK1 is formed by the coordinated actions of the FLZ domain and intrinsically disordered regions. *J. Biol. Chem.* 293 (34), 13134–13150. doi: 10.1074/jbc.RA118.002073

Jang, J. (2016). Arginine-rich motif-tandem CCCH zinc finger proteins in plant stress responses and post-transcriptional regulation of gene expression. *Plant Sci.* 252, 118–124. doi: 10.1016/j.plantsci.2016.06.014

Jan, A., Maruyama, K., Todaka, D., Kidokoro, S., Abo, M., Yoshimura, E., et al. (2013). OsTZF1, a CCCH-tandem zinc finger protein, confers delayed senescence and stress tolerance in rice by regulating stress-related genes. *Plant Physiol.* 161, 1202–1216. doi: 10.1104/pp.112.205385

Jiang, A.-L., Xu, Z.-S., Zhao, G.-Y., Cui, X.-Y., Chen, M., Li, L.-C., et al (2014). Genome-wide analysis of the C3H zinc finger transcription factor family and drought responses of members in aegilops tauschii. *Plant Mol. Biol. Report* 32, 1241–1256.

Jin, Y., Liu, L., Zhang, S., He, R., Wu, Y., Chen, G., et al. (2016). Cadmium exposure to murine macrophages decreases their inflammatory responses and increases their oxidative stress. *Chemosphere.* 144, 168–175. doi: 10.1016/j.chemosphere.2015.08.084

Jin, Y., Wang, M., Fu, J., Xuan, N., Zhu, Y., Lian, Y., et al. (2007). Phylogenetic and expression analysis of ZnF-AN1 genes in plants. *Genomics.* 90 (2), 265–275. doi: 10.1016/j.ygeno.2007.03.019

Joazeiro, C. A., and Weissman, A. M. (2000). RING finger proteins: Mediators of ubiquitin ligase activity. *Cell* 102, 549–552. doi: 10.1016/s0092-8674(00)00077-5

Jonak, C., Nakagami, H., and Hirt, H. (2004). Heavy metal stress. activation of distinct mitogen-activated protein kinase pathways by copper and cadmium. *Plant Physiol.* 136 (2), 3276–3283.

Joo, H., Lim, C. W., and Lee, S. C. (2019). Roles of pepper bZIP transcription factor CaATBZ1 and its interacting partner RING-type E3 ligase CaASRF1 in modulation of ABA signalling and drought tolerance. *Plant J.* 100, 399–410. doi: 10.1111/tpj.14451

Joo, H., Lim, C. W., and Lee, S. C. (2020). The pepper RING-type E3 ligase, CaATIR1, positively regulates abscisic acid signalling and drought response by modulating the stability of CaATBZ1. *Plant Cell Environ. Cell Environ.* 43, 1911–1924. doi: 10.1111/pce.13789

Jozefczak, M., Bohler, S., Schat, H., Horemans, N., Guisez, Y., Remans, T., et al. (2015). Both the concentration and redox state of glutathione and ascorbate influence the sensitivity of arabidopsis to cadmium. *Ann. Bot.* 116, 601–612. doi: 10.1093/aob/mcv075

Kang, J. S., Singh, H., Singh, G., Kang, H., Kalra, V. P., and Kaur, J. (2017). Abiotic stress and its amelioration in cereals and pulses: A review. *Int. J. Curr. Microbiol. Appl. Sci.* 6, 1019–1045. doi: 10.20546/ijcmas.2017.603.120

Kanneganti, V., and Gupta, A. K. (2008). Overexpression of OsiSAP8, a member of stress associated protein (SAP) gene family of rice confers tolerance to salt, drought and cold stress in transgenic tobacco and rice. *Plant Mol. Biol.* 66 (5), 445–462. doi: 10.1007/s11103-007-9284-2

Kao, C. H. (2017). Mechanisms of salt tolerance in rice plants: Cell wall-related genes and expansins. *J. Taiwan Agric. Res.* 66, 87–93. doi: 10.6156/JTAR/2017.06602.01

Katny, M. A. C., Hoffmann-Thoma, G., Schrier, A. A., Fangmeier, A., Jäger, H. J., and van Bel, A. J. (2005). Increase of photosynthesis and starch in potato under elevated CO_2 is dependent on leaf age. *J. Plant Physiol.* 162 (4), 429–438. doi: 10.1016/j.jplph.2004.07.005

Kaur, H., Kaur, H., Kaur, H., and Srivastava, S. (2022). The beneficial roles of trace and ultratrace elements in plants. *Plant Growth Regul.*, 1–18. doi: 10.1007/s10725-022-00837-6

Keilin, D., and Mann, T. (1940). Carbonic anhydrase. purification and nature of the enzyme. *Biochem.J.* 34 (8-9), 1163. doi: 10.1042/bj0341163

Khan, M., Samrana, S., Zhang, Y., Malik, Z., Khan, M. D., and Zhu, S. (2020). Reduced glutathione protects subcellular compartments from Pb-induced ROS injury in leaves and roots of upland cotton (Gossypium hirsutum l.). *Front. Plant Sci.* 11. doi: 10.3389/fpls.2020.00412

Kielbowicz-Matuk, A. (2012). Involvement of plant C(2)H(2)-type zinc finger transcription factors in stress responses. *Plant Sci.* 185, 78–85. doi: 10.1016/j.plantsci.2011.11.015

Kim, J. C., Lee, S. H., Cheong, Y. H., Yoo, C. M., Lee, S. I., Chun, H. J., et al. (2001). A novel cold-inducible zinc finger protein from soybean, SCOF-1, enhances cold tolerance in transgenic plants. *Plant J.* 25, 247–259. doi: 10.1046/j.1365-313x.2001.00947.x

Kim, J. H., Lee, H. J., and Park, C. M. (2017). HOS1 acts as a key modulator of hypocotyl photo morphogenesis. *Plant Signal. Behav.* 12, e1315497. doi: 10.1080/15592324.2017.1315497

Kimura, M., Yamamoto, Y. Y., Seki, M., Sakurai, T., Sato, M., Abe, T., et al. (2003). Identification of arabidopsis genes regulated by high light stress using cDNA microarray. *Photochem. Photobiol.* 77, 226–233. doi: 10.1562/0031-8655(2003)077<0226:ioagrb>2.0.co;2

Kochańczyk, T., Drozd, A., and Krężel, A. (2015). Relationship between the architecture of zinc coordination and zinc binding affinity in proteins–insights into zinc regulation. *Metallomics* 7 (2), 244–257. doi: 10.1039/C4MT00094C

Kochańczyk, T., Nowakowski, M., Wojewska, D., Kocyła, A., Ejchart, A., Koźmiński, W., et al. (2016). Metal-coupled folding as the driving force for the extreme stability of Rad50 zinc hook dimer assembly. *Sci. Rep.* 6 (1), 1–12. doi: 10.1039/c4mt00094c

Kodaira, K., Qin, F., Tran, L. P., Maruyama, K., Kidokoro, S., Fujita, Y., et al. (2011). Arabidopsis Cys2/His2 zinc-finger proteins AZF1 and AZF2 negatively regulate abscisic acid-repressive and auxin-inducible genes under abiotic stress conditions. *Plant Physiol.* 157, 742–756. doi: 10.1104/pp.111.182683

Ko, J. H., Yang, S. H., and Han, K. H. (2006). Upregulation of an arabidopsis RING-H2 gene, XERICO, confers drought tolerance through increased abscisic acid biosynthesis. *Plant Journal: For Cell Mol. Biol.* 47 (3), 343–355. doi: 10.1111/j.1365-313X.2006.02782.x

Kovtun, Y., Chiu, W. L., Tena, G., and Sheen, J. (2000). Functional analysis of oxidative stress-activatedmitogenactivated protein kinase cascade in plants. *PANS* 97, 2940–2945. doi: 10.1073/ pnas.97.6.2940

Ku, Y. S., Sintaha, M., Cheung, M. Y., and Lam, H. M. (2018). Plant hormone signaling crosstalks between biotic and abiotic stress responses. *Int. J. Mol. Sci.* 19, 3206. doi: 10.3390/ijms19103206

Laity, J. H., Lee, B. M., and Wright, P. E. (2001). Zinc finger proteins: New insights into structural and functional diversity. *Curr. Opin. Struct. Biol.* 11, 39–46. doi: 10.1016/S0959-440X(00)00167-6

Larcher, W. (2003). *Physiological plant ecology: Ecophysiology and stress physiology of functional groups* (Berlin/Heidelberg, Germany: Springer), 345–437.

Lawrence, S. D., Blackburn, M. B., Shao, J., and Novak, N. G. (2022). The response to cabbage looper infestation in arabidopsis is altered by lowering levels of Zat18 a q-type C2H2 zinc finger protein. *J. Plant Interaction.* 17 (1), 198–205. doi: 10.1080/17429145.2021.2024285

Lee, S. J., Jung, H. J., Kang, H., and Kim, S. Y. (2012). Arabidopsis zinc finger proteins AtC3H49/AtTZF3 and AtC3H20/AtTZF2 are involved in ABA and JA responses. *Plant Cell Physiol.* 53, 673–686. doi: 10.1093/pcp/pcs023

Lima, J. M., Nath, M., Dokku, P., Raman, K., Kulkarni, K., Vishwakarma, C., et al. (2015). Physiological, anatomical and transcriptional alterations in a rice mutant leading to enhanced water stress tolerance. *AoB Plant* 7, plv023. doi: 10.1093/aobpla/plv023

Lim, C. W., Baek, W., and Lee, S. C. (2017). The pepper RING-type E3 ligase CaAIRF1 regulates ABA and drought signaling *via* CaADIP1 protein phosphatase degradation. *Plant Physiol.* 173, 2323–2339. doi: 10.1104/pp.16.01817

Lim, C. W., Baek, W., and Lee, S. C. (2018). Roles of pepper bZIP protein Ca DILZ 1 and its interacting partner RING-type E3 ligase Ca DSR 1 in modulation of drought tolerance. *Plant J.* 96, 452–467. doi: 10.1111/tpj.14046

Lim, S. D., Cho, H. Y., Park, Y. C., Ham, D. J., Lee, J. K., and Jang, C. S. (2013). The rice RING finger E3 ligase, OsHCI1, drives nuclear export of multiple substrate proteins and its heterogeneous overexpression enhances acquired thermo tolerance. *J. Exp. Bot.* 64, 2899–2914. doi: 10.1093/jxb/ert143

Lin, Y. F., and Aarts, M. G. (2012). The molecular mechanism of zinc and cadmium stress response in plants. *Cell Mol. Life Sci.* 69, 3187–3206. doi: 10.1007/s00018-012-1089-z

Lin, C. Y., and Lin, L. Y. (2018). The conserved basic residues and the charged amino acid residues at the alpha-helix of the zinc finger motif regulate the nuclear

transport activity of triple C2H2 zinc finger proteins. *PloS One* 13, e0191971. doi: 10.1371/journal.pone.0191971

Lin, P., Pomeranz, M., Jikumaru, Y., Kang, S. G., Hah, C., Fujioka, S., et al. (2011). The arabidopsis tandem zinc finger protein AtTZF1 affects ABA- and GA-mediated growth, stress and gene expression responses. *Plant J.* 65, 253–268. doi: 10.1111/j.1365-313X.2010.04419.x

Lin, L., Wu, J., Jiang, M., and Wang, Y. (2021). Plant mitogen-activated protein kinase cascades in environmental stresses. *Int. J. Mol. Sci.* 22, 1543. doi: 10.3390/ijms22041543

Lipiec, J., Doussan, C., Nosalewicz, A., and Kondracka, K. (2013). Effect of drought and heat stresses on plant growth and yield: A review. *Int. Agrophys.* 27, 463–477. doi: 10.2478/intag-2013-0017

Lippuner, V., Cyert, M., and Gasser, C. (1996). Two classes of plant cDNA clones differentially complement yeast calcineurin mutants and increase s alt tolerance of wild-type yeast. *J. Biol. Chem.* 271 (22), 12859–12866. doi: 10.1074/jbc.271.22.12859

Liu, Y., Khan, A. R., and Gan, Y. (2022). C2H2 zinc finger proteins response to abiotic stress in plants. *Int. J. Mol. Sci.* 23, 2730. doi: 10.3390/ijms23052730

Liu, X. M., Kim, K. E., Kim, K. C., Nguyen, X. C., Han, H. J., Jung, M. S., et al. (2010). Cadmium activates arabidopsis MPK3 and MPK6 *via* accumulation of reactive oxygen species. *Phytochemistry* 71 (5–6), 614–618. doi: 10.1016/j.phytochem.2010.01.005

Liu, S., Kracher, B., Ziegler, J., Birkenbihl, R. P., and Somssich, I. E. (2015). Negative regulation of ABA signaling by WRKY33 is critical for arabidopsis immunity towards botrytis cinerea 2100. *Life* 4, e07295. doi: 10.7554/eLife.07295.033

Liu, Y., Xu, C., Zhu, Y., Zhang, L., Chen, T., Zhou, F., et al. (2018). The calcium-dependent kinase OsCPK24 functions in cold stress responses in rice. *J. Integr. Plant Biol.* 60, 173–188. doi: 10.1111/jipb.12614

Li, D., Xu, X., Hu, X., Liu, Q., Wang, Z., Zhang, H., et al. (2015). Genome-wide analysis and heavy metal-induced expression profiling of the HMA gene family in *Populus trichocarpa*. *Front. Plant Sci.* 6, 1149. doi: 10.3389/fpls.2015.01149

Li, S., Zhao, B., Yuan, D., Duan, M., Qian, Q., Tang, L., et al. (2013). Rice zinc finger protein DST enhances grain production through controlling Gn1a/OsCKX2 expression. *Proceed. Natl. Acad. Sci. United States Amer.* 110 (8), 3167–3172. doi: 10.1073/pnas.1300359110

Logemann, E., Birkenbihl, R. P., Rawat, V., Schneeberger, K., Schmelzer, E., and Somssich, I. E. (2013). Functional dissection of the PROPEP2 and PROPEP3 promoters reveals the importance of WRKY factors in mediating microbe-associated molecular pattern-induced expression. *New Phytol.* 198, 1165–1177. doi: 10.1111/nph.12233

Lopes, K. L., Rodrigues, R. A., Silva, M. C., Braga, W. G., and Silva-Filho, M. C. (2018). The zinc-finger thylakoid-membrane protein FIP is involved with abiotic stress response in arabidopsis thaliana. *Front. Plant Sci.* 9, 504. doi: 10.3389/fpls.2018.00504

Luo, X., Bai, X., Zhu, D., Li, Y., Ji, W., Cai, H., et al. (2012). GsZFP1, a new Cys2/His2-type zinc-finger protein, is a positive regulator of plant tolerance to cold and drought stress. *Planta* 235 (6), 1141–1155. doi: 10.1007/s00425-011-1563-0

Lv, Q., Zhang, L., Zan, T., Li, L., and Li, X. (2020). Wheat RING E3 ubiquitin ligase TaDIS1 degrade TaSTP *via* the 26S proteasome pathway. *Plant Sci.* 296, 110494. doi: 10.1016/j.plantsci.2020.110494

Lyu, T., and Cao, J. (2018). Cys(2)/His(2) zinc-finger proteins in transcriptional regulation of flower development. *Int. J. Mol. Sci.* 19, 2589. doi: 10.3390/ijms19092589

Mainuddin, M., Bell, R. W., Gaydon, D. S., Kirby, J. M., Glover, M., Akanda, M. A. R., et al. (2019). An overview of the Ganges coastal Zone: Climate, hydrology, land use and vulnerability. *J. Ind. Soc Coast. Agric. Res.* 37 (2), 1–11.

Mainuddin, M., Maniruzzaman, M., Gaydon, D. S., Sarkar, S., Rahman, M. A., Sarangi, S. K., et al. (2020). A water and salt balance model for the polders and islands in the Ganges delta. *J. Hydrol* 587, 125008. doi: 10.1016/j.jhydrol.2020.125008

Maret, W., Albrecht Messerschmidt, W. B., and Cygler, M. (2004). *Handbook of metalloproteins* (Boca Raton, USA: CRC Press).

Maret, W., and Li, Y. (2009). Coordination dynamics of zinc in proteins. *Chem. Rev.* 109 (10), 4682–4707. doi: 10.1021/cr800556u

Martin, R. C., Glover-Cutter, K., Baldwin, J. C., and Dombrowski, J. E. (2012). Identification and characterization of a salt stress-inducible zinc finger protein from festuca arundinacea. *BMC Res. Notes* 5, 66. doi: 10.1186/1756-0500-5-66

Mateos Fernández, R., Petek, M., Gerasymenko, I., Juteršek, M., Baebler, Š., Kallam, K., et al. (2022). Insect pest management in the age of synthetic biology. *Plant Biotechnol. J.* 20 (1), 25–36. doi: 10.1111/pbi.13685

Mazumder, M. K., Moulick, D., and Choudhury, S. (2022). Iron (Fe3+)-mediated redox responses and amelioration of oxidative stress in cadmium (Cd2+) stressed mung bean seedlings: A biochemical and computational analysis. *J. Plant Biochem. Biotechnol.* 31 (1), 49–60. doi: 10.1007/s13562-021-00654-4

Miller, J., McLachlan, A. D., and Klug, A. (1985). Repetitive zinc-binding domains in the protein transcription factor IIIA from xenopus oocytes. *EMBO J.* 4 (6), 1609–1614. doi: 10.1002/j.1460-2075.1985.tb03825.x

Mishra, S., Srivastava, S., Tripathi, R. D., Govindarajan, R., Kuriakose, S. V., and Prasad, M. N. V. (2006). Phytochelatin synthesis and response of antioxidants during cadmium stress in bacopa monnieri l. *Plant Physiol. Biochem.* 44 (1), 25–37. doi: 10.1016/j.plaphy.2006.01.007

Mittler, R., Vanderauwera, S., Gollery, M., and Van Breusegem, F. (2004). Reactive oxygen gene network of plants. *Trend. Plant Sci.* 9, 490–498. doi: 10.1016/j.tplants.2004.08.009

Mostofa, M. G., Seraj, Z. I., and Fujita, M. (2015). Interactive effects of nitric oxide and glutathione in mitigating copper toxicity of rice (Oryza sativa l.) seedlings. *Plant Signaling Behav.* 10 (3), e991570. doi: 10.4161/15592324.2014.991570

Moulick, D., Chowardhara, B., and Panda, S. K. (2019). "Agroeco-toxicological aspect of arsenic (As) and cadmium (Cd) on field crops and its mitigation: current status and future prospect," in *Plant-metal interactions* (Cham: Springer), 217–246. doi: 10.1007/978-3-030-20732-8_11

Moulick, D., Ghosh, D., and Santra, S. C. (2016a). An assessment of some physicochemical properties and cooking characteristics of milled rice and associated health risk in two rice varieties of arsenic contaminated areas of West Bengal, India. *Int. J. Res. Agric. Food Sci.* 6, 44–55.

Moulick, D., Ghosh, D., and Santra, S. C. (2016b). Evaluation of effectiveness of seed priming with selenium in rice during germination under arsenic stress. *Plant Physiol. Biochem.* 109, 571–578. doi: 10.1016/j.plaphy.2016.11.004

Moulick, D., Ghosh, D., Skalicky, M., Gharde, Y., Mazumder, M. K., Choudhury, S., et al. (2022). Interrelationship among rice grain arsenic, micronutrients content and grain quality attributes: An investigation from genotype× environment perspective. *Front. Environ. Sci.* 25 (27). doi: 10.3389/fenvs.2022.857629

Moulick, D., Samanta, S., Sarkar, S., Mukherjee, A., Pattnaik, B. K., Saha, S., et al. (2021). Arsenic contamination, impact and mitigation strategies in rice agro-environment: An inclusive insight. *Sci. Total Environ.* 800, 149477. doi: 10.1016/j.scitotenv

Moulick, D., Santra, S. C., and Ghosh, D. (2017). Seed priming with Se alleviate as induced phytotoxicity during germination and seedling growth by restricting as translocation in rice (*Oryza sativa* l cv IET-4094). *Ecotoxicol Environ. Safety.* 145, 449–456. doi: 10.1016/j.ecoenv.2017.07.060

Moulick, D., Santra, S. C., and Ghosh, D. (2018a). Effect of selenium induced seed priming on arsenic accumulation in rice plant and subsequent transmission in human food chain. *Ecotoxicol Environ. Safety.* 152, 67–77. doi: 10.1016/j.ecoenv.2018.01.037

Moulick, D., Santra, S. C., and Ghosh, D. (2018b). Rice seed priming with se: a novel approach to mitigate as induced adverse consequences on growth, yield and as load in brown rice. *J. Hazardous Material.* 355, 187–196. doi: 10.1016/j.jhazmat.2018.05.017

Moulick, D., Santra, S. C., and Ghosh, D. (2018c). Seed priming with Se mitigates as-induced phytotoxicity in rice seedlings by enhancing essential micronutrient uptake and translocation and reducing as translocation. *Environ. Sci. Poll. Res.* 25 (27), 26978–26991. doi: 10.1007/s11356-018-2711-x

Moulick, D., Santra, S. C., and Ghosh, D. (2018d). "Consequences of paddy cultivation in arsenic-contaminated paddy fields of lower Indo-Gangetic plain on arsenic accumulation pattern and selected grain quality traits: A preliminary assessment", in *Mech. of Arsenic Toxic. and Tolerance in Plants*. Ed. M. Hasanuzzaman (Singapore: Springer), 49–78. doi: 10.1007/978-981-13-1292-2_3

Mueller, N. D., Gerber, J. S., Johnston, M., Ray, D. K., Ramankutty, N., and Foley, J. A. (2012). Closing yield gaps through nutrient and water management. *Nat.* 490, 254–257. doi: 10.1038/nature11420

Mukherjee, A., and Hazra, S. (2022). "Impact of elevated CO2 and O3 on field crops and adaptive strategies through agro-technology," in *Response of field crops to abiotic stress* (Boca Raton, USA: CRC Press), 177–190.

Mukhopadhyay, A., Vij, S. ,. A., and Tyagi, A. K. (2004). Overexpression of a zinc-finger protein gene from rice confers tolerance to cold, dehydration, and salt stress in transgenic tobacco. *Proceed. Natl. Acad. Sci. United States Amer* 101 (16), 6309–6314. doi: 10.1073/pnas.0401572101

Nawkar, G. M., Kang, C. H., Maibam, P., Park, J. H., Jung, Y. J., Chae, H. B., et al. (2017). HY5, a positive regulator of light signaling, negatively controls the unfolded protein response in arabidopsis. *Proc. Nat. Acad. Sci.* 21, 14(8):2084–2089. doi: 10.1073/pnas.1609844114

Nedelkoska, T. V., and Doran, P. M. (2000). Hyper accumulation of cadmium by hairy roots of thlaspi caerulescens. *Biotechnol. Bioeng.* 67, 607–615. doi: 10.1002/(SICI)1097-0290(20000305)67:5<607::AID-BIT11>3.0.CO;2-3

Nguyen, T. P., and Ho, T. B. (2012). Detecting disease genes based on semi-supervised learning and protein–protein interaction networks. *Artif. Intell. Med.* 54 (1), 63–71.

Noman, A., Aqeel, M., Khalid, N., Islam, W., Sanaullah, T., Anwar, M., et al. (2019). Zinc finger protein transcription factors: Integrated line of action for plant antimicrobial activity. *Microbial. Pathogen.* 132, 141–149. doi: 10.1016/j.micpath.2019.04.042

Nouman, W., Anwar, F., Gull, T., Newton, A., Rosa, E., and Domínguez-Perles, R. (2016). Profiling of polyphenolics, nutrients and antioxidant potential of germplasm's leaves from seven cultivars of *Moringa oleifera* lam. *Ind. Crop Prod.* 83, 166–176. doi: 10.1016/j.indcrop.2015.12.032

Nouman, W., Basra, S. M. A., Yasmeen, A., Gull, T., Hussain, S. B., Zubair, M., et al. (2014). Seed priming improves the emergence potential, growth and antioxidant system of moringa oleifera under saline conditions. *Plant Growth Regul.* 73, 267–278. doi: 10.1007/s10725-014-9887-y

Ogawa, I., Nakanishi, H., Mori, S., and Nishizawa, N. K. (2009). Time course analysis of gene regulation under cadmium stress in rice. *Plant Soil.* 325, 97. doi: 10.1007/s11104-009-0116-9

Oh, T. R., Yu, S. G., Yang, H. W., Kim, J. H., and Kim, W. T. (2020). AtKPNB1, AtKPNB1, an arabidopsis importin-b protein, is downstream of the RING E3 ubiquitin ligase AtAIRP1 in the ABA-mediated drought stress response. *Plant.* 252, 93. doi: 10.1007/s00425-020-03500-4

O'Malley, R. C., Huang, S. C., Lewsey, M. G., Bartlett, A., Nery, J. R., Galli, M., et al. (2016). Cistrome and epicistrome features shape the regulatory DNA landscape. *Cell.* 165, 1280–1292. doi: 10.1016/j.cell.2016.04.038

Opdenakker, K., Remans, T., Vangronsveld, J., and Cuypers, A. (2012). Mitogen activated protein (MAP) kinases in plant metal stress: Regulation and responses in comparison to other biotic and abiotic stresses. *Int. J.Mol. Sci.* 13, 7828–7853. doi: 10.3390/ijms13067828

Opipari, A. W., Boguski, M. S., and Dixit, V. M. (1990). The A20 cDNA induced by tumor necrosis factor alpha encodes a novel type of zinc finger protein. *J. Biol. Chem.* 265 (25), 14705–14708. doi: 10.1016/S0021-9258(18)77165-2

Osakabe, Y., Osakabe, K., Shinozaki, K., and Tran, L. S. P. (2014). Response of plants to water stress. *Front. Plant Sci.* 5. doi: 10.3389/fpls.2014.00086

Osorio, C. E. (2019). The role of orange gene in carotenoid accumulation: Manipulating chromoplasts toward a colored future. *Front. Plant Sci.* 10. doi: 10.3389/fpls.2019.01235

Parida, A. K., and Das, A. B. (2005). Salt tolerance and salinity effects on plants: A review. *Ecotoxic. Environ. Saf.* 60, 324–349. doi: 10.1016/j.ecoenv.2004.06.010

Park, Y. C., Chapagain, S., and Jang, C. S. (2018). The microtubule-associated RING finger protein 1 (OsMAR1) acts as a negative regulator for salt-stress response through the regulation of OCPI2 (*O. sativa* chymotrypsin protease inhibitor 2). *Planta* 247 (4), 875–886. doi: 10.1007/s00425-017-2834-1

Park, Y. C., Lim, S. D., Moon, J. C., and Jangand Jang, C. S. (2019). A rice really interesting new gene h 2-type e 3 ligase, OsSIRH2-14, enhances salinity tolerance *via* ubiquitin/26 s proteasome-mediated degradation of salt-related proteins. *Plant Cell Environ.* 42 (11), 3061–3076. doi: 10.1111/pce.13619

Parraga, G., Horvath, S. J., Eisen, A., Taylor, W. E., Hood, L., Young, E. T., et al. (1988). Zinc-dependent structure of a single-finger domain of yeast *ADR1*. *Science* 241 (4872), 1489–1492. doi: 10.1126/science.3047872

Pi, B., He, X., Ruan, Y., Jang, J. C., and Huang, Y. (2018). Genome-wide analysis and stress-responsive expression of CCCH zinc finger family genes in *Brassica rapa*. *BMC Plant Biol.* 18 (1), 1–15. doi: 10.1186/s12870-018-1608-7

Poorter, H., Van Berkel, Y., Baxter, R., Den Hertog, J., Dijkstra, P., Gifford, R. M., et al. (1997). The effect of elevated CO2 on the chemical composition and construction costs of leaves of 27 C3 species. *Plant Cell Environ.* 20 (4), 472–482. doi: 10.1046/j.1365-3040.1997.d01-84.x

Pradhan, S., Kant, C., Verma, S., and Bhatia, S. (2017). Genome-wide analysis of the CCCH zinc finger family identifies tissue specific andstress responsive candidates in chickpea (*Cicer arietinum* l.). *PloS One* 12, e0180469. doi: 10.1371/journal.pone.0180469

Qin, X., Huang, S., Liu, Y., Bian, M., Shi, W., Zuo, Z., et al. (2017). Overexpression of a RING finger ubiquitin ligase gene AtATRF1 enhances aluminium tolerance in arabidopsis thaliana. *J. Plant Biol.* 60, 66–74. doi: 10.1007/s12374-016-0903-9

Qu, J., Kang, S. G., Wang, W., Musier-Forsyth, K., and Jang, J. C. (2014). The arabidopsis thaliana tandem zinc finger 1 (AtTZF1) protein in RNA binding and decay. *Plant J.* 78, 452–467. doi: 10.1111/tpj.12485

Raja, V., Majeed, U., Kang, H., Andrabi, K. I., and John, R. (2017). Abiotic stress: Interplay between ROS, hormones and MAPKs. *Environ. Exp. Bot.* 137, 142–157. doi: 10.1016/j.envexpbot.2017.02.010

Reliene, R., and Schiestl, R. H. (2006). Glutathione depletion by buthionine sulfoximine induces DNA deletions in mice. *Carcinogenesis* 27 (2), 240–244. doi: 10.1093/carcin/bgi222

Rhodes, D., and Klug, A. (1986). An underlying repeat in some transcriptional control sequences corresponding to half a double helical turn of DNA. *Cell* 46 (1), 123–132. doi: 10.1016/0092-8674(86)90866-4

Riaz, M., Arif, M. S., Ashraf, M. A., Mahmood, R., Yasmeen, T., Shakoor, M. B., et al. (2019). A comprehensive review on rice responses and tolerance to salt stress. *Adv.Rice Res. Abiotic Stress. Tolerance* (Amsterdam: Elsevier), 133–158. doi: 10.1016/b978-0-12-814332-2.00007-1

Rizhsky, L., Davletova, S., Liang, H., and Mittler, R. (2004). The zinc finger protein Zat12 is required for cytosolic ascorbate peroxidase 1 expression during oxidative stress in arabidopsis. *J. Biol. Chem.* 279 (12), 11736–11743. doi: 10.1074/JBC.M313350200

Rodriguezcazorla, E., Ortunomiquel, S., Candela, H., Baileysteinitz, L. J., Yanofsky, M. F., Martinezlaborda, A., et al. (2018). Ovule identity mediated by pre-mRNA processing in arabidopsis. *PloS Genet.* 14, e1007182. doi: 10.1371/journal.pgen.1007182

Rodriguez, M. C., Petersen, M., and Mundyand Mundy, J. (2010). Mitogen-activated protein kinase signaling in plants. *Annu. Rev. Plant Biol.* 61, 621–649. doi: 10.1146/annurev-arplant-042809-112252

Romero, I., Alegria-Carrasco, E., de Pradena, A. G., Vazquez-Hernandez, M., Escribano, M. I., Merodio, C., et al. (2019). WRKY transcription factors in the response of table grapes (cv. *Autumn royal*) to high CO_2 levels and low temperature. *Postharvest Biol. Technol.* 150, 42–51. doi: 10.1016/j.postharvbio.2018.12.011

Rosales, R., Romero, I., Fernandez-Caballero, C., Escribano, M. I., Merodio, C., and Sanchez- Ballesta, M. T. (2016). Low temperature and short-term high-CO2 treatment in postharvest storage of table grapes at two maturity stages: effects on transcriptome profiling. *Front. Plant Sci.* 7, e1020. doi: 10.3389/fpls.2016.01020

Rossel, J. B., Wilson, I. W., and Pogson, B. J. (2002). Global changes in gene expression in response to high light in arabidopsis. *Plant Physiol.* 130, 1109–1120. doi: 10.1104/pp.005595

Roychoudhury, A., Paul, S., and Basu, S. (2013). Cross-talk between abscisic acid-dependent and abscisic acid-independent pathways during abiotic stress. *Plant Cell Rep.* 32, 985–1006. doi: 10.1007/s00299-013-1414-5

Roy, D., Vishwanath, P. D., Sreekanth, D., Mahawar, H., and Ghosh, D. (2022). "Salinity and osmotic stress in field crops: Effects and way out," in *Response of field crops to abiotic stress: Current status and future prospects*. Eds. S. Choudhury and D. Moulick (Boca Raton, USA: CRC Press), 123. doi: 10.1201/9781003258063-11

Rushton, P. J., Somssich, I. E., Ringler, P., and Shen, Q. J. (2010). WRKY transcription factors. *Trend. Plant Sci.* 15, 247–258. doi: 10.1016/j.tplants.2010.02.006

Saad, R. B., Hsouna, A. B., Saibi, W., Hamed, K. B., Brini, F., and Ghneim-Herrera, T. (2018). A stress-associated protein, LmSAP, from the halophyte *Lobularia maritima* provides tolerance to heavy metals in tobacco through increased ROS scavenging and metal detoxification processes. *J. Plant Physiol.* 231, 234–243. doi: 10.1016/j.jplph.2018.09.019

Sagar, L., Praharaj, S., Singh, S., Attri, M., Pramanick, B., Maitra, S., et al. (2022). Drought and heat stress tolerance in field crops: Consequences and adaptation strategies. response of field crops to abiotic stress: Current status and future prospects. In *Response of field crops to abiotic stress: Current status and future prospects*. Eds. S Choudhury and D Moulick (Boca Raton, USA: CRC Press), 91-102.

Saha, B., Chowardhara, B., Chowra, U., and Panda, C. K. (2022). Aluminum toxicity and ionic homeostasis in plants. response of field crops to abiotic stress: Current status and future prospects. In *Response of field crops to abiotic stress: Current status and future prospects*. Eds. S Choudhury and D Moulick (Boca Raton, USA: CRC Press), 79-90.

Saha, B., Chowardhara, B., Kar, S., Devi, S. S., Awasthi, J. P., Moulick, D., et al. (2019). "Advances in heavy metal-induced stress alleviation with respect to exogenous amendments in crop plants," in *Priming and pretreatment of seeds and seedlings* (Singapore: Springer), 313–332. doi: 10.1007/978-981-13-8625-1_15

Sahoo, S., Borgohain, P., Saha, B., Moulick, D., Tanti, B., and Panda, S. K. (2019). "Seed priming and seedling pre-treatment induced tolerance to drought and salt stress: recent advances," in *Priming and pretreatment of seeds and seedlings* (Singapore: Springer), pp.253–pp.263. doi: 10.1007/978-981-13-8625-1_12

Sah, S. K., Reddy, K. R., and Li, J. (2016). Abscisic acid and abiotic stress tolerance in crop plants. *Front. Plant Sci.* 7. doi: 10.3389/fpls.2016.00571

Sakamoto, H., Maruyama, K., Sakuma, Y., Meshi, T., Iwabuchi, M., Shinozaki, K., et al. (2004). Arabidopsis Cys2/His2-type zinc-finger proteins function as transcription repressors under drought, cold, and high-salinity stress conditions. *Plant Physiol.* 136, 2734–2746. doi: 10.1104/pp.104.046599

Sarkar, S., Gaydon, D. S., Brahmachari, K., Poulton, P. L., Chaki, A. K., Ray, K., et al. (2022). Testing APSIM in a complex saline coastal cropping environment. *Environ. Model. Software* 147, 105239. doi: 10.1016/j.envsoft.2021.105239

Schmitz, R. J., Hong, L., Michaels, S., and Amasino, R. M. (2005). FRIGIDA-ESSENTIAL 1 interacts genetically with FRIGIDA and FRIGIDALIKE 1 to promote the winter-annual habit of arabidopsis thaliana. *Develop.* 132, 5471–5478. doi: 10.1242/dev.02170

Seok, H., Nguyen, L. V., Park, H., Tarte, V. N., Ha, J., Lee, S., et al. (2018). Arabidopsis non-TZF gene AtC3H17 functions as a positive regulator in salt stress response. *Biochem. Biophys. Res. Commun.* 498, 954–959. doi: 10.1016/j.bbrc.2018.03.088

Seok, H. Y., Woo, D. H., Park, H. Y., Lee, S. Y., Tran, H. T., Lee, E. H., et al. (2016). AtC3H17, a non-tandem CCCH zinc finger protein, functions as a nuclear transcriptional activator and has pleiotropic effects on vegetative development, flowering and seed development in arabidopsis. *Plant Cell Physiol.* 57, 603–615. doi: 10.1093/pcp/pcw013

Seong, S. Y., Shim, J. S., Bang, S. W., and Kim, J. K. (2020). Overexpression of OsC3H10, a CCCH-zinc finger, improves drought tolerance inRice by regulating stress-related genes. *Plant.* 9, 1298. doi: 10.3390/plants9101298

Seo, M., Peeters, A. J., Koiwai, H., Oritani, T., Marion-Poll, A., Zeevaart, J. A., et al. (2000). The arabidopsis aldehyde oxidase 3 (AAO3) gene product catalyzes the final step in abscisic acid biosynthesis in leaves. *Proceed. Natl. Acad. Sci.* 97 (23), 12908–12913. doi: 10.1073/pnas.220426197

Shah, A. A., Riaz, L., Siddiqui, M. H., Nazar, R., Ahmed, S., Yasin, N. A., et al. (2022). Spermine-mediated polyamine metabolism enhances arsenic-stress tolerance in phaseolus vulgaris by expression of zinc-finger proteins related genes and modulation of mineral nutrient homeostasis and antioxidative system. *Environ. pollut.* 300, 118941. doi: 10.1016/j.envpol.2022.118941

Shaikhali, J., de Dios Barajas-Lopéz, J., Ötvös, K., Kremnev, D., Garcia, A. S., Srivastava, V., et al. (2012). The CRYPTOCHROME1-dependent response to excess light is mediated through the transcriptional activators zinc finger protein expressed in inflorescence meristem LIKE1 and ZML2 in arabidopsis. *Plant Cell.* 24 (7), 3009–3025. doi: 10.1105/tpc.112.100099

Shalmani, A., Muhammad, I., Sharif, R., Zhao, C., Ullah, U., Zhang, D., et al. (2019). Zinc finger-homeodomain genes: Evolution, functional differentiation, and expression profiling under flowering-related treatments and abiotic stresses in plants. *Evol. Bioinform.* 15, 1176934319867930. doi: 10.1177/1176934319867930

Shimberg, G. D., Michalek, J. L., Oluyadi, A. A., Rodrigues, A. V., Zucconi, B. E., Neu, H. M., et al. (2016). Cleavage and polyadenylation specificity factor 30: An RNA-binding zinc-finger protein with an unexpected 2Fe–2S cluster. *Proceed. Nation Acad. Sci.* 113 (17), 4700–4705. doi: 10.1073/pnas.1517620113

Shi, X., Wu, Y., Dai, T., Gu, Y., Wang, L., Qin, X., et al. (2018). JcZFP8, a C2H2 zinc finger protein gene from *Jatrophacurcas*, influences plant development in transgenic tobacco. *Electronic. J. Biotechnol.* 34, 76–82. doi: 10.1016/j.ejbt.2018.05.008

Singh, A., Kumar, A., Yadav, S., and Singh, I. K. (2019). Reactive oxygen species-mediated signaling during abiotic stress. *Plant Gene.* 18, 100173. doi: 10.1016/j.plgene.2019.100173

Sinha, A. K., Jaggi, M., Raghuram, B., and Tutejaand Tuteja, N. (2011). Mitogen-activated protein kinase signaling in plants under abiotic stress. *Plant Signal. Behav.* 6, 196–203. doi: 10.4161/psb.6.2.14701

Smekalova, V., Doskocilova, A., Komis, G., and Samaj, J. (2014). Crosstalk between secondary messengers, hormones and MAPK modules during abiotic stress signalling in plants. *Biotechnol. Adv.* 32, 2–11. doi: 10.1016/j.biotechadv.2013.07.009

Steinhorst, L., and Kudla, J. (2014). Signaling in cells and organisms – calcium holds the line. *Curr. Opin. Plant Biol.* 22, 14–21. doi: 10.1016/j.pbi.2014.08.003

Stohs, S. J., and Bagchi, D. (1995). Oxidative mechanisms in the toxicity of metal ions. *Free Radic. Biol. Med.* 18, 321–336. doi: 10.1016/0891-5849(94)00159-H

Stone, S. L. (2019). Role of the ubiquitin proteasome system in plant response to abiotic stress. *Int. Rev. Cell Mol. Biol.* 343, 65–110. doi: 10.1016/bs.ircmb.2018.05.012

Ströher, E., Wang, X., Roloff, N., Klein, P., Husemann, A., and Dietz, K. (2009). Redox-dependent regulation of the stress-induced zinc-finger protein SAP12 in arabidopsis thaliana. *Mol. Plant* 2 (2), 357–367. doi: 10.1093/mp/ssn084

Suh, J. Y., Kim, S. J., Oh, T. R., Cho, S. K., Yang, S. W., and Kim, W. T. (2016). Arabidopsis tóxicos en levadura 78 (AtATL78) mediates ABA-dependent ROS signaling in response to drought stress. *Biochem. Biophys. Res. Commun.* 469, 8–14. doi: 10.1016/j.bbrc.2015.11.061

Sun, T., Zhou, F., Huang, X. Q., Chen, W. C., Kong, M. J., Zhou, C. F., et al. (2019). ORANGE represses chloroplast biogenesis in etiolated arabidopsis cotyledons *via* interaction with TCP14. *Plant Cell.* 31, 2996–3014. doi: 10.1105/tpc.18.00290

Suzuki, N., Koizumi, N., and Sano, H. (2001). Screening of cadmium-responsive genes in arabidopsis thaliana: Screening of cadmium-responsive genes in arabidopsis thaliana. *Plant Cell Environ.* 24 (11), 1177–1188. doi: 10.1046/j.1365-3040.2001.00773.x

Swatek, K. N., Usher, J. L., Kueck, A. F., Gladkova, C., Mevissen, T. E., Pruneda, J. N., et al. (2019). Insights into ubiquitin chain architecture using ub-clipping. *Nat.* 572, 533–537. doi: 10.1038/s41586-019-1482-y

Takahashi, F., Kuromori, T., Sato, H., and Shinozaki, K. (2018). Regulatory gene networks in drought stress responses and resistance in plants. *Adv. Exp. Med. Biol.* 1081, 189–214. doi: 10.1007/978-981-13-1244-1_11

Tattini, M., Landi, M., Brunetti, C., Giordano, C., Remorini, D., Gould, K. S., et al. (2014). Epidermal coumaroyl anthocyanins protect sweet basil against excess light stress: Multiple consequences of light attenuation. *Physiol. Plant* 152 (3), 585–598. doi: 10.1111/ppl.12201

Thorpe, G. W., Reodica, M., Davies, M. J., Heeren, G., Jarolim, S., Pillay, B., et al. (2013). Superoxide radicals have a protective role during H_2O_2 stress. *Mol. Biol. Cell.* 24, 2876–2884. doi: 10.1091/mbc.e13-01-0052

Tian, M., Lou, L., Liu, L., Yu, F., Zhao, Q., Zhang, H., et al. (2015). The RING finger E3 ligase STRF1 is involved in membrane trafficking and modulates salt-stress response in arabidopsis thaliana. *Plant J.* 82, 81–92. doi: 10.1111/tpj.12797

Tonnang, H. E., Sokame, B. M., Abdel-Rahman, E. M., and Dubois, T. (2022). Measuring and modelling crop yield losses due to invasive insect pests under climate change. curr. opin. *Insect Sci.* 50, 100873. doi: 10.1016/j.cois.2022.100873

Tognetti, V. B., Van Aken, O., Morreel, K., Vandenbroucke, K., van de Cotte, B., De Clercq, I., et al. (2010). Perturbation of indole-3-butyric acid homeostasis by the UDPglucosyltransferase UGT74E2 modulates arabidopsis architecture and water stress tolerance. *Plant Cell* 22, 2660–2679. doi: 10.1105/tpc.109.071316

Tripathi, R. D., Tripathi, P., Dwivedi, S., Dubey, S., Chatterjee, S., Chakrabarty, D., et al. (2012). Arsenomics: Omics of arsenic metabolism in plants. *Front. Physiol.* 3. doi: 10.3389/fphys.2012.00275

Tsai, T. M., and Huang, H. J. (2006). Effects of iron excess on cell viability and mitogen-activated protein kinase activation in rice roots. *Physiol. Plant* 127, 583–592. doi: 10.1111/j.1399-3054.2006.00696.x

Ullah, A., Nadeem, F., Nawaz, A., Siddique, K. H., and Farooq, M. (2022). Heat stress effects on the reproductive physiology and yield of wheat. *J. Agron. Crop Sci.* 208 (1), 1–17. doi: 10.1111/jac.12572

Upadhyay, M. K., Majumdar, A., Srivastava, A. K., Bose, S., Suprasanna, P., and Srivastava, S. (2022). Antioxidant enzymes and transporter genes mediate arsenic stress reduction in rice (*Oryza sativa* l.) upon thiourea supplementation. *Chemosphere* 292, 133482. doi: 10.1016/j.chemosphere.2021.133482

Vaičiukynė, M., Žiauka, J., Žūkienė, R., Vertelkaitė, L., and Kuusienė, S. (2019). Abscisic acid promotes root system development in birch tissue culture: A comparison to aspen culture and conventional rooting-related growth regulators. *Physiol. Plant* 165 (1), 114–122. doi: 10.1111/ppl.12860

Vallee, B. L., and Neurath, H. (1954). Carboxypeptidase, a zinc metalloprotein. *J.Amer.Chem. Soc* 76 (19), 5006–5007. doi: 10.1021/ja01648a088

Verma, N., Giri, S. K., Singh, G., Gill, R., and Kumar, A. (2022). Epigenetic regulation of heat and cold stress responses in crop plants. *Plant Gene.* 29, 100351. doi: 10.1016/j.plgene.2022.100351

Wang, F., Tong, W., Zhu, H., Kong, W., Peng, R., Liu, Q., et al. (2016). A novel Cys2/His2 zinc finger protein gene from sweetpotato, IbZFP1, is involved in salt and drought tolerance in transgenic arabidopsis. *Planta* 243 (3), 783–797. doi: 10.1007/s00425-015-2443-9

Wang, K., Ding, Y., Cai, C., Chen, Z., and Zhu, C. (2019). The role of C2H2 zinc finger proteins in plant responses to abiotic stresses. *Physiol. Plant* 165, 690–700. doi: 10.1111/ppl.12728

Wang, B., Fang, R., Chen, F., Han, J., Liu, Y., Chen, L., et al. (2020). A novel CCCH-type zinc-finger protein SAW1 activates OsGA20ox3to regulate gibberellin homeostasis and anther development in rice. *J. Integr. Plant Biol.* 62, 1594–1606. doi: 10.1111/jipb.12924

Wang, Y., Liao, Y., Quan, C., Li, Y., Yang, S., Ma, C., et al. (2022a). C2H2-type zinc finger OsZFP15 accelerates seed germination and confers salinity and drought tolerance of rice seedling through ABA catabolism. *Environ. Expe. Bot.* 199, 104873. doi: 10.1016/j.envexpbot.2022.104873

Wang, W., Liu, B., Xu, M., Jamil, M., and Wang, G. (2015). ABA-induced CCCH tandem zinc finger protein OsC3H47 decreases ABA sensitivity and promotes drought tolerance in oryza sativa. *Biochem. Biophy. Res. Commun.* 464 (1), 33–37. doi: 10.1016/j.bbrc.2015.05.087

Wang, L., Xu, Y., Zhang, C., Ma, Q., Joo, S., Kim, S., et al. (2008). OsLIC, a novel CCCH-type zinc finger protein with transcription activation, mediates rice architecture *via* brassinosteroids signaling. *PloS One* 3, e3521. doi: 10.1371/journal.pone.0003521

Wang, D. R., Yang, K., Wang, X., and You, C. X. (2022b). A C2H2-type zinc finger transcription factor, MdZAT17, acts as a positive regulator in response to salt stress. *J. Plant Physiol.* 275, 153737. doi: 10.1016/j.jplph.2022.153737

Wawrzynski, A., Kopera, E., Wawrzynska, A., Kaminska, J., Bal, W., and Sirko, A. (2006). Effects of simultaneous expression of heterologous genes involved in phytochelatin biosynthesis on thiol content and cadmium accumulation in tobacco plants. *J. Exp. Bot.* 57, 2173–2182. doi: 10.1093/jxb/erj176

Wei, C. Q., Chien, C. W., Ai, L. F., Zhao, J., Zhang, Z., Li, K. H., et al. (2016). The arabidopsis b-box protein BZS1/BBX20 interacts with HY5 and mediates

strigolactone regulation of photo morphogenesis. *J. Genet. Genomics* 43, 555–563. doi: 10.1016/j.jgg.2016.05.007

Wu, X. C., Cao, X. Y., Chen, M., Zhang, X. K., Liu, Y. N., Xu, Z. S., et al. (2010). Isolation and expression pattern assay of a C3HC4-type RING zinc finger protein gene GmRZFP1 in *Glycine max* (L.). *J. Plant Genet. Res.* 11, 343–348.

Xie, M., Sun, J., Gong, D., and Kong, Y. (2019). The roles of arabidopsis C1-2i subclass of C2H2-type zinc-finger transcription factors. *Genes* 10, 653. doi: 10.3390/genes10090653

Xiong, L., Gong, Z., Rock, C. D., Subramanian, S., Guo, Y., Xu, W., et al. (2001). Modulation of abscisic acid signal transduction and biosynthesis by an Sm-like protein in arabidopsis. *Dev. Cell.* 1 (6), 771–781. doi: 10.1016/S1534-5807(01)00087-9

Xiong, L., Lee, H., Ishitani, M., and Zhu, J. K. (2002). Regulation of osmotic stress-responsive gene expression by thelos6/aba1 locus inarabidopsis. *J. Biol. Chem.* 277 (10), 8588–8596. doi: 10.1074/jbc.M109275200

Xiong, L., and Zhu, J. K. (2003). Regulation of abscisic acid biosynthesis. *Plant Physiol.* 133 (1), 29–36. doi: 10.1104/pp.103.025395

Xu, Z., Dong, M., Peng, X., Ku, W., Zhao, Y., and Yang, G. (2019). New insight into the molecular basis of cadmium stress responses of wild paper mulberry plant by transcriptome analysis. *Ecotoxicol. Environ. Safety.* 171, 301–312. doi: 10.1016/j.ecoenv.2018.12.084

Xu, D. Q., Huang, J., Guo, S. Q., Yang, X., Bao, Y. M., Tang, H. J., et al. (2008). Overexpression of a TFIIIA-type zinc finger protein gene ZFP252 enhances drought and salt tolerance in rice (*Oryza sativa* l.). *FEBS Lett.* 582 (7), 1037–1043. doi: 10.1016/j.febslet.2008.02.052

Xu, L., Liu, T., Xiong, X., Liu, W., Yu, Y., and Cao, J. (2020). AtC3H18L is a stop-codon read-through gene and encodes a novel non-tandem CCCH zinc-finger protein that can form cytoplasmic foci similar to mRNP granules. *Biochem. Biophys. Res. Commun.* 528, 140–145. doi: 10.1016/j.bbrc.2020.05.081

Xu, X., Li, W., Yang, S., Zhu, X., Sun, H., Li, F., et al. (2022). Identification, evolution, expression and protein interaction analysis of genes encoding b-box zinc-finger proteins in maize. *J. Integr. Agric.* 8, 91. doi: 10.1016/j.jia.2022.08.091

Yaghoubian, I., Ghassemi, S., Nazari, M., Raei, Y., and Smith, D. L. (2021). Response of physiological traits, antioxidant enzymes and nutrient uptake of soybean to azotobacter chroococcum and zinc sulfate under salinity. *South Afr. J. Bot.* 143, 42–51. doi: 10.1016/j.sajb.2021.07.037

Yang, Y., Ma, C., Xu, Y., Wei, Q., Imtiaz, M., Lan, H., et al. (2014). A zinc finger protein regulates flowering time and abiotic stress tolerance in chrysanthemum by modulating gibberellin biosynthesis. *Plant Cell* 26 (5), 2038–2054.

Yang, Z., and Chuand Chu, C. (2011). "Towards understanding plant response to heavy metal stress," in *Abiotic stress in plants - mechanisms and adaptations* (InTech.), 59–78. doi: 10.5772/24204

Yang, K., Li, C. Y., An, J. P., Wang, D. R., Wang, X., Wang, C. K., et al. (2021). The C2H2-type zinc finger transcription factor MdZAT10 negatively regulates drought tolerance in apple. *Plant Physiol. Biochem.* 167, 390–399. doi: 10.1016/j.plaphy.2021.08.014

Yan, Z., Shi, H., Liu, Y., Jing, M., and Han, Y. (2020). KHZ1 and KHZ2, novel members of the autonomous pathway, repress the splicing efficiency of FLC pre-mRNA in arabidopsis. *J. Exp. Bot.* 71 (4), 1375–1386. doi: 10.1093/jxb/erz499

Yin, K., Lv, M., Wang, Q., Wu, Y., Liao, C., Zhang, W., et al. (2016). Simultaneous bioremediation and biodetectionbio-detection of mercury ion through surface display of carboxylesterase E2 from pseudomonas aeruginosa PA1. *Water Res.* 103, 383–390. doi: 10.1016/j.watres.2016.07.053

Yin, J., Wang, L., Zhao, J., Li, Y., Huang, R., Jiang, X., et al. (2020). Genome-wide characterization of the C2H2 zinc-finger genes in *Cucumis sativus* and functional analyses of four CsZFPs in response to stresses. *BMC Plant Biol.* 20 (1), 1–22. doi: 10.1186/s12870-020-02575-1

Yu, G.-H., Jiang, L.-L., Ma, X.-F., Xu, Z.-S., Liu, M.-M., Shan, S.-G., et al. (2014). A soybean C2H2-type zinc finger gene GmZF1 enhanced cold tolerance in transgenic arabidopsis. *PloS One* 9 (10), e109399. doi: 10.1371/journal.pone.0109399

Yuan, J., Chen, D., Ren, Y., Zhang, X., and Zhao, J. (2008). Characteristic and expression analysis of ACCEPTED MANUSCRIPT a metallothionein gene, OsMT2b, down-regulated by cytokinin suggests functions in root development and seed embryo germination of rice. *Plant Physiol.* 146, 1637–1650. doi: 10.1104/pp.107.110304

Yuan, S., Li, X., Li, R., Wang, L., Zhang, C., Chen, L., et al. (2018). Genome-wide identification and classification of soybean C2H2 zinc finger proteins and their expression analysis in legume-rhizobium symbiosis. *Front. Microbiol.* 9, 126. doi: 10.3389/fmicb.2018.00126

Yuce, K., and Ozkan, A. I. (2020). "Cys2His2 zinc finger proteins boost survival ability of plants against stress conditions," in *Plant stress physiology* (London: Intech Open). doi: 10.5772/intechopen.92590

Yu, L. X., Shen, X., and Setter, T. (2015). L. molecular and functional characterization of two drought-induced zinc finger proteins, ZmZnF1 and ZmZnF2 from maize kernels. *Environ. Expe. Bot.* 111, 13–20. doi: 10.1016/j.envexpbot.2014.10.004

Zang, D., Li, H., Xu, H., Zhang, W., Zhang, Y., Shi, X., et al. (2016). An arabidopsis zinc finger protein increases abiotic stress tolerance by regulating sodium and potassium homeostasis, reactive oxygen species scavenging and osmotic potential. *Front. Plant Sci.* 7. doi: 10.3389/fpls.2016.01272

Zeng, D.-E., Hou, P., Xiao, F., and Liu, Y. (2015). Overexpression of arabidopsis XERICO gene confers enhanced drought and salt stress tolerance in rice (Oryza sativa l.). *J. Plant Biochem. Biotechnol.* 24 (1), 56–64. doi: 10.1007/s13562-013-0236-4

Zhang, C., Hou, Y., Hao, Q., Chen, H., Chen, L., Yuan, S., et al. (2015). Genome-wide survey of the soybean GATA transcription factor gene family and expression analysis under low nitrogen stress. *PloS One* 10, e0125174. doi: 10.1371/journal.pone.0125174

Zhang, Y., Lan, H., Shao, Q., Wang, R., Chen, H., Tang, H., et al. (2016). An A20/AN1-type zinc finger protein modulates gibberellins and abscisic acid contents and increases sensitivity to abiotic stress in rice (Oryza sativa). *J. Exp. Bot.* 67 (1, January), 315–326. doi: 10.1093/jxb/erv464

Zhang, X., Shang, F., Huai, J., Xu, G., Tang, W., Jing, Y., et al. (2017). A PIF1/PIF3-HY5-BBX23 transcription factor cascade affects photo morphogenesis. *Plant Physiol.* 174 (4), 2487–2500. doi: 10.1104/pp.17.00418

Zhang, T., Wang, X., Lu, Y., Cai, X., Ye, Z., and Zhang, J. (2014). Genome-wide analysis of the cyclin gene family in tomato. *Int. J. Mol. Sci.* 15 (1), 120–140. doi: 10.3390/ijms15010120

Zhang, D., Xu, Z., Cao, S., Chen, K., Li, S., Liu, X., et al. (2018). An uncanonical CCCH-tandem zinc-finger protein represses secondary wall synthesis and controls mechanical strength in rice. *Mol. Plant* 11, 163–174. doi: 10.1016/j.molp.2017.11.004

Zhang, W., Yin, K., Li, B., and Chen, L. (2013). A glutathione s-transferase from Proteus mirabilis involved in heavy metal resistance and its potential application in removal of Hg2+. *J. Hazard Mater.* 261, 646–652. doi: 10.1016/j.jhazmat.2013.08.023

Zhang, H., Sun, Z., Feng, S., Zhang, J., Zhang, F., Wang, W., et al. (2022). The C2H2-type zinc finger protein PhZFP1 regulates cold stress tolerance by modulating galactinol synthesis in petunia hybrida. *J. Exp. Bot.* 73 (18), 6434–6448. doi: 10.1093/jxb/erac274

Zou, X., Seemann, J. R., Neuman, D., and Shen, Q. J. (2004). A WRKY gene from creosote bush encodes an activator of the abscisic acid signaling pathway. *J. Biol. Chem.* 279 (53), 55770–55779. doi: 10.1074/jbc.M408536200

Zou, X., Shen, Q. J., and Neuman, D. (2007). An ABA inducible WRKY gene integrates responses of creosote bush (*Larrea tridentata*) to elevated CO2 and abiotic stresses. *Plant Sci.* 172, 997–1004. doi: 10.1016/j.plantsci.2007.02.003

frontiers | Frontiers in Plant Science

TYPE Original Research
PUBLISHED 10 January 2023
DOI 10.3389/fpls.2022.1092411

OPEN ACCESS

EDITED BY
Poonam Yadav,
Banaras Hindu University, India

REVIEWED BY
Arnab Majumdar,
Jadavpur University, India
Atsushi Fukushima,
Kyoto Prefectural University, Japan
Bedabrata Saha,
Agricultural Research Organization (ARO), Israel

*CORRESPONDENCE
Yu Wu
hhyyw20030105@126.com

SPECIALTY SECTION
This article was submitted to Plant Abiotic Stress, a section of the journal Frontiers in Plant Science

RECEIVED 08 November 2022
ACCEPTED 21 December 2022
PUBLISHED 10 January 2023

CITATION
Mao C, Li L, Yang T, Gui M, Li X, Zhang F, Zhao Q and Wu Y (2023) Transcriptomics integrated with widely targeted metabolomics reveals the cold resistance mechanism in *Hevea brasiliensis*. *Front. Plant Sci.* 13:1092411. doi: 10.3389/fpls.2022.1092411

Transcriptomics integrated with widely targeted metabolomics reveals the cold resistance mechanism in *Hevea brasiliensis*

Changli Mao, Ling Li, Tian Yang, Mingchun Gui, Xiaoqin Li, Fengliang Zhang, Qi Zhao and Yu Wu*

The Center of Molecular Biology, Yunnan Institute of Tropical Crops, Xishuangbanna, China

The rubber tree is the primary source of natural rubber and is mainly cultivated in Southeast Asian countries. Low temperature is the major abiotic stress affecting the yield of the rubber tree. Therefore, uncovering the cold resistance mechanism in the rubber tree is necessary. The present study used RNA-sequencing technology and ultra-performance liquid chromatography-tandem mass spectrometry (UPLC-MS/MS) to analyze the transcriptomic and metabolomic changes in two rubber tree clones with different cold resistance capacities (temperature-sensitive Reyan 8-79 and cold-resistant Yunyan 77-4) at 0 h, 2 h, 6 h, and 20 h of exposure to 4°C. Independent analysis of the transcriptome and metabolitome showed that under prolonged low-temperature treatment, Yunyan 77-4 expressed more genes involved in regulating enzyme activity, changing cell permeability, and synthesizing significant metabolites, such as flavonoids and amino acids, than Reyan 8-79. The KEGG annotation and enrichment analysis identified arginine metabolism and biosynthesis of flavonoids as the major pathway associated with cold resistance. Integrated transcriptome and metabolome analysis showed that the increase in the expression of genes modulated flavonoid biosynthesis, arginine biosynthesis, and anthocyanins biosynthesis, resulting in higher levels of metabolites, such as naringenin chalcone, apigenin, dihydroquercetin, cyanidin 3-glucoside, L-arginosuccinate, N-acetyl-ornithine, ornithine, and N-acetyl-glutamate, in Yunyan 77-4 than in Reyan 8-79 after prolonged low-temperature treatment. Phylogenetic analysis identified the genes, such as CHS (*gene356*) and F3H (*gene33147*) of flavonoid biosynthesis and NAGS (*gene16028, gene33765*), ArgC (*gene2487*), and ASS (*gene6161*) of arginine biosynthesis were the key genes involved in the cold resistant of rubber tree. Thus, the present study provides novel insights into how rubber clones resist cold and is a valuable reference for cold-resistance breeding.

KEYWORDS

multi-omics analysis, transcriptomics, metabolomics, cold-resistance, rubber tree

Introduction

The rubber tree (*Hevea brasiliensis* Muell. Arg. 2n = 36), a typical tropical tree from the Amazon Basin, is the primary source of natural rubber. It is mainly grown in the warm, humid rain forests within 0–5°C latitude near the equator and is well adapted to the humid tropics between 10°C south and 10°C north of the equator (Vinod et al., 2010). Natural rubber obtained from *H. brasiliensis* has strong elasticity and toughness and is used to make products such as shoes, tires, and medical equipment (Gronover et al., 2011; Priyadarshan, 2011). During the late 1970s, rubber trees were planted in the Southeast Asian non-traditional rubber planting areas of, such as northeast India, the highlands, and coastal regions of Vietnam and southern China (2009; Raj et al., 2005).

In non-traditional rubber planting areas, abiotic stresses affect the growth and production of rubber. Among the various abiotic stresses, low temperature is a key limiting factor for *Hevea*, a temperature-sensitive plant. Typically, a rubber tree that faces one or more cold advection for more than 20 days in winter suffers cold damage characterized by leaf fall, dead branches, and bark blasting (Wang et al., 2012; Chen et al., 2013a). Subsequently, the tree will undergo a series of physiological and biochemical dysfunctions, such as changes in the cell structure, protoplasm colloidal properties, water status, cell osmotic pressure, photosynthesis, respiration, substance metabolism, and protective enzymes (Lin and Yang, 1994; Mai et al., 2009; Wang, 2010; Wang et al., 2012; Tian et al., 2016). Moreover, research has proven that temperatures below 15°C significantly delay seed germination and decrease the germination rate of rubber (Yan and Cao, 2009). At temperatures below 5°C, rubber tree displays branch and stem exsiccation, which affects plant growth (Mo et al., 2009). Thus, low temperatures reduce rubber yield by 8% to 40%, depending on clones (Roy et al., 2003).

Several abiotic factors, such as low/high temperatures, drought, and salinity, limit plant productivity. These abiotic stresses, especially chilling,affect model transduction, transcriptional processing, translation, and post-translational protein modification, resulting in different metabolites (Rodríguez et al., 2005; Zhang et al., 2022a). Researchers have elucidated the regulatory network of many species under cold stress (Sonna et al., 2002; Shinozaki et al., 2003). Currently, the CBF (C-repeat binding factor) genetic network, known to regulate cold acclimation of *Arabidopsis thaliana*, is one of the well-established pathways associated with cold stress response (Cook et al., 2004). CBFs, the cryogenic signaling transcription factors, interact with the phytochrome-interacting transcription factor PIF3, stabilize the red light and temperature receptor phyB and finally enhance freezing resistance (Jiang et al., 2020). Studies based on the transcriptome, metabolome, and proteome analyses have identified numerous cold-responsive genes from *Momordica charantia* (Niu et al., 2020), *Oryza sativa* (Chen et al., 2003; Maruyama et al., 2014; Pan et al., 2020), *Prunus mume* (Zhuo et al., 2018), and various other species (Rezaie et al., 2020; Bu et al., 2021; Li et al., 2022a; Wang et al., 2022). Moreover, research has found significant enrichment of genes involved in phosphorylation, membrane and protein kinase activity, photosynthesis, photoreception, photoreaction, and beta-trehalose-phosphate synthase in Lanzhou lily (*Lilium davidii*) under cold stress (Tian et al., 2020). Recent studies based on multi-omics revealed the cold resistance mechanism of *Triticum aestivum* (Lu et al., 2020), *Cinnamomum cassia* (Li et al., 2021), *Cryptomeria fortunei* (Zhang et al., 2022b), and various other species (Zhao et al., 2019; Xu et al., 2020), providing a deeper understanding of the genetic response of plants under low-temperature stress.

Most of these earlier studies on low-temperature stress response focused on species with robust tolerance. Only a few studies have been carried out on tropical plants, such as the rubber tree. Recently, a few cold-resistance genes, *HbCBF2* and *HbICEs*, were cloned from the rubber tree, and the expression levels of *HbICEs* were found to be significantly higher in cold-resistant rubber clones than in cold-sensitive ones (Cai et al., 2008; Quan et al., 2017; Li et al., 2022b). With the rapid development of sequencing technology and the completion of whole-genome sequencing, transcriptomics has been used to analyze the cold resistance mechanism of the rubber tree. Transcriptome analysis identified numerous regulators of the cold stress response in rubber tree, including M-type MADS, MYB (v-myb avian myeloblastosis viral oncogene homolog), MYB-related, and NAC (NAM, ATAF1/ATAF2, and CUC2) (Gong et al., 2018). Meanwhile, a comparative analysis of the transcriptome of two clones with different cold resistance capacities revealed that phytohormone signaling, heat shock modules, and reactive oxygen species (ROS) scavengers mediate cold tolerance in the rubber tree (Deng et al., 2018). Studies have also identified the early gene expression profile contributing to cold resistance (Cheng et al., 2018) and the differences in the response strategies among germplasms under low-temperature treatment (Mantello et al., 2019). These reports showed a rapid and intensive response at gene expression levels in the cold-resistance rubber clones than in the cold-sensitive ones. Moreover, coexpression network analysis indicated that the general reaction of rubber trees to short-term cold exposure involves downregulation of gibberellin (GA) signaling, complex regulation of jasmonic acid (JA) signaling, increase in programmed cell death (PCD), and upregulation of ethylene response factor genes (Da et al., 2021). However, most reports on rubber are based on transcriptome analysis, and studies on the metabolite differences are rare. Multi-omics approaches showed differences in gene expression and metabolite levels between tobacco cultivars with different tolerance levels (Jin et al., 2017) and proved the significance of ABA/JA signaling and proline biosynthesis in wheat's cold tolerance (Zhao et al., 2019). Although the cold resistance genes of rubber trees have been

cloned, and the cold resistance mechanism has been analyzed based on the transcriptome, the tolerance mechanism based on a multi-omics approach has not been reported.

Therefore, the present study analyzed the transcriptome and the metabolome of two *Hevea* clones with different cold resistance capacities to characterize the differential genes and metabolites associated with the cold stress response. This study, based on the integration and interpretation of transcriptome and metabolome data sets, will improve our knowledge of the metabolic changes caused by transcriptional regulation after cold stress and reveal the main regulatory genes. We believe the present study's findings will propose novel candidates for cold resistance breeding in *Hevea*.

Materials and methods

Plant materials and low-temperature treatment

The bud-grafted plants of the rubber tree clones, namely Yunyan 77-4 (Triploid, cold-resistant clone) (Li, 2005; Li et al., 2009) and Reyan 8-79 (cold-sensitive clone), were used in this study. The seedlings were cultivated in the rubber tree breeding nursery of Yunnan Institute of Tropical Crops, Yunnan, China, and the one-year-old plants were subjected to low-temperature treatment in an artificial box precooled from room temperature to 28°C and 4°C at a cooling rate of 4°C/h. The plants were exposed to continuous low-temperature treatment (4°C) for 2, 6, and 20 h under a 12 h/12 h dark/light cycle, 10,000 lx light intensity, and 75% relative humidity; plants grown at room temperature were used as the control (0 h). We collected twenty-four treatment samples (leaves), including Y0H, Y2H, Y6H, and Y20H from Yunyan 77-4 and R0H, R2H, R6H, and R20H from Reyan 8-79 at 0, 2, 6, and 20 h after exposure to cold stress, maintaining three biological replicates per treatment; Y0H and R0H were used as the control samples (28°C, 0 h). Nine seedlings per clone were treated, of which three formed a replicate. At each treatment time point, the middle leaflet was collected from the second strata, the veins were removed, and the leaves were cut into 1 cm × 1 cm pieces; these pieces were mixed and divided into three parts for RNA-Seq, metabolite analysis, and quantitative real-time polymerase chain reaction (qRT-PCR). The leaf samples were frozen in liquid nitrogen immediately after collection and stored in an ultra-low temperature (-80°C) freezer.

Transcriptome analysis

RNA extraction, quantification, and sequencing

Total RNA was extracted from the 24 samples using TRIzol reagent (Invitrogen, Carlsbad, USA) according to the manufacturer's instructions, followed by poly(A) mRNA enrichment with the oligo (dT) magnetic beads and fragmentation with the fragmentation buffer. The first-strand cDNA was synthesized from this fragmented mRNA (template) using random hexamers, followed by second-strand synthesis using dNTPs, RNase H, and DNA polymerase I. The short, double-stranded cDNA was purified with AMPure XP beads and subjected to end repair; then, an A-tail was added, and a sequencing adaptor was connected, followed by fragment size selection with AMPure XP beads. Finally, the cDNA libraries were obtained by PCR enrichment. Before sequencing, the quality of the cDNA library was assessed using Agilent 2100 Bioanalyzer (Agilent Technologies, Inc. Waldbronn, Germany), and the concentration was measured using a Qubit 2.0 fluorometer (Life Technologies, Carlsbad, CA, USA). Transcriptome sequencing was performed on an Illumina NovaSeq6000 platform (Illumina, San Diego, CA, United States). The Beijing Biomarker Biotechnology Co., Ltd (Beijing, China) performed RNA sequencing and transcriptome assembly for the 24 libraries (eight leaf samples with three replicates each).

Data analysis

The adaptor sequences, ambiguous reads with unknown nucleotides > 5%, or low-quality sequences withQ20 < 20% (percentage of sequences with sequencing error rates < 1%) were removed from the RNA-seq raw data by a perl script. The high-quality reads were mapped to the rubber tree (*Hevea brasiliensis*) genome (the assembly number: ASM1045892v1, https://www.ncbi.nlm.nih.gov/data-hub/genome/GCA_010458925.1/) using Tophat2.0.8 software under the below parameter: "read-realign-edit-dist" was set to "0", and the remaining parameters used the default values (Kim et al., 2013). Fragments per kilobase of transcript per million mapped fragments (FPKM) were used as an index to measure the gene expression levels based on the RNA-seq data. The differentially expressed genes (DEGs) between the two rubber tree clones at the three stages of cold treatment were analyzed using the DESeq2 (an online analysis tool in the OmicShare cloud platform, https://www.omicshare.com/tools/Home/Soft/diffanalysis); genes with a fold change ≥ 2 and a false discovery rate (FDR) < 0.01 were defined as differentially expressed. Here, the FDR was obtained by correcting the differential significance p-value based on the multiple hypothesis test and the Benjamini-Hochberg method. Further, gene clustering, KEGG (Kyoto Encyclopedia of Genes and Genomes) and KO (KEGG Orthology) (Kanehisa et al., 2016) functional annotation, and enrichment analysis were performed for these DEGs using the OmicShare cloud platform (https://www.omicshare.com/tools/).

Quantitative real-time polymerase chain reaction

Eight DEGs were selected for qRT-PCR validation of the RNA-seq data using three technical replicates per sample. The

qRT-PCR was performed on a LightCycler480 fluorescence quantitative PCR instrument (Rotkreuz, Switzerland) using the rubber actin gene (Primer sequence5'-3': Forward-CAAGGGTGAATACGATGAGTCTG, Reverse-GCCTCTCA CTAGCAGCCATAAC) as the internal reference. The qRT-PCR primers were designed with the Primer Premier5.0 software (Supplementary Table 1), and the relative gene expression levels were calculated following the $2^{-\Delta\Delta CT}$ method (Livak and Schmittgen, 2001).

Metabolomic analysis

Sample preparation and metabolite extraction

The leaf samples were freeze-dried in a lyophilizer (Scientz-100, Ningbo Scientz Biotechnology Co. Ltd., Ningbo, Zhejiang, China) and crushed in a blender (MM 400, Retsch) at 30 Hz for 1.5 min. Approximately 100 mg of the powder was dissolved in 1.2 mL of 70% methanol, vortexed every 30 min for 30 s, six times, and stored overnight in a refrigerator (4°C). The following day, the extract was centrifuged at 12,000 rpm for 10 min, and the supernatant was filtered through a microporous filter membrane (0.22 μm) into a sample vial. The metabolites in each sample extract were then analyzed using ultra-performance liquid chromatography-tandem mass spectrometry (UPLC-MS/MS).

Metabolite detection and qualitative and quantitative analyses

Widely targeted metabolomic analysis based on UPLC-MS/MS was performed at the Metware Biotechnology Co., Ltd. (Wuhan, Hubei, China). An AB Sciex high-resolution according to their standard procedure as follow: the widely targeted metabolomics uses high-resolution mass spectrometry AB sciex TripleTOF660 for qualitative detection of mixed samples, and then uses AB sciex4500 QTRAP for quantification, the operation parameters were as follows: ion source, turbo spray; source temperature 550°C; ion spray voltage (IS) 5500 V (positive ion mode)/-4500 V (negative ion mode); ion source gas I (GSI), gas II (GSII), curtain gas (CUR) were set at 50, 60, and 25.0 psi, respectively; the collision-activated dissociation (CAD) was high. Using multiple reaction monitoring (MRM), high-resolution mass spectrometry for accurate qualitative, triple quadrupole mass spectrometry with high sensitivity, high specificity and excellent quantitation capabilities as a complementary tool. Identification was conducted by match of mass spectrum to reference library MetWare database (MWDB) (Chen et al., 2013b) based on the accurate mass, secondary (MS2) fragments, isotope distribution, and retention time (RT). Here, both of MS tolerance and MS2 tolerance were set to 20 ppm, and the RT offset to a maximum of 0.2 minutes. A quality control (QC) sample was analyzed after every tenth test sample to ensure the reproducibility of the analysis.

Metabolite data analysis

The orthogonal partial least squares discriminant analysis (OPLS-DA) and principal component analysis (PCA) were carried out on all the samples to identify the putative biomarkers after data normalization. Finally, the metabolites with variable importance in projection (VIP) ≥ 1 and fold change ≥ 2 or ≤ 0.5 were defined as the differentially accumulated metabolites (DAMs).

Integrated analysis of metabolomic and transcriptomic data

The transcriptome and metabolome were normalized to investigate the relationship between the changes in the genes and the metabolites of rubber tree clones with different cold resistance capacities. Further, a PCA was performed on the transcriptome and metabolome to visualize the differences in the transcriptome and metabolome between the sample groups. Then, all differential genes and metabolites were simultaneously mapped to the KEGG database to identify the significant pathways associated with both DEGs and DAMs. Pearson correlation coefficients (PCC) were calculated for the DEGs and DAMs of each group, and the metabolites and genes with 0.8 ≤ PCC ≤ -0.8 were considered significantly correlated. Then, the PCC values were ranked to screen the strongly correlated genes and metabolites under different treatments and confirm the key regulatory genes and metabolites of the rubber tree clones responsible for low-temperature resistance. PCA and KEGG pathway enrichment were conducted on the Omicshare analysis cloud platform (https://www.omicshare.com/tools/). The phylogenetic analysis was performed following the maximum likelihood (ML) method in MEGA 7.0 (Felsenstein, 1978).

Results

Transcriptome analysis of rubber tree clones with different cold resistance capacities

Approximately 41.24–64.27 M 100 bp pair-end, high-quality sequences were obtained from the raw RNA-seq data after quality control (QC) (Supplementary Table 2). About 73.33% to 89.22% of the clean reads aligned to unique locations on the rubber tree reference genome and 5.31% to 13.2% to multiple locations (Supplementary Table 2). The gene expression density diagram for the rubber samples at different durations after cold exposure indicated similar trends in gene abundance and gene expression density. Moreover, the log FPKM values were concentrated in the [-2, 2] interval for all transcripts of the samples (Figure 1). The correlation heatmap (Supplementary Figure 1A) and PCA plot (Supplementary Figure 1B) showed similarities among replicates of

the same sample and apparent differences among the different cold-resistance rubber tree clones, indicating the reliability of the data.

DEGs identification and verification

A total of 7330 DEGs were identified between Reyan 8-79 and Yunyan 77-4 after 2 h, 6 h, and 20 h of exposure to cold temperature (Figure 2A); 872 DEGs were common to both clones and three treatment durations. The numbers of DEGs of the different groups are listed in Table 1. Detailed examination of the data revealed that for the Reyan 8-79 vs. Yunyan 77-4 comparisons, the downregulated genes were more than the upregulated genes at 0 h and 2 h, while the upregulated genes were more at 6 h and 20 h.

Subsequent gene ontology (GO) analysis indicated that the terms "catalytic activity" and "binding" were prominent in the "molecular function" ontology, "cell" and "cell part" in the "cellular component" ontology, and "metabolic process" and "cellular process" in the "biological process" ontology (Supplementary Figures 2A–D). The KEGG pathway enriched by the DEGs were

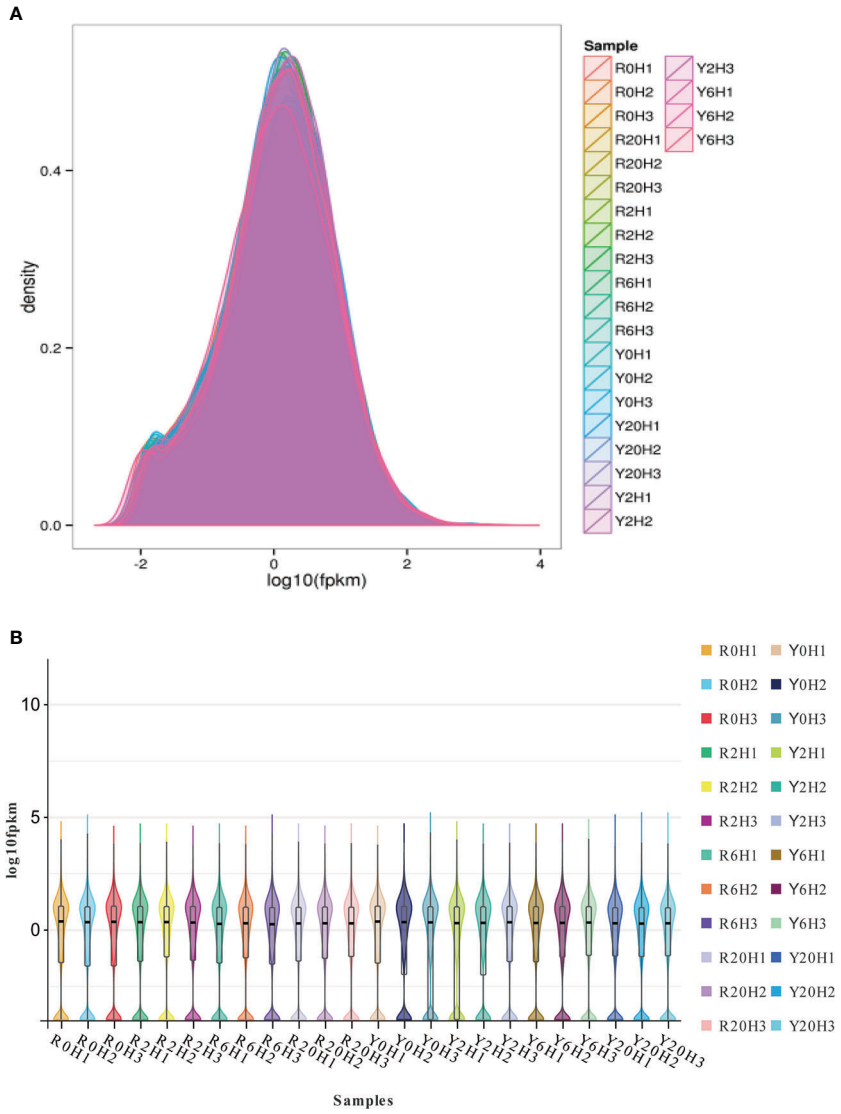

FIGURE 1
The gene expression density diagram and the violin plot for the transcripts of the rubber tree samples. **(A)** Gene expression density diagram. Comparison of FPKM density distribution. The curves in different colors represent different samples; the abscissa indicates the log value of the FPKM and the ordinate indicates the probability density. **(B)** Violin plot. The upper and lower ends of the lines represent the maximum and minimum of non-outliers; the upper and lower edges of the rectangles represent the third and first quartiles of the data; the center dot represents the median of the data.

10.3389/fpls.2022.1092411

"Plant-pathogen interaction", "Starch and sucrose metabolism", "Carbon metabolism", "Plant hormone signal transduction", and "Biosynthesis of amino acid" (Supplementary Figures 2E–H). The "Glycolysis/Gluconeogenesis" pathway was enriched at 0 h, whereas the "Biosynthesis of amino acids", "Carbon metabolism", "Glycolysis/Gluconeogenesis", and "Terpenoid backbone biosynthesis" pathways were enriched at 6 h. Meanwhile, only the " Biosynthesis of amino acids" pathway was significantly enriched at 20 h (Figures 2B–E).

Metabolites of the rubber tree clones with different cold resistance capacities

Furthermore, we performed a UPLC-MS/MS-based widely targeted metabolome analysis to identify the DAMs of the rubber tree clones under low-temperature treatment. The metabolites were qualitatively and quantitatively analyzed using MWDB and MRM, respectively. The total ions current (TIC) of the QC sample and the multimodal detection map in

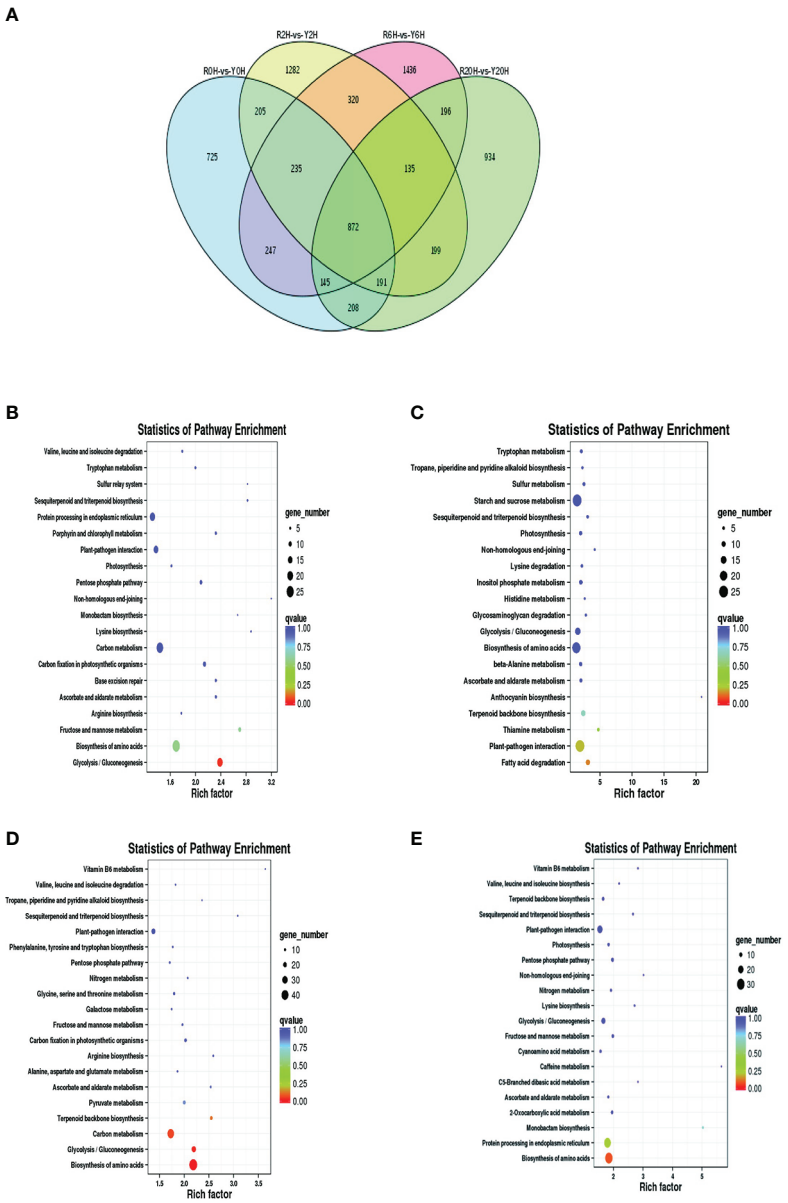

FIGURE 2
Statistics and KEGG enrichment analysis of DEGs. **(A)** Venn diagram of DEGs between Reyan 8-79 and Yunyan 77-4. KEGG enrichment of DEGs of **(B)** R0H_vs_Y0H, **(C)** R2H_vs_Y2H, **(D)** R6H_vs_Y6H, and **(E)** R20H_vs_Y20H comparisons. The horizontal coordinate indicates the Rich factor of each pathway (Rich factor was calculated as the ratio of the number of differentially expressed genes annotated in a pathway to the number of all genes annotated in this pathway), and the vertical coordinate is the pathway's name. The dot color represents the *p*-value; the redder it is, the more significant the enrichment. The size of the dots represents the number of differential metabolites enriched in the pathway.

TABLE 1 Summary of the differentially expressed genes and differentially accumulated metabolites.

Group	DEGs	Upregulated DEGs	Downregulated DEGs	DAMs	Upregulated DAMs	Downregulated DAMs
R0H_vs_Y0H	2828	1440	1388	180	155	25
R2H_vs_Y2H	3439	1490	1949	127	97	30
R6H_vs_Y6H	3586	2040	1546	166	113	53
R20H_vs_Y20H	2880	1627	1253	213	176	37

MRM indicated similar RTs and peak intensities between samples, while the MS occurrence varied among the time points. Analysis of the TIC plots of the MS detection test and the various QC samples showed high overlap in the TIC metabolite detection curve (Supplementary Figures 3A, B). All the substances detected in the samples are shown on the multinodal map. The present study identified 846 metabolites from the samples, including a large proportion of "Flavonoids", "Amino acids and derivatives", "Others", and "Lipids" (Figure 3A). PCA for all samples, including the QC sample, showed large differences between groups and less variability within groups (Figure 3B). Meanwhile, the OPLS-DA showed large differences between the two clones under the same treatment period. The validation of the OPLS-DA model showed that the p-value was less than 0.005 in all groups (R0H vs. Y0H, R2H vs. Y2H, R6H vs. Y6H, and R20H vs. Y20H), indicating the reliability of the OPLS-DA model is reliable (Supplementary Figures 3C–F).

DAM identification and verification

Further, to assess the metabolic differences and group the samples, the OPLS-DA was performed. In the OPLS-DA, Q2 > 0.9 indicates an excellent predictive ability (Chung et al., 2019). The permutation tests for the OPLS-DA model yielded Q^2 and R^2X ranging from 0.818–0.936 and 0.659–0.691, respectively, with a p-value < 0.05 (Supplementary Figures 3C–F), indicating that the model fitted well and have good predictive ability, and the groups were separated well. The study identified 180 (155 upregulated and 25 downregulated), 127 (97 and 30), 166 (113 and 53), and 213 (176 and 37) DAMs from the R0H vs. Y0H, R2H vs.Y2H, R6H vs. Y6H, and R20H vs. Y20H pairwise comparisons, respectively (Table 1), based on the OPLS-DA results and the screening criteria (VIP ≥ 1; fold change ≥ 2 and ≤ 0.5) (Supplementary Table 3). Of these, 180 metabolites were common to all groups. The DAMs showed obvious differences between Yunyan 77-4 and Reyan 8-79. Interestingly, the DAMs associated with cold resistance in other species, such as glucose and putrescine, were not accumulated in the rubber tree; however, flavonoids, lipids, and amino acids exhibited huge differences between the rubber tree clones with different cold resistance capacities. Moreover, the content of flavonoids in the cold-resistant clone Yunyan 77-4 was higher than that in the cold-sensitive clone Reyan 8-79 at room temperature and 4°C; the content of amino acids in Yunyan 77-4 was also higher than that in Reyan 8-79 at room temperature and after 4°C exposure for 2 h. Meanwhile, after 6 h of exposure to 4°C, the content of amino acids in Yunyan 77-4 was lower than that in Reyan 8-79, and after 20 h, the amino acid content was almost the same in both the clones. The lipids were higher in Yunyan 77-4 than in Reyan 8-79 at room temperature, but higher in Reyan 8-79 than in Yunyan 77-4 at 4°C after 2 h and 6 h of exposure. However, the difference between these clones was not obvious at room temperature after 20 h. Heatmap analysis of the DAMs showed that the flavonoid terms "Dihydroflavonol" and "Biflavones" in Yunyan 77-4 vs. Reyan 8-79 groups increased with prolonged exposure to low temperature (Supplementary Figure 4, Supplementary Table 4). Further KEGG analysis showed that the DAMs enriched the "Metabolic pathway", "Flavonoid biosynthesis", "Biosynthesis of secondary metabolites", "Arginine and proline metabolism", and "Anthocyanin biosynthesis" classes (Supplementary Figure 5A). Among these, the DAMs in Yunyan 77-4 vs. Reyan 8-79 at all treatment duration enriched the "Anthocyanin biosynthesis" pathway; the DAMs of R0H vs. Y0H and R2H vs. Y2H enriched the "Flavone and flavonol biosynthesis", and the DAMs of R20H vs. Y20H enriched the "Isoflavonoid biosynthesis". Meanwhile, the "Arginine and proline metabolism" pathway was the most important pathway in all groups (Supplementary Figure 5B). We also performed the enrichment analysis for the upregulated and downregulated DAMs separately. The downregulated DAMs enriched the "Phenylpropanoid biosynthesis" at 0 h and 2 h of exposure to low temperature, the "Tropane, piperidine, and pyridine alkaloid biosynthesis"; "Biosynthesis of various plant secondary metabolites"; "Arginine biosynthesis"; "Phenylalanine, tyrosine, and tryptophan biosynthesis"; "Phenylpropanoid biosynthesis" at 6 h, and the "Purine metabolism" at 20 h. Meanwhile, the upregulated DAMs enriched the "Biosynthesis of flavonoid" term at all treatment durations (Supplementary Figure 6).

10.3389/fpls.2022.1092411

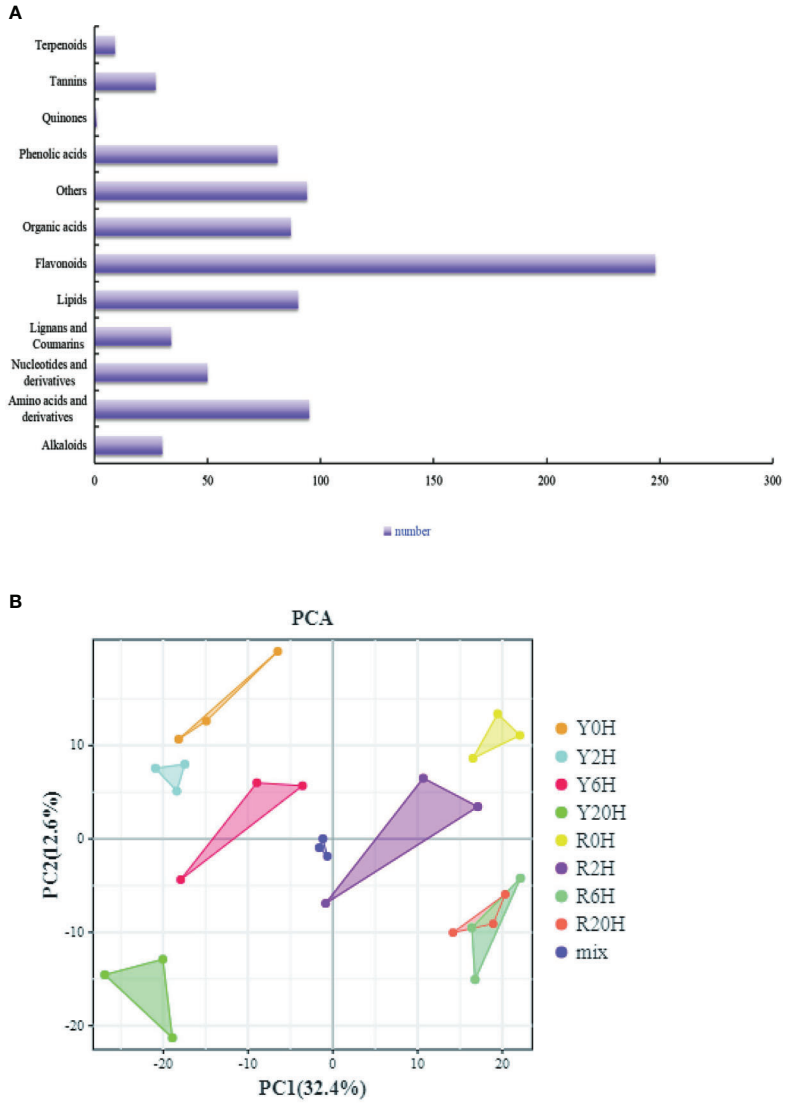

FIGURE 3
Overall analysis of the metabolites. **(A)** All identified metabolites. **(B)** PCA plot of all samples, including the QC sample.

Integrated analysis of the transcriptomic and metabolomic data reveals the cold resistance mechanism of rubber tree

We then integrated the transcriptome and metabolome data sets to understand the mechanisms underlying cold resistance in the rubber tree. The PCA of transcriptome and metabolome showed that Y20H accounted for the first principal component, and the two clones at room temperature (0 h) accounted for most of the second principal component. Then, the DEGs and DAMs were simultaneously mapped to the KEGG pathway map to assess the relationship between genes and metabolites better. The KEGG enrichment and pathway analysis showed that the DAMs and DEGs enriched "Flavonoid biosynthesis", "Biosynthesis of amino acids", and "Arginine and proline metabolism" pathways at 0 h; "Anthocyanin biosynthesis" and "Arginine and proline metabolism" were significantly enriched at 2 h. Interestingly, "Flavonoid biosynthesis" was significantly enriched in addition to "Amino acid biosynthesis" at 6 h and 20 h of exposure to 4°C (Supplementary Figure 7A). Further, the heatmap based on the PCC between DEGs and DAMs ($0.8 \leq PCC \leq -0.8$) showed that flavonoids were the highest at all time points, followed by phenolic acids, organic acids, tannins, and amino acids and derivatives (Supplementary Figure 7B). Thus, the integrated analysis identified flavonoids, arginine, and anthocyanins as the key metabolites regulating cold resistance in the rubber tree.

Identification of the cold resistance genes associated with the biosynthesis of flavonoids, arginine, and anthocyanins

The enrichment analysis integrating DEGs and DAMs revealed flavonoid biosynthesis, arginine biosynthesis, and anthocyanin biosynthesis as the predominant metabolic pathways related to cold resistance in rubber trees. Then, to identify the key genes regulating these pathways under low temperatures, a phylogenetic analysis was performed between the genes that demonstrated a good correlation with metabolites of the flavonoid and anthocyanin biosynthetic pathway in this study and similar to the cold resistance genes of the same pathway in *Arabidopsis thaliana* (Li et al., 2017). The ML phylogenetic tree showed the highest similarity for *gene10192*, *gene21405*, *gene9468*, and *gene36729* of the rubber tree with the cold-resistance genes *ATUGT79B3*, *ATUGT79B2*, *AtMYB75*/*PAP1*, and *ATDFR* of *A. thaliana* (Figure 4A). Further KEGG annotation and enrichment analysis confirmed that *gene27178*, *gene7125*, *gene28839*, *gene31599*, *gene356*, and *gene05278* participated in the biosynthesis and metabolism of rubber flavonoids. Integrated analysis of the DEGs and DAMs with $0.8 \leq PCC \leq -0.8$ data and related to flavonoid biosynthesis and metabolism during cold resistance in the rubber tree (Figure 4B) revealed that flavonoids, anthocyanins, and flavones were biosynthesized from *p*-coumaroyl-CoA through the action of chalcone synthase (CHS) under cold stress in the resistant clone. Generally, under low temperatures, among the intermediates of the flavonoid pathway, apigenin and kaempferol are involved in flavone and flavonol biosynthesis, while cyanidin is involved in anthocyanin biosynthesis. The content of kaempferol and cyanidin was lower in Yunyan 77-4 than in Reyan 8-79, while that of apigenin was higher at room temperature or low temperature. Additionally, heatmap clustering of the genes (FPKM values) and metabolites (content) involved in the cryogenic regulation of flavonoid biosynthesis and anthocyanin biosynthesis showed differences in the expression of flavonoid biosynthetic genes and the content of flavonoids between the two rubber tree clones (Figure 4C). Specifically, Yunyan 77-4 exhibited the highest content of flavonoids and expression of flavonoid-related genes under prolonged low-temperature treatment; however, the trend in this relationship between the genes and metabolites was not found in Reyan 8-79 (Figure 4C).

Similarly, to search for key genes involved in arginine biosynthesis under low temperatures, we performed another phylogenetic analysis using the arginine biosynthesis related-genes annotated in this study and the arginine decarboxylase (ADC) genes reported in *A. thaliana* (*AtADC1*: *AT2G16500*; *AtADC2*: *AT4G34710*), *Cucumis sativus* (*CuADC*, Sequence ID: NM_001308900.2), and *Solanum lycopersicum* (SlADC, Sequence ID: NM_001247720.2). The ML tree showed that *gene2487, gene33765*, *gene9849*, *gene6161*, and *gene2702* were highly similar to the reported ADC genes of *A. thaliana*, *C. sativus*, and *S. lycopersicum* (Figure 5A). The KEGG annotation and enrichment analysis showed that these genes belonged to the members of the Arg gene family, confirming their role in arginine biosynthesis. The pathway in the rubber tree elucidated based on these observation is demonstrated in Figure 5B. In addition to the genes mentioned above, *gene16028*, *gene35888*, and *PB.8216* also participated in arginine biosynthesis in the rubber tree. Additionally, the heatmap showed a higher arginine content in Yunyan 77-4 than in Reyan 8-79 before cold exposure; however, almost an opposite trend was observed in *gene2487* and *gene33765*. These genes displayed a higher expression level in Reyan 8-79 but did not increase the content of the associated metabolites of arginine biosynthesis, such as N-acetyl-glutamyl-P (Figure 5C), resulting in a weak cold resistance of Reyan 8-79. Thus, our observation suggested that the differences in the expression patterns of genes involved in the biosynthesis of flavonoids and arginine led to differences in the content of flavonoids, arginine, and their intermediates, resulting in different cold resistance capacities between the clones.

Quantitative real-time polymerase chain reaction

Finally, qRT-PCR was performed to validate the RNA-Seq data and confirm the expression levels of eight genes associated with the arginine and flavonoid biosynthesis pathway in different samples (Supplementary Table 4). The expression patterns of these genes obtained by qRT-PCR showed good consistency with the RNA-Seq results, indicating the reliability of the transcriptome data (Figure 6).

Discussion

In the present study, the cold-resistance clone Yunyan77-4 and the cold-sensitive clone Reyan 8-79 were exposed to 4°C for different durations, and the response was analyzed. The DEGs identified between the two rubber tree clones based on transcriptome sequencing mainly enriched the glycolysis/gluconeogenesis pathway at room temperature and the biosynthesis of amino acids at 6 h under low temperature. These observations indicated that Yunyan 77-4 expressed more genes under prolonged low-temperature treatment than Reyan 8-79. Meanwhile, KEGG analysis suggested that the rubber tree responds to cold stress by regulating enzyme activity, changing cell permeability, and synthesizing significant metabolites. Subsequent metabolome analysis

10.3389/fpls.2022.1092411

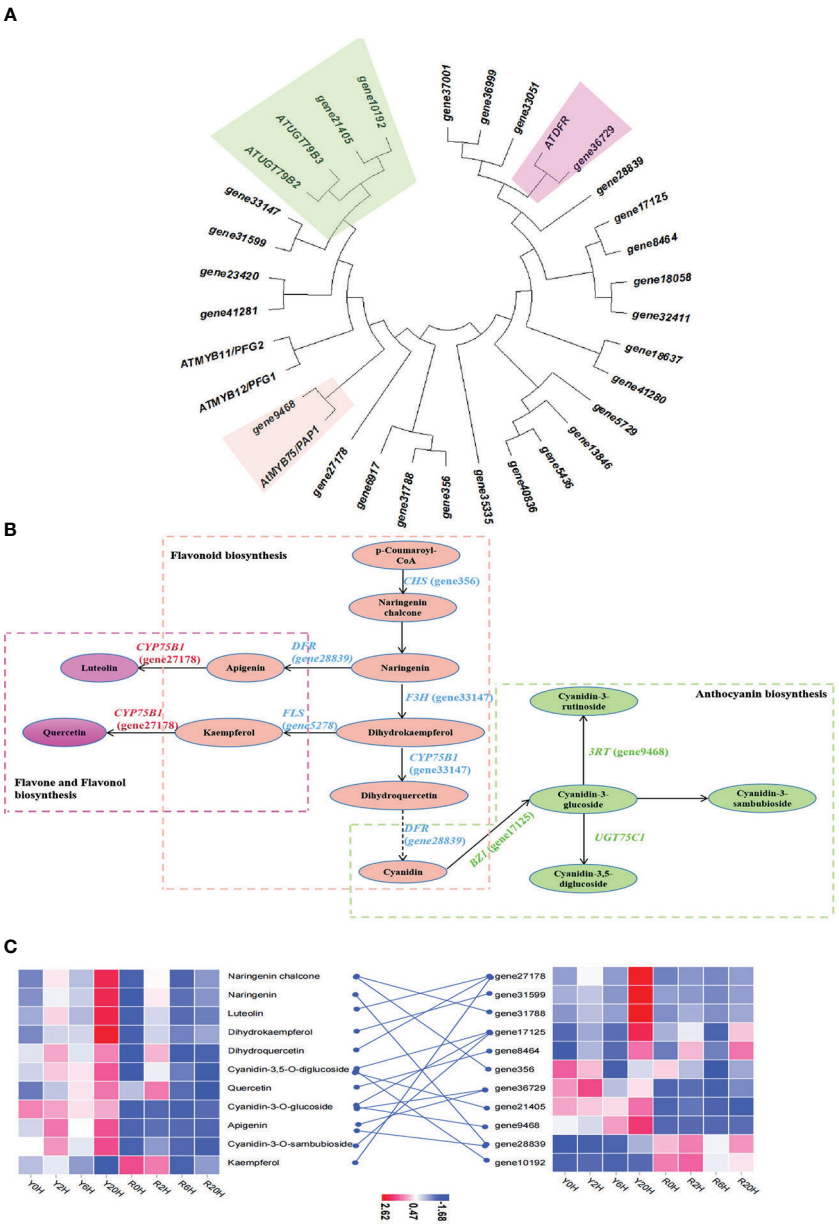

FIGURE 4
Metabolites and genes involved in flavonoid biosynthesis and anthocyanin biosynthesis. **(A)** Maximum likelihood phylogenetic tree of the key genes of the flavonoid and anthocyanin biosynthetic pathways. The colored blocks highlight the relationship between genes involved in flavonoid, anthocyanin, and flavone biosyntheses identified in this study and the genes of the same pathway in *Arabidopsis thaliana*. **(B)** Flavonoid biosynthetic mechanisms associated with cold resistance in the rubber tree. The green dashed box represents anthocyanin biosynthesis, the orange dashed box represents flavonoid biosynthesis, and the pink dashed box represents flavone and flavonol biosynthesis. Ellipses in the same color represent the same pathway, and the names in parentheses beginning with the term "gene" are the IDs of the genes annotated in this study. **(C)** The heatmap of metabolites and genes involved in flavonoid biosynthesis, anthocyanin biosynthesis, and flavone biosynthesis based on the FPKM of key genes and the content of metabolites.

indicated that under prolonged treatment, the DAMs increased, and Yunyan 77-4 had higher metabolite content than Reyan 8-79. Arginine biosynthesis and flavonoid and anthocyanin biosyntheses were significantly enriched at 0 h and 2 h in Yunyan 77-4; however, enrichment of arginine biosynthesis reduced at 6 h and 20 h, while the biosynthesis of flavonoids and anthocyanins remained significantly enriched. In addition, 97 (93 upregulated and 3 downregulated), 63 (57 and 5), 74 (68 and 5), and 123 (117 and 5) flavonoids were found differentially accumulated in Reyan 8-79 compared with Yunyan 77-4 at 0 h, 2 h, 6 h, and 20 h, respectively. The cold-resistant clone Yunyan 77-4 had a higher content of flavonoids than the cold-sensitive

10.3389/fpls.2022.1092411

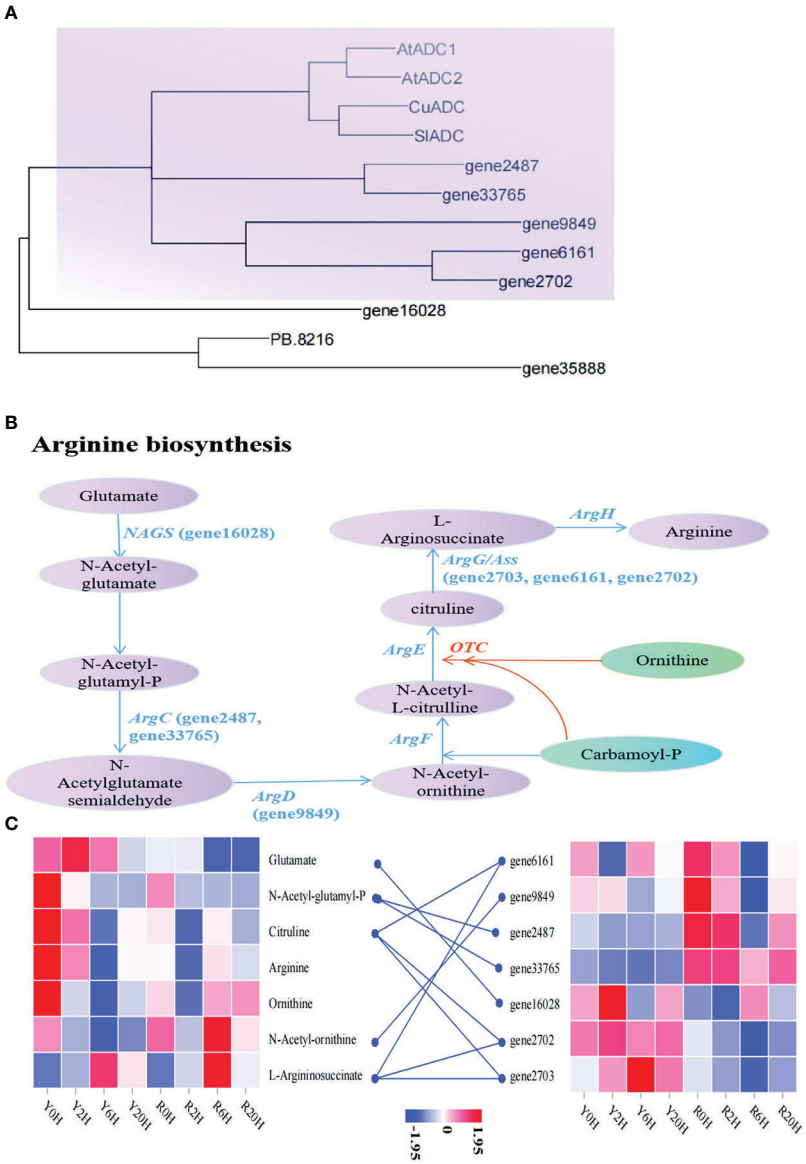

FIGURE 5
Metabolites and genes involved in arginine biosynthesis **(A)** Maximum likelihood phylogenetic tree of the key genes in arginine biosynthetic pathway. The colored blocks highlight the relationship between genes involved in arginine biosynthesis identified in this study and the genes of the same pathway in *Arabidopsis thaliana*, *Cucumis sativus*, and *Solanum lycopersicum*. **(B)** Arginine biosynthetic mechanisms associated with cold resistance in the rubber tree. The name in parentheses beginning with the term "gene" are the IDs of the genes annotated in this study. **(C)** The heatmap of metabolites and genes involved in arginine biosynthesis based on the FPKM of key genes and the content of metabolites.

Reyan 8-79. As the treatment prolonged, the species and content of flavonoids in the cold-resistant clone increased and attained more elevated levels than in the temperature-sensitive clone. These observations indicate that the cold-resistant rubber tree shows more robust gene expression than the temperature-sensitive one for adjusting enzyme activity, changing cell permeability, and synthesizing metabolites.

Integrated transcriptome and metabolome analysis revealed significant enrichment of the arginine and proline metabolism pathway at 2 h; however, the enrichment was reduced with prolonged treatment (6 h and 20 h), while flavonoid biosynthesis was enriched. The primary reason for this change in Yunyan 77-4 is the upregulation in the genes encoding CHS, flavanone 3-hydroxylase (F3H), and FDR involved in flavonoid biosynthesis, and the high content of flavonoids, including naringenin, chalcone, and dihydrokaempferol. Moreover, Yunyan 77-4 exhibited higher expression levels of genes involved in flavonoid biosynthesis and accumulation of flavonoids and anthocyanins than Reyan 8-79 after low-temperature exposure for 6 h and 20 h. The arginine biosynthetic genes encoding N-

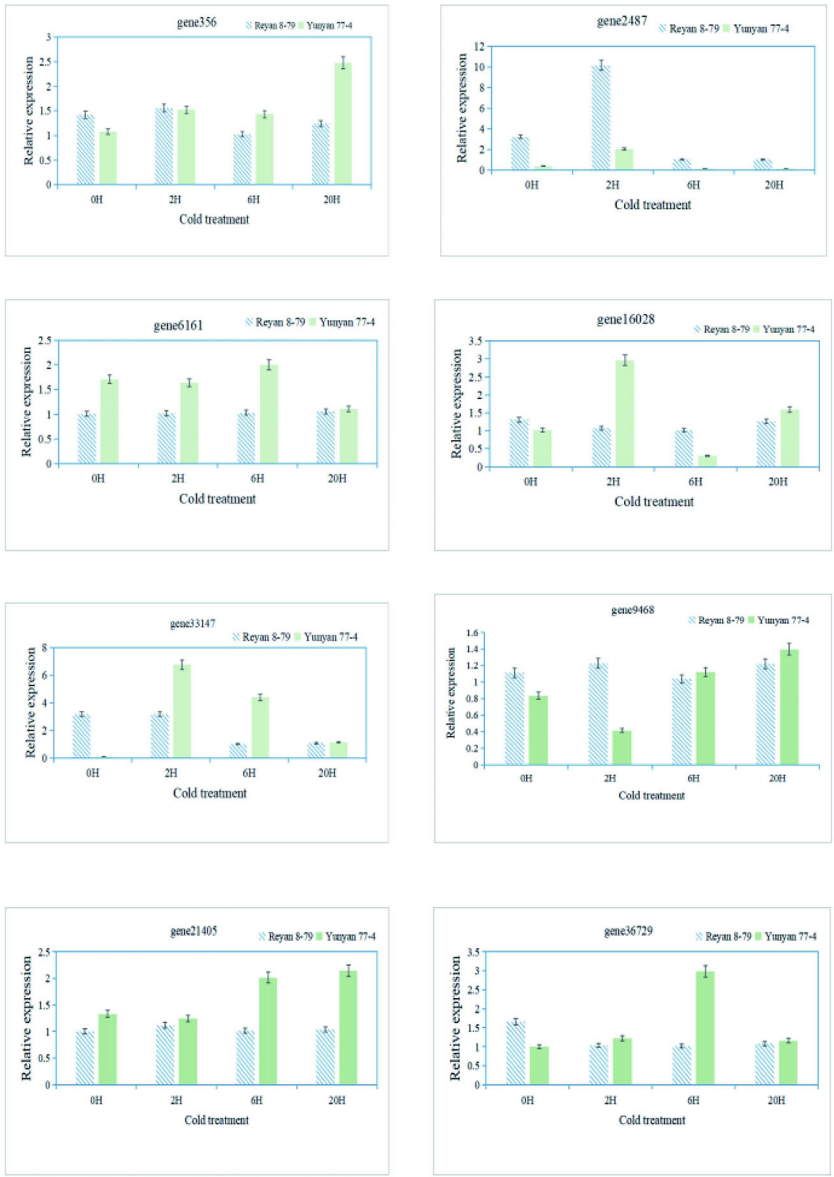

FIGURE 6
qRT-PCR validation of the transcript levels of DEGs of the arginine and flavonoid biosynthetic pathway.

acetylglutamate synthase (NAGS, *gene16028* in this study), N-acetyl-gamma-glutamyl-phosphate reductase (ArgC, *gene2487*, *gene33765*), and argininosuccinate synthase (Ass, *gene2703*, *gene6161*, *gene2702*), and the metabolites L-arginosuccinate, N-acetyl-ornithine, ornithine, and N-acetyl-glutamate were significantly different between the two rubber tree clones under low temperature. KEGG analysis indicated arginine biosynthesis was significantly enriched only at 6 h in Yunyan 77-4. The NAGS gene and N-acetyl-glutamate regulated by this gene were upregulated at 2 h, the ArgC gene and N-acetyl-ornithine content were downregulated at 6 h and 20 h, and the ASS gene was upregulated at all time points. Moreover, arginine content was consistently higher in Yunyan 77-4 than in Reyan 8-79. Arginine, the primary form in which organic nitrogen is stored and transported in plants, is a key precursor of polyamine biosynthesis and plays an important role in growth, development, and stress regulation (Winter et al., 2015). Overexpression of NAGS in *A. thaliana* increased salt and drought tolerance (Mary et al., 2009). Thus, the present study's results indicate that the resistant clone synthesizes arginine and its precursors under the action of Arg genes, providing better cold tolerance. In addition, the two clones showed differences in glutamate and related genes and ornithine. Therefore, we speculated that the treatment

duration obviously influenced arginine biosynthesis, and NAGS, ArgC, and Ass genes were necessary for low-temperate response in the rubber tree.

In plants, flavonoids participate in many processes associated with biotic and abiotic stresses (Samanta et al., 2011). Flavonoid content and type vary based on the development phase and tissues (Makoi and Ndakidemi, 2011; Choi et al., 2012). In this study, the continuous low-temperature treatment upregulated the expression of flavonoid biosynthetic genes and the accumulation of flavonoids and anthocyanins in the rubber tree, consistent with the reports in other species, such as grape and *A. thaliana* (Azuma et al., 2012; Nakabayashi et al., 2014). After cold treatment for 6 h, the CHS and F3H genes were upregulated in Yunyan 77-4. These two genes probably promoted the accumulation of flavonoids, such as apigenin and dihydroquercetin (Dao et al., 2011), the key substrates for anthocyanin, flavone, and flavonol biosynthesis. The correlation observed between the increased content and CHS and F3H upregulation confirmed this hypothesis. Similarly, low temperatures upregulated the CHS gene in barley (*Hordeum vulgare*) and provided stress tolerance (Lee et al., 2019). Moreover, other genes of this pathway (CYP75B1: *gene27178*; FDR: *gene28839*; 3RT: *gene9468*) (Figure 4C) were upregulated in the cold-resistant clone, and the content of the related metabolites increased accordingly. Thus, the observations indicate that the accumulation of flavonoids in the cold-resistant rubber tree also contributed to their enhanced cold resistance.

Conclusion

The study found that the variations in the level of flavonoids, glutamate, and ornithine led to the difference in the cold resistance capacity between Yunyan 77-4 and Reyan 8-79. The content of flavonoids, especially the intermediates of anthocyanin biosynthetic pathway, was higher in Yunyan 77-4 than in Reyan 8-79 at room temperature and low temperature. During the early stage of cold stress, more glutamates were synthesized in the cold-resistant rubber tree clone. With prolonged exposure, compounds of the arginine biosynthetic pathway, such as L-arginosuccinate, N-acetyl-ornithine, N-acetyl-glutamate, and ornithine, were accumulated more in Yunyan 77-4 than in Reyan 8-79. The study also found differences in the content of naringenin chalcone, apigenin, dihydroquercetin, and cyanidin-3-glucoside of flavonoid biosynthetic pathway between the two rubber tree clones, with variations in the expression of the genes regulating their biosyntheses. Thus, the study suggests that flavonoid biosynthetic genes, such as CHS (*gene356*) and F3H (*gene33147*), and the arginine biosynthetic genes, including NAGS (*gene16028*), ArgC (*gene2487*, *gene33765*), and Ass (*gene6161*), play key roles in regulating cold resistance of the rubber tree. However, the role of transcription factors, such as CBF1 and MYB, in regulating these genes remains unclear. Thus, the study provides an empirical basis for future investigations on the molecular and biochemical mechanisms underlying cold resistance in the rubber tree and the genes identified in present study may be used as candidate to develop improved new cold-resistant varieties.

Data availability statement

The original contributions presented in the study are publicly available. This data can be found here: https://dataview.ncbi.nlm.nih.gov/object/PRJNA855273?reviewer=fam1jekvgc6ts689hp1ihtrt1c, PRJNA855273.

Author contributions

CM: writing - original draft, proofreading, metabolomic test, data curation, analysis, and visualization. LL: material preparation and transcriptomic data analysis. TY and XL: metabolome data analysis. MG: experimental seedling preparation. FZ and QZ: manuscript proofreading. YW: supervision, project administration, and funding acquisition. All authors contributed to the article and approved the submitted version.

Funding

We gratefully acknowledge the financial support provided by the National Key R&D Program of China (2019YFD1001102-01), and the Sci-Tech Innovation System Construction for Tropical Crops Grant of Yunnan Province (RF2021-2), and The YITC Science fund for Distinguished Young Scholars (QNCZ2020-1; QNCZ2022-2).

Acknowledgments

We thank the staff of Beijing Biomarker Biotechnology Co., Ltd. (Beijing, China) for their support during the transcriptomic sequencing and Wuhan Metware Biotechnology Co., Ltd. (Wuhan, China) for their support during the metabolome data analysis.

Conflict of interest

The authors declare that the research was conducted in the absence of any commercial or financial relationships that could be construed as a potential conflict of interest.

Publisher's note

All claims expressed in this article are solely those of the authors and do not necessarily represent those of their affiliated organizations, or those of the publisher, the editors and the reviewers. Any product that may be evaluated in this article, or claim that may be made by its manufacturer, is not guaranteed or endorsed by the publisher.

Supplementary material

The Supplementary Material for this article can be found online at: https://www.frontiersin.org/articles/10.3389/fpls.2022.1092411/full#supplementary-material

References

Azuma, A., Yakushiji, H., Koshita, Y., and Kobayashi, S. (2012). Flavonoid biosynthesis-related genes in grape skin are differentially regulated by temperature and light conditions. *Planta* 236, 1067–1080. doi: 10.1007/s00425-012-1650-x

Bu, X., Wang, X., Yan, J., Zhang, Y., Zhou, S., Sun, X., et al. (2021). Genome-wide characterization of b-box gene family and itsroles in responses to light quality and cold stress in tomato. *Front. Plant Science* 12. doi: 10.3389/fpls.2021.698525

Cai, H., Hu, Y., Huang, H., and Cheng, H. (2008). Cloning and expression analysis of HbCBF2 gene in *Hevea brasiliensis*. *Trop. Agric. Sci. Technol.* 31(1-5), 12.

Chen, J., Dong, Y., Wang, Y., Liu, Q., Zhang, J., and Chen, S. (2003). An AP2/EREBP-type transcription-factor gene from rice is cold-inducible and encodes a nuclear-localized protein. *Theor. Appl. Genet.* 107, 972–979. doi: 10.1007/s00122-003-1346-5

Cheng, H., Chen, X., Fang, J., An, Z., Hu, Y., and Huang, H. (2018). Comparative transcriptome analysis reveals an early gene expression profile that contributes to cold resistance in *Hevea brasiliensis* (the para rubber tree). *Tree Physiol.* 38, 1409–1423. doi: 10.1093/treephys/tpy014

Chen, Y., Tan, Z., Fan, J., Zhou, S., and Xue, J. (2013a). Classification of chilling injury in hevea rubber based on meteorological conditions. *Trop. Agric. Sci. Technol.* 36, 7–11.

Chen, W., Gong, L., Guo, Z., Wang, W., Zhang, H., Liu, X., et al. (2013b). A novel integrated method for large-scale detection, identification, and quantification of widely targeted metabolites: application in the study of rice metabolomics. *Mol. Plant* 6 (6), 1769–1780. doi: 10.1093/mp/sst080

Choi, S., Ahn, J., Kim, H., Im, N., Kozukue, N., Levin, C., et al. (2012). Changes in free amino acid, protein, and flavonoid content in jujube (*Ziziphus jujube*) fruit during eight stages of growth and antioxidative and cancer cell inhibitory effects by extracts. *J. Agric. Food Chem.* 60, 10245–10255. doi: 10.1021/jf302848u

Chung, I., Kim, J., Han, J., Kong, W., Kim, S., Yang, Y., et al. (2019). Potential geo-discriminative tools to trace the origins of the dried slices of shiitake (*Lentinula edodes*) using stable isotope ratios and OPLS-DA. *Food Chem.* 295, 505–513. doi: 10.1016/j.foodchem.2019.05.143

Cook, D., Fowler, S., Fiehn, O., and Thomashow, M. (2004). A prominent role for the CBF cold response pathway in configuring the low-temperature metabolome of *Arabidopsis*. *Roceedings Natl. Acad. Sci.* 101, 15243–15248. doi: 10.1073/pnas.0406069101

Dao, T., Linthorst, H., and Verpoorte, R. (2011). Chalcone synthase and its functions in plant resistance. *Phytochem. Rev.* 10, 397–412. doi: 10.1007/s11101-011-9211-7

Da, S. C.C., Bajay, S. K., Aono, A. H., Francisco, F. R., Junior, R. B., Souza, A. P.D., et al. (2021). Novel insights into the cold resistance of *Hevea brasiliensis* through coexpression networks, bioRxiv print. pp.1–27. doi: 10.1101/2021.11.02.466997

Deng, X., Wang, J., Li, Y., Wu, S., Yang, S., Chao, J., et al. (2018). Comparative transcriptome analysis reveals phytohormone signalings, heat shock module and ROS scavenger mediate the cold-tolerance of rubber tree. *Sci. Rep.* 8, 1–16. doi: 10.1038/s41598-018-23094-y

Felsenstein, J. (1978). Cases in which parsimony or compatibility methods will be positively misleading. *Systematic Biol.* 27 (4), 401–410. doi: 10.1093/sysbio/27.4.401

Gong, X., Yan, B., Hu, J., Yang, C., Li, Y., Liu, J., et al. (2018). Transcriptome profiling of rubber tree (*Hevea brasiliensis*) discovers candidate regulators of the cold stress response. *Genes Genomics* 40, 1181–1197. doi: 10.1007/s13258-018-0681-5

Gronover, C., Wahler, D., and Prüfer, D. (2011). "Natural rubber biosynthesis and physic-chemical studies on plant derived latex," in *Biotechnology of biopolymers*. Ed. M. Elnashar (Croatia: InTech).

Jiang, B., Shi, Y., Peng, Y., Jia, Y., Yan, Y., Dong, X., et al. (2020). Cold-induced CBF–PIF3 interaction enhances freezing tolerance by stabilizing the phyB thermosensor in *Arabidopsis*. *Mol. Plant* 13, 894–906. doi: 10.1016/j.molp.2020.04.006

Jin, J., Zhang, H., Zhang, J., Liu, P., Chen, X., Li, Z., et al. (2017). Integrated transcriptomics and metabolomics analysis to characterize cold stress responses in Nicotiana tabacum. *BMC Genomics*. 18 (1), 1–15. doi: 10.1186/s12864-017-3871-7

Kanehisa, M., Sato, Y., Kawashima, M., Furumichi, M., and Tanabe, M. (2016). KEGG as a reference resource for gene and protein annotation. *Nucleic Acids Res.* 44 (D1), D457–D462. doi: 10.1093/nar/gkv1070

Kim, D., Pertea, G., Trapnell, C., Pimentel, H., Kelley, R., and Salzberg, S. L. (2013). TopHat2: accurate alignment of transcriptomes in the presence of insertions, deletions and gene fusions. *Genome Biol.* 14, R36. doi: 10.1186/gb-2013-14-4-r36

Lee, K., Rahman, M., Song, Y., Ji, C., Choi, G., Kim, K., et al. (2019). Cold stress-induced regulation of differentially expressed genes in barley (*Hordeum vulgare* l.) leaves. *J. Anim. Plant Sci.* 29, 1673–1679.

Li, M. (2005). Cold-resistance physiological appraise to rubber tree new varietied of 'Yunyan 77-4' and 'Yunyan77-2'. *Trop. Agric. Sci. Technol.* 28, 1–6,3.

Li, W., Fu, Y., Lv, W., Zhao, S., Feng, H., Shao, L., et al. (2022a). Characterization of the early gene expression profile in *Populus ussuriensis* under cold stress using PacBio SMRT sequencing integrated with RNA-seq reads. *Tree Physiol.* 42, 646–663. doi: 10.1093/treephys/tpab130

Li, P., Li, Y., Zhang, F., Zhang, G., Jiang, X., Yu, H., et al. (2017). The *Arabidopsis* UDP-glycosyltransferases UGT79B2 and UGT79B3, contribute to cold, salt and drought stress tolerance *via* modulating anthocyanin accumulation. *Plant J.* 89 (1), 85–103. doi: 10.1111/tpj.13324

Lin, M., and Yang, H. (1994). Physiological responses of *Hevea brasiliensis* during the chilling injury. *Chin. J. Trop. Crops* 15, 7–11.

Li, Y., Quan, C., Yang, S., Wu, S., Shi, M., Wang, J., et al. (2022b). Functional identification of ICE transcription factors in rubber tree. *Forests* 13, 52. doi: 10.3390/f13010052

Livak, K., and Schmittgen, T. (2001). Analysis of relative gene expression data using real-time quantitative PCR and the $2^{-\Delta\Delta CT}$ method. *Methods* 25, 402–408. doi: 10.1006/meth.2001.1262

Li, X., Xing, B., Liu, X., Jiang, X., Lu, H., Xu, Z., et al. (2021). Network pharmacology-based research uncovers cold resistance and thermogenesis mechanism of cinnamomum *cassia*. *Fitoterapia* 149, 104824. doi: 10.1016/j.fitote.2020.104824

Li, H., Zhou, T., Ning, L., and Li, G. (2009). Cytological identification and breeding course of *Hevea* 'Yunyan 77-2' and 'Yunyan 77-4'. *J. Trop. Subtropical Botany* 17, 602–605. doi: 10.3969/j.issn.1005-3395.2009.6.2323

Lu, Q., Guo, F., Xu, Q., and Cang, J. (2020). LncRNA improves cold resistance of winter wheat by interacting with miR398. *Funct. Plant Biol.* 47, 544–557. doi: 10.1071/FP19267

Mai, J., Herbette, S., Vandame, M., Kositsup, B., Kasemsap, P., Cavaloc, K., et al. (2009). Effect of chilling on photosynthesis and antioxidant enzymes in *Hevea brasiliensis* muell. arg. *Trees* 23, 863–874. doi: 10.1007/s00468-009-0328-x

Makoi, J., and Ndakidemi, P. (2011). Changes in plant growth, nutrient dynamics and accumulation of flavonoids and anthocyanins by manipulating the cropping systems involving legumes and cereals-a review. *Aust. J. Agric. Engineering* 2, 56–65.

Mantello, C., Boatwright, L., da Silva, C., Scaloppi, E., de Souza Goncalves, P., Barbazuk, W., et al. (2019). Deep expression analysis reveals distinct cold-response strategies in rubber tree (*Hevea brasiliensis*). *BMC Genomics* 20, 1–20. doi: 10.1186/s12864-019-5852-5

Maruyama, K., Urano, K., Yoshiwara, K., Morishita, Y., Sakurai, N., Suzuki, H., et al. (2014). Integrated analysis of the effects of cold and dehydration on rice metabolites, phytohormones, and gene transcripts. *Plant Physiol.* 164, 1759–1771. doi: 10.1104/pp.113.231720

Mary, S., Dimitris, A., Diamanto, L., Georgios, M., Vasileios, F., and Irene, P. (2009). Over-expression of a tomato n-acetyl-L-glutamate synthase gene (SlNAGS1) in *Arabidopsis thaliana* results in high ornithine levels and increased tolerance in salt and drought stresses. *J. Exp. Botany* 60, p.1859–p.1871. doi: 10.1093/jxb/erp072

Mo, T., Zhang, Y., Huang, J., and Xie, H. (2009). Comprehensive evaluation of cold resistance of 31 *Hevea* clones. *Chin. J. Trop. Crops* 30 (5), 637–643. doi: 10.1007/978-1-4020-9623-5_5

Nakabayashi, R., Yonekura-Sakakibara, K., Urano, K., Suzuki, M., Yamada, Y., Nishizawa, T., et al. (2014). Enhancement of oxidative and drought tolerance in *Arabidopsis* by overaccumulation of antioxidant flavonoids. *Plant J.* 77, 367–379. doi: 10.1111/tpj.12388

Niu, Y., Liu, Z., He, H., Han, X., Qi, Z., and Yang, Y. (2020). Gene expression and metabolic changes of *Momordica charantia* l. seedlings in response to low temperature stress. *PloS One* 15, e0233130. doi: 10.1371/journal.pone.0233130

Pan, Y., Liang, H., Gao, L., Dai, G., Chen, W., Yang, X., et al. (2020). Transcriptomic profiling of germinating seeds under cold stress and characterization of the cold-tolerant gene LTG5 in rice. *BMC Plant Biol.* 20, 1–17. doi: 10.1186/s12870-020-02569-z

Priyadarshan, P. (2011). Biology of *Hevea* rubber. *Springer*. p6. doi: 10.1007/978-3-319-54506-6

Quan, C., Li, Y., and Tian, W. (2017). Molecular cloning and expression analysis of HbICE2 in rubber tree (*Hevea brasiliensis* muell. arg.). *J. Trop. Biol.* 8, 133–140. doi: 10.15886/j.cnki.rdswxb.2017.02.001

Raj, S., Das, G., Pothen, J., and Dey, S. (2005). Relationship between latex yield of *Hevea brasiliensis* and antecedent environmental parameters. *Int. J. Biometeorol.* 49, 189–196. doi: 10.1007/s00484-004-0222-6

Rezaie, R., Mandoulakani, B., and Fattahi, M. (2020). Cold stress changes antioxidant defense system, phenylpropanoid contents and expression of genes involved in their biosynthesis in *Ocimum basilicum* l. *Sci. Rep.* 10, 1–10. doi: 10.1038/s41598-020-62090-z

Rodríguez, M., Canales, E., and Borrás-Hidalgo, O. (2005). Molecular aspects of abiotic stress in plants. *Biotecnologia Aplicada.* 22, 1–10.

Roy, S., Das, G., Pal, T. K., Alam, B., Raj, S., and Dey, S. K. (2003). Studies on yield and biochemical sub-components of latex of rubber trees (Hevea brasiliensis) with a special reference to the impact of low temperature in a non-optimal environment. *Journal of Rubber Research.* 6(4), 241–257.

Samanta, A., Das, G., and Das, S. (2011). Roles of flavonoids in plants. *Int. J. Pharm. Sci. technol.* 6, 12–35.

Shinozaki, K., Yamaguchi-Shinozaki, K., and Seki, M. (2003). Regulatory network of gene expression in the drought and cold stress responses. *Curr. Opin. Plant Biol.* 6, 410–417. doi: 10.1016/S1369-5266(03)00092-X

Sonna, L., Fujita, J., Gaffin, S., and Lilly, C. (2002). Invited review: effects of heat and cold stress on mammalian gene expression. *J. Appl. Physiol.* 92, 1725–1742. doi: 10.1152/japplphysiol.01143.2001

Tian, X., Xie, J., and Yu, J. (2020). Physiological and transcriptomic responses of lanzhou lily (*Lilium davidii*, var. unicolor) to cold stress. *PloS One* 15, e0227921. doi: 10.1371/journal.pone.0227921

Tian, Y., Yuan, H., Xie, J., Deng, J., Dao, X., and Zheng, Y. (2016). Effect of diurnal irradiance on night-chilling tolerance of six rubber cultivars. *Photosynthetica* 54, 374–380. doi: 10.1007/s11099-016-0192-z

Vinod, K., Meenattoor, J., Reddy, Y., Priyadarshan, P., and Chaudhuri, D. (2010). Ontogenetic variations in flush development are indicative of low temperature tolerance in *Hevea brasiliensis* clones. *Annal For. Res.* 53, 95–105. doi: 10.15287/afr.2010.102

Wang, B. (2010). *Plant biology under stress* (Higher education press). p179–194

Wang, X., Li, W., Gao, X., Wu., C., and Zhang, X. (2012). Physiological characteristics of *Hevea brasiliensis* in response to low temperature stress and its regulation mechanisms. *Plant Physiol. J.* 48, 318–324. doi: CNKI:SUN:ZWSL.0.2012-04-004

Wang, X., Wu, Y., Sun, M., Wei, X., Huo, H., Yu, L., et al. (2022). Dynamic transcriptome profiling revealed key genes and pathways associated with cold stress in castor (*Ricinus communis* l.). *Ind. Crops Products* 178, 114610. doi: 10.1016/j.indcrop.2022.114610

Winter, G., Todd, C., Trovato, M., Forlani, G., and Funck, D. (2015). Physiological implications of arginine metabolism in plants. *Front. Plant Science* 6. doi: 10.3389/fpls.2015.00534

Xu, J., Chen, Z., Wang, F., Jia, W., and Xu, Z. (2020). Combined transcriptomic and metabolomic analyses uncover rearranged gene expression and metabolite metabolism in tobacco during cold acclimation. *Sci. Rep.* 10, 1–13. doi: 10.1038/s41598-020-62111-x

Yan, X., and Cao, M. (2009). Effect of seed coat and enviromental temperature on the germination of *Hevea brasiliensis* seeds. *J. Trop. Subtropical Botany* 17 (6), 584–589. doi: CNKI:SUN:RYZB.0.2009-06-014

Zhang, H., Zhu, J., Gong, Z., and Zhu, J. (2022a). Abiotic stress responses in plants. *Nat. Rev. Genet.* 23, 104–119. doi: 10.1038/s41576-021-00413-0

Zhang, Y., Yang, L., Hu, H., Yang, J., Cui, J., Wei, G., et al. (2022b). Transcriptome and metabolome changes in Chinese cedar during cold acclimation reveal the roles of flavonoids in needle discoloration and cold resistance. *Tree Physiol.* doi: 10.1093/treephys/tpac046

Zhao, Y., Zhou, M., Xu, K., Li, J., Li, S., Zhang, S., et al. (2019). Integrated transcriptomics and metabolomics analyses provide insights into cold stress response in wheat. *Crop J.* 7, 857–866. doi: 10.1016/j.cj.2019.09.002

Zhuo, X., Zheng, T., Zhang, Z., Zhang, Y., Jiang, L., Ahmad, S., et al. (2018). Genome-wide analysis of the NAC transcription factor gene family reveals differential expression patterns and cold-stress responses in the woody plant *Prunus mume*. *Genes* 9, 494. doi: 10.3390/genes9100494

frontiers | Frontiers in Plant Science

TYPE Original Research
PUBLISHED 15 March 2023
DOI 10.3389/fpls.2023.1129114

OPEN ACCESS

EDITED BY
Guanlin Li,
Jiangsu University, China

REVIEWED BY
Juan B. Arellano,
Institute of Natural Resources and Agrobiology of Salamanca, Spanish National Research Council (CSIC), Spain
Dinakaran Elango,
Iowa State University, United States

*CORRESPONDENCE
Jinggui Fang
2013151@njau.edu.cn
Lingfei Shangguan
shangguanlf@njau.edu.cn

†These authors have contributed equally to this work

SPECIALTY SECTION
This article was submitted to Plant Abiotic Stress, a section of the journal Frontiers in Plant Science

RECEIVED 21 December 2022
ACCEPTED 24 February 2023
PUBLISHED 15 March 2023

CITATION
Yang Y, Xia J, Fang X, Jia H, Wang X, Lin Y, Liu S, Ge M, Pu Y, Fang J and Shangguan L (2023) Drought stress in 'Shine Muscat' grapevine: Consequences and a novel mitigation strategy–5-aminolevulinic acid. *Front. Plant Sci.* 14:1129114. doi: 10.3389/fpls.2023.1129114

Drought stress in 'Shine Muscat' grapevine: Consequences and a novel mitigation strategy–5-aminolevulinic acid

Yuxian Yang[1,2†], Jiaxin Xia[1,2†], Xiang Fang[2,3†], Haoran Jia[1,2], Xicheng Wang[4], Yiling Lin[1,2], Siyu Liu[1,2], Mengqing Ge[1,2], Yunfeng Pu[5], Jinggui Fang[1,2*] and Lingfei Shangguan[1,2*]

[1]College of Horticulture, Nanjing Agricultural University, Nanjing, Jiangsu, China, [2]Fruit Crop Variety Improvement and Seedling Propagation Engineering Research Center of Jiangsu Province, Nanjing, Jiangsu, China, [3]School of Agronomy and Horticulture, Jiangsu Vocational College of Agriculture and Forestry, Jurong, Jiangsu, China, [4]Institute of Pomology, Jiangsu Academy of Agricultural Sciences, Nanjing, Jiangsu, China, [5]College of Life Sciences, Tarim University, Alar, Xinjiang, China

Drought is a common and serious abiotic stress in viticulture, and it is urgent to select effective measures to alleviate it. The new plant growth regulator 5-aminolevulinic acid (ALA) has been utilized to alleviate abiotic stresses in agriculture in recent years, which provided a novel idea to mitigate drought stress in viticulture. The leaves of 'Shine Muscat' grapevine (*Vitis vinifera* L.) seedlings were treated with drought (Dro), drought plus 5-aminolevulinic acid (ALA, 50 mg/L) (Dro_ALA) and normal watering (Control) to clarify the regulatory network used by ALA to alleviate drought stress in grapevine. Physiological indicators showed that ALA could effectively reduce the accumulation of malondialdehyde (MDA) and increase the activities of peroxidase (POD) and superoxide dismutase (SOD) in grapevine leaves under drought stress. At the end of treatment (day 16), the MDA content in Dro_ALA was reduced by 27.63% compared with that in Dro, while the activities of POD and SOD reached 2.97- and 5.09-fold of those in Dro, respectively. Furthermore, ALA reduces abscisic acid by upregulating *CYP707A1*, thus, relieving the closure of stomata under drought. The chlorophyll metabolic pathway and photosynthetic system are the major pathways affected by ALA to alleviate drought. Changes in the genes of chlorophyll synthesis, including *CHLH*, *CHLD*, *POR*, and *DVR*; genes related to degradation, such as *CLH*, *SGR*, *PPH* and *PAO*; the *RCA* gene that is related to Rubisco; and the genes *AGT1* and *GDCSP* related to photorespiration form the basis of these pathways. In addition, the antioxidant system and osmotic regulation play important roles that enable ALA to maintain cell homeostasis under drought. The reduction of glutathione, ascorbic acid and betaine after the application of ALA confirmed the alleviation of drought. In summary, this study revealed the mechanism of effects of drought stress on grapevine, and the alleviating effect of ALA, which provides a new concept to alleviate drought stress in grapevine and other plants.

KEYWORDS

grapevine, drought stress, ALA, transcriptome, metabolome, alleviation

1 Introduction

With the intensification of global warming, the occurrence of drought stress will be more frequent, which will exacerbate problems with agricultural cultivation (Chaves et al., 2010). Drought seriously affects plant growth and development and reduces the growth rate of crops. This is primarily because drought affects the leaf size, stem elongation and root proliferation, stomatal movement, and water and nutrient relations of plants (Farooq et al., 2012). Under conditions of water shortage, plant leaves wither, and the edges turn yellow, which inhibits leaf development (Fanizza and Ricciardi, 2015). Furthermore, drought can result in the destruction of chloroplasts and photosynthetic machinery, which leads to a reduction in the content of chlorophyll and a significant decrease in the efficiency of plant photosynthesis (Cornic and Massacci, 1996; Reddy et al., 2004; Farooq et al., 2009; Zargar et al., 2017). The reduction in photosynthesis primarily occurs owing to stomatal or non-stomatal factors (Bota et al., 2004; Zhou et al., 2007). Moreover, drought will cause oxidative stress in plants from the cellular level, the closure of stomata, and the inhibition of photosynthetic electron transport chain, which results in the overproduction of reactive oxygen species (ROS) (Moran et al., 1994; Sade et al., 2011; Hasanuzzaman et al., 2013). Plants have evolved efficient mechanisms to adapt to drought. Stomatal closure is the first reaction to reduce transpiration under drought, which is primarily maintained by the accumulation of phytohormones, such as ABA (Pirasteh-Anosheh et al., 2016). Antioxidant and scavenging defense systems are the important bases of drought tolerance. The activities of enzymatic components, such as superoxide dismutase (SOD) and peroxidase (POD), as well as the contents of non-enzymatic components, such as glutathione (GSH), ascorbate (AsA) and α-tocopherol will change in response to oxidative stress under drought (Terzi and Kadioglu, 2006; Laxa et al., 2019). Moreover, osmotic accumulation (OA) is also a key mechanism of drought tolerance in plants, which involves the accumulation of organic solutes, such as proline, betaine (N, N, N-trimethyl glycine), soluble sugars, and sugar alcohols, and a series of inorganic salt ions, such as Ca^{2+}, K^{+} and Cl^{-}, to reduce the cell osmotic potential and maintain water relationship (Serraj and Sinclair, 2002; Fang and Xiong, 2015). Together, these mechanisms provide drought tolerance to plants.

Various exogenous applications of substances have been proposed to mitigate drought, which is the most common and harmful abiotic stress. For example, the combined application of 24-epibrassinolide and spermine alleviates drought-induced oxidative stress in maize (*Zea mays* L.) (Talaat et al., 2015). The application of melatonin can improve the drought tolerance of loquat (*Eriobotrya japonica* L.) seedlings (Wang et al., 2021a). The exogenous application of betaine and potassium fertilizer can improve water relationship and the yield of wheat (*Triticum aestivum* L.) under drought conditions (Raza et al., 2014). The application of exogenous glycine betaine and salicylic acid can improve the water relationship of hybrid sunflower (*Helianthus*) under conditions of water shortage (Hussain et al., 2009). As a non-toxic endogenous plant growth regulator, 5-aminolevulinic acid (ALA) has a substantial potential to alleviate abiotic stress on plants. Studies have shown that ALA can improve photosynthesis, photosystem efficiency, and the antioxidant capacity of plants (Memon et al., 2009). ALA also has the potential to alleviate some common abiotic stresses in plants, including salinity, temperature, and drought stresses (Hodgins and Van Huystee, 1986; Watanabe et al., 2000; Phung et al., 2011; Zhang et al., 2012). However, most of these studies focused on physiological aspects, and the exact mechanism of action of ALA's mitigating effect still needs to be fully elucidated.

There is a large and growing global market for grapes (*V. vinifera*) and grape-based products. In addition to its huge economic value, as the first fruit crop whose whole genome was sequenced (Jaillon et al., 2007), many studies related to grapevine have been reported, making grapevine the model perennial fruit crop species (Gambetta et al., 2020). During the process of viticulture, vineyards are often affected by various abiotic stresses, of which drought is the most serious. Most vineyards face prolonged drought during the summer, thus, limiting grapevine growth (Lovisolo et al., 2016). ALA, a plant growth regulator that can enhance plant stress resistance, could provide a new concept to reduce drought damage in vineyards. In this study, leaves of the grapevine cultivar 'Shine Muscat' ('SM') (*Vitis labruscana* × *Vitis vinifera*) were used as research materials. The leaves were classified into control, drought treatment (Dro), and drought plus ALA (Dro_ALA) treatment. The morphological and physiological characteristics of three treated leaves were measured to examine the content of malondialdehyde (MDA) and the activities of antioxidant enzymes, such as SOD and POD. Furthermore, we combined transcriptomic and metabolome analyses to compare differentially expressed genes (DEGs) and differentially abundant metabolites (DAMs) between the ALA-treated group and the non-treated group under drought stress. The purpose of this study was to determine the protective mechanism of exogenous ALA on grapevine leaves under drought and to construct the regulatory network of drought resistance in grapevine leaves, thus, providing theoretical support for subsequent related studies.

2 Materials and methods

2.1 Plant materials, treatments, and sampling

Two-year-old 'SM' grapevines were grown in the heliogreenhouse (relative humidity of ~85% and a temperature regime of 25 °C day/15 °C night) of the Baima Teaching and Research Base of Nanjing Agricultural University, Nanjing, China (31°36′36″ N, 119°10′48″ E). They were used as the plant material for this study. Equal proportions of perlite, peat and horticultural vermiculite (1:1:1, v/v/v) were used to grow the grape seedlings. First, each pot of seedling soil was flooded with water and then allowed to dry out. Ten days after the watering had stopped was defined as 0 d, and the soil water content was below 9% at this time. The leaves in the Dro_ALA treatment was sprayed with 50 $mg{\cdot}L^{-1}$ ALA on both sides until the leaf surface was

soaked once every three days from 0 d. The same amount of distilled water was sprayed on the leaves for the Dro treatment. The control plants were watered daily to field capacity. Leaves were collected at 0, 2, 4, 6, 8, 10, 12, 14, and 16 days, and phenotypic observations and physiological indices were measured.

2.2 Measurement of physiological and biochemical responses

The content of MDA and activities of POD and SOD were measured as previously described (Beauchamp and Fridovich, 1971; Zheng and Van Huystee, 1992; Tewari et al., 2002). Cellulose acetate glue was applied to the leaf surface to form a thin layer, and the glue was dried into a thin film, which was imaged in an automatic positive fluorescence microscope (DM6 B; Leica Microsystems, Wetzlar, Germany). The stomatal apertures were also measured using this system. The soil water content (WC) was determined by the gravimetric method (Little et al., 1998). Each sample had three biological replicates.

2.3 Transcriptome and metabolome sequencing and multi-omics analysis

Transcriptome sequencing was performed on samples from the 16th day of the treatments. Total RNA was extracted and sequenced as described by Huang et al. (2020). Reads obtained from the sequencing machines included raw reads that contained adapters or low-quality bases that would affect the following assembly and analysis. Thus, to obtain high quality clean reads, the reads were further filtered by FASTP version 0.18.0 (Chen et al., 2018). The parameters were as follows: (1) removal of the reads that contained adapters; (2) removal of the reads that contained > 10% of unknown nucleotides (N); and (3) removal of low quality reads that contained > 50% of low quality (Q-value ≤ 20) bases. $|\log_2$ fold change (FC)$| \geq 1.0$ and adjusted *P*-value (p_{adj}) < 0.05 were used as the screening criteria for DEGs. Metabolome sequencing was determined by liquid chromatography-mass spectrometry (LC-MS) based on high-performance liquid chromatography (HPLC) (UltiMate 3000; Thermo Fisher Scientific, Waltham, MA, USA) and mass spectrometry (Q Exactive; Thermo Fisher Scientific). As for DAMs, the variable importance in the projection (VIP) value of a multivariate statistical analysis of orthogonal projections to latent structure discriminant analysis (OPLS-DA) and the *t*-test *P*-values of univariate statistical analysis were combined to screen the metabolites with significant differences between the different comparison groups (VIP > 1 and *P*-value < 0.05) (Saccenti et al., 2014). The transcriptomic and metabolomic data were integrated by a two-way orthogonal partial least squares (O2PLS) analysis (Bylesjö et al., 2007) using the Omics PLS package. Pearson correlation coefficients were calculated to integrate the metabolome and transcriptome data. Gene and metabolite pairs were ranked in the descending order of absolute correlation coefficients. The top 50 genes and metabolites were selected for heatmap analysis using pheatmap packages in the R project. Additionally, the top 250 pairs of genes and metabolites (with an absolute Pearson correlation > 0.5) were subjected to metabolite-transcript network analysis using igraph packages in the R project (Csardi and Nepusz, 2006). Cytoscape software (version 3.6.1) was used to visualize the pairs of genes and metabolites.

2.4 Analysis of the experimental results

The DEGs and DAMs between the groups were measured to analyze the major response of the 'SM' grapevine to drought stress and the mitigating effects of ALA. Comparison groups were established as follows: (I) DEGs and DAMs between the control versus Dro (control *vs.* Dro) comparison group were analyzed to determine the effect of drought stress on grapevine. (II) The control versus Dro_ALA (control *vs.* Dro_ALA) comparison group was used to analyze the difference between the ALA treatment after drought stress and the control treatment, and (III) The alleviating effect of ALA on drought stress was determined by analyzing the DEGs and DAMs between the Dro and Dro_ALA (Dro *vs.* Dro_ALA) treatments.

2.5 Statistical analysis

TBtools software (version 1.0692) and MapMan software (version 3.6.0) were used to analyze the functions of DEGs (Thimm et al., 2004). The data were expressed as the mean ± standard deviation (SD). A one-way analysis of variance (ANOVA) was used to analyze the data. Tukey's multi-range test was conducted using GraphPad Prism software (version 8.0.2) (GraphPad Software, San Diego, CA, USA) to determine significant differences between and within groups at $P < 0.05$ (Saccenti et al., 2014).

2.6 Validation of RNA-seq using RT-qPCR

Ten DEGs were randomly selected for quantitative reverse transcription PCR (RT-qPCR) analysis to verify the precision and repetitiveness of the transcriptome analytical results. Purified RNA samples were reverse-transcribed using the Revert Aid^{TM} First-Strand cDNA Synthesis Kit (Fermentas, Glen Burnie, MD, USA) following the manufacturer's instructions. Real-time quantitative reverse transcription PCR (qRT-PCR) was performed using a Quantagene q225 system (Kubo Tech, Beijing, China). Specific primers were designed using Primer Premier 5 software (Table S1; Premier Biosoft, Palo Alto, CA, USA). The *V. vinifera* actin gene (*VvActin*, AB073011) was used as the internal control gene. Each sample had three replicates. Gene expression was calculated using the $2^{-\Delta\Delta CT}$ method (Livak and Schmittgen, 2001).

3 Results

3.1 ALA can alleviate drought stress on grapevine leaves by increasing the activity of antioxidant enzymes

The leaf morphology of 'SM' grapevine seedlings was significantly affected by drought treatment. Under drought

conditions, the leaves first wilted on the fourth day, and they were significantly withered and became yellowed on the tenth and the 16th days, respectively. The leaves were already producing significant drought symptoms. However, the Dro_ALA leaves showed only mild symptoms of drought stress (Figures 1A-C and S1). The drought-induced MDA accumulation in grapevine leaves was significantly reduced by the ALA treatment, and on the tenth day, the MDA content in Dro_ALA leaves was 28.94% lower than that in the Dro leaves (Figure 1D and Table S2). The POD activity in the Dro treatment kept increasing until the sixth day, and then it gradually decreased, while the POD activity in Dro_ALA was higher than that in the Dro treatment (Figure 1E and Table S2). The activity of SOD increased first and then decreased under drought. In the Dro_ALA treatment, the SOD activity showed the same trend as that in the Dro, which peaked on the fourth day and then decreased. However, the SOD activity in the ALA treatment group decreased more slowly (Figure 1F and Table S2). These results indicate that exogenous ALA may effectively prevent 'SM' grapevine seedlings from prolonged drought by increasing the activity of antioxidant enzymes. Moreover, on the 16th day, the symptoms of drought stress were evident, so the leaf samples of the control, Dro and Dro_ALA plants from the 16th day of treatment were collected for transcriptome and metabolome sequencing.

3.2 Mechanisms of the response of grapevine leaves to drought and ALA

The control, Dro, and Dro_ALA samples were subjected to RNA-seq and metabolome analyses (Table S3). A total of 6,326, 5,790, and 2,680 DEGs (Figure 2A) and 255, 147, and 327 DAMs (Figure 2B) were detected between the three comparison groups (control *vs.* Dro; control *vs.* Dro_ALA; and Dro *vs.* Dro_ALA). The intersection of different numbers of DEGs in each comparison is shown in Figure 2A. We demonstrated the correlation of each sample in Figures S2 and S3 and Tables S3 and S4, and we found that the DEGs significantly correlated with the DAMs (PCC) > 0.8 (Figure S4). Details of the DEGs and DAMs are shown in Tables S5-S20. A Gene Ontology (GO) analysis indicated that 'thylakoid', 'thylakoid part', 'chloroplast', and 'chloroplast part' were enriched in the control *vs.* Dro and control *vs.*

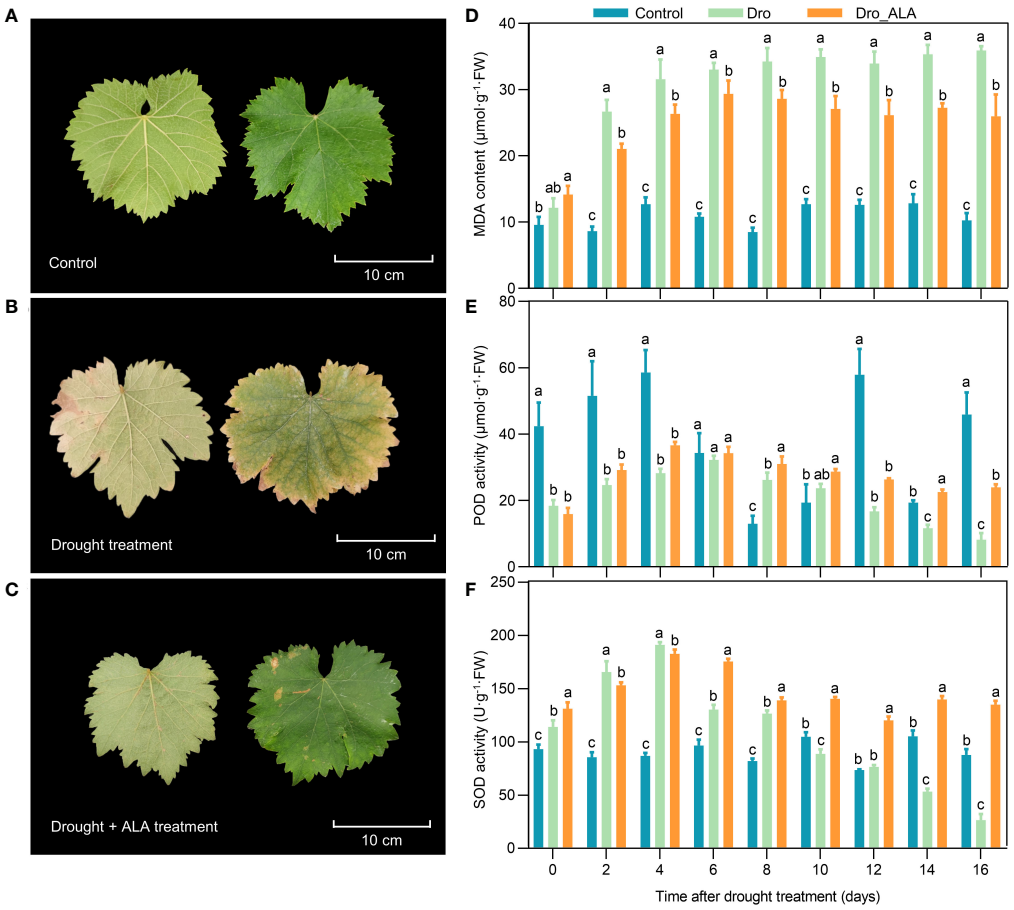

FIGURE 1
Leaf phenotype observation and physiological index determination **(A)** Leaf phenotype of control on the 16th day. **(B)** Leaf phenotype of drought treatment (Dro) on the 16th day. **(C)** Leaf phenotype of drought plus 5-aminolevulinic acid treatment (Dro_ALA) on the 16th day. **(D)** Malondialdehyde (MDA) content changes with time under control, Dro and Dro_ALA groups. **(E)** Peroxidase (POD) activity changes with time under control, Dro and Dro_ALA groups. **(F)** Superoxide dismutase (SOD) activity changes with time under control, Dro and Dro_ALA groups. In Figure 1C, the left side of each picture shows the bottom surface of the leaf, and the right side shows the top side of the leaf. Different letters in a column indicate significance of difference between treatments ($P \leq 0.05$).

10.3389/fpls.2023.1129114

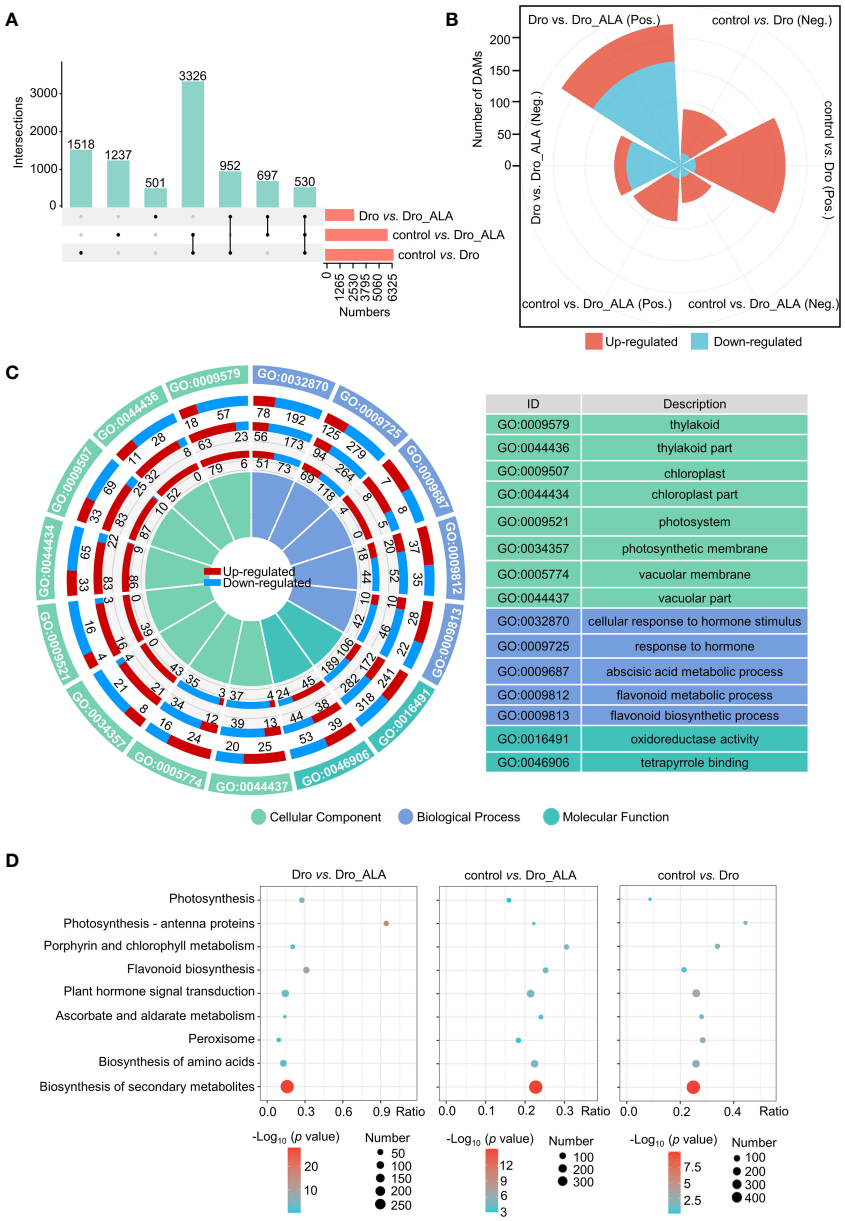

FIGURE 2
Functional annotations of total DEGs and DAMs. **(A)** Upset plot of DEGs between control and drought treatment (control *vs.* Dro); control and drought plus 5-aminolevulinic acid treatment (control *vs.* Dro_ALA); drought and drought and 5-aminolevulinic acid treatment (Dro *vs.* Dro_ALA). **(B)** Statistics of significant difference of DAMs between control *vs.* Dro, control *vs.* Dro_ALA, and Dro *vs.* Dro_ALA. The threshold of significant difference was VIP≥1 and T-test P<0.05.(Pos. means positive and Neg. means negative) **(C)** Information about key GO terms of control *vs.* Dro, control *vs.* Dro_ALA, and Dro *vs.* Dro_ALA. The first circle represents the GO ID, the second circle represents the DEGs between control *vs.* Dro, the third circle for control *vs.* Dro_ALA, and the fourth for Dro *vs.* Dro_ALA. Red and blue indicate up-regulated and down-regulated DEGs, respectively. **(D)** Information about key pathways in the KEGG enrichment pathways of control *vs.* Dro, control *vs.* Dro_ALA, and Dro *vs.* Dro_ALA.

Dro_ALA comparison group. This result suggests that drought could affect chlorophyll anabolism. In the meantime, the enrichment of 'photosystem', 'photosynthesis membrane' in the control *vs.* Dro and control *vs.* Dro_ALA indicated that photosynthesis was affected under drought stress (Figures 2C and S5; Table S17). Consistent with this, the Kyoto Encyclopedia of Genes and Genomes (KEGG) enrichment analysis of the DEGs revealed that 'porphyrin and chlorophyll metabolism', 'photosynthesis-antenna proteins,' and 'photosynthesis' were significantly enriched in the control *vs.* Dro comparison group (Figures 2D and S6; Table S18). In the control *vs.* Dro_ALA comparison group, most of the DEGs in GO terms that were related to chlorophyll metabolism and photosynthesis were upregulated (Figures 2C and S5; Table S17), indicating that ALA could play a positive role in mitigating the inhibition of photosynthesis in grapevine under drought. Furthermore, phytohormones play a role in drought tolerance, and ALA alleviates drought in grapevine. 'Response to hormone,' 'cellular response to hormone stimulus' in GO and 'plant hormone signal transduction' in KEGG were significantly enriched. Moreover, the enrichment of molecular function, such as 'oxidoreductase activity' in GO and 'peroxisome' and 'ascorbate and

aldarate metabolism' in the KEGG analysis in each comparison group showed that antioxidant systems also play a vital role in drought resistance in grapevine and the process of alleviating drought stress by ALA (Figures 2D and S6; Table S18). The KEGG analysis of the metabolome also detected enriched terms, such as the 'biosynthesis of secondary metabolism' (Figure S7 and Table S19). Moreover, qRT-PCR was used to validate the reliability of RNA-seq (Figure S8; Table S1). The function of DEGs was analyzed using MapMan software as shown in Tables S20 and S21.

3.3 ALA inhibits stomatal closure induced by abscisic acid in grapevine leaves under drought stress

In this study, the grapevine stomatal aperture was found to be significantly reduced compared with the control under drought. Although it was still smaller than the control, the stomatal aperture increased after the ALA treatment (Figures 3A, B; Table S22). In the 16th day, the stomatal aperture of control was 103.7% larger than that of Dro, while Dro_ALA was 58.4% larger than that of Dro. (Figures 3A, B, Table S22). It is a consensus that ABA induces plants to close their stomata to resist stress under drought (Bray, 1997; Buckley, 2019; Ilyas et al., 2020). The DEGs of factors associated with ABA synthase, such as neoxanthin synthase (*ABA4*, $|\log_2 FC| = 1.26$) and 9-*cis*-epoxycarotenoid dioxygenase6 (*NCED*6, $|\log_2 FC| = 3.35$) were significantly upregulated in the control *vs.* Dro comparison. Simultaneously, in the Dro treatment, the genes of factors related to the decomposition of ABA, such as abscisic acid 8'-hydroxylase (*CYP707A1*, *CYP707A2*, and *CYP707A4*), were expressed at lower levels than those in the control. This led to the accumulation of endogenous ABA under drought. In the metabolome, (S)-abscisic acid (POS_M265T406; Log_{10} content from 8.71 to 8.82) increased after drought treatment, which was consistent with the results described above. It is worth noting that the upregulation of *ABF2* ($|\log_2 FC| = 1.48$), an ABRE-binding bZIP factor, was also detected as upregulated in the control *vs.* Dro comparison, which confirmed the accumulation of ABA (Figure 3C). The downregulation of some genes, such as *ABA4* ($|\log_2 FC| = 0.53$), *NCED6* ($|\log_2 FC| = 0.41$), and *ABF2* ($|\log_2 FC| = 0.04$), were detected in the Dro *vs.* Dro_ALA comparison. Moreover, *CYP707A1* ($|\log_2 FC| = 1.79$) was significantly upregulated after the application of ALA. In the metabolome, the content of (S)-abscisic acid in Dro_ALA was lower than that of Dro (Log_{10} content from 8.82 to 8.70). These findings suggest that ALA could primarily reduce the accumulation of ABA by accelerating the degradation of ABA, thus, resulting in the re-enlargement of stomatal aperture.

3.4 ALA alleviates the inhibition of photosynthesis by drought on grapevine leaves

Phenotypic observations showed that the leaves suffered from severe chlorosis under drought (Figures 1 and S1), which could be related to the degradation of chlorophyll. In the control *vs.* Dro comparison, the level of expression of *glutamyl-tRNA reductase* (*HEMA1*) was downregulated by 31.2%, which led to the inhibition of endogenous ALA formation (Figure 3D; Table S25). Transcripts involved in the factors of protoporphyrin synthesis, such as porphobilinogen synthase (*ALAD*), porphobilinogen deaminase (*PBGD*), coproporphyrinogen III oxidase (*CPOX*), and protoporphyrinogen oxidase (*PPOX*), were all maintained at low levels of expression under drought conditions (Figure 3D; Table S25). The genes for protochlorophyllide oxidoreductase (*POR*) and divinyl chlorophyllide a 8-vinyl-reductase (*DVR*) were also downregulated in the control *vs.* Dro comparison (Figure 3D; Table S25). These results indicate that chlorophyll biosynthesis is inhibited under drought stress. In contrast, chlorophyll conjugation and degradation genes, such as the genes that encode chlorophyllide a oxygenase (*CAO*), chlorophyllase (*CLH*), magnesium dechelatase (*SGR*), and pheophorbide a oxygenase (*PAO*), were all downregulated in the control *vs.* Dro comparison. Changes in these genes led to a reduction in chlorophyll accumulation in grapevine leaves under drought (Figure 3D; Table S25). In porphyrin metabolism, an increase of L-glutamate (Log_{10} content from 8.52 to 8.85) and L-threonine (Log_{10} content from 8.52 to 8.85) were detected (Figures 3E and S9).

In this study, the application of ALA upregulated the levels of expression of genes related to chlorophyll synthesis and inhibited the levels of expression of the genes related to degradation. Compared with Dro, the levels of expression of genes, such as *HEMA1*, *ALAD*, *PBGD*, *CPOX*, and *PPOX*, all increased in Dro_ALA. Simultaneously, in the Dro *vs.* Dro_ALA comparison, *CHLH*, *CHLD*, *POR*, and *DVR* were all upregulated, indicating that the inhibition of chlorophyll synthesis was relieved. Moreover, the downregulation of *CLH*, *SGR*, *PPH*, and *PAO* was detected in Dro *vs.* Dro_ALA, which resulted in the inhibition of chlorophyll degradation (Figure 3D; Table S25). In the metabolome, the contents of L-glutamate (Log_{10} content from 8.85 to 8.72) and biliverdin (Log_{10} content from 7.91 to 8.11) increased, while those of heme (Log_{10} content from 7.67 to 6.80) and L-threonine (Log_{10} content from 8.79 to 8.39) decreased (Figures 3E and S9). These combined effects resulted in an increase in chlorophyll synthesis and a decrease in chlorophyll degradation after the application of ALA.

The photosynthetic electron transport chains were also inhibited under drought. A comparison of Dro to the Control showed that approximately 66% DEGs that are involved in photosynthesis were downregulated (Figure 3F; Table S24). Eight of the 14 DEGS related to photosystem II were downregulated in the Control *vs.* Dro comparison. Most of them were associated with the LHC-II complex and PSII assembly and maintenance. The functions of cytochrome b6/f complex, photosystem I, and ATP synthase complex were also inhibited, and the corresponding three, five and one DEGs detected in the control *vs.* Dro, respectively, were all downregulated. Furthermore, seven of the DEGs related to the NADH dehydrogenases were downregulated in the control *vs.* Dro. As a vital enzyme in the Calvin cycle, the activity of Rubisco was also inhibited under drought. This could be owing to the downregulation of DEGs related to the CPN20 auxiliary co-chaperone (*CPN20*, $|\log_2 FC| = 7.21$) and BSD2 assembly factor (*BSD2*). The downregulation of genes described above resulted in

10.3389/fpls.2023.1129114

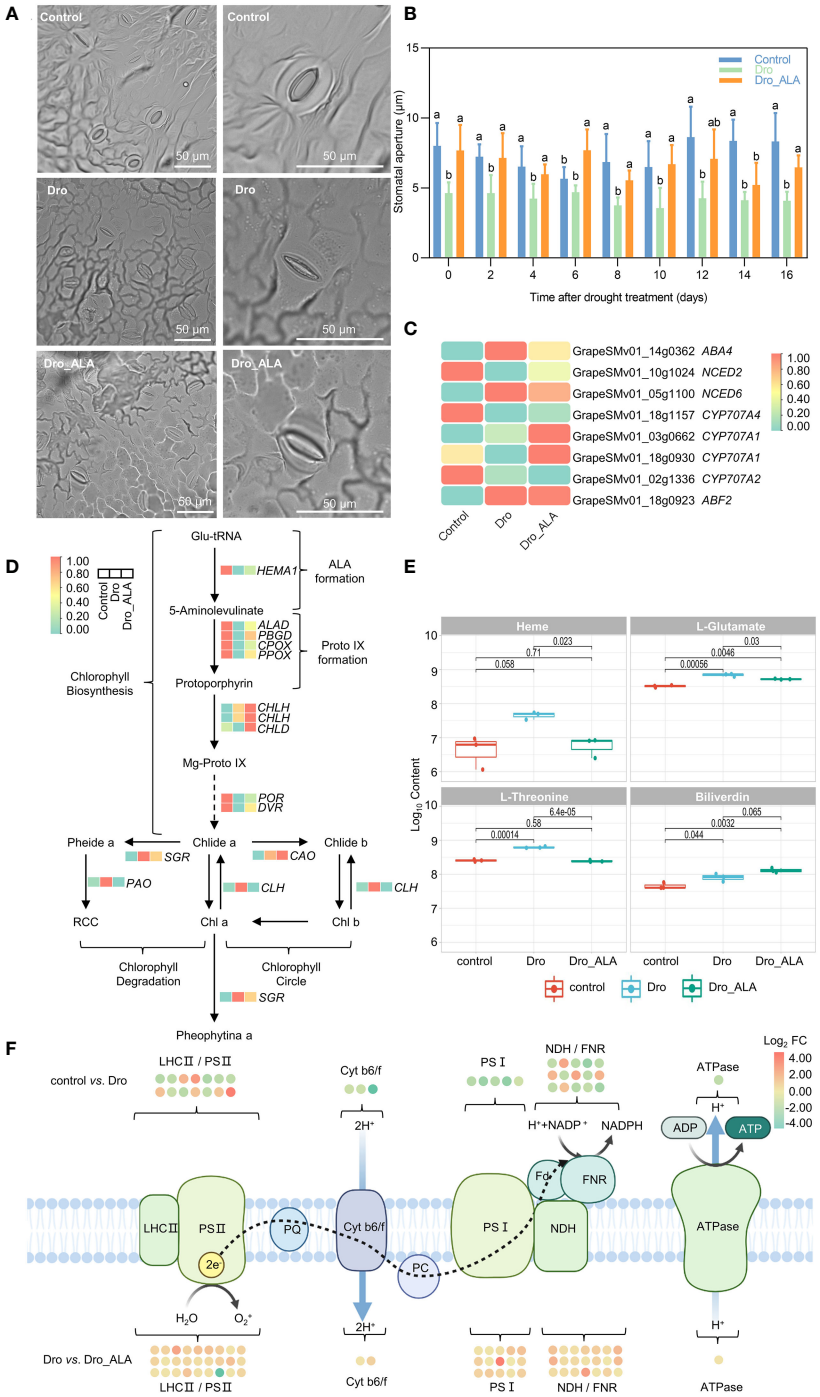

FIGURE 3
Stomatal movement, chlorophyll metabolism and photosynthesis in grapevine leaves under drought stress and drought plus ALA treatment. **(A)** Stomatal aperture observation of control, drought treatment (Dro), and drought plus 5-aminolevulinic acid treatment (Dro_ALA) on the 16th day (via upright fluorescent microscope). **(B)** Variation of stomatal aperture with drought treatment time. **(C)** Key DEGs related to phytohormones action between control *vs.* Dro, control *vs.* Dro_ALA, and Dro *vs.* Dro_ALA. **(D)** Pathway of chlorophyll metabolism and key genes in grapevine under drought stress and drought plus 5-aminolevulinic acid treatment. Arrows (↑) and (↓) indicate up-regulation and down-regulation, respective. Red indicates the control vs. Dro comparison group and blue indicates the Dro vs. Dro_ALA comparison group. **(E)** Key metabolites in chlorophyll metabolism pathway under control, Dro and Dro_ALA treatments. **(F)** Effects of drought and drought plus 5-aminolevulinic acid on photosynthesis. Each dots represents a DEG, green and red indicate up-regulation and down-regulation, respectively. Different letters indicate significant differences among experimental groups ($p < 0.05$).

a significant decrease in the photosynthetic efficiency under drought stress. Moreover, the DEGs related to glycolate oxidase (*GLO1*), glutamate-glyoxylate transaminase (*GGAT2*), and serine-glyoxylate transaminase (*AGT1*) were all maintained at high levels of expression in Dro, which resulted in enhanced photorespiration (Table S20). This could further weaken photosynthesis.

In the Dro *vs.* Dro_ALA comparison, only two of 82 DEGs related to photosynthesis were downregulated, and most of them

were also downregulated in the control *vs.* Dro treatment (Figure 3F; Table S24). Changes in the DEGs associated with PSII (26 upregulated and one downregulated), cytb6/f complex (four upregulated), PSI (15 upregulated), ferredoxin electron carrier (one upregulated), ferredoxin $NADP^+$ oxidoreductase (FNR) (three upregulated), NDH complex (17 upregulated) and ATP synthase complex (one upregulated) were detected (Table S24). A significant upregulation of the DEGs related to the activity, assembly, and regulation of Rubisco, such as *CPN60B4*, *RBCX1*, *RBCX2*, *BSD2*, and *RCA*, was detected after ALA treatment, indicating that the inhibition of Rubisco under drought was relieved. Moreover, treatment with ALA led to upregulation of the genes that encoded serine-glyoxylate transaminase (*AGT1*), glycine dehydrogenase component P-protein of the glycine cleavage system (*GDCSP*), aminomethyl transferase component T-protein of the glycine cleavage system (*GDCST*), and lipoamide-containing component H-protein of the glycine cleavage system (*GDCSH*), which indicated that ALA reduces photorespiration, and thus, alleviates drought stress (Table S21).

3.5 ALA alleviates oxidative stress in grapevine leaves

In this study, the upregulation of NADPH oxidase (*RBOHA*, 21.52-29.21 fragments per kilobase of transcripts per million mapped reads [FPKM]) related to ROS generation was detected in the control *vs.* Dro comparison, indicating that there is a mass production of ROS under drought stress (Table S26). Drought inhibited the expression of some genes related to antioxidant scavenging. For example, the DEGs related to iron superoxide dismutase (*FSD3* and *FSD2*) and copper/zinc superoxide dismutase (*SODCP*) were significantly downregulated (Figure 4C; Table S26). The genes of some low-molecular weight scavengers, such as phosphomannose isomerase (*PMI*), related to the biosynthesis of ascorbate also showed a similar trend. The α-, β-, γ-, and δ-forms of tocopherol are active antioxidants that are primarily located in chloroplast membranes where they detoxifying singlet oxygen and lipid peroxy radicals (Munné-Bosch, 2005). In the control *vs.* Dro comparison group, the genes related to tocopherol biosynthesis, such as *VTE1* and *VTE3*, were both downregulated (Figure 4B and Table S26). As expected, the levels of α-tocopherol and ascorbate were indeed decreased in the metabolome (Figure S10; Table S27). In the ascorbate-glutathione cycle, the level of expression of the gene related to ascorbate peroxidase (*APX*, 20.97 to 6.46 FPKM) was also suppressed. The chloroplast redox homeostasis was disrupted under drought stress, which could inhibit the photosynthesis of grapevine leaves even further. DEGs related to typical 2-Cys peroxiredoxin (*2-CysPrx*), atypical 2-Cys peroxiredoxin (*PrxQ*), M-type thioredoxin (*TRM*) and atypical thioredoxin (*ACHT*) maintained low levels of expression. Simultaneously, the levels of monodehydroascorbate reductase (*MDHAR*, 29.26 to 31.50 FPKM) in the ascorbic acid-glutathione (AsA-GSH) cycle and γ-glutamyl cysteine ligase (GSH) associated with glutathione biosynthesis were upregulated. The DEGs related to catalase (*CAT*, 305.9 to 747.97 FPKM), glutathione peroxidase (*GPX6*, 238.037 to 429.523 FPKM), and type-2 peroxiredoxin (*PrxII*) showed the same trend (Figure 4C; Table S26). In contrast, the DEGs associated with glutathione degradation, such as glutathione reductase (*GR*, 92.6 to 77.30 FPKM), γ-glutamyl cyclotransferase (*GGCT*), oxoprolinase (*OXP*), and dehydroascorbic acid reductase (*DHAR*, 42.34 to 26.08 FPKM), were downregulated (Figure 4C and Table S26). This could indicate that the glutathione content was increased to remove the ROS. Together, changes in the genes described above led to the accumulation of intracellular ROS, which caused drought oxidative stress. The metabolome data were consistent with the results described above and showed that the contents of glutathione, L-cysteine and oxidized glutathione increased (Figure S10; Table S27).

The application of ALA inhibited the generation of ROS, *RBOHA*, *RBOHB*, and *RBOHC*, which were all downregulated in the Dro *vs.* Dro_ALA comparison group (Table S26). ALA could enhance the function of ROS scavenging system in grapevine under drought stress. A comparison of Dro with Dro_ALA showed that *FSD3*, *FSD2* and *SODCP* restored upregulation (Figure 4C; Table S26). In addition, the upregulation of *VTE1* and *VTE3* indicated that tocopherol was resynthesized, and the content of α-tocopherol increased in the metabolome (Figure S10 and Table S27). In the AsA-GHS cycle, ascorbate peroxidase (*APX*) and glutathione peroxidase (*GPX8*), and the genes related to type-2 peroxiredoxin (*PrxII*) all tended to be downregulated after application with ALA (Figure 4C; Table S26). This suggests that the drought stress was easing. The effect of ALA on photosynthesis was shown in the recovery of chloroplast redox homeostasis, and the genes of atypical 2-Cys peroxiredoxin (*PrxQ*), M-type thioredoxin (*TRM1*), and atypical thioredoxin (*ACHT*) were significantly upregulated. These processes reduce the production of ROS and ease the cellular damage caused by drought stress. In the metabolome of the Dro *vs.* Dro_ALA comparison group, the contents of glutathione and ascorbate decreased (Figure S10; Table S27). Changes in the genes and metabolites described above suggest that ALA does alleviate the oxidative stress caused by drought.

3.6 Osmotic regulation under drought stress

OA has often been considered to be a key mechanism of the resistance of plants to drought stress (Serraj and Sinclair, 2002). Proline has long been thought to accumulate in plants that experience water restriction (Verslues and Sharma, 2010). Pyrroline-5-carboxylate synthetase (*PRO2*, 52.19 to 202.07 FPKM), ornithine aminotransferase (*OAT*, 15.88 to 60.90 FPKM) and PHR1 transcription factor (*PHR1*, 3.61 to 13.42 FPKM) involved in the regulation of proline synthesis were significantly upregulated in the Control *vs.* Dro comparison group (Table S28). Consistent with this result, increased levels of L-proline were detected in the metabolome (Figure 4D; Table S29). As a quaternary ammonium compound, betaine (N, N, N-trimethyl glycine) is also a vital solute involved in osmotic regulation. Betaine aldehyde dehydrogenase (BADH) catalyzes the conversion of betaine aldehyde to betaine (Weretilnyk and Hanson, 1990). *BADH4* associated with BADH tended to be

10.3389/fpls.2023.1129114

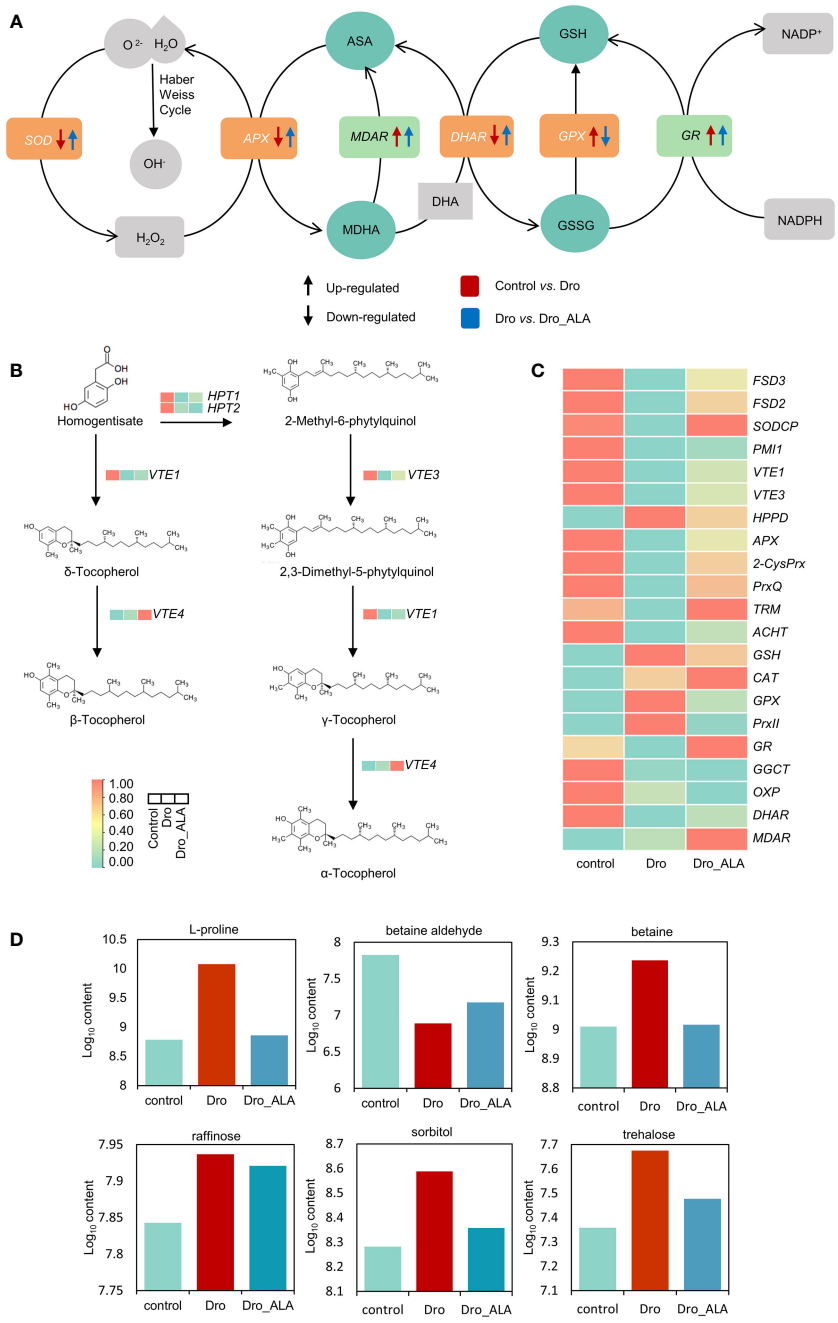

FIGURE 4
Cellular homeostasis under drought treatment and drought plus ALA treatment. **(A)** AsA-GSH cycle of grapevine leaves under drought stress and drought plus 5-aminolevulinic acid treatments, Arrows (↑) and (↓) represent up-regulation and down-regulation, respectively. Red and blue represent control *vs.* Dro and Dro *vs.* Dro_ALA groups, respectively. **(B)** Biosynthesis of tocopherol in grapevine leaves under control, under drought stress and drought plus 5-aminolevulinic acid treatments. Red and green represent higher and lower expression, respectively. **(C)** Information of DEGs related to antioxidant system of grapevine in control, Dro and Dro _ALA. **(D)** Information of important DAMs related to osmotic regulation and autophagy of grapevine in control, Dro and Dro _ALA. (Dro represents drought treatment; Dro_ALA represents drought plus 5-aminolevulinic acid treatment).

upregulated after drought stress, and this corresponded to a significant decrease in the contents of betaine aldehyde and an increase in the content of betaine in the metabolome (Figure 4D; Table S29). The contents of some soluble sugars and sugar alcohol also changed. For example, trehalose, raffinose, and sorbitol were all elevated under water deficiency (Figure 4D; Table S29). A sharp decrease in proline content (Log_{10} content from 10.08 to 8.86) was detected in the metabolome of Dro *vs.* Dro_ALA comparison group, which was caused by the downregulation of *PRO2* (202.07 to 101.14 FPKM), *OAT* (60.90 to 33.71 FPKM), and *PHR1* (13.42 to 7.64 FPKM). In this study, *BADH4* was downregulated, which resulted in an increase in betaine aldehyde, and a decrease in betaine (Figure 4D; Tables S28 and 29). The decrease in the contents of soluble sugars and sugar alcohols also indicated that

drought stress tended to be alleviated after the application of ALA. The contents of raffinose, sorbitol, and trehalose all decreased in the Dro *vs*. Dro_ALA comparison group (Figure 4D; Table S29). These results indicate that the cell homeostasis tends to moderate.

4 Discussion

4.1 ALA uses multiple synergistic mechanisms to alleviate drought stress

Exogenous plant growth regulators are widely used to alleviate drought stress in grapevine. For example, exogenous melatonin can improve the resistance of wine grape 'Riesling' seedlings to water deficiency by alleviating PSII damage and protecting the chloroplasts (Meng et al., 2014). The application of exogenous 24-epibrassinolide (EBR) has also been shown to alleviate the inhibition of drought stress on grape photosynthesis by increasing the content of chlorophyll and alleviating stomatal and non-stomatal limitations on photosynthetic performance (Wang et al., 2015). Consistent with this, ALA alleviates the stomatal closure caused by drought and thus, moderates the decrease in photosynthesis to some extent (Figures 3A, B; Table S22). As a precursor of chlorophyll biosynthesis, ALA can directly increase chlorophyll synthesis and inhibit chlorophyll degradation under drought stress (Figure 3D). The inhibition of photosynthetic electron transport chain was also relieved by ALA under drought (Figure 3F). This also impacted the genes related to Rubisco and alleviated photorespiration (Table S24). Exogenous growth regulators can also alleviate the imbalance of grapevine cell homeostasis caused by drought stress. Strigolactones upregulate the antioxidant enzyme genes *CAT1* and *APX6* to alleviate drought stress in 'Cabernet Sauvignon' seedlings (Wang et al., 2021b). The application of ABA increases the contents of proline and soluble sugars and the activities of SOD and POD in 'Red Globe' grape. ALA mitigated drought in a manner similar to that of the study described above. In this study, the application of exogenous ALA reduced the contents of MDA and inhibited the production of ROS in 'SM' seedlings under drought, activated antioxidant system by upregulating *FSD* and *SODCP* and increased the content of α-tocopherol and other non-enzymatic antioxidant scavengers (Figure 4C, D). Therefore, this study provides a novel idea for ALA to alleviate grapevine drought stress.

4.2 Mitigating effects of ALA on grapevine photosynthesis under drought stress

The formation of ALA is a rate-limiting step in chlorophyll biosynthesis (Beale, 1990), and many studies (Kosar et al., 2015; Wang et al., 2018; Rasheed et al., 2020) have shown that ALA enhances the resistance of plants to drought stress by enhancing photosynthesis. For example, pretreatment with ALA increases stomatal conductance and thus, stabilizes photosynthesis in wheat under drought. Rasheed et al. (2020) demonstrated that ALA alleviates the drought stress of sunflower (*H. annuus* L.) by protecting chlorophyll from degradation. The exogenous application of ALA alleviates drought stress by enhancing the chlorophyll pigments of spring wheat seedlings. However, these studies are based on physiological indicators, and the changes in genes and metabolites during drought were unclear. In our study, ALA treatment significantly increased the stomatal aperture during drought (Figure 3A, B; Table S22). ALA leads to an increase in the level of expression of *CYP707A1* under drought, which reduces the content of ABA and leads to further stomatal opening (Figure 3C). In addition, ROS are important signals that regulate stomatal closure (Song et al., 2014), our study shows that the antioxidant system reduces ROS production after ALA application, which may also lead to stomatal reopening, but the specific mechanism is still unclear. GSH plays a role in stomatal movement, it is generally believed that increased GSH content leads to stomatal opening. For example, studies on the negative regulation of glutathione in *Arabidopsis* thaliana on stomatal closure induced by methyl jasmonate have been reported (Akter et al., 2013). In this study, although we detected stomatal opening caused by ALA, GSH content decreased after application of ALA, which was inconsistent with the above study. We hypothesized that GSH did not play a major role in ROS reduction and stomatal opening after ALA application. Although the inhibition of water lost by transpiration that is limited by the closure of stomata induced by ABA is an important mechanism to improve drought tolerance in plants (Li et al., 2006), a previous study indicated that the closure of stomata induced by ABA does not increase plant sensitivity to drought stress (An et al., 2016). In this study, we hypothesized that during mild drought, the positive effect of stomatal opening and enhancing photosynthesis by ALA was greater than the negative effect of water loss caused by transpiration. Nevertheless, the molecular mechanisms behind the paradox between the prohibition of stomatal opening and an enhancement of drought tolerance merits further study. As for non-stomatal factors, first, after the application of ALA, genes related to chlorophyll synthesis, such as *HEMA1*, *ALAD*, PBGD, *CPOX*, and *PPOX*, were significantly upregulated, while the levels of expression of *CLH*, *SGR*, *PPH*, and *PAO* were downregulated, which resulted in the inhibition of chlorophyll degradation (Figure 3D and Table S25). Consistent with the DEGs, the contents of L-glutamate and biliverdin increased, while those of heme and L-threonine decreased. These changes in the genes and metabolites together serve as the basis for ALA to alleviate the loss of chlorophyll in grape leaves under drought (Figures 3D, E and S9). It is worth mentioning that the relation between porphyrin metabolism and the content of L-glutamate and L-threonine is not well followed. Our data support the results that the above metabolites are related to porphyrin and chlorophyll metabolism, the specific mechanisms are still meriting further study. Furthermore, Cai et al. (2020) found that spraying 10 mg/L ALA on the leaves alleviated the reduction in the activities of PSI and PSII reaction centers induced by PEG 6000, electron transport activity, and photosynthetic performance indices in strawberry (*Fragaria* × *annanasa* Duch. cv. 'Benihoppe'). The transcriptomic data showed that ALA upregulated the genes related to PSII and those related to the cytochrome B6/F complex in plants that had been subjected to drought stress (Figure 3F), which was consistent with our conclusions above. Notably, ALA treatment alleviates drought stress by upregulating the levels of expression of *AGT1*, *GDCSP*, *GDCST* and *GDCSH*, and thus, reducing

photorespiration. To our knowledge, this concept has not been mentioned in other papers. Therefore, we hypothesize that ALA enhances photosynthesis and reduces photorespiration by promoting chlorophyll accumulation and alleviating the inhibition of photosynthetic electron transport chain, thus, alleviating drought stress. However, the specific photosynthetic indices related to this effect still merit further study and determination.

4.3 Effects of ALA on grapevine cell homeostasis under drought stress

There is a consensus that drought causes an imbalance in plant cell homeostasis. It has been reported that the foliar application of 3 μM ALA can not only increase the activities of SOD, CAT, GPX, GSH-Px, APX, DHAR, MDHAR, and GR but also increase the contents of AsA and GSH in cucumber (*Cucumis sativus* L.) under drought (Li et al., 2011). Similarly, we found that treatment with ALA significantly increased the activities of POD and SOD activities in 'SM' leaves over time. Furthermore, treatment with ALA upregulated antioxidant enzymes, such as *FSD*, *SODCP*, *APX*, *MDAR*, *DHAR*, and *GR*, under drought (Figure 4C), which could explain the increase in ALA antioxidant enzyme activity from a genetic perspective. In contrast to the results of the study described above, we found that the application of ALA reduced the levels of AsA and GSH in the metabolome (Figures 4A and S10). This could be owing to different results observed when different concentrations of ALA were sprayed in different types of drought mitigation. OA is a fundamental mechanism of drought adaptation in higher plants (Sanders and Arndt, 2012), Ji-Xuan et al. (2017) suggested that 50 mg L^{-1} of ALA could increase the contents of soluble proteins and the sugars and proline of Chinese ryegrass (*Leymus chinensis* [Trin.] Tzvel) to alleviate drought stress (Song et al., 2017). In the metabolome, we found that spraying ALA caused a sharp decrease in the contents of proline in grapevine leaves, which was caused by the downregulation of *PRO2*, *OAT*, and *PHR1*. In contrast to that study, the contents of raffinose, sorbitol, and trehalose all decreased after the application of ALA (Figure 4D) and alternatively, they were involved in the alleviation of drought by ALA. Autophagy plays an important role in the resistance of plants to drought stress (Tang and Bassham, 2022). Nevertheless, no study has reported that ALA alleviates drought stress by affecting autophagy. We found that many autophagy-related genes (ARGs) were highly expressed in the transcriptome of control *vs.* Dro comparison group, only one out of seven key ARGs that were identified were downregulated (Table S28). Among them, *ATG11* and *ATG2* were DEGs that play an important role in drought response. *ATG8F*, *ATG8I* and *ATG8C* were also expressed at high levels. After ALA treatment, the ARGs detected in the control *vs.* Dro comparison group were all downregulated (Table S28). Owing to the lack of direct experimental evidence, we anticipate that there will be subsequent studies on whether ALA affects plant drought tolerance by affecting autophagy. Nonetheless, our study interpreted the role of ALA in the maintenance of grapevine cell homeostasis

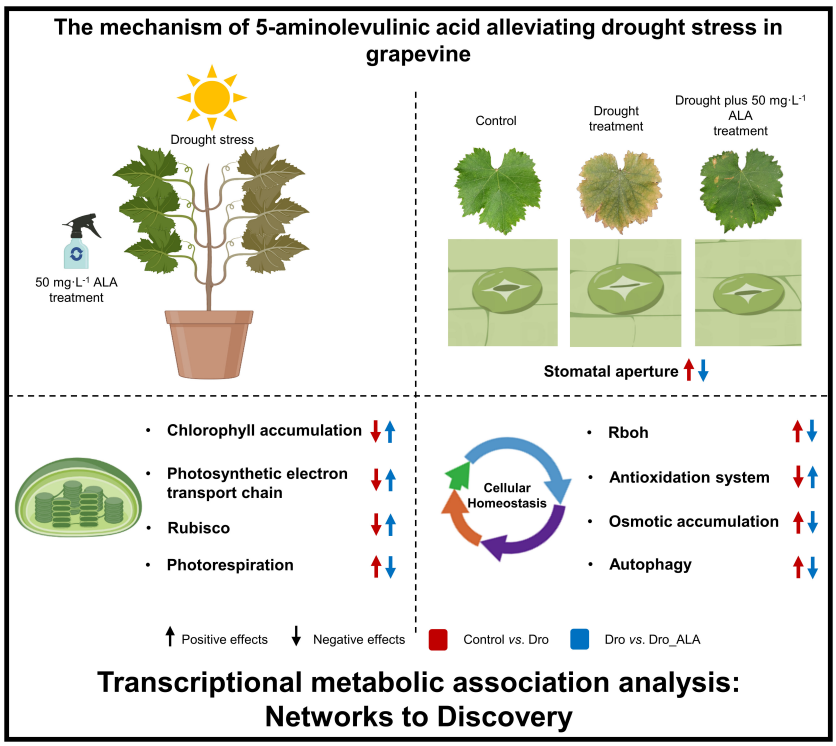

FIGURE 5
Regulation network of 5-aminolevulinic acid to mitigate drought stress in grapevine.

under drought from the perspectives of genes and metabolites, and it was our goal that this study could provide some ideas for future studies on the mitigation of abiotic stress by ALA.

5 Conclusion

In this study, we confirmed that ALA can mitigate drought stress in grapevine. Stomatal movement, the chlorophyll biosynthetic pathway, metabolic pathway, photosynthetic mechanism, and cellular homeostasis constitute the basis of ALA's regulatory network for alleviating drought stress. First, the application of ALA upregulated the genes related to ABA degradation, thus, inhibiting the stomatal closure induced by ABA, which alleviates the inhibition of drought on photosynthesis to some extent. The current data indicate that the DEGs associated with chlorophyll biosynthesis, such as *HEMA1*, *ALAD*, *PBGD*, *CPOX*, *PPOX, CHLH*, *CHLD*, *POR*, and *DVR*, were upregulated after ALA treatment, while the chlorophyll degradation genes *CLH*, *SGR*, *PPH*, and *PAO*, were downregulated, thus, mitigating the inhibition of chlorophyll accumulation caused by drought. ALA treatment also alleviated the inhibition of photosynthetic electron transport chain by drought. The genes related to Rubisco activity were upregulated by ALA, and photorespiration was attenuated. ALA down-regulated *RBOH*, thus, reducing the production of ROS and activating the antioxidant system, which changed the contents of antioxidants, such as tocopherol, ascorbate, and glutathione, to reduce the oxidative damage induced by ROS. *FSD* and *SODCP* were also restored to high levels of expression after the application of ALA. In addition, the decrease in the contents of betaine, raffinose, sorbitol and trehalose indicated that the degree of drought stress was reduced after the ALA had been applied. Therefore, this study explains the regulatory network of ALA to mitigate drought stress in grapevine (Figure 5) and provides a new concept to study the regulatory network of grapevine drought stress and apply plant growth regulators to alleviate other abiotic stresses.

Data availability statement

The datasets presented in this study can be found in online repositories. The names of the repository/repositories and accession number(s) can be found below: https://www.ncbi.nlm.nih.gov/, PRJNA769649.

Author contributions

YY wrote the original draft of the manuscript, managed and formalized the data. YY, JX, XF and HJ conducted the experiment. YY and YL carried out statistical analysis. JF and SL provided funds. XW, MG, SL, YP and XF polished the manuscript. All authors contributed to the article and approved the submitted version.

Funding

This project was funded by the National Key Research and Development Project [grant number: 2018YFD1000300], Natural Science Foundation of Jiangsu Province [grant number: BK20201321], Jiangsu Agricultural Science and Technology Innovation Fund [grant number: CX(21)2027], National Natural Science Foundation of China [grant number: 31772283], Postdoctoral Research Fund Project of Jiangsu Province [grant number: 2020Z052], the Fundamental Research Funds for the Central Universities [grant number: KYLH201903], Priority Academic Program Development of Jiangsu Higher Education Institutions (PAPD), and President's Foundation of Tarim University [grant number: NMLH201902].

Acknowledgments

We thank the Bioinformatics Center at Nanjing Agricultural University for computational support.

Conflict of interest

The authors declare that the research was conducted in the absence of any commercial or financial relationships that could be construed as a potential conflict of interest.

Publisher's note

Supplementary material

The Supplementary Material for this article can be found online at: https://www.frontiersin.org/articles/10.3389/fpls.2023.1129114/full#supplementary-material

References

Akter, N., Okuma, E., Sobahan, M. A., Uraji, M., Munemasa, S., Nakamura, Y., et al. (2013). Negative regulation of methyl jasmonate-induced stomatal closure by glutathione in arabidopsis. *J. Plant Growth Regul.* 32 (1), 208–215. doi: 10.1007/s00344-012-9291-7

An, Y., Liu, L., Chen, L., and Wang, L. (2016). ALA inhibits ABA-induced stomatal closure *via* reducing H_2O_2 and Ca^{2+} levels in guard cells. *Front. Plant Sci.* 7. doi: 10.3389/fpls.2016.0048

Beale, S. I. (1990). Biosynthesis of the tetrapyrrole pigment precursor, δ-aminolevulinic acid, from glutamate. *Plant Physiol.* 93 (4), 1273–1279. doi: 10.1104/pp.93.4.1273

Beauchamp, C., and Fridovich, I. (1971). Superoxide dismutase: improved assays and an assay applicable to acrylamide gels. *Analytical Biochem.* 44 (1), 276–287. doi: 10.1016/0003-2697(71)90370-8

Bota, J., Medrano, H., and Flexas, J. (2004). Is photosynthesis limited by decreased rubisco activity and RuBP content under progressive water stress? *New Phytol.* 162 (3), 671–681. doi: 10.1111/j.1469-8137.2004.01056.x

Bray, E. A. (1997). Plant responses to water deficit. *Trends Plant Sci.* 2 (2), 48–54. doi: 10.1016/S1360-1385(97)82562-9

Buckley, T. N. (2019). How do stomata respond to water status? *New Phytol.* 224 (1), 21–36. doi: 10.1111/nph.15899

Bylesjö, M., Eriksson, D., Kusano, M., Moritz, T., and Trygg, J. (2007). Data integration in plant biology: the O2PLS method for combined modeling of transcript and metabolite data. *Plant J.* 52 (6), 1181–1191. doi: 10.1111/j.1365-313X.2007.03293.x

Cai, C., He, S., An, Y., and Wang, L. (2020). Exogenous 5-aminolevulinic acid improves strawberry tolerance to osmotic stress and its possible mechanisms. *Physiologia Plantarum* 168 (4), 948–962. doi: 10.1111/ppl.13038

Chaves, M., Zarrouk, O., Francisco, R., Costa, J., Santos, T., Regalado, A., et al. (2010). Grapevine under deficit irrigation: hints from physiological and molecular data. *Ann. Bot.* 105 (5), 661–676. doi: 10.1093/aob/mcq030

Chen, S., Zhou, Y., Chen, Y., and Gu, J. (2018). Fastp: an ultra-fast all-in-one FASTQ preprocessor. *Bioinformatics* 34 (17), i884–i890. doi: 10.1093/bioinformatics/bty560

Cornic, G., and Massacci, A. (1996). Leaf photosynthesis under drought stress. In: N. R. Baker (eds) *Photosynthesis and the environment*. Dordrecht: Springer. 5. doi: 10.1007/0-306-48135-9_14

Csardi, G., and Nepusz, T. (2006). The igraph software package for complex network research. *InterJournal Complex Syst.* 1695 (5), 1–9.

Fang, Y., and Xiong, L. (2015). General mechanisms of drought response and their application in drought resistance improvement in plants. *Cell. Mol. Life Sci.* 72 (4), 673–689. doi: 10.1007/s00018-014-1767-0

Fanizza, G., and Ricciardi, L. (2015). Influence of drought stress on shoot, leaf growth, leaf water potential, stomatal resistance in wine grape genotypes (*Vitis vinifera* l.). *VITIS-Journal Grapevine Res.* 29, 371. doi: 10.5073/vitis.1990.29.special-issue.371-381

Farooq, M., Hussain, M., Wahid, A., and Siddique, K. H. M. (2012). Drought Stress in Plants: An Overview. In: Aroca, R. (eds) *Plant Responses to Drought Stress*. Springer, Berlin, Heidelberg. doi: 10.1007/978-3-642-32653-0_1

Farooq, M., Wahid, A., Kobayashi, N., Fujita, D., Basra, S. M. A., Lichtfouse, E., et al. (2009). "Plant Drought Stress: Effects, Mechanisms and Management," in *Sustainable Agriculture*, eds. E. Lichtfouse, M. Navarrete, P. Debaeke, S. Véronique and C. Alberola. (Dordrecht: Springer Netherlands), 153–188. doi: 10.1007/978-90-481-2666-8_12

Gambetta, G. A., Herrera, J. C., Dayer, S., Feng, Q. S., Hochberg, U., and Castellarin, S. D. (2020). The physiology of drought stress in grapevine: towards an integrative definition of drought tolerance (vol 71, pg 4658, 2020). *J. Exp. Bot.* 71 (18), 5717–5717. doi: 10.1093/jxb/eraa245

Hasanuzzaman, M., Nahar, K., Gill, S. S., and Fujita, M. (2013). Drought stress responses in plants, oxidative stress, and antioxidant defense. In *Climate Change and Plant Abiotic Stress Tolerance* (eds N. Tuteja and S. S. Gill). 209–250. doi: 10.1002/9783527675265.ch09

Hodgins, R., and Van Huystee, R. (1986). Porphyrin metabolism in chill stressed maize (*Zea mays* l.). *J. Plant Physiol.* 125 (3-4), 325–336. doi: 10.1016/S0176-1617(86)80154-7

Huang, Y., Liang, D., Xia, H., Lin, L. J., Wang, J., and Lv, X. L. (2020). Lignin and quercetin synthesis underlies berry russeting in 'Sunshine muscat' grape. *Biomolecules* 10 (5), 690. doi: 10.3390/biom10050690

Hussain, M., Malik, M. A., Farooq, M., Khan, M. B., Akram, M., and Saleem, M. F. (2009). Exogenous glycinebetaine and salicylic acid application improves water relations, allometry and quality of hybrid sunflower under water deficit conditions. *J. Agron. Crop Sci.* 195 (2), 98–109. doi: 10.1111/j.1439-037X.2008.00354.x

Ilyas, M., Nisar, M., Khan, N., Hazrat, A., Khan, A. H., Hayat, K., et al. (2020). Drought tolerance strategies in plants: A mechanistic approach. *J. Plant Growth Regul.* 40, 1–19. doi: 10.1007/s00344-020-10174-5

Jaillon, O., Aury, J. M., Noel, B., Policriti, A., Clepet, C., Casagrande, A., et al. (2007). The grapevine genome sequence suggests ancestral hexaploidization in major angiosperm phyla. *Nature* 449 (7161), 463–467. doi: 10.1038/nature06148

Ji-Xuan, S., Anjum, S., Zong, X., Yan, R., Wang, L., Yang, A., et al. (2017). "Combined foliar application of nutrients and 5-aminolevulinic acid (ALA) improved drought tolerance in leymus chinensis by modulating its morpho-physiological characteristics. *Crop Pasture Sci.* 68, 474–482. doi: 10.1071/CP16187

Kosar, F., Akram, N., and Ashraf, M. (2015). Exogenously-applied 5-aminolevulinic acid modulates some key physiological characteristics and antioxidative defense system in spring wheat (*Triticum aestivum* l.) seedlings under water stress. *South Afr. J. Bot.* 96, 71–77. doi: 10.1016/j.sajb.2014.10.015

Laxa, M., Liebthal, M., Telman, W., Chibani, K., and Dietz, K.-J. (2019). The role of the plant antioxidant system in drought tolerance. *Antioxidants* 8 (4), 94. doi: 10.3390/antiox8040094

Li, S., Assmann, S. M., and Albert, R. (2006). Predicting essential components of signal transduction networks: a dynamic model of guard cell abscisic acid signaling. *PloS Biol.* 4 (10), e312. doi: 10.1371/journal.pbio.0040312

Li, D. M., Zhang, J., Sun, W. J., Li, Q., Dai, A. H., and Bai, J. G. (2011). 5-aminolevulinic acid pretreatment mitigates drought stress of cucumber leaves through altering antioxidant enzyme activity. *Scientia Hortic.* 130 (4), 820–828. doi: 10.1016/j.scienta.2011.09.010

Little, K., Metelerkamp, B., and Smith, C. (1998). A comparison of three methods of soil water content determination. *South Afr. J. Plant Soil* 15 (2), 80–89. doi: 10.1080/02571862.1998.10635121

Livak, K. J., and Schmittgen, T. D. (2001). Analysis of relative gene expression data using real-time quantitative PCR and the $2^{-\Delta\Delta CT}$ method. *methods* 25 (4), 402–408. doi: 10.1006/meth.2001.1262

Lovisolo, C., Lavoie-Lamoureux, A., Tramontini, S., and Ferrandino, A. (2016). Grapevine adaptations to water stress: new perspectives about soil/plant interactions. *Theor. Exp. Plant Physiol.* 28 (1), 53–66. doi: 10.1007/s40626-016-0057-7

Memon, S. A., Hou, X., Wang, L., and Li, Y. (2009). Promotive effect of 5-aminolevulinic acid on chlorophyll, antioxidative enzymes and photosynthesis of pakchoi (*Brassica campestris* ssp. *chinensis* var. communis tsen et Lee). *Acta Physiologiae Plantarum* 31 (1), 51. doi: 10.1007/s11738-008-0198-7

Meng, J. F., Xu, T. F., Wang, Z. Z., Fang, Y. L., Xi, Z. M., and Zhang, Z. W. (2014). The ameliorative effects of exogenous melatonin on grape cuttings under water-deficient stress: antioxidant metabolites, leaf anatomy, and chloroplast morphology. *J. Pineal Res.* 57 (2), 200–212. doi: 10.1111/jpi.12159

Moran, J. F., Becana, M., Iturbe-Ormaetxe, I., Frechilla, S., Klucas, R. V., and Aparicio-Tejo, P. (1994). Drought induces oxidative stress in pea plants. *Planta* 194 (3), 346–352. doi: 10.1007/BF00197534

Munné-Bosch, S. (2005). The role of α-tocopherol in plant stress tolerance. *J. Plant Physiol.* 162 (7), 743–748. doi: 10.1016/j.jplph.2005.04.022

Phung, T.-H., Jung, H.-i., Park, J.-H., Kim, J.-G., Back, K., and Jung, S. (2011). Porphyrin biosynthesis control under water stress: sustained porphyrin status correlates with drought tolerance in transgenic rice. *Plant Physiol.* 157 (4), 1746–1764. doi: 10.1104/pp.111.188276

Pirasteh-Anosheh, H., Saed-Moucheshi, A., Pakniyat, H., and Pessarakli, M. (2016). Stomatal responses to drought stress. In *Water Stress and Crop Plants*, P. Ahmad (Ed.). doi: 10.1002/9781119054450.ch3

Rasheed, R., Yasmeen, H., Hussain, I., Iqbal, M., Ashraf, M. A., and Parveen, A. (2020). Exogenously applied 5-aminolevulinic acid modulates growth, secondary metabolism and oxidative defense in sunflower under water deficit stress. *Physiol. Mol. Biol. Plants* 26 (3), 489–499. doi: 10.1007/s12298-019-00756-3

Raza, M., Saleem, M., Shah, G., Khan, I., and Raza, A. (2014). Exogenous application of glycinebetaine and potassium for improving water relations and grain yield of wheat under drought. *J. Soil Sci. Plant Nutr.* 14 (2), 348–364. doi: 10.4067/S0718-95162014005000028

Reddy, A. R., Chaitanya, K. V., and Vivekanandan, M. (2004). Drought-induced responses of photosynthesis and antioxidant metabolism in higher plants. *J. Plant Physiol.* 161 (11), 1189–1202. doi: 10.1016/j.jplph.2004.01.013

Saccenti, E., Hoefsloot, H. C. J., Smilde, A. K., Westerhuis, J. A., and Hendriks, M. M. W. B. (2014). Reflections on univariate and multivariate analysis of metabolomics data. *Metabolomics* 10 (3), 361–374. doi: 10.1007/s11306-013-0598-6

Sade, B., Soylu, S., and Soylu, E. (2011). Drought and oxidative stress. *Afr. J. Biotechnol.* 10 (54), 11102–11109. doi: 10.5897/AJB11.1564

Sanders, G. J., and Arndt, S. K. (2012). Osmotic Adjustment Under Drought Conditions. In: R. Aroca (eds) *Plant Responses to Drought Stress*. Springer, Berlin, Heidelberg. doi: 10.1007/978-3-642-32653-0_8

Serraj, R., and Sinclair, T. (2002). Osmolyte accumulation: can it really help increase crop yield under drought conditions? *Plant Cell Environ.* 25 (2), 333–341. doi: 10.1046/j.1365-3040.2002.00754.x

Song, J.-X., Anjum, S. A., Zong, X.-F., Yan, R., Wang, L., Yang, A.-J., et al. (2017). Combined foliar application of nutrients and 5-aminolevulinic acid (ALA) improved drought tolerance in leymus chinensis by modulating its morpho-physiological characteristics. *Crop Pasture Sci.* 68 (5), 474–482. doi: 10.1071/CP16187

Song, Y., Miao, Y., and Song, C. P. (2014). Behind the scenes: the roles of reactive oxygen species in guard cells. *New Phytol.* 201 (4), 1121–1140. doi: 10.1111/nph.12565

Talaat, N. B., Shawky, B. T., and Ibrahim, A. S. (2015). Alleviation of drought-induced oxidative stress in maize (*Zea mays* l.) plants by dual application of 24-epibrassinolide and spermine. *Environ. Exp. Bot.* 113, 47–58. doi: 10.1016/j.envexpbot.2015.01.006

Tang, J., and Bassham, D. C. (2022). Autophagy during drought: function, regulation, and potential application. *Plant J.* 109 (2), 390–401. doi: 10.1111/tpj.15481

Terzi, R., and Kadioglu, A. (2006). Drought stress tolerance and the antioxidant enzyme system. *Acta Biologica Cracoviensia Ser. Botanica* 48, 89–96. doi: 10.1016/j.jep.2005.09.020

Tewari, R. K., Kumar, P., Sharma, P. N., and Bisht, S. S. (2002). Modulation of oxidative stress responsive enzymes by excess cobalt. *Plant Sci.* 162 (3), 381–388. doi: 10.1016/S0168-9452(01)00578-7

Thimm, O., Bläsing, O., Gibon, Y., Nagel, A., Meyer, S., Krüger, P., et al. (2004). MAPMAN: a user-driven tool to display genomics data sets onto diagrams of metabolic

pathways and other biological processes. *Plant J.* 37 (6), 914–939. doi: 10.1038/s41598-022-14606-y

Verslues, P. E., and Sharma, S. (2010). Proline metabolism and its implications for plant-environment interaction. *Arabidopsis Book/American Soc. Plant Biologists* 8, 3. doi: 10.1199/tab.0140

Wang, D., Chen, Q., Chen, W., Guo, Q., Xia, Y., Wang, S., et al. (2021a). Physiological and transcription analyses reveal the regulatory mechanism of melatonin in inducing drought resistance in loquat (*Eriobotrya japonica* lindl.) seedlings. *Environ. Exp. Bot.* 181, 104291. doi: 10.1016/j.envexpbot.2020.104291

Wang, W.N., Min, Z., Wu, J.R., Liu, B.C., Xu, X.l., Fang, Y.l., et al. (2021b). Physiological and transcriptomic analysis of Cabernet sauvginon (*Vitis vinifera* l.) reveals the alleviating effect of exogenous strigolactones on the response of grapevine to drought stress. *Plant Physiol. Biochem.* 167, 400–409. doi: 10.1016/j.plaphy.2021.08.010

Wang, Y., Wei, S., Wang, J., Su, X., Suo, B., Qin, F., et al. (2018). Exogenous application of 5-aminolevulinic acid on wheat seedlings under drought stress enhances the transcription of psbA and psbD genes and improves photosynthesis. *Braz. J. Bot.* 41 (2), 275–285. doi: 10.1007/s40415-018-0455-y

Wang, Z., Zheng, P., Meng, J., and Xi, Z. (2015). Effect of exogenous 24-epibrassinolide on chlorophyll fluorescence, leaf surface morphology and cellular ultrastructure of grape seedlings (*Vitis vinifera* L.) under water stress. *Acta Physiologiae Plantarum* 37, 1729. doi: 10.1007/s11738-014-1729-z

Watanabe, K., Tanaka, T., Hotta, Y., Kuramochi, H., and Takeuchi, Y. (2000). Improving salt tolerance of cotton seedlings with 5-aminolevulinic acid. *Plant Growth Regul.* 32 (1), 97–101. doi: 10.1023/A:1006369404273

Weretilnyk, E. A., and Hanson, A. D. (1990). Molecular cloning of a plant betaine-aldehyde dehydrogenase, an enzyme implicated in adaptation to salinity and drought. *Proc. Natl. Acad. Sci.* 87 (7), 2745–2749. doi: 10.1199/tab.0140

Zargar, S. M., Gupta, N., Nazir, M., Mahajan, R., Malik, F. A., Sofi, N. R., et al. (2017). Impact of drought on photosynthesis: Molecular perspective. *Plant Gene* 11, 154–159. doi: 10.1016/j.plgene.2017.04.003

Zhang, J., Li, D.-M., Gao, Y., Yu, B., Xia, C.-X., and Bai, J.-G. (2012). Pretreatment with 5-aminolevulinic acid mitigates heat stress of cucumber leaves. *Biol. Plantarum* 56 (4), 780–784. doi: 10.1007/s10535-012-0136-9

Zheng, X., and Van Huystee, R. (1992). Peroxidase-regulated elongation of segments from peanut hypocotyls. *Plant Sci.* 81 (1), 47–56. doi: 10.1016/0168-9452(92)90023-F

Zhou, Y., Lam, H. M., and Zhang, J. (2007). Inhibition of photosynthesis and energy dissipation induced by water and high light stresses in rice. *J. Exp. Bot.* 58 (5), 1207–1217. doi: 10.1093/jxb/erl291

frontiers | Frontiers in Plant Science

TYPE Original Research
PUBLISHED 29 March 2023
DOI 10.3389/fpls.2023.1115782

OPEN ACCESS

EDITED BY
Guanlin Li,
Jiangsu University, China

REVIEWED BY
Dinakaran Elango,
Iowa State University, United States
Rufeng Wang,
Shanghai University of Traditional Chinese Medicine, China
Mingzhi Zhu,
Hunan Agricultural University, China

*CORRESPONDENCE
Guihua Li
liguihua@gdaas.cn

†These authors have contributed equally to this work

SPECIALTY SECTION
This article was submitted to Plant Abiotic Stress, a section of the journal Frontiers in Plant Science

RECEIVED 04 December 2022
ACCEPTED 09 March 2023
PUBLISHED 29 March 2023

CITATION
Fu M, Jahan MS, Tang K, Jiang S, Guo J, Luo S, Luo W and Li G (2023) Comparative analysis of the medicinal and nutritional components of different varieties of *Pueraria thomsonii* and *Pueraria lobata*. *Front. Plant Sci.* 14:1115782. doi: 10.3389/fpls.2023.1115782

Comparative analysis of the medicinal and nutritional components of different varieties of *Pueraria thomsonii* and *Pueraria lobata*

Mei Fu[1†], Mohammad Shah Jahan[2†], Kang Tang[1,3], Shizheng Jiang[1,3], Juxian Guo[1], Shanwei Luo[1], Wenlong Luo[1] and Guihua Li[1*]

[1]Guangdong Key Laboratory for New Technology Research of Vegetables, Vegetable Research Institute, Guangdong Academy of Agricultural Sciences, Guangzhou, China, [2]Department of Horticulture, Faculty of Agriculture, Sher-e-Bangla Agricultural University, Dhaka, Bangladesh, [3]College of Horticulture, South China Agricultural University, Guangzhou, China

Pueraria thomsonii and *Pueraria lobata* are important medicinal plants with unique chemical compositions that are widely used in traditional Chinese medicine. To compare the nutritional and medicinal profiles of these two species, we analyzed the flavonoid, dietary fiber, total starch, and crude protein contents of one *P. lobata* and three *P. thomsonii* varieties using ultra-performance liquid chromatography-tandem mass spectrometry, enzyme weight, acid hydrolysis, and Kjeldahl methods. Furthermore, we used principal component analysis and hierarchical clustering heatmap analysis to separate the data obtained from the *P. thomsonii* and *P. lobata* samples. We detected 279 flavonoid compounds in the two *Pueraria* species, including 90 isoflavones and 78 flavonoids. A large proportion of isoflavones and flavonoids were more abundant in *P. lobata* than in *P. thomsonii*. The total starch content was significantly higher in *P. thomsonii* than in *P. lobata*. By contrast, the soluble dietary fiber, insoluble dietary fiber, and crude protein contents were substantially lower in *P. thomsonii* than in *P. lobata*. Taken together, our results demonstrate that *P. lobata* is better suited for use as a medicine, whereas *P. thomsonii* is better suited as an edible food, and provide a theoretical foundation for developing *P. thomsonii* and *P. lobata* germplasm resources.

KEYWORDS

***Puerariae thomsonii*, *Puerariae lobatae*, flavonoids, starch, dietary fiber**

Introduction

Pueraria, belonging to the Leguminosae family, is a genus of perennial semi-woody vine that originated in southern, eastern, and southeast Asia. More than 20 species belong to the genus *Pueraria*; among them, *P. thomsonii* and *P. lobata* are economically important food and medicinal plants. *P. thomsonii* contains a higher starch content than *P. lobata* and

is known as starch kudzu. *P. lobata* contains abundant isoflavones, particularly puerarin, and is known as kudzu in the Chinese Pharmacopoeia (Wong et al., 2011). At present, most cultivated varieties of *Pueraria* are *P. thomsonii*, while *P. lobata* mostly consists of wild varieties.

Starch in plant-derived foods is the primary source of calories in the human diet. Starch is a type of polysaccharide that is composed of D-glucose monomers. Plants produce starch granules in storage organs such as seeds, aerial and root tubers, and bulbs. Numerous studies have explored the physicochemical characteristics of starch and its modifications (Sangseethong et al., 2005; Liu et al., 2021). *Pueraria* plants produce abundant starch, making them a potential source of starch for use in the food and industrial sectors. *Pueraria* starch can be processed into various cakes, cold drinks, vermicelli, and highly nutritional therapeutic foods. Over the past two decades, numerous *P. thomsonii* cultivars have been developed in China with the wide use of *Pueraria* starch. Dietary fiber is another essential component of the *Pueraria* genus. Used to treat constipation, for detoxification, and to lower blood cholesterol and triglyceride levels (Bazzano, 2008; Trottier et al., 2012; Soliman, 2019; Cronin et al., 2021), dietary fiber is classified based on its solubility. Soluble dietary fiber is soluble in water, can absorb water and expand, and can be digested by microorganisms in the large intestine. By contrast, insoluble dietary fiber does not dissolve in water and cannot be digested in the human gut. Several studies have investigated the nutritional profiles of *P. lobata* and *P. thomsonii* roots (Wong et al., 2015; Shang et al., 2021).

In addition to its nutritional value, *Pueraria* has medicinal properties and is a key component of several traditional Chinese medicines. The root tubers of these plants are rich in bioactive ingredients, particularly flavonoids and isoflavonoids, and their associated derivatives (Wong et al., 2011; Jóźwiak et al., 2018; Wagle et al., 2019). The bioactive components of *Pueraria* have many pharmacological applications. For instance, these components are used to treat cardiovascular and cerebrovascular diseases, hypolipidemia (high cholesterol), hyperglycemia (high blood sugar), and high blood pressure, as well as to inhibit cancer cell activity, expand blood vessels in the brain, and enhance the oxygen supply to the brain (Meezan et al., 2005; Hien et al., 2010; Zhao et al., 2012; Kim et al., 2014; Liu et al., 2015). Therefore, much effort has focused on isolating and identifying the pharmacological constituents of *Pueraria* and analyzing their biosynthetic pathways (Wang et al., 2015; Gao et al., 2016; Wang et al., 2016; Wang et al., 2017; Mocan et al., 2018; Wang et al., 2019). Several common active ingredients, such as daidzin, daidzein, puerarin, and genistin, have been detected in *P. lobata* and *P. thomsonii* (Wong et al., 2011; Wong et al., 2015). Moreover, five isoflavones were detected in *P. lobata* and *P. thomsonii* by near-infrared spectroscopy (NIRS) (Lau et al., 2009). Likewise, 13 isoflavones were identified in both *P. lobata* and *P. thomsonii* using quantitative proton nuclear magnetic resonance (H-NMR) spectrometry (Chen et al., 2014). Although previous studies have offered a glimpse of the active substances present in *P. lobata* and *P. thomsonii*, the research methods employed in these studies are time-consuming and the number of detected active substances is small. Thus, these methods are unlikely to fully reflect the differences between the metabolite complement of *P. lobata* and *P. thomsonii*.

Metabolomics uses cutting-edge analytical techniques to systematically and comprehensively analyze the metabolic contents of organisms (Nicholson and Wilson, 2003). Ultra-performance liquid chromatography-tandem mass spectrometry (UPLC-MS/MS) is commonly used for metabolome studies. In addition to being highly sensitive and highly accurate, this technique offers high resolution and high throughput. UPLC-MS/MS can simultaneously detect numerous metabolites and is widely used in fields such as botany, zoology, and food science (Li et al., 2020; Zou et al., 2020; Li et al., 2021; Zhao et al., 2021). Notably, metabolomics approaches have not been widely used to analyze the pharmacological constituents of these two *Pueraria* species.

To compare the bioactive compositions of these two important *Pueraria* species, we used UPLC-MS/MS to analyze the flavonoid metabolite profiles of three cultivated *P. thomsonii* varieties and one wild *P. lobata* variety. We also analyzed the total starch, dietary fiber, and crude protein contents of these plants. Our results provide a basis for evaluating the medicinal and dietary potential of *P. lobata* and *P. thomsonii* roots and serve as a reference for developing *Pueraria* germplasm resources.

Materials and methods

Plant materials

Four *Pueraria* varieties were used as test materials. Three cultivated *P. thomsonii* varieties [Heshui (HS), Fogang (FG), and Guilin (GL)] were collected from the experimental field at Foshan Institute of Agricultural Sciences, Gaoming District, Foshan City, Guangdong Province, China. The *P. lobata* variety [Zhangjiajie (YS)] was collected from Yanghuping Town, Yongding District, Zhangjiajie, Hunan Province, China. All plant materials were harvested in December 2021.

Sample preparation

The samples were prepared and the metabolites were extracted according to the following steps. Roots were freeze-dried and ground into powder. Approximately 0.1 g of powder was dissolved in 1.2 mL of 70% (v/v) methanol. To ensure that the powder was completely dissolved, samples were vortexed for 30 s every 30 min at least 6 times, and then stored at 4°C overnight. After centrifugation at 12,000 rpm for 10 min, the supernatant was collected and filtered (SCAA-104, 0.22 μm pore size; ANPEL, Shanghai, China) before being used for UPLC-MS/MS analysis.

UPLC-MS/MS analysis conditions

Flavonoids were profiled on a UPLC-ESI-MS/MS system (UPLC, SHIMADZU Nexera X2) with a C18 column. The two solvents for UPLC consisted of 0.04% (v/v) acetic acid in water (A)

and 0.04% (v/v) acetic acid in acetonitrile (B). The gradient program was as follows: (A:B) 95:5 (v/v) at 0 min, 5:95 (v/v) at 11.0 min, 5:95 (v/v) at 12.0 min, 95:5 (v/v) at 12.1 min, and 95:5 (v/v) at 15.0 min; flow rate 0.40 mL/min. A 4-μL sample was injected and the column temperature was maintained at 40°C. For MS, the metabolites were detected on a triple quadrupole–linear ion trap mass spectrometer (API 6500 Q TRAP AB Sciex, CA, USA). The ion source gases were injected at a pressure ranging from 25 to 60 psi. Instrument troubleshooting and mass calibration were performed using 10 μM and 100 μM polypropylene glycol. Multiple reaction monitoring (MRM) mode was used to scan the metabolites. Optimized de-clustering potential (DP) and collision energy (CE) values were used for each MRM transition.

Determination of Dietary fiber, starch, and crude protein

The crude protein contents were quantified by the Kjeldahl method with slight modifications (Rizvi et al., 2022). Briefly, 200 mg of each sample was ground into fine powder and placed into a 300-mL digestion tube. Five mL sulfuric acid and 2 g accelerator were added to each tube after wetting the sample. Each mixture was incubated at 250 ° for 30 min on a digester. The temperature was raised to 400 ° when H_2SO_4 decomposed and emitted while smoke. Each tube was removed from the digester when the solution had turned brownish black. Protein contents were analyzed on an automated protein analyzer.

The enzyme gravimetric method (Nishibata et al., 2009) was used to extract dietary fiber from the samples with slight modifications. Briefly, 100 g of each sample was dried and crushed into fine powder. Each powdered sample was transferred into a high-foot bottle designed to detect dietary fiber. Afterwards, 40 mL of 0.05 ml/L MES-Tris buffer was added and stirred until the sample was completely mixed. The samples were treated with different enzymes, and the treated samples were used to detect the soluble and insoluble dietary fiber.

Total starch content was determined according to the acid hydrolysis method (Rose et al., 1991) with minor modifications. Briefly, 200 mg powdered sample was placed into a 15-mL centrifuge tube to remove the fat and soluble sugars from the sample. Initially, the material was washed several times with a total volume of 150 mL absolute ethanol and 10 mL distilled water. The washed material was transferred into a 50-mL conical flask after removal of the ethanol solution. Subsequently, 3 mL of hydrochloric acid was added to the conical flask and the flask was placed in a boiling water bath for 2 h. Each sample was allowed to cool to room temperature before the pH was adjusted to 7.0. The sample was further incubated for 10 min after adding 2 mL of lead acetate solution, transferred to a 50-mL volumetric flask and diluted with water. Afterwards, the material was filtered and the filtrate was used to quantify total starch contents.

Data processing

The metabolome analysis was performed by Beijing Biomarker Biotechnology Co., Ltd. Compounds were identified by comparing their ionization spectra with a self-built database. Quantitative analysis was performed using the MRM mode. The data were processed using Analyst 1.6.3 software. Unsupervised principal component analysis (PCA) was performed in R-3.1.1. The results of hierarchical cluster analysis (HCA) of the samples and metabolites are presented as heatmaps. HCA was performed in R using normalized signal intensities of metabolites and displayed as histograms. Similarly, supervised multiple regression orthogonal partial least squares discriminant analysis (OPLS-DA) was performed in R using ropls (R-3.1.1). OPLS-DA modeling was validated with a permutation test (200 permutations). The prediction parameters of the OPLS-DA model included R2X, R2Y, and Q2Y; R2X and R2Y represent the interpretation rate of the built model to the X and Y matrices, respectively, and Q2Y represents the prediction ability of the model. When R2Y and Q2Y parameters are closer to 1, the model is more stable and reliable, and can be used to screen differentially accumulated metabolites (DAMs). Based on the results of OPLS-DA, we analyzed the variable importance in projection (VIP) of the OPLS-DA model from the obtained multivariate analysis. DAMs were determined based on VIP value ≥ 1 and p-value < 0.05. The metabolites selected from different comparison groups were presented as volcano plots, plotted in R (R-3.1.1). Each point in the volcano plot represents a metabolite, and the size of the scatter represents the VIP value of the OPLS-DA model. The larger the scatter, the greater the VIP value, and the more reliable the screened differential metabolite is.

Results

PCA of flavonoid metabolites in *Pueraria thomsonii* and *Pueraria lobata*

We profiled the flavonoid metabolites in one *P. lobata* variety [Zhangjiajie (YS)] and three *P. thomsonii* varieties [Heshui (HS), Fogang (FG), and Guilin (GL)] using UPLC-MS/MS. We performed a PCA to better characterize the overall metabolite differences among the four *Pueraria* varieties and the degree of variability between samples within the same variety. As displayed in the PCA score chart (Figure 1A), the contribution by PC1 was 93.10% and that of PC2 was 4.18%. The flavonoid metabolites among the four *Pueraria* varieties were clearly distinguished on the two-dimensional graph, and replicates within the same group clustered, indicating the repeatability and reliability of our data. Moreover, YS was clearly separated from HS, FG, and GL, indicating that *P. thomsonii* and *P. lobata* differ substantially in their metabolite profiles. We identified 279 flavonoid metabolites in the four varieties, consisting of 90 flavonoids, 78 isoflavones, 38 flavonols, 32 dihydroflavones, 15 chalcones, 7 other flavonoids, 6 dihydroflavonols, 6 flavanols, 4 anthocyanins, and 3 proanthocyanidins (Figure 1B, Supplementary Table S1). The flavonoid metabolites in the four varieties are presented as a heatmap following homogenization (Figure 1C). The composition of flavonoid metabolites in YS differed notably from those in HS, FG, and GL, indicating that the flavonoid metabolite compositions of the two species differ substantially.

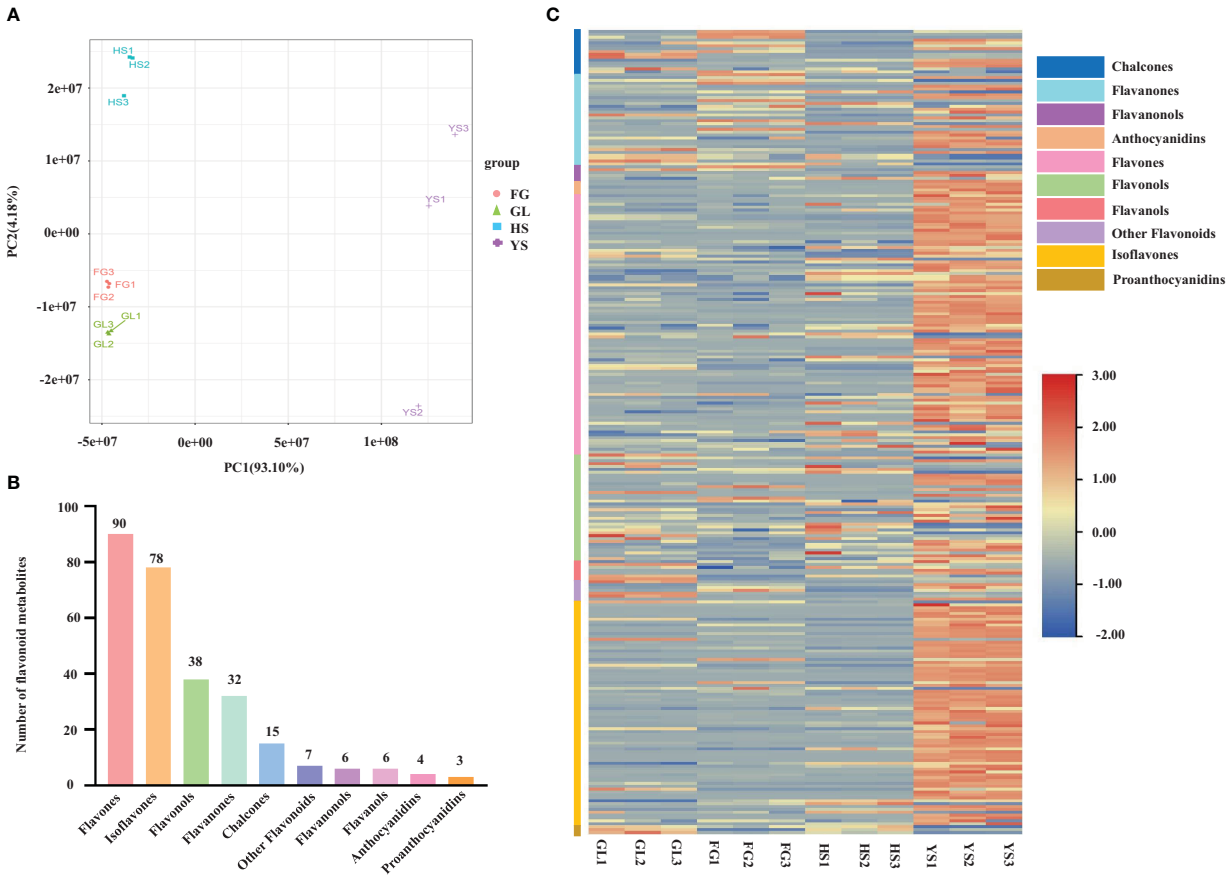

FIGURE 1
Principal component analysis and metabolite profiles of *P. thomsonii* and *P. lobata*. **(A)** PCA of all samples. **(B)** Classification and quantification of all detected metabolites. **(C)** Heatmap of flavonoid metabolites in *P. thomsonii* and *P. lobata*. HS, *P. thomsonii* variety [Heshui (HS)]; FG, *P. thomsonii* variety [Fogang (FG)]; GL, *P. thomsonii* variety [Guilin (GL)]; YS, *P. lobata* variety [Zhangjiajie (YS)].

OPLS-DA of flavonoid metabolites among the different *Pueraria* varieties

We used supervised orthogonal signal correction to evaluate the differences in metabolite composition between samples within the same variety, and applied an orthogonal partial least squares-discriminant analysis (OPLS-DA) model to emphasize the distinctions among varieties. OPLS-DA is effective at identifying DAMs as it can be used to optimize population differences. R2X, R2Y, and Q2Y are important parameters for evaluating the OPLS-DA model. Values of R2Y and Q2Y closer to 1 reflect a more stable and reliable model. In addition, Q2Y values above 0.5 are indicative of an effective model, while Q2Y values above 0.9 are indicative of an excellent model. We used the OPLS-DA model to compare the flavonoid metabolite composition of YS vs. HS (R2X=0.913, R2Y=1, Q2Y=0.998; Figure 2A), YS vs. FG (R2X=0.947, R2Y=1, Q2Y=0.999; Figure 2B), YS vs. GL (R2X=0.920, R2Y=1, Q2Y=0.998; Figure 2C), HS vs. FG (R2X=0.841, R2Y=1, Q2Y=0.990; Figure 2D), HS vs. GL (R2X=0.868, R2Y=1, Q2Y=0.989; Figure 2E), and FG vs. GL (R2X=0.805, R2Y=1, Q2Y=0.981; Figure 2F). The high values for R2X, R2Y, and Q2Y in all pairwise comparisons indicate that these analyses were repeatable and reliable and were suitable to screen for DAMs.

Volcano plot analysis of DAMs among the different *Pueraria* varieties

We used a VIP value ≥ 1 and $p < 0.05$ as criteria to screen for DAMs. The metabolites that differed between pairs of samples (YS vs. HS, YS vs. FG, YS vs. GL, HS vs. FG, HS vs. GL, and FG vs. GL) are presented as volcano plots in Figure 3 and the quantification are given in Supplementary Table S2. The blue dots in the figure represent down-regulated DAMs, and the red dots represent up-regulated DAMs. We identified 205 significant differentially accumulated flavonoid metabolites between YS and HS, of which 180 were down-regulated in HS compared with YS and 25 were up-regulated in HS compared with YS; 205 between YS and FG (172 down-regulated in FG compared with YS and 33 up-regulated in FG compared with YS); 210 between YS and GL (176 down-regulated in GL compared with YS and 34 up-regulated in GL compared with YS); 129 between HS and FG (57 down-regulated in FG compared with HS and 72 up-regulated in FG compared with HS); 128 between HS and GL (59 down-regulated in GL compared with HS and 69 up-regulated in GL compared with HS); and 120 between FG and GL (65 down-regulated in GL compared with FG and 55 up-regulated in GL compared with FG). These results verify that the complement of flavonoid metabolites differs substantially between YS, HS, FG, and GL.

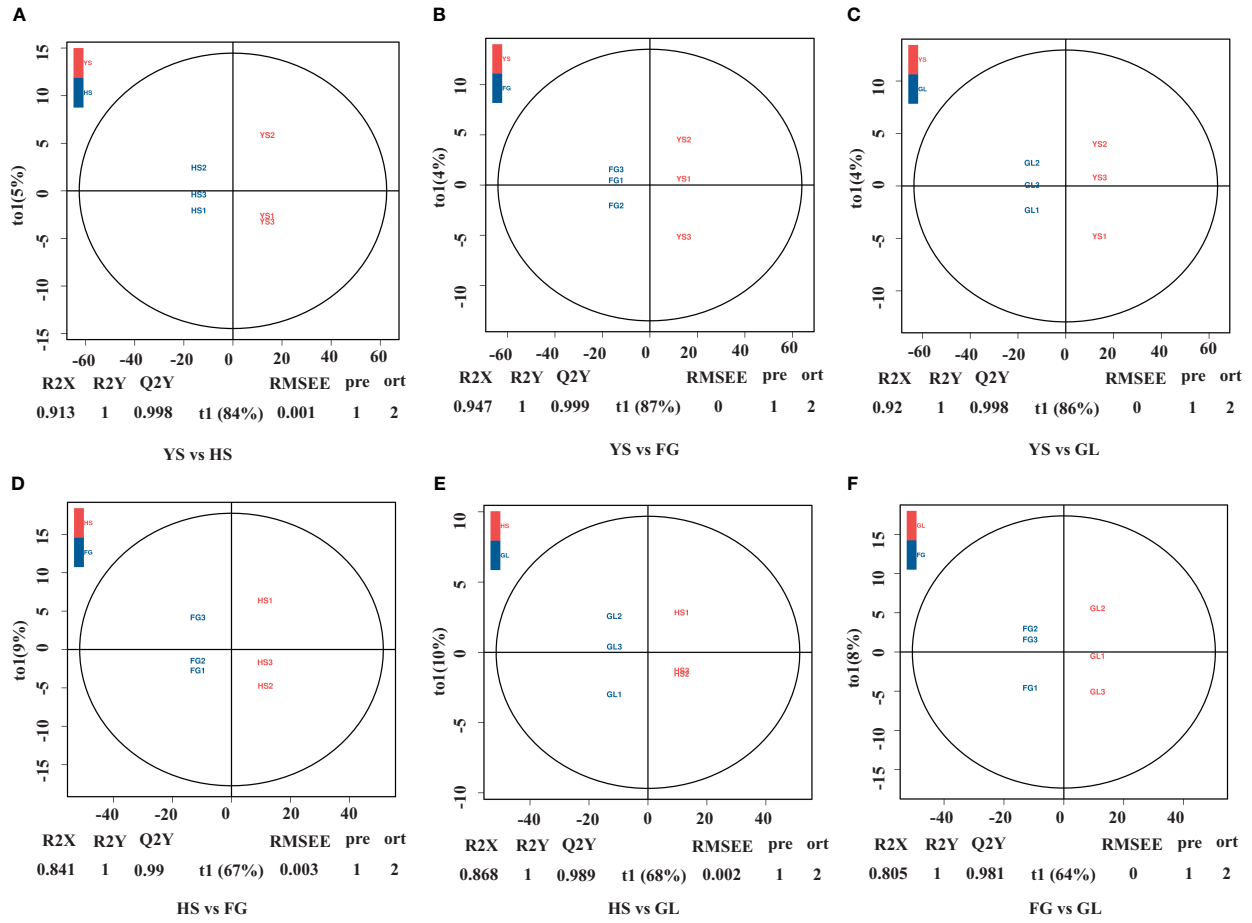

FIGURE 2
Differential flavonoid accumulation analysis using orthogonal signal correction and orthogonal partial least squares-discriminant analysis. HS, FG, GL, *P. thomsonii* varieties; YS, *P. lobata* variety. Pairwise comparisons YS vs. HS **(A)**, YS vs. FG **(B)**, YS vs. GL **(C)**, HS vs. FG **(D)**, HS vs. GL **(E)**, and FG vs. GL **(F)**.

Venn diagram and HCA analysis of common DAMs among the different *Pueraria* varieties

We screened for DAMs that were shared among the different varieties, as shown in the Venn diagram in Figure 4. The number of differentially accumulated flavonoid metabolites in YS vs. HS, YS vs. FG, and YS vs. GL was 205, 205, and 210, respectively; however, we identified 167 DAMs in common between each of these comparisons, reflecting the difference between the one *P. lobata* variety (YS) and the three *P. thomsonii* varieties (HS, FG, and GL) (Figure 4A). We detected only 54 common DAMs between HS vs. FG, HS vs.GL, and FG vs. GL (Figure 4B). These results show that the flavonoid metabolites that underlie the differences between YS vs. HS, YS vs. FG, and YS vs. GL are essentially identical. Furthermore, fewer DAMs were common in comparisons of the three *P. thomsonii* varieties (i.e., 54) than in comparisons of *P. lobata* and each *P. thomsonii* variety (i.e., 167). We next classified the 167 common DAMs into subgroups (Supplementary Table S3), of which 59 isoflavones and 55 flavonoids were the major components (Figure 5). Compared to *P. thomsonii*, most of the more abundant isoflavones and flavonoids in *P. lobata* were puerarin, daidzein, genistein, biochanin A, acacetin, apigenin, and tricin, and their glycosyl and methyl derivatives. However, the isoflavones and flavonoids mentioned above displayed no clear difference among the three *P. thomsonii* varieties. We further analyzed DAMs among the three *P. thomsonii* varieties. Among these metabolites, 12 metabolites including garbanzol, licoflavonol*, 8-Prenylkaempferol, neobavaisoflavone, and pratensein showed drastic differences in the pairwise comparisons between *P. thomsonii* varieties (Table 1), thus defining metabolite signatures that can be used as markers to distinguish the three *P. thomsonii* varieties.

Apart from isoflavones and flavonoids, we detected eight chalcones, four anthocyanins, three flavanols, and 18 dihydroflavones that were differentially accumulated in comparisons of *P. lobata* and each *P. thomsonii* variety (Figure 6). Among these metabolites, the four anthocyanins peonidin-3-O-glucoside, delphinidin-3-O-sambubioside, pelargonidin-3-O-glucoside, and rosinidin-3-O-glucoside were more abundant in *P. lobata* than in *P. thomsonii* (Figure 6B). These results indicate that *P. lobata* accumulated higher levels of

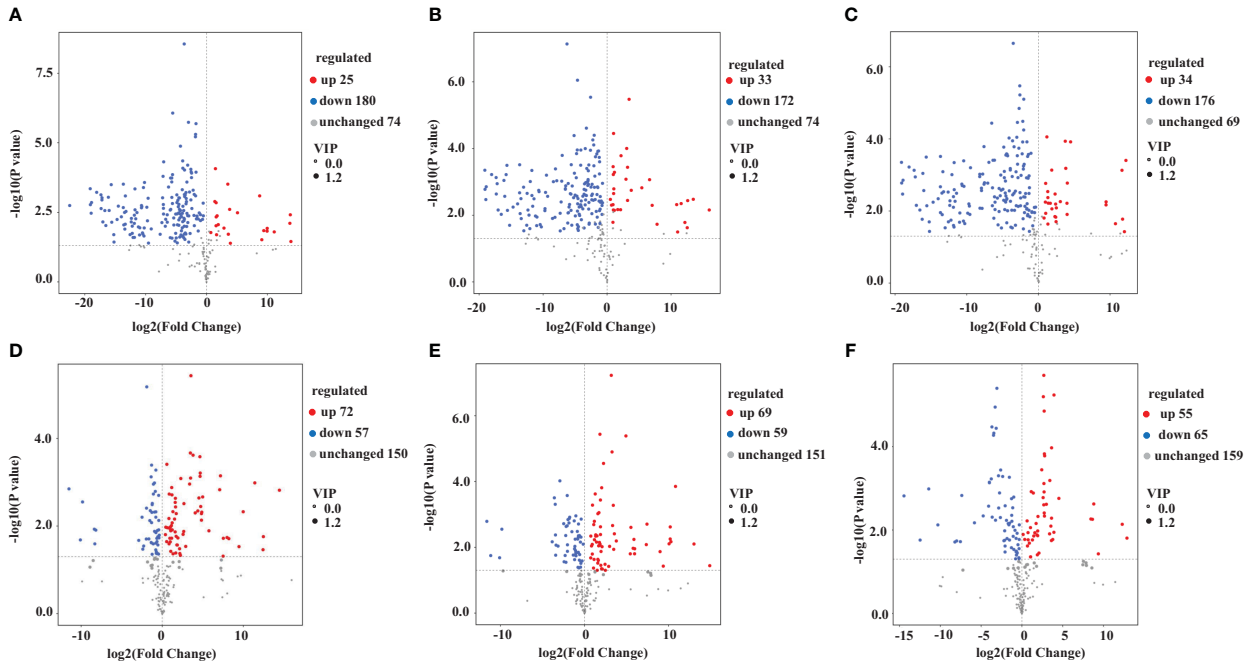

FIGURE 3
Volcano plot of the differentially accumulated metabolites among the different *Pueraria* varieties. Pairwise comparisons YS vs. HS **(A)**, YS vs. FG **(B)**, YS vs. GL **(C)**, HS vs. FG **(D)**, HS vs. GL **(E)**, and FG vs. GL **(F)**.

flavonoids than *P. thomsonii*. We also detected high amounts of anthocyanin in *P. lobata*. In addition, of the top 10 least abundant DAMs identified in the YS vs. HS, YS vs. FG, and YS vs. GL pairwise comparisons, seven were shared (Figure 7): 6-C-methylkaempferol-3-glucoside, kaempferol-3-O-(2''-O-acetyl) glucuronide, 4,6-dimethoxyisoflavone-7-O-glucoside, biochanin A-7-O-glucoside (Sissotrin), acacetin-7-O-glucoside (tilianin)*, prunetin-5-O-glucoside, and acacetin-7-O-galactoside*. These substances can therefore be used as markers to distinguish between *P. lobata* and *P. thomsonii*.

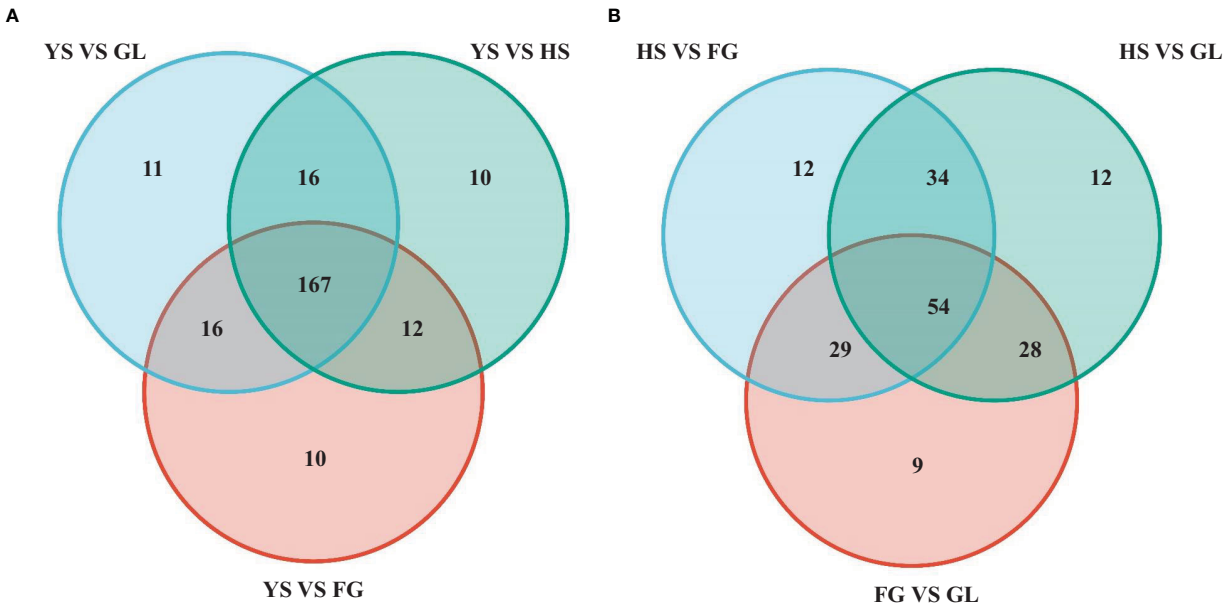

FIGURE 4
Venn diagram of common differentially accumulated metabolites. HS, FG, GL, *P. thomsonii* varieties; YS, *P. lobata* variety. **(A)** Common differentially accumulated metabolites in comparisons of P. lobata and each P. thomsonii variety. **(B)** Common differentially accumulated metabolites in comparisons of the three P. thomsonii varieties.

10.3389/fpls.2023.1115782

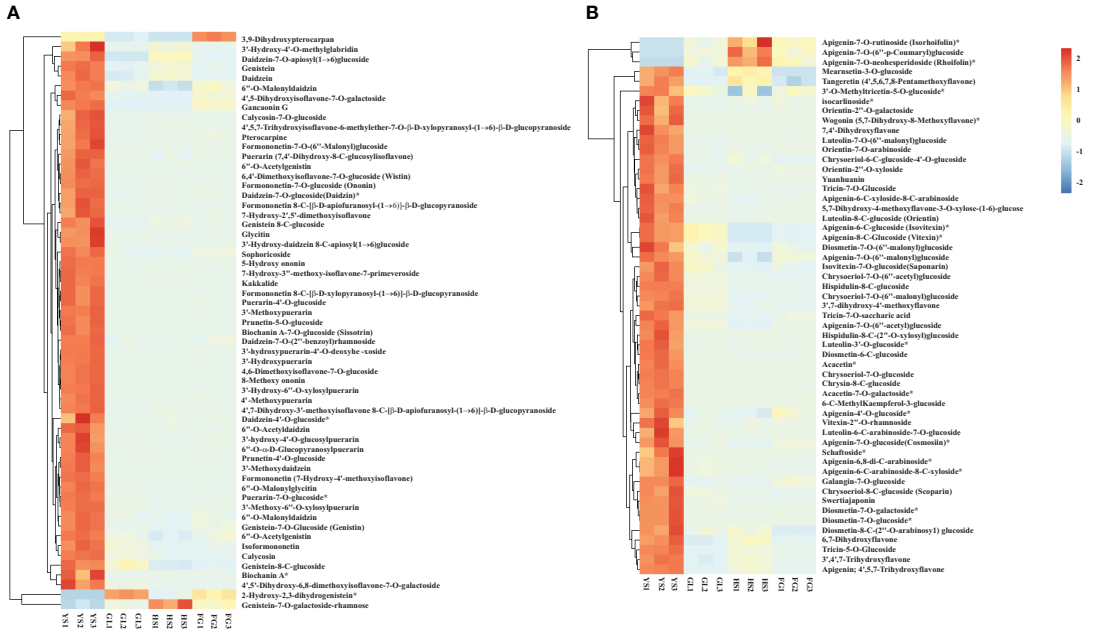

FIGURE 5
Heatmap of selected differentially accumulated metabolites. **(A)** isoflavones; **(B)** flavones in *P. thomsonii* and *P. lobata*. HS, FG, GL, *P. thomsonii* varieties; YS, *P. lobata* variety. The asterisk indicates that this substance has isomers.

Comparative analysis of starch, dietary fiber, and crude protein in *Pueraria thomsonii* and *Pueraria lobate*

In addition to flavonoids, nutrients such as starch, dietary fiber, and crude protein contribute to the nutritional value of *P. thomsonii* and *P. lobata*. We quantified the dietary fiber, total starch, and crude protein contents of *P. thomsonii* and *P. lobata* roots using enzyme gravimetry, acid hydrolysis, and the Kjeldahl method, respectively. The *P. thomsonii* varieties contained more starch than the *P. lobata* variety. We observed the lowest total starch content in YS (449.85 ± 2.61 mg/g sample), and the highest starch content in GL (629.93 ± 3.73 mg/g), followed by FG (618.24 ± 3.54 mg/g) and HS (613.50 ± 1.93 mg/g) (Table 2).

P. thomsonii is known for its low fiber content. Indeed, per 100 g of sample, we measured the highest insoluble dietary fiber content

TABLE 1 Differentially accumulated compounds among the three *P. thomsonii* varieties.

Class	Compounds	HS vs. GL		HS vs. FG		FG vs. GL	
		log2FC	VIP	log2FC	VIP	log2FC	VIP
Flavonols	Garbanzol	7.43	1.21	2.90	1.14	4.53	1.25
Flavonols	Licoflavonol*	13.02	1.20	9.47	1.15	3.55	1.23
Flavonols	8-Prenylkaempferol	5.97	1.19	2.58	1.18	3.39	1.22
Isoflavones	Neobavaisoflavone	2.12	1.10	4.99	1.21	-2.87	1.25
Isoflavones	Pratensein	10.19	1.20	7.51	1.11	2.68	1.23
Isoflavones	Glyceollin III	7.35	1.20	9.99	1.21	-2.64	1.24
Chalcones	Licoagrochalcone D*	5.96	1.18	2.17	1.11	3.78	1.21
Other Flavonoids	Licoisoflavanone*	5.88	1.20	2.25	1.11	3.63	1.24
Other Flavonoids	Licoflavone A	2.03	1.10	4.88	1.21	-2.85	1.24
Other Flavonoids	Licoflavone C	3.55	1.19	5.76	1.19	-2.21	1.20
Other Flavonoids	Licoisoflavone A*	5.97	1.19	2.58	1.18	3.39	1.22
Other Flavonoids	(3R)-Vestitol	10.82	1.21	7.19	1.22	3.64	1.25

The asterisk indicates that this substance has isomers.

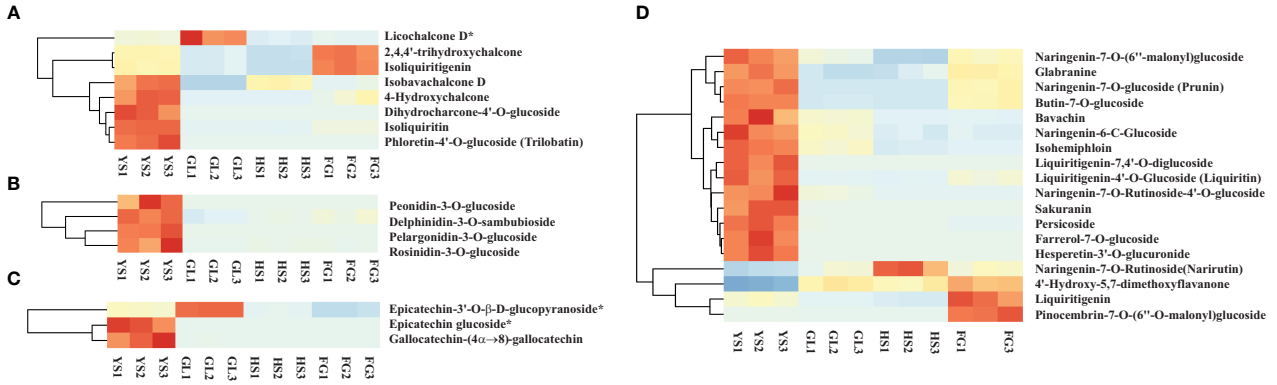

FIGURE 6
Heatmap of selected differentially accumulated metabolites. **(A)** chalcones; **(B)** anthocyanins; **(C)** flavanols; **(D)** dihydroflavones in *P. thomsonii* and *P. lobata*. HS, FG, GL, *P. thomsonii* varieties; YS, *P. lobata* variety.

in YS (10.23 ± 0.28 g), followed by HS (4.26 ± 0.14 g), FG (3.75 ± 0.35 g), and GL (3.24 ± 0.25 g). Per 100 g of sample, we detected the highest soluble dietary fiber content in YS (3.81 ± 0.30 g), followed by GL (0.88 ± 0.03 g), HS (0.29 ± 0.05 g), and FG (0.17 ± 0.03 g) (Table 2).

The *P. lobata* variety contained the highest crude protein content of the four varieties tested. Per kilogram of sample, the crude protein content was highest in YS (106.24 ± 0.70 g), followed by GL (81.40 ± 0.59 g), HS (72.82 ± 0.91g), and FG (70.95 ± 0.41 g) (Table 2). These results demonstrate that the nutritional compositions of *P. thomsonii* and *P. lobata* differ substantially, while those of the three *P. thomsonii* varieties are similar to each other.

Discussion

Pueraria species are found throughout Asia, with China being the leading producer. *Pueraria* is predominantly used in traditional Chinese medicine and as an edible food. The metabolic profiles of *Pueraria* plants have not been extensively investigated. Using UPLC-MS/MS, we identified 279 flavonoid metabolites in *P. lobata* and *P. thomsonii* (Figure 1B). PCA and HCA indicated that the metabolite constituents of YL, HS, FG, and GL differ markedly, with YL being clearly distinguishable from HS, FG, and GL (Figure 1), supporting the notion that the flavonoid metabolite compositions vary among different *Pueraria* species.

Isoflavones and flavonoids are essential bioactive ingredients of *P. lobata* and *P. thomsonii*. Isoflavones are predominantly found in legumes such as soybean (*Glycine max*) and have essential functions in plant protection and nodule formation (Li et al., 2015). Five isoflavones were identified in the roots of *P. thomsonii* and *P. lobata* plants, including puerarin, formononetin-7-O-glycoside, biochanin A-7-O-glucoside, 7-hydroxy-3''-methoxy-isoflavone-7-primeveroside, and genistein-8-C-apiosyl(1→6)glucoside(Shang et al., 2021). Furthermore, 13 isoflavones were previously detected by H-NMR spectrometry in *P. thomsonii* and *P. lobata*, including puerarin, puerarin 6''-O-xylopyranoside, daidzin, genistin, and mononetin (Chen et al., 2014). In another study, puerarin, genistin, daidzin, and daidzein were the main ingredients identified in *P. thomsonii* and *P. lobata* samples collected from Australia, China, and the USA (Wong et al., 2015). Here, we determined that 59 isoflavones accumulated to a greater degree in *P. lobata* than in *P. thomsonii* (Figure 5). The major isoflavones identified here were puerarin, daidzein, genistein, acacetin, and biochanin A, as well as their glycosylated or methylated derivatives, and these altered metabolites significantly affect the pharmacological activities of isoflavone products (Zhou et al., 2014; Egan, 2020; Wang et al., 2020). Here, we established that puerarin, genistin, and daidzein, and their derivatives, are the major isoflavones in *P. thomsonii* and *P. lobata*. Our results were consistent with studies mentioned above. In addition to the isoflavone metabolites mentioned above, our study revealed isoflavone metabolites that had not been identified in previous studies of *Pueraria* plants. These metabolites can be used as biomarkers to distinguish between *P. lobata* and *P. thomsonii*.

The contents of 52 flavonoids, particularly acacetin, apigenin, tricin, and their derivatives, were higher in *P. lobata* than in *P. thomsonii* (Figure 5). These flavonoids possess antiplasmodial, antiperoxodant, anti-inflammatory, and anticancer properties (Cai et al., 2004; Kim et al., 2014; Kim et al., 2017; Wu et al., 2018). Our results are consistent with those of a previous UPLC-MS/MS-based analysis (Shang et al., 2021) that had identified 15 flavonoids, including acacetin-7-O-galactoside, kaempferol-7-O-glucoside, and apigenin-7-O-(6''-p-Coumaryl) glucoside. Although *P. lobata* and *P. thomsonii* both contain abundant isoflavones and flavonoids, the isoflavone and flavonoid contents were higher in *P. lobata* than in *P. thomsonii*, which may explain why *P. lobata* is commonly used for medicinal purposes. Our findings suggest that variations in the abundance and composition of flavonoids and isoflavones may contribute to the different uses of *P. lobata* and *P. thomsonii* (Chen et al., 2006; Chen et al., 2014; Shang et al., 2021). In addition to the two main bioactive ingredients (isoflavone and flavonoids), four anthocyanins were more abundant in *P. lobata* than in *P. thomsonii* (Figure 6). Anthocyanins are water-soluble pigments belonging to the flavonoid class. Anthocyanins not only

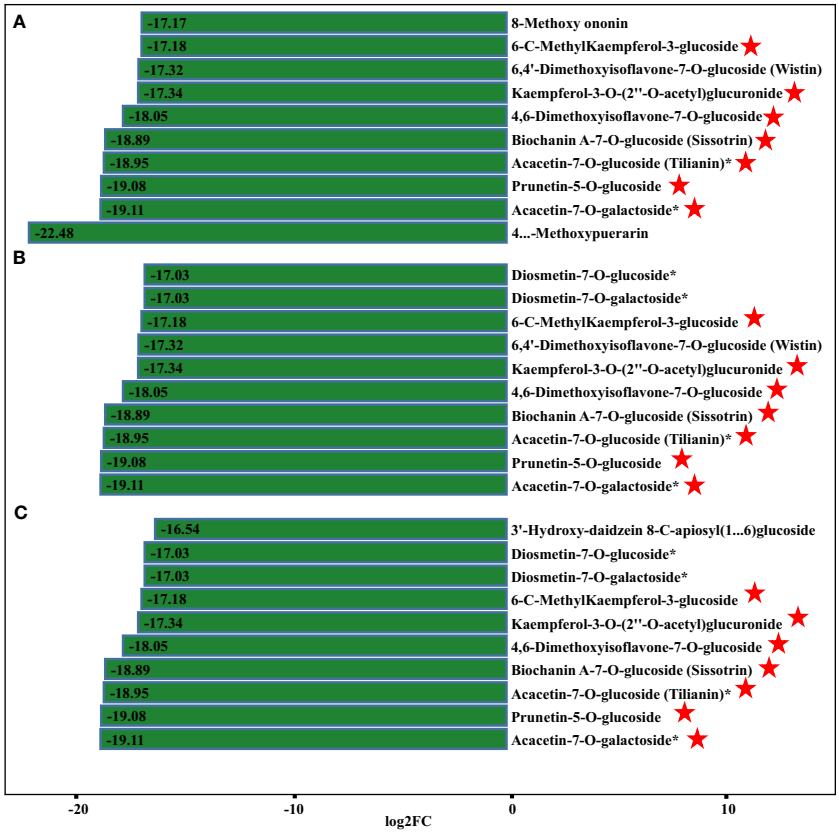

FIGURE 7
Fold-changes of differentially accumulating metabolites. **(A)** YS vs. HS; **(B)** YS vs. FG; **(C)** YS vs. GL. The pentagram represents the common metabolites of the three comparisons.

give plants their color, but also limit the damage caused by biological and abiotic stressors (Abdel-Aal et al., 2006; Gould, 2010; He et al., 2020). Therefore, the high accumulation of anthocyanins in *P. lobata* is consistent with *P. lobata* having a darker color than *P. thomsonii*. Moreover, the anthocyanins mentioned above have not been detected in previous studies focusing on *Pueraria* plants.

Pueraria plants have dual applications as medicine and food, and are used to produce both pharmaceutical ingredients and edible starch (Tanner et al., 1979). The starch paste produced by *P. thomsonii* is transparent and difficult to degrade, and the elastic modulus of *P. thomsonii* starch gel is significantly lower than that of potato (*Solanum tuberosum*) starch gel. As a result, *P. thomsonii* starch can be used as a food ingredient as well as a raw industrial material. A previous study had shown that the total starch content of PTR (*Puerariae Thomsonii Radix*) was higher than that of PLR (*Puerariae Lobatae Radix*) (Wong et al., 2015). In this study, the total starch content of *P. thomsonii* roots was higher than that of *P. lobata* roots (Table 2); thus, *P. thomsonii* will have high utility in the food industry. Indeed, numerous *P. thomsonii* cultivars with high starch yields have been developed in China for use as food.

Dietary fiber improves the human intestinal microbiota and intestinal peristalsis. We observed that *P. thomsonii* had a lower dietary fiber content than *P. lobata* (Table 2). This result was inconsistent with the findings of a previous study (Wong et al., 2015) that established that *P. lobata* roots contained more dietary fiber than *P. thomsonii* roots. This discrepancy may be due to the different varieties used in the two studies. The materials used in the previous study came from three different countries (Australia, China, and the USA), while the materials used in our study all came from China. In addition, the three varieties of *P. thomsonii* used in our study are common cultivated varieties, and have broad market value. Fiber also affects the taste of food. Foods with a high fiber content often lack flavor without processing. For the reasons mentioned above, dietary fiber compounds were found in relatively lower quantities among the three varieties of *P. thomsonii* used in our study. Therefore, *P. thomsonii* with a lower fiber content is useful as food. Crude protein content was higher in *P. lobata* than in *P. thomsonii*. Thus, *P. lobata* has an advantage over *P. thomsonii* in efforts aimed at developing and using crude protein.

Conclusion

Here, we analyzed the flavonoid profiles of four important *Pueraria* varieties (one *P. lobata* variety and three common cultivated *P. thomsonii* varieties) using UPLC-MS/MS. We identified 279 flavonoid metabolites, of which 167 DAMs were common between YS vs. HS, YS vs. FG, and YS vs. GL. We classified these common metabolites into different subgroups, with 59

TABLE 2 Starch, soluble dietary fiber, insoluble dietary fiber, and crude protein contents in *Puerariae Thomsonii* and *Puerariae Lobatae* varieties tested in this study.

Cultivar name	Starch (mg/g)	Insoluble dietary fiber(g/100g)	soluble dietary fiber(g/100g)	Crude protein (g/kg)
ZhangJiaJie(YS)	449.85 ± 2.61c	10.23 ± 0.28a	3.81 ± 0.30a	106.24 ± 0.70a
HeShui(HS)	613.50 ± 1.93b	4.26 ± 0.14b	0.29 ± 0.05c	72.82 ± 0.91c
FoGang(FG)	618.24 ± 3.54b	3.75 ± 0.35bc	0.17 ± 0.03c	70.95 ± 0.41d
GuiLin(GL)	629.93 ± 3.73a	3.24 ± 0.25c	0.88 ± 0.03b	81.40 ± 0.59b

Different letters indicate significant differences (P<0.05), while the same letter indicates no significant differences.

isoflavones and 55 flavonoids. A large proportion of isoflavones and flavonoids were more abundant in *P. lobata* than in *P. thomsonii*. The starch content was significantly higher in the *P. thomsonii* varieties than in the *P. lobata* variety, while the cellulose and crude protein contents were significantly lower in *P. thomsonii* varieties than in the *P. lobata* variety. This study provides insight into the differences in medicinal and nutritional profiles between *P. lobata* and *P. thomsonii*, and serves as a theoretical basis for developing *P. lobata* and *P. thomsonii* germplasm resources.

Data availability statement

The original contributions presented in the study are included in the article/Supplementary Material. Further inquiries can be directed to the corresponding author.

Author contributions

Conceptualization, MF; methodology, KT and SJ; software, WL; resources, JG; writing—original draft preparation, MF and MJ; writing—review and editing, SL; supervision and funding acquisition, GL. All authors contributed to the article and approved the submitted version.

Funding

This research was funded by Guangdong Province key areas research and development plan project, grant number 2022B0202110003. 2022 Provincial Rural Revitalization Strategy Special Fund Seed Industry Revitalization Project, grant number 2022-NBA-00-014 Guangzhou Science and Technology Plan Project, grant number 202102020442.

Conflict of interest

The authors declare that the research was conducted in the absence of any commercial or financial relationships that could be construed as a potential conflict of interest.

Publisher's note

All claims expressed in this article are solely those of the authors and do not necessarily represent those of their affiliated organizations, or those of the publisher, the editors and the reviewers. Any product that may be evaluated in this article, or claim that may be made by its manufacturer, is not guaranteed or endorsed by the publisher.

Supplementary material

The Supplementary Material for this article can be found online at: https://www.frontiersin.org/articles/10.3389/fpls.2023.1115782/full#supplementary-material

SUPPLEMENTARY TABLE 1
Total flavonoid metabolites in the one *P. lobata* and three *P. thomsonii* varieties tested in this study.

SUPPLEMENTARY TABLE 2
Differential metabolites among the different *Pueraria* varieties tested in this study.

SUPPLEMENTARY TABLE 3
List of the 167 common differentially accumulating metabolites in the comparison groups.

References

Abdel-Aal, E.-S. M., Young, J. C., and Rabalski, I. (2006). Anthocyanin composition in black, blue, pink, purple, and red cereal grains. *J. Agric. Food Chem.* 54, 4696–4704. doi: 10.1021/jf0606609

Bazzano, L. A. (2008). Effects of soluble dietary fiber on low-density lipoprotein cholesterol and coronary heart disease risk. *Curr. Atheroscl. Rep.* 10, 473–477. doi: 10.1007/s11883-008-0074-3

Cai, H., Hudson, E. A., Mann, P., Verschoyle, R. D., Greaves, P., Manson, M. M., et al. (2004). Growth-inhibitory and cell cycle-arresting properties of the rice bran constituent tricin in human-derived breast cancer cells *in vitro* and in nude mice *in vivo*. *Br. J. Cancer* 91, 1364–1371. doi: 10.1038/sj.bjc.6602124

Chen, S.-B., Liu, H.-P., Tian, R.-T., Yang, D.-J., Chen, S.-L., Xu, H.-X., et al. (2006). High-performance thin-layer chromatographic fingerprints of isoflavonoids for

distinguishing between radix puerariae lobate and radix puerariae thomsonii. *J. Chromatogr. A* 1121, 114–119. doi: 10.1016/j.chroma.2006.04.082

Chen, Y.-G., Song, Y.-L., Wang, Y., Yuan, Y.-F., Huang, X.-J., Ye, W.-C., et al. (2014). Metabolic differentiations of pueraria lobata and pueraria thomsonii using 1H NMR spectroscopy and multivariate statistical analysis. *J. Pharm. Biomed. Anal.* 93, 51–58. doi: 10.1016/j.jpba.2013.05.017

Cronin, P., Joyce, S. A., O'toole, P. W., and O'connor, E. M. (2021). Dietary fibre modulates the gut microbiota. *Nutrients* 13, 1655. doi: 10.3390/nu13051655

Egan, A. N. (2020). Economic and ethnobotanical uses of tubers in the genus pueraria DC. *Legume* 19, 24.

Gao, Y., Wang, X., and He, C. (2016). An isoflavonoid-enriched extract from pueraria lobata (kudzu) root protects human umbilical vein endothelial cells against oxidative stress induced apoptosis. *J. Ethnopharmacol.* 193, 524–530. doi: 10.1016/j.jep.2016.10.005

Gould, K. S. (2010). "Muriel Wheldale onslow and the rediscovery of anthocyanin function in plants," in C. Santos-Buelga, M. T. Escribano-Bailon and V. Lattanzio. *Recent advances in polyphenol research*. Ames, USA 2, 206–225.

He, Q., Ren, Y., Zhao, W., Li, R., and Zhang, L. (2020). Low temperature promotes anthocyanin biosynthesis and related gene expression in the seedlings of purple head Chinese cabbage (Brassica rapa l.). *Genes* 11, 81. doi: 10.3390/genes11010081

Hien, T. T., Kim, H. G., Han, E. H., Kang, K. W., and Jeong, H. G. (2010). Molecular mechanism of suppression of MDR1 by puerarin from pueraria lobata *via* NF-κB pathway and cAMP-responsive element transcriptional activity-dependent up-regulation of AMP-activated protein kinase in breast cancer MCF-7/adr cells. *Mol. Nutr. Food Res.* 54, 918–928. doi: 10.1002/mnfr.200900146

Jóźwiak, B., Orczykowska, M., and Dziubiński, M. (2018). Rheological properties of kuzu starch pastes with galactomannans. *J. Food Sci. Technol.* 55, 1575–1581. doi: 10.1007/s13197-018-3047-8

Kim, S., Go, G.-W., and Imm, J.-Y. (2017). Promotion of glucose uptake in C2C12 myotubes by cereal flavone tricin and its underlying molecular mechanism. *J. Agric. Food Chem.* 65, 3819–3826. doi: 10.1021/acs.jafc.7b00578

Kim, H. R., Park, C. G., and Jung, J. Y. (2014). Acacetin (5, 7-dihydroxy-4'-methoxyflavone) exhibits *in vitro* and *in vivo* anticancer activity through the suppression of NF-κB/Akt signaling in prostate cancer cells. *Int. J. Mol. Med.* 33, 317–324. doi: 10.3892/ijmm.2013.1571

Lau, C.-C., Chan, C.-O., Chau, F.-T., and Mok, D. K.-W. (2009). Rapid analysis of radix puerariae by near-infrared spectroscopy. *J. Chromatogr. A* 1216, 2130–2135. doi: 10.1016/j.chroma.2008.12.089

Li, J., Hu, Y., Liu, L., Wang, Q., Zeng, J., and Chen, C. (2020). PM2. 5 exposure perturbs lung microbiome and its metabolic profile in mice. *Sci. Total Environ.* 721, 137432. doi: 10.1016/j.scitotenv.2020.137432

Li, X., Li, Y., Zhao, M., Hu, Y., Meng, F., Song, X., et al. (2021). Molecular and metabolic insights into anthocyanin biosynthesis for leaf color change in chokecherry (Padus virginiana). *Int. J. Mol. Sci.* 22, 10697. doi: 10.3390/ijms221910697

Li, L., Lv, Y., Xu, L., and Zheng, Q. (2015). Quantitative efficacy of soy isoflavones on menopausal hot flashes. *Br. J. Clin. Pharmacol.* 79, 593–604. doi: 10.1111/bcp.12533

Liu, D., Ma, L., Zhou, Z., Liang, Q., Xie, Q., Ou, K., et al. (2021). Starch and mineral element accumulation during root tuber expansion period of pueraria thomsonii benth. *Food Chem.* 343, 128445. doi: 10.1016/j.foodchem.2020.128445

Liu, B., Wu, Z., Li, Y., Ou, C., Huang, Z., Zhang, J., et al. (2015). Puerarin prevents cardiac hypertrophy induced by pressure overload through activation of autophagy. *Biochem. Biophys. Res. Commun.* 464, 908–915. doi: 10.1016/j.bbrc.2015.07.065

Meezan, E., Meezan, E. M., Jones, K., Moore, R., Barnes, S., and Prasain, J. K. (2005). Contrasting effects of puerarin and daidzin on glucose homeostasis in mice. *J. Agric. Food Chem.* 53, 8760–8767. doi: 10.1021/jf058105e

Mocan, A., Carradori, S., Locatelli, M., Secci, D., Cesa, S., Mollica, A., et al. (2018). Bioactive isoflavones from pueraria lobata root and starch: Different extraction techniques and carbonic anhydrase inhibition. *Food Chem. Toxicol.* 112, 441–447. doi: 10.1016/j.fct.2017.08.009

Nicholson, J. K., and Wilson, I. D. (2003). Understanding'global'systems biology: metabonomics and the continuum of metabolism. *Nat. Rev. Drug Discovery* 2, 668–676. doi: 10.1038/nrd1157

Nishibata, T., Tashiro, K., Kanahori, S., Hashizume, C., Kitagawa, M., Okuma, K., et al. (2009). Comprehensive measurement of total nondigestible carbohydrates in foods by enzymatic– gravimetric method and liquid chromatography. *J. Agric. Food Chem.* 57, 7659–7665. doi: 10.1021/jf9010565

Rizvi, N. B., Aleem, S., Khan, M. R., Ashraf, S., and Busquets, R. (2022). Quantitative estimation of protein in sprouts of vigna radiate (Mung beans), lens culinaris (Lentils), and cicer arietinum (Chickpeas) by kjeldahl and lowry methods. *Molecules* 27, 814. doi: 10.3390/molecules27030814

Rose, R., Rose, C. L., Omi, S. K., Forry, K. R., Durall, D. M., and Bigg, W. L. (1991). Starch determination by perchloric acid vs enzymes: evaluating the accuracy and precision of six colorimetric methods. *J. Agric. Food Chem.* 39, 2–11. doi: 10.1021/jf00001a001

Sangseethong, K., Ketsilp, S., and Sriroth, K. (2005). The role of reaction parameters on the preparation and properties of carboxymethyl cassava starch. *Starch-Stärke* 57, 84–93. doi: 10.1002/star.200400302

Shang, X., Huang, D., Wang, Y., Xiao, L., Ming, R., Zeng, W., et al. (2021). Identification of nutritional ingredients and medicinal components of pueraria lobata and its varieties using UPLC-MS/MS-based metabolomics. *Molecules* 26, 6587. doi: 10.3390/molecules26216587

Soliman, G. A. (2019). Dietary fiber, atherosclerosis, and cardiovascular disease. *Nutrients* 11, 1155. doi: 10.3390/nu11051155

Tanner, R. D., Hussain, S. S., Hamilton, L. A., and Wolf, F. T. (1979). Kudzu (Pueraria lobata): potential agricultural and industrial resource. *Economic Bot.* 33, 400–412. doi: 10.1007/BF02858336

Trottier, M., Erebara, A., and Bozzo, P. (2012). Treating constipation during pregnancy. *Can. Family Physician* 58, 836–838.

Wagle, A., Seong, S. H., Jung, H. A., and Choi, J. S. (2019). Identifying an isoflavone from the root of pueraria lobata as a potent tyrosinase inhibitor. *Food Chem.* 276, 383–389. doi: 10.1016/j.foodchem.2018.10.008

Wang, X., Fan, R., Li, J., Li, C., and Zhang, Y. (2016). Molecular cloning and functional characterization of a novel (iso) flavone 4′, 7-o-diglucoside glucosyltransferase from pueraria lobata. *Front. Plant Sci.* 7, 387. doi: 10.3389/fpls.2016.00387

Wang, X., Li, S., Li, J., Li, C., and Zhang, Y. (2015). *De novo* transcriptome sequencing in pueraria lobata to identify putative genes involved in isoflavones biosynthesis. *Plant Cell Rep.* 34, 733–743. doi: 10.1007/s00299-014-1733-1

Wang, X., Li, C., Zhou, C., Li, J., and Zhang, Y. (2017). Molecular characterization of the c-glucosylation for puerarin biosynthesis in pueraria lobata. *Plant J.* 90, 535–546. doi: 10.1111/tpj.13510

Wang, X., Li, C., Zhou, Z., and Zhang, Y. (2019). Identification of three (iso) flavonoid glucosyltransferases from pueraria lobata. *Front. Plant Sci.* 10, 28. doi: 10.3389/fpls.2019.00028

Wang, S., Zhang, S., Wang, S., Gao, P., and Dai, L. (2020). A comprehensive review on pueraria: Insights on its chemistry and medicinal value. *Biomed. Pharmacother.* 131, 110734. doi: 10.1016/j.biopha.2020.110734

Wong, K. H., Li, G. Q., Li, K. M., Razmovski-Naumovski, V., and Chan, K. (2011). Kudzu root: traditional uses and potential medicinal benefits in diabetes and cardiovascular diseases. *J. Ethnopharmacol.* 134, 584–607. doi: 10.1016/j.jep.2011.02.001

Wong, K. H., Razmovski-Naumovski, V., Li, K. M., Li, G. Q., and Chan, K. (2015). Comparing morphological, chemical and anti-diabetic characteristics of puerariae lobatae radix and puerariae thomsonii radix. *J. Ethnopharmacol.* 164, 53–63. doi: 10.1016/j.jep.2014.12.050

Wu, W.-Y., Li, Y.-D., Cui, Y.-K., Wu, C., Hong, Y.-X., Li, G., et al. (2018). The natural flavone acacetin confers cardiomyocyte protection against hypoxia/reoxygenation injury *via* AMPK-mediated activation of Nrf2 signaling pathway. *Front. Pharmacol.* 9, 497. doi: 10.3389/fphar.2018.00497

Zhao, X. Z., Li, X. W., Jin, Y. R., Yu, X. F., Qu, S. C., and Sui, D. Y. (2012). Hypolipidemic effects of kaempferide-7-O-(4"-O-acetylrhamnosyl)-3-O-rutinoside in hyperlipidemic rats induced by a high-fat diet. *Mol. Med. Rep.* 5, 837–841. doi: 10.3892/mmr.2011.714

Zhao, M., Ren, Y., Wei, W., Yang, J., Zhong, Q., and Li, Z. (2021). Metabolite analysis of Jerusalem artichoke (Helianthus tuberosus l.) seedlings in response to polyethylene glycol-simulated drought stress. *Int. J. Mol. Sci.* 22, 3294. doi: 10.3390/ijms22073294

Zhou, Y. X., Zhang, H., and Peng, C. (2014). Puerarin: a review of pharmacological effects. *Phytother. Res.* 28, 961–975. doi: 10.1002/ptr.5083

Zou, S., Wu, J., Shahid, M. Q., He, Y., Lin, S., Liu, Z., et al. (2020). Identification of key taste components in loquat using widely targeted metabolomics. *Food Chem.* 323, 126822. doi: 10.1016/j.foodchem.2020.126822

frontiers | Frontiers in Plant Science

TYPE Original Research
PUBLISHED 12 June 2023
DOI 10.3389/fpls.2023.1193284

OPEN ACCESS

EDITED BY
Jose M. Mulet,
Universitat Politècnica de València, Spain

REVIEWED BY
Dinakaran Elango,
Iowa State University, United States
Markus Kuhlmann,
Leibniz Institute of Plant Genetics and Crop Plant Research (IPK), Germany

*CORRESPONDENCE
Alan H. Schulman
alan.schulman@helsinki.fi

RECEIVED 24 March 2023
ACCEPTED 09 May 2023
PUBLISHED 12 June 2023

CITATION
Paul M, Tanskanen J, Jääskeläinen M, Chang W, Dalal A, Moshelion M and Schulman AH (2023) Drought and recovery in barley: key gene networks and retrotransposon response.
Front. Plant Sci. 14:1193284.
doi: 10.3389/fpls.2023.1193284

Drought and recovery in barley: key gene networks and retrotransposon response

Maitry Paul [1,2], Jaakko Tanskanen [1,2,3], Marko Jääskeläinen [1,2], Wei Chang [1,2], Ahan Dalal [4], Menachem Moshelion [4] and Alan H. Schulman [1,2,3]*

[1]HiLIFE Institute of Biotechnology, University of Helsinki, Helsinki, Finland, [2]Viikki Plant Science Centre (ViPS), University of Helsinki, Helsinki, Finland, [3]Production Systems, Natural Resources Institute Finland (LUKE), Helsinki, Finland, [4]The Robert H. Smith Institute of Plant Sciences and Genetics in Agriculture, The Hebrew University of Jerusalem, Rehovot, Israel

Introduction: During drought, plants close their stomata at a critical soil water content (SWC), together with making diverse physiological, developmental, and biochemical responses.

Methods: Using precision-phenotyping lysimeters, we imposed pre-flowering drought on four barley varieties (Arvo, Golden Promise, Hankkija 673, and Morex) and followed their physiological responses. For Golden Promise, we carried out RNA-seq on leaf transcripts before and during drought and during recovery, also examining retrotransposon *BARE*1expression. Transcriptional data were subjected to network analysis.

Results: The varieties differed by their critical SWC (Θ_{crit}), Hankkija 673 responding at the highest and Golden Promise at the lowest. Pathways connected to drought and salinity response were strongly upregulated during drought; pathways connected to growth and development were strongly downregulated. During recovery, growth and development pathways were upregulated; altogether, 117 networked genes involved in ubiquitin-mediated autophagy were downregulated.

Discussion: The differential response to SWC suggests adaptation to distinct rainfall patterns. We identified several strongly differentially expressed genes not earlier associated with drought response in barley. *BARE1* transcription is strongly transcriptionally upregulated by drought and downregulated during recovery unequally between the investigated cultivars. The downregulation of networked autophagy genes suggests a role for autophagy in drought response; its importance to resilience should be further investigated.

KEYWORDS

drought, autophagy, barley, resilience (environmental), network analysis, gene expression, *Hordeum vulgare*

1 Introduction

Optimization of the balance between carbon fixed and water lost by transpiration is a central problem for plants. In drought, the challenge to water homeostasis from decreased water potential generates a response by the plant at a critical soil water content (SWC), which leads to stomatal closure, even in daylight, to reduce water loss. The associated dehydration and its consequences are commonly referred to as drought stress. Drought response involves mechanisms and signaling cascades, leading to stomatal closure (Merilo et al., 2015) and to physiological and metabolic changes (Jogawat et al., 2021). Mechanisms to counter dehydration and cellular damage include accumulation of osmolytes to mediate osmotic adjustment (Hildebrandt, 2018) and enzymatic and non-enzymatic scavenging of excess reactive oxygen species (ROS) (Das and Roychoudhury, 2014), as well as changes in the chloroplast proteome (Chen et al., 2021a).

Two contrasting responses to water limitation have been described: isohydric and anisohydric (Sade et al., 2012). Isohydric implies maintenance of constant water potential; many physiological parameters are involved (Scharwies and Dinneny, 2019). Barley has been shown to be diurnally anisohydric (Tardieu and Simonneau, 1998). The terms also have been applied broadly for drought response strategy (Sade et al., 2012), isohydric plants conservating water, closing stomata at a relatively high SWC, sacrificing carbon fixation but delaying plant dehydration. This strategy may reduce risk from early droughts in climates where the probability of precipitation increases during the growing season. An anisohydric plant delays stomatal closure and continues fixing carbon, a strategy consistent with environments having terminal droughts or with those where dry periods are short and show little seasonal variation.

Studies in Arabidopsis indicate that induction of autophagy is needed for drought tolerance (Avin-Wittenberg, 2019). Autophagy is an evolutionarily conserved mechanism for recycling damaged proteins and cellular organelles by transport to the vacuoles or lysosomes for degradation (Chen et al., 2021b). Rewatering at the end of drought may result in the resumption of normal diurnal stomatal opening, recovery of photosynthesis, and the resumption of growth. The occurrence, degree, and rate of recovery strongly depends both on the intensity and duration of drought and on the species; recovery has relatively little studied on its own (Xu et al., 2010; Lawas et al., 2019; Chen et al., 2021b; Qi et al., 2021) but involves the ABA signaling pathway (Cao et al., 2021).

Drought is also well known to induce transcription of transposable elements, particularly retrotransposons (RLX; Wicker et al. (2007). The RLXs have been shown to be transcriptionally induced by stresses ranging from ionizing and UV radiation to drought and heavy metals (Kimura et al., 2001; Grandbastien et al., 2005; Ramallo et al., 2008; Makarevitch et al., 2015; Galindo-Gonzalez et al., 2017). For barley (*Hordum vulgare* L.) RLX, earlier studies indicated that *BARE*1 transcripts and translational products accumulated under drought (Jääskeläinen et al., 2013) and appeared linked to the abscisic acid (ABA) signaling pathway through the ABA-response elements (ABREs) present in the *BARE*1promoter (Jääskeläinen et al., 2013).

Optimization of drought response for an annual crop such as barley is related to the climatic zone for which the plant is bred. In some zones, the probability of drought may be greater early in the growing season (e.g., Nordic conditions, before flowering); in others, the probability of drought increases during seed maturation (Mediterranean basin, as terminal drought) (Rollins et al., 2013; Tao et al., 2017). Here, we focus on pre-flowering drought in four barley cultivars shown in pilot experiments to respond differentially to SWC (Dalal et al., in prep). For one of them (Golden Promise), the goal was to carry out transcriptional analyses for leaves for both genes and the *BARE*1 RLX at physiologically defined time points before, during, and after drought. Gene expression data were then input to network analysis to understand the activated pathways and possible connections to RLX stress response.

2 Materials and methods

2.1 Plant material

Barley cultivars Arvo, Golden Promise ("GP"), Hankkija 673 ("H673"), and Morex were selected from the diversity set of the ERA-NET SusCrop Climbar Project. GP is the standard genotype for transformation in barley (Schreiber et al., 2019), whereas preliminary experiments indicated that Arvo and H673 have high and low stomatal conductance, respectively (Dalal et al., in prep.). Morex is the established reference genome assembly in barley (Beier et al., 2017; Mascher et al., 2017; Mascher et al., 2021).

2.2 Growth conditions

Plants were grown during the winter season in the iCORE functional phenotyping greenhouse (https://plantscience.agri.huji.ac.il/icore-center) under natural sunlight, with moderate temperature control, which closely reflects the natural external environment (Halperin et al., 2017; Galkin et al., 2018) (Figure 1A). There, drought experiments were carried out with a randomized block design on a gravimetric functional phenotyping platform (Dalal et al., 2020; Gosa SC et al, 2022) (Plantarray, PA 3.0, PlantDitech Ltd., Yavne, Israel), which allows simultaneous standardized control of drought treatment with continuous monitoring of multiple physiological parameters. The platform comprises temperature-compensated load cells (lysimeters) for simultaneous and continuous gravimetric monitoring of water relations in the soil–plant–atmosphere continuum (SPAC) under dynamic environmental conditions (Halperin et al., 2017).

Seeds were sown in germination trays and then transplanted at the 3- to 4-leaf stage (2 weeks old) to pots. Before transplanting, seedling roots were carefully washed to remove the original soil,

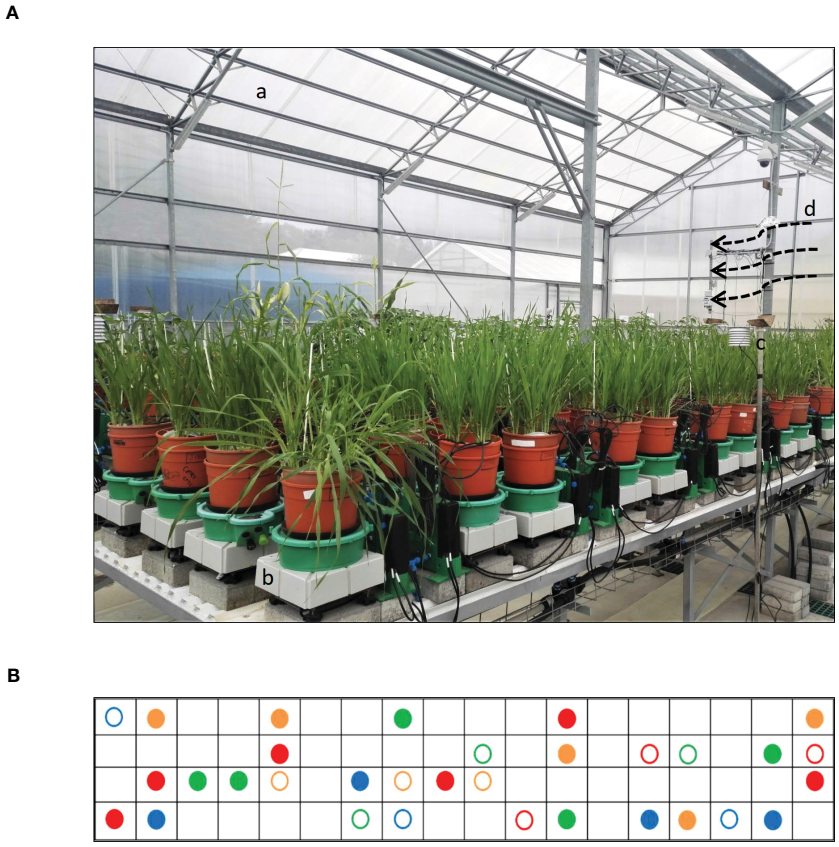

FIGURE 1
Experimental setup. **(A)** Lysimeters of gravimetric functional phenotyping platform, comprising 72 lysimeter platforms with soil probes and four weather stations. The setup features: (a) minimally controlled greenhouse, (b) lysimeter platform, (c) weather station, and (d) cooling vent. **(B)** Table diagram for sample pots distributed according to a randomized block design. Filled circles are drought treatments; empty circles are well-watered (controls). Arvo, orange; GP, red; H673, green; Morex, blue.

planted into potting soil ["Bental 11", Tuff Marom Golan, Israel; four per 3.9-liter pot; Dalal et al. (2020)], and then placed onto lysimeters (Dalal et al., 2019; Gosa SC et al, 2022). Each cultivar was grown in four to six biological replicates for the drought treatment and in three biological replicates for the controls, which were maintained under well-irrigated conditions (Figure 1B). The plants were grown at 18°C–25°C, 20%–35% relative humidity, and 10-h light/14-h dark, typical of the greenhouse's semi-controlled conditions as affected by the external Mediterranean winter. Temperature, humidity, and photosynthetically active radiation (PAR) were monitored as described earlier (Dalal et al., 2020; Gosa SC et al, 2022). The vapor pressure deficit (VPD) ranged between 0.2 and 4.0 kPa in the greenhouse and represented typical weather fluctuations during winters in Central Israel (Figure 2B).

2.3 Experimental design

To mimic the onset of a drought, the experiment was divided into five phases on the lysimeter platform: (i) well watered, (ii) dry phase I (iii), rewatering I (iv), dry phase II, and (v) rewatering II (Figure 2A). For the well-watered phase (first 12 days) and for the controls throughout, plants daily received three nighttime irrigations at 3-h intervals to reach field capacity. The volumetric water content (VWC) was calculated with the SPAC analytical software embedded in the Plantarray system (Figure 3). In dry phase I, the system was set to irrigate droughted plants to 80% of their own previous day's transpiration, so that these would be subjected to gradual water stress from days 13 to 24, followed by rewatering (rewatering I) on the night of day 25. Dry phase II extended from days 26 to 41 with the same irrigation parameters as dry phase I, until the time when the droughted plants reached <100 g of daily transpiration (DT; around 20% to 30% of controls) (Figure 4D). Rewatering II began on day 42. Daily night irrigation was given to all plants until day 44. At that point, several irrigation cycles were used to moisten the soil and to ensure a laterally uniform SWC in the pots. VPD data were continuously monitored (Figure 2B).

2.4 Sampling and isolation of RNA

Second leaves from the youngest tillers were collected for RNA analysis: time point 1 (T1) on the last day of the well-watered phase (day 12); T2, on the last day of dry phase II (day 41); T3, last day of rewatering II (day 44). Well-watered control samples at the same

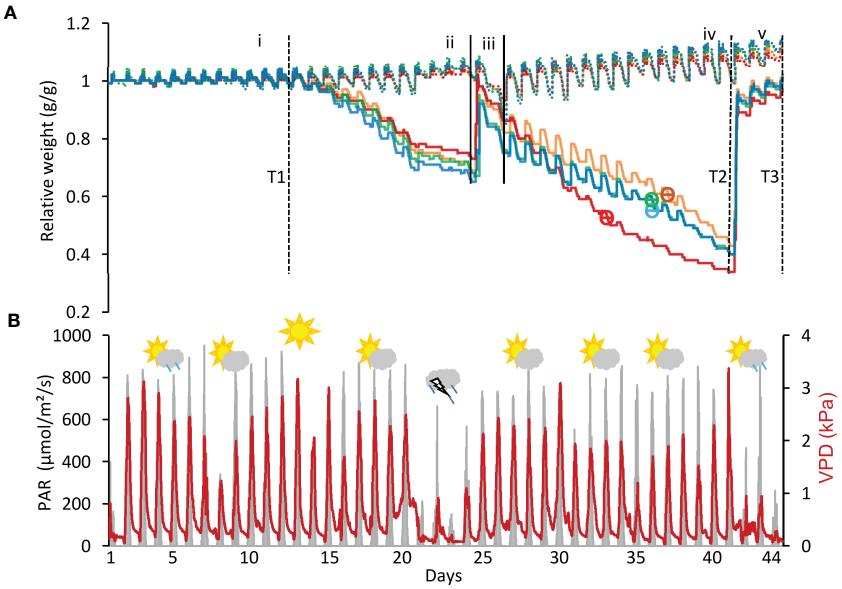

FIGURE 2
Key system parameters during drought and recovery. **(A)** Relative change in system weight of all control and drought-treated pots. The experiment is divided into five phases:(i)well-watered,(ii)dry phase I,rewatering I, (iv) dry phase II, and (v) rewatering II. Drought samples, solid lines; well-irrigated controls, dashed. Cultivars are Arvo, orange; Golden Promise (GP), red; Hankkija 673 (H673), green; Morex, blue. Day of Θ crit indicated by Θ on the cultivars' curves. Time points (T) for collection of RNA from leaf samples are: T1, last day of well-watered; T2, last day of drought; T3, last day of recovery. **(B)** Photosynthetically active radiation (PAR) and vapor pressure deficit (VPD) over the course of the experiment. The weather symbols depict conditions outdoors during this time each symbol representing the average of five days.

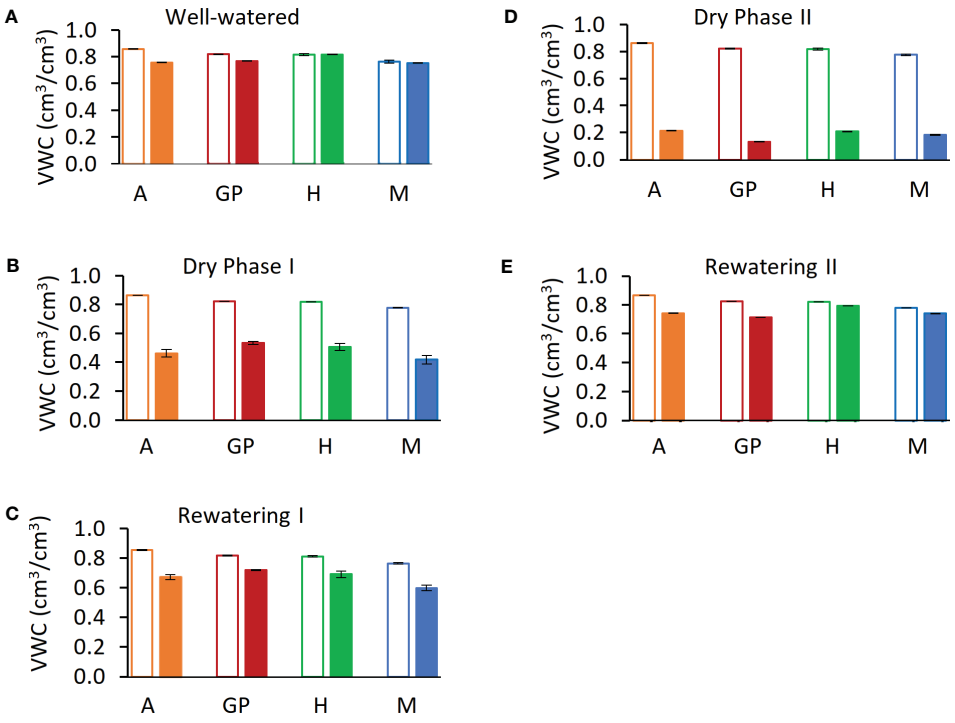

FIGURE 3
Calculated soil volumetric water content (VWC) during five phases of the experiment. **(A)** Day 12, last day of well-watered (phase i). **(B)** Day 24, last day of dry phase I **(C)** Day 25, last day of rewatering I **(D)** Day 41, dry phase II. **(E)** Day 44, last day of rewatering II. Solid bars represent drought samples; empty bars represent controls. Arvo (A), orange; red, Golden Promise (GP), green; Hankkija 673 (H); blue, Morex (M)..

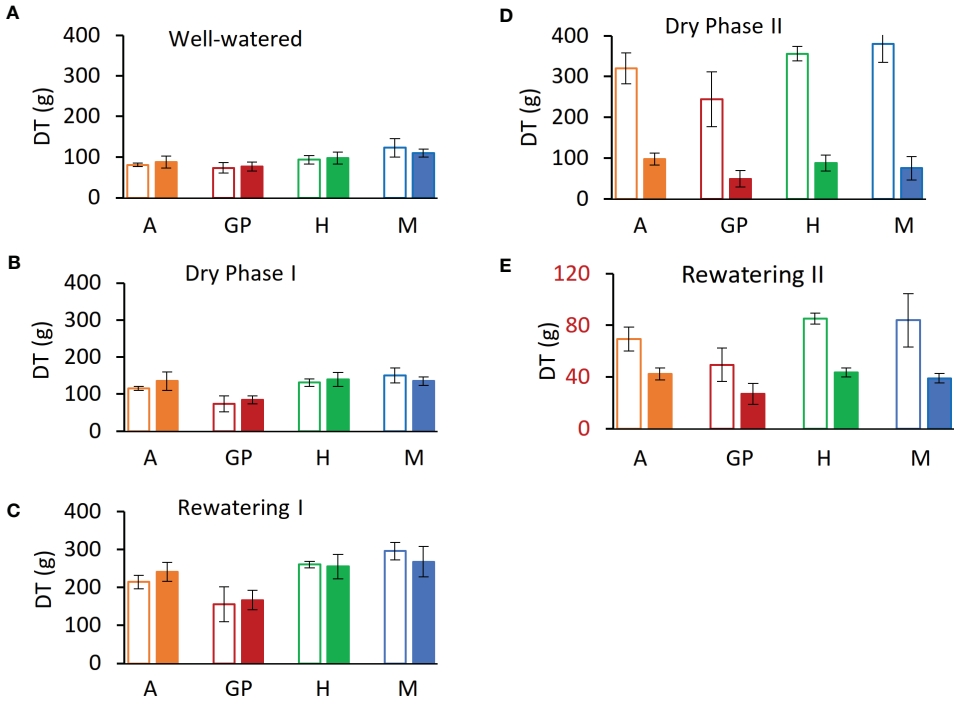

FIGURE 4
Daily transpiration (DT) at the end of each experimental phase. **(A)** Day 12, last day of well-watered (phase i). **(B)** Day 24, last day of dry phase I **(C)** Day 25, last day of Rewatering I **(D)** Day 41, dry phase II. **(E)** Day 44, last day of rewatering II. Solid bars represent drought samples, empty bars controls. Orange represents Arvo (A); red, Golden Promise (GP); green, Hankkija 673 (H); blue, Morex (M).

growth stages were collected at T2 and T3. For RNA extraction, leaf samples were collected in liquid N2 and later ground and stored in TRIzol reagent (Invitrogen). Total RNA was extracted from the leaf samples with the Direct-zol RNA Miniprep Plus kit according to the manufacturer's (Zymo Research Europe GmbH) guidelines. RNA (1 µg) from each sample was treated with Ambion® DNase I (RNase-free; Applied Biosystems) in a 20-µl reaction mixture for 90 min at 37°C to remove remaining DNA. An RNeasy MinElute Cleanup Kit (Qiagen) was used to purify and concentrate the RNA from the DNase treatments. RNA quantity and quality were checked both spectrophotometrically (NANODROP-2000 spectrophotometer, Thermo Scientific) and by agarose gel electrophoresis.

2.5 qPCR analysis

Reverse transcription to cDNA was carried out in reactions containing 200 ng of total RNA, 1 µl of Invitrogen™ SuperScript® IV Reverse Transcriptase (RT) (Thermo Fisher Scientific), 1 µl of 10 mM deoxynucleotide triphosphates (dNTPs; Thermo Scientific),, and 0.5 µl of 10 µM primer E1820 (AAGCAGTGGTAACAACGCA GAGTACT30NA) as the oligo(dT) primer (Chang et al., 2013). For qPCR, 10 µl of reactions comprised 0.5 µl of cDNA as template, 5 µl of SsoAdvanced™ Universal SYBR® Green Supermix, 0.1 µl of each forward and reverse primer, and 4.3 µl of water. Reactions were run on a CFX 384 Real-Time PCR detection system (Bio-Rad) in three technical replicates as follows: activation for 2 min at 94°C; 40 cycles comprising denaturation for 30 s at 94°C, annealing for 30 s at 56°C, and extension for 1 min at 72°C. Relative quantification of the cDNA product was made by the 2– **ΔΔCT** method (Livak and Schmittgen, 2001). All primers used for qPCR are listed in Supplementary Table S1. The amplification efficiency of all the primers has been checked; R2 was from 0.97 to 0.99.

2.6 RNA-seq and network analysis

Three sets of biological replicates from each time point and their corresponding controls were taken from cv. GP for RNA-seq analysis. Libraries were constructed using the TruSeq Stranded Total RNA kit with plant cytoplasmic and chloroplast ribosomal RNA removal (Illumina); adaptors were TruSeq adaptors. FastQC (Andrews, 2010) was used to check the quality control metrics of the raw reads and to trim the RNA-seq data. Adapter sequences were removed with Trimmomatic (Bolger et al., 2014). The STAR alignment method (Dobin et al., 2013) served to map sequence reads to the GP genome (GPV1.48, Ensembl Plants). Next, to quantify transcript expression, the Salmon tool was applied (Patro et al., 2017). Differentially expressed genes (DEGs) and principal component analysis (PCA) plots were obtained with DESeq2 (Love et al., 2014; Hong et al., 2020). Multidimensional scaling (MDS) plots were used to verify the approximate expression differences between sample replicates.

From the clean reads, those with pADJ value < 0.05 for their fold change were run in g:Profiler for functional enrichment analysis and to obtain a Gene Matrix Transposed (GMT) file for

Cytoscape (Reimand et al., 2019). Cytoscape_v3.8.2 was then used to develop network clusters for biological pathways. The parameters used were false discovery rate (FDR) q-value cutoff = 1, node cutoff = 0.5, edge cutoff = 0.375, and significance threshold for functional enrichment $p \leq 0.01$.

3 Results

3.1 Whole-plant water relations over the course of drought and recovery

Four barley varieties (Arvo, GP, H673, and Morex), which, in preliminary experiments, differed in their water use strategies, were placed on lysimeters and measured through the four experimental phases. Transpiration and plant weight were followed continuously. The SWC at which the transpiration rate drops in response to drought [Θ critical point (Θ_{crit})] was calculated from the data.

*Daily transpiration.*Analysis of DT of the four varieties on the Plantarray platform revealed variation in their transpiration both between the varieties (Figure 4, Supplementary Figure S1) and day by day (Figure 5A, Supplementary Figures S1A–C). All plants were exposed to similar changes in PAR and VPD simultaneously (Figure 1), which were monitored throughout the experiment (Figure 2B); from days 21 to 23, the cloudy and rainy weather outside the minimally controlled greenhouse reduced the PAR and VPD within, lowering DT. For the well-watered control plants of all varieties, DT gradually increased along with plant size over the course of the experiment, closely matched by the droughted plants, which then diverged following the onset of dry phase II. The overall DT of Morex is the highest, followed by H673, Arvo, and GP. The DT of droughted Morex plants diverged from controls by day 20 (Supplementary Figure S1C) and H673 by day 25 (Supplementary Figure S1B), whereas Arvo and GP only by day 30 (Figure 5A, Supplementary Figure S1A). A complete return to control whole-plant transpiration was not observed for any of the varieties before termination of the experiment on day 44; all plants showed low DT between days 42 and 44, linked to low VPD and PAR.

3.2 Effect of drought on the plant growth and transpiration

Changes in net plant weight as a measure of growth were calculated from the Plantarray system as before (Halperin et al., 2017). The high rate of growth observed for all varieties between days 2 and 9 (Figure 5B, Supplementary Figures S2A–C) corresponds to the peak in PAR during the same period (Figure 2B). The control plants showed similar trends in growth rates throughout the experiment. The droughted plants of all four varieties displayed specific growth rates lower than their well-watered controls during drought: first in Morex (day 23), then Arvo (day 29), and then both H673 and GP (on day 30) (Supplementary Figure S2, Figure 5B). The relative effect of drought on the growth rate of the four varieties is most apparent when the rate of change is considered.

The Θ_{crit} was calculated for all varieties (Figure 6) on the basis of midday whole-plant transpiration (Halperin et al., 2017). The transpiration rates of all four varieties remained constant up to a VWC of 0.55 and then declined, with the VWC at the Θ_{crit} differing by variety. Arvo, H673, and Morex display similar initial transpiration rates, whereas GP was about 30% lower. The H673 Θ_{crit} occurred at 0.53 VWC on day 36, Arvo at 0.52 on day 37, Morex at 0.46 on day 36, and GP at 0.42 already on day 33.

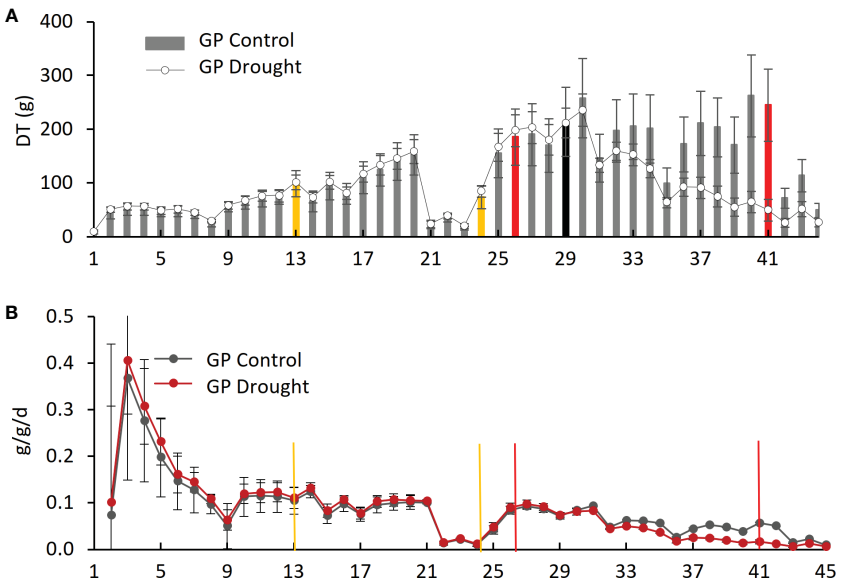

FIGURE 5
Daily transpiration and plant weight over the experimental period for Golden Promise (GP). **(A)** Daily transpiration (DT). The black bar represents the divergence of drought from control plants. **(B)** Daily specific change in plant weight (g/g/d). Yellow bars represent the start and end of dry phase I, and red bars show the start and end of dry phase II.

Following stomatal closure at Θ_{crit}, weight (water) loss preceded at different rates among the varieties. Although GP had the lowest initial transpiration rate (Figure 6), it declined the fastest, whereas Arvo, with a high transpiration rate, declined the slowest.

3.3 Gene expression analysis

An average of 33 million reads per sample were generated by RNA-seq, which showed the expression of approximately 27,000 genes. To check the quality of the gene expression, DESeq2 dispersion estimates were made to reflect the variance in gene expression for a given mean value; values were adjusted as the basis for significance testing (Supplementary Figure S3). PCA of differential gene expression showed an alignment of all groups of samples along PC1 and a narrow dispersion of all control groups along PC2 (Supplementary Figure S4). Movement of the expression pattern during the course of the experiment shows a shift within PC2 during drought and then a return to near the position of the control groups for the recovery samples (Supplementary Figure S4), consistent with ongoing physiological recovery. Of the genes detected, those differentially expressed (DEGs) with adjusted $p < 0.01$ include 611 that were upregulated and 643 downregulated in drought compared to the well-watered controls samples taken on the same day, whereas 697 were upgregulated and 282 downregulated during recovery compared with the controls on the same day (Supplementary Tables S2–S5).

RNA-seq reads were annotated by reference to the cv. Morex genome (release 2), transcript expression was quantified, and DEGs were identified. In the drought samples, the most highly upregulated gene compared to the well-watered control was for glutathione s-transferase (Table 1), with 3-million-fold more expression than control; in the samples from plants undergoing recovery, this gene dropped by 8.6-fold compared with drought. Altogether, 44 genes showed more than 100-fold upregulation and 218 genes over 10-fold upregulation compared to controls (Supplementary Table S2). The most downregulated gene was for a cytochrome P450 family protein (Table 2), with around 3,000-fold less expression than control. Conversely, among the DEGs in recovery compared to drought, this gene showed the third highest upregulation, 195-fold (Supplementary Table S7). Altogether, nine genes showed more than 100-fold downregulation and 53 genes over 10-fold downregulation (Supplementary Table S3).

In the recovery samples, compared to the controls that never experienced drought, the most upregulated gene was annotated as a leguminosin group485 secreted peptide, having 16-billion-fold more expression than in the controls (Table 3). This gene has been reported in *Medicago truncatula* root during root nodulation, with gene ID Medtr5g064530 and Medtr2g009450. However, a BLASTp of the transcript corresponding to the barley gene (HORVU.MOREX.r2.5HG0428280.1) has its best match (89% identity, Expected value (*E*-value) of 2e-36) to a serine/threonine-protein phosphatase 7 (PP7) long-form homolog for barley (XP_044965344.1). Four genes showed more than 100-fold upregulation and 58 genes over 10-fold upregulation (Supplementary Table S4). Compared to the drought samples, 139 genes showed more than 10-fold upregulation. The most upregulated, compared with drought (635X; Supplementary Table S7), was annotated as for a "bifunctional inhibitor/lipid-transfer protein/seed storage 2S albumin superfamily protein," a protein type reported to have diverse functions (Wei and Zhong, 2014).

The most downregulated transcript in recovery compared to control corresponded to a superfamily *Copia* RLX, which automatic annotation designated as a "retrovirus-related Pol polyprotein", having around 8-million-fold less expression than the control (Table 4). When drought and recovery DEGs were compared, the most strongly downregulated (1.8-million fold) transcript likewise was annotated as a "Pol polyprotein from transposon *Tnt*1-94", i.e., a superfamily *Copia* RLX (Supplementary Table S6). Of the top 20 repressed in recovery compared with drought samples (Supplementary Table S6), three were annotated as dehydrins (435- to 1634-fold downregulated) and three as heat-shock proteins (188- to 627-fold downregulated). Compared to controls, overall, three genes showed more than 100-fold downregulation and nine genes more than 10-fold downregulation (Supplementary Table S5). Compared to drought samples, 222 genes in the recovery

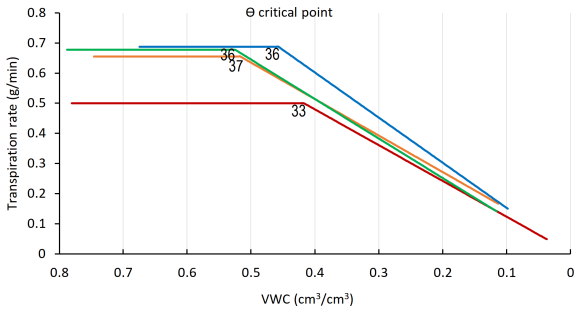

FIGURE 6
Θ critical point (Θ_{crit}), for midday whole-plant transpiration versus calculated VWC. The inflection points in the fitted transpiration lines indicate the Θ_{crit}. Arvo, orange; Golden Promise, red; Hankkija 673 (H673), green; Morex, blue. Day on which the Θ_{crit} occurred is indicated by a number adjacent to the inflection point..

TABLE 1 Top 20 upregulated genes, drought phase.

Ensembl_gene_id	Description	log2 FC[1]	padj[2]
HORVU.MOREX.r2.5HG0441700	Glutathione s-transferase	21.49	5.6E-07
HORVU.MOREX.r2.6HG0456270	Linalool synthase	13.20	9.4E-05
HORVU.MOREX.r2.6HG0516720	Dehydrin	11.76	9.4E-18
HORVU.MOREX.r2.5HG0395660	U-box domain containing protein	10.67	6.2E-03
HORVU.MOREX.r2.5HG0429440	Dehydrin	10.31	3.4E-05
HORVU.MOREX.r2HG0053260	NOT FOUND	10.17	2.1E-03
HORVU.MOREX.r2.3HG0242240	Coiled-coil domain-containing protein 18	9.89	7.6E-12
HORVU.MOREX.r2.3HG0184850	Trypsin inhibitor	9.44	5.5E-09
HORVU.MOREX.r2.4HG0328360	Branched-chain amino acid aminotransferase	9.38	5.6E-04
HORVU.MOREX.r2.3HG0186590	Basic 7S globulin 2	9.28	2.1E-04
HORVU.MOREX.r2.7HG0593880	Cysteine-rich/transmembrane domain A–like protein	9.19	2.3E-03
HORVU.MOREX.r2.3HG0201230	DWNN domain	9.13	1.9E-04
HORVU.MOREX.r2.7HG0620080	Carbonic anhydrase	9.00	2.7E-03
HORVU.MOREX.r2.2HG0149830	Caleosin	8.39	4.3E-05
HORVU.MOREX.r2.3HG0184880	Trypsin inhibitor	8.38	6.9E-11
HORVU.MOREX.r2.3HG0245240	Disulfide isomerase	8.35	4.6E-07
HORVU.MOREX.r2.5HG0356770	Germin-like protein	8.09	8.1E-04
HORVU.MOREX.r2.5HG0402770	Basic helix-loop-helix (bHLH) DNA-binding superfamily protein	8.04	2.7E-05
HORVU.MOREX.r2.2HG0149820	Caleosin	7.75	9.0E-03
HORVU.MOREX.r2.6HG0512380	2-oxoglutarate (2OG) and Fe (II)-dependent oxygenase superfamily protein	7.61	1.7E-03

[1]FC, fold change; [2]padj, adjusted *p*-value.

phase showed more than 10-fold downregulation and 140 showed more than 10-fold upregulation. To place the very many significantly DEGs into a biological context, we undertook a network analysis, as described below.

3.4 Network analysis

3.4.1 Upregulated networks under drought stress

When drought-treated plants were compared to the well-watered controls of the same age, a simple pattern of three clusters with two nodes, each comprising the upregulated genes, was seen (Figure 7). Detailed information on key nodes with the clusters is presented in Supplementary Table S8. Cluster A, which has the highest statistical significance and contains 113 genes, is annotated as "response to water" (GO:0009415) and to "acid chemical" (GO:0001101), meaning any process that responds to the availability of water (e.g., under drought), or to an anion. In this cluster, the dehydrin genes have the highest differential expression, ranging from 100- to 3458-fold upregulation during drought, followed by the late-embryogenesis-abundant (LEA) protein Lea14 at 60-fold (Supplementary Table S12). Both are associated with physiological drought; dehydrin is a drought-inducible LEA II protein (Kosová et al., 2014). Conversely, three dehydrins are among the top 20 downregulated DEGs in recovery vs. drought (Supplementary Table S6). Of the other two clusters, one (cluster B) comprises nodes for response to salt stress (GO:0009651) and osmotic stress (GO:0006970), together with 126 genes (Supplementary Table S8). In cluster B, the most strongly upregulated genes are for a serine-threonine protein kinase (Supplementary Table S12), which is a family well connected to drought response (Saddhe et al., 2021) and salt stress (GO:0009651; 19-fold), and for an uncharacterized transcription factor (18-fold). Drought, salt, and osmotic stress response pathways are well-known to overlap (Buti et al., 2019). The third cluster C, with 250 genes, is associated with negative regulation of protein metabolic processes in two nodes (GO:0051248 and GO:0032269). These nodes contain multiple proteinase inhibitors, including a trypsin/amylase inhibitor such as was earlier shown to confer drought tolerance (Xiao et al., 2013), that are strongly upregulated in drought (64- to 694-fold).

3.4.2 Downregulated networks under drought stress

During the drought stress, eight clusters, comprising 48 nodes, were downregulated (Figure 7B). All are related to processes of growth and development. The cluster with the highest significance and with the greatest number of genes (B) is related to metabolism

TABLE 2 Top 20 downregulated genes, drought phase.

Ensembl_gene_id	Description	log2 FC1	padj2
HORVU.MOREX.r2.3HG0191820	Cytochrome P450 family protein	−11.71	6.0E-08
HORVU.MOREX.r2.3HG0268430	Basic helix-loop-helix (BHLH) family transcription factor	−9.82	3.1E-03
HORVU.MOREX.r2.4HG0346330	Cortical cell-delineating protein	−9.46	2.6E-09
HORVU.MOREX.r2.4HG0346340	Cortical cell-delineating protein	−9.28	4.7E-08
HORVU.MOREX.r2.2HG0158510	Bifunctional inhibitor/lipid-transfer protein/seed storage 2S albumin superfamily protein	−8.79	4.5E-05
HORVU.MOREX.r2.4HG0288340	translation initiation factor	−7.73	4.0E-07
HORVU.MOREX.r2.7HG0561840	MYB-related transcription factor	−7.69	4.0E-09
HORVU.MOREX.r2.5HG0369380	Glutaredoxin family protein	−7.29	1.0E-04
HORVU.MOREX.r2.3HG0268450	Basic helix-loop-helix (bHLH) DNA-binding superfamily protein	−6.98	2.3E-03
HORVU.MOREX.r2.7HG0548630	Pollen Ole e 1 allergen/extensin	−6.56	7.0E-09
HORVU.MOREX.r2.5HG0356760	Glutaredoxin family protein	−6.47	2.6E-03
HORVU.MOREX.r2.5HG0412710	CRT-binding factor	−6.45	1.5E-04
HORVU.MOREX.r2.2HG0165830	Pollen Ole e 1 allergen/extensin	−6.39	1.3E-09
HORVU.MOREX.r2.4HG0330890	Beta-xylosidase	−6.20	1.6E-03
HORVU.MOREX.r2.3HG0268330	Dicer-like 3	−5.83	4.2E-07
HORVU.MOREX.r2.2HG0079590	Avr9/Cf-9 rapidly elicited protein	−5.72	2.9E-03
HORVU.MOREX.r2.7HG0623060	Aquaporin	−5.61	4.4E-03
HORVU.MOREX.r2.6HG0455680	Pollen Ole e 1 allergen/extensin	−5.57	1.1E-07
HORVU.MOREX.r2.5HG0438030	Leucine-rich repeat receptor-like protein kinase family protein	−5.47	1.3E-05
HORVU.MOREX.r2.2HG0160110	Orexin receptor type 2	−5.39	1.0E-07

[1]FC, fold change; [2]padj, adjusted p-sub>value.

of carboxylic acids and anions and comprises 3,600 genes. These are involved in nutrient supply, plant development, and processes including cell wall signaling, guard mother cell division, and pathogen virulence (Polko and Kieber, 2019). The key nodes in this cluster include metabolism of organic acids (GO:0006082), oxoacids (GO:0043436), cellular amino acids (GO:0006520), carboxylic acids (GO:0019752), and small molecules (GO:0044281) (Supplementary Table S9). The other interconnected clusters are associated with cluster A (654 genes), which concerns the regulation of photosynthesis, (e.g., photosystem genes, 2- to 5-fold downregulated): purine ribonucleotide metabolism, transfer RNA (tRNA) aminoacylation translation, pigment biosynthesis, and tetraterpenoid biosynthesis. A second set of linked clusters downregulated under drought stress comprises plastid translation organization (cluster G, 83 genes; GO:00032544 and GO:0009657) and pigment, including chlorophyll and carotenoid, biosynthesis (cluster E, 1588 genes; cluster F, 136 genes). A small cluster (H, 10 genes) unlinked to others is annotated as concerning plant ovary development (GO:0032544) although, given that leaf samples were analyzed, the function appears to be otherwise. Detailed information on the key nodes and clusters can be found in Supplementary Tables S9, S13. Hence, the downregulated pathways are manifold and generally involved in growth and development.

3.4.3 Upregulated networks during recovery

Recovery is the process of restoring the physiological and molecular functions from drought-induced damage (Chen et al., 2021). As described above, gene networks related to the growth and development were downregulated during drought. In turn, during recovery, many associated with growth, plastidial function, and energy metabolism were upregulated, organized in five linked clusters of interconnected nodes (Figure 8A). Cluster A has 2597 genes and concerns cell wall metabolism (Supplementary Table S10). Its nodes include those for carbohydrate (GO:0005975), polysaccharide (GO:0005976), glucan (GO:0006073), and xyloglucan (GO:0010411) metabolism, “cell wall organization or biogenesis”, “external encapsulation structure organization” (GO:0045229), and hemicellulose metabolism (GO:0010410). Genes for biosynthesis of xyloglucan, an abundant component of the primary cell wall, were particularly strongly induced, up to 239-fold over the control plants that did not experience drought. Two of the clusters (B, 2522 genes; C, 7842 genes) include nodes associated with protein biosynthesis that were downregulated during drought but are upregulated during recovery. These include nodes for ribosome biogenesis (GO:0042254), ncRNA metabolism (GO:0034660), ribosomal RNA (rRNA) processing (GO:0006364), ribonucleoprotein complex assembly (GO:0022618), maturation of large subunit rRNA (GO:0000463), translation (GO:0006412),

TABLE 3 Top 20 upregulated genes during the recovery phase.

Ensembl_gene_id	Description	log2 FC[1]	padj[2]
HORVU.MOREX.r2.5HG0428280	Leguminosin group485 secreted peptide	33.95	5.4E-10
HORVU.MOREX.r2.5HG0406650	Nucleolar-like protein	7.59	2.4E-03
HORVU.MOREX.r2.7HG0563500	Fasciclin-like arabinogalactan protein	7.11	2.7E-04
HORVU.MOREX.r2HG0002090	Arginine decarboxylase	6.73	3.9E-03
HORVU.MOREX.r2.7HG0604490	Xyloglucan endotransglucosylase/hydrolase	6.25	3.4E-03
HORVU.MOREX.r2.2HG0083580	Cytochrome P450	5.57	9.3E-03
HORVU.MOREX.r2.4HG0340230	translation initiation factor	5.54	1.1E-03
HORVU.MOREX.r2.2HG0179370	Cytochrome P450	5.51	1.0E-02
HORVU.MOREX.r2.7HG0579230	MLG (mixed-linkage glucan) synthase, Biosynthesis of MLG (cell wall polysaccharide	5.33	6.3E-04
HORVU.MOREX.r2HG0072930	Thiamine-phosphate synthase	5.05	6.7E-15
HORVU.MOREX.r2.6HG0519350	Heparanase	5.05	2.2E-04
HORVU.MOREX.r2.2HG0141350	3-Oxoacyl-[acyl-carrier-protein] synthase	4.86	4.4E-08
HORVU.MOREX.r2.3HG0183950	Glycosyltransferase	4.81	2.5E-03
HORVU.MOREX.r2.5HG0355750	Bidirectional sugar transporter SWEET	4.80	3.5E-05
HORVU.MOREX.r2.7HG0558300	Glycosyltransferase	4.78	4.4E-03
HORVU.MOREX.r2.5HG0349900	Receptor-like protein kinase	4.67	2.4E-05
HORVU.MOREX.r2.6HG0516480	F-box protein SKIP8	4.52	1.5E-13
HORVU.MOREX.r2.4HG0318550	MYB transcription factor	4.44	5.4E-03
HORVU.MOREX.r2.6HG0502520	4-coumarate: coenzyme A ligase, Flavonoid biosynthesis	4.39	7.9E-03
HORVU.MOREX.r2.7HG0594280	Beta-galactosidase	4.33	6.7E-03

[1]FC, fold change; [2]padj, adjusted p-value.

peptide biosynthesis and metabolism (GO:0043043 and GO:0006518), amide biosynthesis (GO:0043604), and tRNA aminoacylation and metabolism (GO:0043039 and GO:0006399). Consistent with reactivation of leaf function, plastid and chloroplast organization processes (GO:0009657 and GO:0009658) were upregulated. One unlinked cluster, for "quinone process" (GO:1901663), nevertheless, also indicates upregulation of photosynthetic function and growth, as plastoquinone and ubiquinone serve in the electron transport chains, respectively, of photosynthesis and aerobic respiration. Descriptions of the clusters and their nodes are found in Supplementary Tables S10, S14.

3.4.4 Downregulated networks during recovery

The networks of genes downregulated during recovery, when compared to the controls, form six clusters (Figure 8B). Cluster F (13 genes in one node) is associated with the de-repression of genes associated with organelle organization (GO:0010638). Cluster A has nine nodes, each with a single gene, for processes spanning cell wall macromolecules (GO:0010981), carbohydrate metabolism (GO:0010676), trichome papilla formation (GO:1905499), among others. Descriptions of the clusters and their nodes are presented in Supplementary Tables S11 and S15.

Of the other five clusters of genes downregulated during recovery, notably, three (B, D, and E) contain altogether 117 networked autophagy-related genes (ATGs) involved in ubiquitin-mediated autophagy (Figure 8B). The largest cluster (B) has six nodes, including ones with genes concerned with autophagosome organization and assembly. Two unlinked ATG clusters (D and E) consist of a single node each. One is for genes involved in protein K63- linked de-ubiquitination (GO:0070536). In this cluster, the genes for deubiquitinating enzyme AMSH1 are also observed. The other cluster with its single node concerns genes involved in protein neddylation (GO:0045116), the process by which the ubiquitin-like protein NEDD8 is conjugated to its target proteins in a manner analogous to ubiquitination.

The reduction in expression of the ATGs genes is modest, compared with the controls, around two-fold at most. However, of the six gene clusters with reduced expression during recovery, the top three most strongly reduced are all for ATGs genes. The *p*-values of the ATG nodes are all highly significant (mean of 0.01). Among the ATGs, the most strongly downregulated are autophagy-related protein 101 (−1.76X), beclin 1 (−1.7X), and autophagy-related protein 3 (−1.48X), all in cluster B (autophagy); a 26S proteasome regulatory subunit (−1.98X), in cluster D (protein K63-linked deubiquitination); and ubiquitin-conjugating enzyme E2 (−1.57X), in cluster E (neddylation). When gene expression levels at recovery are compared to that at drought, a similar picture emerges for ATGs (Supplementary Table S15). While only a few are significant at padj = 0.05, most show the same trends.

TABLE 4 Top 20 downregulated genes during the recovery phase.

Ensembl_gene_id	Description	log2 FC[1]	padj[2]
HORVU.MOREX.r2.7HG0531380	Retrovirus-related Pol polyprotein from transposon TNT 1-94	−23.01	1.188E-10
HORVU.MOREX.r2.4HG0321820	Plant protein 1589 of Uncharacterized protein function	−7.39	2.631E-05
HORVU.MOREX.r2.3HG0253380	ATP-dependent Clp protease adapter protein ClpS	−6.74	9.786E-03
HORVU.MOREX.r2.4HG0280100	Staurosporin and temperature sensitive 3-like A	−4.50	1.056E-04
HORVU.MOREX.r2.3HG0188940	AP2/B3 transcription factor family protein	−4.31	2.280E-04
HORVU.MOREX.r2.2HG0093560	Flowering-promoting factor 1-like protein 1	−3.70	3.800E-03
HORVU.MOREX.r2.4HG0280110	Staurosporin and temperature sensitive 3-like A/Haloacid dehalogenase-like hydrolase	−3.68	8.266E-05
HORVU.MOREX.r2.7HG0581730	NAC domain-containing protein	−3.64	1.844E-03
HORVU.MOREX.r2.2HG0138540	DNA helicase homolog	−3.51	6.905E-03
HORVU.MOREX.r2.5HG0357350	2-Oxoglutarate and Fe (II)-dependent oxygenase superfamily protein	−3.04	7.989E-03
HORVU.MOREX.r2.2HG0093550	Flowering-promoting factor 1–like protein 1	−2.89	6.611E-04
HORVU.MOREX.r2.2HG0173810	Unidentified	−2.87	2.376E-03
HORVU.MOREX.r2.4HG0279680	Lysine–tRNA ligase	−2.85	1.142E-03
HORVU.MOREX.r2.2HG0091470	NAC domain protein	−2.83	1.016E-04
HORVU.MOREX.r2.6HG0522770	Inosine-5′-monophosphate dehydrogenase	−2.82	6.337E-04
HORVU.MOREX.r2.3HG0259320	Transmembrane protein	−2.76	1.878E-06
HORVU.MOREX.r2.4HG0346330	Cortical cell-delineating protein	−2.68	3.434E-03
HORVU.MOREX.r2.2HG0152820	Hsp70-Hsp90 organizing protein 1	−2.53	1.247E-03
HORVU.MOREX.r2.2HG0133410	SNF1-related protein kinase regulatory subunit gamma 1	−2.52	1.255E-03
HORVU.MOREX.r2.5HG0357520	NAC domain-containing protein/Tetratricopeptide repeat (TPR)-like superfamily protein (LC)	−2.51	2.664E-04

[1]FC, fold change; [2]padj, adjusted p-value.

3.5 *BARE* response during drought and recovery

For all four varieties during drought and recovery (Table 5, Supplementary S16), the mRNA levels matching the *BARE gag* region was analyzed by qPCR; in GP, additionally, the abundance of mRNA containing the 5′ untranslated leader (UTL) regions corresponding to expression from TATA1 and TATA2 (Chang and Schulman, 2008), respectively, for the genomic RNA (gRNA) and mRNA, was measured (Table 5). As an indicator of general stress response, *hsp17* expression was examined; putative *hsp17* and *hsp21* were among the most strongly downregulated genes in recovery vs. drought (Supplementary Table S6).

Drought-induced expression of both *hsp17* and of *BARE* (*gag*) was significantly higher (Supplementary Tables S17, S18) in GP and Arvo over the well-watered control (Table 5, Supplementary S16). During recovery, *BARE gag* and *hsp17* were downregulated in Arvo and GP (down 2.2X, Arvo; 1.3X, GP), but not in H673 (up 2.9X over control), suggesting delayed recovery in H673 (Table 5, Supplementary S16). Notably, in Morex, *gag* levels but not *hsp17* showed an inverse pattern from the other lines: decreasing 1.8-fold under drought but increasing 1.7-fold during recovery (Supplementary Table S16). We additionally followed the expression of the 5′ UTLs corresponding to both the gRNA (TATA1) and the mRNA (TATA2) of *BARE* in GP. TATA1 was more strongly upregulated than TATA2 under drought (Table 5, Supplementary S17). During recovery, TATA1 and HSP17 expression were below that of the well-watered control, whereas TATA2 was near to control levels. On the protein level (Supplementary Figure S5), *BARE* Pol, produced from the TATA2 mRNA, showed a strong drought response, which decreased but was still above the control during recovery.

4 Discussion

Drought tolerance and resilience are important traits for wild plants and commonly sought for crops. For crops, in contrast to wild species, not only the production of viable seed but also high yield is desirable. Hence, trade-offs between drought tolerance and concomitant stomatal water loss and CO_2 uptake are relevant to breeding. Drought under field conditions is complex, affected by many factors: ambient heat, humidity, VPD, and their diurnal fluctuations; soil structure and hydration profile; soil and root microbiomes; the length and completeness of rain cessation (Scharwies and Dinneny, 2019). Likewise, experimental droughts in greenhouses and growth chambers can differ greatly from each other and from those in the field. Here, we sought to correlate transcriptional to physiological responses in barley on a precision feedback lysimeter

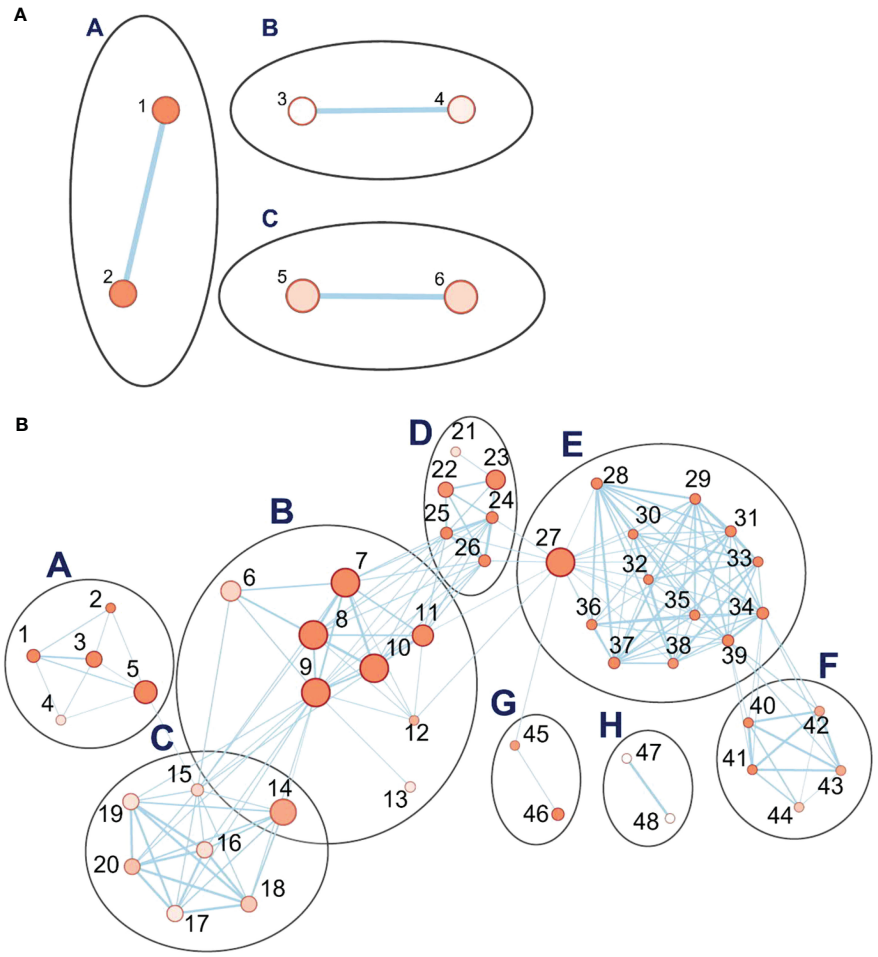

FIGURE 7
Pathway enrichment analysis of differentially expressed genes (DEGs) during the drought phase. **(A)** The set of three clusters of nodes containing upregulated genes. **(B)** Eight interlinked clusters of interlinked nodes containing genes downregulated during the drought phase. Pathway nodes are shown as small circles connected by lines (edges) if the pathways share many genes. Nodes are colored by enrichment score, and the thickness of lines according to the number of genes shared by the connected pathways. The clusters are A, photosynthesis; B, acid metabolic process; C, purine metabolic process; tRNA aminoacylation translation; E, pigment biosynthesis; F, tetraterpenoid process; G, plastid translation organization; H, plant ovary development. Nodes are numbered; descriptions for upregulated and downregulated genes are organized by node number in Supplementary Tabless S8, S9, respectively.

platform with well-controlled soil and watering as well as continuous data collection. We recorded VPD and PAR continuously throughout the experiment, as well as the DT and increase in plant weight. The platform itself was in a greenhouse that closely reflected natural external environmental conditions beyond.

4.1 Physiological response of four barley varieties to drought and rewatering

We analyzed the drought and recovery responses of four barley varieties for which pilot experiments showed a difference in transpiration rates and Θ_{crit}. We have not tracked leaf water potential but rather the stomatal response to SWC; we use the terms anisohydric and isohydric as equivalent to Θ_{crit} at comparatively low and high SWC, respectively. The SWC at which drought response is invoked is genotype-dependent; the two strategies can be found within genotypes of the same species such as barley or wheat (*Triticum aestivum* L.), which have both spring- and autumn-sown types that thereby experience contrasting rainfall patterns (Tao et al., 2017) depending on the cultivation region (Galle et al., 2013).

Morex, having the highest DT rate, reached Θ_{crit} at VWC 0.46 cm^3/cm^3 on day 36, whereas GP reached Θ_{crit} at the lowest VWC, 0.42 cm^3/cm^3, already on day 33 and continued to dehydrate at the fastest rate, but with the lowest initial transpiration rate. Hence, the rate of water loss after Θ_{crit} was not linked to the initial transpiration rate, as GP dried the fastest and Arvo the slowest. Our interpretation is that GP is therefore the most anisohydric of the four. As bred in the UK, GP may be able to manage the risk as SWC falls because of its low transpiration rate and the relatively balanced precipitation throughout the growing season. Morex also reaches Θ_{crit} at a comparatively low VWC but, nevertheless, maintains weight as well as H673, which has Θ_{crit} at the highest VWC, so would appear to manage water loss well. Arvo appears to be the most isohydric; it, like H673, responds at a high Θ_{crit} and maintains its weight best during drought. This is consistent with Arvo and H673 being varieties from Finland, where droughts

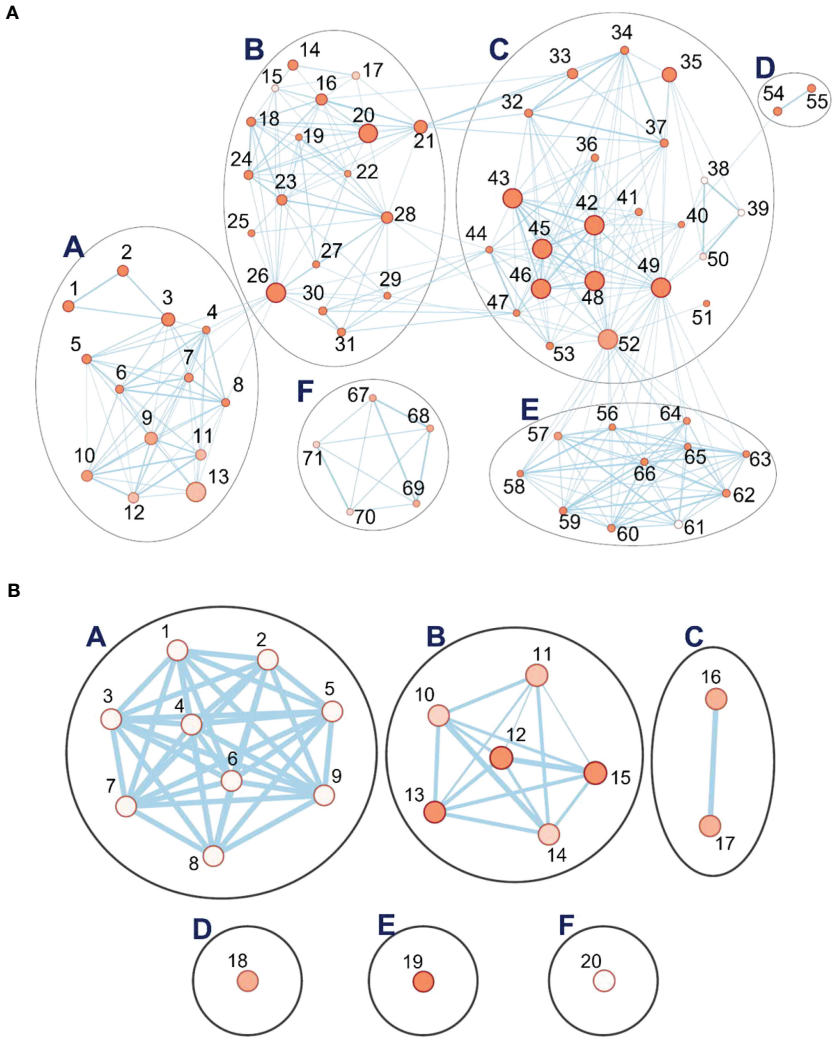

FIGURE 8
Pathway enrichment analysis of differentially expressed genes (DEGs) during the recovery phase. **(A)** Six interlinked clusters of interlinked nodes containing upregulated genes. **(B)** Six clusters of nodes containing downregulated genes. Pathway nodes are shown as small circles connected by lines (edges) if the pathways share many genes. Nodes are colored by enrichment score, and the thickness of lines according to the number of genes shared by the connected pathways. The clusters are A, positive regulation process; B, autophagy; C, response to sucrose and disaccharide; D, protein K63; E, protein neddylation; F, positive regulation of organelle. Pathway nodes are shown as small circles connected by lines (edges) if the pathways share many genes. Nodes are colored by enrichment score, and the thickness of lines according to the number of genes shared by the connected pathways. Nodes are numbered; descriptions for upregulated and downregulated genes are organized by node number in Supplementary Tables S10, S11, respectively.

occur early in the growing season and can persist for weeks, but where the probability of precipitation increases as the season progresses (Tao et al., 2017). All lines responded to rewatering by increasing specific weight gain (g/g), GP being the lowest, but none returned to control rates during the three days that recovery was followed. Full recovery may require longer.

4.2 Gene networks and differential expression in Golden Promise during drought and recovery

We focused gene expression analyses on GP, as the standard line for transformation and editing. *Drought*: Networks of genes responding to drought, salt, and acid, as well as negative regulators of metabolism, were upregulated following Θ_{crit}. Among individual genes, *glutathione s-transferase* (*GST*) was most upregulated (3 × 106-fold) over the control; at the sampling point early in recovery, it had dropped by 8.6-fold relative to drought samples. GST expression is associated with drought tolerance in barley (Rezaei et al., 2013); it scavenges drought-produced ROS for detoxification (Guo et al., 2009). Likewise, increased GST expression was observed under cold and osmotic stress in a potato genotype tolerant to these (Guo et al., 2009). The second most highly upregulated (447X) gene is chloroplastic linalool synthase (XP_044955412), a terpenoid biosynthetic enzyme; its expression fell 70-fold in recovery relative to drought. In rice, the bHLH family transcription factor *RERJ1* is drought-induced, leading to jasmonate (JA) biosynthesis

TABLE 5 Relative expression of *hsp17*and BARE transcripts in Golden Promise during the drought and recovery phases along with TATA1- and TATA2-driven mRNA levels.

DROUGHT				
Samples	*hsp17* **	*gag***	TATA1**	TATA2**
Control 1	1.50 ± 0.08	0.66 ± 0.17	0.49 ± 0.09	0.60 ± 0.11
Control 2	2.75 ± 0.38	1.19 ± 0.09	0.83 ± 0.05	0.40 ± 0.01
Drought 1	8.01 ± 1.96	4.78 ± 0.30	5.15 ± 0.82	1.78 ± 0.24
Drought 2	4.06 ± 0.10	3.52 ± 0.79	2.12 ± 0.20	0.87 ± 0.19
RECOVERY				
Samples	*hsp17*	*gag*	TATA1*	TATA2
Control 1	0.64 ± 0.03	1.17 ± 0.07	0.57 ± 0.08	1.03 ± 0.13
Control 2	0.39 ± 0.09	0.35 ± 0.14	1.33 ± 0.12	0.59 ± 0.04
Recovery 1	0.38 ± 0.05	0.36 ± 0.11	0.23 ± 0.01	0.97 ± 0.08
Recovery 2	0.37 ± 0.02	0.73 ± 0.11	0.61 ± 0.07	1.06 ± 0.21

Values are given as means ± SD of three technical replicates for each plant. The asterisks indicate the significance level of *$p< 0.05$ and **$p< 0.005$ analyzed using a non-parametric Mann–Whitney U-test.

and induction of linalool synthase (Valea et al., 2022). In barley, 98 among 135 detected phenolic and terpenoid compounds (linolool was not investigated) were shown to change in expression as result of drought stress (Piasecka et al., 2017). Our observed induction of linolool synthase here is consistent with a role in ABA/JA-mediated stomatal closure as reported for Arabidopsis (Munemasa et al., 2019). *Dehydrin* (*Dhn*) transcripts were also highly upregulated, 3500X over control, and among the most strongly downregulated in recovery vs. drought. Dehydrins, along with other late embryogenesis abundant (LEA) proteins such as LEA14 (also upregulated here), protect enzymes from dehydration and other environmental stresses (Liu et al., 2017). Differential *Dhn* expression was shown in cultivated and wild (*H. spontaneum*) barley to be correlated with drought tolerance (Suprunova et al., 2004; Kosová et al., 2014), likewise in *Brachypodium distachyon* (Decena et al., 2021), wheat (Brini et al., 2007; Wang et al., 2014), and rice (Verma et al., 2017).

Networks for photosynthetic and plastidial processes, metabolism, and ovary development were downregulated during drought, consistent with earlier reports for some individual genes from these processes: ribulose 1,5-bisphosphate carboxylase small subunit (*rbcS*), chlorophyll a/b-binding protein (*cab*), and components of photosystems I and II (Seki et al., 2002; Narusaka et al., 2004). Here, the most strongly downregulated gene was for cytochrome P450 (*CYP*), which conversely was the third most strongly upregulated in recovery vs. drought. The *CYP* genes are widely distributed in plants and animals (Shiota et al., 2000), forming a large family, 45 in wheat (Li and Wei, 2020), playing multiple roles (McKinnon et al., 2008), including in biotic and abiotic stress response (Li and Wei, 2020). In rice, 83 *OsCYPs* are differentially expressed, of which six are strongly induced and three are strongly downregulated, during drought (Wei and Chen, 2018).

Two genes for cortical cell delineating protein were highly (−705X and −621X) repressed during drought; while associated with roots, they appear to have a role in cell division and elongation (Isayenkov et al., 2020). These, too, had their expression strongly upregulated during recovery vs. drought. Downregulated almost as strongly (−442X) was a gene of the *bHLH* family. This widespread family of transcription factors has been shown in various plants, including wheat, to be integrated into ABA- and JA-mediated signaling, ROS scavenging, and stomatal closure, as well as to play multiple roles in development (Yang et al., 2016; Guo et al., 2021). Given that *bHLH* is strongly induced by drought and ABA, the pattern seen here suggests that induction occurs before Θ_{crit} and that its downregulation thereafter may be linked to suppression of developmental processes.

Recovery: During the recovery phase, gene networks connected to growth and to chloroplast development were upregulated; these processes were downregulated under drought. The putative *PP7*, here the most upregulated individual gene vs. control during recovery, has shown to be highly expressed in Arabidopsis stomata (Andreeva et al., 1999), to regulate phytochrome signaling (Andreeva et al., 1999) and to be involved also in Arabidopsis chloroplast development (Xu et al., 2019), a function that would be consonant with recovery in the barley system.

Notably, autophagy processes were downregulated. Autophagy mechanisms are conserved in eukaryotes for turning over unwanted cytoplasmic components and maintaining homeostasis during stress (Marshall and Vierstra, 2018; Bao, 2020; Tang and Bassham, 2022). Mutant or silenced individual autophagy genes (*atg5,ATG6, atg7*, *ATG8d,*and *ATG18h*), variously in Arabidopsis, tomato, and wheat (Liu et al., 2009; Marshall and Vierstra, 2018; Zhu et al., 2018; Li et al., 2019), reduced drought tolerance. In barley, a mutant of autophagosome formation gene *ATG6* (*Beclin 1*) was upregulated under various abiotic stresses including drought, whereas its knockdown resulted in yellowing leaves in dark and H_2O_2 treatments (Zeng et al., 2017). We confirmed that *ATG6* is identical to 3HG0280440.1 (Morex assembly vers3) and saw a 1.47X reduction in recovery vs. drought (adjusted $p= 0.01$). While these studies indicated the importance of individual autophagy

components in mediating abiotic stress response including drought, the autophagy network as a whole had not been examined. During recovery, along with *ATG6*, we observed a downregulation of many other *ATG*s in nodes connected either to initiation of autophagy, vesicle nucleation, expansion, or autophagosome formation. The likely importance of the suppression of autophagy during recovery is indicated by COST1 (constitutively stressed 1), attenuating autophagy in Arabidopsis under optimal growth conditions; *cost1* mutants are highly drought tolerant but very small, growing slowly (Bao et al., 2020). Of the two *COST1* matches in the barley genome, expression of HORVU.MOREX.r2.4HG0296600.1 was not seen; for HORVU.MOREX.r2.6HG0480550, expression was almost identical in drought and recovery samples and regarding the controls.

4.3 Response of retrotransposon *BARE* to drought and recovery

BARE, of which the reference genome contains 20,258 full-length copies and 6,216 solo LTRs (Mascher et al., 2021), carries out the various stages of the RLX lifecycle: It is transcribed, translated, and forms virus-like particles (Jääskeläinen et al., 2013). While the *BARE* LTR promoter was earlier shown to carry ABREs (Suoniemi et al., 1996), the capsid protein Gag to be more strongly expressed under drought (Jääskeläinen et al., 2013), and *BARE* copy number variations and insertional polymorphism patterns to be consistent with long-term drought activation (Kalendar et al., 2000), *BARE* transcription has not earlier been linked to physiologically characterized drought. Here, we found that *BARE* transcription, as measured by qPCR from the *gag* coding region, increased following Θ_{crit} in GP, Arvo, and H673, as did the gene for heat-shock protein *HSP17,* a marker for drought stress (Guo et al., 2009); Morex, however, showed *HSP17* response but no increased *BARE* transcription. For Arvo and GP, both the *BARE gag* and *HSP17* were strongly lower in the samples taken after rewatering, whereas H673 had apparently not entered recovery, given that the *HSP17* level was still elevated. Divergent *BARE* levels in different varieties are consistent with those seen earlier (Jääskeläinen et al., 2013), where GP showed a stronger response on the Gag protein level than did cv. Bomi. For GP, we also examined the drought response for the two transcripts, one driven by TATA1, which produces the gRNA that will be reverse transcribed, and another by TATA2, which produces the translatable mRNA. In drought, TATA1 was more strongly induced than TATA2, whereas, during recovery, TATA1 showed lower expression than in control samples, perhaps indicating post-transcriptional silencing of the *BARE* gRNA. Consonant with the qPCR results, the most strongly downregulated gene in the recovery RNA-seq (HORVU.MOREX.r2.7HG0531380) matches best a superfamily *Copia* integrase domain (KAE8773625.1; 65% similar residues, *E*-value 7×10^{-101}), likely from the *Hopscotch* family.

5 Conclusions

Using a precision phenotyping platform, we have identified barley varieties whose transpiration rates drop (Θ_{crit}) at different points as soil dries during drought, which may mirror adaptation to pre-flowering vs. terminal drought or to droughts of varying length. The timing of droughts regarding phenology is expected to shift across Europe over the coming decades (Appiah et al., 2023). Using Θ_{crit} as a guidepost, we carried out a global analysis of gene expression in the transformable variety GP in response to drought and rewatering and placed the DEGs into the context of biological pathways. We identified several strongly DEGs not earlier associated with drought response in barley, including for linalool synthase, cortical cell delineating protein, and long-form PP7. These data will serve to establish candidate genes from phenotyped mapping populations and diversity sets and for analysis of the many drought tolerance QTLs heretofore identified (Zhang et al., 2017; Moualeu-Ngangue et al., 2020). We were able to confirm that the *BARE* RLX family is strongly transcriptionally upregulated by drought and downregulated during recovery unequally between cultivars and that the two *BARE* promoters are differentially drought responsive. Consistent with what may be a general epigenetic deregulation of RLXs and DNA transposons (Pontes et al., 2009; Wei et al., 2014), *Dicer-like 3* (*DCL3*) was downregulated 57-fold compared to the well-watered control during the drought phase (Supplementary Table S3); full analysis of transposable element expression under drought and recovery is currently in progress. In the context of recovery rate and resilience, which is key to maintenance of crop yields in the face of climate change, our observation that the autophagy gene network is downregulated during recovery is worthy of further investigation; we are currently constructing a higher resolution timeline.

Data availability statement

The datasets presented in this study can be found in online repositories. The names of the repository/repositories and accession number(s) can be found in the article/Supplementary Material.

Author contributions

MP carried out the physiological experiments and expression assays, analyzed the data, and wrote the manuscript; JT was responsible for bioinformatics analyses; MJ carried out protein expression analyses; WC contributed to qPCR analyses; AD contributed to physiological experiments; MM and AS designed the experiments; AS revised the manuscript and was project P.I. All authors contributed to the article and approved the submitted version.

Funding

Funding was provided by the Finnish Ministry of Agriculture and Forestry (Decision 153/03.01.02, ClimBar project), the Academy of Finland (Decision 292726, BARISTA project) and by the Academy of Finland (Decision 314961) for project

"Retrostress". MP was supported in part by a BRAVE Erasmus Mundus scholarship.

Acknowledgments

We acknowledge Anne-Mari Narvanto for excellent technical assistance and Triin Vahisalu for useful discussions on the physiology and molecular biology of drought response.

Conflict of interest

The authors declare that the research was conducted in the absence of any commercial or financial relationships that could be construed as a potential conflict of interest.

Publisher's note

Supplementary material

The Supplementary Material for this article can be found online at: https://www.frontiersin.org/articles/10.3389/fpls.2023.1193284/full#supplementary-material

References

Andreeva, A. V., Kearns, A., Hawes, C. R., Evans, D. E., and Kutuzov, M. A. (1999). PP7, a gene encoding a novel protein Ser/Thr phosphatase, is expressed primarily in a subset of guard cells in *Arabidopsis thaliana*. *Physiol. Plant* 106, 219–223. doi: 10.1034/j.1399-3054.1999.106211.x

Andrews, S. (2010). *FASTQC. a quality control tool for high throughput sequence data*. Available at: http://www.bioinformatics.babraham.ac.uk/projects/fastqc

Appiah, M., Bracho-Mujica, G., Ferreira, N., Schulman, A., and Rötter, R. (2023). Projected impacts of sowing date and cultivar choice on the timing of heat and drought stress in spring barley grown along a European transect. *Field Crops Res.* 291, 108768. doi: 10.1016/j.fcr.2022.108768

Avin-Wittenberg, T. (2019). Autophagy and its role in plant abiotic stress management. *Plant Cell Environ.* 42, 1045–1053. doi: 10.1111/pce.13404

Bao, Y. (2020). Links between drought stress and autophagy in plants. *Plant Signal Behav.* 15, 1779487. doi: 10.1080/15592324.2020.1779487

Bao, Y., Song, W. M., Wang, P. P., Yu, X., Li, B., Jiang, C. M., et al. (2020). COST1 regulates autophagy to control plant drought tolerance. *Proc. Natl. Acad. Sci. U.S.A.* 117, 7482–7493. doi: 10.1073/pnas.1918539117

Beier, S., Himmelbach, A., Colmsee, C., Zhang, X. Q., Barrero, R. A., Zhang, Q., et al. (2017). Construction of a map-based reference genome sequence for barley, *Hordeum vulgare* l. *Sci. Data* 4, 170044. doi: 10.1038/sdata.2017.443

Bolger, A. M., Lohse, M., and Usadel, B. (2014). Trimmomatic: a flexible trimmer for illumina sequence data. *Bioinformatics* 30, 2114–2120. doi: 10.1093/bioinformatics/btu170

Brinii, F., Hanin, M., Irar, S., Pagès, M., and Masmoudi, K. (2007). Functional characterization of DHN-5, a dehydrin showing a differential phosphorylation pattern in two Tunisian durum wheat (*Triticum durum* desf.) varieties with marked differences in salt and drought tolerance. *Plant Sci.* 172, 20–28. doi: 10.1016/j.plantsci.2006.07.011

Buti, M., Baldoni, E., Formentin, E., Milc, J., Frugis, G., Lo Schiavo, F., et al. (2019). A meta-analysis of comparative transcriptomic data reveals a set of key genes involved in the tolerance to abiotic stresses in rice. *Int. J. Mol. Sci.* 20, 5662. doi: 10.3390/ijms20225662

Cao, L., Lu, X., Wang, G., Zhang, Q., Zhang, X., Fan, Z., et al. (2021). Maize ZmbZIP33 is involved in drought resistance and recovery ability through an abscisic acid-dependent signaling pathway. *Front. Plant Sci.* 12, 629903. doi: 10.3389/fpls.2021.629903

Chang, W., Jaaskelainen, M., Li, S. P., and Schulman, A. H. (2013). *BARE* retrotransposons are translated and replicated via distinct RNA pools. *PloS One* 8, e72270. doi: 10.1371/journal.pone.0072270

Chang, W., and Schulman, A. H. (2008). *BARE* retrotransposons produce multiple groups of rarely polyadenylated transcripts from two differentially regulated promoters. *Plant J.* 56, 40–50. doi: 10.1111/j.1365-313X.2008.03572.x

Chen, H., Dong, J., and Wang, T. (2021a). Autophagy in plant abiotic stress management. *Int. J. Mol. Sci.* 22, 4075. doi: 10.3390/ijms22084075

Chen, S., Li, P., Tan, S., Pu, X., Zhou, Y., Hu, K., et al. (2021b). Combined proteomic and physiological analysis of chloroplasts reveals drought and recovery response mechanisms in *Nicotiana benthamiana*. *Plants* 10, 1127. doi: 10.3390/plants10061127

Dalal, A., Bourstein, R., Haish, N., Shenhar, I., Wallach, R., and Moshelion, M. (2019). Dynamic physiological phenotyping of drought-stressed pepper plants treated with "productivity-enhancing" and "survivability-enhancing" biostimulants. *Front. Plant Sci.* 10, 905. doi: 10.3389/fpls.2019.00905

Dalal, A., Shenhar, I., Bourstein, R., Mayo, A., Grunwald, Y., Averbuch, N., et al. (2020). A telemetric, gravimetric platform for real-time physiological phenotyping of plant-environment interactions. *J. Vis. Exp.* 162, 10.3791/61280. doi: 10.3791/612804

Das, K., and Roychoudhury, A. (2014). Reactive oxygen species (ROS) and response of antioxidants as ROS-scavengers during environmental stress in plants. *Front. Environ. Sci.* 2, 53. doi: 10.3389/fenvs.2014.00053

Decena, M. A., Galvez-Rojas, S., Agostini, F., Sancho, R., Contreras-Moreira, B., Des Marais, D. L., et al. (2021). Comparative genomics, evolution, and drought-induced expression of dehydrin genes in model *Brachypodium* grasses. *Plants* 10, 2664. doi: 10.3390/plants10122664

Dobin, A., Davis, C. A., Schlesinger, F., Drenkow, J., Zaleski, C., Jha, S., et al. (2013). STAR: ultrafast universal RNA-seq aligner. *Bioinformatics* 29, 15–21. doi: 10.1093/bioinformatics/bts635

Galindo-Gonzalez, L., Mhiri, C., Deyholos, M. K., and Grandbastien, M. A. (2017). LTR-Retrotransposons in plants: engines of evolution. *Gene* 626, 14–25. doi: 10.1016/j.gene.2017.04.051

Galkin, E., Dalal, A., Evenko, A., Fridman, E., Kan, I., Wallach, R., et al. (2018). Risk-management strategies and transpiration rates of wild barley in uncertain environments. *Physiol. Plant* 164, 412–428. doi: 10.1111/ppl.12814

Galle, A., Csiszar, J., Benyo, D., Laskay, G., Leviczky, T., Erdei, L., et al. (2013). Isohydric and anisohydric strategies of wheat genotypes under osmotic stress: biosynthesis and function of ABA in stress responses. *J. Plant Physiol.* 170, 1389–1399. doi: 10.1016/j.jplph.2013.04.010

Gosa SC, G. B., Patil, R., Mencia, R., and Moshelion, M. (2022). Diurnal stomatal apertures and density ratios affect whole-canopy stomatal conductance, water-use efficiency and yield. *BioRxiv*. doi: 10.1101/2022.01.06.475121

Grandbastien, M. A., Audeon, C., Bonnivard, E., Casacuberta, J. M., Chalhoub, B., Costa, A. P., et al. (2005). Stress activation and genomic impact of *Tnt1* retrotransposons in solanaceae. *Cytogenet. Genome Res.* 110, 229–241. doi: 10.1159/000084957

Guo, P., Baum, M., Grando, S., Ceccarelli, S., Bai, G., Li, R., et al. (2009). Differentially expressed genes between drought-tolerant and drought-sensitive barley genotypes in response to drought stress during the reproductive stage. *J. Exp. Bot.* 60, 3531–3544. doi: 10.1093/jxb/erp194

Guo, J. R., Sun, B. X., He, H. R., Zhang, Y. F., Tian, H. Y., and Wang, B. S. (2021). Current understanding of bHLH transcription factors in plant abiotic stress tolerance. *Int. J. Mol. Sci.* 22, 4921. doi: 10.3390/ijms22094921

Halperin, O., Gebremedhin, A., Wallach, R., and Moshelion, M. (2017). High-throughput physiological phenotyping and screening system for the characterization of plant-environment interactions. *Plant J.* 89, 839–850. doi: 10.1111/tpj.13425

Hildebrandt, T. M. (2018). Synthesis versus degradation: directions of amino acid metabolism during arabidopsis abiotic stress response. *Plant Mol. Biol.* 98, 121–135. doi: 10.1007/s11103-018-0767-0

Hong, Y., Ni, S. J., and Zhang, G. P. (2020). Transcriptome and metabolome analysis reveals regulatory networks and key genes controlling barley malting quality in responses to drought stress. *Plant Physiol. Biochem.* 152, 1–11. doi: 10.1016/j.plaphy.2020.04.029

Isayenkov, S., Hilo, A., Rizzo, P., Moya, Y. A. T., Rolletschek, H., Borisjuk, L., et al. (2020). Adaptation strategies of halophytic barley *Hordeum marinum* ssp. *marinum* to high salinity and osmotic stress. *Int. J. Mol. Sc.* 21, 9019.

Jääskeläinen, M., Chang, W., Moisy, C., and Schulman, A. H. (2013). Retrotransposon *BARE* displays strong tissue-specific differences in expression. *New Phytol.* 200, 1000–1008. doi: 10.1111/nph.12470

Jogawat, A., Yadav, B., Chhaya,, Lakra, N., Singh, A. K., and Narayan, O. P. (2021). Crosstalk between phytohormones and secondary metabolites in the drought stress tolerance of crop plants: a review. *Physiol. Plant* 172, 1106–1132. doi: 10.1111/ppl.13328

Kalendar, R., Tanskanen, J., Immonen, S., Nevo, E., and Schulman, A. H. (2000). Genome evolution of wild barley (*Hordeum spontaneum*) by *BARE-1* retrotransposon dynamics in response to sharp microclimatic divergence. *Proc. Natl. Acad. Sci. U.S.A.* 97, 6603–6607. doi: 10.1073/pnas.110587497

Kimura, Y., Tosa, Y., Shimada, S., Sogo, R., Kusaba, M., Sunaga, T., et al. (2001). *OARE-1*, a *Ty1-Copia* retrotransposon in oat activated by abiotic and biotic stresses. *Plant Cell Physiol.* 42, 1345–1354. doi: 10.1093/pcp/pce171

Kosová, K., Vítámvás, P., and Prášil, I. T. (2014). Wheat and barley dehydrins under cold, drought, and salinity – what can LEA-II proteins tell us about plant stress response? *Front. Plant Sci.* 5,343. doi: 10.3389/fpls.2014.00343

Lawas, L. M. F., Erban, A., Kopka, J., Jagadish, S. V. K., Zuther, E., and Hincha, D. K. (2019). Metabolic responses of rice source and sink organs during recovery from combined drought and heat stress in the field. *Gigascience* 8, giz102. doi: 10.1093/gigascience/giz102

Li, Y. B., Cui, D. Z., Sui, X. X., Huang, C., Huang, C. Y., Fan, Q. Q., et al. (2019). Autophagic survival precedes programmed cell death in wheat seedlings exposed to drought stress. *Int. J. Mol. Sci.* 20, 5777. doi: 10.3390/ijms20225777

Li, Y. X., and Wei, K. F. (2020). Comparative functional genomics analysis of cytochrome P450 gene superfamily in wheat and maize. *BMC Plant Biol.* 20, 93. doi: 10.1186/s12870-020-2288-7

Liu, Y., Song, Q., Li, D., Yang, X., and Li, D. (2017). Multifunctional roles of plant dehydrins in response to environmental stresses. *Front. Plant Sci.* 8,1018. doi: 10.3389/fpls.2017.01018

Liu, Y., Xiong, Y., and Bassham, D. C. (2009). Autophagy is required for tolerance of drought and salt stress in plants. *Autophagy* 5, 954–963. doi: 10.4161/auto.5.7.9290

Livak, K. J., and Schmittgen, T. D. (2001). Analysis of relative gene expression data using real-time quantitative PCR and the 2(-delta delta C(T)) method. *Methods* 25, 402–408. doi: 10.1006/meth.2001.1262

Love,M.I.,Huber,W.,andAnders,S.(2014).Moderatedestimationoffoldchangeanddispersion for RNA-seq data with DESeq2. *Genome Biol.* 15, 550. doi: 10.1186/s13059-014-0550-8

Makarevitch, I., Waters, A. J., West, P. T., Stitzer, M., Hirsch, C. N., Ross-Ibarra, J., et al. (2015). Transposable elements contribute to activation of maize genes in response to abiotic stress. *PloS Genet.* 11:e1004915. doi: 10.1371/journal.pgen.10049156

Marshall, R. S., and Vierstra, R. D. (2018). Autophagy: the master of bulk and selective recycling. *Ann. Rev. Plant Biol.* 69, 173–208. doi: 10.1146/annurev-arplant-042817-040606

Mascher, M., Gundlach, H., Himmelbach, A., Beier, S., Twardziok, S. O., Wicker, T., et al. (2017). A chromosome conformation capture ordered sequence of the barley genome. *Nature* 544, 427–433. doi: 10.1038/nature22043

Mascher, M., Wicker, T., Jenkins, J., Plott, C., Lux, T., Koh, C. S., et al. (2021). Long-read sequence assembly: a technical evaluation in barley. *Plant Cell* 33, 1888–1906. doi: 10.1093/plcell/koab077

McKinnon, R. A., Sorich, M. J., and Ward, M. B. (2008). Cytochrome P450 part 1: multiplicity and function. *J. Pharm. Pract. Res.* 38, 55–57. doi: 10.1002/j.2055-2335.2008.tb00798.x

Merilo, E., Jalakas, P., Laanemets, K., Mohammadi, O., Horak, H., Kollist, H., et al. (2015). Abscisic acid transport and homeostasis in the context of stomatal regulation. *Mol. Plant* 8, 1321–1333. doi: 10.1016/j.molp.2015.06.006

Moualeu-Ngangue, D., Dolch, C., Schneider, M., Leon, J., Uptmoor, R., and Stutzel, H. (2020). Physiological and morphological responses of different spring barley genotypes to water deficit and associated QTLs. *PloS One* 15, e0237834. doi: 10.1371/journal.pone.0237834

Munemasa, S., Hirao, Y., Tanami, K., Mimata, Y., Nakamura, Y., and Murata, Y. (2019). Ethylene inhibits methyl jasmonate-induced stomatal closure by modulating guard cell slow-type anion channel activity via the OPEN STOMATA 1/SnRK2.6 kinase-independent pathway in arabidopsis. *Plant Cell Physiol.* 60, 2263–2271. doi: 10.1093/pcp/pcz121

Narusaka, Y., Narusaka, M., Seki, M., Umezawa, T., Ishida, J., Nakajima, M., et al. (2004). Crosstalk in the responses to abiotic and biotic stresses in arabidopsis: analysis of gene expression in cytochrome P450 gene superfamily by cDNA microarray. *Plant Mol. Biol.* 55, 327–342. doi: 10.1007/s11103-004-0685-1

Patro, R., Duggal, G., Love, M. I., Irizarry, R. A., and Kingsford, C. (2017). Salmon provides fast and bias-aware quantification of transcript expression. *Nat. Methods* 14, 417–419. doi: 10.1038/nmeth.4197

Piasecka, A., Sawikowska, A., Kuczynska, A., Ogrodowicz, P., Mikolajczak, K., Krystkowiak, K., et al. (2017). Drought-related secondary metabolites of barley (*Hordeum vulgare* l.) leaves and their metabolomic quantitative trait loci. *Plant J.* 89, 898–913. doi: 10.1111/tpj.13430

Polko, J. K., and Kieber, J. J. (2019). 1-aminocyclopropane 1-carboxylic acid and its emerging role as an ethylene-independent growth regulator. *Front. Plant Sci.* 10,1602. doi: 10.3389/fpls.2019.01602

Pontes, O., Costa-Nunes, P., Vithayathil, P., and Pikaard, C. S. (2009). RNA Polymerase V functions in arabidopsis interphase heterochromatin organization independently of the 24-nt siRNA-directed DNA methylation pathway. *Mol. Plant* 2, 700–710. doi: 10.1093/mp/ssp006

Qi, M., Liu, X., Li, Y., Song, H., Yin, Z., Zhang, F., et al. (2021). Photosynthetic resistance and resilience under drought, flooding and rewatering in maize plants. *Photosynth Res.* 148, 1–15. doi: 10.1007/s11120-021-00825-3

Ramallo, E., Kalendar, R., Schulman, A. H., and Martinez-Izquierdo, J. A. (2008). *Reme1*, a *Copia* retrotransposon in melon, is transcriptionally induced by UV light. *Plant Mol. Biol.* 66, 137–150. doi: 10.1007/s11103-007-9258-4

Reimand, J., Isserlin, R., Voisin, V., Kucera, M., Tannus-Lopes, C., Rostamianfar, A., et al. (2019). Pathway enrichment analysis and visualization of omics data using g: Profiler, GSEA, cytoscape and EnrichmentMap. *Nat. Protoc.* 14, 482–517. doi: 10.1038/s41596-018-0103-9

Rezaei, M. K., Shobbar, Z. S., Shahbazi, M., Abedini, R., and Zare, S. (2013). Glutathione s-transferase (GST) family in barley: identification of members, enzyme activity, and gene expression pattern. *J. Plant Physiol.* 170, 1277–1284. doi: 10.1016/j.jplph.2013.04.005

Rollins, J. A., Drosse, B., Mulki, M. A., Grando, S., Baum, M., Singh, M., et al. (2013). Variation at the vernalisation genes *Vrn-H1* and *Vrn-H2* determines growth and yield stability in barley (*Hordeum vulgare*) grown under dryland conditions in Syria. *Theor. Appl. Genet.* 126, 2803–2824. doi: 10.1007/s00122-013-2173-y

Saddhe, A. A., Karle, S. B., Aftab, T., and Kumar, K. (2021). With no lysine kinases: the key regulatory networks and phytohormone cross talk in plant growth, development and stress response. *Plant Cell Rep.* 40, 2097–2109. doi: 10.1007/s00299-021-02728-y

Sade, N., Gebremedhin, A., and Moshelion, M. (2012). Risk-taking plants: anisohydric behavior as a stress-resistance trait. *Plant Signal Behav.* 7, 767–770. doi: 10.4161/psb.20505

Scharwies, J. D., and Dinneny, J. R. (2019). Water transport, perception, and response in plants. *J. Plant Res.* 132, 311–324. doi: 10.1007/s10265-019-01089-8

Schreiber, M., Barakate, A., Uzrek, N., Macaulay, M., Sourdille, A., Morris, J., et al. (2019). A highly mutagenised barley (cv. golden promise) TILLING population coupled with strategies for screening-by-sequencing. *Plant Methods* 15, 99. doi: 10.1186/s13007-019-0486-9

Seki, M., Narusaka, M., Ishida, J., Nanjo, T., Fujita, M., Oono, Y., et al. (2002). Monitoring the expression profiles of 7000 arabidopsis genes under drought, cold and high-salinity stresses using a full-length cDNA microarray. *Plant J.* 31, 279–292. doi: 10.1046/j.1365-313X.2002.01359.x

Shiota, N., Kodama, S., Inui, H., and Ohkawa, H. (2000). Expression of human cytochromes P450 1A1 and P450 1A2 as fused enzymes with yeast NADPH-cytochrome P450 oxidoreductase in transgenic tobacco plants. *Biosci. Biotechnol. Biochem.* 64, 2025–2033. doi: 10.1271/bbb.64.2025

Suoniemi, A., Narvanto, A., and Schulman, A. H. (1996). The *BARE*-1 retrotransposon is transcribed in barley from an LTR promoter active in transient assays. *Plant Mol. Biol.* 31, 295–306. doi: 10.1007/BF00021791

Suprunova, T., Krugman, T., Fahima, T., Chen, G., Shams, I., Korol, A., et al. (2004). Differential expression of dehydrin genes in wild barley, *Hordeum spontaneum*, associated with resistance to water deficit. *Plant Cell Environ.* 27, 1297–1308. doi: 10.1111/j.1365-3040.2004.01237.x

Tang, J., and Bassham, D. C. (2022). Autophagy during drought: function, regulation, and potential application. *Plant J.* 109, 390–401. doi: 10.1111/tpj.15481

Tao, F. L., Rotter, R. P., Palosuo, T., Diaz-Ambrona, C. G. H., Minguez, M. I., Semenov, M. A., et al. (2017). Designing future barley ideotypes using a crop model ensemble. *Eur. J. Agron.* 82, 144–162. doi: 10.1016/j.eja.2016.10.012

Tardieu, F., and Simonneau, T. (1998). Variability among species of stomatal control under fluctuating soil water status and evaporative demand: modelling isohydric and anisohydric behaviours. *J. Exp. Bot.* 49, 419–432. doi: 10.1093/jxb/49.Special_Issue.419

Valea, I., Motegi, A., Kawamura, N., Kawamoto, K., Miyao, A., Ozawa, R., et al. (2022). The rice wound-inducible transcription factor RERJ1 sharing same signal transduction pathway with OsMYC2 is necessary for defense response to herbivory and bacterial blight. *Plant Mol. Biol.* 109, 651–666. doi: 10.1007/s11103-021-01186-0

Verma, G., Dhar, Y. V., Srivastava, D., Kidwai, M., Chauhan, P. S., Bag, S. K., et al. (2017). Genome-wide analysis of rice dehydrin gene family: its evolutionary conservedness and expression pattern in response to PEG induced dehydration stress. *PloS One* 12, e0176399. doi: 10.1371/journal.pone.0176399

Wang, Y., Xu, H., Zhu, H., Tao, Y., Zhang, G., Zhang, L., et al. (2014). Classification and expression diversification of wheat dehydrin genes. *Plant Sci.* 214, 113–120. doi: 10.1016/j.plantsci.2013.10.005

Wei, K. F., and Chen, H. Q. (2018). Global identification, structural analysis and expression characterization of cytochrome P450 monooxygenase superfamily in rice. *BMC Genomics* 19, 35. doi: 10.1186/s12864-017-4425-8

Wei, L., Gu, L., Song, X., Cui, X., Lu, Z., Zhou, M., et al. (2014). Dicer-like 3 produces transposable element-associated 24-nt siRNAs that control agricultural traits in rice. *Proc. Natl. Acad. Sci. U.S.A.* 111, 3877–3882. doi: 10.1073/pnas.1318131111

Wei, K., and Zhong, X. (2014). Non-specific lipid transfer proteins in maize. *BMC Plant Biol.* 14, 281. doi: 10.1186/s12870-014-0281-8

Wicker, T., Sabot, F., Hua-Van, A., Bennetzen, J. L., Capy, P., Chalhoub, B., et al. (2007). A unified classification system for eukaryotic transposable elements. *Nat. Rev. Genet.* 8, 973–982. doi: 10.1038/nrg2165

Xiao, Y., Huang, X., Shen, Y., and Huang, Z. (2013). A novel wheat alpha-amylase inhibitor gene, TaHPS, significantly improves the salt and drought tolerance of transgenic arabidopsis. *Physiol. Plant* 148, 273–283. doi: 10.1111/j.1399-3054.2012.01707.x

Xu, D. R., Marino, G., Klingl, A., Enderle, B., Monte, E., Kurth, J., et al. (2019). Extrachloroplastic PP7L functions in chloroplast development and abiotic stress tolerance. *Plant Physiol.* 180, 323–341. doi: 10.1104/pp.19.00070

Xu, Z., Zhou, G., and Shimizu, H. (2010). Plant responses to drought and rewatering. *Plant Signal Behav.* 5, 649–654. doi: 10.4161/psb.5.6.11398

Yang, T. R., Yao, S. F., Hao, L., Zhao, Y. Y., Lu, W. J., and Xiao, K. (2016). Wheat bHLH-type transcription factor gene TabHLH1 is crucial in mediating osmotic stresses tolerance through modulating largely the ABA-associated pathway. *Plant Cell Rep.* 35, 2309–2323. doi: 10.1007/s00299-016-2036-5

Zeng, X., Zeng, Z., Liu, C., Yuan, W., Hou, N., Bian, H., et al. (2017). A barley homolog of yeast ATG6 is involved in multiple abiotic stress responses and stress resistance regulation. *Plant Physiol. Biochem.* 115, 97–106. doi: 10.1016/j.plaphy.2017.03.013

Zhang, X., Shabala, S., Koutoulis, A., Shabala, L., and Zhou, M. (2017). Meta-analysis of major QTL for abiotic stress tolerance in barley and implications for barley breeding. *Planta* 245, 283–295. doi: 10.1007/s00425-016-2605-4

Zhu, T., Zou, L., Li, Y., Yao, X., Xu, F., Deng, X., et al. (2018). Mitochondrial alternative oxidase-dependent autophagy involved in ethylene-mediated drought tolerance in *Solanum lycopersicum*. *Plant Biotechnol. J.* 16, 2063–2076. doi: 10.1111/pbi.12939

frontiers | Frontiers in Plant Science

TYPE Original Research
PUBLISHED 08 August 2023
DOI 10.3389/fpls.2023.1150909

OPEN ACCESS

EDITED BY
Poonam Yadav,
Banaras Hindu University, India

REVIEWED BY
Angelika Mustroph,
University of Bayreuth, Germany
Ritesh Kumar,
Boyce Thompson Institute (BTI), United States
Achuit K. Singh,
Indian Institute of Vegetable Research (ICAR), India
Vivek P. Chimote,
Mahatma Phule Krishi Vidyapeeth, India

*CORRESPONDENCE
Suresh Gawande
sureshgawande76@gmail.com

RECEIVED 25 January 2023
ACCEPTED 19 July 2023
PUBLISHED 08 August 2023

CITATION
Gedam PA, Khandagale K, Shirsat D, Thangasamy A, Kulkarni O, Kulkarni A, Patil SS, Barvkar VT, Mahajan V, Gupta AJ, Bhagat KP, Khade YP, Singh M and Gawande S (2023) Elucidating the molecular responses to waterlogging stress in onion (*Allium cepa* L.) leaf by comparative transcriptome profiling. *Front. Plant Sci.* 14:1150909. doi: 10.3389/fpls.2023.1150909

Elucidating the molecular responses to waterlogging stress in onion (*Allium cepa* L.) leaf by comparative transcriptome profiling

Pranjali A. Gedam[1], Kiran Khandagale[1], Dhananjay Shirsat[1], A. Thangasamy[1], Onkar Kulkarni[2], Abhijeet Kulkarni[2], Swaranjali S. Patil[3], Vitthal T. Barvkar[3], Vijay Mahajan[1], Amar Jeet Gupta[1], Kiran P. Bhagat[4], Yogesh P. Khade[1], Major Singh[1] and Suresh Gawande[1]*

[1]Indian Council of Agricultural Research (ICAR)-Directorate of Onion and Garlic Research, Pune, India, [2]Bioinformatics Centre, Savitribai Phule Pune University, Pune, India, [3]Department of Botany, Savitribai Phule Pune University, Pune, India, [4]Indian Council of Agricultural Research (ICAR)-Directorate of Floriculture Research, Pune, India

Introduction: Waterlogging is a major stress that severely affects onion cultivation worldwide, and developing stress-tolerant varieties could be a valuable measure for overcoming its adverse effects. Gathering information regarding the molecular mechanisms and gene expression patterns of waterlogging-tolerant and sensitive genotypes is an effective method for improving stress tolerance in onions. To date, the waterlogging tolerance-governing molecular mechanism in onions is unknown.

Methods: This study identified the differentially expressed genes (DEGs) through transcriptome analysis in leaf tissue of two onion genotypes (Acc. 1666; tolerant and W-344; sensitive) presenting contrasting responses to waterlogging stress.

Results: Differential gene expression analysis revealed that in Acc. 1666, 1629 and 3271 genes were upregulated and downregulated, respectively. In W-344, 2134 and 1909 genes were upregulated and downregulated, respectively, under waterlogging stress. The proteins coded by these DEGs regulate several key biological processes to overcome waterlogging stress such as phytohormone production, antioxidant enzymes, programmed cell death, and energy production. The clusters of orthologous group pathway analysis revealed that DEGs contributed to the post-translational modification, energy production, and carbohydrate metabolism-related pathways under waterlogging stress. The enzyme assay demonstrated higher activity of antioxidant enzymes in Acc. 1666 than in W-344. The differential expression of waterlogging tolerance related genes, such as those related to antioxidant enzymes, phytohormone biosynthesis, carbohydrate metabolism, and transcriptional factors, suggested that significant

fine reprogramming of gene expression occurs in response to waterlogging stress in onion. A few genes such as ADH, PDC, PEP carboxylase, WRKY22, and Respiratory burst oxidase D were exclusively upregulated in Acc. 1666.

Discussion: The molecular information about DEGs identified in the present study would be valuable for improving stress tolerance and for developing waterlogging tolerant onion varieties.

KEYWORDS

waterlogging, onion, transcriptome, RNA-sequencing, differential gene expression

Introduction

Water is a prerequisite for plant growth; however, excess soil moisture or prolonged soil saturation causes waterlogging stress that adversely affects several plant developmental processes. Every year, approximately 17 million km^2 of land area and 16% of global agriculture production are challenged by flooding stress (Kaur et al., 2020). The reasons for waterlogging in the field is soil type, poor soil drainage, and unpredictable and intense rainfall. Waterlogging affects plant vegetative growth as well as strongly influences its reproductive growth, leading to yield loss and sometimes complete crop failure. In the context of global climate change, the area under waterlogging stress has been increasing every year since the 1990s, affecting 10%–16% of soils and approximately 80% of the yield losses of economically important crops (Shabala, 2011).

Onion (*Allium cepa* L.) is a significantly valuable crop cultivated globally on approximately 7.1 million-hectare land area. The annual bulb production is 136 million tonnes (FAO, 2021). Next to China, India is the second largest onion producer contributing to 22% of global production (Priyadarshini et al., 2021). Depending on the amount and distribution of rainfall, onion in India is cultivated as both a rainfed and irrigated crop during the monsoon and post-monsoon seasons, respectively. Waterlogging or soil flooding due to heavy rainfall occurs in a substantial part of the world. In India, the monsoon is the major irrigation water source for *Kharif* onion crops (July–December). Erratic monsoon rains lead to frequent waterlogging episodes. Onion is extremely sensitive to waterlogging stress as it is a shallow-rooted crop (Pelter et al., 2004). Heavy and prolonged rainfall at almost all growth stages restrains crop growth with 50%–70% yield losses, indicating that the onion crop is sensitive to waterlogging (Ghodke et al., 2018). Thus, waterlogging is a grave environmental threat limiting onion production during monsoons. To attain adequate onion production during monsoons, genotypes that can withstand short or prolonged waterlogging conditions must be identified. In our previous study, we screened diverse onion genotypes for waterlogging tolerance and then grouped them as tolerant and sensitive based on their phenotypic and physiological traits (Gedam et al., 2022).

In waterlogged soil, the main reason for plant growth inhibition and mortality is a low oxygen diffusion rate that creates a hypoxic condition in roots, thereby shifting the energy-related aerobic respiration pathway to the anaerobic fermentation mode and declining plant root activity, permeability, and growth (Zhou et al., 2020). This disturbs a series of morphological, physiological, and biochemical mechanisms, thereby limiting plant development, gas exchange, and photosynthesis-related processes. Waterlogging triggers the production of reactive oxygen species (ROS) that are detrimental to the cellular membrane components. They also inactivate various enzyme activities, cause oxidation of proteins and membrane lipids, and damage nucleoproteins (Yeung et al., 2018).

Plants respond to waterlogging stress by undergoing a series of phenotypic, physiological, biochemical, and molecular alterations. Changes in leaf and root morphological and anatomical structures are the first visual morphological adaptations that occur in response to stress. Likewise, physiological and molecular regulatory mechanisms, such as reduction in stomatal conductance, a decline in photosynthesis, activation of certain hormonal biosynthesis and signaling pathways, induction of antioxidant enzyme systems, and modulation of certain genes and transcription factors, are triggered in response to waterlogging stress (Pan et al., 2021; Wu et al., 2022). Plant hormonal regulation is a crucial player in plant development and stress response. Ethylene is a key hormone regulating the waterlogging stress response in plants. It is synthesized by 1-aminocyclopropane-1-carboxylic acid (ACC) synthase and ACC oxidase. Ethylene and ROS signaling leads to programmed cell death (PCD) in root tissues, thereby resulting in aerenchyma formation that mediates gaseous exchange during waterlogging (Khan et al., 2020). Salicylic acid (SA) is another phytohormone involved in activating antioxidants and aerenchyma formation (Koramutla et al., 2022) during waterlogging and hypoxia conditions. Energy crisis is common under waterlogging stress and is caused by limited oxygen supply. Therefore, anaerobic fermentation is initiated for maintaining ATP production through glycolysis by oxidation of NADH to NAD^+. The higher expression of *pyruvate decarboxylase (PDC)* and *alcohol dehydrogenase (ADH)* was reported in waterlogging-tolerant genotypes, which helps to

meet the temporary demand of ATP with alcohol fermentation (Xu et al., 2014; Luo et al., 2017; Zhang et al., 2017; Shen et al., 2021). Further, overexpression of these genes also reported to be associated with better performance of transgenic plants under waterlogging conditions than wild-type plants (Komatsu et al., 2011; Tougou et al., 2012; Zhang et al., 2016). Transcription factors are a critical player in regulating gene expression in response to stress. Gene regulation under the waterlogging or hypoxic condition depends on group VII *Ethylene Response Factors* (*ERFs*). They act as master inducers of several hypoxia-responsive genes (Gibbs et al., 2011; Gasch et al., 2016). The aforementioned adaptive processes facilitate acclimatization of the plant to the detrimental consequences of waterlogging stress.

RNA-Seq technology is a powerful and cost-effective tool for conducting the high-throughput plant transcriptome analysis and thus identifying candidate genes associated with various stress-responsive metabolic pathways. This technology has been efficiently used for understanding the expression pattern of key genes and transcription factors associated with waterlogging stress-responsive metabolic pathways in crops such as potatoes and cassava (Park et al., 2020; Cao et al., 2022). Although roots are the key part affected by waterlogging, researchers have also investigated the waterlogging stress response in the leaf tissues of soybean (Chen et al., 2016), peanut (Zeng et al., 2021), and pigeon pea (Tyagi et al., 2022).

To date, no study has highlighted the molecular mechanism governing waterlogging stress tolerance in onion crops. The present study compared the waterlogging-tolerant onion genotype with the sensitive one at the transcriptional level to identify waterlogging tolerance-associated key genes and related pathways. Both genotypes were selected based on previous findings of phenotypic and biochemical responses under the waterlogging condition (Gedam et al., 2022). To the best of our knowledge, this study is the first to investigate the molecular mechanism underlying waterlogging tolerance in onion.

Material and methods

Plant material

Two onion genotypes (*Allium cepa* L.) with contrasting responses to waterlogging stress were used. The genotype Acc. 1666 exhibited a high tolerance to waterlogging stress, whereas W-344 was highly sensitive (Gedam et al., 2022). The experiment was conducted at the ICAR-Directorate of Onion and Garlic Research, Pune, India (N 18°84′, E 73°88′, H 553.8 m). Seedlings of both genotypes were raised in plastic pots (100 × 150 × 60 cm, height × length × width) filled with a 1:3 ratio of farm yard manure and clay loam soil. The recommended fertilizer and plant protection measures were followed to grow healthy seedlings. The experiment was conducted in a completely randomized block design with 10 replications per treatment for each genotype. The seedlings were raised under ambient growth conditions and irrigated after every 36 h until the 5–6 leaf stage.

Waterlogging treatment

After 45 days of seedling transplantation, half of the pots for each genotype were placed in a tank where the water level was maintained 4 cm above the soil surface to induce waterlogging stress (Figure S1). Each pot contained 10 seedlings, and the waterlogged condition was maintained for 72 h. The remaining half pots were maintained in ambient growth conditions throughout the experiment under a rain-out shelter. The leaf samples were collected from both control and waterlogged plants before the stress was relieved, immediately frozen in liquid nitrogen, and stored at −80°C.

Morphological and physiological traits

The phenotypic traits, namely plant height, leaf length, and the number of leaves per plant, were recorded 72 h after the stress treatment (control and waterlogging) in five replications from both genotypes. The fourth fully expanded leaf was cut, and leaf area was measured using the leaf area meter. The seedlings from both control and waterlogged pots were carefully uprooted and washed after the stress period, and their shoot and root lengths were recorded. Leaf total chlorophyll content was quantified using the method of Hiscox and Israelstam (1979). Leaf tissue (0.05 g) was weighed and placed in a test tube containing 10 mL dimethyl sulfoxide. The test tubes were incubated at 60°C for 1 h in water bath and allowed to cool at room temperature for 30 min. Absorbance was recorded at 645 and 663 nm by using a UV–visible spectrophotometer (Thermo Fisher Scientific, Waltham, MA, USA). The total chlorophyll content was calculated using the following formula given by Arnon (1949):

$$\text{Chlorophyll content} = \frac{(20.2 \times \text{OD645} + 8.02 \times \text{OD663}) \times \text{Volume of the extract}}{1000 \times \text{Weight of the sample}}$$

where OD_{663} and OD_{645} are absorbances at 663 and 645 nm, respectively.

Lipid peroxidation in onion leaves was estimated using the protocol of Heath and Packer (1968). The lipid peroxidation level was measured in terms of thiobarbituric acid reactive substance (TBARS) contents by reading absorbance at 532 nm by using a spectrophotometer. The TBARS content level is expressed as µmol g^{-1} FW. The hydrogen peroxide level was quantified using the method of Rao et al. (1997). The onion leaf sample (1 g) was pulverized using liquid nitrogen, followed by the addition of 10 mL ice-cooled acetone. The homogenate was filtered, and 4 mL of titanium reagent (This reagent was prepared according to the method of Teranishi et al., 1974); then, 5 mL of ammonium solution was added to form a titanium hydroperoxide complex. The mixture was centrifuged at 10000 g for 10 min, and the precipitate obtained was dissolved in 10 mL of 2 M sulphuric acid and recentrifuged. The absorbance of the supernatant was read at 415 nm by using the UV–Visible spectrophotometer. The H_2O_2 concentration was computed by referring to the standard curve and is expressed as µmol H_2O_2 g^{-1} FW.

Antioxidant enzyme activity

Leaf samples were harvested at 72 h of waterlogging from both control and stressed plants of both genotypes. Catalase (CAT), ascorbate peroxidase (APX), superoxide dismutase (SOD), and peroxidase (POD) were assayed. Enzyme extraction was performed by grinding the leaf tissue in liquid nitrogen and extracting it in phosphate buffer (0.1 M) of pH 7.2, as described by Roylawar and Kamble (2017). Catalase activity was measured by recording the change in absorbance at 240 nm (Volk and Feierabend, 1989) due to H_2O_2 decomposition. For CAT activity estimation, 3 mL of the reaction mixture was formed by adding 0.1 M potassium phosphate buffer (pH 7.0), 30 mM H_2O_2, and distilled water to the enzyme extract. One unit of CAT activity was recorded as the amount of enzyme that used 1 mmol H_2O_2 per minute. SOD activity was determined according to the method of Beauchamp and Fridovich (1971). SOD activity was measured by adding the enzyme extract to a reaction mixture containing phosphate buffer (50 mM, pH 7.8), riboflavin (60 mM), methionine (20 mM), EDTA (1 mM), nitro-blue tetrazolium (1 mM), and distilled water. The absorbance was recorded at 560 nm after illuminating the sample under light for 20 min. One unit of SOD activity was considered as the amount of enzyme that caused 50% inhibition of NBT reduction in light compared with that in tubes without the enzyme. APX activity was determined by adding the enzyme extract to the reaction mixture containing Tris-HCL buffer (5 M, pH 7.6), Na_2EDTA (0.1 mM), ascorbic acid (0.5 mM) and distilled water. The reaction was initiated by adding H_2O_2, and the activity was measured by recording the reduction in ascorbate at 290 nm, as described by Nakano and Asada, 1987. POD activity was estimated according to the method of Castillo et al. (1984), wherein the enzyme extract was added to the reaction mixture comprising phosphate buffer (50 mM, pH 6.1), guaiacol (16 mM), H_2O_2 (2 mM), and distilled water. The POD activity involved the oxidation of guaiacol to tetra-guaiacol and was determined by reading the absorbance at 470 nm.

RNA isolation and library preparation

Total RNA was isolated from the leaf tissues of control and waterlogged plants of both genotypes by using the RNeasy Plant Mini Kit (Qiagen, Germany). For each treatment, RNA was isolated from the leaf samples of three plants that were considered as one replicate. Three such independent biological replicates were used in the present study. Total RNA from each replicate was quantified and qualified using NanoDrop 1000 (Thermo Fisher Scientific, Waltham, MA, USA) and through 1% agarose gel analysis. Further, the RIN value of the isolated RNA was determined using Agilent 2100 Bioanalyzer (Agilent Technologies, Palo Alto, CA, USA). An equal amount of high-quality RNA from each replicate of the control and stressed samples of each genotype was used for library preparation. In total, 12 next-generation sequencing libraries were prepared using the NEBNext®Ultra™ RNA Library Preparation Kit for Illumina® (NEB, Ipswich, MA, USA) as per the manufacturer's protocol. The libraries were then sequenced in the paired-end mode with 150 × 2 read length by using the Illumina Hi-Seq 2500 platform.

Transcriptome data analysis

The raw reads were filtered using the FastQC tool v0.12.1 with Q > 30, and only qualifying paired-end reads were considered for the analysis. The onion genome sequence v. 1.2 was downloaded from https://www.oniongenome.wur.nl/ with annotation files. The genome index was built using the STAR aligner with runModegenomeGenerate. The filtered high-quality paired reads were aligned to the reference genome and quantified using STAR aligner v. 2.7.10 (https://github.com/alexdobin/STAR). DESeq2 in R package was used for differential gene expression profiling between the control and treated samples of both genotypes. Differentially expressed transcripts were selected based on the following cut-offs: log2 fold change = 2 and p = 0.05. In addition to the information from the annotation file, the transcriptome was annotated using the DIAMOND BLASTX v. 2.0.9.147 (https://ab.inf.uni-tuebingen.de/software/diamond) tool against the UniProt/SwissProt database (https://www.uniprot.org/) and plant TFDB (http://planttfdb.cbi.pku.edu.cn/), with an e-value cut-off of $\leq 10^{-2}$. UniProt/SwissProt ID mapping functionality was used to obtain gene ontology (GO) and pathway annotation for the transcripts.

Validation of DEGs under waterlogging stress through quantitative real-time PCR analysis

The expression of the randomly selected differentially expressed transcripts encoding waterlogging stress-responsive genes was validated through qRT-PCR (Table 1). RNA was isolated from the same samples that were employed for the transcriptome analysis. For each sample, three replicates were used in the study. RNA was treated with *DNase-I* (Fermentas, Lithuania) to eliminate DNA contamination. First-strand cDNA was synthesized from 1 µg RNA by using the RevertAid First Strand cDNA synthesis kit (Fermentas, Lithuania) following the manufacturer's protocol. Primer-BLAST (https://www.ncbi.nlm.nih.gov/tools/primer-blast/) was used to design primers for selected genes where *AcActin* was used as a reference gene. The expression of selected genes was analyzed in the Realflex2 Master Cycler (Eppendorf, Germany). The reaction was carried out in 10 µL mixture containing 1× SYBR Green I master mix (Roche, Germany), 1 µL cDNA, and 1 µM of each primer. The relative gene expression and fold change were calculated using the $2^{-\Delta\Delta CT}$ method (Livak and Schmittgen, 2001).

Statistical analysis

One-way analysis of variance was performed to analyze data by using SAS software (version 9.3; SAS Institute, Cary, NC, USA). The results are presented as the mean ± standard error. The differences

TABLE 1 Details of primers used for the validation of RNAseq data.

Transcript ID	Transcript Name	Primer sequence (5′-3′)	Product size (bp)
g107775	ACC Oxidase	GATCCTGCCCTGTTGACTTT	175
		CCAACACCCTATGCTTCACA	
g346683	Lipoxygenase	CCATGTATGCTCGTCCTGTC	163
		AGATGTCCAAATCGCTCGTC	
g165028	Alcohol dehydrogenase	GCCGGTCAGGTTATCAAGTG	134
		CTGACCCTTAGCTTCCCAGA	
g325946	Pyruvate decarboxylase	ATGTTGTCGGGTGATACTGC	199
		AGCTTCCATCACCAATGCAA	
g125872	WRKY70	ACACCGTCCAAAGAGAACAC	120
		CTCCCAATCTGTCATCCACC	
g238720	MYB1R1	TGGAAAAGGAGATTGGCGAG	156
		TCAGCAGTCGTTCCAACATC	
g444194	Respiratory burst oxidase	AGCGGTTCGTGAGAAAAAGT	142
		GATAGCAGGGCATTTGACGA	
Housekeeping gene	*AcActin*	GCACCAAGAGCAGTATTC	183
		CCAAATCTTCTCCATGTCA	

in the mean values were compared using Duncan's multiple range test where a p value of<0.05 represented statistical significance.

Results

Physiological and biochemical parameters under waterlogging stress

To understand the waterlogging tolerance mechanism in onion, physiological and biochemical analyses were conducted using waterlogging-tolerant (Acc. 1666) and sensitive (W-344) genotypes. Phenotypic traits such as plant height, leaf length, number of photosynthetically active leaves, and leaf area in the tolerant genotype were significantly better than those in the sensitive genotype under both water regimes (Figure S2). The aforementioned traits markedly declined in W-344 during stress, reflecting its poor growth performance under waterlogging stress. However, Acc. 1666 could maintain its plant height and photosynthetically active leaves to continue its growth in a stressful environment. Acc. 1666 maintained its chlorophyll level, whereas W-344 exhibited a significant reduction in the chlorophyll level under waterlogging stress (Figure 1). The H_2O_2 level was elevated in the sensitive genotype (W-344) but not in the tolerant genotype, under waterlogging stress (Figure 2). Further, antioxidant enzyme activities were induced due to waterlogging in both

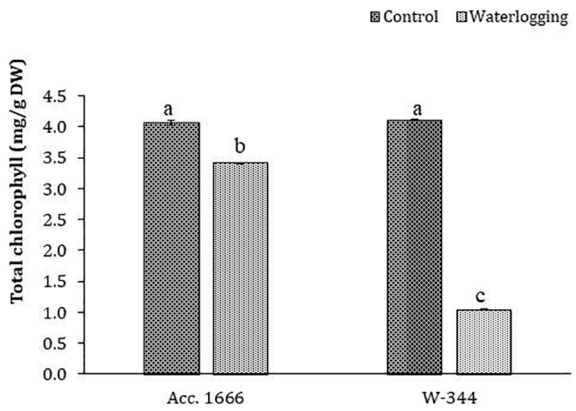

FIGURE 1
Chlorophyll content in contrasting onion genotypes after waterlogging stress. The different letters indicate statistically significant differences at p< 0.05.

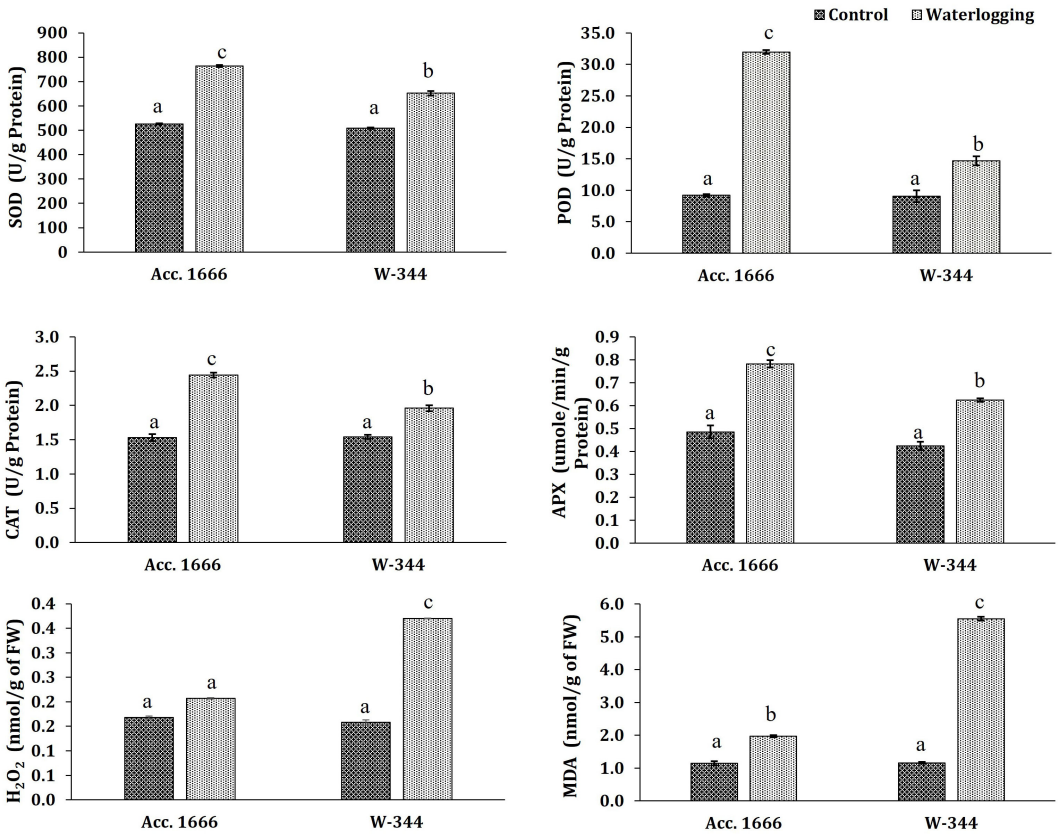

FIGURE 2
Effects of waterlogging stress on antioxidant enzyme activity in contrasting onion genotypes under waterlogging stress. Values are expressed as the average of three replicates, each consisting of three plants pooled together. The different letters indicate statistically significant differences at $p< 0.05$).

genotypes. Significantly higher levels of SOD, CAT, POD, and APX activities were observed in Acc. 1666 than in W-344 under waterlogging (Figure 2). This increase in antioxidant enzyme activity facilitated the tolerant genotype Acc. 1666 to withstand waterlogging with minimum growth damage.

RNA-seq and *de novo* transcriptome assembly

Paired-end RNA sequencing of control and waterlogged samples of Acc.1666 and W-344 genotypes yielded 41194433 to 51240147 raw reads, respectively. The quality check analysis yielded 79%–85% high-quality reads for use in further analysis. The overall alignment rate of these reads with the onion reference genome was 84%–90% (Table 2). The raw RNA sequencing data were submitted to the NCBI (BioProject: PRJNA926808).

Differential gene expression

Differential gene expression (control *vs.* treatment) was analyzed using aligned reads of the waterlogging-tolerant (Acc. 1666) and sensitive (W-344) onion genotypes. In Acc. 1666, 1629 and 3271 genes were upregulated and downregulated, respectively, under the waterlogging condition. While in W-344, 2134 and 1909 genes were upregulated and downregulated, respectively, in response to waterlogging stress. The DEGs were further analyzed using the Venn diagram. Among the upregulated and downregulated DEGs, 137 and 399 DEGs, respectively, were common in both genotypes. By contrast, 340 DEGs were common in both genotypes but were upregulated in Acc. 1666 and downregulated in W344. Similarly, 350 DEGs were common in both genotypes but were downregulated in Acc. 1666 and upregulated in W344 (Figure 3A). Principal component analysis was also performed based on the top 500 most variable genes that grouped the sample with respective treatments. PC1 and PC2 explained more than 93% variation (Figure 3B). The top 1000 significant DEGs are schematically represented using a heatmap (Figure S3). Details of DEGs, such as gene count, fold change, and functional annotation, are given in Excel S1.

Functional annotation of transcripts expressed in onion under waterlogging stress

The differentially expressed transcripts from both Acc. 1666 and W-344 were grouped into three categories based on the GO

10.3389/fpls.2023.1150909

TABLE 2 Summary of RNA-seq data and its alignment with reference onion genome.

Control/ Treatment	File Name	Bio Replicate	Total reads	Total HQ reads	Percentage HQ reads	Overall alignment with Onion ref genome
Control	1666_C1	BioRep1	93859624	76782844	81.81%	87.14%
	1666_C2	BioRep2	82388866	67921678	82.44%	87.37%
	1666_C3	BioRep3	76703980	60804856	79.27%	87.00%
Waterlogging	1666_WL	BioRep1	96634572	77980830	80.70%	88.65%
	1666_WL2	BioRep2	90456116	72938486	80.63%	89.21%
	1666_WL3	BioRep3	102480294	91617856	89.40%	89.71%
Control	344_C1	BioRep1	98707754	80641202	81.70%	90.07%
	344_C2	BioRep2	91684122	75300356	82.13%	90.05%
	344_C3	BioRep3	92127778	76191504	82.70%	89.91%
Waterlogging	344_WL1	BioRep1	90564764	75667990	83.55%	85.88%
	344_WL2	BioRep2	98237482	83470436	84.97%	85.28%
	344_WL3	BioRep3	95782168	82197786	85.82%	84.76%

annotation as biological processes (BP), cellular components (CC), and molecular functions (MF). In the waterlogging-tolerant genotype Acc. 1666, GO terms such as ATP binding (153), metal ion binding (79), and DNA binding (49), which belonged to the MF category, and terms such as protein phosphorylation (54), regulation of DNA-templated transcription (26), and RNA modification (20), which belonged to the BP category, were upregulated in response to waterlogging stress. Similarly, in the waterlogging-sensitive genotype W-344, GO terms such as ATP binding (143), metal ion binding (79), and DNA binding (62), which belonged to the MF category; terms such as protein phosphorylation (56), proteolysis (24), and phosphorylation (23), which belonged to the BP category; and terms such as membrane (214), nucleus (122), and cytoplasm (33), which belonged to the CC category, were upregulated under waterlogging stress. Several DEGs in the onion genotypes contributed to GO terms involved in the plant waterlogging stress responses. The upregulated DEGs contributed majorly to GO terms belonging to the BP category, such as hydrogen peroxide catabolic process [GO:0042744], response to oxidative stress [GO:0006979], and carbohydrate metabolic process [GO:0005975], and those belonging to the MF category, such as heme binding [GO:0020037], peroxidase activity [GO:0004601], ATP binding [GO:0005524], and calmodulin binding [GO:0005516]. Downregulated DEGs majorly contributed to the GO terms such as photosynthesis, light harvesting in photosystem I [GO:0009768], fatty acid biosynthesis process [GO:0006633], abscisic acid-activated signaling pathway [GO:0009738], chlorophyll binding [GO:0016168], and heme binding [GO:0020037], which belonged to the CC category in the onion transcriptome in response to waterlogging stress. Figure 4 presents the top 10 upregulated and downregulated GO terms in each category.

According to the analyses of distribution of clusters of orthologous groups in DEGs from Acc. 1666 and W-344, majorly

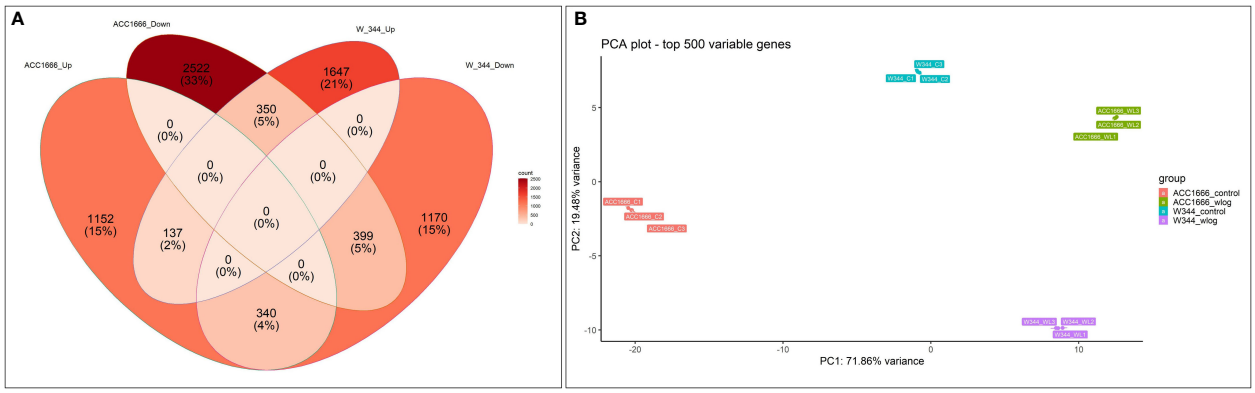

FIGURE 3
Differential gene expression pattern shown by waterlogging tolerant (Acc. 1666) and sensitive (W-344) onion genotypes under waterlogging stress using Venn diagram **(A)** and PCA **(B)**.

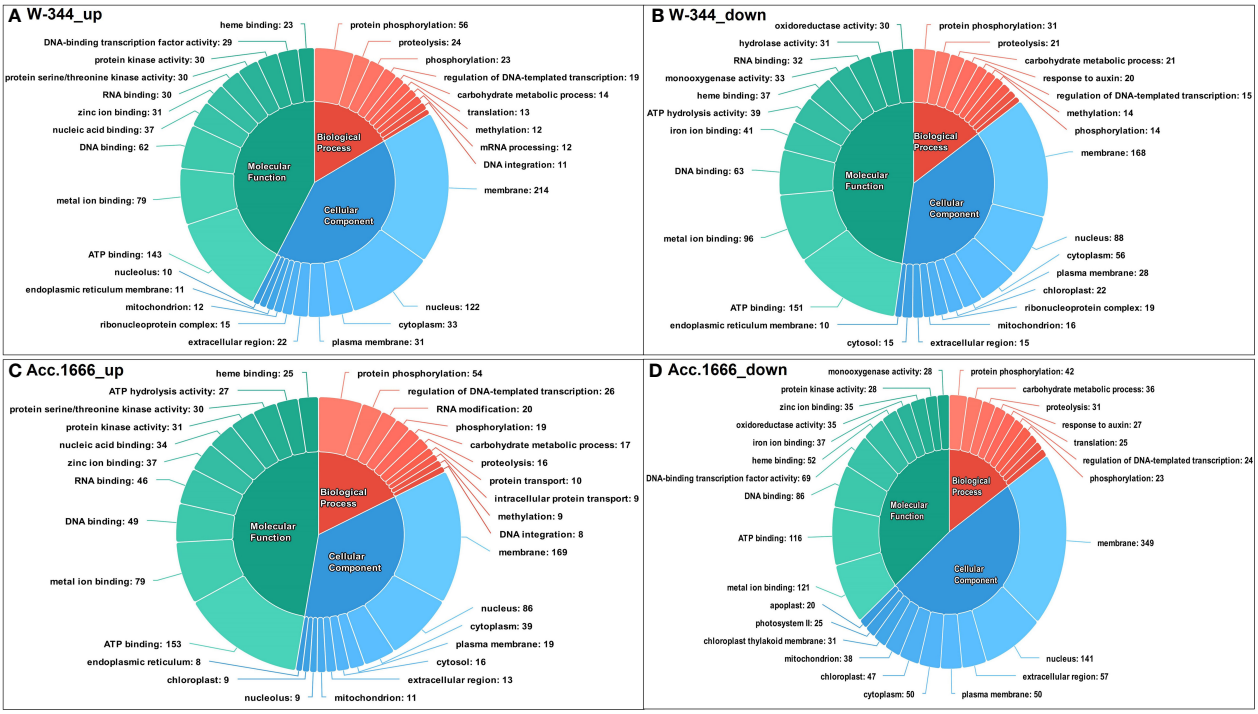

FIGURE 4
Functional annotation of differentially expressed transcripts in response to waterlogging stress in onion genotypes using Gene Ontology (GO); **(A)** Upregulated GO terms in W-344, **(B)** Downregulated GO terms in W-344, **(C)** Upregulated GO terms in Acc. 1666, **(D)** Downregulated GO terms in Acc. 1666.

belonged pathways for DNA replication and repair, post-translational modification signal transduction etc. (Figure S4). The transcription factor distribution was also analyzed for DEGs in contrasting onion genotypes under waterlogging stress (Figure S5). DEG transcripts were blasted against the plant TFDB to identify various transcription factors in the RNA-seq data. Of the identified transcription factors in both genotypes, some such as *ERF*, *bHLH*, *NFY*, *NAC*, and *bZIP* were found to be dominant in both genotypes under waterlogging stress.

DEG expression in response to waterlogging stress

Phytohormone biosynthesis and signaling pathway genes

Several transcripts for phytohormone biosynthesis and signaling were differentially expressed in response to waterlogging stress in both the waterlogging-tolerant (Acc. 1666) and sensitive (W-344) genotypes (Table 3). Transcripts for phenylalanine

TABLE 3 DEGs for phytohormone in contrasting onion genotypes in response to waterlogging stress.

Transcript id	Protein name	Acc. 1666		W-344	
		Fold change	Regulation	Fold change	Regulation
g11149	Phenylalanine ammonia-lyase	–	neutral	-2.4	down
g278967	Phenylalanine ammonia-lyase	–	neutral	-2.2	down
g346683	Lipoxygenase	2.3	up	-2.3	down
g78441	Lipoxygenase	2	up	-2	down
g125937	Lipoxygenase	–	–	-4.3	down
g58476	Lipoxygenase	-2	down	–	neutral
g174553	Lipoxygenase	–	neutral	4.9	up
g373200	9-cis-epoxycarotenoid dioxygenase	2.1	up	–	neutral
g239942	9-cis-epoxycarotenoid dioxygenase	–	neutral	-2.4	down
g107775	1-aminocyclopropane-1-carboxylate oxidase	2.3	up	–	neutral

-, indicate the no fold change in the gene express, representing the neutral gene regulation.

ammonia lyase, a key enzyme involved in SA biosynthesis, was neutral in Acc. 1666 and downregulated by −2.4-fold in W-344. Similarly, the transcript for the enzyme involved in jasmonic acid (JA) biosynthesis, such as lipoxygenase, also exhibited differential expression in response to waterlogging stress. The transcript (g346683) coding for lipoxygenase in *Allium cepa* was upregulated by 2.3-fold in Acc. 1666 and downregulated in W344. Another gene involved in JA biosynthesis (12-oxophytodienoate reductase-1) was downregulated in both genotypes. The key gene encoding an enzyme [i.e., 9-cis-epoxycarotenoid dioxygenase (*NCED*)] involved in the ABA biosynthesis pathway was upregulated (2.3-fold) in Acc. 1666 but downregulated by 2.4-fold in W-344. One gene transcript for 1-aminocyclopropane-1-carboxylate oxidase, which is involved in ethylene biosynthesis, was upregulated. Another transcript was downregulated in Acc. 1666, whereas it was neutral in the sensitive genotype.

Energy production, carbon metabolism, and photosynthesis

Gene encoding sucrose phosphate synthase was upregulated in Acc. 1666, while that encoding sucrose synthase was upregulated in W-344. Transcripts for invertase were upregulated by 4–6 fold in both genotypes under waterlogging stress. In addition, several genes involved in the carbohydrate catabolic pathway were found to be differentially expressed in the present investigation. A key gene in photosynthesis and carbon fixation, that is, *PEP carboxylase*, was exclusively upregulated (up to 5-fold) in the tolerant genotype Acc. 1666 but downregulated in W-344 (up to 3-fold). Similarly, several photosynthesis-related genes were differentially expressed in response to waterlogging stress. The majority of the photosynthesis-related genes were downregulated and a few were upregulated in both genotypes. For example, transcripts (g539704, g9297) for the photosystem II 10-kDa polypeptide were upregulated in Acc. 1666 but downregulated in W-344. Expression of genes in anaerobic fermentation like *PDC* and *ADH* were upregulated in Acc. 1666 but their gene count was low.

PCD, aerenchyma, and cell wall-related genes

Genes involved in PCD and aerenchyma development were differentially expressed under waterlogging stress in onion. Proteases such as ubiquitin-like protease, ubiquitin-specific protease 17, and 26S protease regulatory subunit were differentially expressed. Ubiquitin-like protease was upregulated in both onion genotypes, and 26S protease regulatory subunit was upregulated in Acc. 1666 but downregulated in W-344. Similarly, several other serine, aspartate, and cysteine peptidases were differentially expressed. Cell wall modification is among the plants' responses to stress. In the present study, several cell wall modification-related genes were differentially expressed under the waterlogging condition such as *Expansins, Xyloglucan endotrans-glucosylase/hydrolase (XTH), Cellulase synthase, Extensin*, and *Polygalacturonases*. In Acc. 1666, nine transcripts for *Expansin* were downregulated and none was upregulated, while in W-344, four transcripts are upregulated and three were downregulated. Similarly, *XTH*, another cell wall biosynthesis-related gene, was mostly downregulated under waterlogging stress in both genotypes. Only one *XTH* gene was upregulated in Acc. 1666. One transcript for polygalacturonase was upregulated and five were downregulated in Acc. 1666, while three transcripts were upregulated and two were downregulated in W-344.

Transcription factors

Waterlogging stress induced the expression of several transcription factors in the present study. *WRKY 70, WRKY44, WRKY22*, and *WRKY17* were upregulated by 10-, 3.8-, 2.8-, and 2.3-folds, respectively, whereas *WRKY19* was downregulated in Acc. 1666. In W-344, *WRKY12* and *WRKY40* were upregulated by 2.5- and 2.1-folds, respectively, whereas *WRKY70* was downregulated by 9.1 fold. Transcripts for the *NF-Y* transcription factor were upregulated by 4.6-fold in Acc. 1666 and downregulated by 3.2-fold in W-344. Several MYB transcription factors were differentially expressed in onion in response to waterlogging stress. Among *MYB* transcription factors, *MYB4* and *MYB29* were differentially upregulated in Acc. 1666 but downregulated in W-344. *MYB1R1* was upregulated in Acc.1666 alone. ERFs are key players in the response to various biotic and abiotic stresses in plants. ERFs in onion also exhibited differential expression under waterlogging. The majority of ERFs were downregulated in the present study. *ERF03, ERF34, ERF12, ERF39, ERF14, ERF12, ERF11*, etc. were downregulated, whereas *ERF53* and *AP2/ERF* domain-containing genes were upregulated.

ROS-scavenging genes

Under waterlogging or hypoxia stress, antioxidant enzymes have a key role in alleviating oxidative stress induced due to ROS overproduction. Several genes encoding antioxidant enzymes were differentially regulated in onion in the present investigation. Six transcripts in Acc. 1666 and 5 in W-344 for peroxidases were upregulated, whereas 17 transcripts in Acc. 1666 and 5 in W-344 were downregulated. One transcript for CAT was upregulated in Acc. 1666, whereas none exhibited upregulation in W-344. Similarly, one transcript for CAT was downregulated in Acc. 1666, whereas three were downregulated in W-344. A transcript for APX was downregulated by 2-fold in Acc. 1666, while that for monodehydroascorbate reductase was downregulated by 2.9-fold in W-344. Other important enzymes in stress response, such as ubiquinol oxidase having alternative oxidase activity, methionine sulfoxide reductase with antioxidative activity, and respiratory burst oxidase D, were also upregulated in Acc. 1666 and downregulated in W-344. SOD was also differentially expressed in the present experiment. In both genotypes, one transcript of SOD was upregulated and the other one was downregulated. *Glutathione S-*

transferase (GST) genes were differentially expressed. *GSTU1* and *GSTF1* were upregulated, whereas *GSTU3*, *GSTF2*, and *GSTF3* were downregulated in Acc. 1666. In W-344, *GSTU3* and *GSTU17* were upregulated, whereas *GSTU7*, *GSTF4*, and *GSTT3* were downregulated.

Phenylalanine metabolic pathway

Genes related to the phenylalanine metabolic pathway were downregulated in the susceptible genotype (W-344), such as *PAL, 4-coumarate:CoA ligase, and caffeic acid 3-O-methyltransferase*, by 2.4, 4.6, and 2.3-folds, respectively. By contrast, *PAL* was neutral and *4-coumarate:CoA ligase* was induced by 7.9-fold in the tolerant genotype (Acc. 1666) under the waterlogging condition. Similarly, some genes involved in flavonoid biosynthesis (such as *Flavonol synthase, Flavanone 3-hydroxylase, Isoflavone 2'-hydroxylase*, and *CYP71BE30*) were also downregulated in the susceptible genotype (W-344).

Pathogenesis-related proteins

In this study, transcripts for the defense response and pathogenesis-related proteins were also differentially expressed in response to waterlogging stress. The putative disease-resistant protein *RGA3, RGA4*, defensin, etc. were upregulated in both genotypes. By contrast, protein *TIFY* (jasmonate ZIM domain-containing protein), *MLO*-like protein, pathogenesis-related protein 10c, etc. were downregulated in both genotypes under waterlogging stress.

Validation of DEGs under waterlogging stress through qRT-PCR

For validating the results of the transcriptome analysis through qRT-PCR, seven DEGs belonging to the categories such as antioxidant enzymes, anaerobic fermentation, phytohormones, and transcription factors and involved in waterlogging stress responses were selected randomly (Table 1). The gene expression level in qRT-PCR and RNA-seq exhibited a good correlation, proving the reliability of RNA-seq data (Figure 5).

Discussion

Morpho-physiological responses to waterlogging stress in onion

Onion being a shallow-rooted crop is highly sensitive to water stresses, that is, both drought and waterlogging (Pelter et al., 2004). Waterlogging is commonly caused by excess rainfall during monsoons and hinders normal plant growth and survival (Ghodke et al., 2018). Our previous study reported that during the waterlogging condition, the growth of the sensitive genotype was more severely affected than that of its tolerant counterpart. Physiological and morphological alterations were also reported in different onion genotypes in response to waterlogging stress (Gedam et al., 2022). In the present study, the physiological and molecular alterations in the leaves of the two contrasting onion genotypes (waterlogging-tolerant: Acc. 1666; waterlogging-sensitive: W-344) were investigated in response to waterlogging stress.

After 72 h of waterlogging treatment, W-344 exhibited a sensitive phenotype with reduced plant height and leaf length, whereas Acc. 1666 exhibited better plant growth with more photosynthetically active leaves, higher chlorophyll content, and good plant architecture. Leaf area and chlorophyll content are vital physiological traits severely affected under a water stress environment (Kozlowski, 1997). This may be due to a reduction in leaf cell division and elongation in the sensitive genotype. By contrast, the tolerant genotype maintained its higher leaf area and chlorophyll content under stressful environments. At the onset of waterlogging stress, photosynthesis, transpiration, and nutrient mobilization in plants are disturbed along with the degradation of photosynthetic pigments such as chlorophyll, which decreases the net photosynthesis rate (Kaur et al., 2019; Zhang et al., 2023). Consequently, the assimilate partitioning towards the leaves and developing bulbs might be hampered, accelerating premature leaf senescence. The higher photosynthesis ability, as reflected by a

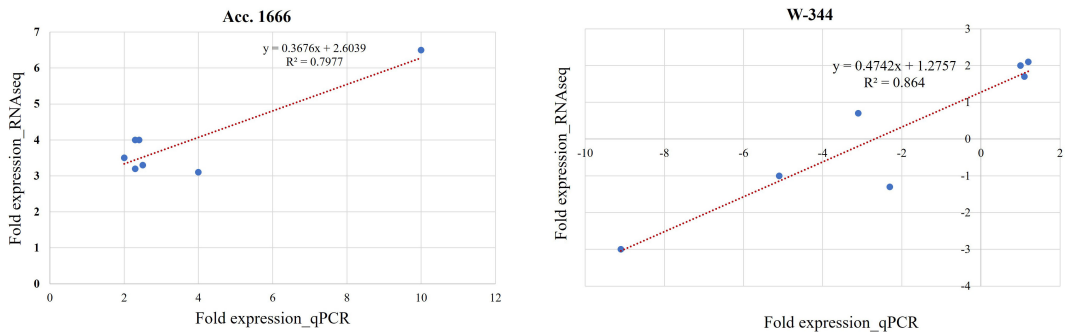

FIGURE 5
Validation of selected DEGs by qPCR analysis in Acc. 1666 and W-344. Each reaction was performed in triplicate. A good correlation was observed between RNA-Seq and qPCR data at of Acc. 1666 (R^2 = 79 and W-344 (R^2 = 0.86) after waterlogging stress in onion.

higher chlorophyll content in the tolerant genotype (Acc. 1666), is among the tolerance mechanisms that might help the plant to withstand the waterlogging condition. Consistently, the low chlorophyll content and poor plant phenotype with senesced leaves reflected the higher sensitivity of W-344 to waterlogging stress. The adverse effects of waterlogging stress with growth inhibition, poor plant architecture, and reduced photosynthesis and consequent low biomass and yield production have been described in sesame (Wei et al., 2013; Keya et al., 2022).

Phytohormonal responses to waterlogging stress in onion

SA is a well-known phytohormone with a key role in various plant developmental processes including plant response to biotic and abiotic stresses. SA imparts tolerance to waterlogging stress by stimulating antioxidant enzyme activity, PCD, aerenchyma formation, adventitious root development, and improvement in the photosynthetic efficiency in various plants (Koramutla et al., 2022). Similarly, JA plays a protective role in the waterlogging condition (Kamal and Komatsu, 2016). The genes involved in JA and SA biosynthesis and signaling were more highly upregulated in the tolerant genotype (Acc. 1666) than in the sensitive counterpart (W-344). ABA is among the key plant hormones involved in plant water stress response and such as stomatal closure and aerenchyma formation. ABA promotes suberin deposition in cell wall to regulate abiotic stress responses (Shimamura et al., 2014; Zhao et al., 2021). *NCED* is a key enzyme in ABA biosynthesis, and its expression is correlated with abiotic stress tolerance in several plants (Gong et al., 2010). In the present study, *NCED* transcripts were significantly upregulated in the leaves of the waterlogging-tolerant genotype (Acc. 1666), whereas they were downregulated in the sensitive genotype. The very-long-chain fatty acids (VLFCAs) constitute the primary components of suberin in plants, and they directly participate in ethylene biosynthesis by stimulating production of 1-aminocyclopropane-1-carboxylic acid (ACC), a precursor of ethylene. The enhanced ethylene synthesis induces aerenchyma formation in root cortical cells (Yamauchi et al., 2015). Therefore, it is suggested that the ABA promoted suberin deposition in the cell wall is utilized for ethylene biosynthesis, leading to the degradation of ABA and the production of ethylene, which, in turn, induces aerenchyma formation in root cortical cells under flooding condition. Along with growth regulation, ethylene plays a major role in tolerance to abiotic and biotic stresses in plants. ACC oxidase is an ethylene biosynthesis enzyme that converts the precursor ACC to ethylene. The *ACC oxidase* gene was upregulated in the tolerant onion genotype. The gene has also been reported to be upregulated in other species such as *Arabidopsis* (Ramadoss et al., 2018), cotton (Christianson et al., 2010), and cucumber (Qi et al., 2012) in response to waterlogging stress.

Energy production and carbon metabolism

The energy crisis is well-known in the waterlogging or hypoxia condition. Thus, modulating the expression of energy and glycolysis-related genes might help plants to overcome these adversities. The low oxygen level due to hypoxia leads to reduced ATP production (Crawford and Brändle, 1996). Under such conditions, plants need to maintain their energy level (ATP) through glycolysis and anaerobic fermentation pathways to sustain their growth and other developmental processes (Liu et al., 2020). Energy homeostasis and metabolism-related gene regulation is important in combating the adverse effect of waterlogging stress. During waterlogging, sucrose metabolism is also affected, which then hampers the source–sink relationship and ultimately leads to yield penalty (Zeng et al., 2021). In Acc. 1666, along with sucrose breakdown genes, the sucrose biosynthesis gene (SPS) was upregulated in the tolerant genotype, while all sucrose-metabolizing genes were upregulated. SPS promotes plant growth and confers abiotic stress tolerance to tomato plants (Zhang et al., 2022). In the present experiment, due to waterlogging conditions, only the roots were hypoxic, while the leaves remained in aerobic conditions. However, it is possible that some sort of signaling from the roots induced the expression of fermentation-related genes such as *PDC* and *ADH* in the leaves. Similar findings have also been reported in mungbean and cotton, where the induced expression of *PDC* and *ADH* was observed in the leaves when the roots were subjected to hypoxic conditions (Sreeratree et al., 2022; Christianson et al., 2010). Photosynthesis is highly sensitive to waterlogging stress, and several transcripts related to photosynthesis were differentially expressed in onion due to waterlogging. PEP carboxylase is among the key enzymes in C4 photosynthesis and was upregulated in Acc. 1666 but downregulated in W-344. This might have affected photosynthesis, and ultimately, carbon fixation under the stressful condition (Zhang et al., 2023). The findings thus proved that the tolerant genotype accumulates more energy by activating the alternate energy metabolism pathway under waterlogging stress, which might be responsible for its better adaptability than the sensitive genotype.

PCD, aerenchyma, and cell wall-related genes

Plants employ several strategies to overcome prolonged waterlogging-induced oxygen deficiency. Here, the transcriptional reprogramming in leaves, and not in roots, was studied, and several genes involved in PCD and aerenchyma formation and encoding for cell wall-related enzymes were found to be differentially expressed in onion leaves in response to waterlogging stress. The study findings are consistent with those of previous studies in soybean (Chen et al., 2016), peanut (Zeng et al., 2021), and pigeon pea (Tyagi et al., 2022). In these studies, leaf tissue was used for transcriptome profiling to explore the molecular mechanism regulating the waterlogging tolerance mechanism in these crops. In addition to ROS scavenging and phytohormone biosynthesis and signaling genes, PCD-regulating genes were differentially expressed in the present study. PCD is involved in aerenchyma development under waterlogging stress in several plants (Yamauchi et al., 2018; Ni et al., 2019). In the present study, several genes, such as those encoding for ubiquitin-like protease and 26S protease regulatory subunit, and a few genes for proteases and peptidases were differentially expressed. Along with PCD, cell wall modification is crucial for aerenchyma development in

roots and stems (Arora et al., 2017). Transcripts for xyloglucan-endo-trans-glucosylase/hydrolase, expansin, poly-galacturonase, etc. were differentially expressed in the onion genotype in response to waterlogging stress. Thus, this might be the factor responsible for waterlogging tolerance in Acc. 1666. Previous findings have supported these results, which indicate that anatomical adaptations such as adventitious roots and aerenchyma formation help the plants, such as rice, to withstand submergence or waterlogging (Justin and Armstrong, 1991).

ROS scavenging and antioxidant enzyme activity under waterlogging stress in onion

Hypoxia during waterlogging leads to ROS production in plant roots as well as in leaf tissue (Baxter et al., 2014). The excessive amount of ROS is deleterious to plants, and antioxidant enzymes such as POD, CAT, SOD, and APX have a critical role in regulating ROS levels to avoid oxidative stress (Bansal and Srivastava, 2012). In the present study, significantly higher ROS (H_2O_2) accumulation in the sensitive genotype (W-344) indicates that this genotype experienced higher cellular membrane damage and leaf senescence. By contrast, the H_2O_2 level was comparatively low in the tolerant genotype, indicating less oxidative stress-induced damage and higher membrane stability and functionality under the stress condition. Consistent with low oxidative stress, the activities of various antioxidant enzymes, including SOD, CAT, POD, and APX, were significantly higher in Acc. 1666 as they might be directly involved in ROS scavenging and improving plant survival and growth under the stressful environment. In this study, the tolerance of Acc. 1666 and the sensitivity of W-344 to waterlogging stress was observed. However, waterlogging tolerance is a complex and quantitative trait and needs to be studied in detail by highlighting the adaptive mechanism regulating genes in the tolerant genotype. Information available on the molecular response of onion crops to waterlogging stress is limited. The current study was conducted to highlight the waterlogging tolerance mechanism in onion crops at the transcriptional level by using the RNA-seq approach.

The transcript level of these antioxidant enzyme-encoding genes is usually upregulated in response to abiotic stresses including waterlogging stress. Genes encoding antioxidant enzymes, such as SOD, APX, glutathione peroxidase, CAT, and GST, were differentially expressed in the present analysis. Similarly, the activities of antioxidant enzymes were also increased in response to waterlogging stress. The increased antioxidant enzyme activities under waterlogging stress have been reported in several crops such as wheat (Ma et al., 2022), onion (Dubey et al., 2020), barley (Borrego-Benjumea et al., 2020), and sesame (Sathi et al., 2022). The activities of these enzymes were higher in the tolerant genotypes of pigeon pea, maize, and sorghum (Bansal and Srivastava, 2012; Li et al., 2018; Zhang R. et al., 2019; ; Zhang Y. et al., 2019). The RNA-seq analysis revealed differential expression of antioxidant genes in tomato roots under hypoxia. These antioxidant genes were reported to be associated with aerenchyma development under waterlogging stress in tomato (Safavi-Rizi et al., 2020). In the present study, *Ubiquinol oxidase* having alternate oxidase (*AOX*) activity was upregulated in the tolerant genotype in response to waterlogging. *AOX* upregulation in hypoxia has been reported earlier (Wany et al., 2019; Jayawardhane et al., 2020). The peptide methionine sulfoxide reductase gene was upregulated in Acc. 1666. This enzyme has been reported to be involved in H_2O_2-induced oxidative stress response, ABA treatment, and photooxidative stress (Dai and Wang, 2010; Vieira Dos Santos et al., 2005). The respiratory burst oxidase homolog D (RbohD) gene was upregulated in the tolerant onion genotype. *AtRboh D* is involved in waterlogging response and induces the expression of ethylene biosynthesis genes as well as *ERFs*, *ADH1*, and *PDC1* under the waterlogging condition (Yang and Hong, 2015; Liu et al., 2017). Thus, the RbohD might be involved in plant response to waterlogging stress.

A higher transcript level and more enzyme activities during waterlogging indicate a translational correlation between gene expression and protein-level actions. In the present study, some transcripts for a particular enzyme were upregulated, whereas some were downregulated. However, the enzyme activity was higher under the stress condition. Glanemann et al. (2003) also found a similar disparity between the mRNA abundance and enzyme activity. They stated that predicting enzyme activity from transcriptome data is difficult. The variation in the transcript level at different time points and in tissue types, and resources of translation significantly influence this correlation. Thus, in many scenarios, determining only the mRNA level is not sufficient for predicting the gene product (protein) level. Alternative splicing and post-transcriptional modifications also affect the mRNA–protein correlation (Brar et al., 2012; Liu et al., 2016). This report thus suggests that the high antioxidant enzyme activity confers stress tolerance to the tolerant onion genotype Acc. 1666.

Transcription factor expression under waterlogging stress

Transcription factors act as key regulators of the waterlogging stress response (Valliyodan et al., 2014). In the present study, several transcription factors were differentially expressed in response to waterlogging stress. Members of transcription factor families such as *ERF, WRKY, MYB, NAC*, and *bHLH* are known to be involved in regulating various biotic and abiotic stress responses in onion (Ghodke et al., 2020; Khandagale et al., 2022). These transcription factors are also involved in response to a hypoxic condition caused by waterlogging stress in plants. *WRKY22* was involved in submergence tolerance by positively regulating ethylene-mediated signaling (Hsu et al., 2013). *WRKY40* has also been reported to be upregulated under waterlogging stress in *Arabidopsis* and Kiwifruit (Meng et al., 2020; Wurms et al., 2023). *WRKY70* is known to regulate SA and JA signaling in response to stress and acts as a negative regulator of senescence (Besseau et al., 2012). *NF-Y* regulates ABA synthesis by binding to the *NCED* gene promoter (Bi et al., 2017). In addition to ABA regulation, *NF-Y* improves photosynthesis, activity of antioxidant enzymes (Manimaran et al., 2017), and root length (Han et al., 2013). MYB transcription factors are crucial players in anthocyanin and phenylpropanoid biosynthesis and plant resistance to biotic and abiotic stress. *MYB1R1* expression was induced in hot pepper under waterlogging stress (Zhang R. et al., 2019; Zhang Y. et al., 2019).

Further, *MYBs* are involved in response to the hypoxia and waterlogging stresses (Lee et al., 2007; Fukushima et al., 2016). Ethylene is a gaseous hormone having a vital role in controlling plants' waterlogging responses (Khan et al., 2020). The *ERF* family is a plant-specific transcription factor group regulating plant responses to several abiotic stresses (Muller and Munne-Bosch, 2015). The differential expression of these transcription factors indicates their importance in transcriptional reprogramming during adaptation to the waterlogging condition.

Phenylalanine metabolic pathway

Lignin biosynthesis genes, such as *4-coumarate:CoA ligase* and *caffeic acid 3-O-methyltransferase*, were associated with the waterlogging response in wheat (Nguyen et al., 2016). *Arabidopsis* mutants for these genes accumulated a low amount of lignin than the wild-type plants (Vanholme et al., 2012). Induced expression of *4-coumarate:CoA ligase* was also reported in *Sesbania cannabina* under waterlogging stress (Ren et al., 2017). Similarly, flavonoid biosynthesis-related genes were downregulated in the susceptible onion genotype, whereas these were neutral in the tolerant genotype. RNA-Seq of *Pterocarya stenoptera* and *Brassica napus* leaves revealed that flavonoid synthesis-related genes were associated with the waterlogging stress response (Li et al., 2021; Hong et al., 2023). Thus, upregulation of these genes of the phenylalanine metabolic pathway in the tolerant onion genotype might play some role in conferring waterlogging stress tolerance.

Conclusions

In this study, two contrasting onion genotypes with varying degrees of waterlogging tolerance capacities were subjected to 72 h of waterlogging stress. Morphological and physiological stress indicators revealed that Acc. 1666 exhibited a stronger tolerance to waterlogging than the sensitive genotype W-344. Genes coding for proteins regulating several key biological processes involved in combating waterlogging stress, such as phytohormone production, antioxidant enzymes, PCD, anaerobic fermentation, and energy production, were differentially expressed. Genes such as *ADH, PDC, WRKY22*, and *RbohD* were upregulated in the tolerant genotype and might have been involved in conferring stress tolerance to Acc. 1666. This study provides valuable information about key regulatory genes that can be used in onion breeding programmes aimed at developing waterlogging-tolerant varieties.

Data availability statement

The data from the current study has been made available publically at NCBI with accession no "PRJNA926808".

Author contributions

PG, AT, SG, AK: conceptualization, planning, methodology, supervision, writing-original draft., project administration. KK, DS, KB, YK: methodology, biochemical analysis, statistical analysis. VM, AG: resources. OK, VB: methodology, writing, editing. MS: supervision, funding, and project administration. All authors listed have made a substantial, direct, and intellectual contribution to the work.

Funding

This study was supported by the India Council of Agricultural Research (ICAR)- National Innovations on Climate Resilient Agriculture (NICRA) and ICAR Directorate of Onion and Garlic Research, Pune.

Conflict of interest

The authors declare that the research was conducted in the absence of any commercial or financial relationships that could be construed as a potential conflict of interest.

Publisher's note

Supplementary material

The Supplementary Material for this article can be found online at: https://www.frontiersin.org/articles/10.3389/fpls.2023.1150909/full#supplementary-material

References

Arnon, D. (1949). Estimation of total chlorophyll. *Plant Physiol.* 24, 1–15. doi: 10.1104/pp.24.1.1

Arora, K., Panda, K. K., Mittal, S., Mallikarjuna, M. G., Rao, A. R., Dash, P. K., et al. (2017). RNAseq revealed the important gene pathways controlling adaptive mechanisms under waterlogged stress in maize. *Sci. Rep.* 7 (1), 1–12. doi: 10.1038/s41598-017-10561-1

Bansal, R., and Srivastava, J. P. (2012). Antioxidative defense system in pigeonpea roots under waterlogging stress. *Acta Physiol. Plant* 34, 515–522. doi: 10.1007/s11738-011-0848-z

Baxter, A., Mittler, R., and Suzuki, N. (2014). ROS as key players in plant stress signalling. *J. Exp. Bot.* 65, 1229–1240. doi: 10.1093/jxb/ert375

Beauchamp, C., and Fridovich, I. (1971). Superoxide dismutase: improved assays and an assay applicable to acrylamide gels. *Anal. Biochem.* 44 (1), 276–287. doi: 10.1016/0003-2697(71)90370-8

Besseau, S., Li, J., and Palva, E. T. (2012). WRKY54 and WRKY70 co-operate as negative regulators of leaf senescence in Arabidopsis thaliana. *J. Exp. Bot.* 63, 2667–2679. doi: 10.1093/jxb/err450

Bi, C., Ma, Y., Wang, X. F., and Zhang, D. P. (2017). Overexpression of the transcription factor NF-YC9 confers abscisic acid hypersensitivity in Arabidopsis. *Plant Mol. Biol.* 955, 425–439. doi: 10.1007/s11103-017-0661-1

Borrego-Benjumea, A., Carter, A., Tucker, J. R., Yao, Z., Xu, W., and Badea, A. (2020). Genome-wide analysis of gene expression provides new insights into waterlogging responses in barley (*Hordeum vulgare* L.). *Plants* 9 (2), 240. doi: 10.3390/plants9020240

Brar, G. A., Yassour, M., Friedman, N., Regev, A., Ingolia, N. T., and Weissman, J. S. (2012). High-resolution view of the yeast meiotic program revealed byribosome profiling. *Science* 335, 552–557. doi: 10.1126/science.1215110

Cao, M., Zheng, L., Li, J., Mao, Y., Zhang, R., Niu, X., et al. (2022). Transcriptomic profiling suggests candidate molecular responses to waterlogging in cassava. *PloS One* 17 (1), e0261086. doi: 10.1371/journal.pone.0261086

Castillo, F. J., Penel, C., and Greppin, H. (1984). Peroxidase release induced by ozone in Sedum album leaves: involvement of Ca2+. *Plant Physiol.* 74 (4), 846–851. doi: 10.1104/pp.74.4.846

Chen, W., Yao, Q., Patil, G. B., Agarwal, G., Deshmukh, R. K., Lin, L., et al. (2016). Identification and comparative analysis of differential gene expression in soybean leaf tissue under drought and flooding stress revealed by RNA-Seq. *Front. Plant Sci.* 7, 1044. doi: 10.3389/fpls.2016.01044

Christianson, J. A., Llewellyn, D. J., Dennis, E. S., and Wilson, I. W. (2010). Global gene expression responses to waterlogging in roots and leaves of cotton (*Gossypium hirsutum* L.). *Plant Cell Physiol.* 51 (1), 21–37. doi: 10.1093/pcp/pcp163

Crawford, R. M. M., and Brändle, R. (1996). Oxygen deprivation stress in a changing environment. *J. Exp. Bot.* 47 (2), 145–159. doi: 10.1093/jxb/47.2.145

Dai, C., and Wang, M. H. (2010). Expression pattern of a peptide methionine sulfoxide reductase gene from tomato (*Solanum lycopersicum*) in response to abiotic and oxidative stresses. *J. Korean Soc. Appl. Biol. Chem.* 53 (2), 127–132. doi: 10.3839/jksabc.2010.022

Dubey, S., Kuruwanshi, V. B., Ghodke, P. H., and Mahajan, V. (2020). Biochemical and yield evaluation of onion (*Allium cepa* L.) genotypes under waterlogging condition. *Int. J. Chem. Stud.* 8, 2036–2040. doi: 10.22271/chemi.2020.v8.i4v.9926

Food and Agriculture Organization of the United Nation (2020). *FAOSTAT* (Rome: FAO).

Fukushima, S., Mori, M., Sugano, S., and Takatsuji, H. (2016). Transcription factor *WRKY62* plays a role in pathogen defense and hypoxia-responsive gene expression in rice. *Plant Cell Physiol.* 57 (12), 2541–2551. doi: 10.1093/pcp/pcw185

Gasch, P., Fundinger, M., Müller, J. T., Lee, T., Bailey-Serres, J., and Mustroph, A. (2016). Redundant ERF-VII transcription factors bind to an evolutionarily conserved cis-motif to regulate hypoxia-responsive gene expression in Arabidopsis. *Plant Cell* 28 (1), 160–180. doi: 10.1105/tpc.15.00866

Gedam, P. A., Shirsat, D. V., Arunachalam, T., Ghosh, S., Gawande, S. J., Mahajan, V., et al. (2022). Screening of onion (*Allium cepa* L.) genotypes for waterlogging tolerance. *Front. Plant Sci.* 12, 727262. doi: 10.3389/fpls.2021.727262

Ghodke, P., Khandagale, K., Thangasamy, A., Kulkarni, A., Narwade, N., Shirsat, D., et al. (2020). Comparative transcriptome analyses in contrasting onion (Allium cepa L.) genotypes for drought stress. *PloS One* 15 (8), e0237457. doi: 10.1371/journal.pone.0237457

Ghodke, P. H., Shirsat, D. V., Thangasamy, A., Mahajan, V., Salunkhe, V. N., Khade, Y., et al. (2018). Effect of water logging stress at specific growth stages in onion crop. *Int. J. Curr. Microbiol. Appl. Sci.* 7, 3438–3448. doi: 10.20546/ijcmas.2018.701.405

Gibbs, D. J., Lee, S. C., Md Isa, N., Gramuglia, S., Fukao, T., Bassel, G. W., et al. (2011). Homeostatic response to hypoxia is regulated by the N-end rule pathway in plants. *Nature* 479 (7373), 415–418. doi: 10.1038/nature10534

Glanemann, C., Loos, A., Gorret, N., Willis, L. B., O'brien, X. M., Lessard, P. A., et al. (2003). Disparity between changes in mRNA abundance and enzyme activity in Corynebacterium glutamicum: implications for DNA microarray analysis. *Appl. Microbiol. Biotechnol.* 61, 61–68. doi: 10.1007/s00253-002-1191-5

Gong, P. J., Zhang, J. H., Li, H. X., Yang, C. X., Zhang, C. J., Zhang, X. H., et al. (2010). Transcriptional profiles of drought-responsive genes in modulating transcription signal transduction, and biochemical pathways in tomato. *J. Exp. Bot.* 61, 3563–3575. doi: 10.1093/jxb/erq167

Han, X., Tang, S., An, Y., Zheng, D. C., Xia, X. L., and Yin, W. L. (2013). Overexpression of the poplar *NF-YB7* transcription factor confers drought tolerance and improves water-use efficiency in *Arabidopsis*. *J. Exp. Bot.* 64 (14), 4589–4601. doi: 10.1093/jxb/ert262

Heath, R. L., and Packer, L. (1968). Photoperoxidation in isolated chloroplasts: I. Kinetics and stoichiometry of fatty acid peroxidation. *Arch. Biochem. Biophys.* 125 (1), 189–198. doi: 10.1016/0003-9861(68)90654-1

Hiscox, J. D., and Israelstam, G. F. (1979). A method for the extraction of chlorophyll from leaf tissue without maceration. *Can. J. Bot.* 57 (12), 1332–1334. doi: 10.1139/b79-163

Hong, B., Zhou, B., Peng, Z., Yao, M., Wu, J., Wu, X., et al. (2023). Tissue-specific transcriptome and metabolome analysis reveals the response mechanism of *Brassica napus* to waterlogging stress. *Int. J. Mol. Sci.* 24 (7), 6015. doi: 10.3390/ijms24076015

Hsu, F. C., Chou, M. Y., Chou, S. J., Li, Y. R., Peng, H. P., and Shih, M. C. (2013). Submergence confers immunity mediated by the *WRKY22* transcription factor in *Arabidopsis*. *Plant Cell* 25, 2699–2713. doi: 10.1105/tpc.113.114447

Jayawardhane, J., Cochrane, D. W., Vyas, P., Bykova, N. V., Vanlerberghe, G. C., and Igamberdiev, A. U. (2020). Roles for plant mitochondrial alternative oxidase under normoxia, hypoxia, and reoxygenation conditions. *Front. Plant Sci.* 11, 566. doi: 10.3389/fpls.2020.00566

Justin, S., and Armstrong, W. (1991). Evidence for the involvement of ethylene in aerenchyma formation in adventitious roots of rice (*Oryza sativa*). *New Phytol.* 118, 49–62. doi: 10.1111/j.1469-8137.1991.tb00564.x

Kamal, A. H. M., and Komatsu, S. (2016). Jasmonic acid induced protein response to biophoton emissions and flooding stress in soybean. *J. Proteomics* 133, 33–47. doi: 10.1016/j.jprot.2015.12.004

Kaur, G., Singh, G., Motavalli, P. P., Nelson, K. A., Orlowski, J. M., and Golden, B. R. (2020). Impacts and management strategies for crop production in waterlogged or flooded soils: A review. *Agron. J.* 112 (3), 1475–1501. doi: 10.1002/agj2.20093

Kaur, G., Zurweller, B., Motavalli, P. P., and Nelson, K. A. (2019). Screening corn hybrids for soil waterlogging tolerance at an early growth stage. *Agriculture* 9 (2), 33. doi: 10.3390/agriculture9020033

Keya, S. S., Mostofa, M. G., Rahman, M. M., Das, A. K., Rahman, M. A., Anik, T. R., et al. (2022). Effects of glutathione on waterlogging-induced damage in sesame crop. *Ind. Crops Prod.* 185, 115092. doi: 10.1016/j.indcrop.2022.115092

Khan, M. I. R., Trivellini, A., Chhillar, H., Chopra, P., Ferrante, A., Khan, N. A., et al. (2020). The significance and functions of ethylene in flooding stress tolerance in plants. *Environ. Exp. Botany* 179, 104188. doi: 10.1016/j.envexpbot.2020.104188

Khandagale, K., Roylawar, P., Kulkarni, O., Khambalkar, P., Ade, A., Kulkarni, A., et al. (2022). Comparative transcriptome analysis of onion in response to infection by *Alternaria porri* (Ellis) Cifferi. *Front. Plant Sci.* 13, 857306–857306. doi: 10.3389/fpls.2022.857306

Komatsu, S., Thibaut, D., Hiraga, S., Kato, M., Chiba, M., Hashiguchi, A., et al. (2011). Characterization of a novel flooding stress-responsive alcohol dehydrogenase expressed in soybean roots. *Plant Mol. Biol.* 77, 309–322. doi: 10.1007/s11103-011-9812-y

Koramutla, M. K., Tuan, P. A., and Ayele, B. T. (2022). Salicylic acid enhances adventitious root and aerenchyma formation in wheat under waterlogged conditions. *Int. J. Mol. Sci.* 23 (3), 1243. doi: 10.3390/ijms23031243

Kozlowski, T. T. (1997). Responses of woody plants to flooding and salinity. *Tree Physiol.* 17 (7), 490–490. doi: 10.1093/treephys/17.7.490

Lee, T. G., Jang, C. S., Kim, J. Y., Kim, D. S., Park, J. H., Kim, D. Y., et al. (2007). A Myb transcription factor (*TaMyb1*) from wheat roots is expressed during hypoxia: roles in response to the oxygen concentration in root environment and abiotic stresses. *Physiol. Plantarum* 129 (2), 375–385. doi: 10.1111/j.1399-3054.2006.00828.x

Li, W., Mo, W., Ashraf, U., Li, G., Wen, T., Abrar, M., et al. (2018). Evaluation of physiological indices of waterlogging tolerance of different maize varieties in South China. *Appl. Ecol. Environ. Res.* 16, 2059–2072. doi: 10.15666/aeer/1602_20592072

Li, Y., Shi, L. C., Yang, J., Qian, Z. H., He, Y. X., and Li, M. W. (2021). Physiological and transcriptional changes provide insights into the effect of root waterlogging on the aboveground part of *Pterocarya stenoptera*. *Genomics* 113 (4), 2583–2590. doi: 10.1016/j.ygeno.2021.06.005

Liu, Y., Beyer, A., and Aebersold, R. (2016). On the dependency of cellular protein levels on mRNA abundance. *Cell* 165 (3), 535–550. doi: 10.1016/j.cell.2016.03.014

Liu, J., Hasanuzzaman, M., Sun, H., Zhang, J., Peng, T., Sun, H., et al. (2020). Comparative morphological and transcriptomic responses of lowland and upland rice to root-zone hypoxia. *Environ. Exp. Bot.* 169, 103916. doi: 10.1016/j.envexpbot.2019.103916

Liu, B., Sun, L., Ma, L., and Hao, F.-S. (2017). Both AtrbohD and AtrbohF are essential for mediating responses to oxygen deficiency in Arabidopsis. *Plant Cell Rep.* 36, 947–957. doi: 10.1007/s00299-017-2128-x

Livak, K. J., and Schmittgen, T. D. (2001). Analysis of relative gene expression data using real-time quantitative PCR and the $2^{-\Delta\Delta CT}$ method. *Methods* 25 (4), 402–408. doi: 10.1006/meth.2001.1262

Luo, H. T., Zhang, J. Y., Wang, G., Jia, Z. H., Huang, S. N., Wang, T., et al. (2017). Functional characterization of waterlogging and heat stresses tolerance gene pyruvate decarboxylase 2 from *Actinidia deliciosa*. *Int. J. Mol. Sci.* 18 (11), 2377. doi: 10.3390/ijms18112377

Ma, S., Gai, P., Geng, B., Wang, Y., Ullah, N., Zhang, W., et al. (2022). Exogenous melatonin improves waterlogging tolerance in wheat through promoting antioxidant enzymatic activity and carbon assimilation. *Agronomy* 12 (11), 2876. doi: 10.3390/agronomy12112876

Manimaran, P., Venkata Reddy, S., Moin, M., Raghurami Reddy, M., Yugandhar, P., Mohanraj, S. S., et al. (2017). Activation-tagging in indica rice identifies a novel transcription factor subunit, *NF-YC13* associated with salt tolerance. *Sci. Rep.* 7 (1), 9341. doi: 10.1038/s41598-017-10022-9

Meng, X., Li, L., Narsai, R., De Clercq, I., Whelan, J., and Berkowitz, O. (2020). Mitochondrial signalling is critical for acclimation and adaptation to flooding in *Arabidopsis thaliana*. *Plant J.* 103 (1), 227–247. doi: 10.1111/tpj.14724

Muller, M., and Munne-Bosch, S. (2015). Ethylene response factors: a key regulatory hub in hormone and stress signaling. *Plant Physiol.* 169 (1), 32–41. doi: 10.1104/pp.15.00677

Nakano, Y., and Asada, K. (1987). Purification of ascorbate peroxidase in spinach chloroplasts; its inactivation in ascorbate-depleted medium and reactivation by monodehydroascorbate radical. *Plant Cell Physiol.* 28 (1), 131–140. doi: 10.1093/oxfordjournals.pcp.a077268

Nguyen, T. N., Son, S., Jordan, M. C., Levin, D. B., and Ayele, B. T. (2016). Lignin biosynthesis in wheat (Triticum aestivum L.): its response to waterlogging and association with hormonal levels. *BMC Plant Biol.* 16, 1–16. doi: 10.1186/s12870-016-0717-4

Ni, X. L., Gui, M. Y., Tan, L. L., Zhu, Q., Liu, W. Z., and Li, C. X. (2019). Programmed cell death and aerenchyma formation in water-logged sunflower stems and its promotion by ethylene and ROS. *Front. Plant Sci.* 9, 1928. doi: 10.3389/fpls.2018.01928

Pan, J., Sharif, R., Xu, X., and Chen, X. (2021). Mechanisms of waterlogging tolerance in plants: Research progress and prospects. *Front. Plant Sci.* 11, 627331. doi: 10.3389/fpls.2020.627331

Park, S. U., Lee, C. J., Kim, S. E., Lim, Y. H., Lee, H. U., Nam, S. S., et al. (2020). Selection of flooding stress tolerant sweetpotato cultivars based on biochemical and phenotypic characterization. *Plant Physiol. Biochem.* 155, 243–251. doi: 10.1016/j.plaphy.2020.07.039

Pelter, G. Q., Mittelstadt, R., Leib, B. G., and Redulla, C. A. (2004). Effects of water stress at specific growth stages on onion bulb yield and quality. *Agric. Water Manage.* 68 (2), 107–115. doi: 10.1016/j.agwat.2004.03.010

Priyadarshini, E., Jayalakshmi, K., Shalini, M., Chakkravarthy, S. E., Vidhya, M., and Govindarajan, A. (2021). Analysis of onion prices at wholesale level in India–an application of Rescaled Range Analysis. *J. Phys.* 1770 (1), 012107. doi: 10.1088/1742-6596/1770/1/012107

Qi, X. H., Xu, X. W., Lin, X. J., Zhang, W. J., and Chen, X. H. (2012). Identification of differentially expressed genes in cucumber (*Cucumis sativus* L.) root under waterlogging stress by digital gene expression profile. *Genomics* 99 (3), 160–168. doi: 10.1016/j.ygeno.2011.12.008

Ramadoss, N., Gupta, D., Vaidya, B. N., Joshee, N., and Basu, C. (2018). Functional characterization of 1-aminocyclopropane-1-carboxylic acid oxidase gene in *Arabidopsis thaliana* and its potential in providing flood tolerance. *Biochem. Biophys. Res. Commun.* 503 (1), 365–370. doi: 10.1016/j.bbrc.2018.06.036

Rao, M. V., Paliyath, G., Ormrod, D. P., Murr, D. P., and Watkins, C. B. (1997). Influence of salicylic acid on H2O2 production, oxidative stress, and H2O2-metabolizing enzymes (salicylic acid-mediated oxidative damage requires H2O2). *Plant Physiol.* 115 (1), 137–149. doi: 10.1104/pp.115.1.137

Ren, C. G., Kong, C. C., Yan, K., Zhang, H., Luo, Y. M., and Xie, Z. H. (2017). Elucidation of the molecular responses to waterlogging in Sesbania cannabina roots by transcriptome profiling. *Sci. Rep.* 7 (1), 1–12. doi: 10.1038/s41598-017-07740-5

Roylawar, P., and Kamble, A. (2017). β–amino butyric acid mediated changes in cellular redox homeostasis confers tomato resistance to early blight. *Australas. Plant Pathol.* 46 (3), 239–249. doi: 10.1007/s13313-017-0484-1

Safavi-Rizi, V., Herde, M., and Stohr, C. (2020). RNA-Seq reveals novel genes and pathways associated with hypoxia duration and tolerance in tomato root. *Sci. Rep.* 10 (1), 1–17. doi: 10.1038/s41598-020-57884-0

Sathi, K. S., Masud, A. A. C., Falguni, M. R., Ahmed, N., Rahman, K., and Hasanuzzaman, M. (2022). Screening of soybean genotypes for waterlogging stress tolerance and understanding the physiological mechanisms. *Adv. Agric.* 2022, 1–14. doi: 10.1155/2022/5544665

Shabala, S. (2011). Physiological and cellular aspects of phytotoxicity tolerance in plants: the role of membrane transporters and implications for crop breeding for waterlogging tolerance. *New Phytol.* 190 (2), 289–298. doi: 10.1111/j.1469-8137.2010.03575.x

Shen, C., Yuan, J., Ou, X., Ren, X., and Li, X. (2021). Genome-wide identification of alcohol dehydrogenase (ADH) gene family under waterlogging stress in wheat (*Triticum* aestivum). *PeerJ* 9, e11861. doi: 10.7717/peerj.11861

Shimamura, S., Yoshioka, T., Yamamoto, R., Hiraga, S., Nakamura, T., Shimada, S., et al. (2014). Role of abscisic acid in flood-induced secondary aerenchyma formation in soybean (*Glycine max*) hypocotyls. *Plant Prod. Sci.* 17 (2), 131–137. doi: 10.1626/pps.17.131

Sreeratree, J., Butsayawarapat, P., Chaisan, T., Somta, P., and Juntawong, P. (2022). RNA-Seq reveals waterlogging-triggered root plasticity in mungbean associated with ethylene and jasmonic acid signal integrators for root regeneration. *Plants* 11 (7), 930. doi: 10.3390/plants11070930

Teranishi, Y., Tanaka, A., Osumi, M., and Fukui, S. (1974). Catalase activities of hydrocarbon-utilizing Candida yeasts. *Agric. Biol. Chem.* 38 (6), 1213–1220. doi: 10.1080/00021369.1974.10861301

Tougou, M., Hashiguchi, A., Yukawa, K., Nanjo, Y., Hiraga, S., Nakamura, T., et al. (2012). Responses to flooding stress in soybean seedlings with the alcohol dehydrogenase transgene. *Plant Biotechnol.* 29, 301–305. doi: 10.5511/plantbiotechnology.12.0301a

Tyagi, A., Sharma, S., Srivastava, H., Singh, A., Kaila, T., Ali, S., et al. (2022). Transcriptome profiling of two contrasting pigeon pea (*Cajanus cajan*) genotypes in response to waterloging stress. *Front. Genet.* 13, 3757. doi: 10.3389/fgene.2022.1048476

Valliyodan, B., Van Toai, T. T., Alves, J. D., de Fátima P. Goulart, P., Lee, J. D., Fritschi, F. B., et al. (2014). Expression of root-related transcription factors associated with flooding tolerance of soybean (*Glycine max*). *Int. J. Mol. Sci.* 15 (10), 17622–17643. doi: 10.3390/ijms151017622

Vanholme, R., Storme, V., Vanholme, B., Sundin, L., Christensen, J. H., Goeminne, G., et al. (2012). A systems biology view of responses to lignin biosynthesis perturbations in Arabidopsis. *Plant Cell.* 24, 3506–3529. doi: 10.1105/tpc.112.102574

Vieira Dos Santos, C., Cuiné, S., Rouhier, N., and Rey, P. (2005). The *Arabidopsis* plastidic methionine sulfoxide reductase B proteins. Sequence and activity characteristics, comparison of the expression with plastidic methionine sulfoxide reductase A, and induction by photooxidative stress. *Plant Physiol.* 138 (2), 909–922. doi: 10.1104/pp.105.062430

Volk, S., and Feierabend, J. (1989). Photoinactivation of catalase at low temperature and its relevance to photosynthetic and peroxide metabolism in leaves. *Plant Cell Environ.* 12 (7), 701–712. doi: 10.1111/j.1365-3040.1989.tb01630.x

Wany, A., Gupta, A. K., Kumari, A., Mishra, S., Singh, N., Pandey, S., et al. (2019). Nitrate nutrition influences multiple factors in order to increase energy efficiency under hypoxia in *Arabidopsis*. *Ann. Bot.* 123 (4), 691–705. doi: 10.1093/aob/mcy202

Wei, W., Li, D., Wang, L., Ding, X., Zhang, Y., Gao, Y., et al. (2013). Morpho-anatomical and physiological responses to waterlogging of sesame (*Sesamum indicum* L.). *Plant Sci.* 208, 102–111. doi: 10.1016/j.plantsci.2013.03.014

Wu, J., Wang, J., Hui, W., Zhao, F., Wang, P., Su, C., et al. (2022). Physiology of plant responses to water stress and related genes: A review. *Forests* 13 (2), 324. doi: 10.3390/f13020324

Wurms, K. V., Reglinski, T., Buissink, P., Ah Chee, A., Fehlmann, C., McDonald, S., et al. (2023). Effects of drought and flooding on phytohormones and abscisic acid gene expression in kiwifruit. *Int. J. Mol. Sci.* 24 (8), 7580. doi: 10.3390/ijms24087580

Xu, X., Wang, H., Qi, X., Xu, Q., and Chen, X. (2014). Waterlogging-induced increase in fermentation and related gene expression in the root of cucumber (Cucumis sativus L.). *Sci. Hortic.* 179, 388–395. doi: 10.1016/j.scienta.2014.10.001

Yamauchi, T., Colmer, T. D., Pedersen, O., and Nakazono, M. (2018). Regulation of root traits for internal aeration and tolerance to soil waterlogging-flooding stress. *Plant Physiol.* 176 (2), 1118–1130. doi: 10.1104/pp.17.01157

Yamauchi, T., Shiono, K., Nagano, M., Fukazawa, A., Ando, M., Takamure, I., et al. (2015). Ethylene biosynthesis is promoted by very-long-chain fatty acids during lysigenous aerenchyma formation in rice roots. *Plant Physiol.* 169 (1), 180–193. doi: 10.1104/pp.15.00106

Yang, C.-Y., and Hong, C.-P. (2015). The NADPH oxidase Rboh D is involved in primary hypoxia signalling and modulates expression of hypoxia-inducible genes under hypoxic stress. *Environ. Exp. Bot.* 115, 63–72. doi: 10.1016/j.envexpbot.2015.02.008

Yeung, E., van Veen, H., Vashisht, D., Sobral Paiva, A. L., Hummel, M., Rankenberg, T., et al. (2018). A stress recovery signaling network for enhanced flooding tolerance in *Arabidopsis thaliana*. *Proc. Natl. Acad. Sci.* 115 (26), E6085–E6094. doi: 10.1073/pnas.1803841115

Zeng, R., Chen, T., Wang, X., Cao, J., Li, X., Xu, X., et al. (2021). Physiological and expressional regulation on photosynthesis, starch and sucrose metabolism response to waterlogging stress in peanut. *Front. Plant Sci.* 12, 601771. doi: 10.3389/fpls.2021.601771

Zhang, J. Y., Huang, S. N., Wang, G., Xuan, J. P., and Guo, Z. R. (2016). Overexpression of Actinidia deliciosa pyruvate decarboxylase 1 gene enhances waterlogging stress in transgenic *Arabidopsis thaliana*. *Plant Physiol. Biochem.* 106, 244–252. doi: 10.1016/j.plaphy.2016.05.009

Zhang, P., Lyu, D., Jia, L., He, J., and Qin, S. (2017). Physiological and *de novo* transcriptome analysis of the fermentation mechanism of *Cerasus sachalinensis* roots in response to short-term waterlogging. *BMC Genomics* 18, 649. doi: 10.1186/s12864-017-4055-1

Zhang, Y., Ou, L., Zhao, J., Liu, Z., and Li, X. (2019). Transcriptome analysis of hot pepper plants identifies waterlogging resistance related genes. *Chilean J. Agric. Res.* 79 (2), 296–306. doi: 10.4067/S0718-58392019000200296

Zhang, R., Yue, Z., Chen, X., Zhou, Y., Cao, X., and Huang, R. (2023). Effects of waterlogging at different growth stages on the photosynthetic characteristics and grain yield of sorghum (*Sorghum bicolor* L.). *Scientific Reports*, 13 (1), 7212. doi: 10.1038/s41598-023-32478-8

Zhang, Y., Zeng, D., Liu, Y., and Zhu, W. (2022). *SlSPS*, a sucrose phosphate synthase gene, mediates plant growth and thermotolerance in tomato. *Horticulturae* 8 (6), 491. doi: 10.3390/horticulturae8060491

Zhang, R., Zhou, Y., Yue, Z., Chen, X., Cao, X., Xu, X., et al. (2019). Changes in photosynthesis, chloroplast ultrastructure, and antioxidant metabolism in leaves of sorghum under waterlogging stress. *Photosynthetica* 57, 1076–1083. doi: 10.1016/j.cj.2020.08.005

Zhou, W., Chen, F., Meng, Y., Chandrasekaran, U., Luo, X., Yang, W., et al. (2020). Plant waterlogging/flooding stress responses: From seed germination to maturation. *Plant Physiol. Biochem.* 148, 228–236. doi: 10.1016/j.plaphy.2020.01.020

Zhao, Y., Zhang, W., Abou-Elwafa, S. F., Shabala, S., and Xu, L. (2021). Understanding a mechanistic basis of ABA involvement in plant adaptation to soil flooding: The current standing. *Plants* 10 (10), 1982. doi: 10.3390/plants10101982

frontiers | Frontiers in Plant Science

TYPE Original Research
PUBLISHED 23 August 2023
DOI 10.3389/fpls.2023.1245308

OPEN ACCESS

EDITED BY
Poonam Yadav,
Banaras Hindu University, India

REVIEWED BY
Debojyoti Moulick,
Independent researcher, Kolkata, India
Rajkumar U. Zunjare,
Indian Agricultural Research Institute (ICAR), India

*CORRESPONDENCE
Sivalingam Anandhan
anandhans@gmail.com

†These authors have contributed equally to this work

RECEIVED 23 June 2023
ACCEPTED 07 August 2023
PUBLISHED 23 August 2023

CITATION
Manape TK, Soumia PS, Khade YP, Satheesh V and Anandhan S (2023) A glossy mutant in onion (*Allium cepa* L.) shows decreased expression of wax biosynthesis genes.
Front. Plant Sci. 14:1245308.
doi: 10.3389/fpls.2023.1245308

A glossy mutant in onion (*Allium cepa* L.) shows decreased expression of wax biosynthesis genes

Tushar Kashinath Manape[1†], Parakkattu S. Soumia[1†], Yogesh P. Khade[1], Viswanathan Satheesh[2] and Sivalingam Anandhan[1*]

[1]Crop Improvement Section, Indian Council of Agricultural Research (ICAR)-Directorate of Onion and Garlic Research, Pune, Maharashtra, India, [2]Genome Informatics Facility, Office of Biotechnology, Iowa State University, Ames, IA, United States

Cuticular wax is a characteristic feature of land plants that provides protection against both biotic and abiotic stresses. In this study, a glossy mutant lacking an epicuticular wax layer was identified in the γ-irradiated M_2 mutant population of the onion cultivar Bhima Super. The inheritance of the mutant's glossy phenotype was determined to be recessive and single locus. Scanning electron microscopy analysis showed poor accumulation of wax crystals in the glossy mutant, concentrated near the stomata. The plant height, number of leaves per plant, and stomatal parameters of the mutant were similar to the wild-type. RNA-seq was used to comprehend the expression variations of waxy cuticle-related genes in the glossy mutant and its wild-type waxy cultivars. Differential gene expression analysis of the RNA-seq data revealed that the genes involved in wax biosynthesis, such as *AcCER1, AcCER26, AcMAH1*, and *AcWSD1*, were downregulated by 2.72, 1.74, 2.59 and 2.12-fold, respectively, in the glossy mutant respectively. The expression patterns of these four unigenes were validated using semi-quantitative RT-PCR. The glossy mutant displayed a substantial 3.5-fold reduction in cuticular wax load compared to the wild-type due to the significant downregulation of these wax biosynthesis genes. These findings represent early advancements in understanding the molecular mechanisms of wax biosynthesis in onions. Furthermore, they provide a foundation for utilizing the glossy mutant trait in breeding programmes to enhance stress and pest resilience.

KEYWORDS

cuticular wax, glossy, mutant, wax biosynthesis, RNA-seq

Introduction

Onion is an important vegetable crop and is preferred for its flavor profile. India is the second-largest contributor to onion production in the world, with a substantial output of 26,738,000 metric tons. Moreover, India ranks among the top consumers and exporters of onions on a global scale (FAOSTAT, 2021). The leaves of onions display characteristic white wax deposits on their surfaces.

Cuticular wax is an important adaptation of terrestrial plants, forming a protective outer layer on plant surfaces (Edwards et al., 1996; Yeats and Rose, 2013). This layer helps to maintain the water balance of plants by regulating non-stomatal water loss and provides a barrier against a range of biotic and abiotic stresses, including drought, cold, UV radiation, pests and pathogens. The composition of cuticular wax varies between species, as well as within a species between different organs, developmental stages and tissue types (Yeats and Rose, 2013). In addition, environmental factors such as light, drought, humidity temperature can also influence the distribution of cuticular wax within a species. The distribution and chemical composition of cuticular wax can affect a plant's ability to tolerate biotic and abiotic stress (Yeats and Rose, 2013; Serrano et al., 2014; Singh et al., 2018), making it an important trait for breeders to consider when developing crops with improved stress tolerance. The crystal structure of cuticular wax also varies based on its composition and can impact the survival, feeding and oviposition of insects. The wax composition or wax load on the leaf surface has been shown to be important in determining plant tolerance to thrips in onion. Leaf wax composition analysis shows that Hentriacontanone-16 is a major component of cuticular wax that determines the total wax load in leek and onion leaves (Rhee et al., 1998; Munaiz et al., 2020). The wax related phenotype is mainly determined by the quantitative variation in accumulation of hentriacontanone-16 in visually different phenotypes of onion such as waxy, semi-glossy and glossy (Munaiz et al., 2020). Genetic analysis of naturally occurring mutants exhibiting a glossy phenotype in BianGan Welsh onion (Yang et al., 2017) and in the onion varieties 'Australian Brown' and 'White Persian' (Jones et al., 1944; Munaiz and Havey, 2020) has shown that this trait is controlled by a recessive allele and is determined by different loci.

Cuticular wax is composed of a complex mixture of very long chain of fatty acids (VLCFAs) and their derivatives, such as aldehydes, alkanes, ketones, fatty alcohol and even cyclic compounds (Yeats and Rose, 2013). The fatty acids are synthesized in the chloroplast and exported to the endoplasmic reticulum for elongation (Block and Jouhet, 2015). Further, the cuticular wax are synthesized in epidermal cells and deposited on the surface. The biosynthesis of cuticular wax is a complex process that involves the coordination of several genes. These cuticular wax biosynthesis genes have been identified in several plants, including maize, rapeseed, tomato and model plants such as *Arabidopsis* and rice. *Eceriferum 6 (CER6), Eceriferum 10 (CER10), Glossy 8A (GL8A), Glossy 8B (GL8B), Formate dehydrogenase (FDH), Fatty Acid Elongation1 (FAE1), 3-ketoacyl-CoA synthase1 (KCS1) and Protein-tyrosine phosphatase 2 (PAS2)* genes then elongate these C16 and C18 CoA esters to form VLCFAs precursors mediated through long-chain acyl-CoA synthetase (LACS) enzymes. KCS, KCR, HACD, and CER26, which are endoplasmic reticulum-associated fatty acid elongases, work sequentially to synthesize fully saturated long chains acyl-CoA. These acyl-CoAs then enter either the decarbonylation pathway or the acyl reduction pathway. The decarbonylation pathway involves the conversion of long chain fatty acyl-CoAs into aldehydes, alkanes, secondary alcohols and ketones through the action of *FAR, CER1, CER4*, and *MAH1* genes. The acyl reduction pathway, which includes *FAR, CER4*, and *WSD1* genes, converts fully saturated long chain acyl-CoAs into primary alcohols and wax esters. These waxes are transported to plasma membrane by an unknown mechanism and subsequently into the cell wall by ABC transporters (*CER5* and *ABCG*). Further, transport of wax compounds across the cell wall is facilitated by lipid transfer proteins to the final destination at the cuticle (Li-Beisson et al., 2013).

In this study, we report a glossy mutant in onion developed through γ-irradiation mutagenesis. A comparative transcriptome analysis between the glossy mutant and its wild-type counterpart revealed significant differences in the wax biosynthesis pathway genes between the glossy mutant and the wild-type. These observations highlight the importance of comprehending the molecular mechanisms involved in wax biosynthesis in onions, as it holds great potential for enhancing crop quality and resilience to stress.

Materials and methods

Plant material

The present study was conducted during 2019-2022 at the Indian Council of Agricultural Research - Directorate of Onion and Garlic Research (ICAR-DOGR), situated at the latitude (27°19'00.2 N) and longitude (82°25'00.1E) Pune, Maharashtra, India 553.8 meters above sea level. Onion being a biennial crop, its seed production was done during *rabi* season and the subsequent generations were grown in *kharif* during 2019-2021. The glossy mutant phenotype was observed in the seed-germinated M_2 population of γ-irradiation-treated Indian short-day onion cv. Bhima Super (B. Super) mutant line (IR-300-53). Bulbs of the M_2 generation γ-irradiated onion (glossy type) and its non-mutagenized counterpart [wild-type (WT)/waxy], were planted in a greenhouse under a 16/8-h light/dark photoperiod at 25°C. The phenotypic data, including plant height and number of leaves per plant were recorded at 75 days after transplanting (DAT). The glossy mutants were both selfed and outcrossed with the wild-type. Seeds from the subsequent F_1 and M_3 generations were sown in the greenhouse. The F_1 plants were backcrossed with the glossy mutant and the number of glossy and waxy phenotypes were recorded in the M_3, F_1 and BC_1F_1 generations. All plant studies were carried out in accordance with relevant institutional, national, and international guidelines and legislation.

Scanning electron microscopy

Onion leaves are isobilateral, having equal stomatal density on both sides of the leaf. The third leaf from the center of both the WT waxy and M_3 mutant glossy plants were torn into 3×3 mm^2 pieces using tweezers and mounted on aluminium stubs. The leaf specimens were then sputter-coated with gold and examined for the micro-structure analysis using an Environmental Scanning Electron Microscope (ESEM) (FEI, Quanta 200 and ESEM Mode) at Sophisticated Analytical Instrument Facility (SAIF) of Indian

Institute of technology (Bombay, India). Electron micrographs of leaf surfaces from three replicate plants were taken for each line and used to visually estimate the shape of the epicuticular waxes and cuticular striation. The stomatal count was measured using the IMAGEJ software v. 1.43u. Stomatal index was calculated using the formula, Stomatal index (%) = (S/S+E) × 100; where, S and E are the number of stomata and epidermal cells, respectively; in the microscopic field of view (FOV).

Epicuticular wax coverage

The epicuticular wax content was extracted using the colorimetric method as described by Ebercon et al. (1977). Intact onion leaves were immersed in 15 ml distilled chloroform for 10 s and kept in a boiling water bath until the smell of chloroform was no longer detected. A 5 ml wax reagent ($K_2Cr_2O_7$ prepared in conc. H_2SO_4) was added to each tube and kept at 60°C in a water bath for 30 min. After cooling, 12 ml of deionized water was added to each tube, and the solution was filtered through a filter paper. The absorbance was measured at a wavelength of 590 nm using SPECTROstar Nano microplate reader. The wax content was calculated using standard Polyethylene Glycol-3000 and expressed as mg per cm^2.

RNA sequencing, *de novo* assembly and sequence clustering

Total RNA was isolated from 6-weeks-old leaves of wild-type and M_3 generation glossy mutant plants in 2 biological replicates using TRIzol reagent. The mRNA was then isolated and subjected to quality control (QC) before being used for paired-end (PE) library preparation. The libraries were sequenced on the Illumina NovaSeq 6000 platform using 2×150 bp chemistry at Eurofins India Pvt. Ltd. (Bangalore, India). The generated raw sequence datasets were deposited in the NCBI in the Short Read Archive (SRA) database with Bioproject accession number PRJNA943431. The sequenced raw paired-end reads of all samples were processed to obtain clean and high-quality concordant reads using Trimmomatic v0.38 (Bolger et al., 2014) to remove adapters, ambiguous reads (reads with unknown nucleotides "N" larger than 5%), and low-quality sequences (reads with more than 10% quality threshold (QV) < 20 phred score. The resulting high-quality (QV>20) paired-end reads were used for *de novo* assembly using Trinity v2.8.4 (Henschel et al., 2012) with a kmer of 25, and the mapped high quality reads of all samples were pooled together for assembly into transcripts.

CDS prediction, functional annotation and gene ontology analysis

The assembled transcripts were then further clustered together using CD-HIT-EST-4.6 to get unigenes. Only those unigenes which were found to have >90% coverage at 3X read depth were considered for downstream analysis. To identify sample-wise CDS from the pooled set of CDS, reads from each of the samples were mapped onto the final set of pooled CDS sequences using Bowtie mapper v2.4.4 (Langmead and Salzberg, 2012). TransDecoder v5.3.0 was used to predict coding sequences from the unigenes. Functional annotation of the CDS was performed using the DIAMOND program (Buchfink et al., 2015) with BLASTX alignment mode to find the homologous sequences for the genes against non-redundant protein database (NR) from NCBI. Gene ontology (GO) analyses of identified CDS of each sample were carried out using Blast2GO program (Conesa et al., 2005). GO assignments were used to classify the functions of the predicted CDS. GO mapping was used to group identified genes into three main domains: Biological Process (BP), Molecular Function (MF) and Cellular Component (CC). To identify the potential involvement of the predicted CDS in biological pathways, all the identified CDS for each of the samples were mapped to reference canonical pathways in KEGG (Eudicots database) using KEGG automated annotation server, KAAS (Moriya et al., 2007).

Differentially expressed gene analysis

The unigenes were used as the transcriptome reference for quantifying transcript abundance using Salmon version 1.8.0. A reference transcriptome index was created using the salmon "index" command. Transcript quantification was performed using the salmon "quant" command. The read counts generated was used for differential expression analysis with DESeq2 version 1.36.0 (Love et al., 2014). Genes that with absolute log fold change > 1 and adjusted p-value < 0.05 were determined to be differentially expressed geneS (Love et al., 2014; Patro et al., 2017).

Semi-quantitative RT-PCR analysis

Total RNA was isolated from 100 mg shoot tissues of M_3 glossy mutant and wild-type B. Super plants (with 2 biological replicates of each) using RNeasy® Plant Mini kit (Qiagen). The RNA was quantified using Nanodrop (UV/Vis Nano spectrophotometer, Nabi, Metler Toledo). Total RNA (1 µg) was treated with DNase I, RNase free kit (Thermo Scientific) to remove any remaining DNA. First-strand cDNA synthesis was prepared using SuperScript™ IV Reverse Transcriptase kit (Invitrogen) as per manufacturer's instructions and quantified using Nanodrop. First-strand cDNA (30 ng) was used for semi-quantitative RT-PCR analysis to validate the differentially expressed genes involved in the wax-biosynthesis pathway. Gene-specific primer sets were used, and the PCR reactions were performed according to the conditions described in Table S1. PCR products were run on 3% agarose gel and the image was captured with a digital camera under a UV light (Vilber Lourmat, ECX20.W). The band area was calculated using

the ImageJ analyser tool and the band area of the wild-type was compared with the glossy mutant in terms of $\log_2$ fold change.

Statistical analysis

To evaluate the variation in physical parameters between the glossy mutant and wild-type (WT) plants, a one-way analysis of variance (ANOVA) was employed using Statistical Analysis Software, Version 9.2 (Sas Institute, 2009). Mean comparisons were performed using the least significant difference (LSD) approach at a significance level of P=0.05. Chi-square analysis was performed in the segregating populations to understand the segregation pattern of the glossy mutant.

Results

Identification, phenotypic variance and segregation of glossy mutants

Four glossy green mutant phenotypes were observed in the M_2 population of γ-irradiation-treated onion mutant line (B. Super-IR-300-53) (Figure S1). Bulbs from the M_2 glossy mutant phenotype were harvested and planted separately under greenhouse conditions. The average plant height was 49.5 ± 2.2 cm and 57.5 ± 4.8 cm, and the number of leaves per plant was 6.5 ± 0.6 and 6.75 + 0.9 in M_2 glossy mutant and WT; respectively. No significant differences were found between the glossy mutant and wild-type plants, with respect to plant height and number of leaves per plant. M_2 plants were selfed and the subsequent M_3 generation was found to be glossy. F_1 plants derived from the cross between M_2 and WT exhibited the waxy phenotype. However, when F_1 plants were backcrossed with M_3 glossy mutant, the subsequent BC_1F_1 population segregated in a 1:1 ratio (waxy: glossy).

Leaf surface microstructure and morphology

The bright green leaf of glossy mutant was in stark contrast to the glaucous leaf of WT in the experimental field. The color variation of the onion foliage is directly correlated with the amount and type of epicuticular wax deposits. SEM micrographs (Figure 1A) revealed large quantities of spiky, needle-like microscopic wax crystals uniformly covering the leaf surface of waxy WT onion, while in the glossy type, relatively few wax crystals were scattered around the stomatal region alone (Figure 1B). The bright green leaf of glossy mutant (Figure 1D) was distinguishable

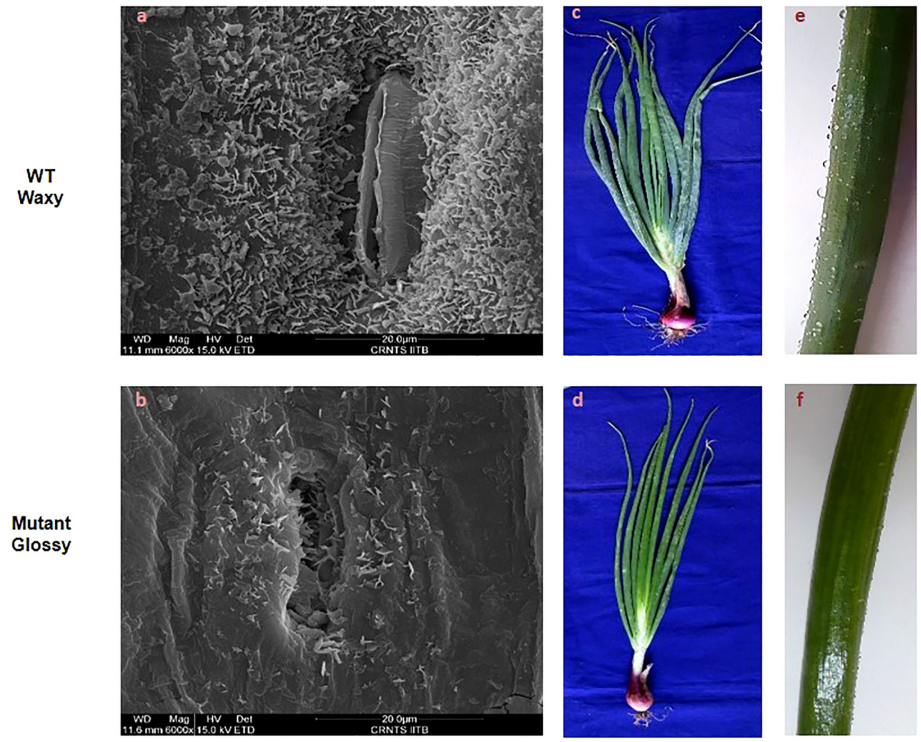

FIGURE 1
Leaf surface microstructure and morphology of WT and glossy mutant. Comparative scanning electron micrographs of leaf surface at magnification of 6000x of **(A)** WT waxy, **(B)** mutant glossy. Large quantities of spiky, needle-like crystals microscopic wax crystals were uniformly covered on the leaf surface of waxy WT onion, whereas in glossy type, relatively few wax crystals were scattered around the stomatal region alone. **(C)** Greenish gray (glaucous) phenotype of WT waxy, **(D)** Shiny glossy green phenotype of mutant glossy. **(E)** WT waxy onion leaf surface showing water droplets due to its hydrophobic nature, **(F)** water droplets were easily adhered and coalesced on to the leaf surface of mutant glossy.

from the waxy leaf of the wild-type onion (Figure 1C). The foliage of the mutant onion appears shiny green, and water droplets easily form and adhere to leaf surfaces after the leaves are sprayed with water (Figure 1F). In contrast, the leaves of wild-type are greenish-grey, due to higher wax deposits (Figure 1E). The glossy leaves of mutant onion showed a wet phenotype (hydrophilic) as water droplets easily adhered onto the surface and coalesced. However, wild-type onion was more hydrophobic as water droplets formed beads due to a dense layer of epicuticular wax. The number of stomata and stomatal index were measured in the glossy mutant and wild-type onions. The results revealed a significant difference between the two genotypes: the mutant had 247 stomata with a stomatal index of 49, while the wild-type had 225 stomata with a stomatal index of 45 (Figure 2).

RNA-seq assembly and analysis

RNA sequencing of 6-week-old leaves of wild-type onion (C1 and C2) and its glossy mutant (G1 and G2) was performed in duplicate using the Illumina platform (NovaSeq6000) with 2 × 150 bp chemistry. After stringent quality assessment and data filtering, a total of 104.33 million paired-end were generated, corresponding to 30.26 Gb of sequence data. Details of high-quality reads, transcripts generated, unigenes identified, predicted CDSs, functional annotation and classification of predicted CDSs, identification of differentially expressed genes (DEGs) and pathway enrichment analysis are summarized in Supplement S1. Before identification of DEGs, the annotated CDs from two biological replicates of each glossy M_3 mutant and wild-type were pooled together independently and expression of unigenes were normalized. A total of 596 annotated unigenes were found to be differentially expressed between wild-type and glossy mutant, with 295 upregulated and 301 downregulated genes in the mutant (Supplementary Sheet S2).

Profiling cuticular wax biosynthesis pathway genes

Out of 301 downregulated unigenes, 4 critical genes related to wax biosynthesis pathway *i.e. AcMAH1, AcWSD1, AcCER1* and *AcCER26* were significantly downregulated in the glossy mutant (Figure 3A). There was 1.74, 2.72, 2.12 and 2.59-fold decrease in the transcripts level of *ECR26, ECR1, WSD1* and *MAH1* genes, respectively (Table 1). To validate the RNA-seq results, expression levels of these genes were evaluated by semi-quantitative PCR, which also showed down-regulation of these genes in the glossy mutant (Figure 3B; Figure S2). Semi-quantitative PCR analysis had shown 1.17, 2.19, 1.61 and 1.95-fold down-regulation of *ECR26, ECR1, WSD1* and *MAH1* genes, respectively. The results of the semi-quantitative PCR were consistent with those of the RNA-seq analysis (Table 1).

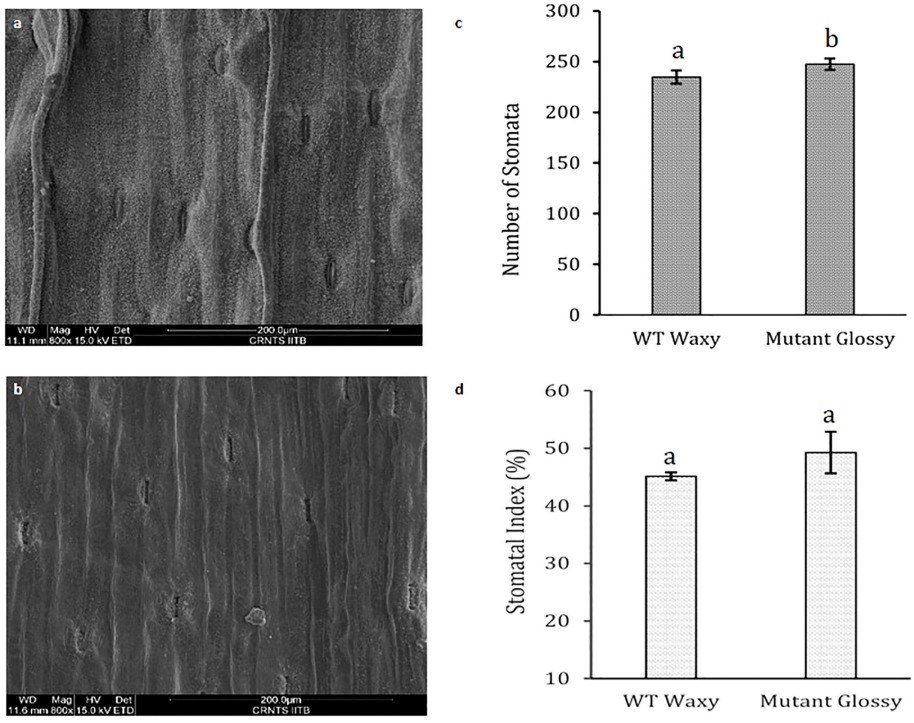

FIGURE 2
Leaf stomatal parameters in WT and glossy mutant. Comparative scanning electron micrographs of leaf surface at magnification of 800x of **(A)** WT waxy, **(B)** mutant glossy, **(C)** Number of stomata in 200 µm length in WT waxy and mutant glossy lines. **(D)** Stomatal index of WT waxy and mutant glossy lines. Stomatal index was calculated in percentage using formula, SI= (S/S+E) x 100 where, S and E are the number of stomata and epidermal cells respectively in 200 µm length microscopic view field. The bars indicate mean ± SE of 3 replicates. The lowercase letters "a and b" indicates the significant difference.

10.3389/fpls.2023.1245308

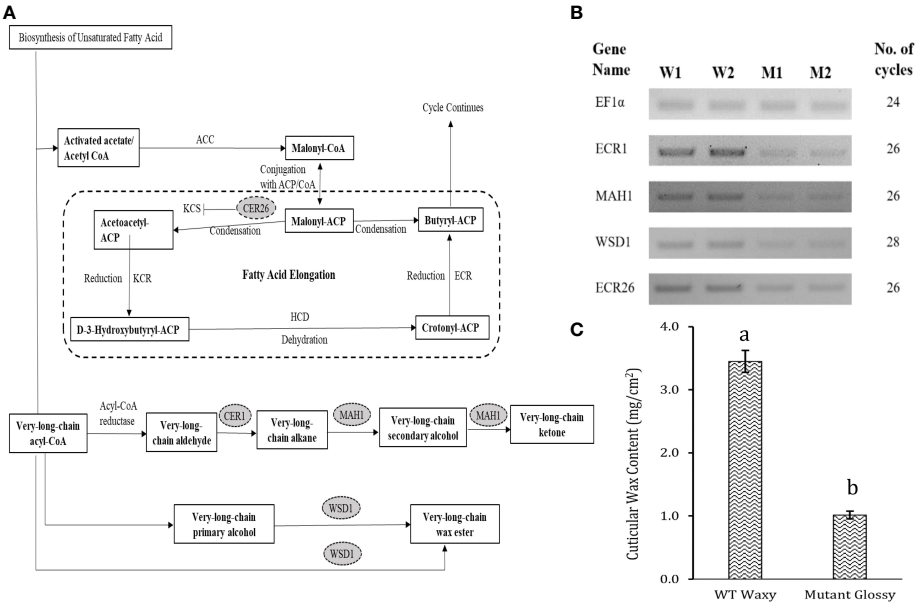

FIGURE 3
Downregulation of cuticular wax biosynthetic genes in the onion glossy mutant. **(A)** Basic cuticular wax biosynthetic pathway. **(B)** Oval highlighted genes were downregulated genes in glossy mutant onion lines by RNA-seq analysis. Question marks and dotted lines indicate unidentified enzymes and processes, respectively, **(B)** Validation of 4 downregulated genes of cuticular wax biosynthesis pathway by semi-quantitative RT-PCR. W1 and W2 indicates 2 biological replicates of WT waxy, whereas M1 and M2 indicates 2 biological replicates of mutant glossy. Total RNA was extracted from 6-week-old shoot tissues and the transcript levels were examined using semiquantitative RT-PCR. **(C)** Epicuticular wax content in WT waxy and mutant glossy lines. The bars indicate mean ± SE of 3 replicates. The lowercase letters "a and b" indicates the significant difference.

Discussion

Segregation pattern of glossy mutant

The F_1 plants derived from the cross between M_2 and WT exhibited a waxy phenotype, revealing no segregation and thereby indicating the possibility of a recessive mutation. When F_1 lines were back-crossed with M_3 glossy mutant lines, BC_1F_1 lines showed an equal mixture of waxy and glossy mutants (Table 2), which confirmed the single-locus recessive gene inheritance of the glossy mutant phenotype. In consistent with our results, several studies had also shown that glossy mutant trait is controlled by single recessive gene/locus in maize (Bianchi et al., 1979), cabbage (Zeng et al., 2017; Liu et al., 2018), Welsh onion (Yang et al., 2017), Barely (Luan et al., 2017) and onion (Munaiz and Havey, 2020).

Epicultricular wax coverage and morphology of glossy mutant

The glossy mutant onion from the present study exhibited a distinct bright green phenotype compared to the WT waxy onion. The type and quantity of epicuticular wax deposits influences leaf color and leaf wettability. Damon and Havey, 2014, had visually classified onions as "glossy" or "semi-glossy," on the basis of low to intermediate amounts of epicuticular waxes. Glossy mutant plants

TABLE 1 Differentially expressed unigenes associated with cuticular wax biosynthesis.

Sl. No.	Unigene ID	SwissProt annotation	COG class annotation	Log_2 fold change			
				Semi-qRT PCR		RNA-seq	
				Waxy WT	Glossy mutant	Waxy WT	Glossy mutant
1	g304621	Protein ECERIFERUM 26	Lipid transport and metabolism	1	-1.17	1	-1.74
2	g367838	Protein ECERIFERUM 1	Lipid transport and metabolism	1	-2.19	1	-2.72
3	g50966	O-acyltransferase WSD1	Lipid transport and metabolism	1	-1.61	1	-2.12
4	g259833	alkane hydroxylase MAH1	Lipid transport and metabolism	1	-1.95	1	-2.59

TABLE 2 Segregation pattern of glossy mutant lines in different populations.

Population	Total no. of plants	Phenotype	
		Waxy WT	Glossy mutant
M2	4	0	4
M3	15	0	15
F1	17	17	0
BC_1F_1	21	11	10*
WT	34	34	0

*Chi square analysis was performed in BC_1F_1 population. Calculated p value is 0.83. The difference was statistically non-significant.

showed significantly fewer wax crystals, mainly concentrated around the stomatal region, giving it a greenish-grey color in contrast to WT. The shape of these wax crystals may vary based on self-assembly as sheet, filiform, tubular, and granular. According to descriptions of epicuticular wax crystals by Jeffree (1986), the spiky crystals on onion foliage are likely formed by a ketone. Studies by Gülz et al. (1992) and Gülz et al. (1993) concluded that characteristic lipid crystals can be observed on leaves if one lipid class comprises at least 40% of the total profile. Therefore, the spiky, needle-like microscopic wax crystals that predominate onion foliage can possibly be ketone(s). The leaves of the glossy mutant exhibit a hydrophilic property, facilitating the easy adhesion and coalescence of water droplets on their surface. In contrast, the wild-type onion has a dense layer of epicuticular wax, rendering it more hydrophobic and causing water droplets to form beads on its surface. These findings are consistent with previous studies conducted on rice and Welsh onion, highlighting the role of epicuticular wax in influencing leaf color, hydrophobicity, and water droplet behavior (Qin et al., 2011; Yang et al., 2017). Our results are in accordance with Yang et al. (2017), where the glossy mutant and wild-type of Welsh onion showed no significant differences in stomatal density.

Cuticular wax biosynthesis genes

The cuticular wax biosynthesis and secretion pathway affects its content and composition. Studies on plant epicuticular wax biosynthesis have revealed ketones, including hentriacontanone-16, derived from the decarbonylation pathway involving aldehydes and alkanes as intermediates (Kunst and Samuels, 2003). Previous studies have provided a strong evidence that hentriacontanone-16 is the predominant epicuticular wax on onion (Damon et al., 2014) and leek (Rhee et al., 1998) foliage. The proteins MAH1 and CER1 are involved in the decarbonylation pathway, where CER1 converts long chain aldehydes to alkanes and MAH1 converts alkanes into secondary alcohols and ketones (Aarts et al., 1995; Greer et al., 2007). According to Jeffree (1986), the spikey wax crystals deposited on onion foliage is likely to be ketone which is in accordance with our results.

Mutations in the *cer1* gene result in glossy green stems with decreased wax deposition in *Arabidopsis*, while mutations in the *mah1* gene lead to glaucous inflorescence stems without affecting epicuticular wax crystals (Aarts et al., 1995; Greer et al., 2007). WSD1 participates in the acyl reduction pathway, and involved in synthesis of wax esters, a component of wax. *Arabidopsis wsd1* mutant had significantly reduced wax ester levels in the stem wax (Li et al., 2008). Leaf surface wax biosynthesis was broadly affected in glossy mutant of *B. napus* due to suppression of *CER1* and other wax-related genes (*MAH1, WSD1, CAC3, FATB, ABCG28, etc.*). Previous research has shown that upregulation of *CER1*, *WSD1* and *MAH1* genes triggered biosynthesis and deposition of cuticular wax on the leaves of EMS-mutagenized *Dianthus spiculifolius* plants in the M_2 generation (Zhou et al., 2018). CER26 is involved in the elongation of the very long chain fatty acids of 30 carbons or more, and its mutation substantially decreased the amount of these very long chain fatty acids (Pascal et al., 2013). The mutation, however, did not affect the wax load on leaf or stem. In our study, we observed a significant difference in leaf cuticular wax content between the WT waxy and M_3 glossy mutant lines. The wax load in the WT waxy was 3.5 ± 0.17 mg cm^{-2}, whereas it was 1.0 ± 0.06 mg cm^{-2} in the glossy mutant lines (Figure 3C). Significant suppression of the four 4 critical wax biosynthesis genes (*AcCER1*, *AcMAH1*, *AcWSD1* and *AcCER26*) in our glossy mutant may have disrupted or slowed down the acyl reduction and decarbonylation pathways of wax biosynthesis, resulting in 3.5 times lower cuticular wax load in the glossy mutant than the WT waxy.

Our research findings indicated that within the wax biosynthesis pathway, *CER1* displayed the highest significant downregulation among the four downregulated genes. These results are consistent with the earlier study by Pu et al. (2013), which showed notable downregulation of *CER1* (4.13-fold) and mild downregulation of other wax biosynthesis-related genes, including *MAH1, WSD1, CAC3, FATB, ABCG28*, and *FAR* (ranging from 1.38 to 1.80-fold), in the glossy mutant of *Brassica napus*. Another study conducted by Liu et al. (2014) also revealed downregulation of four wax biosynthesis pathway genes, namely *LACS2, ECR3 (WAX2 isoform 1), ECR3 (Fatty acid hydroxylase* superfamily*), and ABCG12* (1.3 to 1.55-fold), with *LACS2* exhibiting the most substantial downregulation (5-fold) in glossy mutant of Welsh onion. The variation in downregulated genes and their expression levels in glossy mutants might be influenced by the specific genotype and the regulatory gene that was prabably mutated. The glossy mutant has potential applications in breeding. For instance, the male sterile parent could act as a reliable indicator for eliminating rogue plants in hybrid seed production, as well as in genetic studies focused on wax biosynthesis and export. Compared to the waxy-type, the glossy phenotype of onion has been associated with significantly less epicuticular wax and has been found resistant to thrips infestation (Damon et al., 2014). The quantity of epicuticular wax deposition is directly to insect resistance in various crops such as *Sorghum bicolor* (Starks and Weibel, 1981), *Triticum aestivum* (Lowe et al., 1985), *Brassica oleracea* var. *capitata* (Voorrips et al., 2008) and *Allium cepa* (Damon et al., 2014). Additionally, novel genes associated with cuticular wax biosynthesis potentially serve as valuable genetic resources for enhancing drought resistance in crops (Xue et al., 2017). Considering these factors, we anticipate that our glossy mutant phenotype could offer a potential advantage in onion breeding, contributing to the development of lines with increased resistance to biotic and abiotic stressors.

Conclusion

The wax layer on the epidermal surface provides protection to terrestrial plants from UV radiation, water loss and gas exchange, and biotic stresses. In this study, we isolated a glossy mutant from the M_2 population of γ-irradiated onion mutant lines in variety B. Super. The glossy trait is controlled by a recessive locus. The mutant accumulates wax poorly on the leaf surface, and we show that there is a concomitant downregulation of four structural genes in the wax biosynthesis pathway, namely *AcCER1*, *AcCER26*, *AcWSD1*, and *AcMAH1*, which potentially explains the reduction in wax accumulation. Single gene inheritance indicates that the mutation could be within a regulatory gene that controls these structural genes. Therefore, it would be worthwhile to map this regulatory locus using markers identified around this locus. Additionally, the glossy mutant can be a valuable addition to studies on both abiotic and biotic stress in plant breeding. We will conduct further investigation to determine the influence of cuticle thickness and the epicuticular waxes in conferring resistance to onion plants against various environmental stressors and pests.

Data availability statement

All data are included in the article. RNA-seq raw data is available at the NCBI database (https://www.ncbi.nlm.nih.gov/bioproject/PRJNA943431).

Author contributions

TM and SA conceived and designed the experiments. TM, SS, and YK conducted all the experiments. TM and SS drafted the manuscript. SA and VS carried out the data analysis and manuscript editing. SA supervised the entire work.

Funding

This research work was supported by a grant from Indian Council of Agricultural Research- ICAR National Fellow project (Project code: HORTDOGRSOL201700800088).

Acknowledgments

Authors are highly thankful to Dr. Major Singh, Former Director, ICAR-DOGR, Pune for his suggestions during the entire work.

Conflict of interest

The authors declare that the research was conducted in the absence of any commercial or financial relationships that could be construed as a potential conflict of interest.

Publisher's note

Supplementary material

The Supplementary Material for this article can be found online at: https://www.frontiersin.org/articles/10.3389/fpls.2023.1245308/full#supplementary-material

References

Aarts, M. G., Keijzer, C. J., Stiekema, W. J., and Pereira, A. (1995). Molecular characterization of the *CER1* gene of arabidopsis involved in epicuticular wax biosynthesis and pollen fertility. *Plant Cell* 7 (12), 2115–2127. doi: 10.1105/tpc.7.12.2115

Bianchi, G., Avato, P., and Salamini, F. (1979). Glossy mutants of maize. *Hered.* 42 (3), 391–395. doi: 10.1038/hdy.1979.42

Block, M. A., and Jouhet, J. (2015). Lipid trafficking at endoplasmic reticulum–chloroplast membrane contact sites. *Curr. Opin. Cell Biol.* 35, 21–29. doi: 10.1016/j.ceb.2015.03.004

Bolger, A. M., Lohse, M., and Usadel, B. (2014). Trimmomatic: a flexible trimmer for Illumina sequence data. *Bioinformatics* 30 (15), 2114–2120. doi: 10.1093/bioinformatics/btu170

Buchfink, B., Xie, C., and Huson, D. H. (2015). Fast and sensitive protein alignment using Diamond. *Nat. Methods* 12 (1), 59–60. doi: 10.1038/nmeth.3176

Conesa, A., Götz, S., García-Gómez, J. M., Terol, J., Talón, M., and Robles, M. (2005). Blast2GO: a universal tool for annotation, visualization and analysis in functional genomics research. *Bioinformatics* 21 (18), 3674–3676. doi: 10.1093/bioinformatics/bti610

Damon, S. J., Groves, R. L., and Havey, M. J. (2014). Variation for epicuticular waxes on onion foliage and impacts on numbers of onion thrips. *J. Am. Soc. Hortic. Sci.* 139 (4), 495–501. doi: 10.21273/JASHS.139.4.495

Damon, S. J., and Havey, M. J. (2014). Quantitative trait loci controlling amounts and types of epicuticular waxes in onion. *J. Am. Soc. Hortic. Sci.* 139 (5), 597–602. doi: 10.21273/JASHS.139.5.597

Ebercon, A., Blum, A., and Jordan, W. R. (1977). A rapid colorimetric method for epicuticular wax contest of sorghum leaves 1. *Crop Sci.* 17 (1), 179–180. doi: 10.2135/cropsci1977.0011183X001700010047x

Edwards, D., Abbott, G. D., and Raven, J. A. (1996). "Cuticles of early land plants: a palaeoecophysiological evaluation," in *Plant Cuticles: An Integrated Functional Approach. Environmental Plant Biology*. Ed. G. Kerstiens (Oxford: BIOS Scientific Publishers), 1–31.

FAOSTAT (2021) *Food and Agriculture Organization of the United Nations* (Rome: FAO). Available at: https://www.fao.org/faostat/en/#data/QCL (Accessed 12-07-2023).

Greer, S., Wen, M., Bird, D., Wu, X., Samuels, L., Kunst, L., et al. (2007). The cytochrome P450 enzyme CYP96A15 is the midchain alkane hydroxylase responsible for formation of secondary alcohols and ketones in stem cuticular wax of *Arabidopsis*. *Plant Physiol.* 145 (3), 653–667. doi: 10.1104/pp.107.107300

Gülz, P. G., Müller, E., Herrmann, T., and Lösel, P. (1993). Epicuticular leaf waxes of the hop (*Humulus lupulus*). chemical composition and surface structures. *Z. fur Naturforsch. - Sect. C J. Biosci.* 48 (9-10), 689–696. doi: 10.1515/znc-1993-9-1002

Gülz, P. G., Müller, E., Schmitz, K., Marner, F. J., and Güth, S. (1992). Chemical composition and surface structures of epicuticular leaf waxes of *Ginkgo biloba*,

Magnolia grandiflora and *Liriodendron tulipifera*. *Z. fur Naturforsch. - Sect. C J. Biosci.* 47 (7-8), 516–526. doi: 10.1515/znc-1992-7-805

Henschel, R., Nista, P. M., Lieber, M., Haas, B. J., Wu, L. S., and LeDuc, R. D. (2012). "Trinity RNA-Seq assembler performance optimization," in *XSEDE'12 Proceedings of the 1st Conference of the Extreme Science and Engineering Discovery Environment: Bridging from the eXtreme to the campus and beyond*. New York, United States: Association for Computing Machinery. doi: 10.1145/2335755.2335842

Jeffree, C. E. (1986). The cuticle, epicuticular waxes and trichomes of plants, with reference to their structure, functions and evolution. in Insects and the plant surface. Eds. B. E. Juniper and T. R. E. Southwood. (LondonA: Edward Arnold Publishers Ltd.), 23–64.

Jones, H. A., Clarke, A. E., and Stevenson, F. J. (1944). Studies in the genetics of the onion (*Allium cepa* L.). *Proc. Am. Soc Hortic. Sci.* 44, 479–484.

Kunst, L., and Samuels, A. L. (2003). Biosynthesis and secretion of plant cuticular wax. *Prog. Lipid Res.* 42(1), 51–80. doi: 10.1016/S0163-7827(02)00045-0

Langmead, B., and Salzberg, S. L. (2012). Fast gapped-read alignment with Bowtie 2. *Nat. Methods* 9 (4), 357–359. doi: 10.1038/nmeth.1923

Li, F., Wu, X., Lam, P., Bird, D., Zheng, H., Samuels, L., et al. (2008). Identification of the wax ester synthase/acyl-coenzyme A: diacylglycerol acyltransferase WSD1 required for stem wax ester biosynthesis in *Arabidopsis*. *Plant Physiol.* 148 (1), 97–107. doi: 10.1104/pp.108.123471

Li-Beisson, Y., Shorrosh, B., Beisson, F., Andersson, M. X., Arondel, V., Bates, P. D., et al. (2013). Acyl-lipid metabolism. *Arabidopsis book/American Soc. Plant Biologists* 11, 1–70. doi: 10.1199/tab.0161

Liu, D., Dong, X., Liu, Z., Tang, J., Zhuang, M., Zhang, Y., et al. (2018). Fine mapping and candidate gene identification for wax biosynthesis locus, *BoWax1* in *Brassica oleracea* L. var. capitata. *Front. Plant Sci.* 9. doi: 10.3389/fpls.2018.00309

Liu, Q., Wen, C., Zhao, H., Zhang, L., Wang, J., and Wang, Y. (2014). RNA-Seq reveals leaf cuticular wax-related genes in Welsh onion. *PloS One* 9 (11), e113290. doi: 10.1371/journal.pone.0113290

Love, M. I., Huber, W., and Anders, S. (2014). Moderated estimation of fold change and dispersion for RNA-seq data with DESeq2. *Genome Biol.* 15 (12), 1–21. doi: 10.1186/s13059-014-0550-8

Lowe, H. J. B., Murphy, G. J. P., and Parker, M. L. (1985). Non-glaucousness, a probable aphid-resistance character of wheat. *Ann. Appl. Biol.* 106 (3), 555–560. doi: 10.1111/j.1744-7348.1985.tb03146.x

Luan, H., Shen, H., Zhang, Y., Zang, H., Qiao, H., Tao, H., et al. (2017). Comparative transcriptome analysis of barley (*Hordeum vulgare* L.) glossy mutant using RNA-Seq. *Braz. J. Bot.* 40 (1), 247–256. doi: 10.1007/s40415-016-0328-1

Moriya, Y., Itoh, M., Okuda, S., Yoshizawa, A. C., and Kanehisa, M. (2007). KAAS: an automatic genome annotation and pathway reconstruction server. *Nucleic Acids Res.* 35, W182–W185. doi: 10.1093/nar/gkm321

Munaiz, E. D., Groves, R. L., and Havey, M. J. (2020). Amounts and types of epicuticular leaf waxes among onion accessions selected for reduced damage by onion thrips. *J. Am. Soc Hortic. Sci.* 145 (1), 30–35. doi: 10.21273/JASHS04773-19

Munaiz, E. D., and Havey, M. J. (2020). Genetic analyses of epicuticular waxes associated with the glossy foliage of 'White Persian'onion. *J. Am. Soc. Hortic. Sci.* 145 (1), 67–72. doi: 10.21273/JASHS04840-19

Pascal, S., Bernard, A., Sorel, M., Pervent, M., Vile, D., Haslam, R. P., et al. (2013). The *Arabidopsis cer26* mutant, like the *cer2* mutant, is specifically affected in the very long chain fatty acid elongation process. *Plant J.* 73 (5), 733–746. doi: 10.1111/tpj.12060

Patro, R., Duggal, G., Love, M. I., Irizarry, R. A., and Kingsford, C. (2017). Salmon provides fast and bias-aware quantification of transcript expression. *Nat. Methods* 14 (4), 417–419. doi: 10.1038/nmeth.4197

Pu, Y., Gao, J., Guo, Y., Liu, T., Zhu, L., Xu, P., et al. (2013). A novel dominant glossy mutation causes suppression of wax biosynthesis pathway and deficiency of cuticular wax in *Brassica napus*. *BMC Plant Biol.* 13 (1), 1–14. doi: 10.1186/1471-2229-13-215

Qin, B. X., Tang, D., Huang, J., Li, M., Wu, X. R., Lu, L. L., et al. (2011). Rice *OsGL1-1* is involved in leaf cuticular wax and cuticle membrane. *Mol. Plant* 4 (6), 985–995. doi: 10.1093/mp/ssr028

Rhee, Y., Hlousek-Radojcic, A., Ponsamuel, J., Liu, D., and Post-Beittenmiller, D. (1998). Epicuticular wax accumulation and fatty acid elongation activities are induced during leaf development of leeks. *Plant Physiol.* 116 (3), 901–911. doi: 10.1104/pp.116.3.901

Sas Institute (2009). *SAS Scoring Accelerator 1.5 for Teradata: User's Guide* (Cary, NC, USA: SAS institute).

Serrano, M., Coluccia, F., Torres, M., L'Haridon, F., and Métraux, J. P. (2014). The cuticle and plant defense to pathogens. *Front. Plant Sci.* 5. doi: 10.3389/fpls.2014.00274

Singh, S., Das, S., and Geeta, R. (2018). "Role of cuticular wax in adaptation to abiotic stress: a molecular perspective," in *Abiotic Stress-Mediated Sensing and Signaling in Plants: An Omics Perspective*. Eds. S. Zargar and M. Zargar (Singapore: Springer), 155–182. doi: 10.1007/978-981-10-7479-0_5

Starks, K. J., and Weibel, D. E. (1981). Resistance in bloomless and sparse-bloom sorghum to greenbugs. *Environ. Entomol.* 10 (6), 963–965. doi: 10.1093/ee/10.6.963

Voorrips, R. E., Steenhuis-Broers, G., Tiemens-Hulscher, M., and Van Bueren, E. T. L. (2008). Plant traits associated with resistance to *Thrips tabaci* in cabbage (*Brassica oleracea* var capitata). *Euphytica* 163, 409–415. doi: 10.1007/s10681-008-9704-7

Xue, D., Zhang, X., Lu, X., Chen, G., and Chen, Z. H. (2017). Molecular and evolutionary mechanisms of cuticular wax for plant drought tolerance. *Front. Plant Sci.* 8. doi: 10.3389/fpls.2017.00621

Yang, L., Liu, Q., Wang, Y., and Liu, L. (2017). Identification and characterization of a glossy mutant in Welsh onion (*Allium fistulosum* L.). *Sci. Hortic.* 225, 122–127. doi: 10.1016/j.scienta.2017.05.014

Yeats, T. H., and Rose, J. K. (2013). The formation and function of plant cuticles. *Plant Physiol.* 163 (1), 5–20. doi: 10.1104/pp.113.222737

Zeng, A., Li, J., Wang, J., Song, L., Shi, L., and Yan, J. (2017). Studies of genetic characteristics of two heart-shaped glossy cabbage mutants. *Sci. Hortic.* 226, 91–96. doi: 10.1016/j.scienta.2017.08.033

Zhou, A., Liu, E., Liu, J., Feng, S., Gong, S., and Wang, J. (2018). Characterization of increased cuticular wax mutant and analysis of genes involved in wax biosynthesis in *Dianthus spiculifolius*. *Hortic. Res.* 5 (40), 1–9. doi: 10.1038/s41438-018-0044-z

frontiers | Frontiers in Plant Science

TYPE Original Research
PUBLISHED 01 September 2023
DOI 10.3389/fpls.2023.1211162

OPEN ACCESS

EDITED BY
Poonam Yadav,
Banaras Hindu University, India

REVIEWED BY
Ágnes Szepesi,
University of Szeged, Hungary
Abid Khan,
University of Haripur, Pakistan
Arnab Majumdar,
Jadavpur University, India
Qijie Guan,
University of Mississippi, United States

*CORRESPONDENCE
Shengzuo Fang
fangsz@njfu.edu.cn

RECEIVED 24 April 2023
ACCEPTED 04 August 2023
PUBLISHED 01 September 2023

CITATION
Zhang L, Liu Y, Zhang Z and Fang S (2023) Physiological response and molecular regulatory mechanism reveal a positive role of nitric oxide and hydrogen sulfide applications in salt tolerance of *Cyclocarya paliurus*.
Front. Plant Sci. 14:1211162.
doi: 10.3389/fpls.2023.1211162

Physiological response and molecular regulatory mechanism reveal a positive role of nitric oxide and hydrogen sulfide applications in salt tolerance of *Cyclocarya paliurus*

Lei Zhang[1], Yang Liu[1], Zijie Zhang[1] and Shengzuo Fang[1,2]*

[1]College of Forestry, Nanjing Forestry University, Nanjing, China, [2]Co-Innovation Centre for Sustainable Forestry in Southern China, Nanjing Forestry University, Nanjing, China

As a multifunctional tree species, *Cyclocarya paliurus* leaves are rich in bioactive substances with precious healthy values. To meet the huge requirement of *C. paliurus* leaf production, sites with some environmental stresses would be potential land for developing its plantations due to the limitation of land resources in China. Nitric oxide (NO) and hydrogen sulfide (H_2S) are common gas messengers used to alleviate abiotic stress damage, whereas the mechanism of these messengers in regulating salt resistance of *C. paliurus* still remains unclear. We performed a comprehensive study to reveal the physiological response and molecular regulatory mechanism of *C. paliurus* seedlings to the application of exogenous NO and H_2S under salt stress. The results showed that the application of sodium hydrosulfide (NaHS) and sodium nitroprusside (SNP) not only maintained the photosynthetic capacity and reduced the loss of leaf biomass, but also promoted endogenous NO synthesis and reduced oxidative damage by activating antioxidant enzyme activity and increasing the content of soluble protein and flavonoids. Moreover, transcriptome and metabolome analysis indicated the expression of genes encoding phenylalanine ammonia lyase (PAL), cytochromeP450 (CYP), chalcone synthase (CHS), dihydroflavonol 4-reductase (DFR) and flavonol synthase (FLS) in flavonoid biosynthesis pathway was all up-regulated by the application of NO and H_2S. Meanwhile, 15 transcriptional factors (TFs) such as WRKY, ERF, bHLH and HY5 induced by NO were found to regulated the activities of several key enzymes in flavonoid biosynthesis pathway under salt stress, via the constructed co-expression network. Our findings revealed the underlying mechanism of NO and H_2S to alleviate salt stress and regulate flavonoid biosynthesis, which provides a theoretical basis for establishing *C. paliurus* plantations in the salt stress areas.

KEYWORDS

***Cyclocarya paliurus*, exogenous substance, photosynthetic parameter, antioxidant system, salt stress, transcription factors**

1 Introduction

Salinity is a major environmental factor affecting plant growth and productivity (Guo et al., 2022a). Excessive salt concentration in soil disturbs the osmotic balance, ion transport and metabolic response of plants (Genisel et al., 2015; Mostofa et al., 2015). Salt stress which causes the high concentration of sodium ions in plant cells, not only hinders the absorption of other ions but also interferes with the catalysis of enzyme activity and destroys the nutritional balance (Manishankar et al., 2018). The accumulation of reactive oxygen species such as hydrogen peroxide and superoxide anion in plant cells can seriously damage the structure of various organelles and the biosynthesis of macromolecules (Hazman et al., 2015; Li C. et al., 2017; Ghalati et al., 2020). At present, the area of saline soil in the world has exceeded 800 million hectares and is still expanding (Munns and Tester, 2008). In order to deal with this situation, it is particularly important to reveal the mechanism in response to salt stress and improve the salt tolerance of plants.

Application of exogenous substances on plants is one of the effective methods to alleviate salt stress (Zhang et al., 2019). As important gaseous signal molecules in plants, nitric oxide (NO) and hydrogen sulfide (H_2S) not only have antioxidant properties, but also widely participate in the whole physiological process from seed germination to plant apoptosis (Singh et al., 2015; Mukherjee, 2019). Moreover, the mechanism of NO and H_2S in plant cells has also been widely discussed, including their interaction with related active nitrogen substances, modifying target proteins, and regulating intracellular signal transduction (Khurana et al., 2011; Shen et al., 2018). Importantly, many studies have shown that NO and H_2S are involved in regulating various physiological mechanisms of plants in response to environmental stresses (Begara-Morales et al., 2018; Corpas, 2019; Zhang et al., 2019). For example, NO and H_2S have been reported to regulate plant response strategies to abiotic stresses such as salinization, drought and cold (Shen et al., 2018; Liu et al., 2020; Zhou et al., 2020). Meanwhile, some studies also indicated that H_2S increases the content of S-nitrosothiol and then possibly affects the storage abundance of NO (Singh et al., 2015; Mukherjee, 2019) and the crosstalk relationship between NO and H_2S in cells has become a research hotspot (Singh et al., 2020). For instance, H_2S has been reported to alleviate salt stress of barley seedling via NO-mediated ion homeostasis (Chen et al., 2015). Another finding showed that NO and H_2S enhance the resistance of tomato seedlings to heavy metal stress through sulfur assimilation (Alamri et al., 2020). Thus, the application of exogenous NO and H_2S would be an important way to alleviate abiotic stress of plants, whereas less related information is available in tree species.

Cyclocarya paliurus, as a multifunctional tree species in walnut family, is widely distributed in subtropical areas of China (Fang et al., 2006). Especially its leaves are traditionally used for the production of nutraceutical tea and ingredient of functional foods in China because of its unique taste and rich in bioactive substances with hypoglycemic and hypotensive functions (Fang, 2011). Flavonoids is not only an important bioactive substance but also a key antioxidant in plants in response to abiotic stresses (Li X. et al., 2017). Previous studies have showed that salinity increased the flavonoid content of *C. paliurus* leaves (Zhang et al., 2021). Moreover, exogenous H_2S application has been suggested to induce endogenous NO production, and improve salt tolerance of *C. paliurus* by maintaining fluorescence and enhancing antioxidant activity (Chen et al., 2021). However, the molecular regulation mechanisms of NO and H_2S applications on *C. paliurus* under salt stress still remain unknown.

To meet the huge requirement of *C. paliurus* leaf production, sites with some environmental stresses would be potential land for developing *C. paliurus* plantations due to the limitation of land resources in China, while the coastal saline land has been regarded as a potential area for developing *C. paliurus* resources. Therefore, how to improve the salt tolerance of *C. paliurus* has become particularly urgent in the practices. Moreover, flavonoid is considered not only to be important bioactive substances but also to resist environmental stresses (Maurya and Yadav, 2005; Guo et al., 2022b), so revealing how exogenous substances affect flavonoid biosynthesis in leaves is also important under the salinity condition. The objectives of this research were: (1) to identify the role of NO and H_2S on photosynthetic process and antioxidant capacity of *C. paliurus* under salt stress; (2) to explore the regulatory function of NO and H_2S on *C. paliurus* seedlings in response to salt stress from the perspective of transcriptome and metabolome; (3) to clarify the molecular mechanism of the above signaling molecules acting on the flavonoid pathway. Results from this study may provide new insights into the molecular mechanism of NO and H_2S on alleviating abiotic stress of woody plants.

2 Materials and methods

2.1 Plant materials and treatments

C. paliurus seeds were collected from Yanling county (26° 30′ N, 113° 41′ E) in Hunan province, China, in October 2018. Based on the method of Fang et al. (2006), seeds were treated with exogenous gibberellin A3 and stratification measures to break seed dormancy. In April of 2019, the germinated seeds were sown in nonwoven receptacles (10.0 cm depth and 8.5 cm diameter) and then transferred to the greenhouse at Baima Experimental Base of Nanjing Forestry University (31° 35′ N, 119° 09′ E). The nonwoven receptacles were filled with mixed substrates of peat: soil: perlite: rotting poultry manure = 4: 2: 2: 2 (v/v/v/v). The contents of total N, total P, total K, and organic matter in the substrates were 72.35, 2.19, 9.55, and 73.3 g/kg, respectively.

Salt treatments were performed in July 2019, and a completely random block design was adopted with three replicates for each treatment, and six plants for each replicate. Referring to previous research (Ma et al., 2019), six treatments were set up, including CK (no salt addition and only irrigation with distilled water), SNP (no salt addition, spraying with 0.25mM sodium nitroprusside (a NO donor), and irrigation with distilled water), NaHS (no salt addition, spraying with 0.5mM sodium hydrosulfide (a H_2S donor), and irrigation with distilled water), NaCl (0.4% NaCl treatment and irrigation with 0.4% NaCl solution), SNP+NaCl (0.4% NaCl treatment, spraying with 0.25mM SNP and irrigation with 0.4%

NaCl solution), and NaHS+NaCl (0.4% NaCl treatment, spraying with 0.5mM NaHS and irrigation with 0.4% NaCl solution). To avoid osmotic shock, NaCl solution was gradually added into soil in five times within two days to reach the expected concentrations, while the concentration was calculated based on soil weight. However, the solutions of SNP and NaHS were evenly sprayed on the adaxial and abaxial surfaces of leaves before one day of the salt treatment until completely wetting the leaves. The nonwoven receptacles were placed in plastic pot and trays to prevent salt loss, and irrigation was performed twice a week to keep the field water capacity at 70% - 75%.

Leaf samples were collected for the determination of related indexes 30 days after the salt treatments, in that the phenotypic differences were observed among different treatments (Figure 1). Three plants of each treatment were selected as samples and six expanded mature leaves were collected from the upper position of each sample. These leaves were quickly frozen by liquid nitrogen and kept at -80°C for total RNA extraction and enzyme activity determination. The rest leaves were dried at 70°C and pulverized for the quantitative analysis of flavonoid content.

2.2 Determination of leaf biomass and physiological parameters

2.2.1 Leaf biomass and photosynthetic parameters

Based on the seedling height and ground diameter, three seedlings with uniform growth in each treatment were selected as sample plants for physiological parameters determination. The total leaf biomass was measured by drying the leaves at 70°C for 72 h.

The fourth fully expanded compound leaf of each sample plant was selected to measure photosynthetic parameters by the LI-6400XT photosynthetic system (LI-COR, Inc., Lincoln NE, USA). Photosynthetic parameters including net photosynthetic rate (P_n), transpiration rate (T_r), stomatal conductance (G_s), intercellular CO_2 concentration (C_i) and water use efficiency (WUE) were measured between 8:30–11:00 am 30 days after salt treatments. The operating ambient of the photosynthetic apparatus was set according to the method of Zhang et al. (2022).

2.2.2 Fluorescence parameters and chlorophyll content

Fluorescence parameters of the selected leaves were determined by an FMS-2 portable pulse-modulated fluorometer (Hansatech Instruments Ltd., Norfolk, United Kingdom). After 15 minutes of dark adaptation, the selected leaves were used for the determination of maximal quantum yield of PS II (F_v/F_m), non-photochemical quenching coefficient (NPQ), and electron transfer rate (ETR).

After determining the photosynthetic and fluorescence parameters, fresh leaves were collected from the same part of the seedlings, washed and dried, and extracted with 80% acetone solution to determine the chlorophyll content following the method of Asghar et al. (2016).

2.2.3 NO and soluble protein content

0.3 g fresh leaf powder was ground with 8 ml double distilled water, and then centrifuged for 20 minutes (4°C, 1,2000×g). The contents of endogenous NO and soluble protein in *C. paliurus* leaves were determined according to the instruction of NO oxide determination kit and soluble protein kit (Jiancheng Bioengineering Institute, Nanjing, China) (Usuda et al., 1984; Cantrel et al., 2010).

2.3 Measurement of antioxidant enzyme activity and leaf flavonoid content

2.3.1 Antioxidant enzyme activity

0.3 g fresh leaf samples were homogenized in 50 mM phosphate buffer solution (4.5 ml, containing 0.1 mM ethylene diamine tetra acetic acid and 2 mM dithiothreitol, PH 7.0-7.4). Homogenate was centrifuged at 1,0000×g for 20 min at 4°C, and the supernatant was used for activity analysis of antioxidant enzymes. Antioxidant enzyme activity of *C. paliurus* leaves was detected by a superoxide

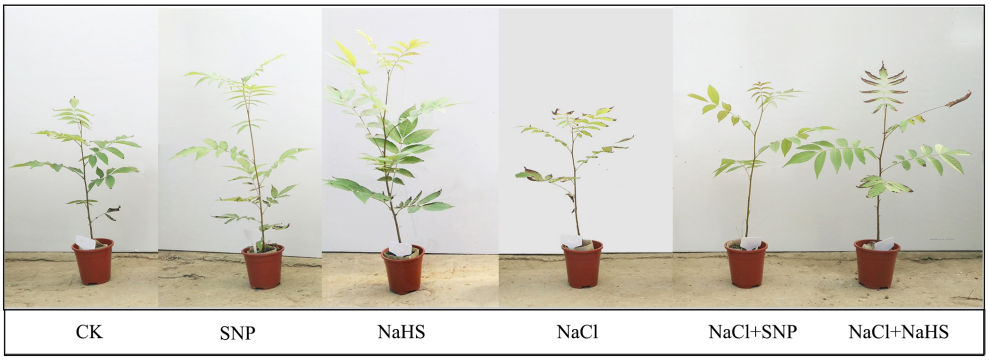

FIGURE 1
Phenotypes of *C. paliurus* seedlings after 30 days of the treatments. Code annotation: CK (no salt addition and only irrigation with distilled water), SNP (no salt addition, spraying with 0.25mM sodium nitroprusside (a NO donor), and irrigation with distilled water), NaHS (no salt addition, spraying with 0.5mM sodium hydrosulfide (a H_2S donor), and irrigation with distilled water), NaCl (0.4% NaCl treatment and irrigation with 0.4% NaCl solution), SNP+NaCl (0.4% NaCl treatment, spraying with 0.25mM SNP and irrigation with 0.4% NaCl solution), and NaHS+NaCl (0.4% NaCl treatment, spraying with 0.5mM NaHS and irrigation with 0.4% NaCl solution), the same below.

dismutase (SOD) kit, peroxidase (POD) kit, catalase (CAT) kit, and malondialdehyde (MDA) kit (Jiancheng Bioengineering Institute, Nanjing, China) (Meloni et al., 2003; Rahnama and Ebrahimzadeh, 2005).

2.3.2 Leaf flavonoid content

Alcohol extraction method was adopted to extract leaf samples for the determination of flavonoid content (Cao et al., 2017). In short, 10 mL 70% (v/v) ethanol mixed with 0.8 g dry leaf powder was ultrasonicated 45 min at 70°C for the preparation of extracting solution. The solution was centrifuged at 10,000 rpm for 10 min when cooling to room temperature, and then separated on C18 solid phase extraction column and filtered through a 0.22 μm polytetrafluoroethylene (PTFE) filter. The total flavonoid content was measured by optimized colorimetry (Bao et al., 2005) and the individual flavonoid content was detected by a high-performance liquid chromatography (HPLC) (Waters Crop., Milford, MA, USA) (Cao et al., 2017).

2.4 Transcriptomic and metabolomic analysis

2.4.1 Transcriptomic analysis and weighted gene co-expression network construction

Transcriptome sequencing was executed by the method of Guo et al. (2020). In brief, the extraction of total RNA from *C. paliurus* leaves was performed using Trizol reagent kit (Invitrogen, Carlsbad, CA, USA). The cDNA fragments were purified with QiaQuick PCR extraction kit (Qiagen, Venlo, The Netherlands). A total of 18 cDNA libraries (six treatments, and three biological replicates for each treatment) were constructed using Illumina HiSeqTM 4000 by Gene Denovo Biotechnology Co. (Guangzhou, China). High-quality clean reads were acquired with filtering the raw reads by Fastp (Version 0.18.0) (Chen et al., 2018), and the mapped reads of each sample were assembled by StringTie v1.3.1 (Pertea et al., 2015; Pertea et al., 2016). The value of FPKM was calculated by StringTie software (max_memory, 30G; seqType, fq; CPU, 10; KMER_SIZE, 31; min_kmer_cov, 11; normalize_reads; normalize_max_read_cov, 50).

In order to expound the interaction between transcription factors and key structural genes in flavonoid biosynthesis pathway, a weighted gene co-expression network analysis was executed by R packages including WGCNA and DESeq2 software (threshold power = 8, min module size = 50). The Pearson correlations between the eigengenes of each module and the abundance of flavonoids were performed using R package ggplot2. The gene regulatory networks between transcription factors and structural genes were constructed with Cytoscape software (Version 3.7.1) (Shannon et al., 2003).

2.4.2 Metabolomics analysis

The extraction of metabolites for leaf samples was performed by UHPLC-QE-MS (Guo et al., 2020). LC-MS/MS analyses were executed by an UHPLC system (1290, Agilent Technologies) with a UPLC HSS T3 column coupled to Q Exactive (Orbitrap MS, Thermo). The mobile phase proportioning and the elution gradient setting were performed by the method of Zhang et al. (2021). The full scan resolution of ESI source was 70000, and MS/MS used a resolution of 17500. The MS raw data was formatted by ProteoWizard and the conversion results were processed by R package XCMS software (version 3.2). The peak annotation was implemented by OSI-SMMS (version 1.0, Dalian Chem Data Solution Information Technology Co. Ltd.) with in-house MS/MS database. Principal component analysis was performed by R package models for the exposition of relevance among samples. And the metabolites were annotated and classified according to the Kyoto Encyclopedia of Genes and Genomics (KEGG) database.

2.5 Statistical analysis

All the statistical analyses were performed using R package models and TBtools software (Version 1.068) (Chen et al., 2020). Differences between samples were determined by one-way analysis of variance (ANOVA) and significant differences were calculated by the least significant difference (LSD) test at $P < 0.05$.

3 Results

3.1 Effects of exogenous NO and H2S on leaf biomass and physiological parameters under salt stress

Exogenous NO and H_2S applications significantly promoted the accumulation of leaf biomass and photosynthetic capacity (Figure 2). Compared with the control, NaHS treatment increased leaf dry weight, T_r, P_n, and WUE by 25%, 33%, 147%, and 63%, respectively. Moreover, salt treatment caused a significant reduction in leaf biomass and photosynthetic parameters of *C. paliurus* seedlings, whereas the application of exogenous NO and H_2S alleviated this reduction ($P < 0.05$) (Figure 2). In comparison with NaCl treatment, SNP + NaCl treatment increased leaf biomass, P_n, and WUE of the seedlings by 18%, 47%, and 59%, respectively.

NPQ represents the proportion of light energy dissipated in the form of heat. The value of NPQ significantly enhanced under NaCl treatment in comparison with CK, indicating that the light energy conversion of *C. paliurus* leaves were inhibited by salt, while exogenous NO and H_2S reduced the NPQ value ($P < 0.05$) (Table 1). Compared with salt-treated plants, applications of NaHS and SNP resulted in an increase in ETR (24%-35%) and F_v/F_m (17%-22%) in *C. paliurus* leaves under salinity. Similarly, the contents of chlorophyll a and b increased significantly with the application of exogenous NO and H_2S ($P < 0.05$) (Table 1).

Exogenous NO and H_2S also significantly affected the content of NO and soluble protein in *C. paliurus* leaves ($P < 0.05$) (Figure 3). Compared with NaCl treatment, the NO content of *C. paliurus* under NaHS+NaCl and SNP+NaCl treatments showed an increase by 35% and 21%, respectively (Figure 3A). Moreover, the NaHS and SNP application significantly promoted soluble protein content under salt stress (Figure 3B).

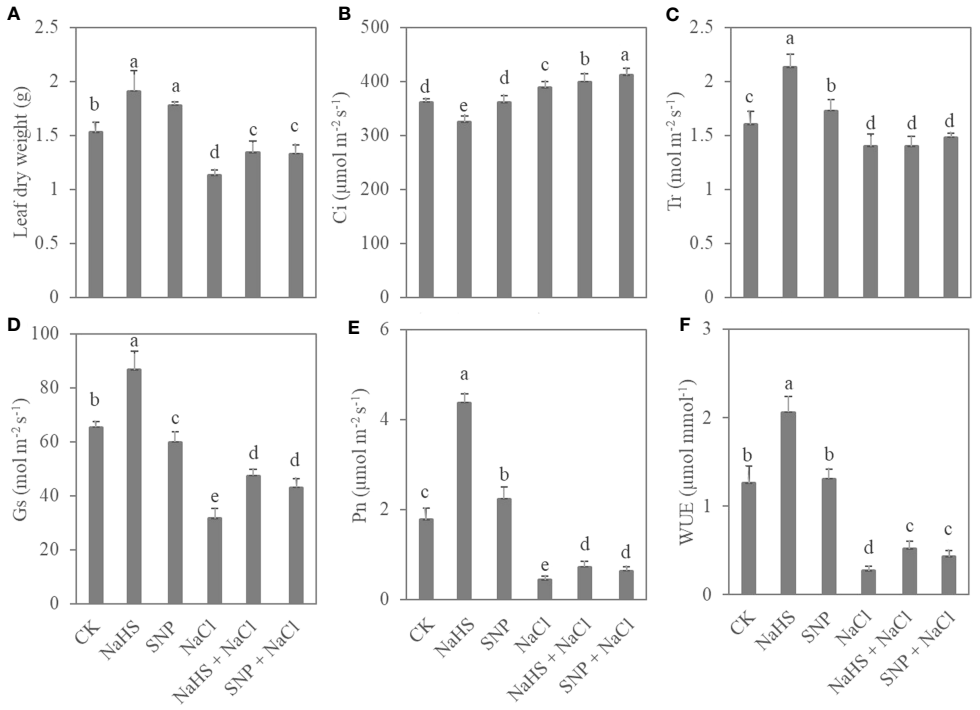

FIGURE 2
Leaf biomass **(A)** and photosynthetic parameters **(B–F)** in *C. paliurus* seedlings of different treatments. Different small letters indicate a significant difference ($P < 0.05$) among the treatments.

3.2 NO and H2S applications promote antioxidant enzyme activities and flavonoid contents under salt stress

Salt treatments significantly affected the activities of antioxidant enzymes in *C. paliurus* leaves (Table 2). Compared with the control, the activities of POD, SOD, and CAT in the leaves under salt treatment decreased 15%, 48% and 60% respectively, whereas the content of MDA increased significantly under salt stress. However, the activities of antioxidant enzymes in leaves were enhanced by exogenous NO and H_2S applications (Table 2). For example, compared with salt-treated plants, SNP+NaCl treatment significantly promoted the activities of POD (70%), SOD (59%), and CAT (129%) in *C. paliurus* leaves. Besides, the content of MDA under NaHS+NaCl and SNP+NaCl treatments significantly decreased in comparison with NaCl treatment ($P < 0.05$). These results suggested that NO and H_2S applications can alleviate oxidative stress response under salinity at a certain extent.

As shown in Table 3, the contents of total flavonoids and seven individual compounds in the leaves under NaHS and SNP treatments showed an overall upward trend when compared with the control. Although the salt stress treatment significantly increased the content of total flavonoids in comparison with CK ($P < 0.05$), compared with salt stress treatment, the treatments of

TABLE 1 Variations in fluorescence parameters and chlorophyll content of *C. paliurus* leaves among different treatments.

Treatments	NPQ	ETR	F_v/F_m	Chl a content (mg g^{-1})	Chl b content (mg g^{-1})
CK	2.17 ± 0.12 c	0.72 ± 0.09 a	0.70 ± 0.06 ab	0.81 ± 0.05 b	0.38 ± 0.04 b
NaHS	1.96 ± 0.14 c	0.68 ± 0.05 a	0.78 ± 0.02 a	1.12 ± 0.06 a	0.41 ± 0.02 ab
SNP	2.17 ± 0.30 c	0.66 ± 0.08 a	0.76 ± 0.02 a	1.21 ± 0.17 a	0.44 ± 0.02 a
NaCl	3.93 ± 0.44 a	0.37 ± 0.04 c	0.54 ± 0.04 c	0.44 ± 0.01 d	0.20 ± 0.02 c
NaHS+NaCl	3.12 ± 0.47 b	0.46 ± 0.05 bc	0.63 ± 0.09 bc	0.61 ± 0.01 c	0.24 ± 0.03 c
SNP+NaCl	3.31 ± 0.22 b	0.50 ± 0.03 b	0.66 ± 0.05 b	0.66 ± 0.06 bc	0.21 ± 0.01 c

Different small letters indicate a significant difference ($P < 0.05$) among the treatments. Code annotation: CK (no salt addition and only irrigation with distilled water), SNP (no salt addition, spraying with 0.25mM sodium nitroprusside (a NO donor), and irrigation with distilled water), NaHS (no salt addition, spraying with 0.5mM sodium hydrosulfide (a H_2S donor), and irrigation with distilled water), NaCl (0.4% NaCl treatment and irrigation with 0.4% NaCl solution), SNP+NaCl (0.4% NaCl treatment, spraying with 0.25mM SNP and irrigation with 0.4% NaCl solution), and NaHS+NaCl (0.4% NaCl treatment, spraying with 0.5mM NaHS and irrigation with 0.4% NaCl solution), the same below.

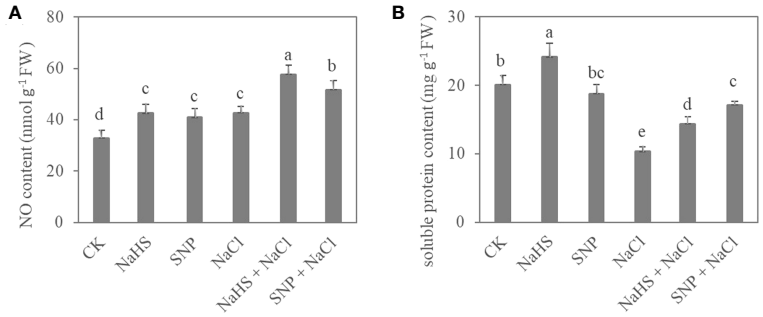

FIGURE 3
NO content **(A)** and soluble protein content **(B)** in *C. paliurus* leaves of different treatments. Different small letters indicate a significant difference ($P < 0.05$) among treatments.

SNP + NaCl and NaHS + NaCl enhanced the total flavonoid content by 27% and 6% respectively. Similarly, the contents of several individual flavonoid compounds, such as quercetin-3-O-glucuronide, kaempferol-3-O-glucuronide, and kaempferol-3-O-glucoside, were also observed to increase significantly ($P < 0.05$). Thus, our results suggested exogenous NO and H_2S can enhance flavonoid contents in the leaves under salt stress to alleviate the oxidative damage.

3.3 Transcriptomic response to NO and H2S applications under salt stress

The sequencing quality of 18 cDNA libraries of *C. paliurus* leaves were summarized in Table S1, and a total of 0.8 billion clean reads were acquired. The proportions of reads mapped to gene of each library ranged from 78.40% to 80.40% (Table S1). Through principal component analysis, an obvious separation between samples under different treatments was shown on the plot (Figure 4A), indicating that salt treatment and the application of exogenous NO and H2S caused intense recombination at transcriptional level. PC1 and PC2 reflected 52.9% and 32.6% information of gene expression among *C. paliurus* samples, respectively. In addition, Pearson product-moment correlation coefficients showed a close correlation between samples under the same treatment (Figure 4B).

By analyzing the transcriptional profile, a large number of differentially expressed genes (DEGs) were identified from the samples between different treatments (Figure 5A). Combined with the results of the five comparison groups, 1248 DEGs were found in all groups, indicating that these genes were susceptible to the factors of salt, NO and H_2S. However, the largest number of specific DEGs (2967 genes) were identified between CK and salt treatments. After further exploring the differences at transcriptional levels among different treatments, it was found that compared with the CK, a total of 9399 genes were up-regulated and 6447 genes were down-regulated under salt treatment (Figure 5B). And the pretreatments of SNP and NaHS before salt treatment resulted in the up-regulation of 4656 and 6493 genes and down-regulation of 8835 and 5262 genes, respectively. According to the enrichment analysis at KEGG pathways, the DEGs between CK and SNP (or NaHS) treatments were found to be enriched in phenylpropanoid biosynthesis, sesquiterpenoid and triterpenoid biosynthesis pathway, and MAPK signaling pathways; and the DEGs between NaCl and SNP + NaCl (or NaHS + NaCl) treatments were enriched at isoquinoline alkaloid biosynthesis, nitrogen metabolism, and flavonoid biosynthesis pathways. In addition, the DEGs among different treatments were collectively enriched in the pathways of

TABLE 2 Variations in antioxidant enzyme activity of *C. paliurus* leaves among different treatments.

Treatments	POD activity (U min^{-1} g^{-1})	SOD activity (U g^{-1})	CAT activity (U min^{-1} g^{-1})	MDA content (μmol g^{-1})
CK	25.21 ± 1.02 bc	385.88 ± 9.08 a	6.44 ± 0.27 c	25.03 ± 2.93 c
NaHS	28.89 ± 2.59 b	417.16 ± 5.87 a	8.08 ± 0.43 b	24.39 ± 1.10 c
SNP	34.08 ± 2.55 a	416.39 ± 10.41 a	9.16 ± 0.73 a	27.86 ± 2.55 c
NaCl	21.49 ± 1.22 c	201.20 ± 27.39 c	2.55 ± 0.53 e	74.75 ± 3.11 a
NaHS+NaCl	27.04 ± 1.54 b	349.30 ± 32.83 b	5.08 ± 0.33 d	63.21 ± 3.62 b
SNP+NaCl	36.63 ± 3.69 a	319.13 ± 14.26 b	5.85 ± 0.19 cd	62.33 ± 1.35 b

Different small letters indicate a significant difference (P < 0.05) among the treatments.

10.3389/fpls.2023.1211162

TABLE 3 Variations in flavonoid content among *C. paliurus* leaf samples of different treatments.

Treatments	Flavonoid contents (mg/g)							
	Total flavonoid	Quercetin-3-O-glucuronide	Quercetin-3-O-galactoside	Isoquercitrin	Kaempferol-3-O-glucuronide	Kaempferol-3-O-glucoside	Quercetin-3-O-rhamnoside	Kaempferol-3-O-rhamnoside
CK	39.42 ± 2.21 e	0.21 ± 0.01 d	0.06 ± 0.01 d	0.06 ± 0.01 c	0.45 ± 0.04 d	0.17 ± 0.02 d	0.05 ± 2.81E-03 b	0.13 ± 0.01 c
NaHS	48.82 ± 3.41 d	0.46 ± 0.06 c	0.17 ± 0.02 c	0.15 ± 0.01 b	2.11 ± 0.05 b	0.46 ± 0.02 b	0.06 ± 9.02E-04 b	0.22 ± 0.02 b
SNP	49.32 ± 2.55 d	0.54 ± 0.06 c	0.14 ± 0.03 c	0.14 ± 0.02 b	1.65 ± 0.15 c	0.28 ± 0.03 c	0.05 ± 1.22E-03 b	0.09 ± 0.01 d
NaCl	52.82 ± 4.02 c	0.19 ± 0.01 d	0.06 ± 0.01 d	0.07 ± 0.01 c	0.4 ± 0.04 d	0.16 ± 0.01 d	0.04 ± 2.15E-03 b	0.06 ± 0.01 d
NaHS+NaCl	67.23 ± 3.22 a	0.71 ± 0.05 b	0.44 ± 0.05 a	0.19 ± 0.02 b	2.16 ± 0.29 b	0.31 ± 0.03 c	0.10 ± 9.82E-03 a	0.35 ± 0.01 a
SNP+NaCl	55.94 ± 1.19 b	0.81 ± 0.06 a	0.31 ± 0.04 b	0.54 ± 0.04 a	2.84 ± 0.16 a	0.6 ± 0.04 a	0.08 ± 8.36E-03 a	0.27 ± 0.03 b

Different small letters indicate a significant difference ($P < 0.05$) among treatments.

ribosome, fatty acid elongation, pyruvate metabolism, citrate cycle and plant hormone signal transduction.

3.4 Metabolomic response to NO and H2S applications under salt stress

As shown in Figure 6A, the distribution of samples from different treatments on the PCA diagram of metabolomic data presented a clear separation, which was consistent with the result of the transcriptional analysis. Among the differentially accumulated metabolites between the treatments of NaCl and SNP + NaCl, the number of up-regulation and down-regulation were 749 and 2382, respectively (Figure 6B). Similarly, the number of up-regulation was much lower than that of down-regulation of differentially accumulated metabolites between the treatments of NaCl and NaHS + NaCl (Figure 6B).

In order to further understand the enrichment information of these metabolites, the top 20 KEGG pathways were shown by bar diagrams (Figures S1A, B). Both two diagrams contained the pathways of flavonoid biosynthesis, flavone and flavonol biosynthesis, and anthocyanin biosynthesis.

3.5 Metabolite accumulation and gene expression in flavonoid biosynthesis pathway

To explore the regulatory effects of NO and H_2S on flavonoid biosynthesis, a schematic diagram was used to clarify the synthesis

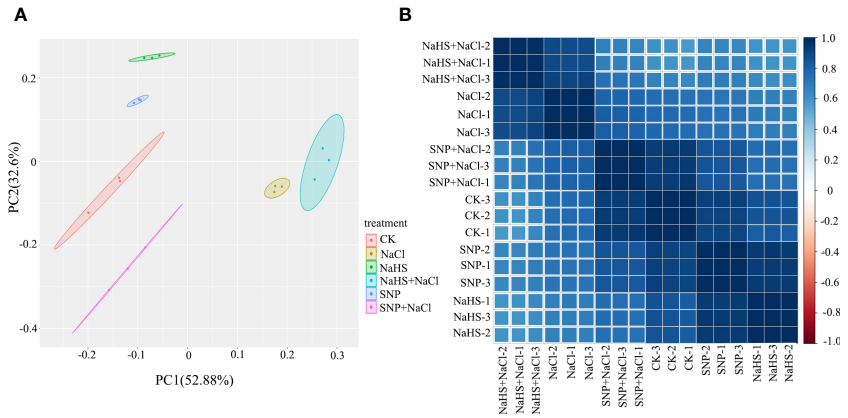

FIGURE 4
PCA score plot and correlation heat map in transcriptomic profile of *C. paliurus* leaf samples. **(A)** Each point in PCA score plot representing an independent biological replicate; **(B)** Pearson product-moment correlation coefficients of the gene expression profile. The blue rectangles represent the positive correlation between the samples, whereas the red rectangles represent the negative correlation.

relationship from phenylalanine in the upstream to flavonoids in the downstream (Figure 7A). A total of 40 DEGs and 17 metabolites with significant differences in abundance between different treatments were screen from the flavonoid biosynthesis pathway (Tables S2, S3), and the expression levels of these genes and metabolites were presented by heatmaps (Figures 7B, C).

Compared with the CK, the treatment of NaHS significantly up-regulated the expression of related genes encoding PAL (phenylalanine ammonia lyase), CYP (cytochromeP450) and 4CL (4-coumarate: coenzyme A ligase). Moreover, when compared with NaCl, the up-regulated genes under the treatment of NaHS + NaCl ran through the entire pathway, whereas the SNP + NaCl treatment only up-regulated the expression of some downstream genes encoding FLS (flavonol synthase), DFR (dihydroflavonol 4-reductase), and F3H (flavonoid 3-hydroxylase) (Figure 7B). Similar to the trend of gene expression, the application of NaHS significantly increased the abundance of a large number of metabolites compared with CK (Figure 7C). Notably, the abundance of metabolites under the treatments of SNP + NaCl and NaHS + NaCl decreased when compared with NaCl treatment, suggesting that the large amount of these metabolites may be used for the synthesis of stress resistant substances in the downstream pathways.

3.6 Gene correlation networks related to flavonoid biosynthesis

The weighted gene co-expression network analysis (WGCNA) indicated that the genes in transcriptional profile of *C. paliurus* samples were divided into 18 modules based on similar expression patterns (Figure 8A). Among them, skyblue module comprised the most genes and brown4 module comprised the least genes, with the number of genes being 6282 and 52 respectively (Figure 8B). Pearson correlation analysis showed that orange module was closely correlated with the seven flavonoid compounds

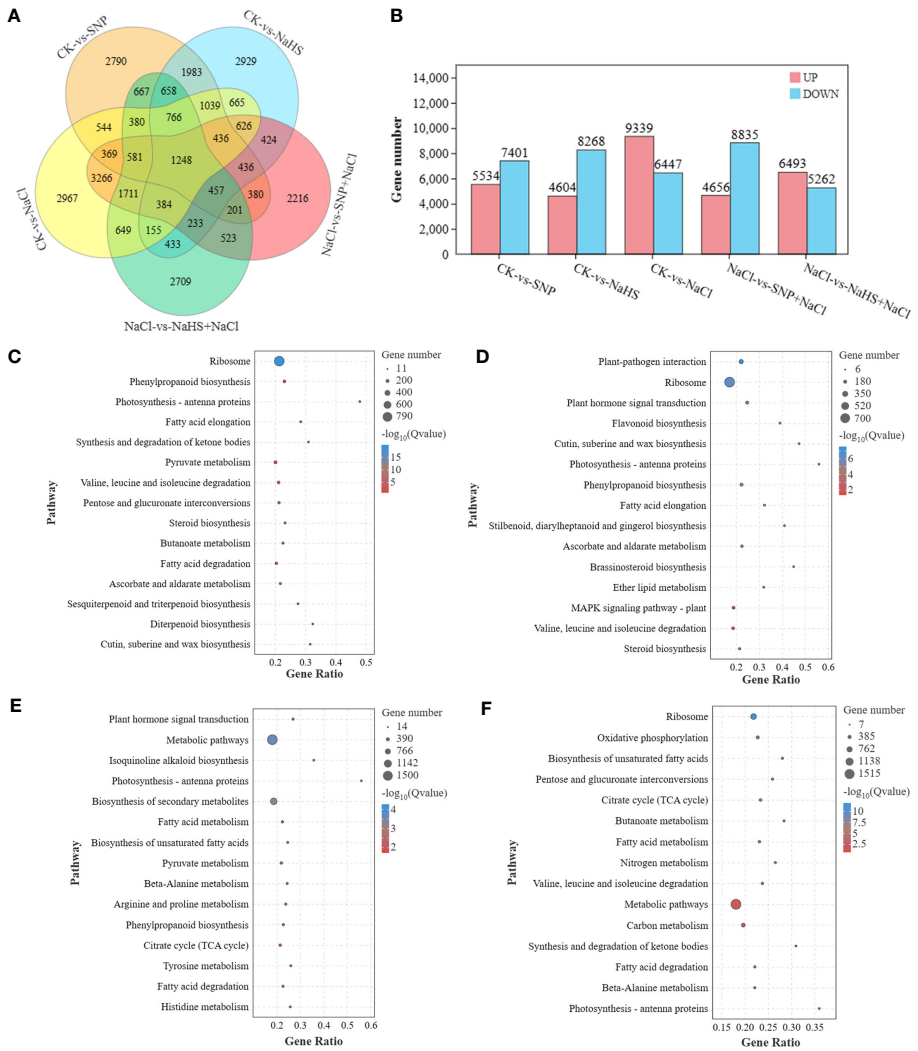

FIGURE 5
The analysis of DEGs in transcriptomic profile of *C. paliurus* samples and the annotation of KEGG enrichment pathway. Venn diagram **(A)** and the number **(B)** of DEGs between different treatments; Top 15 of KEGG enrichment pathway of DEGs between treatments of CK and SNP **(C)**, CK and NaHS **(D)**, Salt and SNP + NaCl **(E)**, and Salt and NaHS + NaCl **(F)**.

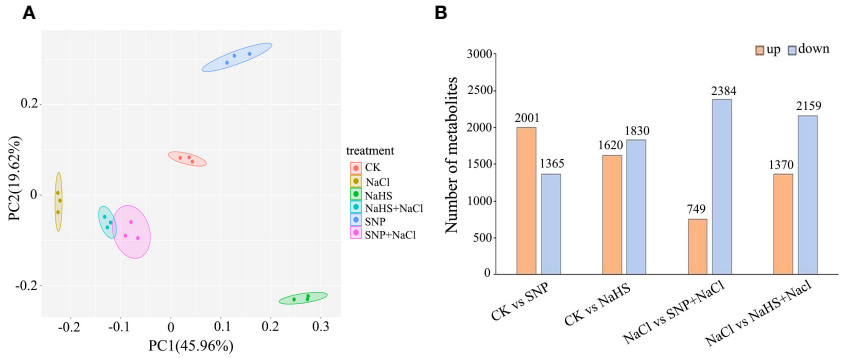

FIGURE 6
PCA score plot and the number of differentially accumulated metabolites in metabolomic profile of *C. paliurus* leaf samples. **(A)** Each point in PCA score plot representing an independent biological replicate; **(B)** The red and blue columns represent the up-regulation and down-regulation of metabolite abundance, respectively.

(Figure 8C), indicating that the eigengenes of this module were related to the accumulation of flavonoids in *C. paliurus* leaves under different treatments. To screen the key regulatory transcription factors (TFs) that may regulate the abundance of flavonoids, a co-expression network based on structural genes and TFs from orange module was constructed (Figure 8D). The results showed that four structural genes FLS (Unigene0041673), CHS (Unigene0033841), PAL (Unigene0040065) and 4CL (Unigene0040344) in the flavonoid pathway were regulated by multiple TFs (Table S4). In the orange module, the four structural genes were positively correlated with 11 TFs, including *ERF*s, *WRKY*s, *HY5*, and so on. Furthermore, the gene encoding 4CL was negatively correlated with *REF12*, *bHLH144*, *GTE7* and *bHLH121*, indicating that the expression of 4CL was inhibited by these four TFs.

4 Discussion

Salt stress, a common abiotic stress in nature, affects agricultural yields significantly, as it can severely inhibit plant growth and development (Ryu and Cho, 2015). Salinity causes osmotic and oxidative stress, interfering with plant photosynthesis (Yang and Guo, 2018). This study indicated that salt stress decreased the net photosynthetic rate, electron transfer rate, chlorophyll content

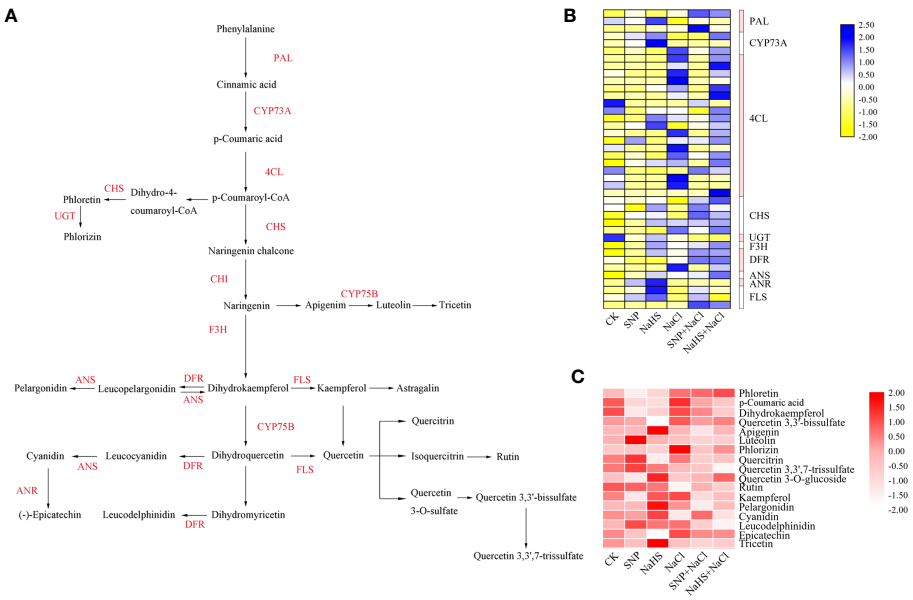

FIGURE 7
Differential expressions of structural genes and metabolites in flavonoid biosynthesis pathway of *C. paliurus* leaf samples. **(A)** Schematic diagram of metabolic relationship and related genes in flavonoid pathway; **(B)** Blue and yellow blocks represent high and low expression of genes, respectively. Enzyme annotation: 4CL, 4-coumarate: coenzyme A ligase; ANR, Anthocyanidin reductase; ANS, Anthocyanidin synthase; CHI, Chalcone isomerase; CHS, Chalcone synthase; CYP, CytochromeP450; DFR, Dihydroflavonol 4-reductase; F3H, Flavonoid 3-hydroxylase; FLS, Flavonol synthase; PAL, Phenylalanine ammonia lyase; UGT, UDP-glycosyltransferase. **(C)** Heat map representing the abundance of metabolites in the flavonoid pathway. And the shade of red in the blocks represents the abundance of metabolites.

and leaf biomass production of *C. paliurus* (Table 1 and Figure 2). However, the values of P_n, WUE, ETR, and F_v/F_m of the plants were significantly increased under NaHS+NaCl and SNP+NaCl treatments compared with those under the sole NaCl treatment, suggesting that NO and H_2S applications play a positive role in regulating photosynthetic rate and light energy conversion efficiency, thus reduce the loss of leaf biomass in salt-treated plants. These results are consistent with previous reports on *Brassica juncea* (Khan et al., 2012), *Glycine max* (Egbichi et al., 2014), and *Matricaria recutita* (Fazelian et al., 2012). Meanwhile, the leaf dry weight, photosynthetic rate and chlorophyll content of the plants under NaHS+NaCl and SNP+NaCl treatments were obviously lower than those in the control (Table 1 and Figure 2), indicating that NO and H_2S application cannot completely eliminate the negative effects caused by salt stress. Chen et al. (2021) showed that H_2S application improved biomass accumulation by maintaining photosynthesis, but we did not study the effect of applying concentration on plants under salt

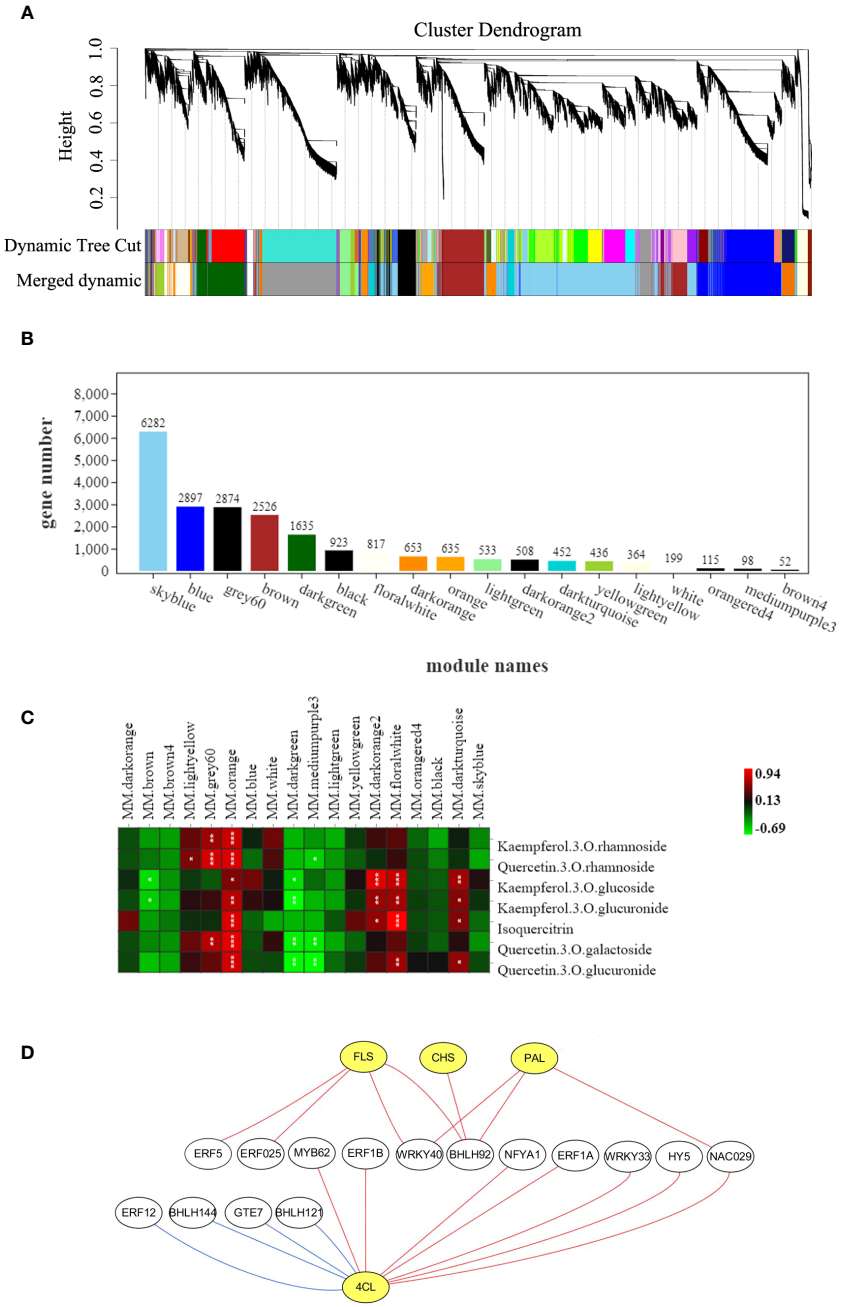

FIGURE 8
Results of the gene co-expression network analysis. **(A)** Cluster dendrogram showing identified modules and the cluster tree of eigengenes in each module; **(B)** The number of genes in each module; **(C)** The heatmap of correlation coefficient between flavonoid contents and module eigengenes "*", "**" and "***" indicate correlations of 0.5-0.6, 0.6-0.7 and 0.7-1, respectively; with the red and green blocks representing positive and negative correlations, respectively; **(D)** Network constructed by selected TFs (white circles) and structural genes (yellow circles) related to flavonoid biosynthesis pathway from orange module. The red line and blue line represent positive correlation and negative correlation, respectively.

stress. Therefore, further research is needed to investigate the regulatory ability of different doses of NO and H_2S on the salt tolerance of *C. paliurus*

NO and H_2S are important messengers among plant cells, and can effectively regulate the physiological response under abiotic stress (Jiang et al., 2020; Goyal et al., 2021). The results from this study showed that the application of SNP and NaHS significantly increased the contents of NO and soluble protein in leaves of *C. paliurus* (Figure 3), inferring a positive regulatory relationship between nitric oxide and protein content. Similarly, previous studies (Chen et al., 2015; Ma et al., 2019) have shown that H_2S-induced NO has a positive regulatory effect on plant protein production and ion homeostasis. Antioxidant enzyme system is activated under salt stress to reduce the accumulation of reactive oxygen species (ROS), while the activities of antioxidant enzymes reflect the ability of plants to cope with the stress (Jin et al., 2013). Our results also showed that the activities of POD, SOD, and CAT under 0.4% NaCl treatment were significantly lower than those in the control group (Table 2), indicating that excessive salinity stress may destroy the normal physiological process and then decrease enzyme activity (Zhang et al., 2021). However, our results showed that the activities of POD, SOD, and CAT were significantly improved with the application of NO and H_2S donors (Table 2). The results from this study also confirm the hypotheses that exogenous NO and H_2S can induce the increase of endogenous NO content and ameliorate salt tolerance of plants (Chen et al., 2021). In addition, NO and H_2S were assumed to mediate antioxidant enzyme activity through persulfidation or S-nitrosation, respectively (Singh et al., 2017; Alamri et al., 2020), however, the translational modifications in these potential ways are need to be further investigated in *C. paliurus*.

Flavonoids are a kind of antioxidants and stress resistant substances in plants (Fini et al., 2011). A large number of studies have shown that plants can promote the production of phenolic metabolites to alleviate salt damage (Hejazi-Mehrizi et al., 2012; Oliveira et al., 2020), which is consistent with our results (Table 2). Here, our result suggested that the contents of total flavonoid and several individual compounds such as kaempferol-3-O-glucoside, quercetin-3-O-rhamnoside and kaempferol-3-O-rhamnoside were the highest under the treatments of SNP + NaCl and NaHS + NaCl (Table 2). These findings indicate that exogenous NO and H_2S may regulate the quantity and composition of flavonoid substances to improve the tolerance to salt stress. Some recent reports have indicated that application of SNP and NaHS to stressed plants resulted in an increase of flavonoid content (Li X. et al., 2017; Chen et al., 2021). Therefore, exogenous NO and H_2S applications may not only be a good way to alleviate abiotic stress, but also contribute to the accumulation of flavonoids in *C. paliurus* leaves.

As a small gas signaling molecular, NO plays a key role in alleviating abiotic stress such as drought, low temperature and salt (Zhao et al., 2004; Abat and Deswal, 2009; Yu et al., 2014). Due to the important functions of NO in plant physiological processes, researches on its regulation mechanism at the molecular level have attracted extensive attention (Imran et al., 2018). In the present study, both salt stress and exogenous NO and H_2S application all led to obviously transcriptional reprogramming in *C. paliurus* leaves (Figures 4A, B), whereas a lots of identified DEGs were enriched in the metabolite pathways such as phenylpropanoid biosynthesis, diterpenoid biosynthesis and flavonoid biosynthesis (Figures 5C–F). It has also been reported that NO mediates the up-regulation of genes related to the metabolism of isoflavonoid, terpenoid and cyanoamino acid in *Medicago sativa* under abiotic stress (Zhao et al., 2019). Furthermore, our results showed the application of SNP and NaHS promoted the activation of plant hormone signal transduction pathway and MAPK signaling pathway (Figures 5C–F). This indicated that NO and H_2S could effectively regulate the expression of genes related to pathways of hormone signaling and flavonoid biosynthesis, thereby improving the content of related hormones and flavonoids. In consistent with previous reports (Yu et al., 2014), exogenous NO and H_2S applications enhance plant tolerance to abiotic stress by mediating a series of physiological and metabolic processes.

As reported, the biosynthesis of various flavonoid metabolites is regulated by PAL, CYP, 4CL and other key enzymes, while the activities of these enzymes are activated or inhibited by a variety of TFs when subjected to diverse stress or environmental factors (Ren et al., 2019; Xu et al., 2020; Qi et al., 2022). Our study found that exogenous NO and H_2S applications enhanced the activities of several enzymes in the flavonoid pathway (Figure 7B), and four genes encoding PAL, 4CL, CHS and FLS were identified to be close correlated with 15 TFs (Figure 8D). Interestingly, most of these TFs, including *ERF*, *MYB*, *WRKY*, *bHLH*, and *HY5*, have been reported to be induced by NO and to be involved in stress responses to various adversity (Imran et al., 2018; Wen et al., 2021).

Overexpression of *WRKY* has been reported to enhance salt tolerance, up-regulate the expression of FLS, DFR, and F3H, and increase accumulation of flavonoid and anthocyanins (Wang et al., 2017; Wang N. et al., 2018). In this research, WRKY TF, one of the factors contributing to increasing flavonoid content, was also observed to promote the up-regulation of genes encoding PAL, 4CL and FLS (Figure 8D). Meanwhile, HY5 is often described to react to light signal and regulate the biosynthesis of flavonoids such as anthocyanins (An et al., 2019), and has recently been suggested to respond to abiotic stresses such as cold and salt (Wang F. et al., 2018; Kovács et al., 2019). In addition, *ERF*, *bHLH*, and *NAC* have also been reported to regulate the expression of structural genes in the flavonoid pathway (Guo et al., 2020; Premathilake et al., 2020) and our results support the viewpoints mentioned above. Notably, *GTE* was observed to inhibit the expression of 4CL in the present study, whereas less information on its related researches is available and more studies on its internal regulatory mechanism on abiotic stress are required. Moreover, it should be aware that both

NO and H_2S are dose-dependent signal molecules, and the single concentration applied in this study may lead to a deviation in the summary of regulatory roles. Therefore, further detailed studies are needed to reveal the signaling pathways and molecular mechanisms of these two gas molecules in mediating plant growth and development under salt stress. However, the effects of NO and H_2S on soil physicochemical properties and soil microbial communities were not explored in this experiment. SNP treatment

has been reported to reduce phytophagous nematode density and soil pH (Gao et al., 2011), while the effects of these factors on the salt tolerance of *C. paliurus* need to be further studied.

5 Conclusion

To sum up, applications of exogenous NO and H_2S under salt stress can promote endogenous NO synthesis, reduce oxidative damage via activating antioxidant enzyme activities and increasing the contents of soluble protein and flavonoids, and thus maintain the photosynthetic capacity of *C. paliurus* seedlings. With the application of the gas messengers (NO and H_2S) under salt stress, the physiological activities and metabolic reactions of the seedlings underwent obvious reprogramming at the molecular level. The messengers activated or inhibited the activity of key enzymes in flavonoid pathway by inducing the expression of TFs such as WRKY, and then affect the accumulation of flavonoid compounds. From the views of physiological response and integrative analysis of metabolome and transcriptome, our study suggests that NO and H_2S applications show a positive role in salt tolerance of *C. paliurus*, even if more researches are required to reveal insight into its molecular mechanism and be verified in the field trial.

Data availability statement

The original contributions presented in the study are publicly available. This data can be found here: National Center for Biotechnology information (NCBI), https://www.ncbi.nlm.nih.gov/bioproject/, PRJNA799813.

Author contributions

LZ: Formal analysis, Data curation, Methodology, Writing - Original Draft, Visualization; YL: Supervision; ZZ: Investigation; SF: Conceptualization, Writing - Review & Editing, Funding acquisition, Project administration.

Funding

This research was supported by the National Natural Science Foundation of China (32071750), the Key Research and Development Program of Jiangsu Province (BE2019388), and the Priority Academic Program Development of Jiangsu Higher Education Institutions (PAPD).

Conflict of interest

The authors declare that the research was conducted in the absence of any commercial or financial relationships that could be construed as a potential conflict of interest.

Publisher's note

Supplementary material

The Supplementary Material for this article can be found online at: https://www.frontiersin.org/articles/10.3389/fpls.2023.1211162/full#supplementary-material

References

Abat, J., and Deswal, R. (2009). Differential modulation of S-nitrosoproteome of *Brassica juncea* by low temperature: change in S-nitrosylation of RuBisCO is responsible for the inactivation of its carboxylase activity. *Proteomics* 9, 4368–4380. doi: 10.1002/pmic.200800985

Alamri, S., Ali, H. M., Khan, M. I. R., Singh, V. P., and Siddiqui, M. H. (2020). Exogenous nitric oxide requires endogenous hydrogen sulfide to induce the resilience through sulfur assimilation in tomato seedlings under hexavalent chromium toxicity. *Plant Physiol. Biochem.* 155, 20–34. doi: 10.1016/j.plaphy.2020.07.003

An, J., Wang, X., Zhang, X., Bi, S., You, C., and Hao, Y. (2019). MdBBX22 regulates UV-B-induced anthocyanin biosynthesis through regulating the function of MdHY5 and is targeted by MdBT2 for 26S proteasome-mediated degradation. *Plant Biotechnol. J.* 17, 2231–2233. doi: 10.1111/pbi.13196

Asghar, T., Jamil, Y., Iqbal, M., Zia-ul-Haq,, and Abbas, M. (2016). Laser light and magnetic field stimulation effect on biochemical, enzymes activities and chlorophyll contents in soybean seeds and seedlings during early growth stages. *J. Photochem. Photobiol. B-Biol.* 165, 283–290. doi: 10.1016/j.jphotobiol.2016.10.022

Bao, J. S., Cai, Y. Z., Sun, M., Wang, G. Y., and Corke, H. (2005). Anthocyanins, flavonols, and free radical scavenging activity of Chinese bayberry (*Myrica rubra*) extracts and their color properties and stability. *J. Agric. Food Chem.* 53, 2327–2332. doi: 10.1021/jf048312z

Begara-Morales, J., Chaki, M., Valderrama, R., Sánchez-Calvo, B., Mata-Pérez, C., Padilla, M., et al. (2018). NO buffering and conditional NO release in stress response. *J. Exp. Bot.* 69, 3425–3438. doi: 10.1093/jxb/ery072

Cantrel, C., Vazquez, T., Puyaubert, J., Rezé, N., Lesch, M., Kaiser, W., et al. (2010). Nitric oxide participates in cold-responsive phosphosphingolipid formation and gene expression in *Arabidopsis thaliana*. *New Phytol.* 189, 415–427. doi: 10.1111/j.1469-8137.2010.03500.x

Cao, Y. N., Fang, S. Z., Yin, Z. Q., Fu, X. X., Shang, X. L., Yang, W. X., et al. (2017). Chemical fingerprint and multicomponent quantitative analysis for the quality evaluation of *Cyclocarya paliurus* leaves by HPLC–Q–TOF–MS. *Molecules* 22, 1927. doi: 10.3390/molecules22111927

Chen, C. J., Chen, H., Zhang, Y., Thomas, H. R., and Xia, R. (2020). TBtools: an integrative toolkit developed for interactive analyses of big biological data. *Mol. Plant* 13, 1194–1202. doi: 10.1016/j.molp.2020.06.009

Chen, J., Wang, W., Wu, F., He, E., Liu, X., Shangguan, Z., et al. (2015). Hydrogen sulfide enhances salt tolerance through nitric oxide-mediated maintenance of ion homeostasis in barley seedling roots. *Sci. Rep.* 5, 12516. doi: 10.1038/srep12516

Chen, P., Yang, W., MinxueWen,, Jin, S., and Liu, Y. (2021). Hydrogen sulfide alleviates salinity stress in *Cyclocarya paliurus* by maintaining chlorophyll fluorescence and regulating nitric oxide level and antioxidant capacity. *Plant Physiol. Biochem.* 167, 738–747. doi: 10.1016/j.plaphy.2021.09.004

Chen, S. F., Zhou, Y. Q., Chen, Y. R., and Gu, J. (2018). fastp: an ultra-fast all-in-one FASTQ preprocessor. *Bioinformatics* 34, i884–i890. doi: 10.1101/274100

Corpas, F. J. (2019). Hydrogen sulfide: a new warrior against abiotic stress. *Trends Plant Sci.* 24, 983–988. doi: 10.1016/j.tplants.2019.08.003

Egbichi, I., Keyster, M., and Ludidi, N. (2014). Effect of exogenous application of nitric oxide on salt stress responses of soybean. *S. Afr. J. Bot.* 90, 131–136. doi: 10.1016/j.sajb.2013.11.002

Fang, S. Z. (2011). Provenance and temporal variations in selected flavonoids in leaves of *Cyclocarya paliurus*. *Food Chem.* 124, 1382–1386. doi: 10.1016/j.foodchem.2010.07.095

Fang, S. Z., Wang, J. Y., Wei, Z. Y., and Zhu, Z. X. (2006). Methods to break seed dormancy in *Cyclocarya paliurus* (Batal)Iljinskaja. *Sci. Hortic.* 110, 305–309. doi: 10.1016/j.scienta.2006.06.031

Fazelian, N., Nasibi, F., and Rezazadeh, R. (2012). Comparison the effects of nitric oxide and spermidin pretreatment on alleviation of salt stress in chamomile plant (*Matricaria recutita* L.). *J. Stress Physiol. Biochem.* 8, 215–223. doi: 10.1007/BF02239382

Fini, A., Brunetti, C., Di Ferdinando, M., Ferrini, F., and Tattini, M. (2011). Stress-induced flavonoid biosynthesis and the antioxidant machinery of plants. *Plant Signaling Behav.* 6, 709–711. doi: 10.4161/psb.6.5.15069

Gao, A. N., Tian, C. P., Hu, Y. L., Chen, Q., and Mao, Z. Q. (2011). Effects of exogenous nitric oxide onphysiological characteristics of seedlings of *Malus hupehensis* Rehd. under continuous cropping. *Sci. Agric. Sin.* 44, 2184–2192. doi: 10.3864/j.issn.0578-1752.2011.10.025

Genisel, M., Erdal, S., and Kizilkaya, M. (2015). The mitigating effect of cysteine on growth inhibition in salt-stressed barley seeds is related to its own reducing capacity rather than its effects on antioxidant system. *Plant Growth Regul.* 75, 187–197. doi: 10.1007/s10725-014-9943-7

Ghalati, R. E., Shamili, M., and Homaei, A. (2020). Effect of putrescine on biochemical and physiological characteristics of guava (*Psidium guajava* L.) seedlings under salt stress. *Sci. Hortic.* 261, 108961. doi: 10.1016/j.scienta.2019.108961

Goyal, V., Jhanghel, D., and Mehrotra, S. (2021). Emerging warriors against salinity in plants – nitric oxide and hydrogen sulphide. *Physiol. Plant* 171, 896–908. doi: 10.1111/ppl.13380

Guo, Y., Gao, C. Y., Wang, M. K., Fu, F. F., El Kassaby, Y. A., Wang, T. L., et al. (2020). Metabolome and transcriptome analyses reveal flavonoids biosynthesis differences in *Ginkgo biloba* associated with environmental conditions. *Ind. Crops Prod.* 158, 112963. doi: 10.1016/j.indcrop.2020.112963

Guo, M., Wang, X. S., Guo, H. D., Bai, S. Y., Khan, A., Wang, X. M., et al. (2022a). Tomato salt tolerance mechanisms and their potential applications for fighting salinity: A review. *Front. Plant Sci.* 13. doi: 10.3389/fpls.2022.949541

Guo, Y., Yu, Y., Wan, Z., Sokhansanj, S., El-Kassaby, Y. A., and Wang, G. (2022b). Evaluation of the potential of pelletized enzyme-treated Ginkgo leaf residues for use as a solid fuel. *Renew. Energy* 201, 305–313. doi: 10.1016/j.renene.2022.10.048

Hazman, M., Hause, B., Eiche, E., Nick, P., and Riemann, M. (2015). Increased tolerance to salt stress in OPDA-deficient rice ALLENE OXIDE CYCLASE mutants is linked with an increased ROS-scavenging activity. *J. Exp. Bot.* 66, 3339–3352. doi: 10.1093/jxb/erv142

Hejazi-Mehrizi, M., Shariatmadari, H., Khoshgoftarmanesh, A., and Dehghani, F. (2012). Copper effects on growth, lipid peroxidation, and total phenolic content of rosemary leaves under salinity stress. *J. Agric. Sci. Technol.* 14, 205–212. doi: 10.1016/j.agsy.2011.10.003

Imran, Q. M., Hussain, A., Lee, S. U., Mun, B. G., Falak, N., Loake, G. J., et al. (2018). Transcriptome profile of NO-induced Arabidopsis transcription factor genes suggests their putative regulatory role in multiple biological processes. *Sci. Rep.* 8, 771. doi: 10.1038/s41598-017-18850-5

Jiang, J., Ren, X., Li, L., Hou, R., Sun, W., Jiao, C., et al. (2020). H2S regulation of metabolism in cucumber in response to salt-stress through transcriptome and proteome analysis. *Front. Plant Sci.* 11. doi: 10.3389/fpls.2020.01283

Jin, G., He, L., Yu, X., Zhang, J., and Ma, M. (2013). Antioxidant enzyme activities are affected by salt content and temperature and influence muscle lipid oxidation during dry-salted bacon processing. *Food Chem.* 141, 2751–2756. doi: 10.1016/j.foodchem.2013.05.107

Khan, M. N., Siddiqui, M. H., Mohammad, F., and Naeem, M. (2012). Interactive role of nitric oxide and calcium chloride in enhancing tolerance to salt stress. *Nitric. Oxide* 27, 210–218. doi: 10.1016/j.niox.2012.07.005

Khurana, A., Khurana, J. P., and Babbar, S. B. (2011). Nitric oxide induces flowering in the duckweed *Lemna aequinoctialis* Welw. (Syn. L. paucicostata Hegelm.) under noninductive conditions. *J. Plant Growth Regul.* 30, 378–385. doi: 10.1007/s00344-011-9199-7

Kovács, H., Aleksza, D., Baba, A. I., Hajdu, A., Király, A. M., Zsigmond, L., et al. (2019). Light control of salt-induced proline accumulation is mediated by ELONGATED HYPOCOTYL 5 in Arabidopsis. *Front. Plant Sci.* 10. doi: 10.3389/fpls.2019.01584

Li, C., Lu, H., Li, W., Yuan, M., and Fu, Y. (2017). A ROP2-RIC1 pathway fine tunes microtubule reorganisation for salt tolerance in Arabidopsis. *Plant Cell Environ.* 40, 1127–1142. doi: 10.1111/pce.12905

Li, X., Zhang, L., Ahammed, G. J., Li, Z. X., Wei, J. P., Shen, C., et al. (2017). Nitric oxide mediates brassinosteroid-induced flavonoid biosynthesis in *Camellia sinensis* L. *J. Plant Physiol.* 214, 145–151. doi: 10.1016/j.jplph.2017.04.005

Liu, F., Zhang, X., Cai, B., Pan, D., Fu, X., Bi, H., et al. (2020). Physiological response and transcription profiling analysis reveal the role of glutathione in H2S-induced chilling stress tolerance of cucumber seedlings. *Plant Sci.* 291, 110363. doi: 10.1016/j.plantsci.2019.110363

Ma, K., Jiang, Y., Yu, Z. Y., Huang, Y. T., Zhan, Y. G., and Fan, G. Z. (2019). H2S-induced NO/SNO positively promotes betulin production in *Betula platyphylla*. *Ind. Crops Prod.* 140, 111608. doi: 10.1016/j.indcrop.2019.111608

Manishankar, P., Wang, N., Köster, P., Alatar, A. A., and Kudla, J. (2018). Calcium signaling during salt stress and in the regulation of ion homeostasis. *J. Exp. Bot.* 69, 4215–4226. doi: 10.1093/jxb/ery201

Maurya, R., and Yadav, P. P. (2005). Furanoflavonoids: an overview. *Nat. Prod. Rep.* 22, 400–424. doi: 10.1039/B505071P

Meloni, D. A., Oliva, M. A., Martinez, C. A., and Cambraia, J. (2003). Photosynthesis and activity of superoxide dismutase, peroxidase and glutathione reductase in cotton under salt stress. *Environ. Exp. Bot.* 49, 69–76. doi: 10.1016/S0098-8472(02)00058-8

Mostofa, M., Saegusa, D., Fujita, M., and Tran, L. S. (2015). Hydrogen sulfide regulates salt tolerance in rice by maintaining Na^+/K^+ balance, mineral homeostasis and oxidative metabolism under excessive salt stress. *Front. Plant Sci.* 6. doi: 10.3389/fpls.2015.01055

Mukherjee, S. (2019). Recent advancements in the mechanism of nitric oxide signaling associated with hydrogen sulfide and melatonin crosstalk during ethylene-induced fruit ripening in plants. *Nitric. Oxide* 82, 25–34. doi: 10.1016/j.niox.2018.11.003

Munns, R., and Tester, M. (2008). Mechanisms of salinity tolerance. *Annu. Rev. Plant Biol.* 59, 651–681. doi: 10.1146/annurev.arplant.59.032607.092911

Oliveira, D., Mota, T., Salatta, F., Sinzker, R., Koncitikova, R., Kopecný, D., et al. (2020). Cell wall remodeling under salt stress: Insights into changes in polysaccharides, feruloylation, lignification, and phenolic metabolism in maize. *Plant Cell Environ.* 43, 2172–2191. doi: 10.1111/pce.13805

Pertea, M., Kim, D., Pertea, G. M., Leek, J. T., and Salzberg, S. L. (2016). Transcript-level expression analysis of RNA-seq experiments with HISAT, StringTie and Ballgown. *Nat. Protoc.* 11, 1650–1667. doi: 10.1038/nprot.2016.095

Pertea, M., Pertea, G. M., Antonescu, C. M., Chang, T. C., Mendell, J. T., and Salzberg, S. L. (2015). StringTie enables improved reconstruction of a transcriptome from RNA-seq reads. *Nat. Biotechnol.* 33, 290–295. doi: 10.1038/nbt.3122

Premathilake, A. T., Ni, J., Shen, J., Bai, S., and Teng, Y. (2020). Transcriptome analysis provides new insights into the transcriptional regulation of methyl jasmonate-induced flavonoid biosynthesis in pear calli. *BMC Plant Biol.* 20, 388. doi: 10.1186/s12870-020-02606-x

Qi, Y.-L., Xue, L.-J., El-Kassaby, Y. A., and Guo, Y. (2022). Identification and comparative analysis of conserved and species-specific microRNAs in four populus sections. *Forests* 13, 873. doi: 10.3390/f13060873

Rahnama, H., and Ebrahimzadeh, H. (2005). The effect of NaCl on antioxidant enzyme activities in potato seedlings. *Biol. Plant* 49, 93–97. doi: 10.1007/s10535-005-3097-4

Ren, G., Cui, J., Xiang, X., Cao, Y., Wei, S., Chang, J., et al. (2019). Flavonoid biosynthesis pathway participating in salt resistance in a landrace sweet sorghum revealed by RNA-Sequencing comparison with grain sorghum. *J. Agric. Sci.* 11, 63. doi: 10.5539/jas.v11n6p63

Ryu, H., and Cho, Y. (2015). Plant hormones in salt stress tolerance. *J. Plant Biol.* 58, 147–155. doi: 10.1007/s12374-015-0103-z

Shannon, P., Markiel, A., Ozier, O., Baliga, N., Wang, J., Ramage, D., et al. (2003). Cytoscape: a software environment for integrated models of biomolecular interaction networks. *Genome Res.* 13, 2498–2504. doi: 10.1101/gr.1239303

Shen, Z. J., Chen, J., Ghoto, K., Hu, W. J., Gao, G. F., Luo, M. R., et al. (2018). Proteomic analysis on mangrove plant *Avicennia marina* leaves reveals nitric oxide enhances the salt tolerance by up-regulating photosynthetic and energy metabolic protein expression. *Tree Physiol.* 38, 1605–1622. doi: 10.1093/treephys/tpy058

Singh, S., Kumar, V., Kapoor, D., Kumar, S., Singh, S., Dhanjal, D. S., et al. (2020). Revealing on hydrogen sulfide and nitric oxide signals co-ordination for plant growth under stress conditions. *Physiol. Plant* 168, 301–317. doi: 10.1111/ppl.13002

Singh, M., Kushwaha, B. K., Singh, S., Kumar, V., Singh, V. P., and Prasad, S. M. (2017). Sulphur alters chromium (VI) toxicity in *Solanum melongena* seedlings: role of sulphur assimilation and sulphur-containing antioxidants. *Plant Physiol. Biochem.* 112, 183–192. doi: 10.1016/j.plaphy.2016.12.024

Singh, V. P., Singh, S., Kumar, J., and Prasad, S. M. (2015). Hydrogen sulfide alleviates toxic effects of arsenate in pea seedlings through up-regulation of the ascorbate–glutathione cycle: possible involvement of nitric oxide. *J. Plant Physiol.* 181, 20–29. doi: 10.1016/j.jplph.2015.03.015

Usuda, H., Ku, M., and Edwards, G. E. (1984). Rates of photosynthesis relative to activity of photosynthetic enzymes, chlorophyll and soluble protein content among ten C4 species. *Funct. Plant Biol.* 11, 509–517. doi: 10.1071/PP9840509

Wang, N., Liu, W., Zhang, T., Jiang, S., Xu, H., Wang, Y., et al. (2018). Transcriptomic analysis of red-fleshed apples reveals the novel role of MdWRKY11

in flavonoid and anthocyanin biosynthesis. *J. Agric. Food Chem.* 66, 7076–7086. doi: 10.1021/acs.jafc.8b01273

Wang, K., Wu, Y. H., Tian, X. Q., Bai, Z. Y., Liang, Q. Y., Liu, Q. L., et al. (2017). Overexpression of *DgWRKY4* enhances salt tolerance in chrysanthemum seedlings. *Front. Plant Sci.* 8. doi: 10.3389/fpls.2017.01592

Wang, F., Zhang, L., Chen, X., Wu, X., Xiang, X., Zhou, J., et al. (2018). SlHY5 integrates temperature, light and hormone signaling to balance plant growth and cold tolerance. *Plant Physiol.* 179, 749–760. doi: 10.1104/pp.18.01140

Wen, W., Wang, R., Su, L., Lv, A., Zhou, P., and An, Y. (2021). MsWRKY11 , activated by MsWRKY22, functions in drought tolerance and modulates lignin biosynthesis in alfalfa (*Medicago sativa* L.). *Environ. Exp. Bot.* 184, 104373. doi: 10.1016/j.envexpbot.2021.104373

Xu, N. T., Liu, S., Lu, Z. G., Pang, S. Y., and Li, W. X. (2020). Gene expression profiles and flavonoid accumulation during salt stress in *Ginkgo biloba* seedlings. *Plants* 9, 1162. doi: 10.3390/plants9091162

Yang, Y., and Guo, Y. (2018). Elucidating the molecular mechanisms mediating plant salt-stress responses. *New Phytol.* 217, 523–539. doi: 10.1111/nph.14920

Yu, M., Lamattina, L., Spoel, S., and Loake, G. (2014). Nitric oxide function in plant biology: a redox cue in deconvolution. *New Phytol.* 202, 1142–1156. doi: 10.1111/nph.12739

Zhang, P., Li, S., Guo, Z., and Lu, S. (2019). Nitric oxide regulates glutathione synthesis and cold tolerance in forage legumes. *Environ. Exp. Bot.* 167, 103851. doi: 10.1016/j.envexpbot.2019.103851

Zhang, L., Zhang, Z. J., Fang, S. Z., Liu, Y., and Shang, X. L. (2021). Integrative analysis of metabolome and transcriptome reveals molecular regulatory mechanism of flavonoid biosynthesis in *Cyclocarya paliurus* under salt stress. *Ind. Crops Prod.* 170, 113823. doi: 10.1016/j.indcrop.2021.113823

Zhang, L., Zhang, Z., Fang, S., Liu, Y., and Shang, X. (2022). Metabolome and transcriptome analyses unravel the molecular regulatory mechanisms involved in photosynthesis of Cyclocarya paliurus under salt stress. *Int. J. Mol. Sci.* 23, 1161. doi: 10.3390/ijms23031161

Zhao, Y., Wei, X., Ji, X., and Ma, W. (2019). Endogenous NO-mediated transcripts involved in photosynthesis and carbohydrate metabolism in alfalfa (*Medicago sativa* L.) seedlings under drought stress. *Plant Physiol. Biochem.* 141, 456–465. doi: 10.1016/j.plaphy.2019.06.023

Zhao, L., Zhang, F., Guo, J., Yang, Y., Li, B., and Zhang, L. (2004). Nitric oxide functions as a signal in salt resistance in the calluses from two ecotypes of reed. *Plant Physiol.* 134, 849–857. doi: 10.1104/pp.103.030023

Zhou, H., Chen, Y., Zhai, F., Zhang, J., Zhang, F., Yuan, X., et al. (2020). Hydrogen sulfide promotes rice drought tolerance via reestablishing redox homeostasis and activation of ABA biosynthesis and signaling. *Plant Physiol. Biochem.* 155, 213–220. doi: 10.1016/j.plaphy.2020.07.038

frontiers | Frontiers in Plant Science

TYPE Original Research
PUBLISHED 09 October 2023
DOI 10.3389/fpls.2023.1265971

OPEN ACCESS

EDITED BY
Jose M. Mulet,
Universitat Politècnica de València, Spain

REVIEWED BY
Viswanathan Satheesh,
Iowa State University, United States
Shen Rao,
Wuhan Polytechnic University, China

*CORRESPONDENCE
Liying Yu
yuliying@vip.sina.com
Chunliu Pan
pchunliu@126.com

RECEIVED 24 July 2023
ACCEPTED 22 September 2023
PUBLISHED 09 October 2023

CITATION
Zhou Y, Yao L, Huang X, Li Y, Wang C, Huang Q, Yu L and Pan C (2023) Transcriptomics and metabolomics association analysis revealed the responses of *Gynostemma pentaphyllum* to cadmium. *Front. Plant Sci.* 14:1265971. doi: 10.3389/fpls.2023.1265971

Transcriptomics and metabolomics association analysis revealed the responses of *Gynostemma pentaphyllum* to cadmium

Yunyi Zhou[1,2], Lixiang Yao[1,2], Xueyan Huang[1,2], Ying Li[1,2], Chunli Wang[1,2], Qinfen Huang[1,2], Liying Yu[1,2]* and Chunliu Pan[1,2]*

[1]Guangxi Traditional Chinese Medicine (TCM) Resources General Survey and Data Collection Key Laboratory, the Center for Phylogeny and Evolution of Medicinal Plants, National Center for TCM Inheritance and Innovation, Guangxi Botanical Garden of Medicinal Plants, Nanning, China, [2]National Engineering Research Center for Southwest Endangered Medicinal Materials Resources Development, Guangxi Botanical Garden of Medicinal Plants, Nanning, China

Gynostemma pentaphyllum an important medicinal herb, can absorb high amounts of cadmium (Cd) which can lead to excessive Cd contamination during the production of medicines and tea. Hence, it is crucial to investigate the response mechanism of *G. pentaphyllum* under Cd stress to develop varieties with low Cd accumulation and high tolerance. Physiological response analysis, transcriptomics and metabolomics were performed on *G. pentaphyllum* seedlings exposed to Cd stress. Herein, *G. pentaphyllum* seedlings could significantly enhance antioxidant enzyme activities (POD, CAT and APX), proline and polysaccharide content subject to Cd stress. Transcriptomics analysis identified the secondary metabolites, carbohydrate metabolism, amino acid metabolism, lipid metabolism, and signal transduction pathways associated with Cd stress, which mainly involved the XTH, EXP and GST genes. Metabolomics analysis identified 126 differentially expressed metabolites, including citric acid, flavonoid and amino acids metabolites, which were accumulated under Cd stress. Multi-omics integrative analysis unraveled that the phenylpropanoid biosynthesis, starch, and sucrose metabolism, alpha-linolenic acid metabolism, and ABC transporter were significantly enriched at the gene and metabolic levels in response to Cd stress in *G. pentaphyllum*. In conclusion, the genetic regulatory network sheds light on Cd response mechanisms in *G. pentaphyllum*.

KEYWORDS

***Gynostemma pentaphyllum*, cadmium tolerance, physiological analysis, gene expression, metabolic level**

1 Introduction

Cadmium (Cd) is a naturally occurring heavy metal, and it is a non-essential element for plant growth. In recent years, the increasingly serious Cd contamination in soil has become an important factor restricting sustainable agricultural development and food health and safety in many regions around the world. Cd can readily be absorbed and transported, and it will accumulate in plant tissues. Plants suffer irreversible damage due to the high toxicity and poor degradability of Cd at elevated concentrations. Cd toxicity causes excessive production of reactive oxygen species (ROS), which affects photosynthesis, water balance, gas exchange, and mineral intake, as well as inhibiting plant growth and organ development (Kumar et al., 2023). Various strategies to detoxify Cd have arisen in plants when they are exposed to Cd stress. As a physical barrier, the plant's cell wall can adsorb and fix Cd by the use of negatively charged substances, and this partially prevents Cd from entering the protoplasts (Meyer et al., 2015; Shi et al., 2015). Some small organic molecules such as phytochelatin, metallothionein and glutahtione in protoplasts are induced to bind and chelate with Cd (Li et al., 2023c). After entering cells, compartmentalization in the plant's transport mechanism will channel the heavy metals to vacuoles (Shi et al., 2015; Xu et al., 2017). In these organelles, the antioxidant enzymes such as POD, SOD, APX and CAT as well as non-enzymatic antioxidants (including proline, soluble sugars and proteins), are activated to remove excess ROS accumulation (Yuan et al., 2013; Shahid et al., 2017). The plant's response to Cd stress has been well studied, clearly understanding the physiology of detoxification strategies. Furthermore, a complicated regulatory network involving numerous genes in Cd tolerance has been identified. Consequently, there is an urgent need to unravel the molecular and metabolic regulatory mechanisms underlying the plant's response to Cd stress.

Recently, there has been significant research on the Cd detoxification molecular mechanisms in plants. The genes involved in the *S*-adenosylmethionine cycle, metal transport, and vacuolar sequestration were found to be regulated differently under Cd stress conditions in maize (Lin et al., 2022). This was also the case for the genes encoding the antioxidant system in rice (Yang et al., 2022). Moreover, the cell wall biosynthesis genes (Casparian strip membrane domain protein (CASP)-like proteins (CSPLs), cell wall protein (CWP), and classical arabinogalactan protein 9-like (CAP9) were identified to play a critical role in Cd detoxification in *Solanum nigrum* (Wang et al., 2022). In addition, some crucial metabolisms that directly protect cells from Cd stress were highlighted. For example, the metabolism of galactose, lipid, and glutathione in buckwheat (Huo et al., 2023), and the ABC transporter, phenylpropanoid biosynthesis and flavonoid biosynthesis pathway in sorghum (Jiao et al., 2023); the unsaturated fatty acids, amino acids (including phenylalanine), nucleotides, sulfur compounds, flavonoids, glutathione and lignin biosynthetic metabolism in *Pistia stratiotes* were also implicated (Wei et al., 2023). The metal-transport genes related to Cd uptake, transport, and detoxification have also been extensively investigated. Such as natural resistance-associated macrophage protein (NRAMP) (Chen et al., 2021), zinc (Zn)-/iron-regulated transporter-like protein (ZIP) (Liu et al., 2019), heavy metal ATPase (HMA) (Qiao et al., 2018) and plant Cd resistance protein (PCR) (Lin et al., 2020). Transcription factors (TFs) have crucial roles in regulating transcription and are important for plants to respond to Cd stress. Recent studies in *Tamarix hispida* have revealed multi-layered transcriptional networks comprising 53 TFs and 54 structural genes, with 341 regulatory relationships predicted, as well as *ThDRE1A*, *ThMYC1* and *ThFEZ*, and modulation of the SOD, CAT and POD activities to scavenge ROS after Cd treatment (Xie et al., 2023). *PvERF15* and *GmWRKY142* were specifically demonstrated to decrease Cd uptake and enhance plant Cd tolerance (Lin et al., 2017; Cai et al., 2020). Hence, it is crucial to construct an accurate molecular regulatory model to identify potential hub genes and metabolites, which is especially important to comprehend the stress response mechanisms in plants.

Gynostemma pentaphyllum (Thunb.) Makino, a well-known economically valuable medicinal plant functioning in health care and disease treatment, belongs to the *Gynostemma* genus of the Cueurbitaeeae family and is widely distributed in subtropical regions of East and Southeast Asia (e.g. China, Vietnam, Laos and Malaysia) (Zhang et al., 2019). The leaves of this medicinal plant contain several saponins, polysaccharides, flavonoids, phytosterols and other bioactive ingredients that effectively act as anti-cancer and anti-atherogenic agents as well as affording neuroprotective and hepatoprotective properties (Su et al., 2021). Apart from its use in traditional Chinese medicine, *G. pentaphyllum* leaves are also utilized in tea production (Long et al., 2023). Due to its diverse range of applications, *G. pentaphyllum* has been praised as "southern ginseng" in China. Moreover, *G. pentaphyllum* has a wide range of ecological adaptations and it has a rapid growth rate. These growth advantages make *G. pentaphyllum* highly capable of accumulating heavy metals in contaminated soil, leading to excessive Cd contamination when it is used for tea (Suntararuks et al., 2008). Research has demonstrated that *G. pentaphyllum* plants possess a high ability to absorb Cd, and its Cd concentration is positively correlated with the concentration of the metal in the soil (Nookabkaew et al., 2016). Currently, the Cd tolerance and accumulation characteristics have been studied in *Gynostemma* plants, and it was found that when they are grown in the presence of high Cd concentrations, this reduced the growth, biomass, and chlorophyll content of three different *Gynostemma* species (Li et al., 2022b). These studies indicated that *Gynostemma* plants have specific tolerance and accumulation characteristics for Cd. Nevertheless, there is still a lack of accurate understanding regarding the Cd tolerance and accumulation characteristics in *G. pentaphyllum*. Currently, there is limited knowledge regarding the molecular mechanisms underlying the response of *G. pentaphyllum* to Cd. In the current study, *G. pentaphyllum* seedlings were chosen and their physiological, genetic and metabolic responses were investigated when subjected to various levels of Cd treatment. This study aimed to investigate the main genes, metabolites and key metabolic pathways associated with *G. pentaphyllum* in response to different levels of Cd stress. This study uncovers how *G. pentaphyllum* responds to Cd stress at both the physiological and

molecular levels. It provides insights into the *G. pentaphyllum* Cd response mechanisms, which can potentially guide the future selection and cultivation of plant varieties with low Cd accumulation and high tolerance varieties.

2 Materials and methods

2.1 Plant material

G. pentaphyllum was obtained from the Guangxi Botanical Garden of Medicinal Plants (Nanning, Guangxi, China). The seeds were germinated on moist perlite, after which seedlings of 3~5 leaf stage were selected and cultivated in hydroponic boxes with the Japanese Yamzaki formula solution (pH 6.0) (Li et al., 2023b). All plants were cultivated at a constant temperature of 25 ± 2°C, with a photoperiod of 14 h/10 h (day/night) and light intensity of 100 μmol m^{-2} s^{-1}). After 7 days of culture, the seedlings were subjected to a hydroponic medium containing different concentrations of $CdCl_2$ (0, 25, 50, 100, 150 and 200 μM) for 7 days, and seedlings grown in Cd-free hydroponic medium were used as controls (Li et al., 2022b). The *G. pentaphyllum* plants were then collected and assessed for height and root length. Fresh leaf samples were acquired for the assessment of physiological indexes as well as transcriptomics and metabolomics analysis. All samples were ground in liquid nitrogen by using a JXFSTPRP-64L grinding instrument (Shanghai, China) and stored at -80°C.

2.2 Determination of physiological indexes

The enzyme activities of superoxide dismutase (SOD), peroxidase (POD), catalase (CAT), L-ascorbate peroxidase (APX), as well as the contents of malondialdehyde (MDA) and proline were assessed and analyzed utilizing the methods as previously described (Pan et al., 2023). Dithizone (DTZ) staining was employed to evaluate Cd localization at the cellular levels as previously described (He et al., 2013). Periodic acid-Schiff (PAS) staining was employed using the Periodic Acid Schiff (PAS) Stain Kit (Beijing Solarbio Technology) by following the manufacturer's instructions. A Zeiss Axioscope 5 microscopy (Zeiss, Germany) was utilized to capture the images. Each experiment utilized three replicates of each treatment regimen.

2.3 High throughput transcriptomics analysis

Fresh leaf samples of Cd0 (CK), Cd25 (LC) and Cd100 (HC) were used in transcriptomics profiling analysis. The total RNA of nine samples from the three conditions was extracted using a Trizol reagent kit (Invitrogen, Carlsbad, CA, USA) according to the manufacturer's instructions. The purity, concentration and integrity of the RNA samples were assessed. The cDNA libraries were prepared using the NEBNext Ultra RNA Library Prep Kit for Illumina (NEB #7530, New England Biolabs, Ipswich, MA, USA). Finally, the cDNA library was sequenced using the Illumina Novaseq 6000 platform in the paired-end mode by Gene Denovo Biotechnology Co., Ltd (Guangzhou, China).

Following the sequencing process, the raw sequence data underwent filtration in order to eliminate low-quality reads (reads with a mass value below 10 and constituting more than 50% of the total bases) by FASTP v0.18.0. The short reads alignment tool Bowtie2 v2.2.8 was used for mapping reads to ribosome RNA (rRNA) database, and the rRNA mapped reads were removed. Then, the clean reads were mapped to the *G. pentaphyllum* reference genome (PRJNA720501, https://www.ncbi.nlm.nih.gov/search/all/?term=PRJNA720501) with HISAT2 v2.2.4. The fragments per kilobase of transcript per million mapped reads (FPKM) for all transcripts were quantified using Trapnell's method (Trapnell et al., 2010). The differential expressed genes (DEGs) were calculated by using the NOISeq method, employing a |log2 (fold change) |>2 and a false discovery rate (FDR) <0.05 (Tarazona et al., 2011). Gene ontology (GO) enrichment analysis was conducted with the GO database (http://www.geneontology.org/), while KEGG pathway enrichment analysis was conducted using the KEGG database (http://www.kegg.jp/).

2.4 Metabonomics profiling analysis

The fresh leaf samples of Cd0 (CK), Cd25 (LC), and Cd100 (HC) were incubated overnight at 4 °C, using 1.0 mL 70% aqueous methanol. The extracts were absorbed and filtered through an SPE cartridge and microporous membrane (0.22 μm pore size) before LC-MS analysis. The metabolomic analysis was conducted utilizing an ultra-performance liquid chromatography-tandem mass spectrometry (UPLC-MS) system. The chromatographic separation was achieved using a Waters C18 column, employing mobile phase A (0.04% acetic acid in water) and mobile phase B (0.05% acetic acid in acetonitrile) and operating at 40°C. Solvent gradient changes were linear for all the steps and these were: 95:5 Phase A/Phase B at 0 min, 5:95 Phase A/Phase B at 11.0 min, 5:95 Phase A/Phase B at 12.0 min, 95:5 Phase A/Phase B at 12.1 min and 95:5 Phase A/Phase B at 15.0 min. The flow rate was 0.4 mL/min, and the injection volume was 2 μL. An electrospray ionization (ESI) mode was employed to acquire the high-resolution mass spectra (HRMS), while operating in the positive ion mode. Further data processing was performed using Analyst 1.6.1 software. Metabolite information was identified by conducting searches in both internal and public databases (MassBank, KNApSAcK, HMDB, MoTo DB, and METLIN). PCA and OPLS-DA were utilized to identify significantly different metabolite levels (p-value < 0.05). Differentially altered metabolites (DAMs) were designated as a log2 fold change (FC) ≥ 2 and FC ≤ 0.5, along with variable importance in projection (VIP) scores > 1. The identified metabolites underwent metabolic pathways analysis using the KEGG database and MetaboAnalyst 4.0 (http://www.metaboanalyst.ca).

2.5 Correlation network analysis of transcriptomics and metabolomics data

Correlation network analysis was utilized to generate and analyze the association characteristics between metabolites and genes. The correlation characteristics between genes and metabolites were obtained using the KEGG pathway shared with genes and metabolites. Bidirectional orthogonal projections to latent structures (O2PLS) were employed to analyze both gene expression and metabolite abundance, and the best models derived from this analysis were derived from integration analysis. Gene-metabolite pairs were ranked by absolute correlation coefficients, which were calculated for gene expression and metabolite abundance. The resulting networks were visualized using the Cytoscape version 3.7.2 software package.

2.6 Quantitative real-time PCR (qRT-PCR) analysis

Fourteen DEGs were selected for qRT-PCR analysis and actin was used as an internal reference gene. The primers used were based on the transcript sequences using Primer 5.0 (Table S6). The qRT-PCR was performed using the LightCycler 96 instrument (Roche, Basel, Switzerland). The $2^{-\Delta\Delta Ct}$ method was employed to calculate the relative expression levels of the genes (Livak and Schmittgen, 2001). When the transcriptomic and qRT-PCR data were combined, the candidate genes appeared to show similar expression patterns (Figure S7).

2.7 Statistical analysis

Statistical analyses were conducted by using SPSS v 26.0 software. All values were expressed as the means ± standard deviations. All the data were tested using one-way ANOVA with Duncan's multiple-range test. The $p < 0.05$ was considered to be statistically significant. The graphs were drawn using GraphPad Prism 8.

3 Results

3.1 Effect of Cd on the growth changes in *Gynostemma pentaphyllum*

With increasing the Cd concentrations, the average root lengths of the Cd treatment groups were significantly reduced by 10.33% ~40.96% compared to that of the control group, except for the Cd5 group (Figure S1A). In addition, with the increase of Cd concentrations, the height of plants also exhibited a notable reduction (Figure S1B). The growth of seedlings displayed visible poisoning symptoms and withered in the Cd200 (200 μM) group. The seedlings treated with Cd25 and Cd100 showed the minimum reduction and significant inhibitory in root length and height, respectively (Figure S1). These also exhibited different growth behavior (Figure 1A), and therefore these two concentrations were chosen for further analysis.

The activities of POD and APX, as well as the concentrations of MDA and proline content, showed a gradual trend with increased Cd stress (Figure 1B). In contrast, there was a notable and consistent decline in SOD activity when compared to the Cd0 group. In addition, the activity CAT was reduced by 24.53% in the Cd 50 group and increased by 22.64% compared with that of the Cd0 group (Figure 1B). Cd-dithizone precipitates were observed in the roots, stems and leaves (Figure 1C). Obvious Cd-dithizone precipitates were also observed in the root tips. Cross-section analysis of the stems showed Cd was mainly located in parenchymatous cells of the cortex. In the leaves, Cd-dithizone precipitates were observed mainly in parenchymatous cells as well as the phloems and xylems of the main veins. However, in the Cd100 group, bright pink polysaccharide staining was seen in the stems and leaves when they were compared with the Cd0 group (Figure 1D). All these results indicated that the *G. pentaphyllum* seedlings could efficiently activate the oxidative enzymes, proline content, Cd transport, and polysaccharides when response to Cd stress.

3.2 Transcriptomics analysis

On average, a total of 42160383 clean reads were obtained from each of the samples (Table S1). The GC content, Q20, and Q30 values of all clear reads were above 45.55%, 97.55%, and 93.16%, respectively, confirming the high reliability of the sequencing outcomes. The clean reads from all samples had a mapping rate of 85.16~86.67% when compared to the reference genome sequence, resulting in the discovery of 25,656 genes. The Pearson correlation coefficient analysis provided evidence of the biological consistency (Figure 2A). In addition, the PCA analysis demonstrated discernible differences in the expression of gene clusters between the control group (Cd0, CK) and the different Cd treatments (Cd25, LC and Cd100, HC) were distinguishable (Figure 2B). 2091 (1018 up- and 1073 down-regulated), 3985 (2010 up- and 1975 down-regulated), and 1811 (1163 up- and 648 down-regulated) DEGs were identified by comparing CK vs LC, CK vs HC, and LC vs HC, respectively (Figure 2C). In all comparison groups, a comprehensive set of 4921 DEGs were screened (Figure 2D and Table S2). Among these, 225 genes were screened that were commonly expressed across all groups (Figure 2D), manifesting that *G. pentaphyllum* activated the expression levels of these genes to cope with varying levels of Cd stress.

3.3 GO and KEGG pathway analysis of DEGs

The GO enrichment analysis confirmed the impact of Cd stress on specific biological functions with the top 20 GO enriched terms (Figure S2 and Table S3). The oxidoreductase activity (GO:0016491), tetrapyrrole binding (GO:0046906) and photosystem (GO:0009521) with enriched GO terms were found

10.3389/fpls.2023.1265971

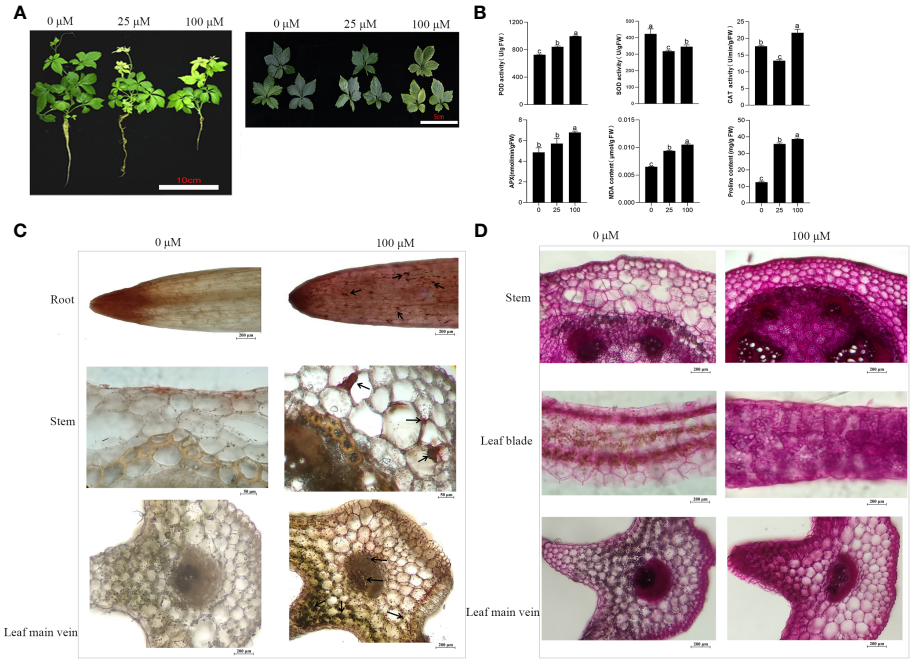

FIGURE 1
Effects of Cd stress in *G. pentaphyllum* seedlings with different concentrations. **(A)** Typical images of the seedlings. **(B)** Antioxidant enzymes (POD, SOD, APX, CAT) activity and MDA, proline content. **(C)** Cd location in the root, stem and leaf. Arrows show the Cd-dithizone precipitates. **(D)** Cell polysaccharides micrographs of stem and leaf. The bars with different lowercase letters represent significant differences based on one-way ANOVA with Duncan's multiple range test ($p < 0.05$).

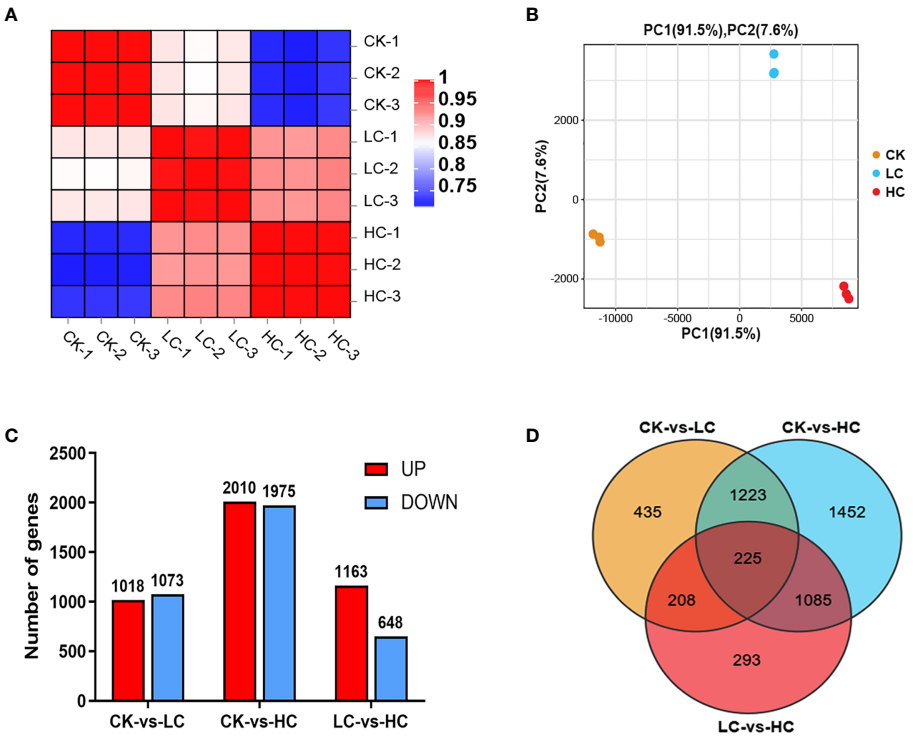

FIGURE 2
Transcriptome data of Cd stress in *G. pentaphyllum* seedlings among the different treatment groups. **(A)** The Pearson correlation coefficient analysis. **(B)** The PCA analysis. **(C)** Analysis of DEGs number. **(D)** Venn graph of DEGs.

mainly in CK vs LC. The protein kinase activity (GO:0004672), protein phosphorylation (GO:0006468) and photosystem (GO:0009521) with enriched GO terms were found mainly in CK vs HC. The DEGs were notably enriched in protein kinase activity (GO:0004672), protein phosphorylation (GO:0006468), and response to chitin (GO:0010200) with LC vs HC comparison. GO analysis indicated that GO terms such as oxidoreductase activity, protein kinase activity and protein phosphorylation could effectively enhance the Cd tolerance of *G. pentaphyllum*.

The KEGG pathway enrichment analysis confirmed the impact of Cd stress on specific biological pathways. A higher number of DEGs were significantly assigned to enrich the metabolic pathways and biosynthesis of secondary metabolites in CK vs LC, CK vs HC, and LC vs HC pairwise groups (Figure S3). In the CK vs LC comparison, several pathways, including phenylpropanoid biosynthesis, plant hormone signal transduction, photosynthesis, starch and sucrose metabolism, alpha-linolenic acid metabolism and flavonoid biosynthesis, showed significant enrichment. The significant enrichment pathways in the comparison between CK and HC included phenylpropanoid biosynthesis, photosynthesis, porphyrin metabolism, starch and sucrose metabolism, MAPK signaling pathway and biosynthesis of various alkaloids. The phenylpropanoid biosynthesis, plant-pathogen interaction, biosynthesis of various alkaloids, MAPK signaling pathway, phenylalanine metabolism and flavonoid biosynthesis were significantly enriched pathways in LC vs HC. According to the KEGG analysis, the response of *G. pentaphyllum* to Cd resulted in the regulation of various pathways, including the biosynthesis of other secondary metabolites, carbohydrate metabolism, amino acid metabolism, lipid metabolism, and signal transduction.

In addition, the detailed functions of the common 225 genes from the three comparison groups were investigated. The xyloglucosyl transferase activity, hydrolase activity, extracellular region, cell wall, oxidoreductase activity and phenylpropanoid metabolic process were mainly enriched in GO terms (Figure 3A). Additionally, these DEGs were categorized based on their involvement in KEGG pathways analysis. The photosynthesis, phenylalanine metabolism, plant hormone signal transduction, indole alkaloid biosynthesis, betalain biosynthesis and MAPK signaling pathway were the most enriched pathways (Figure 3B). These findings indicated that Cd stress had a substantial impact on multiple physiological processes, notably affecting amino acid metabolism, carbon metabolism, signal transduction, and secondary metabolic systems.

3.4 Analysis of genes involved in Cd response

To further elucidate the role of Cd response for 225 genes, the ABC transporters, cell wall, phenylpropanoid biosynthesis, glutathione metabolism, photosynthesis and TFs were selected for analysis (Table 1). There were two genes related to ABC transporters that appeared to be important. ABCG23 (ABC transporter G family member 23) was up-regulated in CK vs HC and LC vs HC, and ABCG8 (ABC transporter family member 8) was down-regulated in all three comparison groups. Three down-regulated xyloglucan endotransglucosylase/hydrolase (XTH31, XTH7 and XTH9) and one down-regulated expansin (EXPA10) involved in the cell wall in the three comparison groups, and two up-regulated XTH23 and XTH2 in CK vs HC and LC vs HC, respectively. Notably, two genes associated with glutathione S-transferase (GST) and related to glutathione metabolism were up-regulated, while six chlorophyll a-b binding protein genes involved in photosynthesis were down-regulated. As many as 12 TFs were also found, underscoring their importance in mediating the Cd response and transportation processes. NAC, ERF4, MYB39, CPRF1 and HSFC1 genes were up-regulated, and bHLH70, COL16, and RL1 genes were down-regulated in three comparison groups. All these *G. pentaphyllum* genes were likely linked to the ability of this species to withstand the response to Cd stress.

3.5 Metabonomics analysis

To explore the response of *G. pentaphyllum* under different Cd stresses, metabolomics analysis was performed using data obtained from UPLC-MS/MS. The control (Cd0, CK) and Cd-treated groups (Cd25, LC and Cd100, HC) were distinguished by PCA and OPLS-DA score plots (Figure S4). In total, 643 metabolites were screened (Figure 4A and Table S4), of which 126 DAMs were identified in all groups (Figure 4B and Table S5). In the CK vs LC, CK vs HC, and LC vs HC comparisons, there were 84, 90 and 81 DAMs, respectively (Figure 4B). The number of DAMs was notably

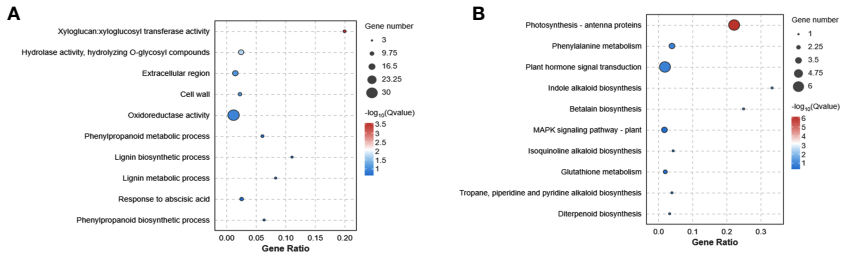

FIGURE 3
The enrichment analysis of GO **(A)** and KEGG **(B)** functional pathways of Cd stress in *G. pentaphyllum*.

10.3389/fpls.2023.1265971

TABLE 1 List of DEGs possibly involved in Cd response of *G. pentaphyllum*.

Unigene ID	Gene annotation	Gene name	Log2 of fold change		
			CK-vs-LC	CK-vs-HC	LC-vs-HC
ABC transporters					
mikado.CM035879.1G2866	ABC transporter G family member 23	ABCG23	-1.20	1.27	2.48
mikado.CM035879.1G3181	ABC transporter G family member 8	ABCG8	-1.08	-2.13	-1.05
cell wall					
mikado.CM035879.1G2690	xyloglucan endotransglucosylase/hydrolase protein 31-like	XTH31	-1.34	-2.51	-1.17
mikado.CM035884.1G2617	xyloglucan endotransglucosylase/hydrolase protein 23	XTH23	-1.98	1.66	3.64
mikado.CM035889.1G1856	xyloglucan endotransglucosylase/hydrolase protein 7	XTH7	-1.68	-2.93	-1.25
mikado.CM035889.1G278	xyloglucan endotransglucosylase/hydrolase protein 9-like	XTH9	-1.03	-2.21	-1.18
mikado.CM035889.1G70	xyloglucan endotransglucosylase/hydrolase 2-like	XTH2	-1.04	2.78	3.82
mikado.CM035882.1G905	expansin-A10-like	EXPA10	-1.73	-2.92	-1.19
Phenylpropanoid biosynthesis					
mikado.CM035879.1G2678	phenylalanine ammonia-lyase-like	PAL	-2.08	-3.99	-1.91
mikado.CM035882.1G2411	phenylalanine ammonia-lyase-like	PAL	-1.52	1.31	2.83
mikado.CM035879.1G2959	peroxidase 2-like	PER2	-4.08	-2.46	1.62
mikado.JAHXMR010000013.1G34	peroxidase 40-like	PER40	-1.31	-2.37	-1.06
Glutathione metabolism					
mikado.CM035881.1G108	glutathione *S*-transferase U9-like	GSTU9	1.10	3.08	1.98
mikado.CM035883.1G1246	glutathione *S*-transferase	GST	2.54	4.24	1.70
Photosynthesis					
mikado.CM035881.1G136	chlorophyll a-b binding protein P4	LHCA-P4	-1.87	-2.91	-1.05
mikado.CM035881.1G1201	chlorophyll a-b binding protein of LHCII type 1-like	CAB	-3.58	-5.41	-1.83
mikado.CM035881.1G1203	chlorophyll a-b binding protein of LHCII type 1-like	CAB	-3.81	-5.01	-1.20
mikado.CM035881.1G1204	chlorophyll a-b binding protein of LHCII type 1-like	CAB	-3.82	-5.16	-1.34
mikado.CM035881.1G1189	chlorophyll a-b binding protein 3	LHCB3	-2.90	-4.09	-1.19
mikado.CM035883.1G565	chlorophyll a-b binding protein 3	LHCB3	-1.41	-2.58	-1.17
Transcription factor					
mikado.CM035879.1G1883	NAC transcription factor 29-like	NAC	1.03	2.63	1.61
mikado.CM035889.1G563	NAC domain-containing protein 35-like	NAC	1.32	3.76	2.44
mikado.CM035881.1G1043	ethylene-responsive transcription factor 4	ERF4	1.02	2.30	1.28
mikado.CM035882.1G1403	zinc finger protein ZAT12-like	ZAT12	-1.09	1.35	2.44
mikado.CM035882.1G3397	transcription factor MYB39	MYB39	1.53	2.94	1.41
mikado.CM035885.1G2092	transcription factor MYB44-like	MYB44	-1.26	1.21	2.47
mikado.CM035887.1G539	transcription factor MYB44-like	MYB44	-1.49	1.19	2.68
mikado.CM035885.1G1089	transcription factor bHLH67	bHLH70	-1.67	-3.20	-1.54
mikado.CM035885.1G894	transcriptional activator TAF-1-like	CPRF1	2.08	3.10	1.02
mikado.CM035886.1G1570	heat stress transcription factor C-1-like	HSFC1	1.03	2.07	1.03

(Continued)

TABLE 1 Continued

Unigene ID	Gene annotation	Gene name	Log2 of fold change		
			CK-vs-LC	CK-vs-HC	LC-vs-HC
mikado.CM035888.1G2676	zinc finger protein CONSTANS-LIKE 16-like	COL16	-1.66	-2.78	-1.12
mikado.CM035889.1G766	protein RADIALIS-like 1	RL1	-4.09	-13.54	-9.45

higher in CK vs HC than in other combinations, indicating that there was a specific impact on the stimulation of certain metabolites by a high concentration of Cd. By performing KEGG enrichment analysis (Figure S5), it was observed that pathways involved with pyruvate metabolism, citrate cycle (TCA cycle), glyoxylate and dicarboxylate metabolism were significantly enriched due to DAMs in pairwise CK vs LC. Arginine and proline metabolism, and the TCA cycle were significantly enriched in pairwise CK vs HC. Flavone and flavonol biosynthesis, valine, leucine and isoleucine biosynthesis were significantly enriched in pairwise LC vs HC. The results strongly implied that these metabolites were essential for *G. pentaphyllum* response to Cd stress.

3.6 Analysis of metabolites involved in Cd response

The Venn diagram analysis showed that 29 DAMs were found to be affected by different Cd concentration treatments (Figure 4C and Table S4). These metabolites showed significant induction with increasing Cd intensity in CK vs LC, CK vs HC, and LC vs HC, including 10 lipids, 7 flavonoids, 3 nucleotides and derivatives, 3 organic acids, 2 amino acids and derivatives, 2 phenolic acids and 2 alkaloids (Figure 4D). Based on the $\log_2$ fold change values, it was evident that 15 DAMs were up-regulated in CK vs LC and CK vs HC, and these included L-isoleucine, L-arginine, 5-aminoimidazole ribonucleotide, and kaempferol-3-O-robinobioside (biorobin). The down-regulated DAMs in CK vs HC and LC vs HC were protocatechuic acid-4-O-glucoside, adenine, guanosine and kaempferol-3-O-(6”-malonyl) galactoside. Therefore, these DAMs can serve as potential candidate markers for the response of *G. pentaphyllum* to Cd stress and act as stimuli for distinguishing exposure to various Cd concentrations.

3.7 Integrated transcriptomics and metabolomics analysis

The histogram depicted the degree of KEGG pathway enrichment when considering both DEGs and DAMs simultaneously (Figure 5). 205 DEGs and 87 DAMs were enriched to 38 metabolic pathways in CK vs LC, 532 DEGs, and 128 DAMs were enriched to 50 metabolic pathways in CK vs HC, and 203 DEGs, and 82 DAMs were enriched to 42 metabolic pathways in LC vs HC. Interestingly, it was intriguing to observe that DEGs and DAMs in CK vs LC were simultaneously significantly enriched in the phenylpropanoid biosynthesis pathway, which was stimulated by low concentrations of Cd. The

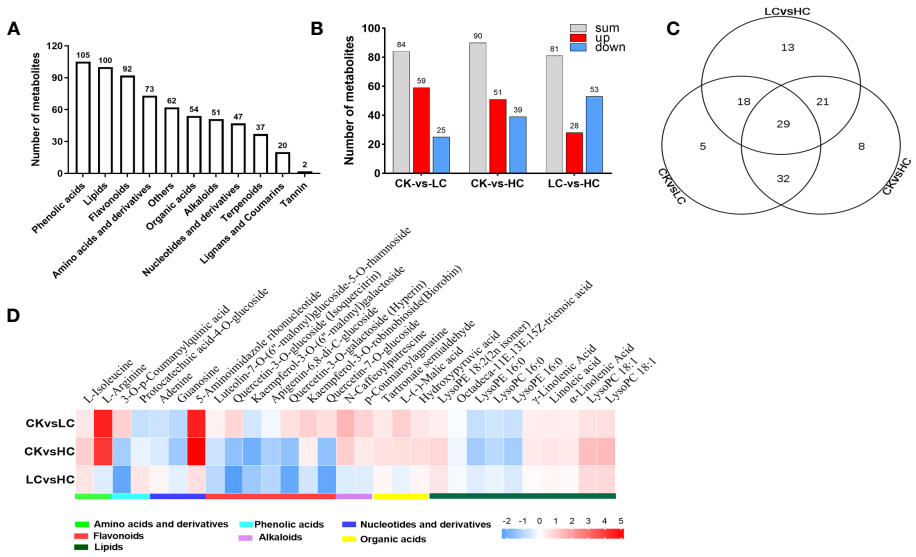

FIGURE 4
Merabolites analysis of *G. pentaphyllum* responding to Cd stress. **(A)** The number of different metabolites types. **(B)** Analysis of DAMs number. **(C)** Venn graph of DAMs. **(D)** Heatmaps of DAMs compared between different groups.

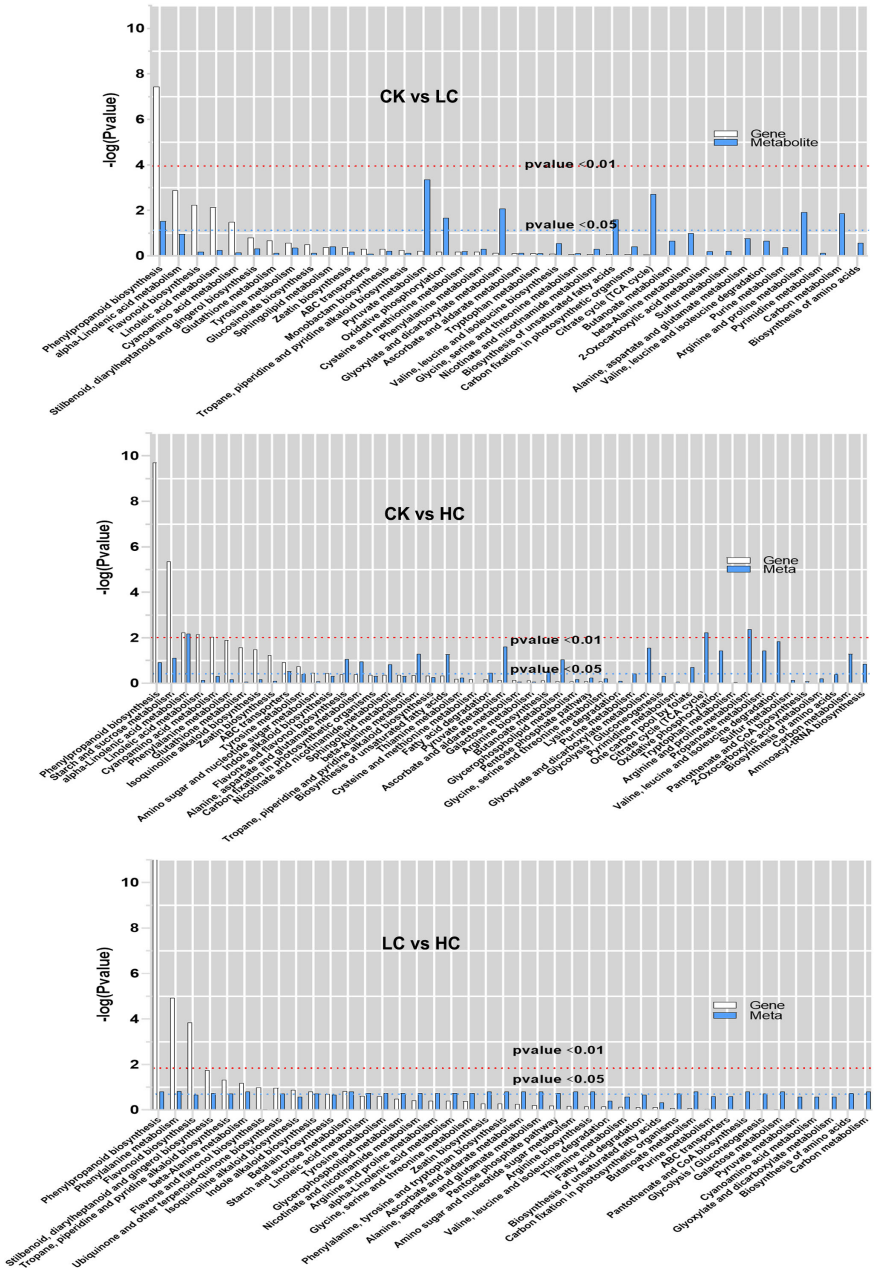

FIGURE 5
KEGG pathway enrichment analysis of DEGs and DAMs in transcriptomic and metabolomics. The abscissa represents metabolic pathways, and the ordinate represents the enriched P-value of DEGs (white) and DAMs (blue), which is represented by -log (p-value) using a threshold of $p < 0.01$ and $p < 0.05$.

phenylpropanoid biosynthesis pathway, starch and sucrose metabolism, alpha-linolenic acid metabolism and ABC transporters were found significantly enriched for DEGs and DAMs simultaneously in CK vs HC. The results suggested that even under high Cd stress, these metabolic pathways were still active and they were stimulated simultaneously to the ABC transporter. The phenylpropanoid biosynthesis pathway, phenylalanine metabolism, beta-alanine metabolism and starch and sucrose metabolism were significantly enriched by DEGs and DAMs simultaneously in LC vs HC, and this showed that these pathways were promoted simultaneously by Cd stress. The phenylpropanoid biosynthesis pathway, starch and sucrose metabolism, alpha-linolenic acid metabolism and ABC transporter were the vital pathways for Cd response of *G. pentaphyllum*.

3.7.1 Potential candidate DEGs and DAMs involved in alpha-linolenic acid metabolism

The 17 genes with significant differences in linolenic acid metabolism were: one PLA2G (secretory phospholipase A2), nine LOX (lipoxygenase), three OPR (12-oxophytodienoic acid reductase), four ACX (acyl-CoA oxidase) genes; and the four

metabolites, a-linolenic acid, 9(S)-HpOTrE, 9(S)-HOTrE and 12-OPDA (Figure 6A). Four ACX, three LOX, three OPR genes, and two metabolites (a-linolenic acid, 9(S)-HOTrE) were up-regulated, while six LOX, one PLA2G gene and two metabolites (9(S)-HpOTrE, 12-OPDA) were down-regulated in Cd treatment, compared to the CK. These findings highlighted ACX, LOX, OPR, and PLA2G as pivotal genes in the alpha-linolenic acid metabolism pathway, which crucially responded to Cd stress. Changes in their expression levels facilitated the synthesis of the crucial metabolites, especially the biosynthesis of jasmonic acid (JA), which is involved in numerous stress responses in plants (Wasternack and Strnad, 2018).

3.7.2 Potential candidate DEGs and DAMs involved in starch and sucrose metabolism

By integrating the analysis of genes and metabolites, 15 DEGs and 5 DAMs were found to be related to starch and sucrose metabolism (Figure 6B). Of these, three SPS (sucrose-phosphate synthase), three SUS (sucrose synthase), two TPS (alpha, alpha-trehalose-phosphate synthase), two AMY (alpha-amylase), one WAXY (granule-bound starch synthase) genes and three metabolites (glucose, alpha-D-glucose-1-phosphate[α-D-Glucose-1P], uridine 5'-diphospho-D-glucose[UDP-glucose]) were up-regulated, while one SUS, one TPS, one TRE (trehalase) genes and two metabolite (D-fructose-6P and trehalose 6-P) were down-regulated in Cd treatment, when compared to the CK. SPS, SUS, TPS, AMY, WAXY, and TRE were identified as key genes in the starch and sucrose metabolism pathway, which significantly responded to Cd stress. The synthesis of the glucose metabolite was triggered by their changes in expression levels.

3.7.3 Potential candidate DEGs and DAMs involved in phenylpropanoid biosynthesis

The 22 genes with significant differences in phenylpropanoid biosynthesis were: thirteen PAL (phenylalanine ammonia-lyase), two C4H (trans-cinnamate 4-monooxygenase), three 4CL (4-coumarate-CoA ligase), three HCT (shikimate O-hydroxy cinnamoyl transferase), one C3H (p-coumaroyl shikimate 3-hydroxylase) genes. There were also six metabolites (phenylalanine, p-coumaric acid, p-coumaroyl-shikimic acid, p-coumaroyl-quinic acid, caffeoylquinic acid and chlorogenic acid) with significant differences (Figure 6C). Nine PAL, two C4H, one 4CL, one HCT gene and three metabolites (p-Coumaric acid, 5-O-p-coumaroylquinic acid, and chlorogenic acid) were up-regulated, while three PAL, two C4H, five 4CL, three HCT, one C3H genes and two metabolites (phenylalanine and p-coumaroyl-shikimic acid) were down-regulated after Cd treatment, when compared to the CK. These results remarkably suggested that Cd stress exerted a substantial influence on the regulation of gene expression and metabolite accumulation in phenylpropanoid biosynthetic pathways of *G. pentaphyllum*.

3.7.4 Potential candidate DEGs and DAMs involved in ABC transporters

A total of 10 ABC transporter family member genes and 5 DAMs were involved in the ABC transporter (Figure 7A). Eight genes and five metabolites were considerably up-regulated, while two genes were significantly down-regulated after Cd treatment, when compared to the CK (Figures 7B, C). These results suggested that the ABC transporter family member gene expression and the accumulation of amino acids within the ABC transporter played important roles in *G. pentaphyllum* response to Cd stress.

3.7.5 Potential candidate TFs involved in Cd response

A network was created depicting the TFs interactions with the key pathway genes to understand the detailed molecular mechanism in response to Cd stress (Figure 8). Five TF families interacted with the phenylpropanoid biosynthesis genes. The ERF and bZIP TFsinteracted with one HCT gene, and three MYB, two MYB_related, and two G2-like TFs interacted with four phenylpropanoid biosynthesis genes (C4H and 4CL), respectively.

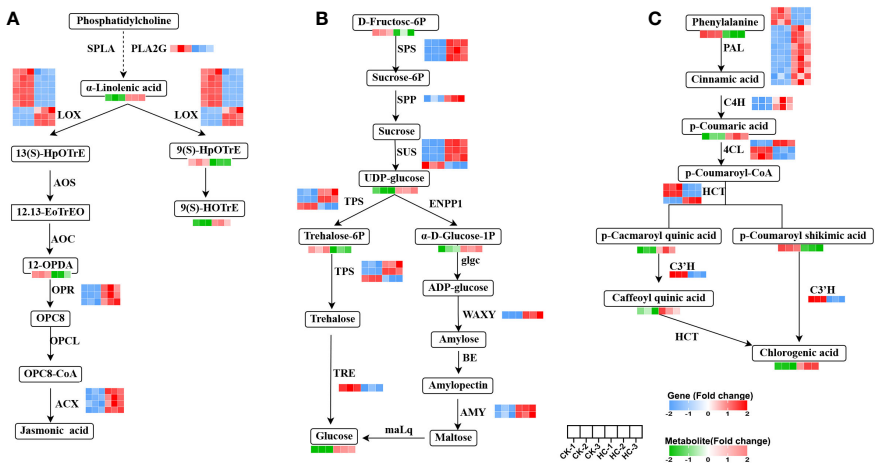

FIGURE 6
Changes of DEGs and DAMs involved in main metabolic pathways in *G. pentaphyllum* with Cd stress. **(A)** Alpha-linolenic acid metabolism. **(B)** Starch and sucrose metabolism. **(C)** Phenylpropanoid biosynthesis pathway.

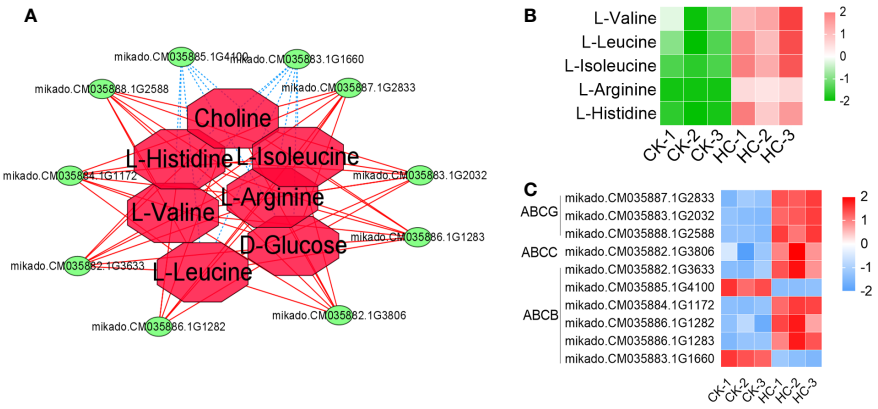

FIGURE 7
Changes of DEGs and DAMs involved in the pathway of ABC transporter in *G. pentaphyllum* with Cd stress. **(A)** The network analysis of DEGs and DAMs. **(B)** Heatmaps of DAMs. **(C)** Heatmaps of DEGs.

Two AMY, one WAXY, one TPS and three SUS genes, which have been demonstrated as hub genes for starch and sucrose metabolism, were also found to be regulated by 10 TF families such as MYB_related, bZIP, BES1 and ERF. Eight TF families interacted with alpha-linolenic acid genes. Four ERF, three bHLH, one WRKY, one GRAS and one AP2 TF interacted with the LOX gene, the FAR TF interacted with four ACX genes, and GATA and MYB TF interacted with the OPR gene, respectively. There were 12 TF families related to MYB, MYB_related, ERF, GRAS, bZIP, WRKY and bHLH which showed significantly different expression levels after Cd treatment (Figure S6). The network analysis indicated that TFs such as MYB, MYB_related, ERF, GRAS, bZIP, WRKY, and bHLH can effectively impact genes associated with phenylpropanoid biosynthesis, starch and sucrose metabolism and alpha-linolenic acid metabolism and improve the Cd response of *G. pentaphyllum*.

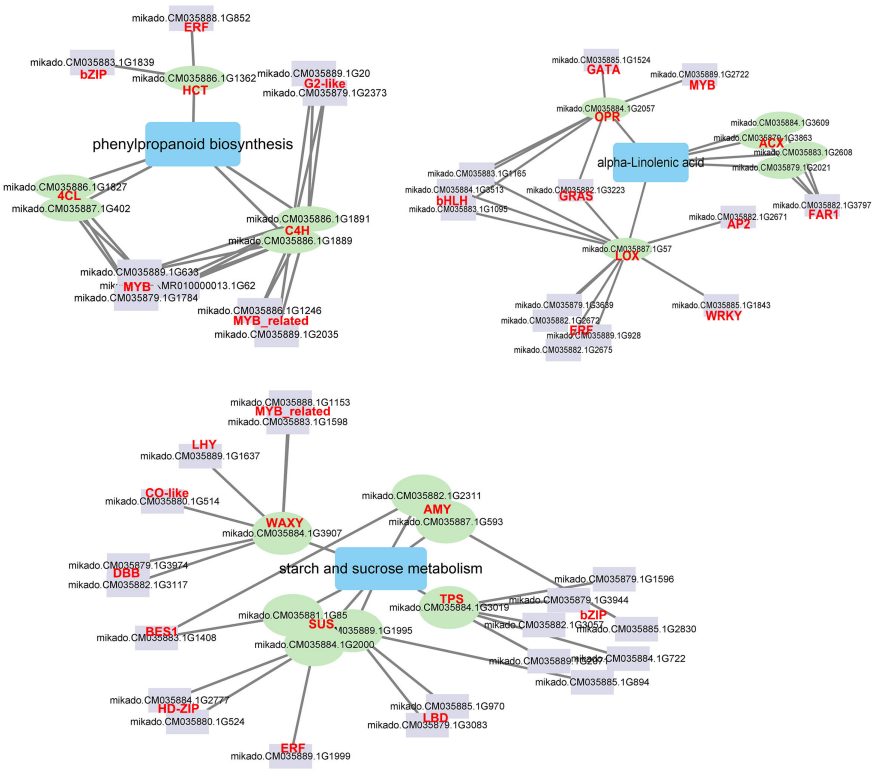

FIGURE 8
The correlation network of TFs and DEGs involved in phenylpropanoid biosynthesis, starch and sucrose metabolism, and alpha-linolenic acid metabolism. The purple rectangle represents TFs, the green circle represents DEGs; the blue rectangle represents metabolic pathway; the line represents interaction with correlation.

4 Discussion

4.1 The effects of Cd on the progression and physiology of *Gynostemma pentaphyllum*

Cd, which is classified as a non-essential heavy metal, can inhibitplant growth which is demonstrated by both physiological and biochemical indicators (Rizwan et al., 2017; Gul et al., 2021). In this study, Cd treatment showed a dwarf phenotype on *G. pentaphyllum*, underscoring the detrimental effects of Cd, and was consistent with previous studies (Li et al., 2022b). Prior research had demonstrated that treatment with Cd in sorghum and wheat seedlings had toxic effects and this was concentration-dependent (Jiao et al., 2023; Zhang et al., 2023). Cd treatment with low concentrations (1.6 mg/L^{-1}) manifested the best stimulatory growth when compared to high concentrations (6.5 mg/L^{-1}) in young peppermint plants (Wang et al., 2023). In this study, *G. pentaphyllum* root growth responds to Cd with stimulation at low doses and inhibition at high doses, as evidenced by the more pronounced growth inhibition in seedlings treated with higher Cd concentrations compared to those treated with lower concentrations (Figures 1A, S1). Previous studies have verified that the Cd accumulation of leaves is higher than that in roots of *Calotropis gigantean* in Cd-polluted environments (Yang et al., 2022). Our results show that Cd mainly accumulates in the root tips, as well as in different structural tissues such as the stems and leaves (Figure 1). Biomass of *G. pentaphyllum* in the aboveground parts is far greater than that of underground portions, and Cd is suggested to be mainly accumulated in the former.

To cope with the cytotoxicity of Cd, plants have developed multiple tolerance mechanisms. The plant's antioxidant defense system, which includes a variety of antioxidant enzymes (POD, SOD, APX and CAT), as well as non-enzymatic antioxidants (proline, soluble sugars and proteins), plays a critical role in scavenging ROS stress generated due to Cd (Rizwan et al., 2016; Rizwan et al., 2017; Li et al., 2023c). Cellulosic polysaccharides, such as pectin, cellulose and hemicellulose, have significant functions in the binding and accumulation of Cd under Cd stress conditions (Wan and Zhang, 2012; Meyer et al., 2015). The activities of POD, CAT, APX, and proline content exhibited a consistent increase with rising concentrations of Cd (Figure 1B). Furthermore, the main components of the cell wall, which are the polysaccharides, were seen to accumulate under Cd stress (Figure 1D). This suggests that activation of antioxidant system and e stimulation of metal binding-related cell wall polysaccharides are the important physiological characteristics of *G. pentaphyllum* in response to Cd exposure.

4.2 The effects of Cd on the transcriptomic and metabolic profiles of *Gynostemma pentaphyllum*

Based on the transcriptomics data, 4921 DEGs were detected across the treatment groups (Figure 2 and Table S2). Analysis of DEGs found that they were associated with specific biological pathways, oxidoreductase activity, protein kinase activity and protein phosphorylation, indicating that the *G. pentaphyllum* seedlings could efficiently activate its defense system and induce the expression of stress-related genes to counter act the Cd toxicity it encountered (Figure S2 and Table S3). In prior studies, it was demonstrated that Cd stress exerted a substantial impact on the expression levels of DEGs which were related to amino acid, carbohydrate, and nucleotide biosynthetic pathways in sorghum and *S. nigrum* (Wang et al., 2022; Jiao et al., 2023). These DEGs exhibited marked induction in the biosynthesis of other secondary metabolites, carbohydrate, amino acid and lipid metabolism, as well as signal transduction pathway, which were stimulated in response of *G. pentaphyllum* to Cd stress (Figure S3). Earlier studies had demonstrated that the XTH gene family was implicated in the production of hemicellulose in the primary cell walls, potentially serving as an essential mechanism for alleviating Cd toxicity in tobacco and *A. thaliana* (Zhu et al., 2013; Han et al., 2014). Studies have also documented that overexpression of *PtoEXPA12* and *TaEXPA2* in tobacco plants increased the resistance to Cd accumulation (Ren et al., 2018; Zhang et al., 2018). XTHs and EXPAs were significantly expressed after Cd treatment to respond to Cd stress (Table 1). In addition, another study showed that XTHs and EXPAs might be candidate genes to regulate cell wall Cd fixation by polysaccharides (Xiao et al., 2020). A greater amount of polysaccharide accumulation was observed in the Cd treatment group (Figure 1D). Therefore, we hypothesized that XTHs and EXPAs could potentially play a role in Cd tolerance by fixation of Cd with cell wall polysaccharides. Nevertheless, further investigations are essential to verify this hypothesis. GST is a crucial enzyme involved in enzymatic detoxification, and it plays a vital role in the ROS-scavenging system by catalyzing the interaction of GST with hydrogen peroxide (Strange et al., 2001). Here we also found that two GST genes were significantly up-regulated after Cd treatment (Table 1), suggesting that high expression of GST genes in the *G. pentaphyllum* may be involved in Cd detoxification, thereby promoting ROS-scavenging. The LHC family gene LHCB3 was found to be specifically expressed after Pb treatment, and it was able to improve the photosynthesis efficiency of *Trifolium pratense* grown under Pb stress (Meng et al., 2022). Notably, the six LHC family genes were down-regulated under Cd stress, and more specifically so at high Cd concentrations (Table 1), when the leaves showed an apparent chlorosis phenotype (Figure 1A), which may regulate the photosynthesis of *G. pentaphyllum*.

From the metabolomics data, 126 DAMs were detected across the treatment groups (Figure 4 and Table S5). These DAMs were involved in pyruvate metabolism, TCA cycle, glyoxylate and dicarboxylate metabolism, arginine and proline metabolism, flavone and flavonol biosynthesis pathway, valine, leucine and isoleucine biosynthesis pathway (Figure S5), indicating that the *G. pentaphyllum* seedlings could efficiently activate these metabolites as a response mechanism to enhancing the tolerance of Cd. The TCA cycle can enhance energy supplies and elevate the Cd stress-related protein levels by increasing the intracellular carbohydrate

content, which ultimately ameliorates Cd toxicity in the roots of *S.nigrum* (Wang et al., 2022). The TCA cycle-related metabolites, citric acid, such as α-ketoglutaric acid, L-(-)-malic acid, succinic acid and fumaric acid, were significantly accumulated after Cd treatment (Tables S3, S4 and Figure 4D), implying that they may play a vital role in maintaining energy support balance during Cd stress. Flavonoids, as secondary metabolites, are mainly used to reduce Cd poisoning through chelation and passivation in plants and these can help to confer Cd resistance (Li et al., 2015; Zhu et al., 2020; Jiao et al., 2023). Flavonoids, including luteolin-7-O-(6''-malonyl) glucoside-5-O-rhamnoside, quercetin-3-O-glucoside (isoquercitrin), quercetin-3-O-galactoside (hyperin), kaempferol-3-O-robinobioside (biorobin) and quercetin-7-O-glucoside were found to be accumulated during Cd treatment (Figure 4D), and there must be is involved in the Cd response of *G. pentaphyllum*. Amino acids can effectively chelate metal ions and reduce the toxic effects of Cd on the rice plant, *Noccaea caerulescens* and *N. praecox* (Zemanová et al., 2017; Xue et al., 2022; Kocaman, 2023). The findings of this study suggest that Cd treatment resulted in significant elevations in the levels of L-isoleucine and L-arginine (Figure 4D), implying that Cd exposure could stimulate the biosynthesis of these amino acids in *G. pentaphyllum*, potentially enhancing stress resistance.

4.3 The effects of Cd on the key metabolic pathways of *Gynostemma pentaphyllum*

Transcriptomics and metabonomics studies have demonstrated that alpha-linolenic acid metabolism plays an important role in tolerance and detoxification to Cd stresses of cotton, rice and fescue, and have identified a significant number of its metabolites and genes that are either induced or inhibited under Cd treatments (Zhu et al., 2018; Zeng et al., 2021; Li et al., 2022a). In this study, a substantial number of DEGs and DAMs were identified that were associated with alpha-linolenic acid metabolism, starch and sucrose metabolism, phenylpropanoid biosynthesis, and ABC transporters as crucial pathways in Cd stress responses in *G. pentaphyllum* seedlings (Figures 5–7). Moreover, alpha-linolenic acid and 12-OPDA metabolites, as well as ACX, LOX, OPR, and PLA2G genes were identified as the key metabolites and genes in this study (Figure 6A), which were related to the production of JA (Ghorbel et al., 2021). JA alleviates Cd toxicity via suppression of Cd uptake and either translocation or reduction of the accumulation of ROS in plants (Lei et al., 2020; Ahmad et al., 2021; Kaushik et al., 2022; Li et al., 2022c). These results suggest that alpha-linolenic acid metabolism was significantly affected by Cd stress, which may have contributed to the impacted key metabolite accumulation and gene expression, thereby promoting JA biosynthesis to alleviate Cd toxicity. Glucose can also alleviate Cd toxicity by enhancing Cd fixation in the cell walls of Arabidopsis roots and sequestering Cd into the vacuoles (Shi et al., 2015). Increased levels of chlorogenic acid in *Kandelia obovata* can reduce Cd and Zn poisoning through its hydroxyl radical scavenging capacity (Chen et al., 2020). It can be speculated that the upregulation of genes involved in the phenylpropanoid biosynthesis pathway together with the increase in chlorogenic acid metabolites is closely related to *G. pentaphyllum* response to Cd stress. The ABC transporter-associated *TaABCC1* and *OsABCC9* genes have been shown to promote Cd compartmentalization in the vacuoles which can enhance Cd tolerance in Cd-tolerant wheat and rice (Yang et al., 2021; Zhang et al., 2023). Our results provide evidence that these key metabolic pathways were significantly responsible for Cd stress, which may have contributed to the impacted key metabolite accumulation and gene expression observed in these conditions.

As crucial transcriptional regulators, WRKY, MYB, and bZIP must play a significant role in the Cd response of plants (Yuan et al., 2018; Li et al., 2023a). Overexpression of *ThDRE1A*, *ThMYC1*, and *ThFEZ* in *T. hispida* decreased the ROS content after Cd treatment by changes in the enzymatic activities of SOD, CAT, and POD (Xie et al., 2023). Overexpression of *PyWRKY75* promoted the absorption and accumulation of Cd, and activated the antioxidant enzymes under Cd stress in poplar (Wu et al., 2022). *PvERF15* positively regulated Cd tolerance by binging to metal response element-binding TF (*PvMTF-1*) (Lin et al., 2017). These findings indicated that TFs are crucial in Cd stress signal transduction, as they interact with various genes associated with Cd uptake, transport, and tolerance, functioning either as transcriptional activators or repressors. Moreover, *AtMYB12* can increase the phenylpropanoid content by activating PAL, C4H, 4CL, and CHS gene expression (Xu et al., 2022). *MeERF72* was found to exert a negative regulatory effect on the expression levels of *MeSuS1* in cassava (Liu et al., 2018). *PuERF12* and *PuMYB44* were identified as candidate TFs that may regulate the expression of *PuLOX2S* in Nanguo pears (Zhang et al., 2022). In this study, MYB, MYB_related, ERF, GRAS, bZIP, WRKY and bHLH could effectively interact with phenylpropanoid biosynthesis, starch and sucrose metabolism and alpha-linolenic acid metabolism pathway genes (Figure 8), suggesting these TFs impact on the accumulation of these metabolites, thereby contributing to the *G. pentaphyllum* response to Cd stress.

A possible model of transcription- and metabolism-driven Cd response mechanisms in *G. pentaphyllum* is shown in Figure 9. Cd could either activate or repress the expression of TFs, including MYB, MYB_related, ERF, GRAS, bZIP, WRKY and bHLH. In addition, phenylpropanoid biosynthesis, starch, and sucrose metabolism, and alpha-linolenic acid metabolism pathway genes were activated and these increased the levels of alpha-linolenic acid, glucose, and chlorogenic acid metabolites. The up-regulated genes such as ABCCs and ABCGs upon Cd application highly activated the synthesis or transport of ABC transporter-related metabolites (L-isoleucine, L-histidine, L-arginine, L-valine, and L-leucine). Taken together, the TFs, ABC transporter genes, and metabolites (i.e. JA, glucose and phenylpropanoid) might all play important roles in *G. pentaphyllum* response to Cd by regulating the activities of antioxidant enzymes and the production of non-enzymatic antioxidants. These would work together to transport, fix, and sequester Cd, thereby inducing the defensive metabolite response for *G. pentaphyllum* to adapt better to the Cd stress. These results provide groundwork for comprehending the Cd response mechanisms in *G. pentaphyllum*. Nevertheless, the functions as well as the biochemical mechanisms of how these TFs, genes, and metabolites perform their tasks require further study.

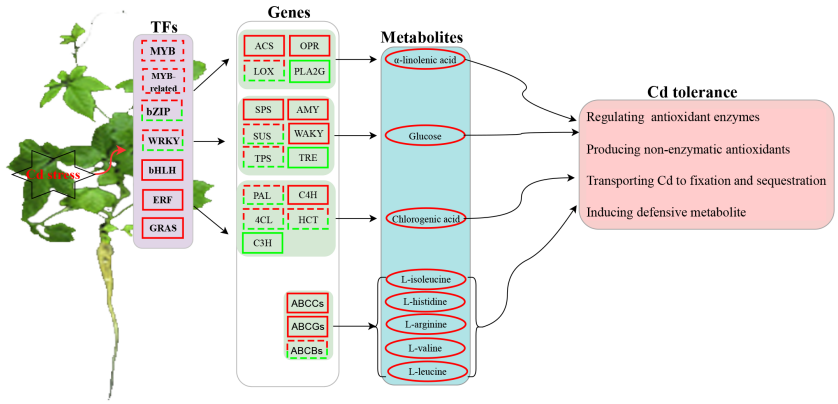

FIGURE 9
A predicted model of transcription- and metabolism-driven mechanisms in *G. pentaphyllum* in response to Cd stress. The square represents the TFs (transcription factors) or genes, and the ellipse represents the metabolites (solid line red: genes up-regulated or metabolites accumulation; solid line green: genes down-regulated; dashed red-green lines: some genes up-regulated or down-regulated).

5 Conclusion

Omics analysis was used to explore the Cd stress response and tolerance mechanism of *G. pentaphyllum*. This study suggests that *G. pentaphyllum* seedlings could significantly activate the POD, CAT and APX enzymatic activities as well as increase the proline and polysaccharide content in response to Cd stress. Transcriptomics analysis revealed that 4921 DEGs responded to Cd stress, and these involved secondary metabolites, carbohydrate metabolism, amino acid metabolism, lipid metabolism, and signal transduction pathways. By using metabolomics analysis, a total of 126 DAMs were identified, and citric acid, flavonoid (diosmetin-7-O-rutinoside, diosmetin-7-O-galactoside and 6-C-methyl kaempferol-3-glucoside) and the amino acids, L-isoleucine and L-arginine were significantly increased after Cd treatment. A large number of candidate genes and metabolites were also identified in alpha-linolenic acid metabolism, starch and sucrose metabolism, phenylpropanoid biosynthesis, and ABC transporters. In addition, MYB, MYB_related, ERF, GRAS, bZIP, WRKY and bHLH TFs may regulate the expression of genes and metabolites accumulation, and all these processes appeared to contribute to *G. pentaphyllum* response to Cd stress.

Data availability statement

The datasets presented in this study can be found in online repositories. The names of the repository/repositories and accession number(s) can be found in the article/Supplementary Material.

Author contributions

YZ: Conceptualization, Data curation, Writing – original draft, Writing – review & editing. LXY: Data Curation, Methodology, Visualization, Investigation. XH: Methodology, Visualization, Investigation. YL: Visualization, Investigation. CW: Visualization, Investigation. QH: Data Curation. LYY: Supervision, Funding acquisition, Resource mobilization, Validation. CP: Project administration, Funding acquisition, Writing – review & editing.

Funding

The authors declare financial support was received for the research, authorship, and/or publication of this article. This work was supported by the National Natural Science Foundation of China (32260071), the National Science Foundation of Guangxi (2021GXNSFAA196027, 2022GXNSFBA035631), the Guangxi Appropriate Technology Development and Promotion project (GZSY-23-06), the Scientific Research funding project of Guangxi Botanical Garden of Medicinal Plants (GYJ202006), and the Key Subjects Construction project of Chinese Medicinal Resources Science (GZXK-Z-20-65).

Acknowledgments

We are grateful to Dr. Dev Sooranna, Imperial College London, for editing the manuscript.

Conflict of interest

The authors declare that the research was conducted in the absence of any commercial or financial relationships that could be construed as a potential conflict of interest.

Publisher's note

All claims expressed in this article are solely those of the authors and do not necessarily represent those of their affiliated organizations, or those of the publisher, the editors and the reviewers. Any product that may be evaluated in this article, or claim that may be made by its manufacturer, is not guaranteed or endorsed by the publisher.

Supplementary material

The Supplementary Material for this article can be found online at: https://www.frontiersin.org/articles/10.3389/fpls.2023.1265971/full#supplementary-material

References

Ahmad, P., Raja, V., Ashraf, M., Wijaya, L., Bajguz, A., and AlYemeni, M. N. (2021). Jasmonic acid (JA) and gibberellic acid (GA(3)) mitigated Cd-toxicity in chickpea plants through restricted cd uptake and oxidative stress management. *Sci. Rep.* 11 (1), 19768. doi: 10.1038/s41598-021-98753-8

Cai, Z., Xian, P., Wang, H., Lin, R., Lian, T., Cheng, Y., et al. (2020). Transcription factor *GmWRKY142* confers cadmium resistance by up-regulating the cadmium tolerance 1-like genes. *Front. Plant Sci.* 11. doi: 10.3389/fpls.2020.00724

Chen, S., Lin, R., Lu, H., Wang, Q., Yang, J., Liu, J., et al. (2020). Effects of phenolic acids on free radical scavenging and heavy metal bioavailability in *kandelia obovata* under cadmium and zinc stress. *Chemosphere* 249, 126341. doi: 10.1016/j.chemosphere.2020.126341

Chen, Y., Li, G., Yang, J., Zhao, X., Sun, Z., and Hou, H. (2021). Role of Nramp transporter genes of Spirodela polyrhiza in cadmium accumulation. Ecotoxicol. *Environ. Saf.* 227, 112907. doi: 10.1016/j.ecoenv.2021.112907

Ghorbel, M., Brini, F., Sharma, A., and Landi, M. (2021). Role of jasmonic acid in plants: the molecular point of view. *Plant Cell Rep.* 40 (8), 1471–1494. doi: 10.1007/s00299-021-02687-4

Gul, I., Manzoor, M., Hashim, N., Shah, G. M., Waani, S. P. T., Shahid, M., et al. (2021). Challenges in microbially and chelate-assisted phytoextraction of cadmium and lead - A review. *Environ. pollut.* 287, 117667. doi: 10.1016/j.envpol.2021.117667

Han, Y., Sa, G., Sun, J., Shen, Z., Zhao, R., Ding, M., et al. (2014). Overexpression of Populus euphratica xyloglucan endotransglucosylase/hydrolase gene confers enhanced cadmium tolerance by the restriction of root cadmium uptake in transgenic tobacco. *Environ. Exp. Bot.* 100, 74–83. doi: 10.1016/j.envexpbot.2013.12.021

He, J., Li, H., Luo, J., Ma, C., Li, S., Qu, L., et al. (2013). A transcriptomic network underlies microstructural and physiological responses to cadmium in Populus x canescens. *Plant Physiol.* 162 (1), 424–439. doi: 10.1104/pp.113.215681

Huo, D., Hao, Y., Zou, J., Qin, L., Wang, C., and Du, D. (2023). Integrated transcriptome and metabonomic analysis of key metabolic pathways in response to cadmium stress in novel buckwheat and cultivated species. *Front. Plant Sci.* 14. doi: 10.3389/fpls.2023.1142814

Jiao, Z., Shi, Y., Wang, J., Wang, Z., Zhang, X., Jia, X., et al. (2023). Integration of transcriptome and metabolome analyses reveals sorghum roots responding to cadmium stress through regulation of the flavonoid biosynthesis pathway. *Front. Plant Sci.* 14. doi: 10.3389/fpls.2023.1144265

Kaushik, S., Sharma, P., Kaur, G., Singh, A. K., Al-Misned, F. A., Shafik, H. M., et al. (2022). Seed priming with methyl jasmonate mitigates copper and cadmium toxicity by modifying biochemical attributes and antioxidants in *Cajanus cajan*. *Saudi J. Biol. Sci.* 29 (2), 721–729. doi: 10.1016/j.sjbs.2021.12.014

Kocaman, A. (2023). Combined interactions of amino acids and organic acids in heavy metal binding in plants. *Plant Signal Behav.* 18 (1), 2064072. doi: 10.1080/15592324.2022.2064072

Kumar, A., Kumari, N., Singh, A., Kumar, D., Yadav, D. K., Varshney, A., et al. (2023). The effect of cadmium tolerant plant growth promoting rhizobacteria on plant growth promotion and phytoremediation: A review. *Curr. Microbiol.* 80 (5), 153. doi: 10.1007/s00284-023-03267-3

Lei, G. J., Sun, L., Sun, Y., Zhu, X. F., Li, G. X., and Zheng, S. J. (2020). Jasmonic acid alleviates cadmium toxicity in Arabidopsis via suppression of cadmium uptake and translocation. *J. Integr. Plant Biol.* 62 (2), 218–227. doi: 10.1111/jipb.12801

Li, Y., Ding, L., Zhou, M., Chen, Z., Ding, Y., and Zhu, C. (2023a). Transcriptional regulatory network of plant cadmium stress response. *Int. J. Mol. Sci.* 24 (5), 4378. doi: 10.3390/ijms24054378

Li, Y., Huang, X., Yu, L., Yao, L., Zhang, Z., He, L., et al. (2022b). Effects of cadmium stress on seedling growth and photosynthetic characteristics of three species of *Gynostemma* plants. *J. Chin. Med. Mater.* 45 (09), 2041–2047. doi: 10.13863/j.issn1001-4454.2022.09.002

Li, Y., Huang, X., Yu, L., Yao, L., Zhou, Y., Wang, C., et al. (2023b). Effects of different hydroponic conditions on the growth and total saponin accumulation of *Gynostemma pentaphyllum*. *Chin. J. Trop. Crops.* 44 (03), 578–588.

Li, J., Lu, H., Liu, J., Hong, H., and Yan, C. (2015). The influence of flavonoid amendment on the absorption of cadmium in Avicennia marina roots. *Ecotoxicol. Environ. Saf.* 120, 1–6. doi: 10.1016/j.ecoenv.2015.05.004

Li, Y., Rahman, S. U., Qiu, Z., Shahzad, S. M., Nawaz, M. F., Huang, J., et al. (2023c). Toxic effects of cadmium on the physiological and biochemical attributes of plants, and phytoremediation strategies: A review. *Environ. pollut.* 325, 121433. doi: 10.1016/j.envpol.2023.121433

Li, L., Yan, X., Li, J., Wu, X., and Wang, X. (2022a). Metabolome and transcriptome association analysis revealed key factors involved in melatonin mediated cadmium-stress tolerance in cotton. *Front. Plant Sci.* 13. doi: 10.3389/fpls.2022.995205

Li, Y., Zhang, S., Bao, Q., Chu, Y., Sun, H., and Huang, Y. (2022c). Jasmonic acid alleviates cadmium toxicity through regulating the antioxidant response and enhancing the chelation of cadmium in rice (Oryza sativa L.). *Environ. pollut.* 304, 119178. doi: 10.1016/j.envpol.2022.119178

Lin, J., Gao, X., Zhao, J., Zhang, J., Chen, S., and Lu, L. (2020). Plant cadmium resistance 2 (*SaPCR2*) facilitates cadmium efflux in the roots of hyperaccumulator *Sedum alfredii* Hance. *Front. Plant Sci.* 11. doi: 10.3389/fpls.2020.568887

Lin, T., Yang, W., Lu, W., Wang, Y., and Qi, X. (2017). Transcription factors PvERF15 and *PvMTF-1* form a cadmium stress transcriptional pathway. *Plant Physiol.* 173 (3), 1565–1573. doi: 10.1104/pp.16.01729

Lin, K., Zeng, M., Williams, D. V., Hu, W., Shabala, S., Zhou, M., et al. (2022). Integration of transcriptome and metabolome analyses reveals the mechanistic basis for cadmium accumulation in Maize. *iScience* 25 (12), 105484. doi: 10.1016/j.isci.2022.105484

Liu, C., Chen, X., Ma, P., Zhang, S., Zeng, C., Jiang, X., et al. (2018). Ethylene responsive factor *MeERF72* negatively regulates sucrose synthase 1 gene in Cassava. *Int. J. Mol. Sci.* 19 (5), 1281. doi: 10.3390/ijms19051281

Liu, X. S., Feng, S. J., Zhang, B. Q., Wang, M. Q., Cao, H. W., Rono, J. K., et al. (2019). *OsZIP1* functions as a metal efflux transporter limiting excess zinc, copper and cadmium accumulation in rice. *BMC Plant Biol.* 19 (1), 283. doi: 10.1186/s12870-019-1899-3

Livak, K. J., and Schmittgen, T. D. (2001). Analysis of relative gene expression data using real-time quantitative PCR and the 2(-Delta Delta C(T)) Method. *Methods* 25 (4), 402–408. doi: 10.1006/meth.2001.1262

Long, T., Hu, R., Cheng, Z., Xu, C., Hu, Q., Liu, Q., et al. (2023). Ethnobotanical study on herbal tea drinks in Guangxi, China. *J. Ethnobiol. Ethnomed.* 19 (1), 10. doi: 10.1186/s13002-023-00579-3

Meyer, C. L., Juraniec, M., Huguet, S., Chaves-Rodriguez, E., Salis, P., Isaure, M. P., et al. (2015). Intraspecific variability of cadmium tolerance and accumulation, and cadmium-induced cell wall modifications in the metal hyperaccumulator Arabidopsis halleri. *J. Exp. Bot.* 66 (11), 3215–3227. doi: 10.1093/jxb/erv144

Nookabkaew, S., Rangkadilok, N., Prachoom, N., and Satayavivad, J. (2016). Concentrations of trace elements in organic fertilizers and animal manures and feeds and cadmium contamination in herbal tea (*Gynostemma pentaphyllum* Makino). *J. Agric. Food Chem.* 64 (16), 3119–3126. doi: 10.1021/acs.jafc.5b06160

Pan, C., Zhou, Y., Yao, L., Yu, L., Qiao, Z., Tang, M., et al. (2023). Amomum tsaoko DRM1 regulate seed germination and improve heat tolerance in Arabidopsis. *J. Plant Physiol.* 286, 154007. doi: 10.1016/j.jplph.2023.154007

Qiao, K., Gong, L., Tian, Y., Wang, H., and Chai, T. (2018). The metal-binding domain of wheat heavy metal ATPase 2 (*TaHMA2*) is involved in zinc/cadmium

tolerance and translocation in Arabidopsis. *Plant Cell Rep.* 37 (9), 1343–1352. doi: 10.1007/s00299-018-2316-3

Ren, Y., Chen, Y., An, J., Zhao, Z., Zhang, G., Wang, Y., et al. (2018). Wheat expansin gene *TaEXPA2* is involved in conferring plant tolerance to Cd toxicity. *Plant Sci. (Amsterdam Neth.)* 270, 245–256. doi: 10.1016/j.plantsci.2018.02.022

Rizwan, M., Ali, S., Adrees, M., Ibrahim, M., Tsang, D. C. W., Zia-Ur-Rehman, M., et al. (2017). A critical review on effects, tolerance mechanisms and management of cadmium in vegetables. *Chemosphere* 182, 90–105. doi: 10.1016/j.chemosphere.2017.05.013

Rizwan, M., Ali, S., Adrees, M., Rizvi, H., Zia-Ur-Rehman, M., Hannan, F., et al. (2016). Cadmium stress in rice: toxic effects, tolerance mechanisms, and management: a critical review. *Environ. Sci. pollut. Res. Int.* 23 (18), 17859–17879. doi: 10.1007/s11356-016-6436-4

Shahid, M., Dumat, C., Khalid, S., Niazi, N. K., and Antunes, P. M. C. (2017). Cadmium bioavailability, uptake, toxicity and detoxification in soil-plant system. *Rev. Environ. Contam. Toxicol.* 241, 73–137. doi: 10.1007/398_2016_8

Shi, Y. Z., Zhu, X. F., Wan, J. X., Li, G. X., and Zheng, S. J. (2015). Glucose alleviates cadmium toxicity by increasing cadmium fixation in root cell wall and sequestration into vacuole in Arabidopsis. *J. Integr. Plant Biol.* 57 (10), 830–837. doi: 10.1111/jipb.12312

Strange, R. C., Spiteri, M. A., Ramachandran, S., and Fryer, A. A. (2001). Glutathione-S-transferase family of enzymes. *Mutat. Res.* 482 (1-2), 21–26. doi: 10.1016/s0027-5107(01)00206-8

Su, C., Li, N., Ren, R., Wang, Y., Su, X., Lu, F., et al. (2021). Progress in the medicinal value, bioactive compounds, and pharmacological activities of *Gynostemma pentaphyllum*. *Molecules* 26 (20), 6249. doi: 10.3390/molecules26206249

Suntararuks, S., Yoopan, N., Rangkadilok, N., Worasuttayangkurn, L., Nookabkaew, S., and Satayavivad, J. (2008). Immunomodulatory effects of cadmium and Gynostemma pentaphyllum herbal tea on rat splenocyte proliferation. *J. Agric. Food Chem.* 56 (19), 9305–9311. doi: 10.1021/jf801062z

Tarazona, S., Garcia-Alcalde, F., Dopazo, J., Ferrer, A., and Conesa, A. (2011). Differential expression in RNA-seq: a matter of depth. *Genome Res.* 21 (12), 2213–2223. doi: 10.1101/gr.124321.111

Trapnell, C., Williams, B. A., Pertea, G., Mortazavi, A., Kwan, G., van Baren, M. J., et al. (2010). Transcript assembly and quantification by RNA-Seq reveals unannotated transcripts and isoform switching during cell differentiation. *Nat. Biotechnol.* 28 (5), 511–515. doi: 10.1038/nbt.1621

Wan, L., and Zhang, H. (2012). Cadmium toxicity: effects on cytoskeleton, vesicular trafficking and cell wall construction. *Plant Signal Behav.* 7 (3), 345–348. doi: 10.4161/psb.18992

Wang, J., Chen, X., Chu, S., You, Y., Chi, Y., Wang, R., et al. (2022). Comparative cytology combined with transcriptomic and metabolomic analyses of *Solanum nigrum* L. in response to Cd toxicity. *J. Hazard. Mater.* 423 (Pt B), 127168. doi: 10.1016/j.jhazmat.2021.127168

Wang, B., Lin, L., Yuan, X., Zhu, Y., Wang, Y., Li, D., et al. (2023). Low-level cadmium exposure induced hormesis in peppermint young plant by constantly activating antioxidant activity based on physiological and transcriptomic analyses. *Front. Plant Sci.* 14. doi: 10.3389/fpls.2023.1088285

Wasternack, C., and Strnad, M. (2018). Jasmonates: news on occurrence, biosynthesis, metabolism and action of an ancient group of signaling compounds. *Int. J. Mol. Sci.* 19 (9), 2539. doi: 10.3390/ijms19092539

Wei, Z., Zhongbing, C., Xiuqin, Y., Luying, S., Huan, M., and Sixi, Z. (2023). Integrated transcriptomics and metabolomics reveal key metabolic pathway responses in Pistia stratiotes under Cd stress. *J. Hazard. Mater.* 452, 131214. doi: 10.1016/j.jhazmat.2023.131214

Wu, X., Chen, Q., Chen, L., Tian, F., Chen, X., Han, C., et al. (2022). A WRKY transcription factor, *PyWRKY75*, enhanced cadmium accumulation and tolerance in poplar. *Ecotoxicol. Environ. Saf.* 239, 113630. doi: 10.1016/j.ecoenv.2022.113630

Xiao, Y., Wu, X., Liu, D., Yao, J., Liang, G., Song, H., et al. (2020). Cell wall polysaccharide-mediated cadmium tolerance between two *Arabidopsis thaliana* ecotypes. *Front. Plant Sci.* 11. doi: 10.3389/fpls.2020.00473

Xie, Q., Wang, Y., Wang, D., Li, J., Liu, B., Liu, Z., et al. (2023). The multilayered hierarchical gene regulatory network reveals interaction of transcription factors in response to cadmium in *Tamarix hispida* roots. *Tree Physiol.* 43 (4), 630–642. doi: 10.1093/treephys/tpac147

Xu, Q., Wang, C., Li, S., Li, B., Li, Q., Chen, G., et al. (2017). Cadmium adsorption, chelation and compartmentalization limit root-to-shoot translocation of cadmium in rice (*Oryza sativa* L.). *Environ. Sci. pollut. Res. Int.* 24 (12), 11319–11330. doi: 10.1007/s11356-017-8775-1

Xu, J., Zhu, J., Lin, Y., Zhu, H., Tang, L., Wang, X., et al. (2022). Comparative transcriptome and weighted correlation network analyses reveal candidate genes involved in chlorogenic acid biosynthesis in sweet potato. *Sci. Rep.* 12 (1), 2770. doi: 10.1038/s41598-022-06794-4

Xue, W., Zhang, C., Huang, Y., Wang, C., Zhang, X., and Liu, Z. (2022). Rice organs concentrate cadmium by chelation of amino acids containing dicarboxyl groups and enhance risks to human and environmental health in Cd-contaminated areas. *J. Hazard. Mater.* 426, 128130. doi: 10.1016/j.jhazmat.2021.128130

Yang, G., Fu, S., Huang, J., Li, L., Long, Y., Wei, Q., et al. (2021). The tonoplast-localized transporter *OsABCC9* is involved in cadmium tolerance and accumulation in rice. *Plant Sci.* 307, 110894. doi: 10.1016/j.plantsci.2021.110894

Yang, J., Li, L., Zhang, X., Wu, S., Han, X., Li, X., et al. (2022). Comparative transcriptomics analysis of roots and leaves under Cd stress in *Calotropis gigantea* L. *Int. J. Mol. Sci.* 23 (6), 3329. doi: 10.3390/ijms23063329

Yuan, J., Bai, Y., Chao, Y., Sun, X., He, C., Liang, X., et al. (2018). Genome-wide analysis reveals four key transcription factors associated with cadmium stress in creeping bentgrass (*Agrostis stolonifera* L.). *PeerJ* 6, e5191. doi: 10.7717/peerj.5191

Yuan, H. M., Liu, W. C., Jin, Y., and Lu, Y. T. (2013). Role of ROS and auxin in plant response to metal-mediated stress. *Plant Signal Behav.* 8 (7), e24671. doi: 10.4161/psb.24671

Zemanová, V., Pavlík, M., and Pavlíková, D. (2017). Cadmium toxicity induced contrasting patterns of concentrations of free sarcosine, specific amino acids and selected microelements in two Noccaea species. *PloS One* 12 (5), e0177963. doi: 10.1371/journal.pone.0177963

Zeng, T., Fang, B., Huang, F., Dai, L., Tang, Z., Tian, J., et al. (2021). Mass spectrometry-based metabolomics investigation on two different indica rice grains (*Oryza sativa* L.) under cadmium stress. *Food Chem.* 343, 128472. doi: 10.1016/j.foodchem.2020.128472

Zhang, H., Ding, Y., Zhi, J., Li, X., Liu, H., and Xu, J. (2018). Over-expression of the poplar expansin gene PtoEXPA12 in tobacco plants enhanced cadmium accumulation. *Int. J. Biol. Macromol.* 116, 676–682. doi: 10.1016/j.ijbiomac.2018.05.053

Zhang, D., Liu, J., Zhang, Y., Wang, H., Wei, S., Zhang, X., et al. (2023). Morphophysiological, proteomic and metabolomic analyses reveal cadmium tolerance mechanism in common wheat (Triticum aestivum L.). *J. Hazard. Mater.* 445, 130499. doi: 10.1016/j.jhazmat.2022.130499

Zhang, X., Su, H., Yang, J., Feng, L., Li, Z., and Zhao, G. (2019). Population genetic structure, migration, and polyploidy origin of a medicinal species *Gynostemma pentaphyllum* (Cucurbitaceae). *Ecol. Evol.* 9 (19), 11145–11170. doi: 10.1002/ece3.5618

Zhang, L., Zhang, L. L., and Kang, L. N. (2022). Promoter cloning of PuLOX2S gene from "Nanguo" pears and screening of transcription factors by Y1H technique. *J. Food Biochem.* 46 (10), e14278. doi: 10.1111/jfbc.14278

Zhu, H., Ai, H., Cao, L., Sui, R., Ye, H., Du, D., et al. (2018). Transcriptome analysis providing novel insights for Cd-resistant tall fescue responses to Cd stress. *Ecotoxicol. Environ. Saf.* 160, 349–356. doi: 10.1016/j.ecoenv.2018.05.066

Zhu, H., Ai, H., Hu, Z., Du, D., Sun, J., Chen, K., et al. (2020). Comparative transcriptome combined with metabolome analyses revealed key factors involved in nitric oxide (NO)-regulated cadmium stress adaptation in tall fescue. *BMC Genomics* 21 (1), 601. doi: 10.1186/s12864-020-07017-8

Zhu, X. F., Wang, Z. W., Dong, F., Lei, G. J., Shi, Y. Z., Li, G. X., et al. (2013). Exogenous auxin alleviates cadmium toxicity in Arabidopsis thaliana by stimulating synthesis of hemicellulose 1 and increasing the cadmium fixation capacity of root cell walls. *J. Hazard. Mater.* 263 (Pt 2), 398–403. doi: 10.1016/j.jhazmat.2013.09.018

frontiers | Frontiers in Plant Science

TYPE Original Research
PUBLISHED 09 November 2023
DOI 10.3389/fpls.2023.1286699

OPEN ACCESS

EDITED BY
Poonam Yadav,
Banaras Hindu University, India

REVIEWED BY
Yiyong Zhu,
Nanjing Agricultural University, China
Hongmei Cai,
Huazhong Agricultural University, China

*CORRESPONDENCE
Shibin Gao
shibingao@163.com

†These authors have contributed equally to this work and share first authorship

RECEIVED 31 August 2023
ACCEPTED 19 October 2023
PUBLISHED 09 November 2023

CITATION
Zhang H, Luo B, Liu J, Jin X, Zhang H, Zhong H, Li B, Hu H, Wang Y, Ali A, Riaz A, Sahito JH, Iqbal MZ, Zhang X, Liu D, Wu L, Gao D, Gao S, Su S and Gao S (2023) Functional analysis of *ZmG6PE* reveals its role in responses to low-phosphorus stress and regulation of grain yield in maize. *Front. Plant Sci.* 14:1286699. doi: 10.3389/fpls.2023.1286699

Functional analysis of *ZmG6PE* reveals its role in responses to low-phosphorus stress and regulation of grain yield in maize

Hongkai Zhang[1,2,3†], Bowen Luo[1,2,3†], Jin Liu[1,2,3], Xinwu Jin[1,2,3], Haiying Zhang[1,2,3], Haixu Zhong[1,2,3], Binyang Li[1,2,3], Hongmei Hu[1,2,3], Yikai Wang[1,2,3], Asif Ali[1], Asad Riaz[4], Javed Hussain Sahito[2,5], Muhammad Zafar Iqbal[2], Xiao Zhang[1,2,3], Dan Liu[1,2,3], Ling Wu[1,2,3], Duojiang Gao[2], Shiqiang Gao[2], Shunzong Su[3] and Shibin Gao[1,2,3*]

[1]State Key Laboratory of Crop Gene Exploration and Utilization in Southwest China, Sichuan Agricultural University, Chengdu, Sichuan, China, [2]Maize Research Institute, Sichuan Agricultural University, Chengdu, Sichuan, China, [3]Key Laboratory of Biology and Genetic Improvement of Maize in Southwest Region, Ministry of Agriculture, Chengdu, Sichuan, China, [4]Centre of Excellence for Plant Success in Nature and Agriculture, The Queensland Alliance for Agriculture and Food Innovation (QAAFI), The University of Queensland, St. Lucia, Brisbane, QLD, Australia, [5]Key Laboratory of Wheat and Maize Crops Science, College of Agronomy, Henan Agricultural University, Zhengzhou, China

A previous metabolomic and genome-wide association analysis of maize screened a glucose-6-phosphate 1-epimerase (*ZmG6PE*) gene, which responds to low-phosphorus (LP) stress and regulates yield in maize's recombinant inbred lines (RILs). However, the relationship of *ZmG6PE* with phosphorus and yield remained elusive. This study aimed to elucidate the underlying response mechanism of the *ZmG6PE* gene to LP stress and its consequential impact on maize yield. The analysis indicated that ZmG6PE required the Aldose_epim conserved domain to maintain enzyme activity and localized in the nucleus and cell membrane. The *zmg6pe* mutants showed decreased biomass and sugar contents but had increased starch content in leaves under LP stress conditions. Combined transcriptome and metabolome analysis showed that LP stress activated plant immune regulation in response to the LP stress through carbon metabolism, amino acid metabolism, and fatty acid metabolism. Notably, LP stress significantly reduced the synthesis of glucose-1-phosphate, mannose-6-phosphate, and β-alanine-related metabolites and changed the expression of related genes. *ZmG6PE* regulates LP stress by mediating the expression of *ZmSPX6* and *ZmPHT1.13*. Overall, this study revealed that *ZmG6PE* affected the number of grains per ear, ear thickness, and ear weight under LP stress, indicating that *ZmG6PE* participates in the phosphate signaling pathway and affects maize yield-related traits through balancing carbohydrates homeostasis.

KEYWORDS

maize, low-phosphorus stress, ZmG6PE, transcriptomics, metabonomics

1 Introduction

Maize (*Zea mays* ssp. *mays*) is a globally imperative food, feed, and industrial feedstock crop (Niu et al., 2020). Growth of maize requires a substantial amount of phosphorus-based fertilizer, but it is a finite and non-renewable resource. It is concerning that phosphate rock is projected to be depleted within the next 100 years (Kochian, 2012). Roots absorb the phosphorus mainly in the form of inorganic phosphate (Pi), but microorganisms and metal cations quickly convert it into unavailable forms by precipitation and fixation (Liu et al., 2005; Chiou and Lin, 2011; Ham et al., 2018). Therefore, determining how to reduce the amount of phosphorus fertilizer while maintaining a high crop yield is an important problem deserving further research.

Plants have evolved complex and sophisticated regulatory systems to adjust to a varying soil phosphate environment to maintain growth. Phosphate starvation-induced (*PSI*) genes are mainly regulated by Phosphate Starvation Response-SYG1/PH081/XPRI (PHR-SPX) modules that play key roles in this network (Puga et al., 2014; Wang et al., 2018). Phosphate Starvation Response (PHR) transcription factors (a sub-family of MYB TFs) positively regulate *PSI* gene expressions by attaching to PHR1 Binding Sequence (P1BS) (Rubio et al., 2001; Zhou et al., 2008). The activities of PHRs are balanced post-transcriptionally by negatively regulating TFs known as SPX-domains containing proteins through recognizing soluble inositol polyphosphates (InsPs) levels in cytosol and preventing the binding of PHRs to P1BS (Wang et al., 2014; Wild et al., 2016). Phosphate Starvation Response (PHR) transcription factors induced the transcription of plasma membrane-localized phosphate transporter (PHT), which is a class of phosphorous transporters playing crucial roles in phosphate uptake/distribution/redistribution in plants and enhances the transmembrane transport of phosphate under LP stress (Gonzalez et al., 2005; Sun et al., 2012). By elucidating the mechanism of phosphorus tolerance, it is possible to effectively improve maize yield while reducing the application of phosphorous fertilizer.

Previous studies have shown that LP stress activates physiological responses in plants, leading to changes in the levels of related metabolites. Under phosphate deficiency stress, plant pile up starch and sugar, which promotes carbon allocation to the root system and facilitates further soil phosphorus excavation. Low-phosphorus (LP) stress affects starch metabolism, inhibits photosynthesis in crop plants, and triggers starch accumulation in leaves (Gibson, 2004; Morcuende et al., 2007). Sucrose upregulated the activities of D-glucuronic acid, 5-O-methylembelin, and N-acetyl-L-phenylalanine during LP conditions (Yang et al., 2020). A metabolome analysis showed that LP stress accelerated glycolysis in the roots of soybean and repressed malic acid synthesis (Li et al., 2022). Under LP conditions, LP-tolerant maize genotypes induce the transcription of genes regulating plant hormone signaling, acid phosphatase, and metabolite, which promote phosphorus absorption and utilization in maize (Jiang et al., 2017).

Metabolomic profiling was conducted on six LP tolerant and sensitive maize inbred lines, and combined with genome-wide association analysis, five genes were identified to be responsive to LP stress. Among them, *ZmG6PE* not only influenced phosphorus content but also responded to LP stress by affecting ear diameter and ear rows (Luo et al., 2019). Glucose-6-phosphate 1-epimerase catalyzes the conversion of anomeric forms of α-D-glucose-6-phosphate to β-D-glucose-6-phosphate at the branch point of D-glucose metabolism (Wurster and Hess, 1972; Wurster and Hess, 1973; Graille et al., 2006). This enzyme is named YMR099C in *Saccharomyces cerevisiae*, and it has an active site with sulfate ion connected by an arginine clamp formed by a side chain of two highly conserved residues of arginine (Graille et al., 2006). A bioinformatics analysis of the budding yeast's entire genome for finding the putative target of transcription factor "GCN4 (a positive transcription factor in yeast, binds general control promoters at all 5' TGACTC 3' sequences)" has shown that GCN4 regulates YMR099C (Schuldiner et al., 1998). Trz1 (a tRNA 3' end processing endonuclease), Nuc1 (a mitochondrial nuclease), and YMR099C form highly stable heterohexamers consisting of two copies of each of the three subunits, which suggests that YMR099C and Trz1 may regulate apoptotic nucleases activity (Ma et al., 2017). Glucose-6-phosphate is an important metabolite in multiple metabolic pathways, such as glycolysis and the pentose phosphate pathway (Wu et al., 2018; He et al., 2021). Glycolysis is a metabolic precursor for producing biomass and supplies cellular energy (Tanner et al., 2018). The pentose phosphate pathway can additionally catalyze the production of nicotinamide adenine dinucleotide phosphate (NADPH) using glucose-6-phosphate dehydrogenase (G6PDH) for providing reductive power (Jiang et al., 2012; Fouquerel et al., 2014). Currently, research on glucose-6-phosphate 1-epimerase mainly focuses on microorganisms and has not been studied in plants (Wurster and Hess, 1972; Wurster and Hess, 1973; Graille et al., 2006). Therefore, the current study would be a reference for investigating the future study of glucose-6-phosphate-1 epimerase in plants.

In sum, ZmG6PE is a glucose-6-phosphate 1-epimerase that regulates carbohydrate homeostasis. ZmG6PE is an enzyme that catalyzes α-D-glucose-6-phosphate to β-D-glucose-6-phosphate and participates in glycolysis and the pentose phosphate pathway. By biochemical, omics, molecular biology, and genetics analysis, the present study found that the gene function of *ZmG6PE* affects maize yield and the mechanism of response to LP stress. This research provides new directions for the improvement of maize yield and the study of LP tolerance mechanisms.

2 Material and methods

2.1 Plant materials and growth conditions

Using the CRISPR/Cas9 (Clustered regularly interspaced short palindromic repeats/CRISPR-associated protein 9) system, the *ZmG6PE* gene was knocked out in the maize inbred line KN5585 by the *Agrobacterium tumefaciens*-mediated transformation method. The mutation site was detected using ZmG6PE-KO-F and R primers (Supplementary Table S1). Maize Research Institute of Sichuan Agricultural University provided the seeds of maize inbred lines 178 and 9782 for the current study.

Seeds were surface disinfected with 2% (V/V) sodium hypochlorite (NaClO) solution for 30 min, then rinsed with ddH_2O 5-6 times to remove the NaClO solution and were

germinated on filter paper in dark conditions at 28 °C for 3 days. Germinated seeds were cultivated in sand and gravel for 7 days, and the seedlings with consistent growth were selected to remove embryos and endosperms. The seedlings were then transferred to plastic containers containing 25 L of half Hoagland nutrient solution concentration for adaptation cultivation for 3 days. Subsequently, the nutrient solution was replaced with normal-phosphorus (NP) (1 mM) or LP (1 μM) solution, also containing 6 mM KNO_3, 4 mM Ca $(NO_3)_2.4H_2O$, 1 mM or 1 μM $NH_4H_2PO_4$, 100 μM EDTA-Fe, 2 mM $MgSO_4.7H_2O$, 46 μM H_3BO_3, 0.146 μM $MnCl_2.4H_2O$, 0.76 μM $ZnSO_4.7H_2O$, 0.016 μM $(NH4)_6Mo_7O_{24}.4H_2O$, and 0.32 μM $CuSO_4.5H_2O$, with a pH of 5.5 (Luo et al., 2019). The nutrient solution was replaced every three days, and the ventilation pump was operated for 8 hours every day.

2.2 Reverse transcription-quantitative polymerase chain reaction (RT-qPCR) analysis

The total RNA was extracted using a Trizol reagent kit (Invitrogen, Thermo Fisher Scientific, Waltham, MA, USA) according to manufacturer's instructions. The reverse transcription of the first strand was performed using the PrimeScript™ II 1st Strand cDNA synthesis kit by following the manual's instructions. The RT-qPCR was carried out using the FastStart Essential DNA Green Master (Roche, Germany) on a CFX96 Real-Time PCR Detection System (Bio-Rad, USA) following the kit's protocol. The total reaction volume consisted of 5 μl 2× FastStart Essential DNA Green Master, with 0.5 μl each of forward and reverse primers and 1 μl of the cDNA template. The amplification procedure was set as follows; initial denaturation at 95 °C for 10 min; then 40 cycles of 95 °C for 5 sec, 60 °C for 15 sec, and 72 °C for 20 sec; and finally, a melting curve process. The quantitative PCR primers were designed using Beacon Designer™ 7 software and shown in Supplementary Table S1. All experiments were conducted thrice with three technical replicates.

2.3 Total phosphorus content measurements in plants

Approximately 0.2 g of dry tissues were digested using H_2SO_4-H_2O_2 at 420 °C to obtain the total phosphorus. Then, phosphorus in the supernatant was measured using Auto Discrete Analyzers (SmartChem 200).

2.4 Measurements of starch and soluble sugar

A starch content kit (Code: G0507W, Grace Biotechnology Co., LTD, Suzhou, China) was used to assay the starch content of maize leaves. The soluble sugar content of maize leaves was determined by a plant soluble sugar content kit (Code: KT-1-Y, Comin Biotechnology Co., LTD, Suzhou, China). The determination of the starch and soluble sugar was carried out strictly according to the operation instructions of the kit.

2.5 Purification and activity analysis of ZmG6PE

The full-length coding sequence of *ZmG6PE* was introduced into the pCold vector and then transformed into Rosetta-competent cells. The optimal protein induction conditions were screened, and the culture broth was scaled up under the optimal conditions. The extracted protein was purified and stored at -80 °C for future use.

Kinetic reactions were carried out at 25 °C in 50 mM KCl, 50 mM imidazole, and 8 mM $MgSO_4$ at pH 7.6. The absorbance values were measured at 340 nm using the SW18-MV Stopped Flow Spectrophotometer (Applied Photophysics, UK). Reactions were started by mixing equivalent volumes of equilibrated 2 mM nicotinamide adenine dinucleotide phosphate ($NADP^+$) and 60 μM glucose-6-phosphate with 160 units/mL glucose-6-phosphate dehydrogenase from *Leuconostoc mesenteroides* (Sigma) and the varying concentrations of ZmG6PE (Graille et al., 2006).

2.6 RNA-seq analysis

For transcriptome analysis, the second fully expanded leaves and the roots of the mutant *zmg6pe* and wild type (WT) plants were harvested and frozen in liquid nitrogen immediately. The Trizol reagent (Invitrogen Life Technologies) was used to isolate total RNA from the leaves and roots following the manual's instructions. RNA's concentration, integrity, and quality were measured and assessed using a NanoDrop™ spectrophotometer (Thermo Scientific). RNA samples were prepared using 3 μg RNA as the initial input material. The RNA-seq and data analysis were carried out by the Shanghai Bioprofile Biotechnology Co., Ltd. (Shanghai, China). The sequencing libraries of the total RNA were constructed using the TruSeq RNA Sample Preparation Kit (Illumina, San Diego, CA, USA), and the RNA libraries were sequenced by the Illumina NovaSeq 6000 platform. Each sample consists of three plants with three replicates.

2.7 Metabolite analysis

For extracting the metabolites, samples were weighed, dried, and transferred into a 1.5 mL Eppendorf tube containing a 5 mm tungsten bead and grounded in a grinding mill for 1 min with 65 Hz power. Metabolite extraction was performed using an ultrasonic shaker with 1 mL precooled acetonitrile, methanol, and H_2O (v:v:v, 2:2:1) at 4 °C for 1 hour. The mixture was placed at -20 °C for 1 hour and then centrifuged at 14,000 rpm for 20 min at 4 °C. The supernatants were collected and placed in a cryogenic vacuum for concentration. Subsequently, the UPLC-ESI-Q-Orbitrap-MS system (UHPLC, Shimadzu Nexera X2 LC-30AD, Shimadzu, Japan) coupled with Q-Exactive Plus (Thermo Scientific, San Jose, CA, USA) was used for Metabolomic profiling.

The MS-DIAL software was used to process the raw MS data for retention time correction, peak alignment, and peak area extraction. The accuracy mass (mass tolerance < 0.02 Da) and MS/MS data (mass tolerance < 0.02 Da) were matched with Kyoto Encyclopedia of Genes and Genomes (KEGG), MassBank, and other available databases, and a standard self-built metabolite library was used to differentiate and recognize the metabolites. Only variables greater than 50% non-zero measured values within at least 1 group were processed in extracted ion features. The samples used in the metabolite analysis were consistent with those used in the RNA-seq analysis.

2.8 Subcellular localization of ZmG6PE

To localize ZmG6PE protein in the cell, a full-length coding sequence of *ZmG6PE* was introduced into pCAMBIA2300-35S-eGFP using the NovoRec® plus One Step PCR Cloning Kit (NovoProtein, Shanghai, China). The constructs were mobilized into an *Agrobacterium* strain GV3101 by the freeze-thaw method and cultured for up to the required density. Then cells were collected and resuspended in a solution comprising 10 mM magnesium chloride and 150 mM acetosyringone (Sigma-Aldrich). Fluorescence signals of the eGFP in *Nicotiana benthamiana* leaves were detected with a confocal microscope (Leica).

3 Results

3.1 ZmG6PE is localized in the nucleus and cell membrane

The subcellular localization of the ZmG6PE protein was determined by introducing the combined vector pCAMBIA2300-P35S: ZmG6PE-eGFP and the nucleus localization signal (NLS) into tobacco leaves using transient transformation. The signals derived from ZmG6PE overlapped with the autofluorescence of NLS (Figure 1A). Similarly, the signals derived from ZmG6PE overlapped with the autofluorescence of the cell membrane localization signal (CMLS) (Figure 1A). These results confirmed the prediction of CELLO v.2.5, showing that the ZmG6PE protein is localized in the nucleus and cell membrane.

3.2 ZmG6PE exhibits glucose-6-phosphate 1-epimerase activity

ZmG6PE protein sequence from 41 to 308 amino acids encodes a conserved domain of Aldose_epim (Supplementary Figure S1A). To explore the critical peptide sequences of ZmG6PE, we divided ZmG6PE into two sections, ZmG6PE-Front (ZmG6PE-F) and ZmG6PE-Behind (ZmG6PE-B). Both sections (ZmG6PE-F and ZmG6PE-B) contained the conserved Aldose_epim domains of ZmG6PE (41 to 308 aa), ZmG6PE-F (41 to 147 aa), and ZmG6PE-B (1 to 161 aa) (Supplementary Figure S1A). Unlike ZmG6PE-B and ZmG6PE-F, the tertiary structure of ZmG6PE had a putative active site pocket (Supplementary Figure S1B). To investigate the biochemical characteristics of ZmG6PE, His-tagged ZmG6PE, ZmG6PE-B, and ZmG6PE-F proteins were expressed in *Escherichia coli* (Supplementary Figure S1C). The enzymatic activity of protein during the interconversion of α- and β-D-glucose-6-phosphate anomers is explained by the specificity of the enzymes participating in sugar metabolism (Figure 1B). Enzyme kinetics and enzyme-linked immunosorbent assay (ELISA) were employed to evaluate the ZmG6PE activity. The results showed that ZmG6PE had glucose-6-phosphate 1-epimerase activity (Figures 1C, D); however, the ZmG6PE protein segments (ZmG6PE-F and ZmG6PE-B) exhibited negligible glucose-6-phosphate 1-epimerase activity (Figures 1C, D).

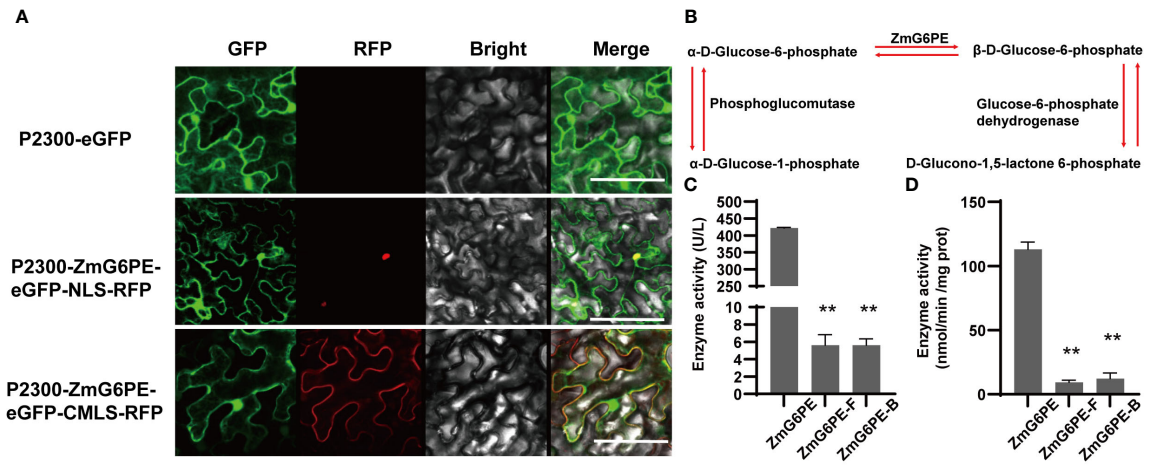

FIGURE 1
Subcellular localization of ZmG6PE and enzyme activity. **(A)** Subcellular localization of ZmG6PE in tobacco leaves, bar = 10 nm. **(B)** Schematic representation of enzymatic reactions involving glucose-6-phosphate anomer. **(C)** Determination of the enzyme activity by the enzyme kinetic method. **(D)** Determination of enzyme activity using an ELISA kit. "**" represents $p < 0.01$ by single factor ANOVA test.

3.3 The *zmg6pe* mutant is sensitive to LP stress

To investigate the functions of *ZmG6PE* in maize, two independent transgenic lines (*zmg6pe-1* and *zmg6pe-2*) were developed using CRISPR/Cas9. The line *zmg6pe-1* has a 421 bp deletion, while *zmg6pe-2* has a 1 bp deletion (Supplementary Figure S2A), thus both result in a truncated protein. During the seedling stage, the fresh weight and phosphorus content in *zmg6pe* decreased compared to WT (Supplementary Figures S2B-D), but there was no significant difference at maturity (Supplementary Figures S2E-G). To determine whether *ZmG6PE* responds to LP stress, 10 days old maize seedlings were further raised in a hydroponic system and treated with 1 mM and 1 μM phosphate conditions for 15 days (Figure 2A and Supplementary Figure S2H). Under both NP and LP conditions, the leaves and roots fresh weight of the *zmg6pe* significantly reduced (Figures 2B, C); LP tolerance coefficients in *zmg6pe* leaves and roots were reduced (Supplementary Figures S2I, J). Starch contents decreased under NP conditions in leaves of *zmg6pe* (Figures 2D). Soluble sugar contents decreased under LP conditions in the leaves of *zmg6pe* (Figures 2E). The phosphorus contents decreased under NP conditions in *zmg6pe* leaves than in WT leaves (Figure 2F). However, the phosphorus content in roots did not significantly change in WT and *zmg6pe* (Figure 2G). It significantly reduced the expression levels of *ZmG6PE* in the leaves and roots of the *zmg6pe* mutant (Figures 2H, I).

3.4 Functional analysis of the *ZmG6PE* gene in response to LP stress

The *zmg6pe* had reduced fresh weight under LP conditions, indicating that *ZmG6PE* responds to LP stress. In order to elucidate the regulatory mechanisms of *ZmG6PE* under LP conditions, comparative transcriptome analysis of leaves and roots was conducted between WT and *zmg6pe* mutant. There were 2072,

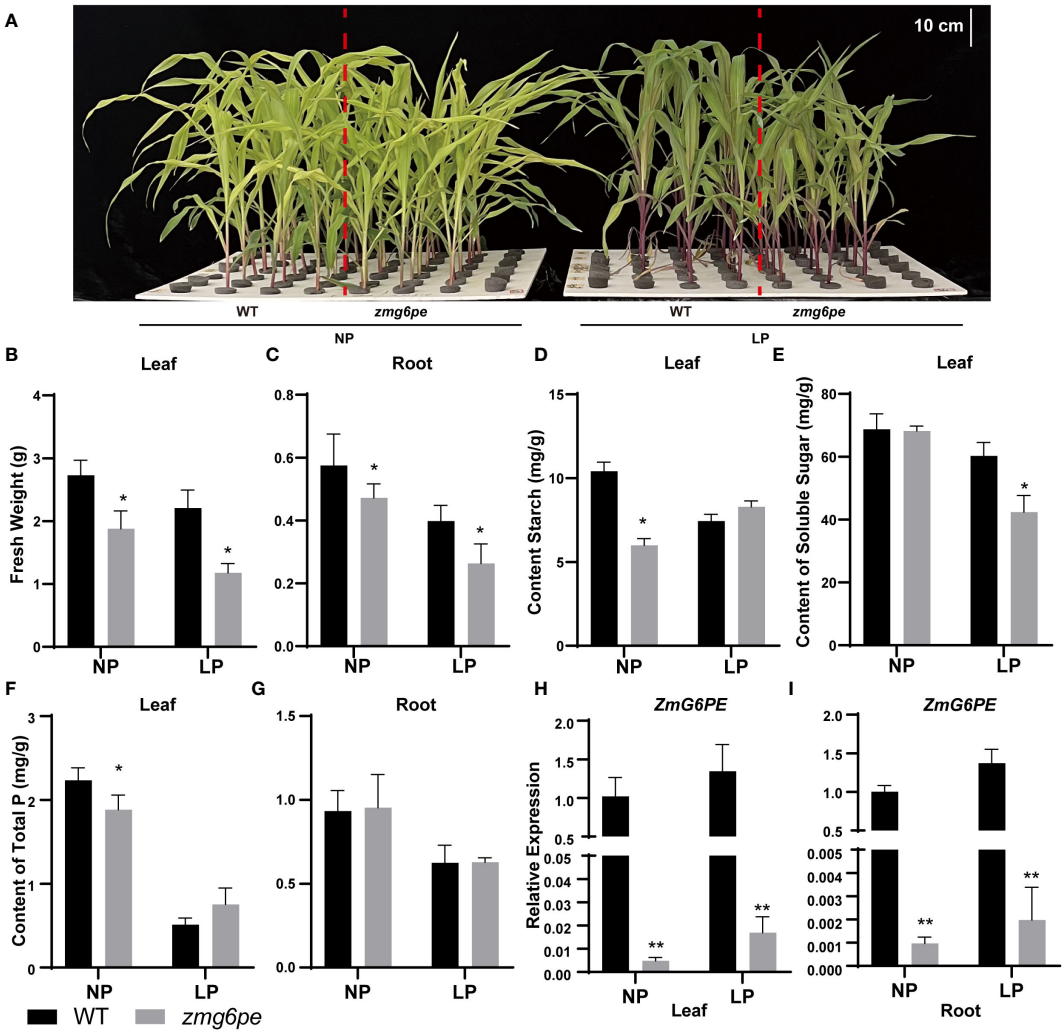

FIGURE 2
Responses of *ZmG6PE* in hydroponic culture with different phosphorous concentrations. **(A)** WT and *zmg6pe* mutants under NP and LP hydroponics. **(B, C)** Fresh weight. **(D)** Starch content. **(E)** Soluble sugar content. **(F, G)** Total phosphorus content. **(H, I)**. The expression levels of *ZmG6PE* gene. "*" represents 0.01< p < 0.05, "**" represents p < 0.01, single factor ANOVA test.

2367, and 504 overlapping differentially expressed genes (DEGs) in leaves (L), roots (R), and both in leaves and the roots (LR), respectively (Supplementary Figure S3A).

KEGG pathway enrichment analysis revealed that terms related to carbon metabolism, amino acid synthesis and metabolism, fatty acid metabolomic pathway, immune regulation, and plant hormones were highly enriched in L (Figure 3A and Supplementary Figure S3B). While terms related to carbon, amino acid and fatty acid metabolisms, amino acid degradation, secondary metabolites, and vitamins were highly enriched in the R (Figure 3B and Supplementary Figure S3C); similarly, the terms related to carbon, amino acid and fatty acid metabolisms, amino acid degradation, immune regulation, and secondary metabolites were enriched in LR (Figure 3C and Supplementary Figure S3D). As such, LP stress activated the immune response system in seedlings, and *ZmG6PE* regulated carbon, amino acid and fatty acid metabolisms, plant hormones, and secondary metabolites in response to LP stress.

3.5 Metabolite analysis of the *ZmG6PE* gene in response to LP stress

Transcriptome KEGG enrichment analysis showed that LP treatment affected carbon and amino acid metabolisms, indicating that LP stress caused variations in the synthesis and metabolism of nitrogen- and carbon-related compounds. To further investigate the function of *ZmG6PE*, comparative metabolomic analyses were performed in *zmg6pe* and WT seedlings under LP and NP conditions. There were 164, 96, and 26 overlapping differentially expressed metabolites (DEMs) found in L, R, and LR, respectively (Supplementary Figure S4A). The metabolomic analysis of L and R samples revealed significant KEGG pathway enrichment in carbon metabolism, amino acid metabolism, genetic material synthesis, and immune regulation, with some more enrichments of fatty acid metabolism, enzymatic activity, and energy metabolism in L (Figures 3D-F and Supplementary Figures S4B-D). These results indicate that LP stress may activate the plant immune response system, whereas *ZmG6PE* affects LP stress by regulating the above-mentioned metabolic pathways.

3.6 Combined analysis revealing *ZmG6PE* involved in KEGG pathways in response to LP stress

A combined transcriptome and metabolome analysis was performed to examine whether there is any association between gene expression patterns and metabolite accumulation. Enrichment analysis revealed 42, 15, and 12 KEGG pathways in L, R, and LR, respectively (Supplementary Figure S5A). In the combined analysis of the KEGG pathways, the carbon metabolism, amino acid synthesis and metabolism, glycolysis/gluconeogenesis, secondary metabolite biosynthesis, and carbon fixation in photosynthesis were found enriched in L (Supplementary Figure S5B). In R, galactose metabolism, starch and sucrose metabolism, carotenoid metabolism, photosynthesis, and secondary metabolite biosynthesis were highly enriched (Supplementary Figure S5C). In LR, significant enrichment was observed in carbon, amino acid and fatty acid metabolisms, and immune regulation (Supplementary Figure S5D). These results indicate that LP stress may activate immune regulation and the *ZmG6PE* gene affects LP stress by regulating primary and secondary metabolism.

The combined network analysis found that α-D-glucose-1 phosphate in the glycolysis/gluconeogenesis pathway and D-mannose-6 phosphate in fructose and mannose metabolism differed significantly (Figure 3G). The pathway map showed significant reductions in α-D-glucose-1 phosphate and D-mannose-6 phosphate. Zm00001eb244910, Zm00001eb121400, Zm00001eb159720, and *ZmG6PE* gene expression levels decreased, while Zm00001eb293670, Zm00001eb018480, Zm00001eb059230, Zm00001eb101090, Zm00001eb283530, Zm00001eb260710, Zm00001eb154520, and Zm00001eb167360 gene expression levels increased. These results indicate that glucose-1-phosphate- and mannose-6-phosphate-related genes and metabolites respond to LP stress.

The pathway map showed significant reduction in β-alanine (Figure 3H). Zm00001eb066680 gene expression level decreased, while Zm00001eb399220, Zm00001eb431200, Zm00001eb189920, Zm00001eb408260, and Zm00001eb420190 gene expression levels increased. These results indicate that β-alanine genes and metabolites respond to LP stress.

3.7 Expression of *ZmSPX2* and *ZmPHT1.13* are down-regulated in *zmg6pe* mutant

Phosphate Starvation Response (PHR) transcriptional factors are the central regulatory factors regulating the activities of LP-responsive genes in the LP regulatory network (Nilsson et al., 2007; Zhou et al., 2008; Lu et al., 2020). The phosphate transporter (PHT) mediates the absorption and transport of Pi in the plant rhizosphere (Shin et al., 2004; Sun et al., 2012). SYG1/PH081/XPRI (SPX) is a negative regulator of PHR, and regulates phosphorus transport and homeostasis in plants (Liu et al., 2010). To further explore the pathways that regulate the phosphorus signal and expression levels of *PSI* genes were investigated. Transcriptome analysis of *PSI* genes revealed that LP treatment promoted the expression of *ZmSPXs* (*ZmSPX1*, *ZmSPX2*, *ZmSPX3*, *ZmSPX4*, and *ZmSPX6*) and *ZmPHTs* (*ZmPHT1.2* and *ZmPHT1.13*), ut the expression of *ZmPHRs* (*ZmPHR1, ZmPHR2*, and *ZmPHR3*) did not show significant changes (Figures 4A–J). Interestingly, regardless of phosphorus status, the expression levels of *ZmSPX2* and *ZmPHT1.13* in *zmg6pe* were significantly lower than WT in both L and R (Figures 4B, J). The RT-qPCR (Figures 4K, L) confirmed the above results, suggesting that *ZmG6PE* is probably involved in responding to LP stress by mediating expressions of *ZmSPX2* and *ZmPHT1.13*. Under LP conditions, the lack of significant differences in phosphorus content between WT and *zmg6pe* mutants might be attributed to the enhanced expression of *ZmSPX2*, which inhibits the expression of *ZmPHRs* and *ZmPHT1.13*.

10.3389/fpls.2023.1286699

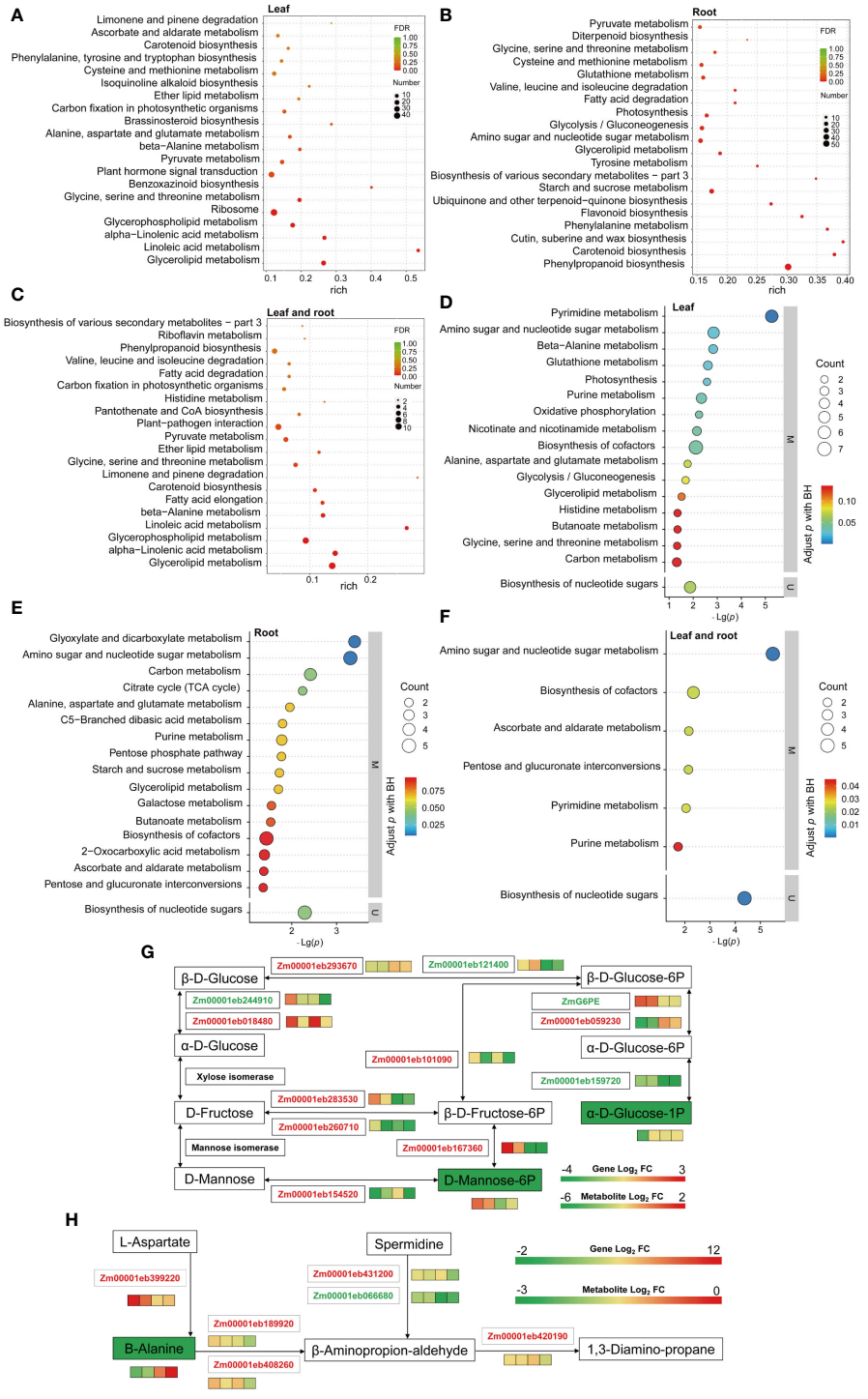

FIGURE 3
KEGG pathway enrichment analysis performed on the DEGs and DEMs, and channel heat map analysis. **(A–C)** KEGG enrichment analysis of the overlapping DEGs in leaves, roots, and shared in leaves and roots, respectively. **(D–F)** KEGG enrichment analysis of the overlapping DEMs in leaves, roots, and shared in leaves and roots, respectively. **(G)** Glycolysis/gluconeogenesis, fructose, and mannose metabolic pathways involve phosphorus transport in leaves and roots. **(H)** The β-alanine metabolism involves phosphorus transport in leaves and roots. Boxes are WT-NP-L vs. WT-LP-L, *zmg6pe*-NP-L vs. *zmg6pe*-LP-L, WT-NP-R vs. WT-LP-R, and *zmg6pe*-NP-R vs. *zmg6pe*-LP-R from left to right. Red and green fonts indicate upregulated and downregulated genes, respectively. Green and red solid squares indicate downregulated and upregulated metabolites, respectively.

10.3389/fpls.2023.1286699

3.8 ZmG6PE regulates the yield-related traits of maize grains

To assess the effects of ZmG6PE on yield-related traits, we investigated the yield-related data for 2021-Qujing (QJ) and 2022-Chongzhou (CZ) grown materials. Results showed that the ear length, ear weight, 100-grain weight, and number of grains per ear were significantly difference in the *zmg6pe* compared to WT (Supplementary Table S2). Besides this, the grain size in *zmg6pe* was significantly smaller (Figure 5A). Moreover, the sugar contents increased, and starch contents decreased in the *zmg6pe* compared to the WT (Figures 5B, C). The phosphate content in the *zmg6pe* was significantly lower than in WT (Figure 5D). The observation of paraffin sections revealed that grain filling in WT was normal at 7 days after pollination (DAP). In contrast, *zmg6pe* showed abnormal grain filling (Figure 5E). At 15 DAP, the starch particles in the WT seeds were fully packed, while *zmg6pe* had irregular cavities. The red box area of the *zmg6pe* had a significantly larger cavity than WT (Figure 5E). The *ZmG6PE* gene expression levels significantly decreased at 7 and 15 DAP in the *zmg6pe* (Figure 5F). The above results demonstrate that the *ZmG6PE* gene affects maize yield.

3.9 Biparental segregation population validation/haplotype analysis

To investigate the effects of ZmG6PE on yield under LP conditions, the yield-related traits of RILs derived from inbred lines 178 and 9782 were measured. The amplification of the *ZmG6PE* gene coding sequences in the inbred lines 178 and 9782

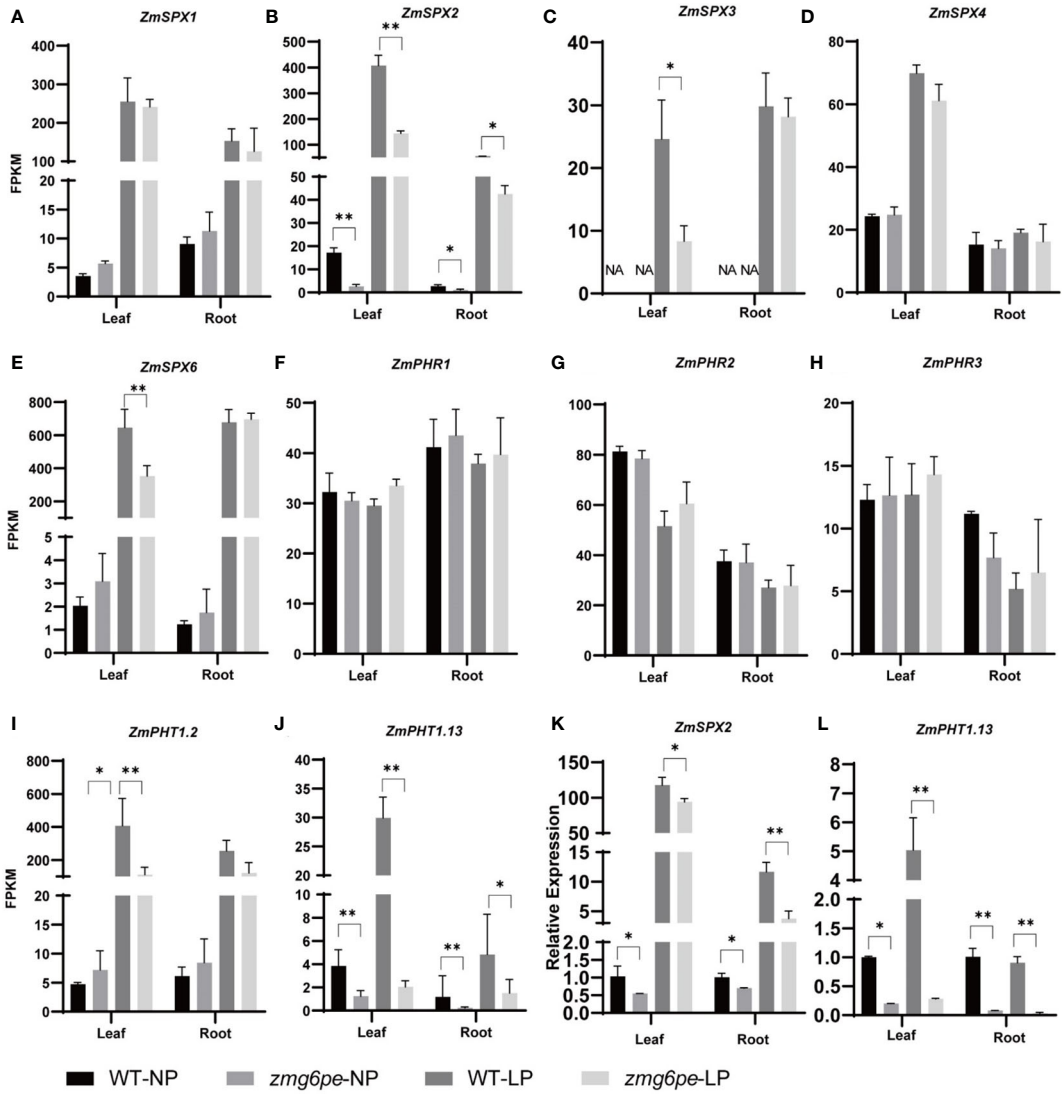

FIGURE 4
Analysis of PSI genes expression levels. **(A–J)** Expression levels (FPKM) of *ZmSPX1*, *ZmSPX2*, *ZmSPX3*, *ZmSPX4*, *ZmSPX6*, *ZmPHR1*, *ZmPHR2*, *ZmPHR3*, *ZmPHT1.2*, and *ZmPHT1.13*, respectively, in leaves and roots under NP and LP conditions. **(K, L)** Expression levels of *ZmSPX2* and *ZmPHT1.13* in leaves and roots under NP and LP, respectively, by RT-qPCR. Values are given as the mean ± SD and indicate the average FPKM values from three biological replicates of RNA-seq libraries. "*" represents $p < 0.05$, and "**" represents $p < 0.01$ by single factor ANOVA test.

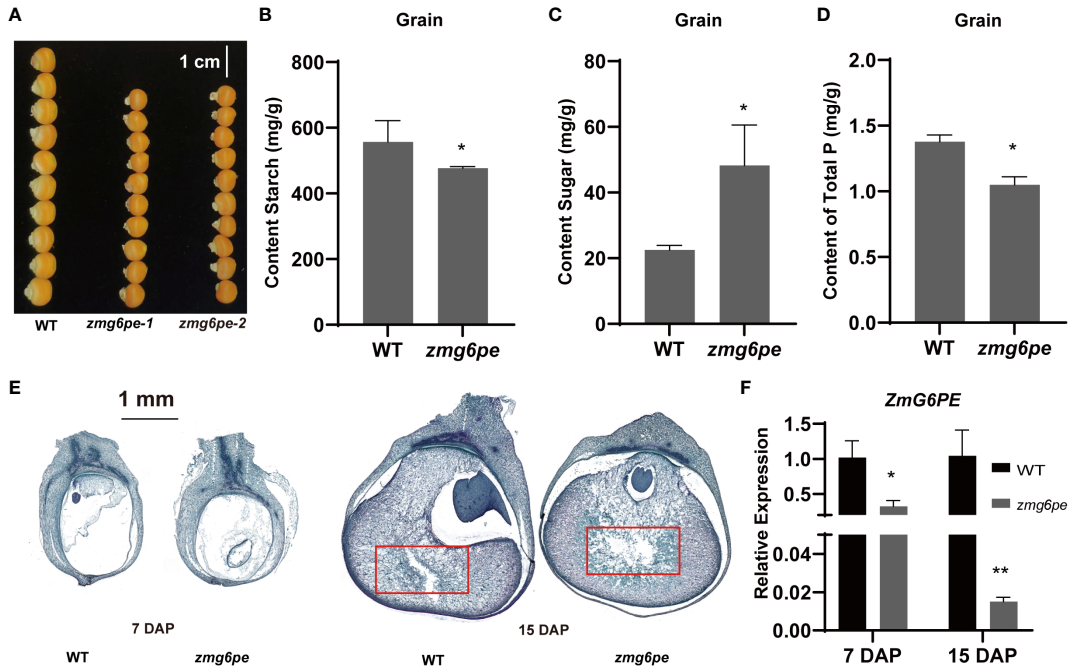

FIGURE 5
Analysis of maize kernel development. **(A)** Grain size. **(B–D)** Content of the grain's starch, sugar, and total phosphorus, respectively. **(E)** Paraffin section of grains at 7 and 15 DAP. **(F)** The expression levels of ZmG6PE in grain were measured at 7 and 15 DAP. "*" represents $p < 0.05$, "**" represents $p < 0.01$ by single factor ANOVA test.

revealed no differences (Supplementary Figure S6A). However, an insertion or deletion (Indel) was detected in the promoter sequence of the *ZmG6PE* gene in two inbred lines, with a 23 bp deletion in inbred line 178 compared to inbred line 9782 (Supplementary Figure S6B), which could be classified into two haplotypes (178 genotypes and 9782 genotypes) (Supplementary Figure S6C). Genotype statistics were performed on the RILs, and the yield-related traits were researched from the Wenjiang Farm in 2013 and the Bifengxia Farm in 2014 under LP conditions. Row number per panicle, number of grains per row, ear length, ear thickness, shaft ear thickness and ear weight of genotype 178 were significantly lower than those of genotype 9782 (Figures 6A–F). In inbred line 9782, the expression of the *ZmG6PE* gene varied with changes in the phosphorus concentration, while in inbred line 178, gene expression was unaffected by the phosphorus concentration (Figure 6G). These results indicate that ZmG6PE plays a role in maize yield and phosphorus content.

4 Discussion

4.1 ZmG6PE is a key enzyme that supports life activities

Anomeric carbon is essential in glycan reactions and quickly provides metabolites for physiological processes (Gomes et al., 2015). Glucose-6-phosphate has two forms of α and β anomers (Wurster and Hess, 1972; Wurster and Hess, 1973; Graille et al., 2006). The isomerization of α-D-glucose-6-phosphate by glucose-6-phosphate isomerase produces fructose 6-phosphate (Aguilar-Pontes et al., 2018). Phosphoglucomutase catalyzes the reversible isomerization of α-D-glucose-6-phosphate to glucose-1-phosphate, which is converted into ADP-glucose (precursor of starch synthesis) by ADP-glucose-pyrophosphorylase (Geigenberger et al., 2004; Zeeman et al., 2007). Combined analysis reveals significant differences in glucose-1-phosphate levels, and starch content reduced in grains, suggesting that ZmG6PE may affect starch synthesis through the modulation of α-D-glucose-6-phosphate. β-D-glucose-6-phosphate participates in pentose phosphate metabolism to provide NADPH for life activities (Efferth et al., 2006; Mamani et al., 2016). Glycolysis and the pentose phosphate pathway occur in the cytoplasm, while the ZmG6PE protein is subcellularly localized in the nucleus and cell membrane. Omics analysis revealed significant enrichment of glycolysis/gluconeogenesis and pentose phosphate pathway-related processes. This suggests that ZmG6PE may indirectly participate in glycolysis and the pentose phosphate pathway by regulating the balance of glucose-6-phosphate. In addition, fructose-6-phosphate and mannose-6-phosphate may be potential substrates of glucose-6-phosphate-1 epimerase, indicating its broad substrate specificity (Graille et al., 2006). Significant differences were also observed in combined analysis for mannose-6-phosphate, indicating that mannose-6-phosphate may serve as a catalytic substrate for ZmG6PE, but further validation is required.

10.3389/fpls.2023.1286699

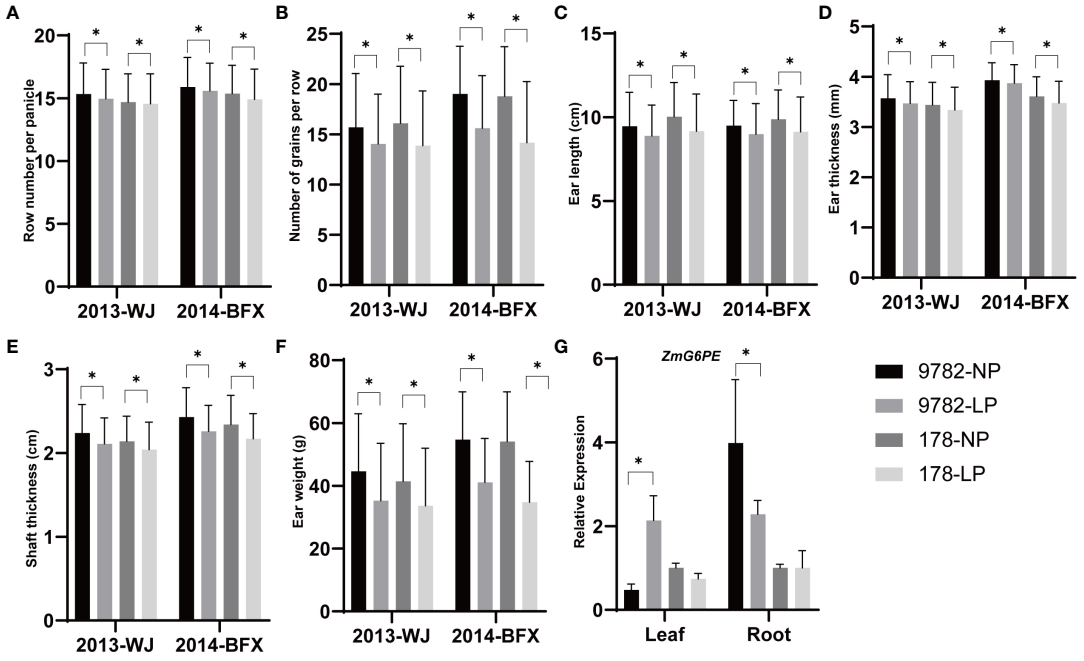

FIGURE 6
Yield-related analysis of the RILs. **(A–F)** Significantly different traits between segregating genotypes of *ZmG6PE*. WJ, Wenjiang Farm; BFX, Bifengxia Farm. **(G)** The gene expression level of *ZmG6PE*. "*" represents $p < 0.05$ by single factor ANOVA test.

4.2 Sugars are key regulators for Pi starvation signaling at the transcriptional level

Sugars are primary metabolites and signaling molecules, and starch is the final product of photosynthesis and the dominant form of energy storage in plants. Phosphorus deficiency makes soluble sugar accumulation in leaves, while exogenously applied sugars can alleviate the phosphorus starvation response (Hermans et al., 2006; Yang et al., 2020). Similarly, LP treatment increases the starch content (Gibson, 2004; Morcuende et al., 2007). The results showed a cascade relationship between carbon metabolism and phosphorus signaling. However, the specific interaction between carbon metabolism and phosphorus remains unclear. ADP-glucosepyrophosphorylase (AGP) Large Subunit 1 (*AGPL1*) and AGP Small Subunit 1 (*AGPS1*) increases the starch and soluble sugar contents in leaves under LP, but the starch and sugar contents do not change significantly in the roots (Meng et al., 2020). The *zmg6pe* mutants had reduced soluble sugar content and increased starch content in the leaves under LP conditions but also had reduced starch content and increased sugar content in the grain. Sugar and starch are the main carbon sources in plants and keep a dynamic balance (Flütsch et al., 2020). Non-metabolizable sugar analogs do not affect the expression of *PSI* genes. Although sugar input appears to be downstream of initial Pi sensing, it is required to complete the *PSI* signaling pathway (Karthikeyan et al., 2007). The cellulose synthase-like family (*OsCSLF6*) gene mutation increases the sugar and phosphorus content, and the expression of sucrose synthase and sucrose transporter genes is also induced in rice (Jin et al., 2015). The overexpression of the sucrose transport (*AtSUC2*) gene promotes sucrose transport and accumulation and enhances *PSI* gene expression and Pi accumulation (Lei et al., 2011). Sucrose and auxin play differential roles in the developmental responses of ontogenetically distinct root traits during Pi deprivation (Jain et al., 2007). Therefore, it is crucial to investigate the potential mechanism of PSI gene expression changes mediated by glycometabolism-related genes.

4.3 Biological pathways involved in response to LP stress

KEGG enrichment analyses of the transcriptomic and metabolomic data showed that amino acids, starch and sugar synthesis, photosynthesis, plant pathogens, ABC transporters, brassinosteroids, plant hormones, and citric acid metabolism responded to LP stress. LP stress significantly increases amino acids in plants (Hernández et al., 2009; Tawaraya et al., 2014; Sung et al., 2015). Plants increase starch content and reduce photosynthesis to avoid anthocyanins accumulation in leaves in LP environments (Wissuwa et al., 2005; Plaxton and Tran, 2011; Pant et al., 2015). The current study analysis showed that LP affected carbon fixation in leaves while starch and sugar synthesis in roots. Phosphorus starvation is also associated with microbial interactions. Under LP conditions, plants establish a mutualistic symbiotic relationship with microorganisms to increase phosphorus acquisition (Smith and Smith, 2011; Oldroyd and Leyser, 2020). These microorganisms may be arbuscular mycorrhizal fungi or species of *Colletotrichum*. ABC transcription proteins are involved in both aluminum tolerance and the inhibition of local phosphate signaling pathways (Dong et al.,

2017). Brassinosteroids and phytohormones respond to LP stress due to the regulation of local phosphorus signaling pathways by hormones interacting with different signals (Kobayashi et al., 2013). Overexpression of citrate synthase and transporter can improve the phosphorus utilization efficiency (PUE) by increasing organic acids secretion (López-Arredondo et al., 2014; Panchal et al., 2021). These pathways have all been reported in plant responses to LP stress. This evidence shows that the design of this research is reasonable and that these pathways are important in response to LP stress.

4.4 LP induces the expression of *ZmSPXs* and *ZmPHTs*

Phosphate Starvation Response (PHR) transcriptional factors are characterized by a conserved MYB domain and can participate in the transcriptional activation of *PSI* genes (Zhou et al., 2008; Guo et al., 2015). Phosphorus transport (PHT) regulates the uptake and transport of phosphorus (Paszkowski et al., 2002). SPX1 and SPX2 interact with PHR through their SPX domains, thereby inhibiting the binding ability of PHR to P1BS (Liu et al., 2010; Wang et al., 2014). Under LP stress, the expression of *ZmSPXs* increased, indicating that *ZmSPXs* inhibited *ZmPHR* and *ZmPHT* activities and affected the absorption and transport of phosphorus. Compared to the WT, the phosphorous content in *zmg6pe* mutant leaves decreased under NP conditions but remained significantly unchanged in *zmg6pe* mutant under LP stress conditions. Combined with the expression analysis, the expression of *ZmSPX2* decreased in the *zmg6pe* mutant under LP stress, indicating that *ZmG6PE* had a stimulative effect on *ZmSPX2*. The regulatory effect of ZmG6PE on ZmSPX2 may be achieved by influencing carbohydrate homeostasis or by modulating the expression of relevant genes in the nucleus. ZmG6PE might play a potential role in coordinating cellular metabolism and gene expression. The mutation of *AGPL1* and *AGPS1* lead to the significant downregulation of *OsSPX2* (Meng et al., 2020). AGPL1/AGPS1 is a starch synthesis enzyme, and ZmG6PE is an enzyme of the glycolysis pathway, suggesting that the carbon balance may affect SPX activity.

4.5 ZmG6PE regulates phosphorus transport and affects maize yield

Based on the above findings, we put forward a working model involving *ZmG6PE* in phosphorus homeostasis maintenance in maize (Figure 7). ZmG6PE is attributed with the capability to modulate the dynamic equilibrium between two carbohydrate sugar and starch. The expression of *ZmSPX2* is subjected to regulation by sugar concentration, while it was found to have no discernible effect on *ZmPHRs* expression. Notably, despite a prominent decrease in *ZmPHT1.13* expression level observed in the *zmg6pe* mutant compared to WT, the unaltered expression of *ZmPHRs* appears to compensate for the deficit by modulating the expression of other *ZmPHTs*. This may account for the absence of significant variations in phosphorus levels under LP conditions between the *zmg6pe* mutant and WT. ZmG6PE is implicated in phosphate uptake through the regulation of *ZmSPX2* and *ZmPHT1.13* expression. Additionally, ZmG6PE exerts an influence on starch synthesis by modulating the α-D-glucose-6-phosphate content, consequently impacting grain filling and altering grain size.

5 Conclusion

The conserved domain of ZmG6PE protein ranges from amino acid 41 to 308, which is identified as the Aldose_epimase domain. It exhibits activity as a glucose-6-phosphate-1-epimerase and may possess substrate diversity. Omics analysis reveals that the *ZmG6PE* gene is involved in LP stress response through pathways, such as amino acid metabolism, carbon metabolism, genetic material biosynthesis, fatty acid metabolism, and immune regulation. Glucose-1-phosphate, mannose-6-phosphate, and β-alanine are identified as marker metabolites in response to LP stress. The *ZmG6PE* gene regulates the expression of *ZmSPX2* and *ZmPHT1.13* by modulating the dynamic balance of carbohydrates, thus participating in phosphate signaling regulation. Mutant studies have demonstrated the impact of ZmG6PE on starch synthesis, grain size, and yield-related traits, while the use of RILs has revealed its influence on yield-related traits

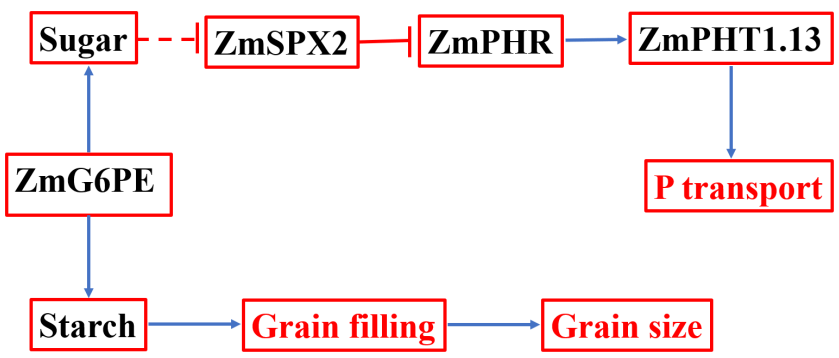

FIGURE 7
If working model for regulating phosphorus homeostasis by ZmG6PE. Solid lines indicate established direct correlations between different genes/proteins and between ZmG6PE, sugar, and starch. The dotted lines indicate indirect correlations between endogenous sugar level and SPX transcript abundance.

and phosphorus content. The *ZmG6PE* gene is a pleiotropic gene that influences maize grain size and responds to LP stress.

Data availability statement

Transcriptomic data has been submitted to the China National Centre for Bioinformatics, Chinese Academy of Sciences, under the accession number CRA010809, and is publicly accessible at https://ngdc.cncb.ac.cn/gsa.

Ethics statement

The manuscript presents research on animals that do not require ethical approval for their study.

Author contributions

HKZ: Writing – original draft, Writing – review & editing, Data curation, Validation. BWL: Writing – review & editing, Supervision. JL: Investigation, Writing – review & editing. XJ: Investigation, Writing – review & editing. HYZ: Data curation, Writing – review & editing. HXZ: Data curation, Writing – review & editing. BYL: Data curation, Writing – review & editing. HH: Data curation, Writing – review & editing. YW: Data curation, Writing – review & editing. AA: Formal Analysis, Writing – review & editing. AR: Formal Analysis, Writing – review & editing. JS: Formal Analysis, Writing – review & editing. MI: Formal Analysis, Writing – review & editing. XZ: Software, Writing – review & editing. DL: Supervision, Writing – review & editing. LW: Supervision, Writing – review & editing. DG: Resources, Writing – review & editing. SQG: Resources, Writing – review & editing. SS: Supervision, Writing – review & editing. SBG: Funding acquisition, Resources, Supervision, Writing – original draft, Writing – review & editing.

Funding

The author(s) declare financial support was received for the research, authorship, and/or publication of this article. This research was supported by the National Key Research and Development Program of China (grant no. 2021YFF1000500 and 2021YFD1200704), the Natural Science Foundation of China (grant no. 32101655), Sichuan Science and Technology Support Project (grant no. 2021YFYZ0027, 2021YFYZ0020) and the earmarked fund for China Agriculture Research System (grant no. CARS-02-09).

Conflict of interest

The authors declare that the research was conducted in the absence of any commercial or financial relationships that could be construed as a potential conflict of interest.

Publisher's note

Supplementary material

The Supplementary Material for this article can be found online at: https://www.frontiersin.org/articles/10.3389/fpls.2023.1286699/full#supplementary-material

References

Aguilar-Pontes, M. V., Brandl, J., McDonnell, E., Strasser, K., Nguyen, T. T. M., Riley, R., et al. (2018). The gold-standard genome of *Aspergillus Niger* NRRL 3 enables a detailed view of the diversity of sugar catabolism in fungi. *Stud. Mycology* 91, 61–78. doi: 10.1016/j.simyco.2018.10.001

Chiou, T., and Lin, S. (2011). Signaling network in sensing phosphate availability in plants. *Annu. Eview Plant Biol.* 62, 185–206. doi: 10.1146/annurev-arplant-042110-103849

Dong, J., Piñeros, M., Li, X., Yang, H., Liu, Y., Murphy, A.S., et al. (2017). An *Arabidopsis* ABC transporter mediates phosphate deficiency-induced remodeling of root architecture by modulating iron homeostasis in roots. *Mol. Plant* 10, 244–259. doi: 10.1016/j.molp.2016.11.001

Efferth, T., Schwarzl, S. M., Smith, J., and Osieka, R. (2006). Role of glucose-6-phosphate dehydrogenase for oxidative stress and apoptosis. *Cell Death Differentiation* 13, 527–528. doi: 10.1038/sj.cdd.4401807

Flütsch, S., Wang, Y., Takemiya, A., Vialet-Chabrand, S. R. M., Klejchová, M., Nigro, A., et al. (2020). Guard cell starch degradation yields glucose for rapid stomatal opening in Arabidopsis. *Plant Cell* 32, 2325–2344. doi: 10.1105/tpc.18.00802

Fouquerel, E., Goellner, E. M., Yu, Z., Gagne, J. P., Barbi, D. M. M., Feinstein, T., et al. (2014). ARTD1/PARP1 negatively regulates glycolysis by inhibiting hexokinase 1 independent of NAD^+ depletion. *Cell Rep.* 8, 1819–1831. doi: 10.1016/j.celrep.2014.08.036

Geigenberger, P., Stitt, M., and Fernie, A. R. (2004). Metabolic control analysis and regulation of the conversion of sucrose to starch in growing potato tubers. *Plant Cell Environ.* 27, 655–673. doi: 10.1111/j.1365-3040.2004.01183.x

Gibson, S. I. (2004). Sugar and phytohormone response pathways: navigating a signalling network. *J. Exp. Bot.* 55, 253–264. doi: 10.1093/jxb/erh048

Gomes, G., Vil', V., Terent'Ev, A., and Alabugin, I. V. (2015). Stereoelectronic source of the anomalous stability of bis-peroxides. *Chem. Sci.* 6, 6783–6791. doi: 10.1039/c5sc02402a

Gonzalez, E., Solano, R., Rubio, V., Leyva, A., and Paz-Ares, J. (2005). PHOSPHATE TRANSPORTER TRAFFIC FACILITATOR 1 is a plant-specific SEC12-related protein that enables the endoplasmic reticulum exit of a high-affinity phosphate transporter in Arabidopsis. *Plant Cell* 17, 3500–3512. doi: 10.1105/tpc.105.036640

Graille, M., Baltaze, J. P., Leulliot, N., Liger, D., Quevillon-Cheruel, S., and van Tilbeurgh, H. (2006). Structure-based functional annotation: yeast *ymr099c* codes for a d-hexose-6-phosphate mutarotase. *J. Biol. Chem.* 281, 30175–30185. doi: 10.1074/jbc.M604443200

Guo, M., Ruan, W., Li, C., Huang, F., Zeng, M., Liu, Y., et al. (2015). Integrative comparison of the role of the phosphate response1 subfamily in phosphate signaling and homeostasis in rice. *Plant Physiol.* 168, 1762–1776. doi: 10.1104/pp.15.00736

Ham, B. K., Chen, J., Yan, Y., and Lucas, W. J. (2018). Insights into plant phosphate sensing and signaling. *Curr. Opin. Biotechnol.* 49, 1–9. doi: 10.1016/j.copbio.2017.07.005

He, Q., Ren, W., Xiang, J., Dabbour, M., Mintah, B. K., Li, Y., et al. (2021). Fermentation of *Saccharomyces cerevisiae* in a 7.5 L ultrasound-enhanced fermenter: Effect of sonication conditions on ethanol production, intracellular Ca^{2+} concentration and key regulating enzyme activity in glycolysis. *Ultrason Sonochemistry* 76, 105624. doi: 10.1016/j.ultsonch.2021.105624

Hermans, C., Hammond, J. P., White, P. J., and Verbruggen, N. (2006). How do plants respond to nutrient shortage by biomass allocation? *Trends Plant Sci.* 11, 610–617. doi: 10.1016/j.tplants.2006.10.007

Hernández, G., Valdés-López, O., Ramírez, M., Goffard, N., Weiller, G., Aparicio-Fabre, R., et al. (2009). Global changes in the transcript and metabolic profiles during symbiotic nitrogen fixation in phosphorus-stressed common bean plants. *Plant Physiol.* 151, 1221–1238. doi: 10.1104/pp.109.143842

Jain, A., Poling, M. D., Karthikeyan, A. S., Blakeslee, J. J., Peer, W. A., Titapiwatanakun, B., et al. (2007). Differential effects of sucrose and auxin on localized phosphate deficiency-induced modulation of different traits of root system architecture in Arabidopsis. *Plant Physiol.* 144, 232–247. doi: 10.1104/pp.106.092130

Jiang, H., Zhang, J., Han, Z., Yang, J., Ge, C., and Wu, Q. (2017). Revealing new insights into different phosphorus-starving responses between two maize (Zea mays) inbred lines by transcriptomic and proteomic studies. *Sci. Rep.* 7, 44294. doi: 10.1038/srep44294

Jiang, S., Zhang, L. F., Zhang, H. W., Hu, S., Lu, M. H., Liang, S., et al. (2012). A novel miR-155/miR-143 cascade controls glycolysis by regulating *hexokinase 2* in breast cancer cells. *EMBO J.* 31, 1985–1998. doi: 10.1038/emboj.2012.45

Jin, C., Fang, C., Yuan, H., Wang, S., Wu, Y., Liu, X., et al. (2015). Interaction between carbon metabolism and phosphate accumulation is revealed by a mutation of a cellulose synthase-like protein, CSLF6. *J. Exp. Bot.* 66, 2557–2567. doi: 10.1093/jxb/erv050

Karthikeyan, A., Varadarajan, D., Jain, A., Held, M., Carpita, N., Raghothama, K.G., et al. (2007). Phosphate starvation responses are mediated by sugar signaling in *Arabidopsis*. *Planta* 225, 907–918. doi: 10.1007/s00425-006-0408-8

Kobayashi, Y., Kobayashi, Y., Sugimoto, M., Lakshmanan, V., Iuchi, S., Kobayashi, M., et al. (2013). Characterization of the complex regulation of atalmt1 expression in response to phytohormones and other inducers. *Plant Physiol.* 162, 732–740. doi: 10.1104/pp.113.218065

Kochian, L. V. (2012). Plant nutrition: rooting for more phosphorus. *Nature* 488, 466–467. doi: 10.1038/488466a

Lei, M., Liu, Y., Zhang, B., Zhao, Y., Wang, X., Zhou, Y., et al. (2011). Genetic and genomic evidence that sucrose is a global regulator of plant responses to phosphate starvation in Arabidopsis. *Plant Physiol.* 156, 1116–1130. doi: 10.1104/pp.110.171736

Li, H., Xu, L., Li, J., Lyu, X., Li, S., Wang, C., et al. (2022). Multi-omics analysis of the regulatory effects of low-phosphorus stress on phosphorus transport in soybean roots. *Front. Plant Sci.* 13. doi: 10.3389/fpls.2022.992036

Liu, J., Samac, D. A., Bucciarelli, B., Allan, D. L., and Vance, C. P. (2005). Signaling of phosphorus deficiency-induced gene expression in white lupin requires sugar and phloem transport. *Plant J.* 41, 257–268. doi: 10.1111/j.1365-313X.2004.02289.x

Liu, F., Wang, Z., Ren, H., Shen, C., Li, Y., Ling, H.Q., et al. (2010). OsSPX1 suppresses the function of OsPHR2 in the regulation of expression of *OsPT2* and phosphate homeostasis in shoots of rice. *Plant J.* 62, 508–517. doi: 10.1111/j.1365-313X.2010.04170.x

López-Arredondo, D. L., Leyva-González, M. A., González-Morales, S. I., López-Bucio, J., and Herrera-Estrella, L. (2014). Phosphate nutrition: improving low-phosphate tolerance in crops. *Annu. Rev. Plant Biol.* 65, 95–123. doi: 10.1146/annurev-arplant-050213-035949

Lu, M., Cheng, Z., Zhang, X., Huang, P., Fan, C., Yu, G., et al. (2020). Spatial divergence of *phr-pht1* modules maintains phosphorus homeostasis in soybean nodules. *Plant Physiol.* 184, 236–250. doi: 10.1104/pp.19.01209

Luo, B., Ma, P., Nie, Z., Zhang, X., He, X., Ding, X., et al. (2019). Metabolite profiling and genome-wide association studies reveal response mechanisms of phosphorus deficiency in maize seedling. *Plant J.* 97, 947–969. doi: 10.1111/tpj.14160

Ma, M., Lazar, N., Pellegrini, O., Lepault, J., Condon, C., et al. (2017). Trz1, the long form rnase Z from yeast, forms a stable heterohexamer with endonuclease Nuc1 and mutarotase. *Biochem. J.* 474, 3599–3613. doi: 10.1042/BCJ20170435

Mamani, S., Moinier, D., Denis, Y., Soulère, L. , Queneau, Y., Talla, E., et al. (2016). Insights into the quorum sensing regulon of the acidophilic *Acidithiobacillus ferrooxidans* revealed by transcriptomic in the presence of an acyl homoserine lactone superagonist analog. *Front. Microbiol.* 71365. doi: 10.3389/fmicb.2016.01365

Meng, Q., Zhang, W., Hu, X., Shi, X., Chen, L., Dai, X., et al. (2020). Two ADP-glucose pyrophosphorylase subunits, OsAGPL1 and OsAGPS1, modulate phosphorus homeostasis in rice. *Plant J.* 104, 1269–1284. doi: 10.1111/tpj.14998

Morcuende, R., Bari, R., Gibon, Y., Zheng, W., Pant, B. D., Bläsing, O., et al. (2007). Genome-wide reprogramming of metabolism and regulatory networks of *Arabidopsis* in response to phosphorus. *Plant Cell Environ.* 30, 85–112. doi: 10.1111/j.1365-3040.2006.01608.x

Nilsson, L., Muller, R., and Nielsen, T. H. (2007). Increased expression of the MYB-related transcription factor, *PHR1*, leads to enhanced phosphate uptake in *Arabidopsis thaliana*. *Plant Cell Environ.* 30, 1499–1512. doi: 10.1111/j.1365-3040.2007.01734.x

Niu, L., Hao, R., Wu, X., Wang, W., Tuberosa, R., et al. (2020). Maize mesocotyl: role in response to stress and deep-sowing tolerance. *Plant Breed.* 139, 466–473. doi: 10.1111/pbr.12804

Oldroyd, G., and Leyser, O. (2020). A plant's diet, surviving in a variable nutrient environment. *Science* 368, eaba0196. doi: 10.1126/science.aba0196

Panchal, P., Miller, A. J., Giri, J., and Manavella, P. (2021). Organic acids: versatile stress-response roles in plants. *J. Exp. Bot.* 72, 4038–4052. doi: 10.1093/jxb/erab019

Pant, B. D., Pant, P., Alexander, E., Huhman, D., Kopka, J., and Scheible, W.R.. (2015). Identification of primary and secondary metabolites with phosphorus status-dependent abundance in *Arabidopsis*, and of the transcription factor phr1 as a major regulator of metabolic changes during phosphorus limitation. *Plant Cell Environ.* 38, 172–187. doi: 10.1111/pce.12378

Paszkowski, U., Kroken, S., Roux, C., and Briggs, S. (2002). Rice phosphate transporters include an evolutionarily divergent gene specifically activated in arbuscular mycorrhizal symbiosis. *Proc. Natl. Acad. Sci.* 99, 13324–13329. doi: 10.1073/pnas.202474599

Plaxton, W. C., and Tran, H. T. (2011). Metabolic adaptations of phosphate-starved plants. *Plant Physiol.* 156, 1006–1015. doi: 10.1104/pp.111.175281

Puga, M. I., Mateos, I., Charukesi, R., Wang, Z., Franco-Zorrilla, J. M., de Lorenzo, L., et al. (2014). Spx1 is a phosphate-dependent inhibitor of PHOSPHATE STARVATION RESPONSE 1 in *Arabidopsis*. *Proc. Natl. Acad. Sci.* 111, 14947–14952. doi: 10.1073/pnas.1404654111

Rubio, V., Linhares, F., Solano, R., Martin, A. C., Iglesias, J., Leyva, A., et al. (2001). A conserved MYB transcription factor involved in phosphate starvation signaling both in vascular plants and in unicellular algae. *Genes Dev.* 15, 2122–2133. doi: 10.1101/gad.204401

Schuldiner, O., Yanover, C., and Benvenisty, N. (1998). Computer analysis of the entire budding yeast genome for putative targets of the GCN4 transcription factor. *Curr. Genet.* 33, 16–20. doi: 10.1007/s002940050303

Shin, H., Shin, H., Dewbre, G., and Harrison, M. (2004). Phosphate transport in *Arabidopsis: Pht1;1* and *Pht1;4* play a major role in phosphate acquisition from both low- and high-phosphate environments. *Plant J.* 39, 629–642. doi: 10.1111/j.1365-313X.2004.02161.x

Smith, S. E., and Smith, F. A. (2011). Roles of arbuscular mycorrhizas in plant nutrition and growth: new paradigms from cellular to ecosystem scales. *Annu. Rev. Plant Biol.* 62, 227–250. doi: 10.1146/annurev-arplant-042110-103846

Sun, S., Gu, M., Cao, Y., Huang, X., Zhang, X., Ai, P., et al. (2012). A constitutive expressed phosphate transporter, OsPht1;1, modulates phosphate uptake and translocation in phosphate-replete rice. *Plant Physiol.* 159, 1571–1581. doi: 10.1104/pp.112.196345

Sung, J., Lee, S., Lee, Y., Ha, S., Song, B., Kim, T., et al. (2015). Metabolomic profiling from leaves and roots of tomato (*Solanum lycopersicum* L.) plants grown under nitrogen, phosphorus or potassium-deficient condition. *Plant Sci.* 241, 55–64. doi: 10.1016/j.plantsci.2015.09.027

Tanner, L. B., Goglia, A. G., Wei, M. H., Sehgal, T., Parsons, L. R., Park, J.O., et al. (2018). Four key steps control glycolytic flux in mammalian cells. *Cell Syst.* 7, 49–62. doi: 10.1016/j.cels.2018.06.003

Tawaraya, K., Horie, R., Shinano, T., Wagatsuma, T., Saito, K., and Oikawa, A. (2014). Metabolite profiling of soybean root exudates under phosphorus deficiency. *Soil Sci. Plant Nutr.* 60, 679–694. doi: 10.1080/00380768.2014.945390

Wang, F., Deng, M., Xu, J., Zhu, X., and Mao, C. (2018). Molecular mechanisms of phosphate transport and signaling in higher plants. *Semin. Cell Dev. Biol.* 74, 114–122. doi: 10.1016/j.semcdb.2017.06.013

Wang, Z., Ruan, W., Shi, J., Zhang, L., Xiang, D., Yang, C., et al. (2014). Rice SPX1 and SPX2 inhibit phosphate starvation responses through interacting with PHR2 in a phosphate-dependent manner. *Proc. Natl. Acad. Sci.* 111, 14953–14958. doi: 10.1073/pnas.1404680111

Wild, R., Gerasimaite, R., Jung, J. Y., Truffault, V., Pavlovic, I., Schmidt, A., et al. (2016). Control of eukaryotic phosphate homeostasis by inositol polyphosphate sensor domains. *Science* 352, 986–990. doi: 10.1126/science.aad9858

Wissuwa, M., Gamat, G., and Ismail, A. M. (2005). Is root growth under phosphorus deficiency affected by source or sink limitations? *J. Exp. Bot.* 56, 1943–1950. doi: 10.1093/jxb/eri189

Wu, H., Liu, J., Chen, S., Zhao, Y. , Zeng, S., Bin, P., et al. (2018). Jejunal metabolic responses to *Escherichia coli* infection in piglets. *Front. Microbiol.* 92465. doi: 10.3389/fmicb.2018.02465

Wurster, B., and Hess, B. (1972). Glucose-6-phosphate-1-epimerase from baker's yeast. A new enzyme. *FEBS Lett.* 23, 341–344. doi: 10.1016/0014-5793(72)80311-9

Wurster, B., and Hess, B. (1973). Enzyme-catalyzed anomerization of D-glucose-6-phosphate. *FEBS Lett.* 38, 33–36. doi: 10.1016/0014-5793(73)80506-x

Yang, A., Kong, L., Wang, H., Yao, X., Xie, F., Wang, H., et al. (2020). Response of soybean root to phosphorus deficiency under sucrose feeding: insight from morphological and metabolome characterizations. *BioMed. Res. Int.* 2020, 2148011–2148032. doi: 10.1155/2020/2148032

Zeeman, S. C., Smith, S. M., and Smith, A. M. (2007). The diurnal metabolism of leaf starch. *Biochem. J.* 401, 13–28. doi: 10.1042/BJ20061393

Zhou, J., Jiao, F., Wu, Z., Li, Y., Wang, X., He, X., et al. (2008). *OPHR2* is involved in phosphate-starvation signaling and excessive phosphate accumulation in shoots of plants. *Plant Physiol.* 146, 1673–1686. doi: 10.1104/pp.107.111443

frontiers | Frontiers in Plant Science

TYPE Original Research
PUBLISHED 08 January 2024
DOI 10.3389/fpls.2023.1284135

OPEN ACCESS

EDITED BY
Jose M. Mulet,
Universitat Politècnica de València, Spain

REVIEWED BY
Jemaa Essemine,
Partner Institute for Computational Biology, China
Francisco Marco,
University of Valencia, Spain

*CORRESPONDENCE
Chao Wu
wuchao@gxib.cn
Hui-Ling Liang
lhl@gxib.cn

†These authors have contributed equally to this work

RECEIVED 28 August 2023
ACCEPTED 15 December 2023
PUBLISHED 08 January 2024

CITATION
Zhang X-J, Wu C, Liu B-Y, Liang H-L, Wang M-L and Li H (2024) Transcriptomic and metabolomic profiling reveals the drought tolerance mechanism of *Illicium difengpi* (Schisandraceae). *Front. Plant Sci.* 14:1284135. doi: 10.3389/fpls.2023.1284135

Transcriptomic and metabolomic profiling reveals the drought tolerance mechanism of *Illicium difengpi* (Schisandraceae)

Xiu-Jiao Zhang†, Chao Wu*†, Bao-Yu Liu, Hui-Ling Liang*, Man-Lian Wang and Hong Li

Guangxi Key Laboratory of Plant Functional Phytochemicals and Sustainable Utilization, Guangxi Institute of Botany, Guangxi Zhuang Autonomous Region and Chinese Academy of Sciences, Guilin, China

Illicium difengpi (Schisandraceae), an endangered medicinal plant endemic to karst areas, is highly tolerant to drought and thus can be used as an ideal material for investigating adaptive mechanism to drought stress. The understanding of the drought tolerance of *I. difengpi*, especially at the molecular level, is lacking. In the present study, we aimed to clarify the molecular mechanism underlying drought tolerance in endemic *I. difengpi* plant in karst regions. The response characteristics of transcripts and changes in metabolite abundance of *I. difengpi* subjected to drought and rehydration were analyzed, the genes and key metabolites responsive to drought and rehydration were screened, and some important biosynthetic and secondary metabolic pathways were identified. A total of 231,784 genes and 632 metabolites were obtained from transcriptome and metabolome analyses, and most of the physiological metabolism in drought-treated *I. difengpi* plants recovered after rehydration. There were more upregulated genes than downregulated genes under drought and rehydration treatments, and rehydration treatment induced stable expression of 65.25% of genes, indicating that rehydration alleviated drought stress to some extent. Drought and rehydration treatment generated flavonoids, phenolic acids, flavonols, amino acids and their derivatives, as well as metabolites such as saccharides and alcohols in the leaves of *I. difengpi* plants, which alleviated the injury caused by excessive reactive oxygen species. The integration of transcriptome and metabolome analyses showed that, under drought stress, *I. difengpi* increased glutathione, flavonoids, polyamines, soluble sugars and amino acids, contributing to cell osmotic potential and antioxidant activity. The results show that the high drought tolerance and recovery after rehydration are the reasons for the normal growth of *I. difengpi* in karst mountain areas.

KEYWORDS

***Illicium difengpi*, drought stress, rehydration, transcriptome, metabolome**

1 Introduction

Drought events are frequent worldwide. It is predicted that extreme drought episodes will become more frequent against the background of global climate change (Dai, 2013). Being sessile, plants are extremely vulnerable to drought stress, which can lead to impaired growth and even death, resulting in enormous yield losses (Bai et al., 2006). Drought stress is thus one of the most serious environmental factors that restricts plant species distribution and diversity and crop productivity (Yang et al., 2020). The southwest karst region of China is the largest and most intensively developed ecologically fragile area among the three largest concentrated karst areas in the world, with a total area of over 500,000 km^2 (Zhang et al., 2012). Due to slow soil formation, shallow soil layers, low organic matter content, and poor soil conservation capabilities, this region experiences geological drought. Even with enough rainfall, after several days of high temperatures and sunny weather, the soil water content decreases, and temporary drought events occur on the surface (Zhao et al., 2022). Drought disasters are the most prominent environmental factors that affect plant growth in karst regions. Short periods of extreme drought are more prone to occur in karst environments, which are characterized by periodic water deficiency. The recovery ability after rehydration is important for the successful adaptation of plants in karst ecosystems prone to drought.

Drought stress activates complex network regulatory mechanisms (Michaletti et al., 2018), which lead to changes in gene expression and biochemical and molecular processes in plants (Golldack et al., 2014). Under soil water deficiency, the optimal water supply is balanced in plant tissues, cell hydration is maintained, and water loss is avoided. The plant accumulates stress-protective metabolites (e.g., tryptophan, trehalose, flavonoids, glutathione, etc.) to prevent acute cell damage and membrane integrity by triggering the antioxidant system and deploying peroxidases (Cramer et al., 2007). Stress-related transcription factors (TFs), such as the MYB, bHLH, NAC, AP2/ERF, NFY and HSF, which specifically bind to *cis*-regulatory elements to activate downstream gene expression in response to stress signals, can be activated under drought stress (Hu et al., 2022). The mechanisms of plants in response to alternating or extreme drought and rehydration have become a research focus in several fields, including environmental and ecological preservation, genetics and breeding improvement (AbdElgawad et al., 2015; Zhao et al., 2022). The physiological and molecular functions in plants can be recovered after rehydration. However, the compensation of rehydration to plant growth after drought stress is often limited. Additionally, large-scale studies using high-throughput genomics have revealed the responses of metabolite accumulation or transcript changes in higher plants under drought and rehydration conditions (Chen et al., 2020; Sousa et al., 2022). However, there is a lack of comprehensive understanding of the mechanisms underlying drought tolerance in terms of transcriptomic and metabonomic integration, especially in endemic plants in karst regions.

Illicium difengpi (Schisandraceae) is a perennial evergreen shrub of *Illicium*, subg. *Cymbostemon*, distributed in the karst region of Guangxi Province with small and isolated populations. *I. difengpi* has high ornamental value, and the stem and root bark of this plant are used for traditional Chinese medicine, but the species is listed on the National Key Protection Plant List (Category II) (http://www.iplant.cn/rep/protlist). *I. difengpi* plants show strong drought resistance and can survive in rocky areas with an elevation of 200~1200 meters, such as on mountain tops, in rocky crevices with soil, or under sparse woodlands on rocky mountains. The leaves of this species have morphological characteristics that enable adaptation to drought stress, such as well-developed leaf veins, thick cuticles and well-developed palisade tissue (Kong et al., 2012). As a drought-tolerant plant, *I. difengpi* has demonstrated strong adaptability to various abiotic stresses, including drought and high temperatures. This makes it a valuable but understudied nonmodel plant resource that can enhance our understanding of the potential molecular mechanisms underlying adaptation and tolerance to drought stress. Research on the drought tolerance of *I. difengpi* has mainly focused on physiological mechanisms (Meng et al., 2019; Wang et al., 2021), few studies having investigated the molecular mechanisms of its adaptation to drought stress (Liu et al., 2022). The drought tolerance of *I. difengpi* has rarely been studied from an omics perspective. Therefore, the present study investigates the transcriptomic and metabolomic responses of the karst endemic medicinal plant *I. difengpi* to drought and rehydration treatment. The objective is to gain a full understanding of drought tolerance mechanisms in *I. difengpi* in terms of transcriptomic and metabolomic profiling.

2 Materials and methods

2.1 Plant materials and water treatments

The experiment was performed at a karst germplasm nursery with a transparent rain shelter (25°4′N, 110°17′E) at the Guangxi Botanical Research Institute in Guangxi, China. Two-year-old plants from seeds collected in Jingxi County, Baise City, Guangxi Province, China, cultivated in plastic pots were subjected to water treatment. *I. difengpi* plants with consistent height (height: 22~24 cm) and leaf number (12~14 leaves) were selected. The plants were subjected to three soil water conditions for 18 days (Figure 1): well-watered treatment (50% of soil water content, water/dry soil, CK), drought stress treatment (10% of soil water content, water/dry soil, DS) and drought–rehydration treatment (rehydration to 50% of soil water content for 3 days after DS treatment for 15 days, DS_R), with four independent biological replicates for each group. After the drought and rehydration treatments, leaf samples (mature functional leaves, from the 2nd to 4th leaves from the top) were collected, frozen in liquid nitrogen, and stored at -80°C for transcriptome, quantitative real-time PCR (RT-qPCR) and metabolome analysis.

2.2 RNA isolation, generation of RNA-seq data and data processing

Total RNA was extracted from the *I. difengpi* samples with Trizol® reagent (Invitrogen, Carlsbad, CA, USA) following the

FIGURE 1
Morphological changes in *I. difengpi* plants during different treatments. CK, well-watered treatment; DS, drought stress treatment; DS_R, drought–rehydration treatment.

manufacturer's instructions. The purity, quantity, and integrity of RNA were assessed on a NanoPhotometer spectrophotometer (IMPLEN, Los Angeles, CA, USA), Qubit RNA Assay Kit in a Qubit 2.0 Fluorometer (Life Technologies, Carlsbad, CA, USA), and RNA Nano 6000 Assay Kit for the Agilent Bioanalyzer 2100 system (Agilent Technologies, Santa Clara, CA, USA).

A total of 1 ug of RNA per sample was used as the input material for library preparation. The mRNA was purified from the total RNA using poly-T oligo-attached magnetic beads. Sequencing libraries from different treatments were constructed with the purified mRNA (100 ng) using the NEBNext® UltraTM RNA Library Prep Kit for lllumina® (NEB, USA) following the manufacturer's instructions, and index codes were added to attribute sequences to each sample. Library sequencing was performed on an lllumina NovaSeq 6000 platform for generation of 150 bp paired end reads. The raw data of *I. difengpi* in this study have been deposited in the NCBI Sequence Read Archive (SRA) under bioproject accession number PRJNA983054.

Clean data were obtained by removing reads containing adapters with an N content greater than 10% and base quality (Q) less than or equal to 10 using the SeqPrep program (https://github.com/jstjohn/SeqPrep) and the Sickle program (https://github.com/najoshi/sickle). FastQC (v 0.12.1) (Andrews, 2010) was used to calculate the GC content, Q20 and Q30 of both the raw and clean data. The clean reads were then *de novo* assembled into unigene sequences using Trinity (v 2.6.6) (Grabherr et al., 2011), and a Python script was employed to extract the longest transcript for each gene as the reference sequence. The reference sequences were further compared against the Nr (Deng et al., 2006), Swiss-Prot (Apweiler et al., 2004), GO (Ashburner et al., 2000), COG (Tatusov et al., 2000), KEGG (Kanehisa et al., 2004) and Pfam (Finn et al., 2013) databases using BLAST (Altschul et al., 1990) for gene functional annotation. Finally, UpSetR (Conway et al., 2017) was utilized to visualize the annotations of these six databases for the genes.

The unigene sequences from each sample back to the reference sequences were mapped using Hisat2 (v 2.4) (Kim et al., 2013). The gene expression levels were calculated from the fragments per kilobase of transcript per million fragments mapped (FRKM) method (Mortazavi et al., 2008) using StringTie (v 1.3.1) (Pertea et al., 2015). DESeq2 (Anders and Huber, 2010) was used to determine the differentially expressed genes (DEGs) with a filtering threshold of fold change ≥2 and FDR < 0.01. The expression levels of the DEGs in each sample were standardized using the built-in *scale* function in R software (v 4.2.2). Principal component analysis (PCA) was performed using the built-in *prcomp* function, and cluster analysis was conducted using the *pheatmap* function to generate an expression heatmap. Gene otology (GO) term enrichment was carried out by mapping all genes to the corresponding terms in the GO database (http://www.geneontology.org/), and pathway analysis was performed based on the KEGG database (https://www.kegg.jp/) using hypergeometric testing to identify significantly enriched GO terms and pathways ($p < 0.05$) compared to the whole-genome background. Visualization of GO terms and pathways was performed using the R package ggplot2 (Villanueva and Chen, 2019) through Hiplot Pro (https://hiplot.com.cn/), a comprehensive web service for biomedical data analysis and visualization.

Reverse transcription was performed using the Monad First Strand cDNA Synthesis Kit. Six genes were selected to verify RNA-Seq data by RT-qPCR with *Actin* as a reference gene. Primers were designed using PRIMER-BLAST (Ye et al., 2012). RT-qPCR was carried out on an ABI7500 Real-Time PCR System (Applied Biosystems). The total reaction volume was 10 μL: 5 μL of MonScriptTM RTIII All-in-one Mix with dsDNase (Monad Biotech Co., Ltd.), 0.7 μL of each forward and reverse primer, 2.55 μL RNase-free water and 1 μL template DNA. The reaction conditions on the thermal cycler were as follows: 95°C for 2 min and 40 cycles of 95°C for 5 s and 60°C for 30 s. Four biological replicates were analyzed in independent runs. The quantification of gene expression levels was calculated as $2^{-\Delta\Delta Ct}$ (Livak and Schmittgen, 2001) relative to the CK samples. The graphs for gene expression were prepared in Microsoft Excel 2007. All primers used in the present study are listed in Supplementary Table S1.

2.3 Sample extraction and metabolome profiling

The leaf samples of *I. difengpi* plants were freeze–dried using a SCIENTZ-100F freeze–dryer under vacuum. The dried samples were ground to a powder using an MM 400 grinder. One hundred milligrams of the powder was dissolved in 1 mL of 70% methanol extraction solution and kept overnight in a refrigerator at 4°C. The mixture was vortexed six times to ensure a thorough extraction during the process. The resulting extract was centrifuged at 12,000 rpm for 10 min, and the supernatant was collected after centrifugation. The supernatant was then filtered through a 0.22-μm-pore-size membrane filter and analyzed by UPLC-MS/MS (UPLC, SHIMADZU CBM30A, https://www.shimadzu.com/; MS/MS, QTRAP® 4500+, https://sciex.com/).

The liquid phase conditions mainly included a Waters ACQUITY UPLC HSS T3 C18 column (1.8 μm, 2.1 mm×100 mm), with mobile phase A as ultrapure water (0.1% formic acid) and mobile phase B as acetonitrile (0.1% formic acid). The gradient elution was as follows: 0 min, water/acetonitrile (95:5 V/V); 10.0 min, water/acetonitrile (5:95 V/V); 11.0 min, water/acetonitrile (5:95 V/V); 11.1 min, water/acetonitrile (95:5 V/V); and 15.0 min, water/acetonitrile (95:5 V/V). The flow rate was 0.4 mL min^{-1}, the column temperature was 40°C, and the injection volume was 2 μL.

The mass spectrometry conditions mainly included an electrospray ionization (ESI) source with a temperature of 550°C, positive ionization at 5500 V and negative ionization at -4500 V. The gas settings were as follows: gas I (GS I) at 55 psi, gas II (GS II) at 60 psi, curtain gas (CUR) at 25 psi, and collision-activated dissociation (CAD) parameters set to high. In the triple-quadrupole (QTRAP) system, each ion pair was scanned and detected based on the optimized declustering potential (DP) and collision energy (CE).

Using the NMDB and public databases (Ren et al., 2022), the *wiff* format raw data obtained from UPLC-MS/MS were subjected to qualitative and quantitative analysis using Analyst (v 1.6.3) (Ren and Chen, 2023). In the qualitative analysis, isotopic signals, duplicate signals of ions containing K^+, Na^+, and NH_4^+ ions, and duplicate signals of ions that were themselves fragments of larger molecules were removed using Microsoft Excel 2007. In the quantitative analysis, all chromatographic peaks in the samples were integrated using multiple reaction monitoring (MRM) mode based on triple-quadrupole mass spectrometry. The integration and calibration of the chromatographic peaks were performed using MultiaQuan (3.0.2, AB SCIEX, Concord, ON, Canada) to achieve metabolite quantification.

Differentially expressed metabolites (DEMs) were selected using the OPLS-DA function (OPLSR.Anal) in the MetaboAnalystR package in R software (v 4.2.2) (Chong and Xia, 2018), with a variable importance in projection (VIP) ≥ 1 and a fold-change of ≥ 1.5 (or ≤ 0.67). The identified DEMs were annotated using the KEGG compound database (https://www.kegg.jp/kegg/compound/) and were analyzed for pathway enrichment using the KEGG pathway database (https://www.kegg.jp/kegg/pathway.html). PCA was performed using the built-in *prcomp* function in R software (4.2.2), and the relative abundances of differentially abundant metabolites in each group were standardized using the built-in *scale* function. K-means clustering analysis was then performed using the R package Mfuzz (Kumar and Matthias, 2007) through Hiplot Pro (https://hiplot.com.cn/).

2.4 Conjoint analysis

The transcriptome and metabolome data were standardized (unit variance scaling) and subjected to statistical analysis to determine their relationships under different treatments. Combining functional analysis, correlation analysis, metabolic regulatory pathways, and functional annotation analysis, key genes or metabolic regulatory pathways involved in the drought resistance mechanism were identified. Genes associated with secondary metabolite biosynthesis and metabolic pathways were taken for analysis. The standardized data were analyzed for correlations using the *cor* function in R software (4.2.2) with a Pearson's correlation coefficient (|PCC|) threshold of ≥ 0.8 and p value ≤ 0.05. Data were organized using Microsoft Excel 2007, and gene expression and metabolite abundance relationships were visualized using Microsoft PowerPoint 2007 and TBtools (v 1.120) (Chen et al., 2018).

3 Results

3.1 *De novo* assembly and annotation

All transcriptome analyses of the three water treatments, CK, DS and DS_R, resulted in a total of 78.20 Gb clean data from 12 samples, with Q20 > 97%, Q30 > 93% and GC content > 46% (Supplementary Table S2). *De novo* assembly generated 231,784 unigene sequences with an average length of 689.19 bp and an N50 of 1,255 bp. The average length of the reference sequence was 552.63 bp, with an N50 length of 712 bp. About 71.09% of the total reads were mapped back onto the reference sequence (Supplementary Tables S2, S3), indicating good sequencing quality. A total of 24,488 genes in the reference sequence were annotated through BLAST analysis against the Nr (22,767), Swiss-Prot (17,323), GO (17,001), COG (14,954), KEGG (9,007) and Pfam (22,123) databases (Figure 2).

A total of 8,739 DEGs in response to CK, DS and DS_R treatment were generated using a stringent threshold fold change ≥ 2 and FDR < 0.01. Both the DS and DS_R treatments induced more upregulated DEGs than downregulated DEGs. Specifically, DS treatment induced 3,301 upregulated DEGs and 2,273 downregulated DEGs, while DS_R treatment induced 2,319 upregulated DEGs and 1,587 downregulated DEGs (Supplementary Figure S1).

The PCA results (Figure 3A) showed distinct gene expression patterns among the different treatment groups. According to PC1, the gene expression under the DS_R treatment was closer to that

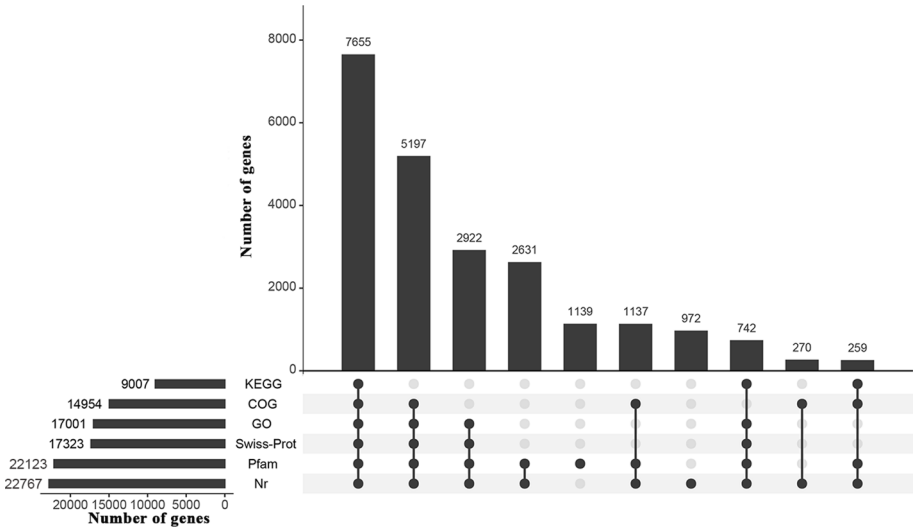

FIGURE 2
UpSet graph showing annotation results of the *I. difengpi* transcriptome against six databases. Nr, non-redundant protein sequence; Swiss-Prot, a manually annotated, non-redundant protein sequence; GO, gene ontology; COG, clusters of orthologous groups of proteins; KEGG, kyoto encyclopedia of genes and genomes; Pfam, homologous protein family.

under the CK treatment, accounting for 47.59% of the total data variation, while PC2 accounted for 30.65% of the total data variation. The hierarchical cluster heatmap of DEGs (Figure 3B) demonstrated significant changes in gene expression patterns during drought stress, with 65.25% of the genes showing a tendency of stable expression after rehydration but also the emergence of some new differentially expressed genes.

To validate the RNA-seq data, RT-qPCR was carried out with 6 genes of interest. (Supplementary Table S4). These genes greatly differed in expression between the three treatments, ranging from 1 to 600 reads per kilobase transcript per million reads (FRKM). The expression levels of the genes determined by RT-qPCR correlated well with those obtained from RNA-seq (R^2 = 0.87) (Supplementary Figure S2), confirming the reliability of the DEGs identified by analyzing the RNA-seq data.

3.2 GO function analysis and KEGG analysis of DEGs

The GO enrichment analysis showed that the DEGs in response to drought stress and rehydration were categorized into 52 functional terms in three categories. Among them, genes associated with metabolic process and cellular process in the category "biological process"; cell, cell parts and organelle in the category "cellular components"; and binding and catalytic activity in the category "molecular function", were the most abundant (Supplementary Figure S3). Among the 20 GO terms with the lowest *p* values in the enrichment analysis, the functional categories in the DS and DS_R treatments were mostly related to chloroplast and photosynthetic components (Figures 4A, B). In the DS treatment, the top 5 enriched biological processes were integral

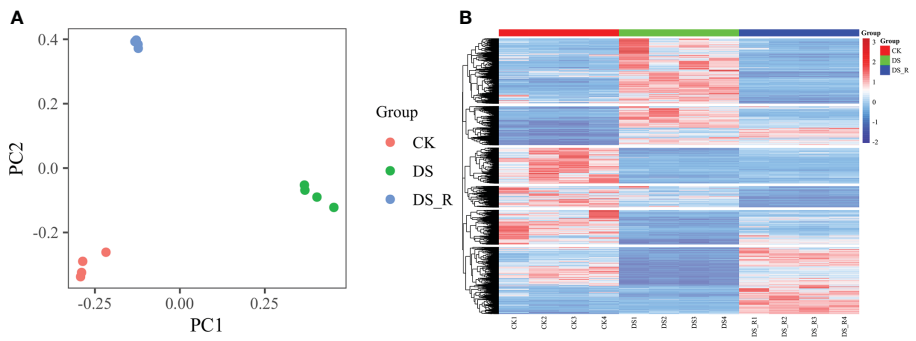

FIGURE 3
Global gene expression profiling of leaves under three soil water treatments. **(A)** Principal component analysis (PCA) of RNA-seq data obtained from leaves of *I difengpi* well-watered (CK), drought stress (DS) and drought–rehydration (DS_R) treatments. **(B)** Hierarchical clustering heatmap of RNA-seq data. The abscissa represents the sample names and hierarchical clustering results, whereas the ordinate represents DEGs and hierarchical clustering results. The expression intensity is indicated as the scale bar, red shading indicates high expression, and blue shading indicates low expression.

component of the membrane, thylakoid part, stress response, chloroplast thylakoid and plastid thylakoid, while under the DS_R treatment, the main enriched categories were defense response, response to stimulus, stress response, ADP binding and cell periphery.

The KEGG enrichment analysis showed 32 and 31 significantly enriched pathways under the DS and DS_R treatments, respectively (Figures 4C, D, $p < 0.05$). Among them, carbon metabolism, phytohormone signal transduction, glyoxylate and dicarboxylate metabolism, starch and sucrose metabolism and photosynthesis were the pathways with the most DEGs under the DS treatment. In the DS_R treatment, starch and sucrose metabolism, phenylpropanoid biosynthesis, amino sugar and nucleotide sugar metabolism, and the cell cycle were the main pathways. In addition, some enriched pathways were shared in common by the DS and DS_R treatments, including glutathione metabolism, flavonoid biosynthesis, nitrogen metabolism, photosynthesis, phenylpropanoid biosynthesis, cyanoamino acid metabolism, photosynthesis-antenna proteins and galactose metabolism. These results indicated that *I. difengpi* responds to drought stress and rehydration by enhancing its energy metabolism, reducing photosynthesis, regulating metabolic pathways and synthesizing metabolites.

3.3 Response TFs under drought and rehydration treatments

A total of 249, 162 and 231 DEGs were identified as encoding TFs in the CK_vs_DS (162 upregulated and 87 downregulated), CK_vs_DS_R (104 upregulated and 58 downregulated) and DS_vs_DS_R comparisons (114 upregulated and 117 downregulated), which could be assigned to 27, 15 and 25 families, respectively (Supplementary Table S5). Compared to the CK treatment, the DS treatment induced the upregulation of several members of the ARR, HSF, bHLH, GRF, B3, MYB, TCP, C2H2 and WRKY TF families (Figures 5A, B). Most members of the MYB, WRKY, bHLH, GRF and B3 gene families continued to be upregulated under DS_R treatment. Additionally, most members of the NAC and AP2/ERF TF families were also upregulated by DS_R treatment.

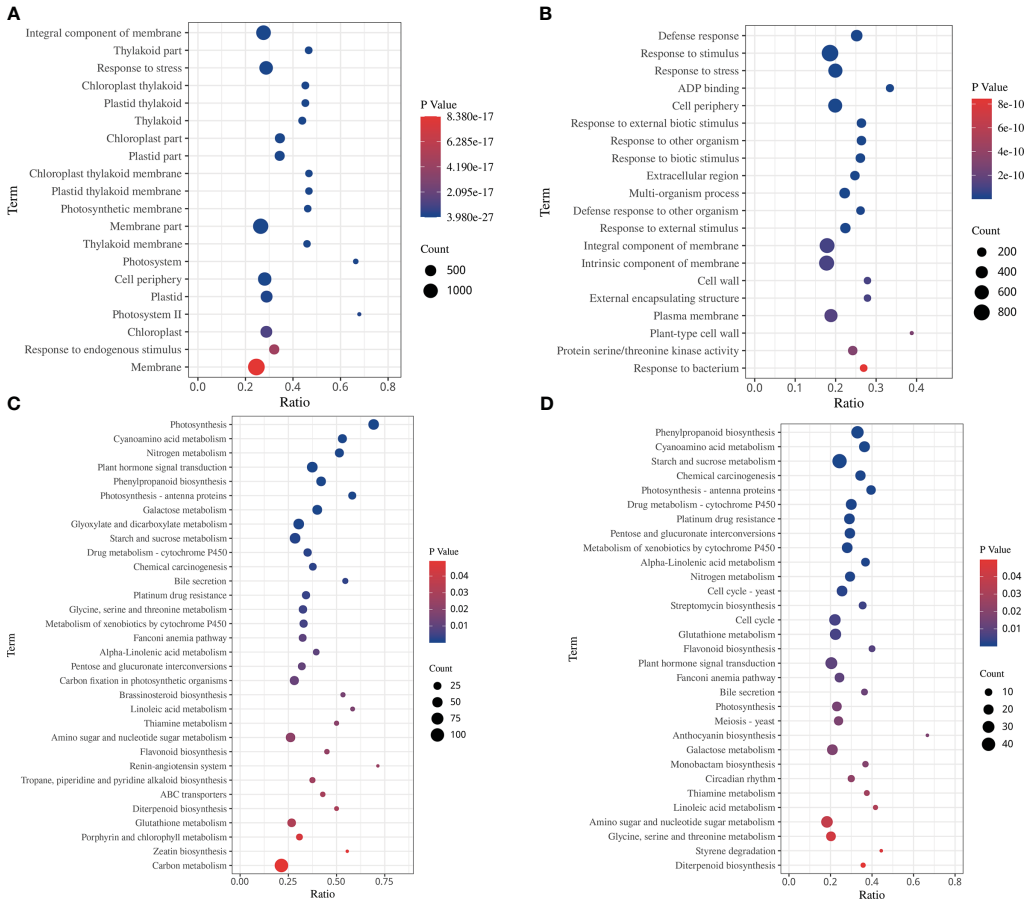

FIGURE 4
Top 20 GO terms and KEGG enrichment of DEGs under soil water treatments. **(A, C)** drought stress treatment. **(B, D)** drought–rehydration treatment. The abscissa represents the ratio of the number of different genes enriched in a pathway to the total number of annotated genes, where a greater ratio corresponds to greater enrichment. Deeper blue shading indicates greater statistical significance in terms of enrichment.

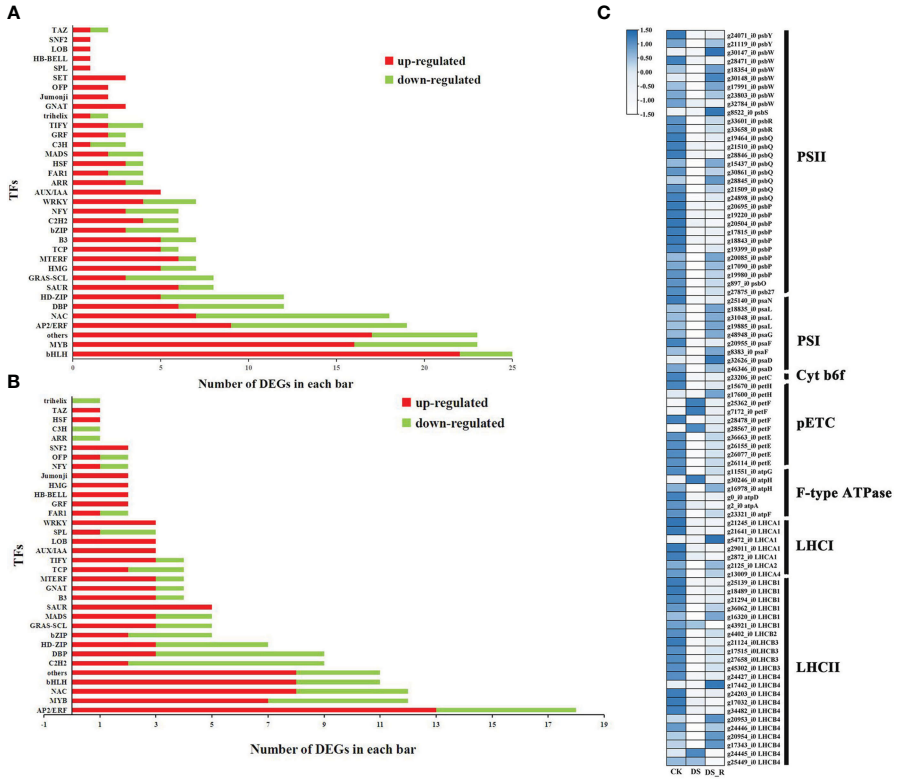

FIGURE 5
Transcription factors (TFs) responsive to drought stress **(A)** and drought–rehydration **(B)** treatment. **(C)** DEGs involved in photosynthesis and photosynthesis-antenna proteins.

3.4 DEGs involved in photosynthesis under drought and rehydration treatments

A total of 86 DEGs were annotated to the photosynthesis and photosynthesis-antenna protein pathways in the DS and DS_R treatments (Figure 5C). Among these, genes related to psaN, psaL, psaG, psaF, psaD, psbY, psbW, psbS, psbR, psbQ, psbP, psbO and psb27 in both photosystem I (PSI) and photosystem II (PSII) were downregulated, and genes related to the photosynthetic electron transport chain (pETC), such as petH, petF and petE, were downregulated under the DS treatment. Additionally, genes related to the cytochrome b6/f complex (Cyt b6f), the F-type ATPase, and the light-harvesting chlorophyll II protein complex, were mostly significantly downregulated under the DS treatment. However, DEGs related to photosynthesis and photosynthesis-antenna protein were mostly significantly upregulated after the DS_R treatment.

3.5 Metabolomics analysis

Metabolomic analysis revealed a total of 632 metabolites in the leaves of *I. difengpi* plants under the CK, DS and DS_R treatments, including 351 in the positive model and 281 in the negative model. The complete list of detected metabolites, along with their corresponding relative peak areas, can be found in Supplementary Table S6. Based on the hierarchical classification of metabolites, the majority of detected compounds were flavones, phenolic acids, flavonols, amino acids and derivatives, saccharides and alcohols (Supplementary Figure S4).

A total of 427 differentially expressed metabolites (DEMs) were identified using the criteria VIP ≥ 1 and fold change ≥ 1.5 or ≤ 0.67. As shown in Supplementary Figure S5, there were 223 and 108 upregulated DEMs and 115 and 115 downregulated DEMs in the DS and DS_R treatments, respectively. In both the DS and DS_R treatments, flavonols and phenolic acids were the main accumulated metabolites in *I. difengpi*. The percentages of flavonols (15.71%) and phenolic acids (9.67%) in the DS treatment were higher than those in the DS_R treatment (10.00% and 9.13%) (Supplementary Figures S6A, B). The OPLS-DA model showed that the prediction parameters R^2X, R^2Y and Q^2 were all higher than 0.7, 1 and 0.9, respectively, indicating the reliability and stability of the OPLS-DA model (Figure 6).

PCA showed clear differences between the CK, DS and DS_R treatments, and the samples of the DS and DS_R treatments were more similar, indicating a high degree of similarity in the metabolomic features between these two treatments (Figure 7A). PC1 and PC2 accounted for 92.10% of the total variation, with PC1 (58.10%) explaining the differences between the DS and DS_R treatments and PC2 (34.00%) explaining the general direction of changes in metabolite concentrations under the DS and DS_R treatments.

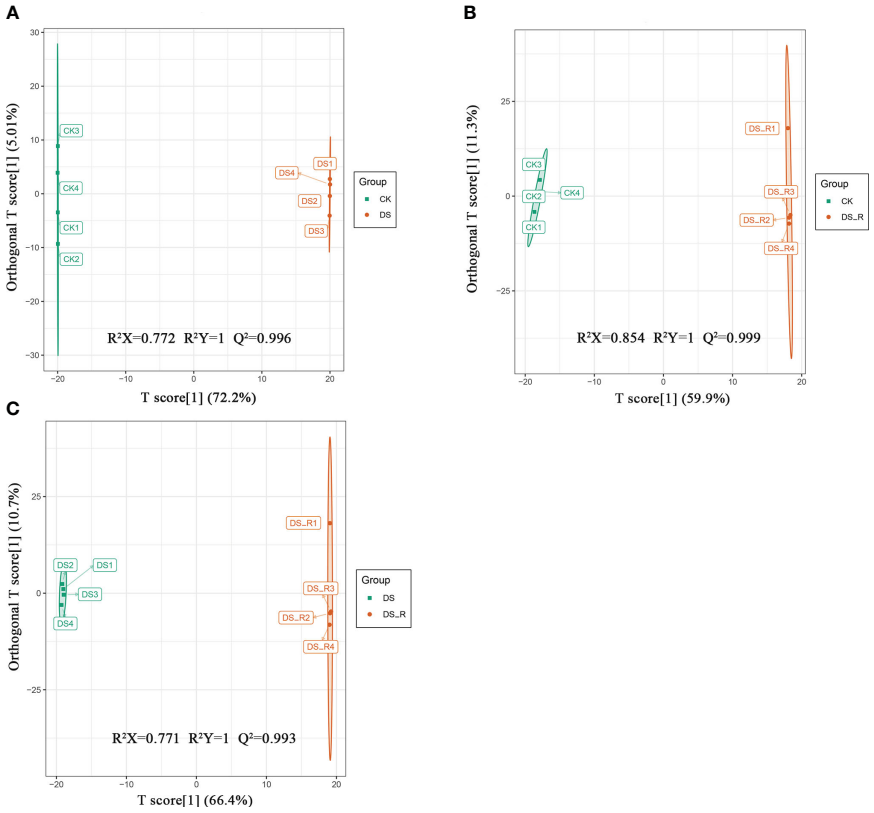

FIGURE 6
OPLS-DA model plots of the metabolites identified between pairs of groups of *I difengpi*. **(A)** Well-watered (CK)_vs_drought stress (DS). **(B)** Well-watered (CK)_vs_Drought−rehydration (DS_R). **(C)** Drought stress (DS)_vs_Drought−rehydration (DS_R). R^2: The interpretation rate of the model to the matrix; Q^2: The prediction ability of the model.

K-means clustering analysis grouped the 427 DEMs into 6 clusters (clusters 1-6, Figure 7B). Cluster 1 showed a decrease in the content of 47 metabolites under the DS treatment, which was restored to CK levels under the DS_R treatment. Cluster 3 exhibited an accumulation of 125 metabolites under the DS treatment, including L-isoleucine, L-leucine, L-serine, quercetin, spermidine and dihydroquercetin, which were restored to the CK level under the DS_R treatment. Clusters 4 and 5 demonstrated an accumulation of 146 metabolites under both DS and DS_R treatments, such as putrescine, L-asparagine, L-tryptophan,

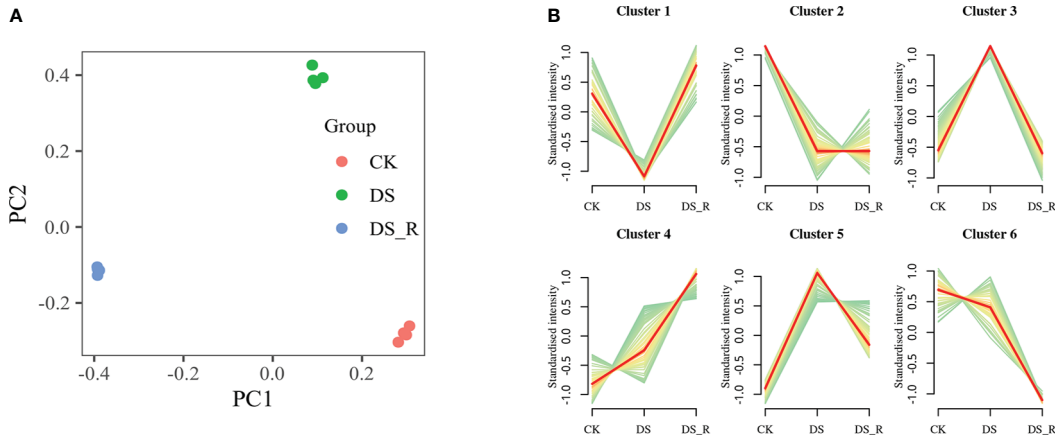

FIGURE 7
Metabolism analysis of leaves under the three soil water treatments. **(A)** PCA of metabolite data obtained from leaves of *I difengpi* plants under well-watered (CK), drought stress (DS) and drought−rehydration treatments (DS_R). **(B)** Differential metabolite K-means diagram. The x-coordinate represents the sample, and the y-coordinate represents the relative content of the standardized metabolite.

glutathione, L-ascorbate, D-sucrose, D-sorbitol and D-trehalose. Clusters 2 and 6 showed a decrease in the contents of 109 metabolites, including naringenin, raffinose and D-inositol, under both DS and DS_R treatments (Supplementary Table S7).

KEGG analysis showed 4 and 3 significantly enriched pathways involved in drought stress and rehydration, respectively (Figures 8A, B, $p < 0.05$). Specifically, there was significant enrichment in starch and sucrose metabolism, galactose metabolism, biosynthesis of secondary metabolites and ABC transporters under the DS treatment. However, under the DS_R treatment, there was significant enrichment of tropane, piperidine, and pyridine alkaloid biosynthesis, beta-alanine metabolism and starch and sucrose metabolism. In particular, four significantly enriched pathways (inositol phosphate metabolism, galactose metabolism, flavonoid biosynthesis and glutathione metabolism) were all found under both DS and DS_R treatments, indicating their close association with the response of *I. difengpi* to drought stress and rehydration.

3.6 Correlation analysis of transcriptome and metabolome data

To screen metabolites and genes in response to drought stress and rehydration, correlation analysis was performed between DEGs and DEMs ($|PCC| \geq 0.8$, $p \leq 0.05$). A total of 1,106 DEGs were found to be correlated with 331 DEMs during drought stress, while 776 DEGs were correlated with 230 DEMs under rehydration. Additionally, common pathways were obtained through the KEGG database for DEGs and DEMs. Supplementary Figure S7 shows that, compared with under the CK treatment, DEGs and DEMs under the DS and DS_R treatments were mapped to 71 and 64 pathways, respectively. Among them, the starch and sucrose metabolism pathways ($p < 0.05$) were significantly enriched under the DS and DS_R treatments. Galactose metabolism, flavonoid biosynthesis, glutathione metabolism and amino acid biosynthesis were also enriched under the DS and DS_R treatments, indicating that these pathways play important roles in *I. difengpi* in response to drought stress and rehydration.

The correlation analysis between DEGs and DEMs in the flavonoid synthesis pathway (Figure 9A) revealed that 6 genes were related to flavonoid synthesis. Among these, the *g9144_i0* gene (naringenin 3-dioxygenase, F3H, EC: 1.14.11.9) was upregulated under DS treatment, but downregulated after DS_R treatment, which promoted dihydroquercetin accumulated under DS treatment but recovered under DS_R treatment. Two genes, including the *g10592_i* gene (shikimate *O*-hydroxycinnamoyl transferase, HCT, EC: 2.3.1.133) were downregulated under both DS and DS_R treatments, which decreased coumaroyl quinic acid content. The *g21120_i* gene (chalcone isomerase, CHI, EC: 5.5.1.6) was upregulated under both DS and DS_R treatments, which decreased naringenin content. The *g32337_i0* gene (chalcone synthase, CHS, EC: 2.3.1.74) was downregulated under DS treatment but upregulated after DS_R treatment, which decreased naringenin chalcone content. Additionally, the *g4437_i0* gene (anthocyanidin synthase, ANS, EC: 1.14.11.9) was upregulated under DS treatment but downregulated after DS_R treatment.

The integrated analysis of the drought stress and rehydration response of *I. difengpi* also showed changes in polyamine metabolism, specifically regarding putrescine and spermidine. As shown in Figure 9B, a total of 3 genes were related to polyamine biosynthesis. The *g15613_i0* gene (ornithine decarboxylase, ODC, EC: 4.1.1.17) was upregulated under both DS and DS_R treatments. This increase in ODC levels could lead to the observed putrescine accumulation. Also, two genes coding for spermidine synthase (SPDS, EC: 2.5.1.16), which catalyzes the conversion of putrescine into spermidine, were upregulated under DS treatment but downregulated during DS_R treatment, correlating with similar changes in spermidine levels.

As shown in Figure 9C, a total of 13 genes were related to galactose metabolism. Two genes, including the *g15119_i0* gene (alpha-galactosidase, galA, EC: 3.2.1.22) were downregulated under both DS and DS_R treatments, which promoted D-sorbitol and melibiose accumulated under DS treatment, but decreased inositol content. Eleven genes, including the *g19280_i0* gene (raffinose synthase, RS, EC: 2.4.1.82), were mostly upregulated under DS treatment but downregulated after DS_R treatment, which decreased raffinose content.

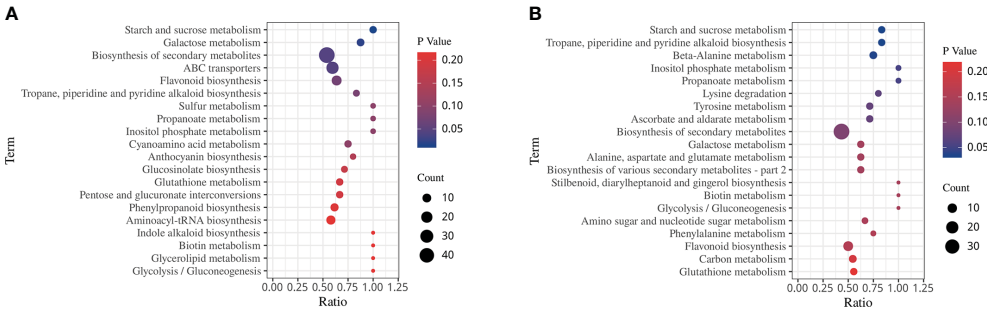

FIGURE 8
KEGG enrichment of DEMs under the three soil water treatments. **(A)** Drought stress treatment. **(B)** Drought–rehydration treatment. The abscissa represents the ratio of the number of different metabolites enriched in a pathway to the total number of metabolites, where a greater ratio corresponds to greater enrichment. Deeper blue shading indicates greater statistical significance in terms of enrichment.

10.3389/fpls.2023.1284135

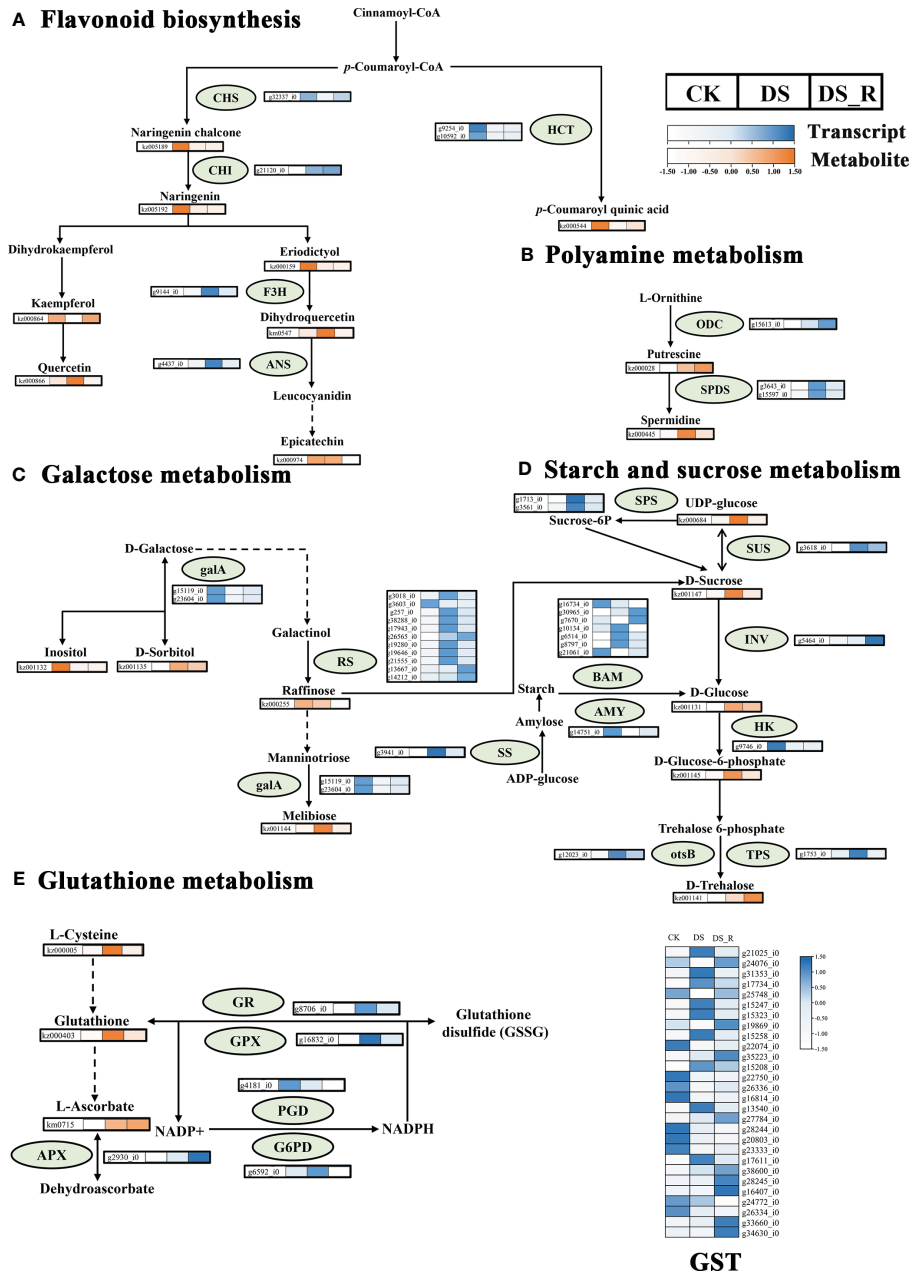

FIGURE 9
Changes in key enzyme activities at the transcript and metabolite levels in response to water treatments. **(A)** Flavonoid biosynthesis. **(B)** Polyamine metabolism; **(C)** Galactose metabolism. **(D)** Starch and sucrose metabolism. **(E)** Glutathione metabolism. HCT, shikimate *O*-hydroxycinnamoyl transferase; CHS, chalcone synthase; F3H, naringenin 3-dioxygenase; CHI, chalcone isomerase; ANS, anthocyanin synthase; SPDS, spermidine synthase; ODC, ornithine decarboxylase; INV, beta-fructofuranosidase; otsB, trehalose 6-phosphate phosphatase; TPS, trehalose phosphate synthase; SUS, sucrose synthase; SPS, sucrose-phosphate synthase; SS, starch synthase; galA, alpha-galactosidase; HK, hexokinase; RS, sucrose galactosyltransferase; BAM, beta-amylase; AMY, alpha-amylase; GST, glutathione S-transferase; GR, glutathione reductase; GPX, glutathione peroxidase; PGD, 6-phosphogluconate dehydrogenase; G6PD, glucose-6-phosphate 1-dehydrogenase; APX, L-ascorbate peroxidase. Dotted arrows indicate multiple enzyme-catalyzed reaction steps. Colored boxes represent the normalized intensity of transcript levels (in blue) and metabolite levels (in orange) across different water treatments. CK, well-watered treatment; DS, drought stress treatment; DS_R, drought–rehydration treatment.

As shown in Figure 9D, a total of 16 genes were related to starch and sucrose metabolism. Among these, the *g5464_i0* gene (beta-fructofuranosidas, INV, EC: 3.2.1.26) was upregulated under DS_R treatments, which promoted D-glucose accumulated. The *g9746_i0* gene (hexokinase, HK, EC: 2.7.1.1) was downregulated under both DS and DS_R treatments, which promoted the accumulated of D-glucose-6-phosphate. The *g12023_i0* gene (trehalose 6-phosphate phosphatases, otsB, EC: 3.1.3.12) and the *g1753_i0* gene (trehalose phosphate synthase, TPS, EC: 2.4.1.15 3.1.3.12), were upregulated under DS treatment, but the g*1753_i0* gene showed stable expression after DS_R treatment, promoted the accumulated of D-trehalose. The *g3618_i0* gene (sucrose synthase, SUS, EC:

2.4.1.13) was upregulated under both DS and DS_R treatments, which promoted UDP-glucose accumulated. Additionally, 7 genes (beta-amylase, BAM, EC: 3.2.1.2) related to starch degradation, were mostly upregulated under DS treatment, while genes related to starch synthesis, such as sucrose-phosphate synthase (SPS, EC: 2.4.1.14) and starch synthase (SS, EC: 2.4.1.21) were upregulated under DS treatment but downregulated during DS_R treatment. The *g14751_i0* gene (alpha-amylase AMY, EC: 3.2.1.1) was downregulated under both DS and DS_R treatments.

The metabolomics analysis showed that glutathione, L-cysteine and L-ascorbate were involved in glutathione metabolism. Five genes were related to glutathione metabolism (Figure 9E). The *g2930_i0* gene (L-ascorbate peroxidase, APX, EC: 1.11.1.11) was upregulated under both DS and DS_R treatments, which promoted the accumulated of L-ascorbate. The *g8706_i0* gene (glutathione reductase, GR, EC: 1.8.1.7) and the *g16832_i0* gene (glutathione peroxidase GPX, EC: 1.11.1.9) were upregulated under DS treatment but downregulated after DS_R treatment, which promoted glutathione accumulated under DS treatment but recovered during DS_R treatment. The *g4181_i0* gene (6-phosphogluconate dehydrogenase, PGD, EC: 1.1.1.44) was downregulated under both DS and DS_R treatment. The *6592_i0* gene (glucose-6-phosphate 1-dehydrogenase, G6PD, EC: 1.1.1.49) was upregulated under DS treatment but recovered after DS_R treatment. Additionally, 28 genes (S-transferase, GST, EC: 2.5.1.18), most of which were upregulated under DS treatment but recovered during DS_R treatment.

Four amino acid metabolism pathways were regulated under drought stress and rehydration (Supplementary Table S8). In the alanine, aspartate and glutamate metabolism, the *g8114_i0* gene (asparagine synthesis, asnB, EC: 6.3.5.4) was upregulated under both DS and DS_R treatments, which promoted L-asparagine accumulated. In the valine, leucine and isoleucine biosynthesis, the *g11815_i0* gene (branched-chain amino acid amino transfer, ilvE, EC: 2.6.1.42) was downregulated under both DS and DS_R treatments, which promoted L-leucine and L-isoleucine accumulated. In the phenylalanine, tyrosine and tryptophan biosynthesis, the *g13599_i0* gene (tryptophan synthase alpha chain, trpA, EC: 4.2.1.20) and the *g9790_i0* gene (tryptophan synthase beta chain, trpB, EC: 4.2.1.20) were downregulated under both DS and DS_R treatments, which promoted L-tryptophan accumulated. In the glycine, serine and threonine metabolism, the *g2861_i0* gene (serine-glyoxylate transaminase, AGXT, EC: 2.6.1.45) was downregulated under DS treatment but upregulated after DS_R treatment, which promoted L-serine accumulated under DS treatment and recovered during DS_R treatment.

4 Discussion

I. difengpi is a naturally drought-tolerant nonmodel plant and an important untapped genetic resource for studying the genetic and metabolic mechanisms underlying drought adaptation. In the present study, transcriptomic and metabolome analytical methods were combined to identify differentially expressed genes and metabolites under drought and rehydration conditions, and we aimed to preliminarily elucidate the molecular mechanisms of the response of *I. difengpi* to drought stress. Next-generation sequencing (NGS) technology, known for its accuracy, speed and low cost, is commonly used to explore unique genetic characteristics in both model and nonmodel plant systems (Unamba et al., 2015; Ren et al., 2022). The GC content represents the stability of DNA as well as the composition of genes and genomes, reflecting evolution, gene structure and gene regulation (Carels et al., 1998), and changes in GC content may reveal adaptability to different climatic conditions. The results in Supplementary Table S2 show that the GC content of the *I. difengpi* transcriptome was 46.59%. This result is similar to previously published data (46.00~48.48%) (Liu et al., 2022). Similarly, in other studies on dicotyledonous plants, the GC content of *Picrorhiza kurrooa* was 44.6% (Gahlan et al., 2012) and that of *Nicotiana benthamiana* was 41.0% (Nakasugi et al., 2013).

Drought can induce the response of various genes, with more upregulated genes than downregulated genes (Wang and Gong, 2017). In the present study, the number of upregulated genes in *I. difengpi* under DS and DS_R treatments was greater than the number of downregulated genes (Supplementary Figure S1), indicating that *I. difengpi* primarily responds to drought stress and rehydration through the upregulation of genes. Upregulation of genes is likely a strategy employed by *I. difengpi* to actively adapt to environmental stress, while downregulation of gene expression helps reduce metabolism, inhibit growth and adapt to adverse conditions. The rehydration process compensates for the damage caused by drought, and the compensatory effect is also influenced by various factors, such as the degree of damage, rehydration time and growth condition of the damaged plant itself. Furthermore, the rehydration treatment reduced the number of DEGs in *I. difengpi* by 29.92% (Supplementary Figure S1), indicating a certain compensatory effect of rehydration, but not complete restoration, and resulting in some new DEGs. The hierarchical clustering heatmap of DEGs shown in Figure 3B illustrates that under rehydration treatment, 65.25% of the genes tended to have stable expression. Taken together, these results indicate that *I. difengpi* actively adapts to or resists drought through upregulated gene expression and exhibits a certain compensatory effect after rehydration, which may partly explain the extreme drought tolerance of *I. difengpi*.

TFs are important upstream regulatory proteins that play a crucial role in plant responses to abiotic and biotic stress (Ning et al., 2011). Figure 5A shows that most members of the six TF families (bHLH, HSF, MYB, ARR, WRKY and C2H2) were upregulated under drought stress treatment, indicating their potential role in positive regulation. The positive regulatory roles of HSF, WRKY, MYB, bHLH, ARR and C2H2 in the plant response to drought stress have been demonstrated in previous studies (Kang et al., 2013b; Yang and Lv, 2022). Additionally, most members of the GRF, TCP and B3 TF families were upregulated, and these TFs are known to regulate various growth and developmental processes, such as leaf development, flower symmetry and bud branching (Liu et al., 2014; Parapunova et al., 2014; Zhang et al., 2014). Furthermore, after rehydration treatment, most members of the MYB, WRKY, bHLH, GRF and B3 gene families continued to be upregulated, suggesting their involvement in regulating the recovery growth of *I. difengpi*.

Under drought stress, stomatal closure interrupts the supply of carbon dioxide to mesophyll cells, inhibiting carbon assimilation and light reactions, leading thereby to a decrease in photosynthetic efficiency (Chaves et al., 2009). The results of this study showed that under drought treatment, the majority of genes involved in PSI, PSII, Cyt b6f, pETC, F-type ATPase and light-harvesting chlorophyll II protein were downregulated (Figure 5C). Furthermore, GO enrichment analysis indicated that the top 20 enriched GO terms were mostly related to photosynthesis (Figures 4A, B), suggesting the inhibition of photosynthesis in *I. difengpi* leaves under drought stress. This further supports the idea that *I. difengpi*, experiencing drought stress, induces stomatal closure to reduce transpiration and consequently decreases photosynthetic capacity. Similar findings have been reported in wheat (Lv et al., 2022). When *I. difengpi* plants were watered again, a majority fraction of photosynthesis-related genes were upregulated, indicating gradual recovery of photosynthesis-related processes from drought stress after rehydration.

Despite the reduction in carbon fixation in leaves under DS treatment, plants accumulate large amounts of water-soluble carbohydrates such as glucose, fructose, sucrose and sorbitol to maintain cell turgor and protect their membrane integrity (Yang et al., 2019). Sucrose is the main soluble product of plant photosynthesis and it is an important regulatory factor in plant cellular metabolism (Xie et al., 2002). The results of the present study showed that under drought stress, genes related to D-sucrose synthesis, such as *SPS*, were upregulated, while genes related to D-sucrose hydrolysis, such as *INV*, were downregulated, promoted the accumulation of D-glucose (Figure 9D). Similar results have been reported in apple trees (Yang et al., 2019). In addition, DS treatment upregulated the expression of *TPS* gene and promoted the accumulation of D-trehalose in *I. difengpi*. TPS converts UDP-glucose into trehalose, thus enhancing the ability of *Selaginella pulvinata* to cope with adverse environments (Seki et al., 2007). Furthermore, *I. difengpi* exhibited higher levels of D-sorbitol under drought conditions. Research by Ranney et al. (1991) found that the osmoregulatory effect of cherry (*Prunus cerasus* and *P. avium* × *pseudocerasus*) under drought stress is mainly driven by sorbitol.

Starch is the main storage carbohydrate in plants (Ballicora et al., 2004). Under drought stress, starch gets hydrolyzed to glucose molecules (such as glucose-6-P and glucose-1-P). These molecules acts as a source of energy through respiration and precursors for the synthesis of sucrose (Geigenberger et al., 1997; Thalmann et al., 2016). The results of this study showed that drought stress downregulated the expression of *AMY* gene and upregulation the expression of *BAM* gene (Figure 9D). The concerted action of AMY and BAM promotes starch degradation, providing energy for plants to withstand drought stress. In summary, under drought treatment, photosynthesis in *I. difengpi* gradually slows, leading to a decrease in the quantity of photosynthetic products. This, in turn, increases the synthesis of D-sucrose, D-glucose, D-sorbitol and D-trehalose, regulating cell osmotic potential and water balance, while stored starch is degraded to provide energy, thereby maintaining normal physiological activities.

Under drought stress, plants produce a large amount of reactive oxygen species (ROS). These excessive ROS can cause damage to plant cells and, in severe cases, lead to plant death (Baxter et al., 2014). To sustain their growth and development, plants respond to drought stress by inducing the expression of genes involved in amino acid and secondary metabolite metabolism, producing large amounts of antioxidant substances such as glutathione, ascorbate, polyamines and flavonoids (Mittler et al., 2004; Alcázar et al., 2011; Nakabayashi et al., 2014).

Flavonoids possess strong antioxidant activity and can minimize the harmful effects of ROS on plants under drought stress (Ma et al., 2014). The major enzymes involved in the formation of various flavonoid compounds include CHS, CHI, F3'H, FLS, F3H, DFR, ANS and UGT. Among them, CHS, CHI, F3'H, FLS and F3H are responsible for the production of flavanols and other flavonoid compounds, while DFR, ANS and UGT are involved in anthocyanin accumulation in later stages (Khusnutdinov et al., 2021). The response of flavonoid content to drought stress varies between different species. Studies conducted in *Arabidopsis thaliana*, for example, have shown significant accumulation of dihydroflavonols and anthocyanins under drought stress (Nakabayashi et al., 2014; Zandalinas et al., 2016). Yang and Lv (2022) found that vitexin and naringenin were significantly increased in *Haloxylon amsenjimodendron* under drought stress. In our study, dihydroquercetin and quercetin significantly accumulated (Figure 9A) under drought stress treatment. Furthermore, genes related to CHI, F3H and ANS showed an upregulated expression under drought stresss treatment, with weaker levels or even downregulated during rehydration. The genes and metabolites related to flavonoids actively respond to drought stress by providing resistance to drought.

The ascorbate–glutathione cycle plays a crucial role in defending against oxidative damage caused by drought stress (Foyer and Noctor, 2011). The protective effect of the ascorbate–glutathione cycle against drought-induced oxidative damage is closely related to the gene expression of key enzymes involved in the regulation of the oxidative state, such as APX, GRC1, DHAR, MDHAR, GPX and GST (Sečenji et al., 2010; Kang et al., 2013a). In this study, drought treatment led to the upregulation of genes related to GPX, GR and APX, as well as the accumulation of glutathione and ascorbate (Figure 9E). This suggests that drought enhances the synthesis capacity of glutathione and ascorbate, which helps alleviate the impact of ROS on plants. The study also found that the genes involved in regulating PGD and G6PD. PGD and G6PD are involved in the conversion of NADP+ to NADPH, catalyzing the production of NADPH as a reducing agent and providing reducing power for the conversion of glutathione disulfide (GSSG) to glutathione (Noctor et al., 2012). This indicates that coenzymes providing reducing power actively respond to drought stress, in addition to the role of reductases under drought stress. Notably, most of the 28 *GST* genes were significantly upregulated under drought stress. GS is encoded by a multigene family that is primarily present in the cytoplasm. It plays a crucial role in combating oxidative stress under biotic and abiotic stresses, acting as a detoxifier for harmful substances inside and outside cells (Dixon et al., 2002). After rehydration, the gene expression and metabolites related to glutathione metabolism decreased, indicating the gradual relief of drought stress.

Amino acids play various roles in regulating plant tolerance to abiotic stress as osmoprotectants, ROS scavengers, and precursors of energy-related metabolites (Less and Galili, 2008). Serine, proline and leucine are important signaling molecules, while other amino acids are precursors of hormones and secondary metabolites with signal transduction functions (Hannah et al., 2010; Szabados and Savouré, 2010; Ros et al., 2014). You et al. (2019) found that *Sesamum indicum* accumulates a large amount of tryptophan, leucine, isoleucine, asparagine, and tyrosine under drought stress. The results of the present study demonstrate that during drought stress, the contents of L-leucine, L-isoleucine, L-serine, L-asparagine and L-tryptophan in *I. difengpi* significantly increased (Supplementary Table S8). Branched-chain amino acids (BCAAs) containing valine, leucine and isoleucine serve multiple functions in drought stress. On the one hand, BCAAs can serve as alternative substrates for respiratory metabolism when plants face drought stress. On the other hand, the catalytic metabolism of BCAAs can provide electrons to the respiratory electron chain under stress conditions (Xu et al., 2021). Aromatic amino acids, including phenylalanine, tyrosine, and tryptophan, can be used to synthesize secondary metabolites that have various functions in abiotic stress (Xu et al., 2019). Therefore, the increase in aromatic amino acids may enhance the accumulation of secondary metabolites. The above results suggest that the accumulation of amino acids in *I. difengpi* under drought conditions may contribute to its drought tolerance.

Polyamines, mainly putrescine, spermidine and spermine, are important growth regulators in plants. When plants are subjected to stress such as water, salinity, and low temperature, polyamines can regulate the physical and chemical properties of cell membranes, remove ROS from the body, and affect the biosynthesis of DNA, RNA, and proteins (Liu et al., 2000; Seiler and Raul, 2005). The results of the present study showed that under drought stress, genes related to putrescine and spermidine synthesis, such as ODC and SPDS, were upregulated, promoted the accumulation of putrescine and spermidine (Figure 9B). This indicates that *I. difengpi* mainly undergoes decarboxylation through the ornithine pathway catalyzed by ornithine decarboxylase to produce putrescine, which is then converted to spermidine as a part of the active response of the plant to drought stress (Takahashi and Kakehi, 2009).

5 Conclusion

As an endangered medicinal plant endemic to the karst region of China, *I. difengpi* has evolved extreme tolerance to drought stress. The present study demonstrated that *I. difengpi* actively responds to drought stress transcriptomically and metabolomically: (i) Defense systems and protective mechanisms are activated rapidly under drought stress to counteract damage. This response is characterized by altering starch and sugar metabolism and promoting photomorphogenesis. (ii) *I. difengpi* has a powerful osmoregulation mechanism, synthesizing metabolites such as D-sucrose, D-trehalose, D-glucose, glutathione, flavonoids, polyamines and amino acids, which helps alleviate the osmotic pressure on the cell membrane. In conclusion, *I. difengpi* exhibits strong drought tolerance by adopting a series of powerful defense and protection measures to delay and minimize drought-induced damage. These findings provide theoretical guidance for the ecological restoration of endemic species in karst regions.

Data availability statement

The datasets presented in this study can be found in online repositories. The names of the repository/repositories and accession number(s) can be found below: https://www.ncbi.nlm.nih.gov/genbank/, PRJNA983054.

Author contributions

X-JZ: Conceptualization, Investigation, Methodology, Supervision, Visualization, Writing – original draft, Writing – review & editing. CW: Conceptualization, Investigation, Methodology, Supervision, Visualization, Writing – original draft, Writing – review & editing. B-YL: Funding acquisition, Project administration, Software, Supervision, Writing – review & editing. H-LL: Investigation, Methodology, Resources, Visualization, Writing – review & editing. M-LW: Funding acquisition, Project administration, Resources, Software, Supervision, Writing – review & editing. HL: Resources, Supervision, Writing – review & editing.

Funding

The author(s) declare financial support was received for the research, authorship, and/or publication of this article. This work was supported by grants from the National Natural Science Foundation of China (32160093); The Guangxi Science and Technology Bases and Talent Project (GuikeAD20297049); The Guangxi Key Research and Development Project (GuikeAB21220024); The Guilin Scientific Research and Technological Development Plan (20220105); and The Guilin Innovation Platform and Talent Plan (20210102-3).

Acknowledgments

We thank Norminkoda Biotechnology Co., Ltd. (Wuhan, China) for their assistance in sequencing data analysis.

Conflict of interest

The authors declare that the research was conducted in the absence of any commercial or financial relationships that could be construed as a potential conflict of interest.

Publisher's note

All claims expressed in this article are solely those of the authors and do not necessarily represent those of their affiliated

organizations, or those of the publisher, the editors and the reviewers. Any product that may be evaluated in this article, or claim that may be made by its manufacturer, is not guaranteed or endorsed by the publisher.

Supplementary material

The Supplementary Material for this article can be found online at: https://www.frontiersin.org/articles/10.3389/fpls.2023.1284135/full#supplementary-material

References

AbdElgawad, H., Farfan-Vignolo, E. R., Vos, D., and Asard, H. (2015). Elevated CO_2 mitigates drought and temperature-induced oxidative stress differently in grasses and legumes. *Plant Sci.* 231, 1–10. doi: 10.1016/j.plantsci.2014.11.001

Alcázar, R., Bitrián, M., Bartels, D., Koncz, C., Altabella, T., and Tiburcio, A. F. (2011). Polyamine metabolic canalization in response to drought stress in Arabidopsis and the resurrection plant Craterostigma plantagineum. *Plant Signal. Behav.* 6 (2), 243–250. doi: 10.4161/psb.6.2.14317

Altschul, S. F., Gish, W., Miller, W., Myers, E. W., and Lipman, D. J. (1990). Basic local alignment search tool. *J. Mol. Bio.* 215 (3), 403–410. doi: 10.1016/S0022-2836(05)80360-2

Anders, S., and Huber, W. (2010). Differential expression analysis for sequence count data. *Genome Biolo.* 11 (10), R106. doi: 10.1038/npre.2010.4282.1

Andrews, S. (2010) *A quality control tool for high throughput sequence data*. Available at: http://www.bioinformatics.babraham.ac.uk/projects/fastqc/.

Apweiler, R., Bairoch, A., Wu, C. H., Barker, W. C., Boeckmann, B., Ferro, S., et al. (2004). UniProt: the universal protein knowledgebase. *Nucleic Acids Res.* 32, D115–D119. doi: 10.1093/nar/gkh131

Ashburner, M., Ball, C. A., Blake, J. A., Botstein, D., Butler, H., Cherry, J. M., et al. (2000). Gene Ontology: tool for the unification of biology. *Nat. Genet.* 25 (1), 25–29. doi: 10.1038/75556

Bai, L., Sui, F., Ge, T., Sun, Z., Lu, Y., and Zhou, G. (2006). Effect of soil drought stress on leaf water status, membrane permeability and enzymatic antioxidant system of maize. *Pedosphere* 16 (3), 326–332. doi: 10.1016/S1002-0160(06)60059-3

Ballicora, M. A., Iglesias, A. A., and Preiss, J. (2004). ADP-Glucose pyrophosphorylase: a regulatory enzyme for plant starch synthesis. *Photosynth. Res.* 79 (1), 1–24. doi: 10.1023/b:pres.0000011916.67519

Baxter, A., Mittler, R., and Suzuki, N. (2014). ROS as key players in plant stress signalling. *J. Exp. Bot.* 65 (5), 1229–1240. doi: 10.1093/jxb/ert375

Carels, N., Hatey, P., Jabbari, K., and Bernardi, G. (1998). Compositional properties of homologous coding sequences from plants. *J. Mol. Evol.* 46 (1), 45–53. doi: 10.1007/PL00006282

Chaves, M. M., Flexas, J., and Pinheiro, C. (2009). Photosynthesis under drought and salt stress: regulation mechanisms from whole plant to cell. *Ann. Bot.* 103 (4), 551–560. doi: 10.1093/aob/mcn125

Chen, C., Xia, R., Chen, H., and He, Y. (2018). TBtools, a toolkit for biologists integrating various HTS-data handling tools with a user-friendly interface. *bioRxiv*, 289660. doi: 10.1101/289660

Chen, Y., Li, C., Yi, J., Yang, Y., Lei, C., and Gong, M. (2020). Transcriptome response to drought, rehydration and re-dehydration in potato. *Int. J. Mol. Sci.* 21 (1), 159. doi: 10.3390/ijms21010159

Chong, J., and Xia, J. (2018). MetaboAnalystR: an R package for flexible and reproducible analysis of metabolomics data. *Bioinformatics* 34 (24), 4313–4314. doi: 10.1093/bioinformatics/bty528

Conway, J. R., Lex, A., and Gehlenborg, N. (2017). UpSetR: an R package for the visualization of intersecting sets and their properties. *Bioinformatics* 33, 2938–2940. doi: 10.1093/bioinformatics/btx364

Cramer, G. R., Ergül, A., Grimplet, J., Tillett, R. L., Tattersall, E. A. R., Bohlman, M. C., et al. (2007). Water and salinity stress in grapevines: early and late changes in transcript and metabolite profiles. *Func. Integr. Genomic.* 7 (2), 111–134. doi: 10.1007/s10142-006-0039-y

Dai, A. (2013). Increasing drought under global warming in observations and models. *Nat. Clim. Change* 3 (1), 52–58. doi: 10.1038/nclimate1633

Deng, Y., Li, J., Wu, S., Zhu, Y., Chen, Y., and He, F. (2006). Integrated nr database in protein annotation system and its localization. *Com. Eng.* 32, 71–72. doi: 10.3969/j.issn.1000-3428.2006.05.026

Dixon, D. P., Lapthorn, A., and Edwards, R. (2002). Plant glutathione transferases. *Genome Biol.* 3 (3), reviews3004.3001–3004.3010. doi: 10.1186/gb-2002-3-3-reviews3004

Finn, R. D., Bateman, A., Clements, J., Coggill, P., Eberhardt, R. Y., Eddy, S. R., et al. (2013). Pfam: the protein families database. *Nucleic Acids Res.* 42, D222–D230. doi: 10.1093/nar/gkt1223

Foyer, C. H., and Noctor, G. (2011). Ascorbate and glutathione: the heart of the redox hub. *Plant Physiol.* 155 (1), 2–18. doi: 10.1104/pp.110.167569

Gahlan, P., Singh, H. R., Shankar, R., Sharma, N., Kumari, A., Chawla, V., et al. (2012). *De novo* sequencing and characterization of *Picrorhiza kurrooa* transcriptome at two temperatures showed major transcriptome adjustments. *BMC Genomics* 13 (1), 126. doi: 10.1186/1471-2164-13-126

Geigenberger, P., Reimholz, R., Geiger, M., Merlo, L., Canale, V., and Stitt, M. (1997). Regulation of sucrose and starch metabolism in potato tubers in response to short-term water deficit. *Planta* 201 (4), 502–518. doi: 10.1007/s004250050095

Golldack, D., Li, C., Mohan, H., and Probst, N. (2014). Tolerance to drought and salt stress in plants: unraveling the signaling networks. *Front. Plant Sci.* 5. doi: 10.3389/fpls.2014.00151

Grabherr, M. G., Haas, B. J., Yassour, M., Levin, J. Z., Thompson, D. A., Amit, I., et al. (2011). Full-length transcriptome assembly from RNA-Seq data without a reference genome. *Nat. Biotechnol.* 29 (7), 644–652. doi: 10.1038/nbt.1883

Hannah, M. A., Caldana, C., Steinhauser, D., Balbo, I., Fernie, A. R., and Willmitzer, L. (2010). Combined transcript and metabolite profiling of *arabidopsis* grown under widely variant growth conditions facilitates the identification of novel metabolite-mediated regulation of gene expression. *Plant Physiol.* 152 (4), 2120–2129. doi: 10.1104/pp.109.147306

Hu, Y., Chen, X., and Shen, X. (2022). Regulatory network established by transcription factors transmits drought stress signals in plant. *Stress Biol.* 2 (1), 26. doi: 10.1007/s44154-022-00048-z

Kanehisa, M., Goto, S., Kawashima, S., Okuno, Y., and Hattori, M. (2004). The KEGG resource for deciphering the genome. *Nucleic Acids Res.* 32, D277–D280. doi: 10.1093/nar/gkh063

Kang, N. Y., Cho, C., and Kim, J. (2013b). Inducible expression of *Arabidopsis* response regulator 22 (ARR22), a type-C ARR, in transgenic *Arabidopsis* enhances drought and freezing tolerance. *PloS One* 8 (11), e79248. doi: 10.1371/journal.pone.0079248

Kang, G. Z., Li, G. Z., Liu, G. Q., Xu, W., Peng, X. Q., and Wang, C. Y. (2013a). Exogenous salicylic acid enhances wheat drought tolerance by influence on the expression of genes related to ascorbate-glutathione cycle. *Bio. Plant.* 57 (4), 718–724. doi: 10.1007/s10535-013-0335-z

Khusnutdinov, E., Sukhareva, A., Panfilova, M., and Mikhaylova, E. (2021). Anthocyanin biosynthesis genes as model genes for genome editing in plants. *Int. J. Mol. Sci.* 22 (16), 8752. doi: 10.3390/ijms22168752

Kim, D., Pertea, G., Trapnell, C., Pimentel, H., Kelley, R., and Salzberg, S. L. (2013). TopHat2: accurate alignment of transcriptomes in the presence of insertions, deletions and gene fusions. *Genome Biol.* 14 (4), R36. doi: 10.1186/gb-2013-14-4-r36

Kong, D., Li, Y., Liang, H., Wang, M., Shi, Y., and Jiang, Y. (2012). Anatomical features of vegetative organs and ecological adaptability of leaf structure of *Illicium difengpi*. *Genomics Appl. Biol.* 31 (3), 282–288. doi: 10.3969/gab.031.000282

Kumar, L., and Matthias, E. F. (2007). Mfuzz: a software package for soft clustering of microarray data. *Bioinformation* 2, 5–7. doi: 10.6026/97320630002005

Less, H., and Galili, G. (2008). Principal transcriptional programs regulating plant amino acid metabolism in response to abiotic stresses. *Plant Physiol.* 147 (1), 316–330. doi: 10.1104/pp.108.115733

Liu, K., Fu, H., Bei, Q., and Luan, S. (2000). Inward potassium channel in guard cells as a target for polyamine regulation of stomatal movements. *Plant Physiol.* 124 (3), 1315–1326. doi: 10.1104/pp.124.3.1315

Liu, B., Liang, H., Wu, C., Huang, X., Wen, X., Wang, M., et al. (2022). Physiological and transcriptomic responses of *Illicium difengpi* to drought stress. *Sustainability* 14 (12), 7479. doi: 10.3390/su14127479

Liu, J., Rice, J. H., Chen, N., Baum, T. J., and Hewezi, T. (2014). Synchronization of developmental processes and defense signaling by growth regulating transcription factors. *PloS One* 9 (5), e98477. doi: 10.1371/journal.pone.0098477

Livak, K. J., and Schmittgen, T. (2001). Analysis of relative gene expression data using real-time quantitative PCR and the 2^{-DDCt} method. *Methods* 25, 402–408. doi: 10.1006/meth.2001.1262

Lv, L., Chen, X., Li, H., Huang, J., Liu, Y., and Zhao, A. (2022). Different adaptive patterns of wheat with different drought tolerance under drought stresses and rehydration revealed by integrated metabolomic and transcriptomic analysis. *Front. Plant Sci.* 13. doi: 10.3389/fpls.2022.1008624

Ma, D., Sun, D., Wang, C., Li, Y., and Guo, T. (2014). Expression of flavonoid biosynthesis genes and accumulation of flavonoid in wheat leaves in response to drought stress. *Plant Physiol. Bioch.* 80, 60–66. doi: 10.1016/j.plaphy.2014.03.024

Meng, X., Wang, M., and Liang, H. (2019). Research progress of medicinal plant *Illicium difengpi* in karst region. *J. Guangxi Acad. Sci.* 35 (01), 13–19. doi: 10.13657/j.cnki.gxkxyxb.20190131.005

Michaletti, A., Naghavi, M. R., Toorchi, M., Zolla, L., and Rinalducci, S. (2018). Metabolomics and proteomics reveal drought-stress responses of leaf tissues from spring-wheat. *Sci. Rep.* 8 (1), 5710. doi: 10.1038/s41598-018-24012-y

Mittler, R., Vanderauwera, S., Gollery, M., and Van Breusegem, F. (2004). Reactive oxygen gene network of plants. *Trends Plant Sci.* 9 (10), 490–498. doi: 10.1016/j.tplants.2004.08.009

Mortazavi, A., Williams, B., McCue, K., and Schaeffer, L. (2008). Mapping and quantifying mammalian transcriptomes by RNA-Seq. *Nat. Methods* 5 (7), 621–628. doi: 10.1038/nmeth

Nakabayashi, R., Yonekura-Sakakibara, K., Urano, K., Suzuki, M., Yamada, Y., Nishizawa, T., et al. (2014). Enhancement of oxidative and drought tolerance in Arabidopsis by overaccumulation of antioxidant flavonoids. *Plant J.* 77 (3), 367–379. doi: 10.1111/tpj.12388

Nakasugi, K., Crowhurst, R. N., Bally, J., Wood, C. C., Hellens, R. P., and Waterhouse, P. M. (2013). *De novo* transcriptome sequence assembly and analysis of RNA silencing genes of *Nicotiana benthamiana*. *PloS One* 8 (3), e59534. doi: 10.1371/journal.pone.0059534

Ning, Y., Jantasuriyarat, C., Zhao, Q., Zhang, H., Chen, S., Liu, J., et al. (2011). The SINA E3 Ligase OsDIS1 negatively regulates drought response in rice. *Plant Physiol.* 157 (1), 242–255. doi: 10.1104/pp.111.180893

Noctor, G., Mhamdi, A., Chaouch, S., Han, Y. I., Neukermans, J., Marquez-Garcia, B., et al. (2012). Glutathione in plants: an integrated overview. *Plant Cell Environ.* 35 (2), 454–484. doi: 10.1111/j.1365-3040.2011.02400.x

Parapunova, V., Busscher, M., Busscher-Lange, J., Lammers, M., Karlova, R., Bovy, A. G., et al. (2014). Identification, cloning and characterization of the tomato TCP transcription factor family. *BMC Plant Biol.* 14 (1), 157. doi: 10.1186/1471-2229-14-157

Pertea, M., Pertea, G. M., Antonescu, C. M., Chang, T. C., Mendell, J. T., and Salzberg, S. L. (2015). StringTie enables improved reconstruction of a transcriptome from RNA-seq reads. *Nat. Biotechnol.* 33 (3), 290–295. doi: 10.1038/nbt.3122

Ranney, T., Bassuk, N., and Whitlow, T. (1991). Osmotic adjustment and solute constituents in leaves and roots of water-stressed cherry (*Prunus*) trees. *J. Am. Soc Hortic. Sci.* 116 (4), 684–688. doi: 10.21273/JASHS.116.4.684

Ren, W., and Chen, L. (2023). Integrated transcriptome and metabolome analysis of salinity tolerance in response to foliar application of β-alanine in Cotton seedlings. *Genes* 14, 1825. doi: 10.3390/genes14091825

Ren, W., Chen, L., Xie, Z. M., and Peng, X. (2022). Combined transcriptome and metabolome analysis revealed pathways involved in improved salt tolerance of *Gossypium hirsutum* L. seedlings in response to exogenous melatonin application. *BMC Plant Biol.* 22 (1), 552. doi: 10.1186/s12870-022-03930-0

Ros, R., Muñoz-Bertomeu, J., and Krueger, S. (2014). Serine in plants: biosynthesis, metabolism, and functions. *Trends Plant Sci.* 19 (9), 564–569. doi: 10.1016/j.tplants.2014.06.003

Sečenji, M., Hideg, É., Bebes, A., and Györgyey, J. (2010). Transcriptional differences in gene families of the ascorbate-glutathione cycle in wheat during mild water deficit. *Plant Cell Rep.* 29 (1), 37–50. doi: 10.1007/s00299-009-0796-x

Seiler, N., and Raul, F. (2005). Polyamines and apoptosis. *J. Cell. Mol. Med.* 9 (3), 623–642. doi: 10.1111/j.1582-4934.2005.tb00493

Seki, M., Umezawa, T., Urano, K., and Shinozaki, K. (2007). Regulatory metabolic networks in drought stress responses. *Curr. Opin. Plant Biol.* 10 (3), 296–302. doi: 10.1016/j.pbi.2007.04.014

Sousa, A. R. d. O., Silva, E.M.d. A., Filho, M. A. C., Costa, M. G. C., Filho, W. d. S. S., Micheli, F., et al. (2022). Metabolic responses to drought stress and rehydration in leaves and roots of three Citrus scion/rootstock combinations. *Sci. Hortic.* 292, 110490. doi: 10.1016/j.scienta.2021.110490

Szabados, L., and Savouré, A. (2010). Proline: a multifunctional amino acid. *Trends Plant Sci.* 15 (2), 89–97. doi: 10.1016/j.tplants.2009.11.009

Takahashi, T., and Kakehi, J.-I. (2009). Polyamines: ubiquitous polycations with unique roles in growth and stress responses. *Ann. Bot.* 105 (1), 1–6. doi: 10.1093/aob/mcp259

Tatusov, R. L., Galperin, M. Y., Natale, D. A., and Koonin, E. V. (2000). The COG database: a tool for genome-scale analysis of protein functions and evolution. *Nucleic Acids Res.* 28 (1), 33–36. doi: 10.1093/nar/28.1.33

Thalmann, M., Pazmino, D., Seung, D., Horrer, D., Nigro, A., Meier, T., et al. (2016). Regulation of leaf starch degradation by abscisic acid is important for osmotic stress tolerance in plants. *Plant Cell* 28 (8), 1860–1878. doi: 10.1105/tpc.16.00143

Unamba, C., Nag, A., and Sharma, R. (2015). Next generation sequencing technologies: the doorway to the unexplored genomics of non-model plants. *Front. Plant Sci.* 6. doi: 10.3389/fpls.2015.01074

Villanueva, R. A. M., and Chen, Z. J. (2019). ggplot2: elegant graphics for data analysis (2nd ed.). *Meas. Interdiscip. Res.* 17 (3), 160–167. doi: 10.1080/15366367.2019.1565254

Wang, D., and Gong, R. (2017). Transcriptome profiling of *Loquat* leaves under drought stress. *Acta Agric. Boreali-Sinica* 32 (1), 60–67. doi: 10.7668/hbnxb.2017.01.010

Wang, M., Huang, L., Liang, H., Wen, X., Liu, H., Ren, H., et al. (2021). Conservation introduction of *Illicium difengpi*, an endangered medicinal plant in southern China is feasible. *Glo. Ecol. Conserv.* 30, e01756. doi: 10.1016/j.gecco.2021.e01756

Xie, Z., jiang, D., Dai, T., and Cao, W. (2002). Sugar signal and its regulation on C/N metabolism gene in plant. *Plant Physiol. Commun.* 4), 399–405. doi: 10.13592/j.cnki.ppj.2002.04.034

Xu, J., Fang, X., Li, Y., and Chen, Y. (2019). General and specialized tyrosine metabolism pathways in plants. *Abiotech* 1 (2), 97–105. doi: 10.1007/s42994-019-00006-w

Xu, X., Legay, S., Sergeant, K., Zorzan, S., Leclercq, C. C., Charton, S., et al. (2021). Molecular insights into plant desiccation tolerance: transcriptomics, proteomics and targeted metabolite profiling in *Craterostigma plantagineum*. *Plant J* 107 (2), 377–398. doi: 10.1111/tpj.15294

Yang, A., Akhtar, S. S., Li, L., Fu, Q., Li, Q., Naeem, M., et al. (2020). Biochar mitigates combined effects of drought and salinity stress in Quinoa. *Agronomy* 10 (6), 912. doi: 10.3390/agronomy10060912

Yang, F., and Lv, G. (2022). Combined analysis of transcriptome and metabolome reveals the molecular mechanism and candidate genes of *Haloxylon* drought tolerance. *Front. Plant Sci.* 13. doi: 10.3389/fpls.2022.1020367

Yang, J., Zhang, J., Li, C., Zhang, Z., Ma, F., and Li, M. (2019). Response of sugar metabolism in apple leaves subjected to short-term drought stress. *Plant Physiol. Bioch.* 141, 164–171. doi: 10.1016/j.plaphy.2019.05.025

Ye, J., Coulouris, G., Zaretskaya, I., Cutcutache, I., Rozen, S., and Madden, T. L. (2012). Primer-blast: a tool to design target-specific primers for polymerase chain reaction. *BMC Bioinf.* 13 (1), 134. doi: 10.1186/1471-2105-13-134

You, J., Zhang, Y., Liu, A., Li, D., Wang, X., Dossa, K., et al. (2019). Transcriptomic and metabolomic profiling of drought-tolerant and susceptible sesame genotypes in response to drought stress. *BMC Plant Biol.* 19 (1), 267. doi: 10.1186/s12870-019-1880-1

Zandalinas, S. I., Sales, C., Beltrán, J., Gómez-Cadenas, A., and Arbona, V. (2016). Activation of secondary metabolism in *citrus* plants is associated to sensitivity to combined drought and high temperatures. *Front. Plant Sci.* 7. doi: 10.3389/fpls.2016.01954

Zhang, Y., Clemens, A., Maximova, S. N., and Guiltinan, M. J. (2014). The *Theobroma cacao* B3 domain transcription factor TcLEC2plays a duel role in control of embryo development and maturation. *BMC Plant Biol.* 14 (1), 106. doi: 10.1186/1471-2229-14-106

Zhang, Z., You, Y., Huang, Y., Li, X., Jinchi, Z., Zhang, D., et al. (2012). Effects of drought stress on *Cyclobalanopsis glauca* seedlings under simulating karst environment condition. *Acta Ecol. Sin.* 32 (20), 6318–6325. doi: 10.5846/stxb201204080492

Zhao, X., Huang, L., Sun, X., Zhao, L., and Wang, P. (2022). Transcriptomic and metabolomic analyses reveal key metabolites, pathways and candidate genes in *Sophora davidii* (Franch.) skeels seedlings under drought stress. *Fron. Plant Sci.* 13. doi: 10.3389/fpls.2022.785702

Frontiers in
Plant Science

Cultivates the science of plant biology and its applications

The most cited plant science journal, which advances our understanding of plant biology for sustainable food security, functional ecosystems and human health.

Discover the latest Research Topics

See more →

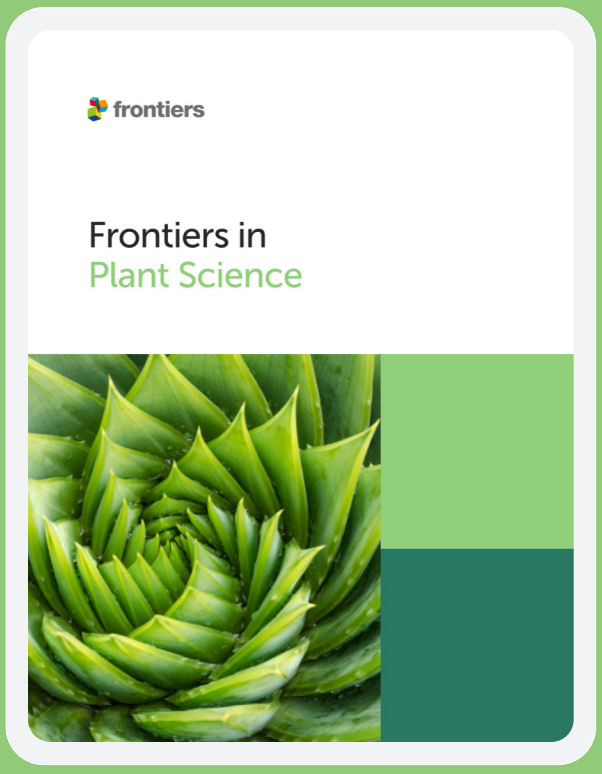

Frontiers

Avenue du Tribunal-Fédéral 34
1005 Lausanne, Switzerland
frontiersin.org

Contact us

+41 (0)21 510 17 00
frontiersin.org/about/contact